Pool-Type LMFBR Plant
1000 MWe Phase A-Extension-2 Design
Volume 6: Heat Transport Systems

Keywords:
Breeder Reactor
LMFBR
Pool-Type Reactor
Nuclear Power Plant

EPRI

EPRI NP-1014
Volume 6
Final Report
June 1979

Prepared by
General Electric Company
Sunnyvale, California

ELECTRIC POWER RESEARCH INSTITUTE

Pool-Type LMFBR Plant
1000 MWe Phase A-Extension-2 Design

PART V: HEAT TRANSPORT SYSTEMS

NP-1014, Volume 6
Research Project 620-20

Final Report, June 1979

Prepared by

GENERAL ELECTRIC COMPANY
Advanced Reactor Systems Department
310 DeGuigne Drive
Sunnyvale, California 94086

Project Manager
S. M. Davies

Prepared for

Electric Power Research Institute
3412 Hillview Avenue
Palo Alto, California 94304

EPRI Project Manager
J. G. Duffy
Nuclear Power Division

PREFACE

This report describes Phase A Extension 2 work performed between August 1 and December 31, 1978 on the design of a large pool-type LMFBR power plant. The work is the result of a team effort by Bechtel Corporation and General Electric Company which was sponsored and guided by Bechtel Corporation and General Electric Company which was sponsored and guided by the Electric Power Research Institute (EPRI). The objective of the work was to complete the conceptual plant design established during Phase A and Phase A Extension 1 during the period from April, 1977 through July, 1978.

The Phase A effort produced an initial description of the overall plant, structures and systems. During Phase A, General Electric developed a conceptual design of the overall nuclear steam supply system (NSSS). It defined specific design approaches for selected NSSS components and subsystems after analyzing various design alternatives. Bechtel assumed responsibility for the intermediate sodium piping arrangement, the access area above the reactor deck and the Balance of Plant (BOP). The resulting integrated plant design provided the necessary seismic data for both the NSSS and the BOP.

The special expertise of several subcontractors was used during Phase A; Byron-Jackson provided a preliminary design of the primary sodium pump, Foster-Wheeler provided a preliminary design of the intermediate heat exchanger (IHX), and CBI Nuclear reviewed the reactor deck design and developed a construction sequence for the overall reactor assembly.

The Phase A effort by General Electric, Bechtel and the subcontractors was funded at a level of nearly 1.7 million dollars. Additionally, General Electric contributed a company-funded effort and both General Electric and Bechtel utilized their backgrounds of prior work on pool-type LMFBRs and extensive interaction with foreign LMFBR organizations. The results of the Phase A work was published by EPRI in April 1978 in report number NP-646, "Pool-Type LMFBR Plant, 1000 MWe Phase A Design."

During Phase A Extension 1, funded at a level of approximately 1.4 million dollars, specific areas established during Phase A received further development and evaluation. These specific areas included the reactor deck, the reactor assembly, the heat transfer system components, the reactor auxiliary systems, and the instrumentation and control systems. Several subcontractors were also used during Phase A Extension 1; Foster-Wheeler designed an alternate IHX, CBI Nuclear evaluated an alternate deck support scheme and further developed the reactor assembly construction sequence, and United Nuclear Industries provided conceptual designs for removable radiation shielding in the deck. The results of the Phase A Extension 1 work was published by EPRI in September 1978 in report number NP-882, "Pool-Type LMFBR Plant, 1000 MWe Phase A-Extension-1 Design."

During Phase A Extension 2, funded at a level of approximately 1.4 million dollars, the reactor assembly, the reactor deck, heat transport systems, auxiliary systems, seismic analysis, maintenance studies, construction studies, a safety approach, and the balance-of-plant design were all brought to levels consistent with a completed concept. Assistance in several specialized areas was supplied by subcontractors; Chicago Bridge and Iron provided a fabrication scheme for the thermal barrier design, Foster-Wheeler developed the IHX design, Bryon-Jackson continued work on the primary sodium pump design, Engineering Decision Analysis Corporation verified and further developed the seismic studies, and CBI Nuclear studied construction of alternate vessel supports and fabrication of the upper internals structure.

"Phase A Extension 1" and "Phase A Extension 2" are frequently shortened to "Extension 1" and "Extension 2" when referred to in this report.

This report of the Phase A Extension 2 work is logically divided into thirteen parts, which have the general title "Pool-Type LMFBR, 1000 MWe Phase A - Extension-2 Design:"

Part I	Executive Summary
Part II	Plant Summary Description
Part III	Reactor Assembly
Part IV	Reactor Deck
Part V	Heat Transport Systems
Part VI	Auxiliary Systems
Part VII	Plant Control and Instrumentation
Part VIII	Seismic Analysis
Part IX	Constructibility and Fabricability

Part X	Maintainability and Inspectibility
Part XI	Safety
Part XII	Balance of Plant - Plant Description
Part XIII	Balance of Plant - Evaluation of Pool-Related Areas

The report is physically divided into twelve volumes as follows:

Volume I	Part I
Volume 2	Part II
Volume 3	Part III, Sections 1 through 2.5
Volume 4	Part III, Sections 2.6 through Appendix IIIB
Volume 5	Part IV
Volume 6	Part V
Volume 7	Parts VI, VII and VIII
Volume 8	Parts IX, X and XI
Volume 9	Part XII
Volume 10	Part XII Appendices
Volume 11	Part XIII
Volume 12	Part XIII Appendices

A Table of Contents for all volumes is included at the end of every volume.

PART V: HEAT TRANSPORT SYSTEMS

Section 1: Introduction and Summary of Phase A and Extensions

CONTENTS

TABLES

FIGURES

1.1 INTRODUCTION

The heat transport systems carry heat from the reactor to the IHXs and from the IHXs to the steam generators. The major components in the primary heat transport system are the primary sodium pumps and IHXs, and the major components in the intermediate heat transport system are the intermediate sodium pumps and steam generators. This section summarizes the history and evolution of the pool reactor heat transport systems and components during previous study phases. In addition, highlights of the current study are summarized.

The sodium piping is not discussed in this section because primary sodium piping is designed as part of the reactor assembly structures (Ref. 1) and the intermediate sodium piping as part of the BOP (Ref. 2). Also, the reactor auxiliary cooling system is reported under the auxiliary systems design task. However, the sodium water reaction pressure relief system (SWRPRS) is treated as part of the intermediate heat transport system. Results of TRANSWRAP analysis which were documented in the Phase A Report (Ref. 3) are summarized in this review.

The principal design criteria for the heat transport systems were established during Phase A (Ref. 4). Consistent with guidelines established by EPRI (Ref. 5), the primary heat transport system incorporates six IHXs and four sodium pumps. General Electric elected to provide each component with shutoff valve capability to facilitate operation with individual components out of service. The use of six IHXs led to the selection of six IHTS loops with a single steam generator module in each IHTS loop. During the initial pool study phase, the following diagrams (Ref. 6) were developed and maintained as reference conditions during subsequent design phases:

- o Plant Heat Balance based on 2903 MWt reactor core, 1000 MWe gross output, and 923 MWe net output (Figure 1-1).

- o PHTS Flow Diagram with tabulated thermal hydraulic conditions for full power (Figure 1-2).

- o IHTS Flow Diagram (Figure 1-3).

- o Hydraulic Profile (Figure 1-4).

1.2 SODIUM - WATER REACTION PRESSURE RELIEF SYSTEM

The analysis of the PLBR sodium water reaction pressure relief system (SWRPRS), based upon double ended guillotine failure of one duplex steam generator tube, was performed at the end of a prior DOE/EPRI loop reactor study and was documented in the Phase A report. This work is considered generally applicable to the reference pool IHTS and steam generator systems. Results indicate a single relief point on the steam generator (SG) module does not provide adequate protection to prevent over pressurization of the IHX. However, replacing the single relief point on the SG shell with two relief points, one on the SG inlet sodium line and one on the outlet line, results in acceptable peak pressures in the IHX.

1.3 PRIMARY PUMP AND IHX

Reference design concepts for the primary pump and IHX were initially established during Phase A (Ref. 7, 8). This EPRI sponsored pool concept plant design study does not include specific studies of the steam generator. Previous PLBR loop work had established a reference steam generator design for a four loop plant for both one and two modules per loop (Ref. 9).

To facilitate systems and building arrangement studies by Bechtel for the pool reactor during Phase A, General Electric established a reference design for a new steam generator size corresponding to one steam generator module per loop and six IHTS loops. Figure 1-5 depicts this steam generator arrangement. Table 1-1 lists the pertinent steam generator data for the Phase A six module plant and the previous Phase II four module plant (Ref. 9).

The following major design studies were conducted for the primary pump and the IHX in the heat transport systems duing Phase A and Extensions:

- o In Phase A, the primary pump was designed for a total system pressure drop of 90 psi, which is consistent with the reference core design. In Extension 2, in order to allow for a new core with higher pressure drop consistent with new EPRI guidance, the primary pump was redesigned to accommodate an increased total system pressure drop of 120 psi.

- In order to accommodate the differential expansion between the IHX tubes and shell, a straight tube design with a bellows on the shell was developed in Phase A; the design was based to a large extent upon CRBR IHX features, including straight tubes. A bent tube design (two tube bends) without bellows on the shell was developed and selected as the reference design in Extension 1. The added tube-to-tube and tube bundle-to-shell flexibility of the bent tube concept was a major factor in selecting it as the new reference design. Studies were made of features to further optimize the bent tube design for Extension 2, including:

  - the potential for using one instead of two tube bends;
  - the possibility of eliminating the primary sodium outer tube row deflector and the lower heat protector; and
  - the development of a conceptual design and an analysis of the diving bell seal for hot pool/cold seal and comparison with the double bellows approach.

Results of the most recent design studies in Extension 2 for the major heat transport components are summarized as follows:

A new primary pump design with slightly larger impeller diameter and slightly greater length than that of the Phase A was established to accommodate the higher total system pressure drop. However, the revised design did not change the deck penetration diameter nor the diameter of the pump support flange. Reference 10 provides additional details of the Byron Jackson pump study.

In an evaluation of one versus two-bend tube geometry, the worst case thermal conditions and displacement resulted when a tube was plugged. The single-bend geometry was found acceptable, with low stress and no tube touching, by locating the bend in the lower bundle region and cutting the plugged tube above the bend.

A simplified inelastic analysis of the lower tubesheet of the IHX verified that the flow deflector and the lower head protector could be eliminated. The diving bell seal was selected over the bellows concept as the reference design because of its lower primary pressure drop, less space requirement and predicted higher reliability. Reference 11 provides additional details of the Foster-Wheeler IHX study.

The impact of using constant speed (one or two-speed) pumps in the heat transport system was investigated during Extension 2. For a saturated steam cycle, a constant speed pump system offers the potential for significant cost reduction, resulting from reduced building space and improved reliability, yet impose no major component design changes nor additional risk to plant operation. However, the variable speed pump is retained as the reference for the first prototype plant because of the anticipated need of operational flexibility in a first-of-a-kind plant.

1.4 OPERATION WITH COMPONENTS OUT OF SERVICE

During Extension 1 plant characteristics and limitations were examined with only four or five of the six IHXs in service or with three of the four primary pumps in operation (Ref. 12). This study was based upon the reference design using variable speed pumps. Results indicated that operation with one component, either an intermediate heat exchanger or primary pump, out-of-service appears acceptable. Operation with two IHXs out-of-service requires further study due to temperature limitations. The pool-type primary system offers the flexibility to operate all of the intermediate heat exchangers and intermediate heat transport loops when a primary system pump is out-of-service.

1.5 PLANT TRANSIENTS

Plant thermal transients occur during normal operation, including startup and shutdown, and during upset, emergency and faulted events. The number of transients and their severity in terms of temperature change rates are important to the structural integrity of the plant. During Phase A the severity of the most important transients such as reactor scram, was determined for a variety of thermal hydraulic and sodium pump control assumptions. In Extension 1 a plant duty cycle was estimated and contained the numbers of all types of events expected during a 40 year plant lifetime. Additionally, the thermal hydraulic model, which described the mixing of post-scram sodium in the hot pool, was improved and used to analyze the effects of different post-scram sodum pump speeds. In a pool-type LMFBR it is expected that the post-scram pump speed can vary between full flow and pony motor flow without an excessively severe hot pool thermal transient. During Extension 1 the post-scram pump speed was tentatively chosen as 50% of full flow, a compromise which minimizes the severity of the hot pool transient without entering the uncertain area of sodium mixing at low flows. During Extension 2 transients involving steam generator blowdown were investigated and found to be benign on the water side of the saturated steam generator. The sodium temperature for the blowdown transient are similar to those where an intermediate pump loses power. The loss of an intermediate pump causes the primary sodium temperature leaving the affected IHX to rise rapidly. Methods of alleviating this effect were further investigated in Extension 2. These studies give confidence that a pool type plant can withstand the most often encountered severe thermal transients and the flexibility exists in the ultimate choice of the post-scram sodium pump speed. Further understanding of post-scram thermal hydraulic behavior in a pool reactor is needed before a final selection of post scram pump speed.

1.6 REFERENCES

1. EPRI NP-646 "Pool-Type LMFBR Plant, 1000 MWe Phase A Design," Part IV, Section 1, April 1978.

2. Ref. 1, Part VII, Section 3.

3. Ref. 1, Part VI, Section 2.

4. Ref. 1, Part II, Sections 1 and 2.

5. This report, Appendix IIA to Part II.

6. Ref. 1, Part II, Section 7.

7. Ref. 1, Part II, Section 3.

8. Ref. 1, Part II, Section 5.

9. GEFR-00099, "Prototype Large Breeder Reactor, Phase II Conceptual Design," Vol. III, Part 2, Ch. 4, June 1977.

10. This report, Appendix VB to Part V.

11. This report, Appendix VA to Part V.

12. This report, Part V, Section 2.4.

TABLE 1-1

STEAM GENERATOR DATA FOR PHASE A AND PHASE II
DOUBLE WALL, STRAIGHT TUBE, 2-1/4 Cr-1 Mo, 1 UNIT/LOOP

	PHASE II	PHASE A
Number of Loops	4	6
Heat Load, MWt per unit	729	486
Water/Steam Flow Rate, lba/hr	4.77×10^6	2.10×10^6
Sodium Flow-Rate, lba/hr	30.5×10^6	20.3×10^6
Outer Tube OD/ID, inches	1.50/1.35	1.50/1.35
Inner Tube OD/ID, inches	1.35/1.22	1.35/1.22
Number of Tubes	2010	1739
Active Tube Length, feet	79	62.5
Total Tube Length, feet	89	66.7
Active OD Heat Transfer Area, $ft.^2$	62,300	42,700
Tube Pitch, inches	2.5	2.5
Bundle Diameter, inches	118	113.6
Vessel Diameter, OD, inches	157.5	148
Overall Length, feet	137.7	109.5
Number of Steam Separators	55	37

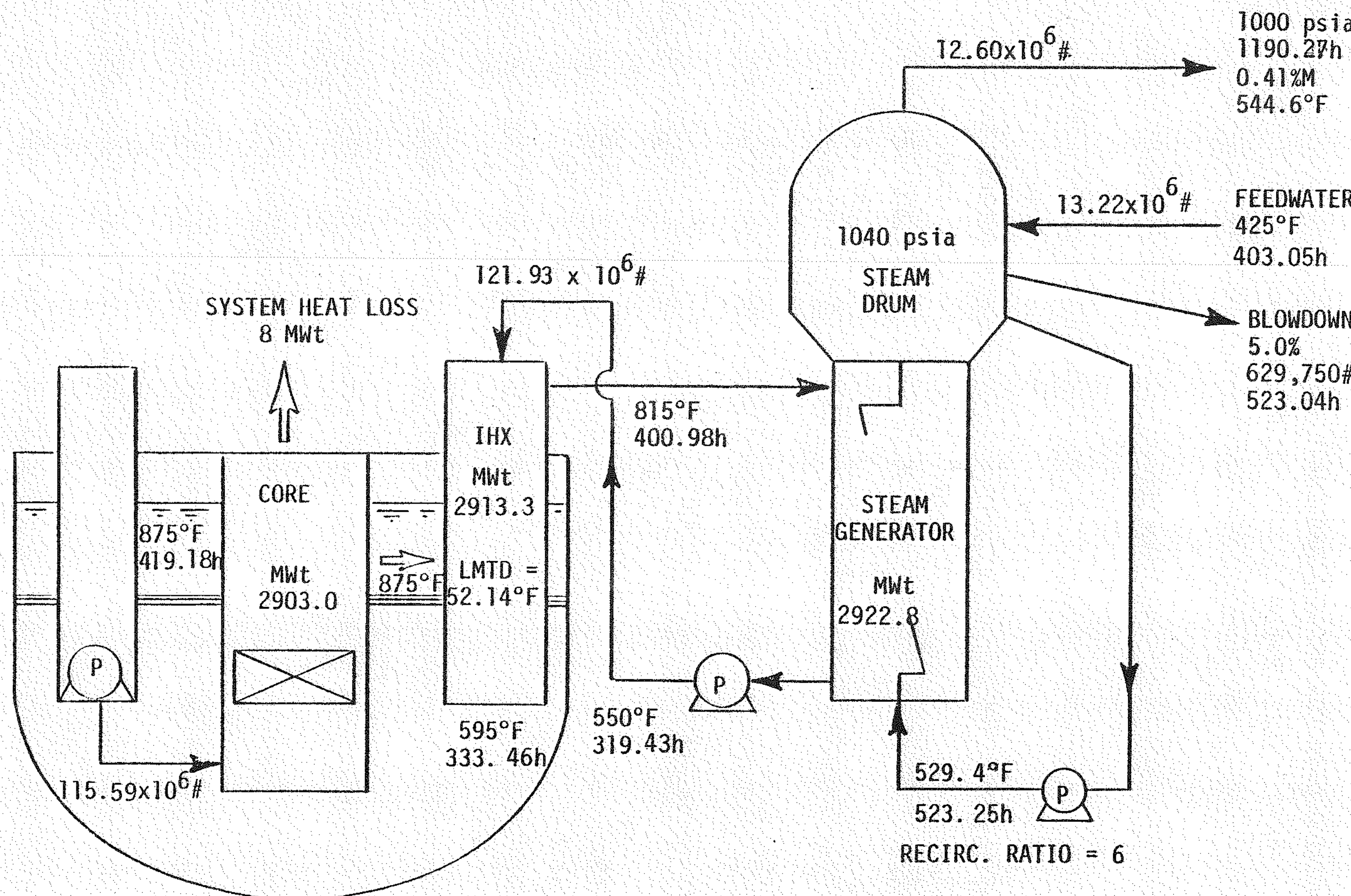

	PRIMARY	INTERMEDIATE	RECIRC.
PUMP HEAD, psi	120	60	45
FLOW/PUMP, gpm	68423*	45960	33175
NO. OF PUMPS	4	6	6
INPUT POWER, MWe	19.3*	10.1	4.9
HEAT ADDED, MWt	18.3*	9.5	4.6
MOTOR EFF.	0.95	0.94	0.93
PUMP EFF.	0.78	0.76	0.85

*Includes 4% core bypass flow.

TURBINE HEAT RATE	=	9974 Btu/kW-hr.
GROSS POWER OUTPUT	=	1001.7 MWe
NET PLANT POWER	=	921.5 MWe
PLANT NET EFFICIENCY	=	31.7%

FIGURE 1-1 PHASE A PLANT HEAT BALANCE DIAGRAM

GENERAL ELECTRIC

UNLESS OTHERWISE SPECIFIED USE THE FOLLOWING:–				
APPLIED PRACTICES	SURFACES	TOLERANCES ON MACHINED DIMENSIONS: FRACTIONS	DECIMALS	ANGLES
	✓	±	±	±

TITLE FLOW DIAGRAM
PHTS AND RACS WITHIN POOL
FIRST MADE FOR

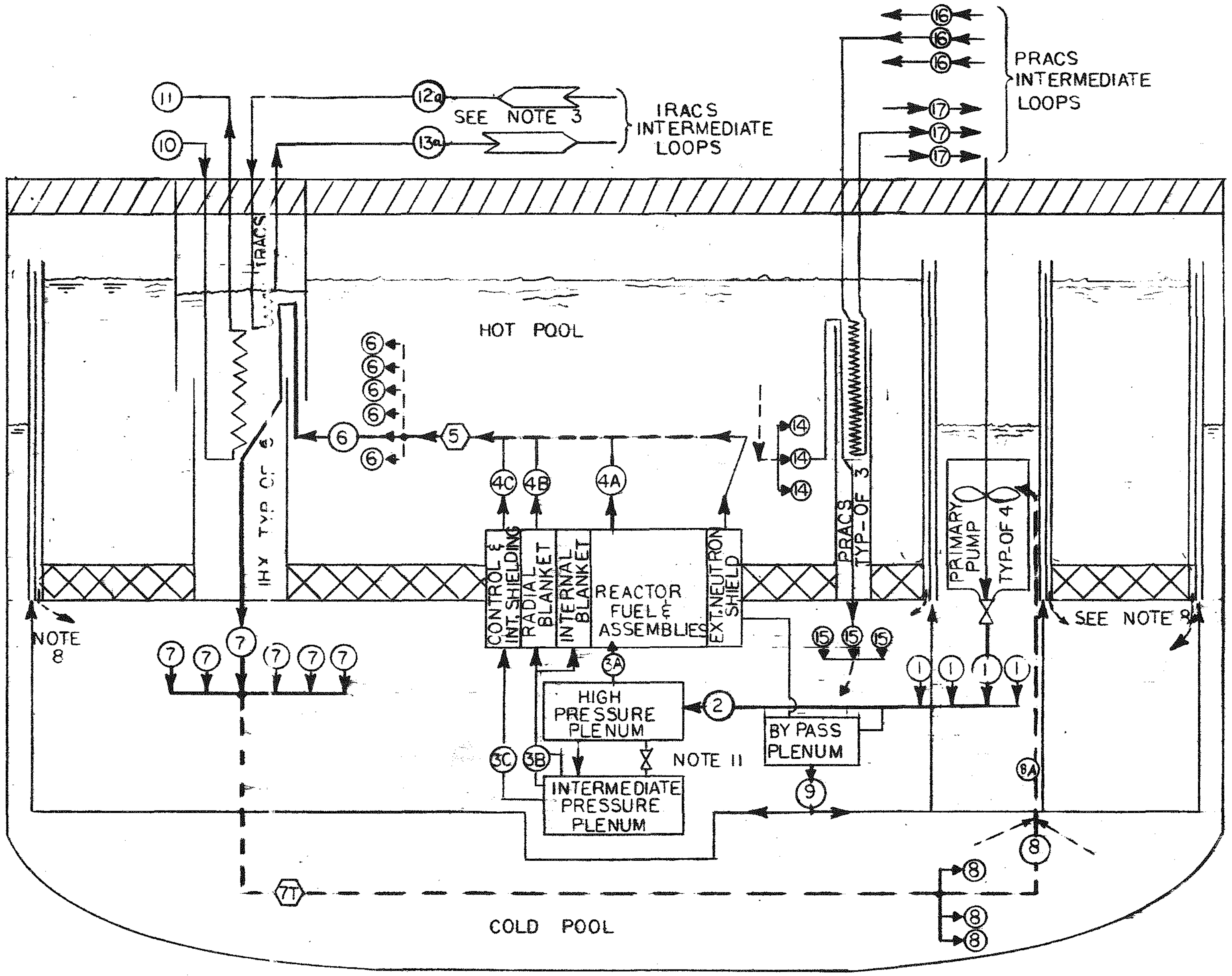

NOTES:
1. IRACS ARE LOCATED ABOVE THE MAIN IHX BUNDLE.
2. THERE ARE 6 IPRACS. THE FLOW IN 12 AND 13 IS PER UNIT.
3. PRACS AND IRACS CONDITIONS SHOWN FOR N-1 CAPACITY:
   2 PRACS = 34 MWT.
   5 IRACS = 34 MWT.
4. POINT 1 DOES NOT INCLUDE SODIUM LEAKAGE THRU PUMP HIGH PRESSURE PIPING SEAL.
5. DARK LINE = MAIN PHTS FLOW PATH.
6. SODIUM FLOW THERMAL BARRIERS ARE PROVIDED AROUND ALL 4 PUMPS AND AROUND THE INSIDE OF THE PRIMARY TANK.
7. IHX PRIMARY SODIUM INLET FLOW SHUTOFF ACCOMPLISHED BY GAS PRESSURIZATION FOR SODIUM LEVEL CONTROL IN IHX.
8. SODIUM FLOWS OUT OF THE THERMAL BARRIERS AND RETURNS DIRECTLY TO THE SODIUM IN THE COLD POOL.
9. PRIMARY SODIUM FLOW THROUGH IRACS ALSO FLOWS THROUGH THE IHX.
10. P. Na = PRIMARY SODIUM.
    I. Na = INTERMEDIATE SODIUM.
    NaK = SODIUM POTASSIUM ALLOY
11. SEE CORE INTERNAL DRAWING FOR DETAIL OF THIS REMOVABLE MAINTAINABLE VALVE
12. DASHED LINES INDICATE SODIUM FLOW PATHS IN BULK COLD OR HOT POOLS

CORE POWER AT 2903 MWT

POINT NO.	1	2	3A	3B	3C	4A	4B	4C	5	6	7	7T	8	9	10	11	12	13	14	15	16	17	8A
TEMP, °F	595	595	595	595	595	923	760	–	875	875	595	595	595	595	550	815	∓	∓	∓	∓	∓	∓	595
FLOW, 10^6 LB/HR	30.05	115.59	TBD	TBD	TBD	TBD	TBD	TBD	115.59	19.27	19.27	115.58	28.90	4.62	20.32	20.32	∓	∓	∓	∓	∓	∓	30.05
PRESSURE, PSIG	*	*	*	*	*	*	*	*	*	*	*	*	*	*	*	*	∓	∓	∓	∓	∓	∓	*
FLUID	P.Na	P.Na	P.Na	P.Na	P.Na	P.Na	P.Na	P.Na	P.Na	P.Na	P.Na	P.Na	P.Na	P.Na	I.Na	I.Na	∓	∓	∓	∓	∓	∓	P.Na

∓ NO FLOW AT FULL POWER ; * TO BE DETERMINED

DESIGN CONDITION FOR DECAY HEAT REMOVAL

	IRACS				PRACS			
POINT NO.	12	13	6	7	14	15	16	17
TEMP, °F	510	830	875	775	875	595	540	820
FLOW, 10^6 LB/HR	.350	.365	.76	.76	.677	.677	.984	.984
PRESSURE, PSIG	*	*	*	*	*	*	*	*
FLUID	NaK	NaK	P.Na	P.Na	P.Na	P.Na	NaK	NaK

FIGURE I-2 PHTS FLOW DIAGRAM

REVISIONS | PRINTS TO

REV. A 11-77, B 1-78, C 2-78, D 1-79, E 3-79, F

MADE BY A. SHAHIN 10-18-77
ISSUED
APPROVALS
AFS-SK-P011

FF-809-P (6-76) PRINTED IN USA

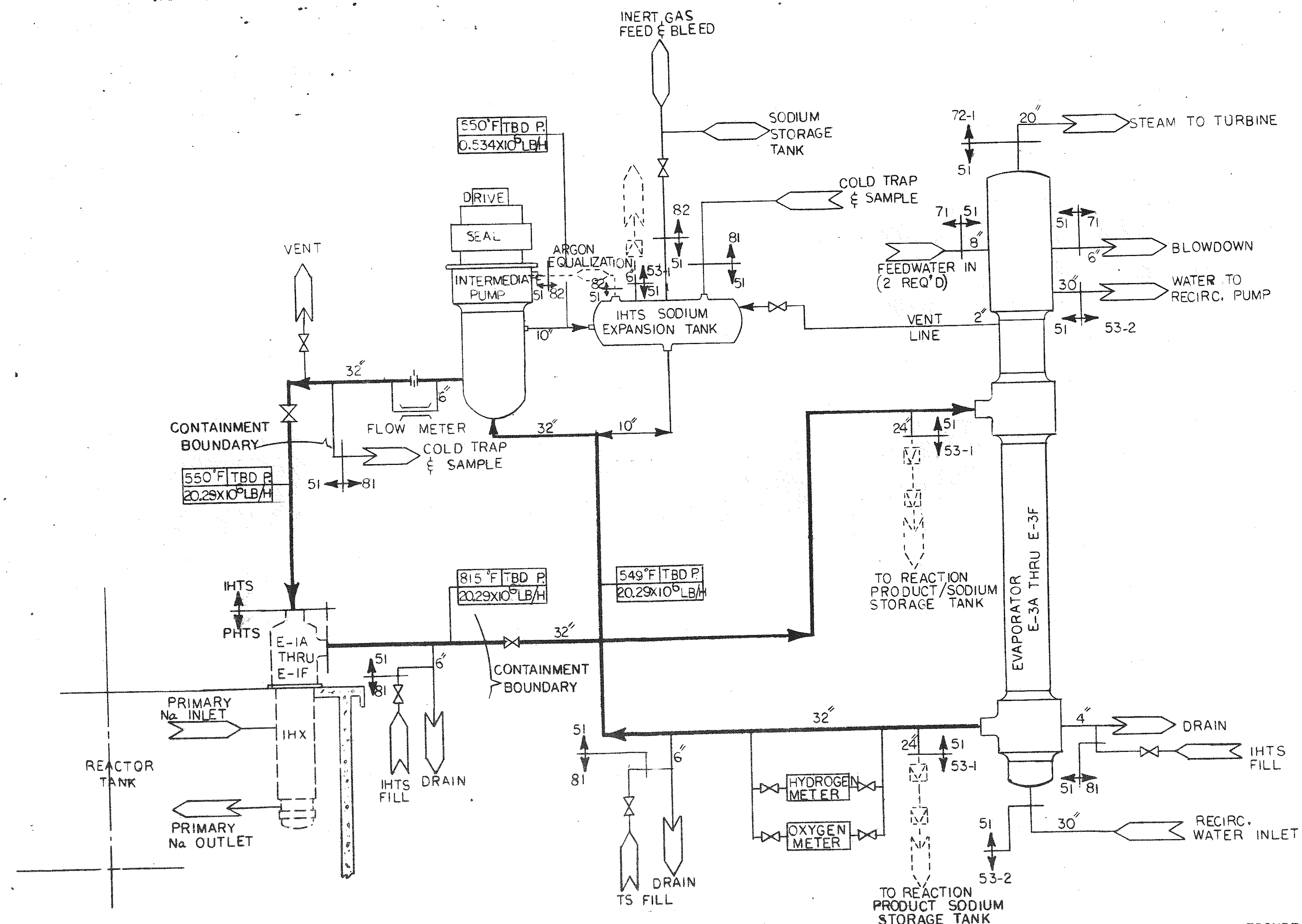

FIGURE 1-3 IHTS FLOW DIAGRAM

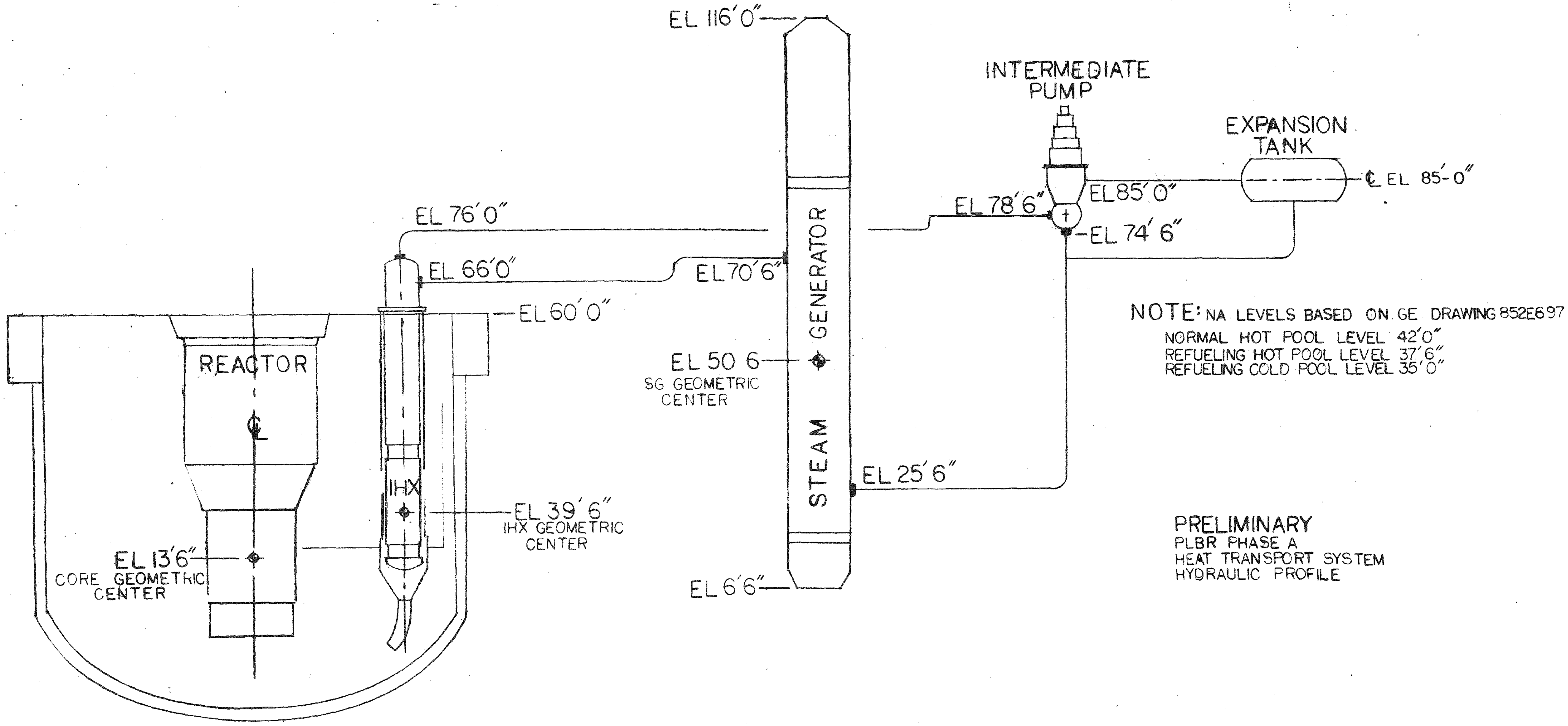

FIGURE 1-4 HTS HYDRAULIC PROFILE

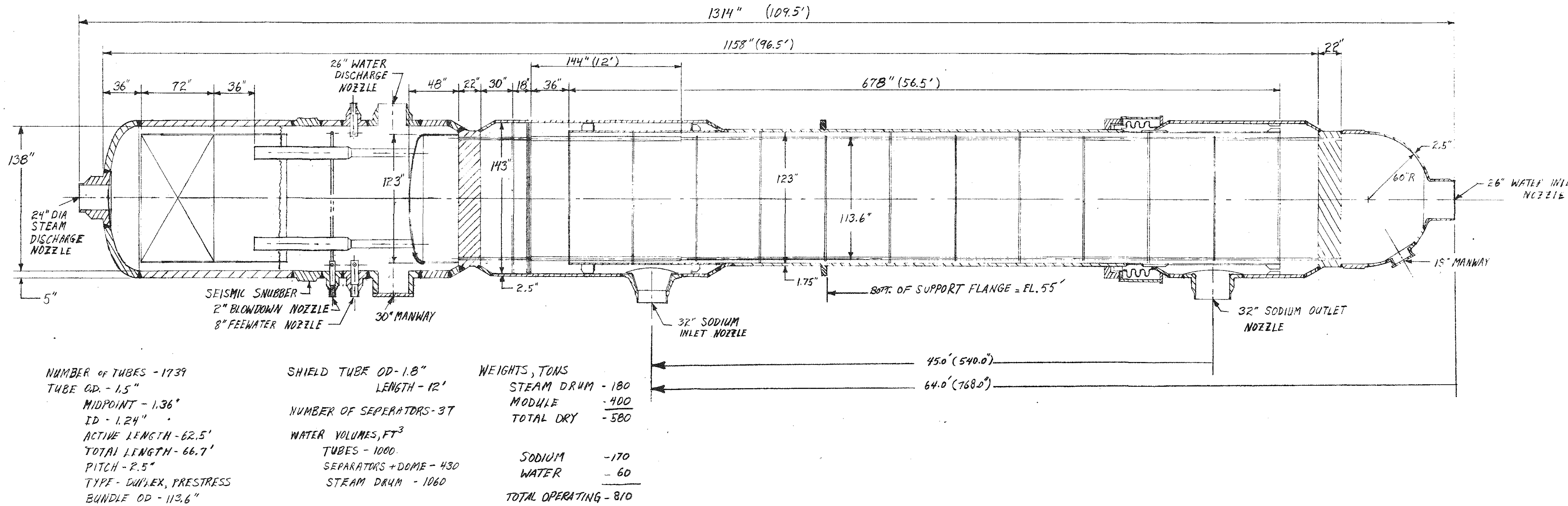

FIGURE 1-5 PHASE A STEAM GENERATOR

PART V: HEAT TRANSPORT SYSTEMS

SECTION 2: WORK PERFORMED DURING EXTENSION 2

SUBSECTION 2.1: IHX DESIGN

CONTENTS

TABLES

FIGURES

1. INTRODUCTION AND SUMMARY

Further studies were made on specific areas of the bent tube IHX design during Phase A Extension 2 of the 1000 MWe Pool-Type LMFBR design study.

A feasibility study, including a thermal stress and a tube wear analysis, showed that the single-bend design was acceptable if every plugged tube is cut in the span above the bend region. (The value of the double-bend design is questionable due to its uncertainty in equally distributing differential tube expansion between the two tubes.) A simplified inelastic analysis of the lower tubesheet verified that both the flow deflector and the lower head protector could be eliminated. Analysis of a proposed new tube support perforation scheme showed that very small improvement was achieved in the shell side sodium flow and thermal distribution. A preliminary design for the IRACS (for decay heat removal) support was developed. A conceptual design of the diving bell seal, for hot pool/cold pool seal at the bottom of the IHX, and a computer code for sizing the seal were developed. Preliminary designs for a 60-in. I.D. and an 80-in. I.D. double bellows hot pool/cold pool seal were also developed. The diving bell seal was selected as the reference design due to its lower primary pressure drop (2.17 psi for one tube bend design), simpler fabrication, less space requirement and the expected higher reliability than the double bellows. The low primary pressure drop as a result of using the diving bell seal provides margins for meeting the design goal of 2.5 psi. Cover gas and sodium level requirements for the IHX were further defined.

Foster Wheeler conducted the bulk of the studies as reported in Appendix VA at the end of Part V. GE conducted the studies on the diving bell seal and determined the cover gas requirements, the sodium level requirements, and the interface characteristics for the IHX.

2. IHX DESIGN

The following are the results and discussions of the further studies on specific areas of the bent tube IHX design, performed during Phase A Extension 2.

2.1 Interface Characteristics

The general arrangement drawings for the IHX are shown in Appendix VA, the Foster-Wheeler report on the IHX.

2.1.1 Deck Penetration Interface

The IHX deck penetration design and the shield plug design, including thermal analysis, structure analysis, shielding analysis and seismic analysis are described in Part IV, Reactor Deck, Subsection 2.1 through 2.8. The deck penetration seals are described in Part VI, Subsection 2.1, Component-to-Deck Seals. The IRACS support has been described in Subsection 2.4 of this report. The new deck penetration and shield plug design have not been incorporated in the drawings in Appendix VA.

2.1.2 IRACS Interface

The IRACS coils are located above the upper tubesheet in the IHX. The IRACS support has been described in Subsection 2.4 of this report. The IRACS will be used for decay heat removal and is described in Part VI, Subsection 2.2, Reactor Auxiliary Cooling Systems. The IRACS consists of an 8-in. pipe helical coil with inlet and outlet piping penetrating the shield plug, as shown in the drawings in Appendix VA.

2.1.3 IHTS Interface

The intermediate sodium from the Intermediate Heat Transport System (IHTS) flows through a 10-in. piping which penetrates the IHX protective cover (at the top of the IHX) and down through the central downcomer, up through the shell side of the tube bundle and the outlet annulus below the upper tubesheet and exit through the piping which penetrates the IHX protective cover.

2.1.4 Reactor Head Compartment Interface

The IHX protective cover which contains the intermediate piping interfaces with the Reactor Head Compartment. The protective cover containing the cooling gas is provided to minimize a sodium fire hazard in case of an intermediate sodium pipe leak.

2.1.5 Cover Gas System

The cover gas requirements for the IHX have been described in 2.6 of this subsection of the report. The sodium levels in the IHX shown in Table 2-8 have not been incorporated in the drawings in Appendix VA. The cover gas piping penetration through the deck is described in Part IV, Reactor Deck, Subsection 2.4. The cover gas system is described in Part XII, Balance of Plant.

2.1.6 Recirculating Gas Cooling System

Nitrogen cooling of the IHX deck penetration and the reactor deck are described in Part IV, Reactor Deck, Subsection 2.1, 2.4 and 2.6.

2.1.7 Core Support System

The diving bell seal located at the bottom of the IHX interfaces with the core support system. They have been described in 2.5.2 of this subsection of the report. The diving bell seal designs shown in Figure 2-1 through Figure 2-4 have not been incorporated in the drawings in Appendix VA.

2.2 One Tube Bend Versus Two Tube Bends

It was identified in Phase A Extension 1 (Ref. 1) that the bent tube IHX design with the two sine wave tube bends and the hot/cold pool double bellows seal had a total primary pressure drop of 3.2 psi, which did not meet the design goal of 2.5 psi. A feasibility study of using one instead of two bends in the IHX tubes, therefore, was conducted in an attempt to reduce the primary pressure drop.

An evaluation of the thermally induced stresses and displacements using a 2-D ANSYS analysis showed that, for the worst case when a plugged-tube results in temperature 100°F colder than its adjacent active tube, tube touching would occur for both the one bend and the two bend designs. It was determined that thermal stresses for the one bend geometry was acceptable because the bend was located in the lower cold end of the bundle and the full $3S_m$ secondary stress range for the allowable bending stress could be used. In addition, tube touching can be eliminated if the plugged tube is cut in the span above the bend region. It was concluded, therefore, that the one bend design is feasible for the bent tube IHX design. See Foster Wheeler's report in Appendix VA for details and Figures.

2.3 Flow Deflector and Lower Head Protector

The results of an ANSYS thermal and thermal stress analysis on the lower tubesheet without the flow deflector (J deflector) and the lower head protector (thermal shield inner head) showed that the maximum linearized thermal bending stress and the peak thermal stress in the perforated region exceeded the ASME Code, Section III, $3S_m$ limit on the elastically calculated secondary stress range. However, a 2-D simplified inelastic analysis of the lower tubesheet verified that both the flow deflector and the lower head protector could be eliminated. The results of the analysis show no fatigue damage and the maximum positive principal strains satisfy the Code Case 1592 allowable strain of 1% for average strains and 2% for surface strains. Furthermore, the new transient data (described in Part V, Subsection 2.3 Thermal Transients for Heat Transport Systems) are less severe than the transient data (from Phase A) which were used in the analysis. See Foster Wheeler's report in Appendix VA for details and Figures.

2.4 Shell Side Sodium Flow and Temperature Distribution

A sodium flow distribution analysis on the shell side of the bent tube IHX design indicates that the bundle entrance velocity is not uniform: the velocity is much higher near the tubesheet area and more sodium flows toward the outer edge of the bundle, as shown in Figure 12 in Appendix VA. An axisymmetric, two-dimensional thermal analysis shows that, due to the lack of cross flow effects, the temperature tends to be higher at the outer edge of the bundle. In order to get radially uniform temperature distribution by diverting more sodium to the outer edge of the bundle, the use of perforated tube supports with non-uniform spacing were investigated.

A flow distribution and thermal distribution analysis were performed for a tube support perforation with 50% perforation for the inner 60% of the bundle and 70% perforation for the outer 40% of the bundle. However, the results show that the improvement made in the thermal distribution is very small compared to the current uniform perforation of 70%. The use of a non-uniform perforation support will also introduce a new uncertainty in flow-induced vibration due to cross flow. Therefore, a uniform perforation of 70% was retained as reference design.

2.5 IRACS Coil Support

A preliminary design for the IRACS coil (for decay heat removal) supports was developed. In order for the IRACS coil support system to result in acceptable coil stresses during seismic events, the coil is supported at four circumferential locations around the helix by split support plates. These support plates are held in place by a shroud which extends down from the shield plug. See Foster Wheeler's report in Appendix VA for details and drawings.

2.6 Diving Bell Seal

A hot pool/cold pool seal at the bottom of the IHX is needed to prevent the primary sodium in the hot pool from leaking around the IHX vessel and into the cold pool. A conceptual design and an analysis for a diving bell seal were developed. Advantages and disadvantages of the diving bell seal design and the double bellows design (in Phase A Extension 1) were identified and evaluated. Based on this study, a reference design for the hot pool/cold pool seal was selected.

2.6.1 Design Requirements

The diving bell seal design must satisfy the following requirements:

- The cover gas barrier in the seal must be maintained under all plant conditions, including normal operating conditions, part load conditions and transient conditions. Table 2-1 and Table 2-2 show the limiting transients for the IHX.

- Ensure that the cover gas in the seal will not be carried over to the core. Provisions must be made to prevent the cover gas in the seal from entering the suction line of the primary pumps.

- Provide the capability for adding cover gas to the seal prior to the IHX operation and in case of loss of the cover gas.

- Since part of the diving bell seal is connected to the core support structure and part of the seal is connected to the IHX, allowances must be provided for axial movement and radial movement of the IHX relative to the core support structure due to thermal expansion and during seismic loadings, as shown in Table 2-3. The axial movement of 2.67 in. and the radial movement of 1.42 in. due to thermal expansion can be accommodated by intentionally off-centering the diving bell seal during its installation. However, the axial movement of 1.5 in. and the radial movement of 0.25 in. due to seismic loadings must be included in the design of the diving bell seal.

2.6.2 Conceptual Design

Figure 2-1 through Figure 2-4 show the conceptual design of the diving bell seal. A double diving bell seal, instead of a single diving bell seal, was selected as referece design to reduce the overall length of the IHX. Although the use of a triple diving bell seal would further reduce the overall length of the IHX, it was not adopted because it would also reduce the space available for the primary sodium discharge piping and result in a higher primary pressure drop.

The double diving bell seal consists of two troughs located at the bottom of the IHX. The troughs are divided into 2.5 in. width, to accommodate the radial movement of the IHX relative to the core support structure, by the two troughs connected to the core support structure. A piping is connected to the bottom of the trough for adding cover gas to the seal. An excess gas outlet piping is provided to prevent the cover gas from entering the suction line of the primary pump and to ensure no cover gas carryover to the reactor core. The excess cover gas will be fed into the reactor cover gas above the sodium pool in the primary tank. The idea of using a sodium level indicator and/or a thermocouple for detecting the loss of the cover gas were rejected because it is doubtful that they will last for 40 years. In addition, maintenance of the instrumentation will be very difficult because of the location of the diving bell seal.

The diving bell seal is designed to maintain the cover gas barrier in the seal during normal plant operating conditions, part load conditions and transient conditions. Before adding cover gas to the seal and with no pump flow, the seal is filled with sodium, as shown in Figure 2-1. The sodium temperature in the seal, under these conditions, will be close to the cold pool temperature (595°F) because of the stagnant sodium in the annulus between the IHX and the core support structure. Figure 2-2 shows the sodium levels in the seal after the cover gas has been added but zero pump flow. Figure 2-3 shows the sodium levels in the seal under normal plant operating conditions when the sum of the differential sodium levels in the two troughs is equivalent to the differential level between the hot pool and the cold pool in the primary tank. The sodium levels in the seal under transient and part load conditions are shown in Figure 2-4.

2.6.3 Computer Modeling

A computer code for sizing the diving bell seal was developed. The flow chart, the code and the nomenclatures for the code are shown in Appendix A, B and C respectively. Table 2-4 shows the results of sizing the double diving bell seal. As we can see from the table, the normal plant operating conditions, when the maximum differential level between the hot pool and the cold pool exists, are the controlling factors in sizing the seal. The cover gas volume and the height of the double diving bell seal required under the transient conditions and the part load conditions are less than that of the normal plant operating conditions. It is determined that a minimum cover gas volume of 39 ft^3 and a minimum height of 3.4 ft will be required for the double diving bell seal.

2.6.4 Diving Bell Seal Versus Double Bellows

In attempts to reduce the primary pressure drop through the IHX, preliminary designs for a 60-in. I.D. and a 80-in. I.D. double bellows (compared to 42-in. I.D. for Phase A Extension 1) for hot pool/cold pool seal were developed, as shown in Table 2-5. The primary pressure drop through the IHX for the double bellows and the diving bell seal, with and without the discharge elbow, are shown in Table 2-6. A 60° discharge elbow is connected to the bottom of the hot pool/cold pool seal to direct the sodium discharging from the IHX into the center of the reactor inlet plenum and away from the primary tank bottom to prevent thermal shocking at the primary tank, especially under transient conditions. For the one tube bend IHX design with the discharge elbow, the primary pressure drop through the IHX with the 60 in. I.D. double bellows with the 80 in. I.D. double bellows and with the diving bell seal will be 2.39 psi, 2.23 psi and 2.17 psi, respectively. The use of a 42-in. I.D. double bellows with one tube bend resulted in a primary pressure drop of 3.11 psi, which exceeded the design goal of 2.5 psi. The lower primary pressure drop for the diving bell seal is due mainly to the more space available for a larger diameter discharge piping.

Table 2-7 shows a comparison of the diving bell seal approach and the double bellows appraoch. The main advantage of the diving bell seal is, due to its lower primary pressure drop, to provide more margins for meeting the design goal of 2.5 psi. In addition, the use of a 60-in I.D. double bellows will require an 18 in. deeper primary tank and a 80 in. I.D. double bellows will require a 3 ft. deeper primary tank for accommodating the discharge elbow. Whereas, the diving bell seal, since it is shorter than the double bellows, does not require any additional space. Furthermore, it is more difficult to fabricate the double bellows and it requires removal of the IHX for maintenance and repair. Therefore, the diving bell seal was selected as the reference design. The double bellows, because it is feasible, was retained as a back-up design.

2.7 Cover Gas/Sodium Level Requirements

Table 2-8 shows the sodium levels in the hot pool, in the cold pool and in the IHX under normal plant operating conditions, transient conditions and during plant startup. Appendix D shows how the hot pool and cold pool levels are determined. Due to the pressure drop through the entrance region of the IHX, the sodium level in the IHX is lower than the hot pool level. The entrance region pressure drop consists of contraction loss to the flow shroud, friction loss in the annulus, 90° turn from the annulus, perforation of the annulus and through the IRACS coils. The sodium levels in the hot pool and the cold pool are also shown in Figure 2-2 in Part III, Subsection 2.1 (General Arrangement for Reactor Assembly).

When an intermediate loop is to be taken out of service for maintenance or for repair, the primary sodium to the IHX can be stopped by a gas valve. It consists in isolating (from the pool cover gas in the primary tank) and pressurizing the cover gas above the sodium in the IHX and depressing the sodium level to below the perforation (for sodium entering) of the annulus. It is calculated that 5 psig and 900 ft^3 of cover gas will be required for this purpose. When the IHX is ready for normal operation, the gas line to the IHX cover gas is opened to make it common to the pool cover gas in the primary tank.

The central downcomer pipe has a double wall with argon gas filled in the space between the walls as a thermal barrier for protection against the temperature gradients across the walls. For the same purpose, the IHX shell also has a double wall with argon gas filled in the space between the walls.

3. REFERENCES

(1) "Pool-Type LMFBR Plant, 1000 MWe Phase A Design", EPRI NP-646, Volumes 1 and 2, Part II, Heat Transport Systems, April, 1978.

TABLE 2-1

Umbrella Transients for IHX

Phase A Extension 2

Event		Number of Events in 40 Years
B-1b	Normal Reactor Scram with Minimum Decay Heat	540
B-14	A Reactor Scram with Minimum Decay Heat and Pony Motor Post-Scram Flow	16
B-4b	A Reactor Scram caused Loss of Pumping Power in One Intermediate Loop	7
B-10	A Reactor Scram Accompanied by the Blowdown of One Steam Generator	6

TABLE 2-2

Transient Conditions for IHX

Event	Pri. Inlet Na Flow	Pri. Outlet Na Flow	Int. Inlet Na Flow	Int. Outlet Na Flow	Pri. Inlet Na Temp.	Pri. Outlet Na Temp.	Int. Inlet Na Temp.	Int. Outlet Na Temp.
B-1b	100% 50%(60 sec)			100% 50%(20 sec)	875°F 570°F(500 sec)	548°F (240 sec)	544°F (120 sec)	815°F 835°F(20 sec) 570°F(500 sec)
B-14	100% 7%(50 sec)			100% 7%(50 sec)	875°F 825°F(40 sec) 695°F(600 sec)	542°F (600 sec)	542°F (600 sec)	815°F 840°F(25 sec) 700°F(100 sec) 650°F(600 sec)
B-4b		100% 41%(80 sec) 46%(400 sec)	100% 12%(100 sec) 10%(400 sec)		640°F(500 sec)	600°F 745°F(80 sec) 610°F(600 sec)	550°F 535°F(300 sec) 540°F(600 sec)	
B-10	100% 50%(60 sec)				620°F (480 sec)	625°F (480 sec)	550°F 835°F(800 sec) 625°F(1800 sec)	625°F (480 sec)

TABLE 2-3

Allowances for Thermal Expansions

and Seismic Loadings

Diving Bell Seal Design

Axial Movement of IHX Relative to the Core Support Structure due to Seismic Loading.	=	1.5 in.
Radial Movement of IHX Relative to the Reactor Deck due to Seismic Loading.	=	0.25 in.
Axial Movement of IHX Relative to the Core Support Structure due to the Thermal Expansion.	=	2.67 in.
Radial Movement of IHX Relative to the Core Support Structure due to Thermal Expansion.	=	1.42 in.

TABLE 2-4

Results of Sizing of Double Diving Bell Seal

Conditions	IHX Pressure psi	Hot Pool Level Change ft	Cold Pool Level Change ft	Velocity ft/sec	Minimum Cover Gas Volume ft^3	Double Diving Bell Seal, Minimum Required Height ft
Normal Plant Operation	2.500	1.667	5.051	5.630	38.002	3.359
Transient Conditions						
B-1b	0.625	0.394	1.241	2.815	9.245	0.818
B-14	0.012	0.008	0.024	0.394	0.183	0.016
B-4b	0.529	0.337	1.061	2.590	7.903	0.699
B-10	0.625	0.396	1.258	2.815	0.351	0.827
Start Up	1.089	0.668	2.115	3.716	15.736	1.392

TABLE 2-5

Double Bellows for IHX

	80"ID	60"ID
Total Length	60"	55"
No. Convolutions/Bellows	8	6
Total No. Convolutions	16	12
Spool Length	39"	39.5"
Convolution Width	3.0"	3.0"
Pitch Diameter	83"	63"
Thickness	0.036"	0.036"
Pitch	1.3"	1.3"
Raddi	0.3"	0.3"
Bellow Length (Each End)	10.4"	7.8"

TABLE 2-6

Primary Pressure Drop Through IHX

	Double Bellows			Diving Bell Seal
	Phase A Ext. 1 42"ID	60"ID	80"ID	
Without Discharge Elbow				
1 Tube Bend	2.96 psi	2.24 psi	2.08 psi	2.02 psi
2 Tube Bends	3.22 psi	2.44 psi	2.26 psi	2.22 psi
With Discharge Elbow				
1 Tube Bend	3.11 psi	2.39 psi	2.23 psi	2.17 psi
2 Tube Bends	3.37 psi	2.59 psi	2.41 psi	2.37 psi

TABLE 2-7

Diving Bell Seal Versus Double Bellows

Diving Bell Seal	Double Bellows
• Primary ΔP of 2.17 PSI for One Tube Bend Design. Allows more Margins for Meeting Design Goal of 2.5 PSI.	• Primary ΔP of 2.39 PSI for 60" I.D. Bellows and 2.23 PSI for 80" I.D. Bellows - Both for One Tube Bend Design.
• No Additional Space Required.	• Requires 18 in. Deeper Primary Tank for 60" I.D. Bellows and 3 ft. Deeper Primary Tank for 80" I.D. Bellows - to - Accommodate Discharge Elbow.
• Little or No Maintenance Required	• Require Removal of IHX for Maintenance and Repair.
• Require Piping for Adding Cover Gas and for Excess Gas Exit.	• No Cover Gas Piping Required.
• Simple Fabrication.	• More Complex Fabrication.
• Although with Cover Gas Provisions, Probably more Reliable due to no Moving Parts.	• Expected Lower Reliability due to Moving Parts.
• Simple and Less Costly Development Tests.	• May need some Development Tests.
	• Probably Cost more due to more Complex Fabrication.
• French Phenix has Operating Experience and Proposed for Super Phenix - although of Different Configuration.	• Proposed for British CDFR.

TABLE 2-8

Sodium Levels in IHX

Conditions	Pressure Drop Through IHX psi	Cold Pool Level	Hot Pool Level	Sodium Level in IHX
Normal Plant Operation:				
at 100% Pump Flow	2.500	(-)25'4"	(-)18'8"	(-)19'8"
at pony motor flow(7% speed)	0.012	(-)20'4"	(-)20'4"	(-)20'4"
Transient Conditions:				
B-1b	0.625	(-)21'7"	(-)19'11"	(-)20'2"
B-14	0.012	(-)20'4"	(-)20'4"	(-)20'4"
B-4b	0.529	(-)21'5"	(-)20'0"	(-)20'3"
B-10	0.625	(-)21'8"	(-)19'11"	(-)20'2"
Plant Startup:				
at 66% flow	1.089	(-)23'11"	(-)21'2"	(-)21'7"
at pony motor flow(7% speed)	0.012	(-)21'10"	(-)21'10"	(-)21'10"
Refueling		(-)20'7"	(-)21'7"	(-)20'7"

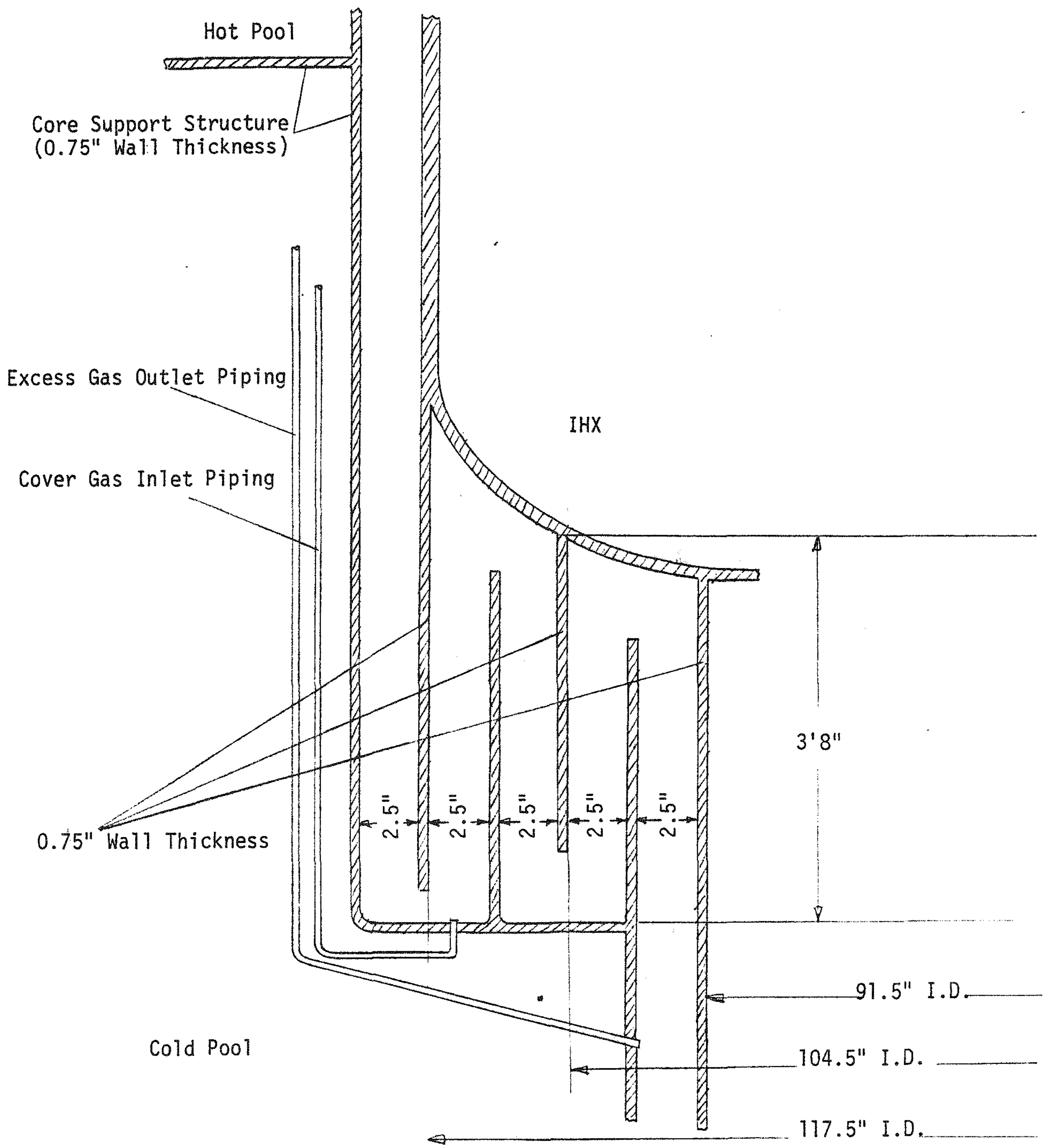

Figure 2-1 Conceptual Design of Double Diving Bell Seal for IHX

Before Adding Cover Gas, with No Pump Flow

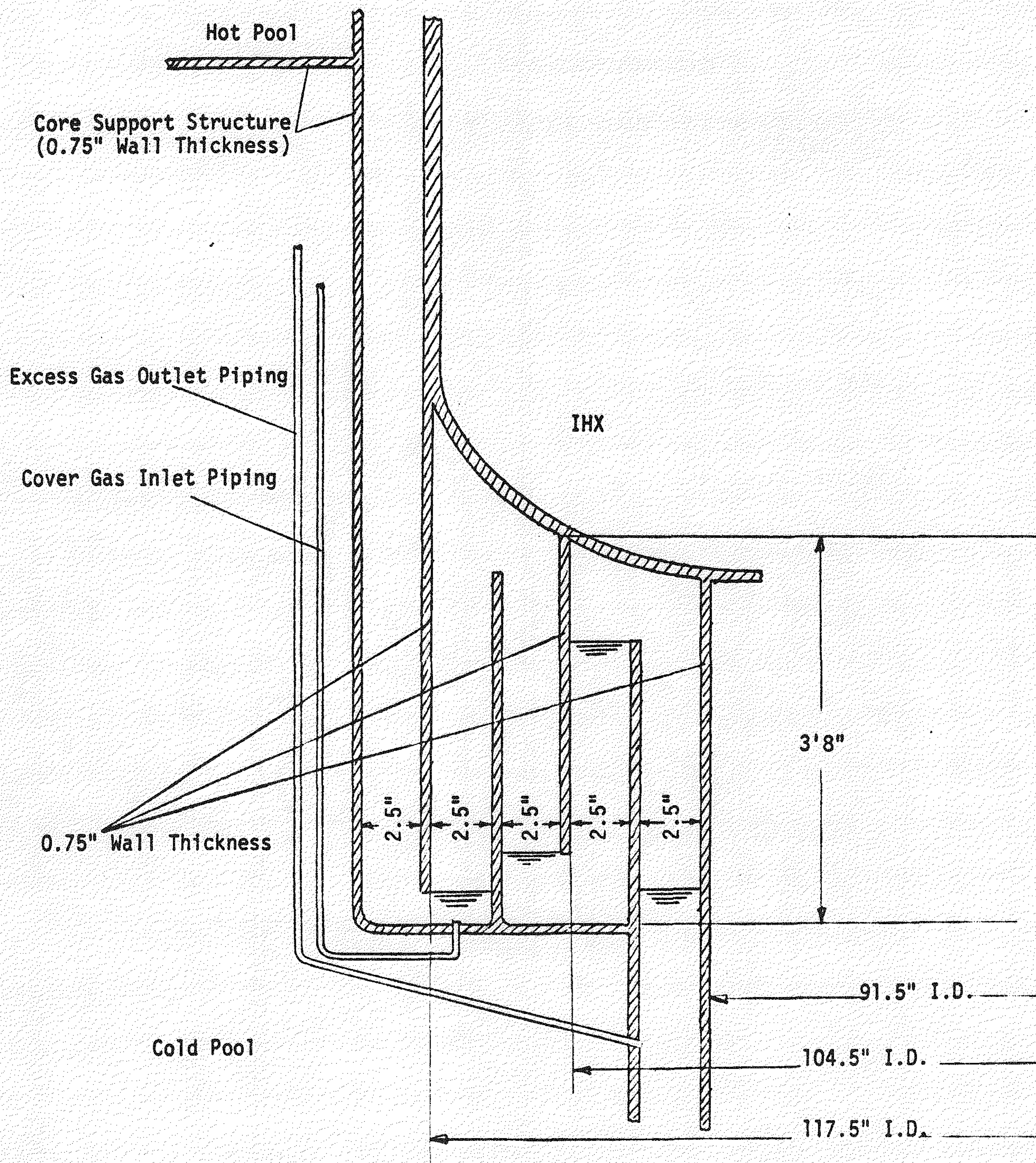

Figure 2-2 Conceptual Design of Double Diving Bell Seal for IHX Cover Gas Added but No Pump Flow

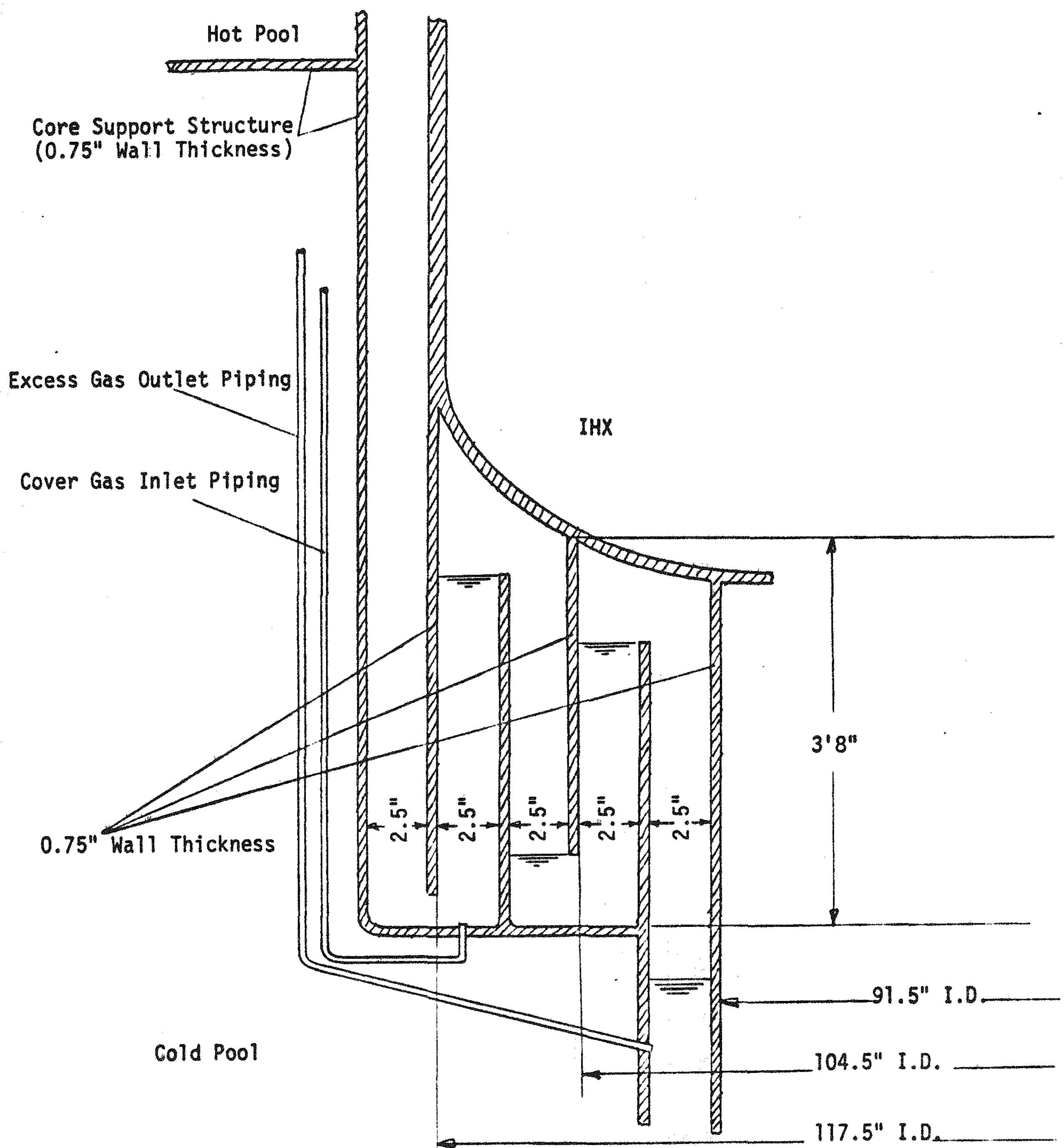

Figure 2-3 Conceptual Design of Double Diving Bell Seal for IHX

Normal Plant Operating Conditions

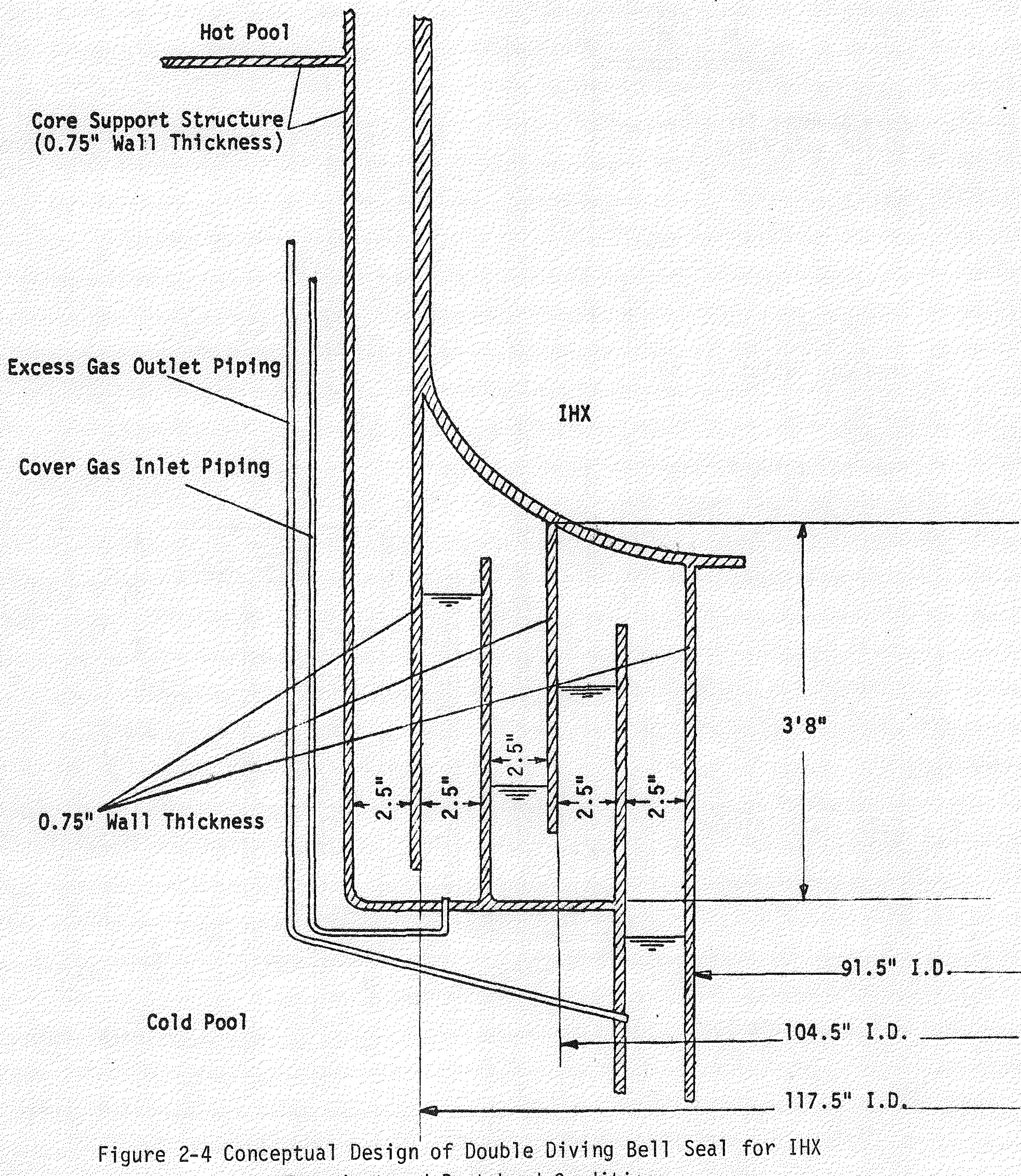

Figure 2-4 Conceptual Design of Double Diving Bell Seal for IHX
Transient and Part Load Conditions

REFERENCE DRAWINGS

DRAWING NO.	DESCRIPTION
51-3145-6-1000	DESIGN LAYOUT
51-3145-5-2001	TUBE LAYOUT & GRID DETAILS
AFS-SK-PB-002	IHX PLUG REGION (G.E.)

DESIGN AND PERFORMANCE DATA

1. PRIMARY FLOW LOCATION - TUBE SIDE
2. DESIGN TEMPERATURES: PRIMARY 900°F. INTERMEDIATE 835°F.
3. OPERATING TEMPERATURES: PRIMARY INLET 875°F. PRIMARY OUTLET 594°F. INTERM. INLET 550°F. INTERM. OUTLET 815°F. IRACS INLET 580°F. IRACS OUTLET 845°F.
4. NUMBER OF TUBES: PRIMARY BUNDLE - 4860 - .875 O.D. x 0.04 MIN. WALL IRACS BUNDLE - 8 625 O.D. x 0.50 WALL COIL.
5. DESIGN PRESSURE: PRIMARY SIDE 10 PSIG INTERM. SIDE 250 PSIG
6. THERMAL RATING: PRIMARY IHX 486 MWt IRACS 3 MWt
7. FLOW RATE: PRIMARY KNa 19.25x10⁶ #/HR. INTERM. KNa 20.29x10⁶ #/HR.
8. PRESSURE DROP: TUBE SIDE 25 PSI SHELL SIDE 27.6 PSI
9. ESTIMATED WEIGHTS:
10. OPERATING PRESSURES: INTERM. SIDE 115 PSIG

NOTES

1. VESSEL DESIGNED AND FABRICATED IN ACCORDANCE WITH ASME B&PV CODE, NUCLEAR VESSELS, SECTION III, CLASS I, 1977 EDITION.
2. DO NOT SCALE THIS DRAWING, USE FIGURE DIMENSIONS ONLY.
3. ALL DIMENSIONS APPLY AT A STANDARD TEMPERATURE OF 70°F.
4. ALL DIMENSIONS ARE IN INCHES.
5. DIMENSIONING IS IN ACCORDANCE WITH ANSI Y14.5, 1973 EDITION.
6. SURFACE FINISH SHALL BE IN ACCORDANCE WITH ANSI B46.1, UNLESS OTHERWISE SPECIFIED THE FOLLOWING SURFACE FINISHES SHALL APPLY:
   a) MATING SURFACES 63
   b) HEAT TRANSFER TUBES 63
   c) TUBE SHEET HOLES 125
   d) ALL OTHER SURFACES 250

PENETRATION SCHEDULE

PENETRATION NO.	DESCRIPTION	PIPE SIZE O.D.	PIPE SIZE WALL	SLEEVE SIZE O.D.	SLEEVE SIZE WALL	OPENING
P1	INTERM. SODIUM INLET	32.00	.500	—	—	—
P2	INTERM. SODIUM OUTLET	32.00	.500	—	—	—
P3	AUX SODIUM INLET	8.625	.500	10.75	.365	—
P4	AUX. SODIUM OUTLET	8.625	.500	10.75	.365	—
P5	MANWAY	—	—	—	—	24.00
P6	ARGON GAS SUPPLY	*	*	—	—	—
P7	COOLING GAS INLET	12.750	.25	—	—	—
P8	COOLING GAS OUTLET	12.750	.25	—	—	—

* TO BE DETERMINED

MATERIAL SPECIFICATION TABLE

MAJOR PART	ASME SPEC.	FWEC SPEC.
FORGINGS	SA-336 TP 304	
NOZZLES	SA-336 TP 304	
HEADS	SA-240 TP 304	
PLATES	SA-240 TP 304	
PIPE	SA-376 TP 304	
TUBING	SA-213 TP 304	

Figure 2-5a Conceptual Design of IHX

Figure 2-5b Conceptual Design of IHX

APPENDIX A

Flow Chart for Diving Bell Seal Modelling

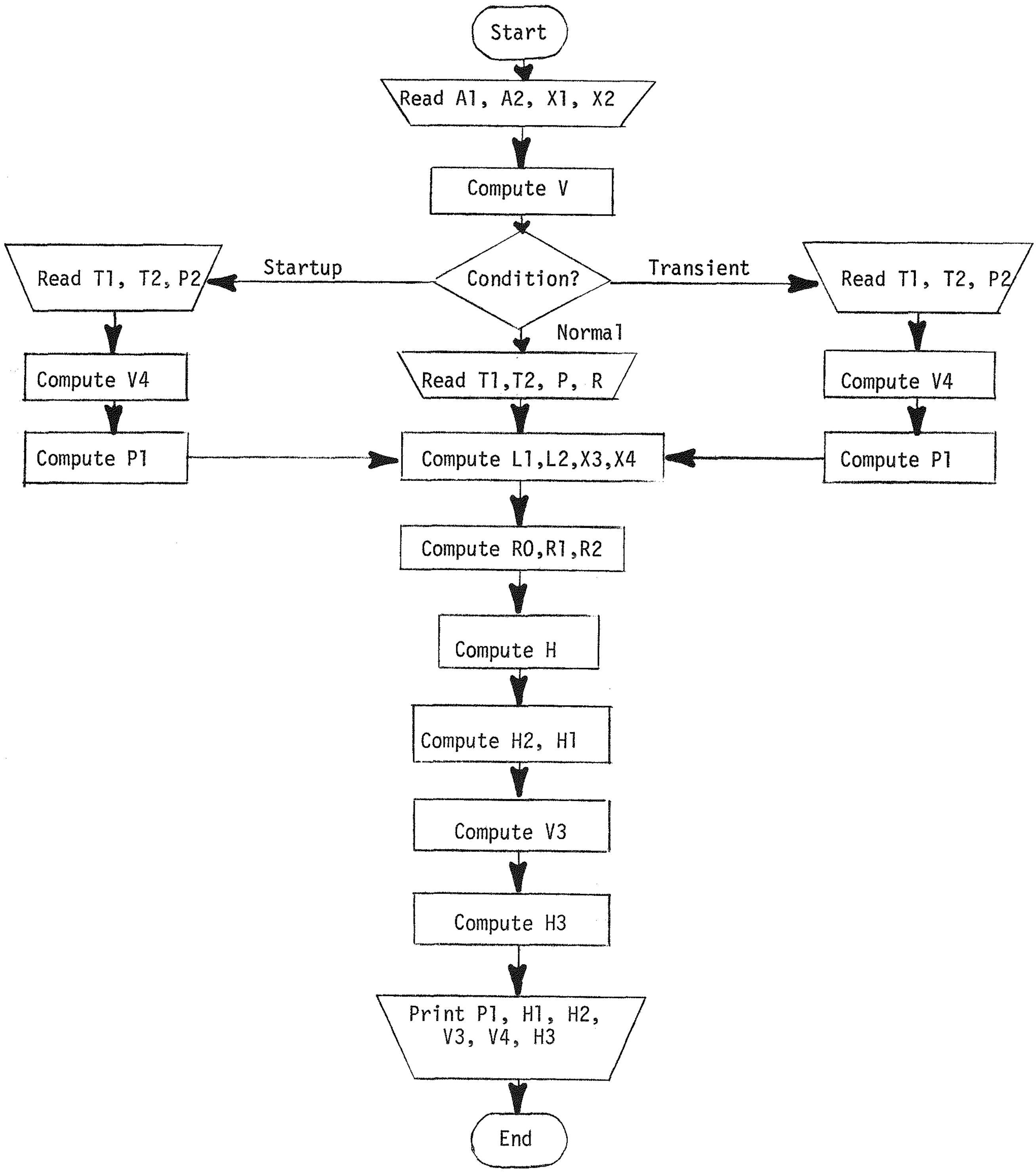

```
FILE FS0053/SEAL;
      11/17/78 AT   15.32638


0010 A1=3063.0
0020 A2=968.0
0030 X1=0.125
0040 X2=0.021
0050 T1=875.0
0060 T2=595.0
0070 M=19.25E6
0080 P=2.5
0090 R=53.59
0100 V=3.094E-7*5.63/5.956*M
0110 P1=P
0120 V4=V
0130 PRINT "NORMAL PLANT OPERATION"
0140 PRINT
0150 PRINT"            IHX      HOT POOL   COLD POOL   VELOCITY   COVER GAS   DOUBLE DIVING"
0160 PRINT"          PRESSURE    LEVEL       LEVEL                  VOLUME      BELL SEAL"
0170 PRINT"                      CHANGE      CHANGE                              DIMENSION"
0180 PRINT"           LB/IN2      FT          FT         FT/SEC      FT3            FT"
0190 PRINT
0200 GOSUB 620
0210 GOSUB 660
0220 PRINT USING 230,P1,H1,H2,V4,V3,H3
0230 :          ##.###     ##.###     ##.###     ##.###     ##.###        ##.###
0240 PRINT
0250 PRINT
0260 PRINT "TRANSIENT CONDITIONS"
0270 PRINT
0280 PRINT"            IHX      HOT POOL   COLD POOL   VELOCITY   COVER GAS   DOUBLE DIVING"
0290 PRINT"          PRESSURE    LEVEL       LEVEL                  VOLUME      BELL SEAL"
0300 PRINT"                      CHANGE      CHANGE                              DIMENSION"
0310 PRINT"           LB/IN2      FT          FT         FT/SEC      FT3            FT"
0320 PRINT
0330 FOR N=1 TO 5
0340 READ T1,T2,P2
0350 GOSUB 590
0360 GOSUB 620
0370 GOSUB 660
0380 IF N=1 GO TO 430
0390 IF N=2 GO TO 460
0400 IF N=3 GO TO 490
0410 IF N=4 GO TO 520
0420 IF N=5 GO TO 550
0430 PRINT USING 440,P1,H1,H2,V4,V3,H3
0440 :    B-1B   ##.###     ##.###     ##.###     ##.###     ##.###        ##.###
0450 GO TO 570
0460 PRINT USING 470,P1,H1,H2,V4,V3,H3
0470 :    B-14   ##.###     ##.###     ##.###     ##.###     ##.###        ##.###
0480 GO TO 570
0490 PRINT USING 500,P1,H1,H2,V4,V3,H3
0500 :    B-4B   ##.###     ##.###     ##.###     ##.###     ##.###        ##.###
```

FS0053/SEAL;

```
0510 GO TO 570
0520 PRINT USING 530,P1,H1,H2,V4,V3,H3
0530 :   B-10   ##.###    ##.###    ##.###     ##.###    ##.###      ##.###
0540 GO TO 570
0550 PRINT USING 560,P1,H1,H2,V4,V3,H3
0560 :START UP  ##.###    ##.###    ##.###     ##.###    ##.###      ##.###
0570 NEXT N
0580 GO TO 810
0590 V4=P2*V
0600 P1=P/V/V*V4*V4
0610 RETURN
0620 L1=6.854E-3*(T1-70.0)
0630 L2=5.817E-3*(T1-70.0)
0640 X3=(L1-L2)/12.0
0650 RETURN
0660 DEF FND(X)=59.566-7.9504E-3*X-0.2872E-6*X*X+0.06035E-9*X*X*X
0670 R1=FND(T1)
0680 R2=FND(T2)
0690 R0=(R1+R2)/2.0
0700 H=P1*144.0/R0
0710 H3=H/2.0
0720 H2=A1*R1*H/(A1*R1+A2*R2)
0730 H1=H-H2
0740 V3=5.92*H1+5.57*H2
0750 RETURN
0760 DATA 570.0,548.0,0.50
0770 DATA 695.0,542.0,0.07
0780 DATA 640.0,610.0,0.46
0790 DATA 620.0,650.0,0.50
0800 DATA 400.0,400.0,0.66
0810 END
```

APPENDIX C

Nomenclature

A1	=	Surface area of hot pool, ft^2.
A2	=	Surface area of cold pool, ft^2.
H	=	Differential level between hot pool and cold pool, ft.
H1	=	Hot pool level change, ft.
H2	=	Cold pool level change, ft.
H3	=	Minimum required height of the double diving bell seal, ft.
L1	=	Thermal expansion of IHX due to hot pool temperature, in.
L2	=	Thermal expansion of the reactor structure due to hot pool temperature, in.
M	=	Mass flow rate of sodium, lb/hr.
M1	=	Increase in sodium mass in hot pool at pump flow, lb.
M2	=	Decrease in sodium mass in cold pool at pump flow, lb.
P	=	Pressure drop across IHX under normal plant operation, psi.
P1	=	Pressure drop across IHX under transient and part load conditions, psi-
P2	=	Fraction of sodium flow rate (velocity) under transient and startup conditions compared to normal plant operating conditions.
R	=	Average density of hot pool and cold pool sodium under normal plant operation, lb/ft^3.
RO	=	Average density of sodium, lb/ft^3.
R1	=	Density of sodium at hot pool temperature, lb/ft^3.
R2	=	Density of sodium at cold pool temperature, lb/ft^3.
T1	=	Hot pool temperature, °F.
T2	=	Cold pool temperature °F.
V	=	Velocity of primary sodium through IHX under normal plant operation, ft/sec.
V1	=	Increase in sodium volume in hot pool at pump flow, ft^3.
V2	=	Decrease in sodium volume in cold pool at pump flow, ft^3.
V3	=	Minimum required volume of cover gas, ft^3.
V4	=	Velocity of sodium under transient and part load conditions, ft/sec.
X1	=	Axial movement of IHX relative to the core support structure due to seismic loading, t.

APPENDIX C (Continued)

X2	=	Radial movement of IHX relative to the reactor deck due to seismic loading, ft.
X3	=	Axial movement of IHX relative to the core support structure due to thermal expansion, ft.
X4	=	Radial movement of IHX relative to the core support structure due to thermal expansion, ft.

APPENDIX D

Determination of Hot Pool and Cold Pool Levels

Since $M_1 = M_2$

and $M_1 = V_1R_1$

$M_2 = V_2R_2$

$V_1 = A_1H_1$

$V_2 = A_2H_2$

Therefore $A_1H_1R_1 = A_2H_2R_2$

Substituting $H_1 = H - H_2$ into the above equation yields:

$$H_2 = \frac{A_1R_1H}{A_1R_1 + A_2R_2}$$

where

M_1 = Increase in Sodium Mass in Hot Pool at Pump Flow, lb.

M_2 = Decrease in Sodium Mass in Cold Pool at Pump Flow, lb.

V_1 = Increase in Sodium Volume in Hot Pool at Pump Flow, ft^3.

V_2 = Decrease in Sodium Volume in Cold Pool at Pump Flow, ft^3.

R_1 = Density of Sodium in Hot Pool, lb/ft^3.

R_2 = Density of Sodium in Cold Pool, lb/ft^3.

H_1 = Rise in Hot Pool Level at Pump Flow, ft.

H_2 = Drop in Cold Pool Level at Pump Flow, ft.

A_1 = Surface Area of Hot Pool, ft^2.

A_2 = Surface Area of Cold Pool, ft^2.

H = Total Differential Level Between Hot Pool and Cold Pool, ft.

PART V: HEAT TRANSPORT SYSTEMS

Section 2: Work Performed During Extension 2

Subsection 2.2: Primary Pump Design

CONTENTS

TABLES

FIGURES

1. INTRODUCTION AND SUMMARY

To allow for a new reactor core with higher pressure drop, the Phase A primary pump design (Ref. 1) was redesigned by Byron Jackson to accommodate a total system pressure drop of up to 120 psi during Phase A Extension 2. The design requirements and the potential inputs of the new pump design on the reactor assembly were evaluated by GE.

The selected pump concept is the same as that of the Phase A: two double-suction impellers in parallel on a single shaft. However, the impeller diameter has been increased from 36 in. to 42 in. to provide for the increase in head to 120 psi. The pump speed remained at 870 rpm, the same as Phase A, to provide a safe margin for NPSH and to avoid cavitation. The selected pump speed is suitable for either a variable speed motor or a constant speed motor. The new pump also is slightly longer than that of Phase A. The new pump did not change the deck penetration diameter and the pump support flange of 96 in. O.D. A structural analysis, shaft dynamic analysis and seismic analysis showed that no insurmountable problems are anticipated with the new pump design. Details of the pump design are described in Appendix VB, the Byron Jackson Report on Primary Pump.

The potential impact of the new pump on the reactor assembly was studied. Areas of further work needed for the reactor assembly were identified.

2. PRIMARY PUMP DESIGN

2.1 Design Requirements

There are four primary pumps in the 1000 MWe Pool-Type LMFBR plant. The pumps are located in the cold pool of the primary tank and suspended from the reactor deck. Figures 2-1 and 2-3 in Part III, Subsection 2.1 (General Arrangement of Reactor Assembly) show the arrangement of the primary pumps, in relation to the IHXs and the cold traps, on the reactor deck and in the primary tank.

The primary pump design must meet the following requirements:

- It must satisfy the operating conditions shown in Table 2-1. Specifically, in order to allow for a new core with 50% increase in pressure drop, the total developed head has been increased from 90 psi (237 ft. of sodium) in Phase A to 120 psi (316 ft. of sodium). In addition, the sodium flow rate to each pump has been increased from 65,820 gpm in Phase A to 68,450 gpm to include the expected sodium flow through the dynamic thermal barriers in the primary tank.

- In sizing the pump, a runout condition of 116% of design flow must be considered so that the plant can be operated with only three of the four pumps running.

- The pump must operate satisfactorily at either constant speed or variable speed.

- The pump design must also satisfy the minimum cold pool level and the pump sodium level shown in Table 2-2. These sodium levels affect not only the available NPSH for the pump but also the location of the intermediate bearing of the long-shaft primary pump. The analysis and the determination of the minimum cold pool level and the pump sodium level are shown in Appendix A.

Table 2-1

Operating Conditions of the Primary Pumps
GE 1000 MWe Pool-Type LMFBR
Phase A Extension 2

Number of Primary Pumps	4
Total Primary Sodium Flow	120.1×10^6 lbs/hr
Operating Flow (Each Pump)	68,450 gpm
Location of Pumps	Cold Pool
Temperature of Cold Pool	595 °F
Total Developed Head	120 psi (316 ft. of sodium)
Code Classification	ASME Section III, Class 1
Seismic Category	1
Operating Reactor Cover Gas	Argon, nearly atmospheric
Design Life	40 years

2.2 Reference Primary Pump Design

The reference pump concept consists of two double-suction impellers in parallel, the same as that of Phase A. The limiting available NPSH remains the predominant factor in the pump selection. However, in order to accommodate the total system pressure drop of 120 psi, the impeller diameter has been increased to 42 in. (from 36 in. in Phase A) but the pump speed retained at 870 rpm (the same as Phase A). The pump speed was retained, for conservatism and reliability, to provide a safe margin for NPSH and to avoid cavitation. The selected pump speed is suitable for either a variable speed motor or a constant speed motor. The shaft length is 36 ft. 8 in., an increase of 2 inches. The total length of the pump, excluding the motor, is 44 ft. 10 in., an increase of 1 ft. 4 inches. The pump length is designed to give an available NPSH of 40 ft. which offers a satisfactory suction specific speed at design flow as well as at run-out flow. The slightly larger impeller diameter and the slightly longer pump did not change the deck penetration diameter of 7 ft. 6 in. nor the pump support flange of 96 in. O.D. for accommodating the pump motor. The maximum diameter at the hydraulic section of the pump, which is the maximum diameter of the withdrawable pump assembly, is 75 in. The required operating pump power is 6,150 horsepower and the estimated total weight of the pump (excluding the motor, the sodium, the insulation and the steel shot) is 104,400 lbs. Table 2-2 shows the major parameters of the primary pump. The performance curves for the pump are shown in Figure 2-2. Since the pump is designed to have an adequate NPSH available for the upper double-suction impellers, the lower doulble-suction impellers have more than adequate NPSH available. In order to prevent gas entrainment due to vortexing into the pump, a diving bell (flow shroud) will be provided to channel the sodium flow to the pump.

The key features of the pump design, with emphasis on those which are new or different from that of the Phase A, are described below. See Appendix VB, Byron Jackson's report, for details of the pump design and the design drawings.

- Impeller

  The pump has two double-suction impellers in parallel. The double-suction impeller has two single-suction impellers designed back-to-back. The two double-suction impeller design further divides the total flow into four suction inlets. The impeller diameter has been increased to 42 in., from 36 in. in Phase A, to obtain the total developed head of 316 ft. of sodium.

- Hydrostatic Bearing

  The hydrostatic bearing is of the same type as in Phase A. However, the size and location of the bearing have been changed, due to an increase in the radial load as a result of the additional pump head, to satisfy the dynamic analysis of the new pump. The bearing has been increased from 16 in. (in Phase A) to 30 in. diameter. In addition, the bearing was moved from its position at the bottom of the pump (in Phase A) to a location between the two impellers. Because the pump is so long another hydrostatic bearing is located below the minimum sodium level to provide a satisfactory bearing span and to allow the use of a smaller shaft.

o Pump Shaft

Since the pump is larger and the horsepower requirement has been increased from Phase A, the size of the shaft has been changed. A coupling is provided at approximately the normal sodium level because the shaft is too long to be made in one piece. The upper shaft (16 in. diameter) and the lower shaft (8.5 in. diameter) are joined by a rigid flanged coupling. The shaft is hollow except in the cold region at the top. A hollow shaft gives maximum rigidity with minimum weight. Furthermore, it gives better stability under thermal transients that a solid shaft. The journal that was at the bottom of the shaft in Phase A has been moved to a location between the two impellers.

o Shaft Seal Cartridge

Because the span between the hydrostatic bearings in the pump and the lower radial bearing in the motor is quite long, an oil lubricated radial bearing is located in the seal area to keep the critical speed a safe margin above the operating speed. Seal leakage tanks are provided to collect oil leakage and to prevent it from going into the sodium.

The shaft seal cartridge includes the two mechanical seals, the pumping ring, the oil lubricated radial bearing and the air-to-oil heat exchanger. A fixture is provided for convenient removal and replacement of the spacer coupling and the seal cartridge assembly without removing the motor.

o Motor Support

Adequate space is provided to allow assembly and removal of the spacer coupling and the shaft seal cartridge. The pump speed is suitable for either a variable speed motor or a constant speed motor. The designs of the motors are discussed in Part VII, Section 2.1, Plant Control. The effects of the constant speed pump on the system are described in Part V, Section 2.4, Fixed-Speed Pump Effects.

- Shut-Off Valve

  A shut-off valve, located at the bottom of the pump, is used to prevent sodium backflow through a disabled pump. Two rods 180 degrees apart provide the vertical motion to open and close the valve. The rods extend vertically to the seal cartridge.

  A stuctural analysis, shaft dynamic analysis and seismic analysis were performed for the new pump design. The analyses shown in Byron Jackson's report in Appendix VB indicate that there are no insurmountable problems with the new pump design.

  Maintenance and inspection requirements for the primary pump, including the maintenance procedures for removal and replacement of the pump and the shaft seal cartridge are described in Part X, Subsection 2.3, Maintainability and Inspectability of the Major Components.

2.3 Pump Concept Selection

The low available NPSH led to the selection of the double-suction impellers. The double-suction design keeps the primary pump diameter as small as practicable. The two, parallel, double-suction impeller design further improves the available NPSH and minimizes the pump diameter. The selected design, two double-suction impellers in parallel, is particularly suitable for the pool-type pump in that all the four suction inlets are immersed in the sodium. In Appendix VB, Byron Jackson has presented design data and drawings to substantiate their claims that large units of four-stage, three-stage and two-stage pumps of double-suction impellers in parallel, have been successfully built, tested and are still in service.

The impeller diameter required for a pump is proportional to the square root of the total developed head of the pump and inversely proportional to the RPM of the pump. The increased total system pressure drop of 120 psi, therefore, can be met by increasing either the impeller diameter or the pump speed, or both. The following pump designs were considered but were not adopted:

- A single-stage double-suction design with 725 rpm variable speed motor was not selected because it required a 50 in. impeller diameter, resulting in an undesirably large pump. Furthermore, it is not suitable for a constant speed motor.
motor was not selected because it required a 50 in. impeller diameter, resulting in an undesirably large pump. Furthermore, it is not suitable for a constant speed motor.

- The use of two stages of double-suction impellers in parallel with a 1000 rpm variable speed motor would require a 36 in. impeller diameter, the same as Phase A. This design is unsuitable for a constant speed motor. The higher pump speed also reduces conservatism and reliability.

- Two stages of double-suction impellers in parallel at 1180 rpm is suitable for either a variable speed motor or a constant speed motor. However, this design has a long shaft (50 ft. 10 in.) which is undesirable not only from the standpoint of shaft dynamics but also from the standpoint of the additional space required in the primary tank. The high pump speed also further reduces the reliability of the pump.

2.4 Potential Impacts on Reactor Assembly

A preliminary study was made of the potential impacts of the new pump design on the reactor assembly. The results are summarized as follows:

- Because the new primary pump is 1 ft. 4 in. longer than that of Phase A, the pump-to-plenum piping seal (a bellows-type expansion joint for the connection between the lower end of the primary pump and the reactor inlet plenum) and the core support structure must be redesigned to match this new elevation of the pump. However, the pump-to-plenum piping seal, which is designed to 150 psig internal pressure, is capable of withstanding the new pump discharge pressure of 120 psi. A less desirable alternative would be to raise the reactor deck to accommodate the new pump length.

- The shut-off valve, connected to the outlet nozzle of the primary pump, was designed to 120 psig of thermal-hydraulic pressure and up to 200 psig of design pressure. Therefore, redesigning of the valve is not required.

- Resizing and redesigning of the fixed flow-splitter and the variable flow-splitter may be required to obtain the desired pressure drop through the splitters.

- Studies are needed to determine if the forged nozzle and the wall thickness of the high pressure plenum are adequate.

3. REFERENCES

(1) "Pool-Type LMFBR Plant, 1000 MWe Phase A Design," EPRI NP-646, Volume 1 and 2, Part II, Heat Transport Systems, April 1978.

TABLE 2-2

Primary Pump Parameters
1000 MWe Pool-Type LMFBR
Phase A Extension 2

Type	Mechanical, two stages of double suction impellers in parallel
Operating Sodium Flow	68,450 gpm
Total Developed Head	316 ft. of sodium (120 psi)
Sodium Temperature	595°F
Operating Speed	870 rpm
NPSH Available	40 ft.
Specific Speed	2,150
Suction Specific Speed, Design	10,000
Suction Specific Speed, Runout	10,900
NPSH Required	26 ft.
Impeller Diameter	42 in.
Pump Efficiency	78%
Pump Power, Design	7,000
Pump Power, Operating	6,150 hp
Shaft Length	36 ft. 8 in.
Max. Hydraulic Section Diameter	75 in.
Pump Length (Excluding Motor)	44 ft. 10 in.
Pump Weight (Excluding motor, sodium, insulation and steel shot)	104,400 lbs

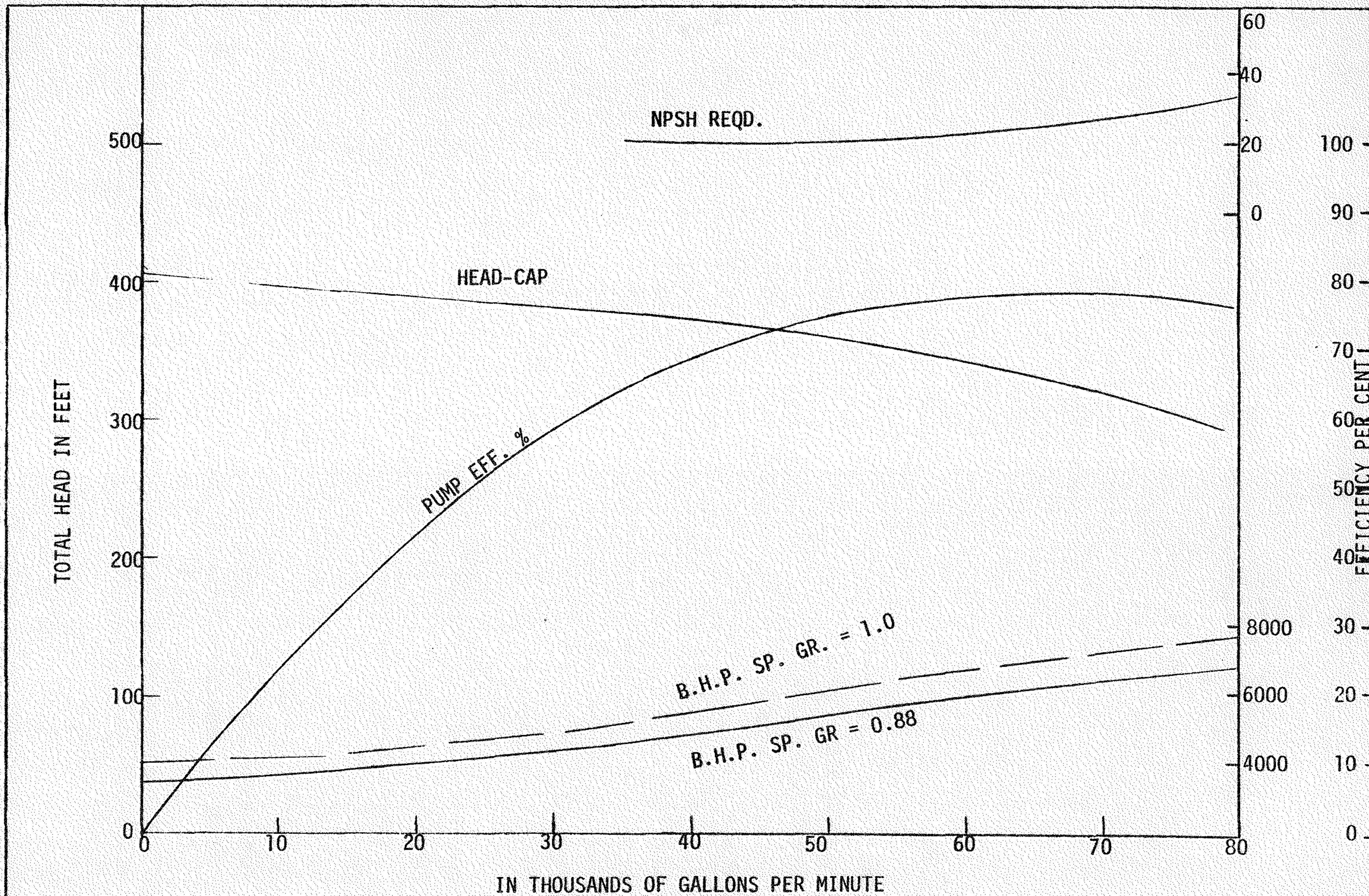

FIGURE 2-1 PERFORMANCE CURVES FOR PRIMARY PUMP

FIGURE 2-2 CONCEPTUAL DESIGN FOR PRIMARY PUMP

BORG WARNER BYRON JACKSON®
BORG-WARNER CORPORATION

IF-8435 V-2.2-11

APPENDIX A: DETERMINATION OF COLD POOL LEVEL AND PUMP SODIUM LEVEL 1000 MWe POOL-TYPE LMFBR PHASE A EXTENSION 2

A-1 Cold Pool Level

At zero sodium flow, the hot pool level is the same as the cold pool level. If the sodium temperatures in both the hot pool and the cold pool are at 595°F, the levels will be at (-) 20'-4", based on the top of the shield deck at 0'-0". During power operation and normal flow, the total differential level between the hot pool and the cold pool is determined by the pressure drop of the primary sodium through the IHX (2.5 psi). The total differential level between the hot pool and the cold pool is equal to the sum of the rise in sodium level in the hot pool and the drop in sodium level in the cold pool. Figure 2-5 in Part II, Subsection 2.1 (Nuclear Steam Supply System) illustrates the relative hot pool and cold pool areas. Since the hot pool surface area (3063 ft^2) is much larger than the cold pool surface area (968 ft^2), the drop in sodium level in the cold pool is much greater than the rise in sodium level in the hot pool. The decrease in sodium mass in the cold pool is equivalent to the increase in sodium mass in the hot pool. However, it should be noted that, due to the simultaneous change in sodium temperatures in the hot pool and the cold pool and the resultant expansion and the contraction of the sodium volume, the decrease in sodium volume in the cold pool is not equal to the increase in sodium volume in the hot pool. Table A-1 shows how the cold pool level during power operation and pump flow conditions are determined. The results of the calculations are shown in Table 2-2. During normal plant operation (cold pool temperature of 595°F and hot pool temperature of 875°F) and 100% pump flow, the minimum cold pool level will be at (-) 25'-4". At pony motor flow (7% speed), the pressure drop across the IHX is approximately proportional to the square of the sodium velocity. It is determined that the differential level between the hot pool and the cold pool is only 0.4", and the minimum cold pool level is nearly equal to (-) 20 ft. 4 inches.

During the plant startup, when both the hot pool and cold pool temperature are at 400°F, the sodium level will be at (-) 21'-10". At 66% pump flow, the minimum cold pool level will be at (-) 23'-11". At pony motor flow, the minimum cold pool level is nearly equal to (-) 21'-10".

Figure 2-2 in Part III, Subsection 2.1 (General Arrangement for Reactor Assembly) shows the sodium levels in the cold pool and the hot pool.

A-2 Pump Sodium Level

The pump sodium level is slightly lower than the cold pool level due mainly to the pressure drop of the primary sodium through the pump inlet flow structure. In order to minimize its effect on the location of the intermediate bearings of the long shaft of the primary pump, a 3" maximum for the differential level between the cold pool level and the pump sodium level at 100% pump flow was selected as a design guide for the pump inlet flow structure. At pony motor flow, the differential level between the cold pool sodium and the pump sodium is negligibly small.

Table A-1

Determination of Cold Pool Level

since $M_1 = M_2$

and
$$M_1 = V_1 D_1$$
$$M_2 = V_2 D_2$$
$$V_1 = V_1 H_1$$
$$V_2 = A_2 H_2$$

we have $A_1\ H_1\ D_1 = A_2\ H_2\ D_2$

substitute $H_1 = H - H_2$ into the above equation, and solve for H_2 we get:

$$H_2 = \frac{A_1\ D_1\ H_1}{A_1\ D_1 + A_2\ D_2}$$

where
M_1 = Increase in sodium mass in hot pool at pump flow, lb.
M_2 = Decrease in sodium mass in cold pool at pump flow, lb.
V_1 = Increase in sodium volume in hot pool at pump flow, ft^3.
V_2 = Decrease in sodium volume in cold pool at pump flow, ft^3.
D_1 = Density of sodium in hot pool, lb/ft^3.
D_2 = Density of sodium in cold pool, lb/ft^3.
H_1 = Rise in hot pool level at pump flow, ft.
H_2 = Drop in cold pool level at pump flow, ft.
H = Total differential level between hot pool and cold pool, ft.
A_1 = surface area of hot pool, ft^2.
A_2 = Surface area of cold pool, ft^2.

Table A-2

Cold Pool Level and Pump Sodium Level

	Cold Pool Level*	Differential Level Between Cold Pool & Pump Sodium Level
Normal Plant Operation:		
at 100% flow	(-) 25'-4"(595°F)	3 in. max.
at pony motor flow (7% speed)	(-) 20'-4"(595°F)	negligible
Plant Startup:		
at 66% flow	(-) 23'-11"(400°F)	
at pony motor flow (7% speed)	(-) 21'-10"(400°F)	

*Based on top of shield deck at 0'-0".

Part V: Heat Transport Systems

Section 2: Work Performed During Extension 2

Subsection 2.3: Thermal Transients

CONTENTS

TABLES

FIGURES

FIGURES

FIGURES

FIGURES

FIGURES

FIGURES

FIGURES

FIGURES

FIGURES

FIGURES

FIGURES

FIGURES

FIGURES

FIGURES

FIGURES

FIGURES

FIGURES

FIGURES

FIGURES

FIGURE NO.	TITLE	PAGE

FIGURES

FIGURES

FIGURES

FIGURES

FIGURES

FIGURES

FIGURES

FIGURES

1. INTRODUCTION AND SUMMARY

This report contains the transient predictions of selected plant duty cycle events for the 1000 MWe Pool-Type LMFBR Plant described in EPRI NP-646 (1). The plant transient predictions were made using a system model called DEMO-POOL (2). This model is based on the DEMO simulation model(3) prepared for the CRBRP with changes necessary to represent a pool system. A list of overall plant design parameters used in the DEMO-POOL simulation is contained in Table 1-1. This effort was directed toward generating transient predictions suitable for use in analysis of system components and for comparison with duty cycle events in loop type LMFBRs.

Data are presented on duty cycle transients for the 1000 MWe Pool-Type LMFBR Plant. These data are suitable for evaluating the impact of pool system transients on component requirements. They are also suitable for comparison with loop-type LMFBR transients to establish whether or not pool and loop systems have significantly different component requirements.

Two possible modes of post-scram sodium pump operation were evaluated. The base case involves a post-scram sodium pump trip to 50 percent speed. This was the basis for evaluation of the majority of the duty cycle events. The possible alternative mode of post scram sodium pump operation, keeping the pumps operating at 100 percent of rated speed, was evaluated for several selected duty cycle events to provide a basis for comparison with the base case transients. In addition, the effect of increased intermediate sodium pump inertia on the temperature transient for two events was evaluated.

Increasing the post-scram pump speed from 50 to 100 percent of rated speed increases the temperature rates for most events analyzed by a factor of two or more. Temperature changes are essentially the same. Increasing the intermediate pump inertia decreases the severity of the loss of power to an intermediate pump but increases the severity of the loss of off-site power events.

Stress analysis is required to determine the impact of plant transients on system components and to determine whether it is better to operate the sodium pumps at 50 or 100 percent of rated speed following a reactor scram. The increased temperature rates associated with full speed post-scram pump operation may or may not have a major impact on component design.

TABLE 1-1

Overall Plant Parameters Used in the
DEMO-POOL Simulation Model

Reactor Power, MWt	2903
Number of Primary Pumps/Intermediate Heat Transport Loops	4/6
Primary Hot Leg Temperature, °F	875
Primary Cold Leg Temperature, °F	595
Intermediate Hot Leg Temperature, °F	815
Intermediate Cold Leg Temperature, °F	550
Primary Pump Flow Rate, 10^6 lb/hr	28.9
Intermediate Loop Flow Rate, 10^6 lb/hr	20.1
Steam Pressure at Turbine Inlet, psia	1000
Steam Temperature at Turbine Inlet, °F	545
Loop Steam Flow Rate, 10^6 lb/hr	2.09
Evaporator Water Inlet Temperature, °F	529
Evaporator Exit Steam Quality	0.167
Steam Drum Pressure, psia	1045

2. DUTY CYCLE EVENT SELECTION

The 1000 MWe Pool-Type LMFBR Plant duty cycle was prepared and reported in EPRI NP-882 (5). It contains lists having the name, transient number and total number of occurrences for duty cycle events in the four ASME Boiler and Pressure Vessel Code, Section III, service levels; Level A Events, Level B Events, Level C Events and Level D Events. These levels were formerly referred to as Normal, Upset, Emergency and Faulted Conditions, respectively. The present analysis is an evaluation of selected duty cycle events from the Level B and Level C Event lists. The events selected for evaluation are listed in Table 2-1.

The application of duty cycle events to analysis of components requires another step not included in either Reference 5 or the present analysis. That step involves the determination of the appropriate number of occurrences during the plant lifetime of specific events selected for component analysis (the umbrella events). Because not all duty cycle events are selected for analysis of specific components, the number of occurrences of the events selected is increased from the number contained in the plant duty cycle to conservatively cover (umbrella) the events deleted from the analysis. Therefore, the number of occurrences of a specific event used in component analysis is, in general, larger and sometimes much larger than that contained in the plant duty cycle (5).

TABLE 2-1

Duty Cycle Events Selected for Evaluation

TRANSIENT NUMBER	TRANSIENT DESCRIPTION
B-1a	Reactor Trip from Full Power with Nominal Decay Heat
B-1b	Reactor Trip from Full Power with Minimum Decay Heat
B-2a	Uncontrolled Rod Insertion
B-2c	Plant Loading at Maximum Rod Withdrawal Rate
B-4b	Loss of Power to One Intermediate Pump
B-10	Inadvertent Isolation and Blowdown of One Steam Generator
B-11	Loss of Feedwater Flow to One Steam Generator Loop
B-14	Loss of Off-Site Power
B-16	Inadvertent Opening of Steam Generator Outlet Steam Line Safety/ Power Relief Valve
B-23a	Uncontrolled Rod Withdrawal from 100% Power
C-7	Water Side Isolation of a Steam Generator with Failure of the Dump Valves to Open

3. BASIS FOR ANALYSIS

The present analysis is based on the assumption that the primary and intermediate sodium pumps are either tripped to half speed or remain at full speed normally following a reactor scram. In addition these pumps are equipped with pony motors that operate at 7% of design speed following the loss of off-site power. The steam generator recirculation pumps are assumed to be tripped following a reactor scram.

The recirculation system provides adequate steam generator water flow by natural circulation after a reactor scram. Steady state full power operation with natural circulation in a recirculation loop would result in a reduced margin between the operating condition and the occurrence of departure from nucleate boiling (DNB) in the evaporator. During the post-scram transient, however, the margin to DNB in the evaporator is not reduced because the DNB quality increases sharply as the water flow is reduced and because of full-power steady-state operation of the evaporator does not occur following the reactor scram and water flow reduction. Short term operation with DNB occurring in the evaporator would be acceptable following a scram but it does not occur except for the steam generator dryout events.

The effectiveness of the hot pool for mitigating temperature transients is somewhat uncertain even at high sodium flow rates. Therefore, it was conservatively assumed that only 50 percent of the sodium in the hot pool participates in the mixing and transient mitigation process at 50 percent pump speed. This was assumed to be the normal post-scram mode of operation.

Minimum and nominal decay heat generation rates based on CRBRP analyses are used to represent power generation rates after a scram. The minimum decay heat data were taken from W-ARD-D-0005(3). These data are based on a power history that ramps from 0 to 10 percent power in 0.5 hours, remains at 10 percent power for 0.5 hours and then ramps to 100 percent power in 0.5 hours at which time the scram occurs. This power history conservatively represents the scrams that might occur shortly after the rise to power following refueling or shortly after the weekly load increases. The nominal decay heat data were taken from W-ARD-D-0090 based on 350 hours of full power operation without adjustment for uncertainties. These data adequately represent decay heating following scrams that might occur during sustained full power operation. This decay power profile was judged appropriate for analysis of most duty cycle events.

4. PLANT TRANSIENTS WITH POST-SCRAM SODIUM PUMP TRIP TO HALF SPEED

A post-scram sodium pump trip to half speed had previously been selected as the most likely compromise between full speed and pony motor pump operation. Therefore, a significant set of duty cycle events have been evaluated on that basis. The results of the evaluation for each of the selected events are contained in the paragraphs that follow.

4.1 B-1a Reactor Trip from Full Power with Nominal Decay Heat

This transient is based on a manual reactor trip from 100 percent power. The primary and secondary control rods start insertion 0.2 seconds later. The primary and intermediate sodium pumps begin coasting down to 50 percent speed 0.5 seconds after the reactor trip. The initial decay heat level for this transient is nominal decay heat which is associated with a reactor in operation for a significant time.

The reactor scram transient with nominal decay heat is shown in Figures 4-1 to 4-12. The primary and intermediate sodium flow coastdowns are shown in Figures 4-1 and 4-2. The 50 percent post-scram pump speed maintains the primary and intermediate sodium flow rates at approximately 50 percent of the rated values. The curve labeled "nuclear reactor power" in Figure 4-1 is the fractional heating rate which includes decay heat. The IHX primary sodium inlet nozzle temperature shown in Figure 4-4 drops from 875 to 580°F in approximately 500 seconds with the majority of the change occurring in 180 seconds. This is also fairly representative of the immediate hot leg temperature transient. The cold leg temperatures are relatively steady as shown in Figures 4-4 and 4-5.

4.2 B-1b Reactor Trip from Full Power with Minimum Decay Heat

The operational sequence for this transient is the same as that described above for Event B-1a. Minimum decay heat levels are used. Minimum time to reach full power level and appropriate uncertainties are used in calculating the minimum decay heat.

The reactor scram transient with minimum decay heat is shown in Figures 4-13 to 4-24. The control rod and pump trip sequence is the same as that described for Event B-1a. The IHX primary inlet nozzle temperature shown in Figure 4-15 is not much different than that shown in Figures 4-4 with nominal decay heat. This demonstrates that decay heat level is not an important parameter when high post-scram flow rates are used.

4.3 B-2a Uncontrolled Rod Insertion

A single control rod is inserted at a rate which causes a 40 percent per minute reduction in reactor thermal power due to an assumed malfunction of the controller on the rod. (This event is not to be confused with a rod drop which is an unlatching of the rod resulting in a free fall of the control rod into the core.) The sodium flows and the turbine admission valve inlet pressure are held constant. It is assumed that this event occurs when the reactor is operating at 100 percent power with correspondingly high system temperatures and nominal reactor decay heating. The operator manually trips the plant at 300 seconds.

The system transient is shown in Figures 4-25 to 4-36. Figures 4-27 and 4-28 show that the primary hot leg temperatures decrease about 270°F prior to the reactor scram while primary cold leg temperatures decrease moderately. The response of the steam generator system is quite smooth and satisfactory. The reactor is essentially shut down prior to the reactor scram which then causes the sodium and water recirculation pumps to be tripped.

4.4 B-2c Plant Loading at Maximum Rod Withdrawal Rate

Two reactor transients were evaluated for this event. The first is based on having variable-speed primary and intermediate sodium pumps which vary sodium flow rates over the 60 to 100 percent power load-following range. The second transient is based on constant-speed primary and intermediate sodium pumps. In that case the sodium flow rates remain constant as the reactor power is changed from 60 to 100 percent power. In both cases the same rate of power increases, 40 percent per minute, was assumed.

4.4.1 Variable Speed Pumps

From initial plant operating conditions of 60 percent thermal power and corresponding part-load flow rates of sodium, water and steam, the station supervisory controller is assumed to require a plant load increase. During the control rod withdrawal, a mechanical malfunction is then assumed to result in the maximum mechanical rod withdrawal speed. The reactor power is assumed to increase from 60 to 100 percent in one minute. The sodium flow rates are assumed to increase from 66 percent primary flow and 72 percent intermediate sodium flow to 100 percent over the same time period. The turbine increases output at the appropriate rate and feedwater flow also functions properly. The result is a rapid ramp increase in reactor power from 60 to 100 percent. No reactor trip occurs.

The plant transient is shown in Figures 4-37 to 4-48. Figures 4-39 and 4-40 show that the primary hot leg temperatures increase approximately 60°F while the primary cold leg temperatures increase approximately 45°F. The intermediate hot leg temperatures increase approximately 55°F while the intermediate sodium cold leg temperatures increase approximately 10°F. The steam system (Figures 4-43 to 4-48) takes approximately 4 to 5 minutes to approach new steady state operating conditions.

4.4.2 Constant Speed Pumps

From initial plant operating conditions of 60 percent thermal power the station supervisory controller is assumed to require a plant load increase. During the control rod withdrawal, a mechanical malfunction is then assumed to result in the maximum mechanical rod withdrawal speed. The reactor power is assumed to increase from 60 to 100 percent in one minute. The sodium flow rates are assumed constant at 100 percent of rated values. The turbine increases output at the appropriate rate and feedwater flow also functions properly. The result is a rapid ramp increase in reactor power from 60 to 100 percent. No reactor trip occurs.

The plant transient is shown in Figures 4-49 to 4-60. Figures 4-51 and 4-52 show that the primary hot leg temperatures increase approximately 135°F while the primary cold leg temperatures increase approximately 20°F. The intermediate hot leg temperatures increase approximately 110°F while the intermediate sodium cold leg temperatures increase approximately 5°F. The steam system (Figures 4-55 to 4-60) takes approximately 4 to 5 minutes to approach new steady state operating conditions.

4.5 B-4b Loss of Power to One Intermediate Pump

The intermediate pump in one loop is assumed to coast down to pony motor speed. The other primary and intermediate pump speeds are assumed to remain at initial values until the reactor/pump trip. A reactor trip is initiated by pump under voltage relays or pump drive shaft tachometers. Following the trip, the remainder of the pumps and the steam/water side are treated as for the normal trip.

The plant transient for this event is presented and discussed in Subsection V-8.4.2 of EPRI NP-882 (6). The primary concern for this event is the primary sodium outlet temperature transient of the affected IHX. The maximum temperature rate for the affected IHX is 2.7°F/sec and the temperature change at the affected IHX primary outlet is 146°F (see Reference 6 for details).

4.6 B-10 Isolation and Blowdown of Steam Generator Components

The events are assumed to be initiated by one of the following: (a) inadvertent operator action (b) spurious activation caused by equipment failure, or (c) operator response to a water-to-sodium leak indication. This transient results in the water-side isolation and dumping of the steam generators in an individual loop. The event terminates at refueling conditions. The water-side of the drained component is subsequently filled with nitrogen gas at 300 psig to maintain water-side pressure higher than the sodium side.

The event is assumed to be initiated by closure of the normally-open isolation valves in this affected loop feedwater and steam lines. Simultaneously, the inlet water dump valves and power relief valves in the affected loop are assumed to open. The steam/water side pressure decreases until the power relief and dump valves are closed. The modules are then pressurized on the water/steam sides with nitrogen at 300 psig. A reactor trip occurs based on low steam drum level. The event is characterized by an up-transient in the affected steam generator and its intermediate sodium loop. The unaffected loops see transients similar to a reactor trip from full power.

Due to the severe cold leg temperature transient in the affected loop, two transients were evaluated. The first assumes that operation of the primary and intermediate sodium pumps will be the same as following a normal scram. In that case the primary and intermediate sodium pump speeds are reduced to 50 percent following the scram. The second transient is based on tripping the affected intermediate loop sodium pump to pony motor speed at the time of isolation and blowdown. This is intended to reduce the severity of the cold leg temperature transient in the affected loop. These transients are presented and discussed in the following paragraphs.

4.6.1 With All Sodium Pumps Tripped to Half Speed Following Scram

In this case all the primary and intermediate sodium pumps are tripped to 50 percent speed following the reactor scram. The resulting system transient is shown in Figures 4-61 to 4-72. Figure 4-69 indicates that the affected steam generator blows down to atmopheric pressure in approximately 30 seconds. The detailed steam side calculation for the affected steam generator was terminated at 40 seconds because the blowdown was essentially completed. This results in lower computer usage with essentially the same consequences. The steam dump flow rate shown in Figure 4-68 is plotted as the percent of normal loop steam flow. The water dump flow rate is plotted as the percent of the normal total loop recirculation water flow rate.

Dumping the water and steam from the affected steam generator causes an eventual dryout of the unit. Prior to the dryout the sodium outlet temperature from the affected unit (Figure 4-66) drops from 550 to 510°F, then it increases to approximately 775°F before beginning to cool. The temperature change at the affected evaporator outlet is approximately 265°F with a maximum rate of approximately 3.5°F/sec. This is a severe transient for the entire cold leg of the affected loop as shown in Figures 4-65 to 4-66.

4.6.2 With Affected IHTS Pump Trip to Pony Motor Speed

The temperature rates in the affected intermediate sodium system cold leg can be reduced from the previous case by tripping the affected intermediate sodium pump to pony motor speed at the time of initiation of the isolation and blowdown. This causes a transient at the affected IHX primary outlet very much like the B-4b Loss-of-Power-to-One-Intermediate-Pump event discussed previously. The system transient is shown in Figures 4-73 to 4-84. Figure 4-76 shows the transient at the affected IHX primary outlet. The temperature change and maximum rate at that location are 146°F and 2.7°F/sec as compared to 220°F and 2.9°F/sec in the previous case. Therefore, tripping the affected IHTS pump to pony motor speed reduces the temperature change at the affected IHX primary outlet but does not signficantly change the maximum rate. The temperature transient at the affected evaporator sodium outlet is shown in Figure 4-78. At that location the temperature change is approximately 229°F and the maximum rate is approximately 0.7°F/sec. This compares to a temperature change of 265°F and a maximum rate of 3.5°F/sec in the previous case. Therefore, tripping the affected IHTS pump to pony motor speed at the time of the scram reduces the temperature change moderately for the cold leg of the intermediate sodium system but reduces the maximum rate by approximately a factor of five. This is a definite improvement over the previous case (Section 4.6.1).

4.7 B-11 Loss of Feedwater to One Steam Generator Loop

This event can be caused by an inadvertent closure of the feedwater control valve to one of the steam generator loops. The reactor will scram on low water level in the steam drum. The transient results in water-side dryout of the affected loop. The event terminates at refueling conditions.

The system transient is shown in Figures 4-85 to 4-96. The large water supply in the steam drum delays the water-side dryout until the intermediate hot leg sodium has cooled following the reactor scram. This is shown in Figure 4-90. The transient is much less severe than the B-10 Isolation and Blowdown for two reasons: 1) the delayed dryout discussed above and 2) the steam drum water temperature doesn't drop prior to the dryout because steam drum pressure is maintained.

4.8 B-14 Loss of Off-Site Power

If the loss of main sodium pump power occurs, the sodium flow will decrease to pony motor flow (driven by emergency power) in all loops. A reactor trip, loss of main condenser and turbine trip will follow. Two auxiliary feed pumps (of 5% capacity each) are available to initially maintain feedwater flow. Sufficient stored water is available to make up for water lost to remove decay and stored heat by dumping steam until the Reactor Auxiliary Cooling Systems are brought on-line.

The system transient is shown in Figures 4-97 to 4-108. The response of the hot pool (Figure 4-99) is based on the two-zone mixing model in DEMO-POOL which conservatively assumed mixing in 50 percent of the volume below the top of the chimneys in the reactor upper internals following pool stratification. The sodium flow coastdowns (Figure 4-97) are based on 5.0 and 6.0 second half-times for the primary and intermediate pumps, respectively. This transient is not as severe for most system components as a reactor scram such as Event B-1a. It does represent a severe test of the reactor vessel cooling system since the hot pool does not cool very rapidly following the scram.

4.9 B-16 Inadvertent Opening of Steam Generator Outlet Steam Line Safety/Power Relief Valve

A steam relief valve is assumed to open at a steam generator outlet steam line. This causes the steam flow from that unit to increase momentarily. The turbine steam flow soon drops by the amount of vented flow and a nearly steady plant operating condition is achieved. It is assumed that the valve cannot be closed. Therefore, after 600 seconds, the plant is assumed to be tripped manually. Feedwater flow in the affected loop is stopped at the time of the plant trip to limit the loss of water inventory. The event is terminated at refueling conditions. This event is also used to provide coverage for small steam line breaks. The major allowable size of break will be determined later.

The system transient is shown in Figures 4-109 to 4-120. Since a relatively steady state condition is achieved shortly after the event is initiated, the transient was calculated based on a manual reactor scram at 300 seconds instead of 600 seconds to save computer time. The results are essentially the same except for the extra delay time.

The plant has 4 safety/power relief valves having a total design steam flow rate equal to the rated steam flow of the loop at 1320 psia (10 percent above the steam generator design pressure). Therefore, opening one valve at normal operating pressure results in a discharge rate of approximately 20 percent of rated loop steam flow as shown in Figure 4-116. Stopping the feedwater flow to the affected loop causes a steam generator dryout. Figure 4-114 shows that the dryout occurs after the intermdeiate hot leg has partially cooled. The transient for the affected steam generator is based on closing the relief valve after dryout. This has no effect on the temperature calculations because the heat transfer between the evaporator tubes and steam is set to zero on dryout. The pressure in the affected steam generator (the "S" loop) shown in Figures 4-117 would drop to atmospheric pressure rather than leveling off above 990 psia if the valve had not been closed after dryout.

4.10 B-23a Uncontrolled Rod Withdrawal from 100 Percent Power

An uncontrolled withdrawal of a control rod was assumed for this analysis to cause the reactor power to rapidly increase from 100 to 115 percent (just below the high flux scram setpoint). A manual reactor trip is assumed to be initiated by the reactor operators 5 minutes after the power increase. Sodium flow rates are maintained at their initial full power values until the reactor trip occurs. The initial decay heat level is the nominal value for sustained full power operation. The system response shows the temperature increases caused by the power increase is followed by a cooling similar to that for a reactor scram from full power but with higher initial temperature and larger temperature changes.

The system transient is shown in Figures 4-121 to 4-132. Figures 4-123 and 4-124 show that primary hot leg temperatures increase 49°F before the scram while primary cold leg temperatures increse only 7°F. Intermediate heat transfer system hot leg temperatures increase approximately 40°F prior to the reactor trip. The reactor trip causes an additional temperature increase due to the partial collapse of the temperature differences across the IHX at low sodium flow rates.

4.11 C-7 Water Side Isolation of a Steam Generator with Failure of the Dump Valves to Open

This transient assumes the same conditions as Event B-10 except the water and steam dump valves on the affected steam generator fail to open. The event is initiated by closure of the normally open isolation valves in the affected loop feedwater and steam lines. The steam and feedwater flows stop. The recirculation water flow through the affected evaporator continues under forced circulation until the reactor trip, then circulation continues under natural convection. The steam pressure in the affected steam generator increases until the safety relief valves open. The reactor trip is initiated on low drum water level in the affected loop. The water side of the affected steam generator dries out at the safety relief valve pressure setting rather than low pressure.

The system transient is shown in Figures 4-133 to 4-144. Figure 4-141 shows the pressurization of the affected steam generator to the safety valve opening pressure (1320 psia). Dryout of the affected steam generator occurs at approximately 120 seconds after the isolation as shown in Figure 4-140. The dryout occurs after the intermediate hot leg has partially cooled. Therefore the cold leg temperature transient in the affected loop is not nearly as severe as the B-10 Isolation and Blowdown.

5. PLANT TRANSIENT WITHOUT POST-SCRAM SODIUM PUMP TRIP

The possible alternative mode of post-scram sodium pump operation, keeping the pumps operating at 100 percent of rated speed, was evaluated for several selected duty cycle events to provide a basis for comparison with the transients in Part 4 of this Subsection. In addition, the effect of increased intermediate sodium pump inertia on the temperature transient for two events was evaluated. The events chosen for comparison are loss of power to one intermediate pump, isolation and blowdown of one steam generator and loss of off-site power. These correspond to Events B-4b, B-10 and B-14 from the plant duty cycle. The analysis of each of these events is described in the following paragraphs:

5.1 B-4b Loss of Power to One Intermediate Pump

The intermediate pump in one loop is assumed to coast down to pony motor speed following the loss of power. The other primary and intermediate pumps are assumed to remain at full speed. A reactor trip is initiated by the pump undervoltage relays. Following the reactor trip, the remainder of the pumps and the steam/ water side are treated the same as for a normal scram. In this case, the primary and intermediate sodium pumps remain at full speed and the steam generator water recirculation pumps are tripped.

This event subjects the affected IHX primary outlet to a fairly severe transient. Therefore, several assumptions were made to produce a conservative transient at that location. These include the use of maximum decay heat, 100 percent hot-pool mixing, a 6 second IHTS pump half-time (as a base case) and the cold-pool bypass of the hot sodium from the affected IHX to the core inlet plenum. These are the same assumptions used to evaluate the transient for an operating procedure involving a post-scram pump trip to half speed in Reference 6.

Three transients were evaluated to establish the effect of intermediate pump inertia. The three cases correspond to IHTS pump half-times of 6, 12 and 24 seconds. The 6 second half-time represents the base case for comparison with Reference 6. The system transients for the three cases are shown in Figures 5-1 to 5-12, 5-13 to 5-24 and 5-25 to 5-36, respectively.

The primary concern for this event is the primary sodium outlet temperature transient from the affected IHX shown in Figures 5-4, 5-16 and 5-28. The increases in primary outlet sodium temperature from the affected IHX for the three cases are 182, 153 and 115°F, respectively, with 6, 12 and 24 second IHTS pump half-times. The maximum temperature rates for the three cases are approximately 6.5, 4.5 and 2.6 °F/sec, respectively. These values compare to an increase of 146°F with a maximum rate of approximately 2.7 °F/sec under similar assumptions but tripping the pumps to half speed. This shows that reducing the post-scram pump speed to 50 percent does more to reduce the transient at the IHX primary outlet than doubling the IHTS pump inertia.

5.2 B-10 Isolation and Blowdown of One Steam Generator

These events are assumed to be initiated by one of the following: (a) inadvertent operator action (b) spurious activation caused by equipment failure, or (c) operator response to a water-to-sodium leak indication. This transient results in the water-side isolation and dumping of the steam generators in an individual loop. The event terminates at refueling conditions. The water-side of the drained component is subsequently filled with nitrogen gas at 300 psig to maintain the water-side pressure higher than the sodium side.

The event is assumed to be initiated by closure of the normally open isolation valves in affected loop feedwater and steam lines. Simultaneously, the inlet water dump valves and power relief valves in the affected loop are assumed to open. The steam/water side pressure decreases until the power relief and dump valves are closed. The modules are then pressurized on the water/steam sides with nitrogren at 300 psig. A reactor trip occurs based on low steam drum level. The event is characterized by an up-transient in the affected steam generator and its intermediate sodium loop. The unaffected loops see transients similar to a reactor trip from full power.

The system transient is shown in Figures 5-37 to 5-48 based on full speed post-scram sodium pump operation. Figure 5-45 indicates that the affected steam generator blows down to atmospheric pressure in approximately 30 seconds. The detailed steam side calculation for the affected steam generator was terminated at 40 seconds because the blowdown was essentially completed. This results in lower computer usage with essentially the same consequences. The steam dump flow rate shown in Figure 5-44 is plotted as the percent of normal loop steam flow. The water dump flow rate is plotted as the percent of the normal total loop recirculation water flow rate.

Dumping the water and steam from the affected steam generator causes an eventual dryout of the unit. Prior to the dryout the sodium outlet temperature from the affected unit (Figure 5-42) drops from 550 to 525°F, then it increases to approximately 765°F before beginning to cool. The temperature change at the affected evaporator outlet is approximately 241°F. This is a severe transient for the entire cold leg of the affected loop as shown in Figures 5-40 to 5-42.

The cold leg temperature changes associated with this event are somewhat less than the corresponding transient in Part 4.6.1 of this Subsection with 50 percent post-scram pump speed. The temperature rates are much higher in the present case, however. Maximum temperature rates at the affected steam generator sodium outlet are approximately 6.2 °F/sec in the present case as compared to 3.5 °F/sec in Part 4.6.1. Temperature rates at the intermediate IHX inlet can be reduced by tripping the affected intermediate sodium pump to pony motor speed at the time of the steam generator isolation. This will also reduce the temperature increase at the primary IHX outlet.

5.3 <u>B-14 Loss of Off-Site Power</u>

Loss of off-site power causes a loss of main sodium pump power and the sodium flow decreases to pony motor flow (driven by emergency power) in all loops. A reactor trip, a loss of main condenser and a turbine trip follow shortly after the event. Two auxiliary feed pumps (5 percent capacity each) are available to initially maintain feedwater flow. Sufficient stored water is available to make up for water lost to remove decay heat and stored heat by dumping steam until the Reactor Auxiliary Cooling Systems are brought on-line.

The system transient for this event is independent of normal post-scram sodium pump main motor speed since power to the main sodium pump motors is lost when the event is initiated. Therefore, the reference system behavior is as shown in Part 4.8 of this Subsection. This is based on primary and intermediate sodium pump coastdown half-times of 5 and 6 seconds, respectively. If the sodium pumps are normally operated at full speed following a reactor scram, the inertia of the intermediate pumps might be increased to provide a milder transient following loss-of-power to an intermediate pump. Therefore, the loss of off-site power event was recalculated using a higher IHTS pump inertia to establish its influence on the intermediate hot leg temperature transient.

The system transient with high-inertia intermediate heat transfer system pumps (half-time = 24 sec) is shown in Figures 5-49 to 5-60. The temperature transient in the primary system is approximately the same as the event in Part 4.8. The intermediate hot leg transient shown in Figures 5-53 and 5-54 is more severe than before. The intermediate IHX outlet temperature drops 160°F in a short period of time (Figure 5-53) due to the mismatch of primary and intermediate pump coast-downs. The maximum temperature rate is approximately 5.2°F/sec.

6. REFERENCES

1. EPRI NP-646, Pool-Type LMFBR Plant, 1000 MWe Phase A Design, April, 1978.

2. EPRI NP-646, Pool-Type LMFBR Plant, 1000 MWe Phase A Design, Part II: Heat Transport Systems, Section 5: Plant Thermal Transient Model, April, 1978.

3. "LMFBR Demonstration Plant Simulation Model (DEMO)", WARD-D-0005, Rev. 3, April 15, 1975.

4. C. A. McGinnis, et al., "CRBRP Decay Power Analysis", WARD-D-0090, January, 1976.

5. EPRI NP-882 Volume 4, Pool-Type LMFBR Plant, 1000 MWe Phase A Extension-1 Design, Part V: Heat Transport System Components, Section 7 Plant Duty Cycle, September, 1978.

6. EPRI NP-882, Volume 4, Pool-Type LMFBR Plant, 1000 MWe Phase A Extension-1 Design, Part V: Heat Transport System Components, Section 8 Plant Transients, September, 1978.

FIGURE 4-1
POOL REACTOR SCRAM FROM FULL POWER WITH NOMINAL DECAY HEAT
RUN DATED 10/04/78
NUMBER PAPGE00

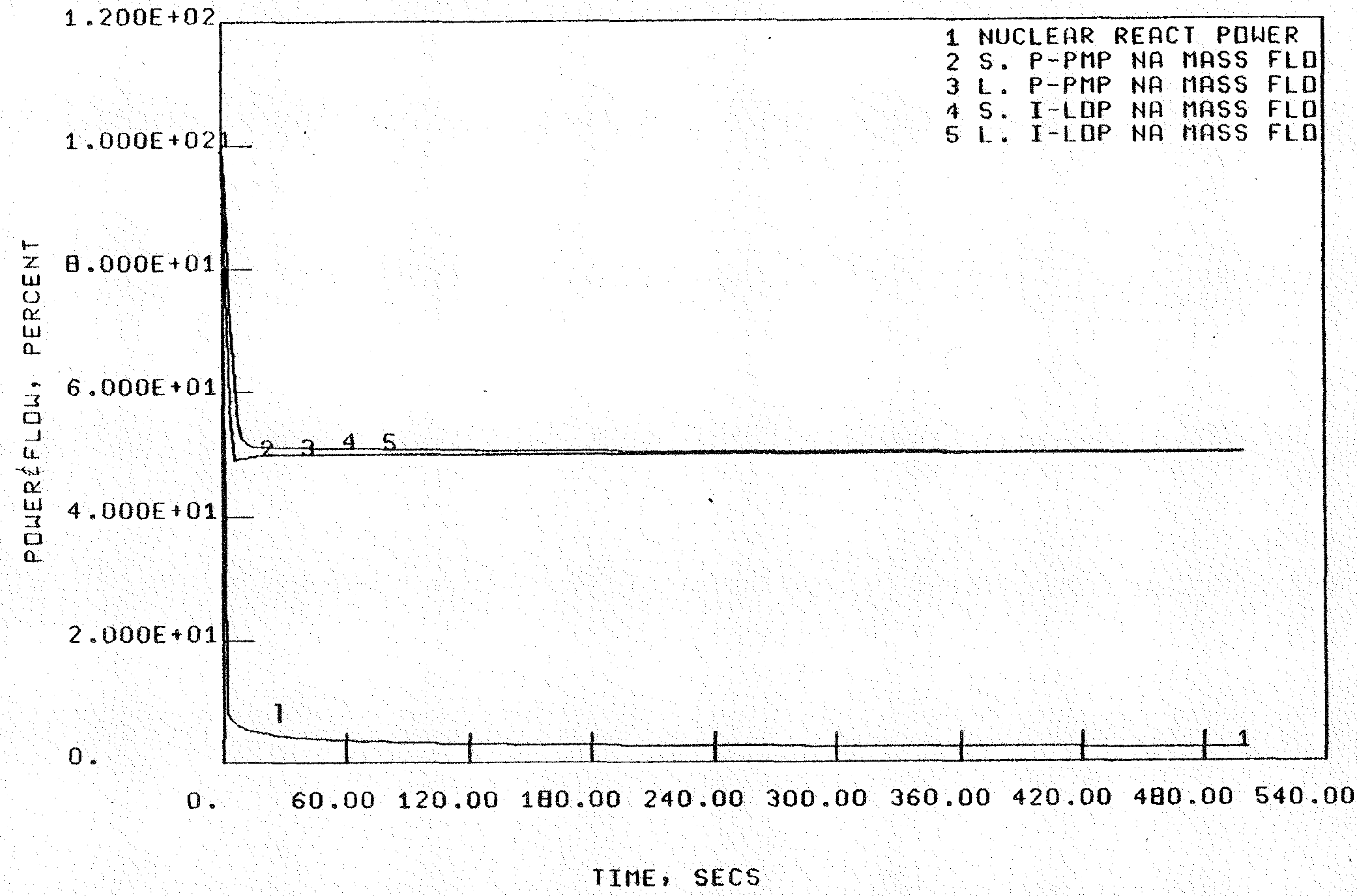

FIGURE 4-2
POOL REACTOR SCRAM FROM FULL POWER WITH NOMINAL DECAY HEAT
RUN DATED 10/04/78
NUMBER PAPGE00

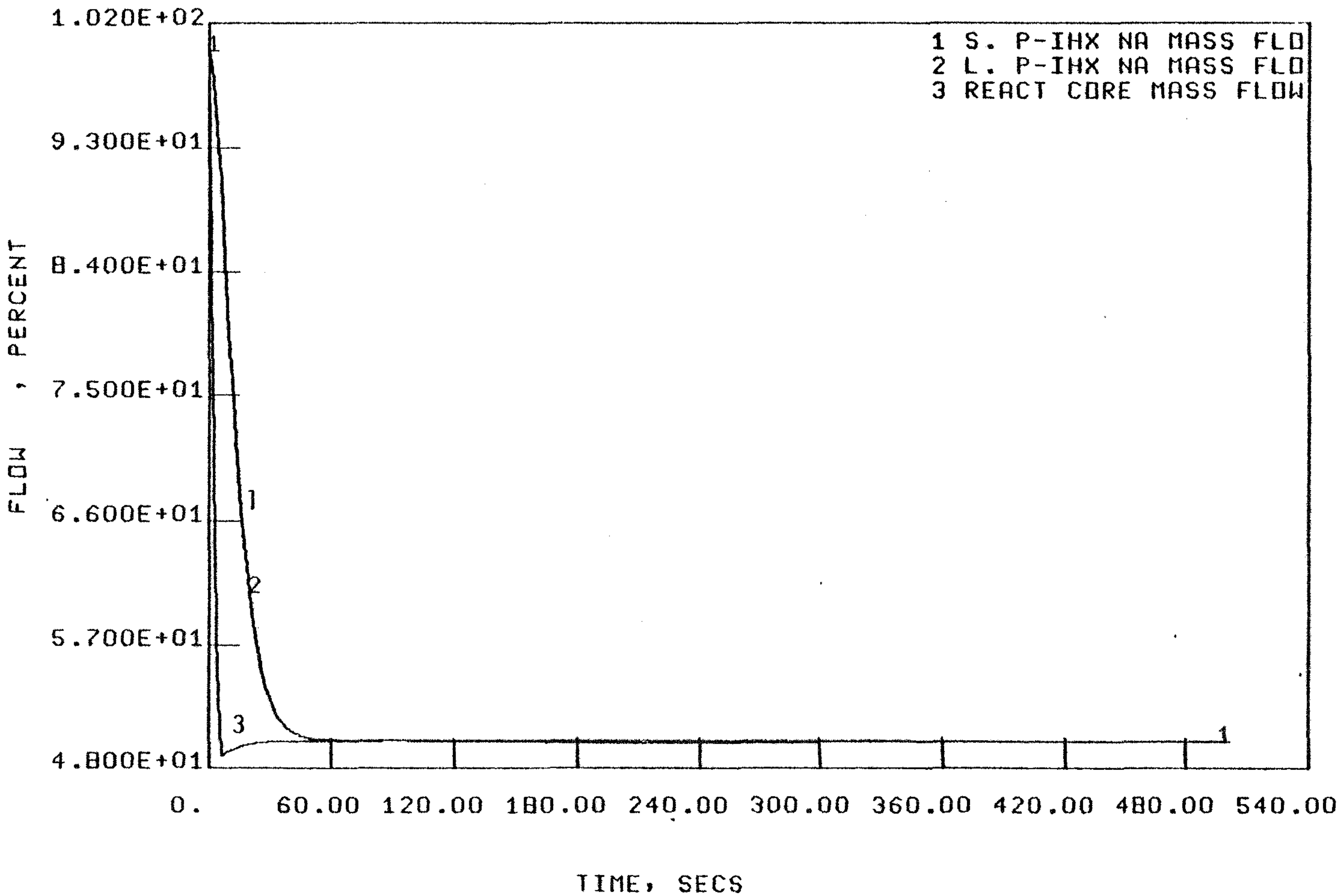

FIGURE 4-3
POOL REACTOR SCRAM FROM FULL POWER WITH NOMINAL DECAY HEAT
RUN DATED 10/04/78
NUMBER PAPGE00

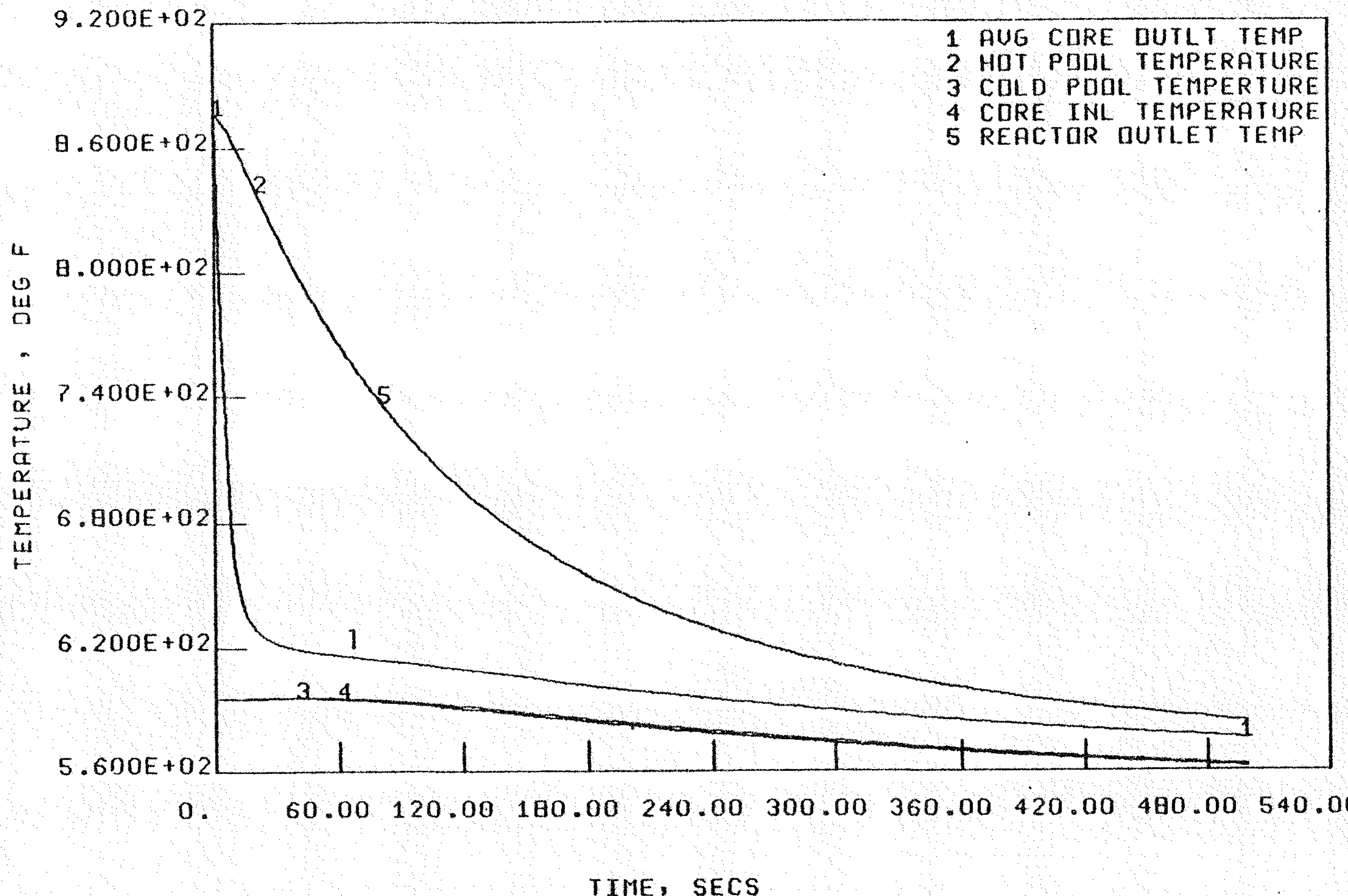

FIGURE 4-4
POOL REACTOR SCRAM FROM FULL POWER WITH NOMINAL DECAY HEAT
RUN DATED 10/04/78
NUMBER PAPGE00

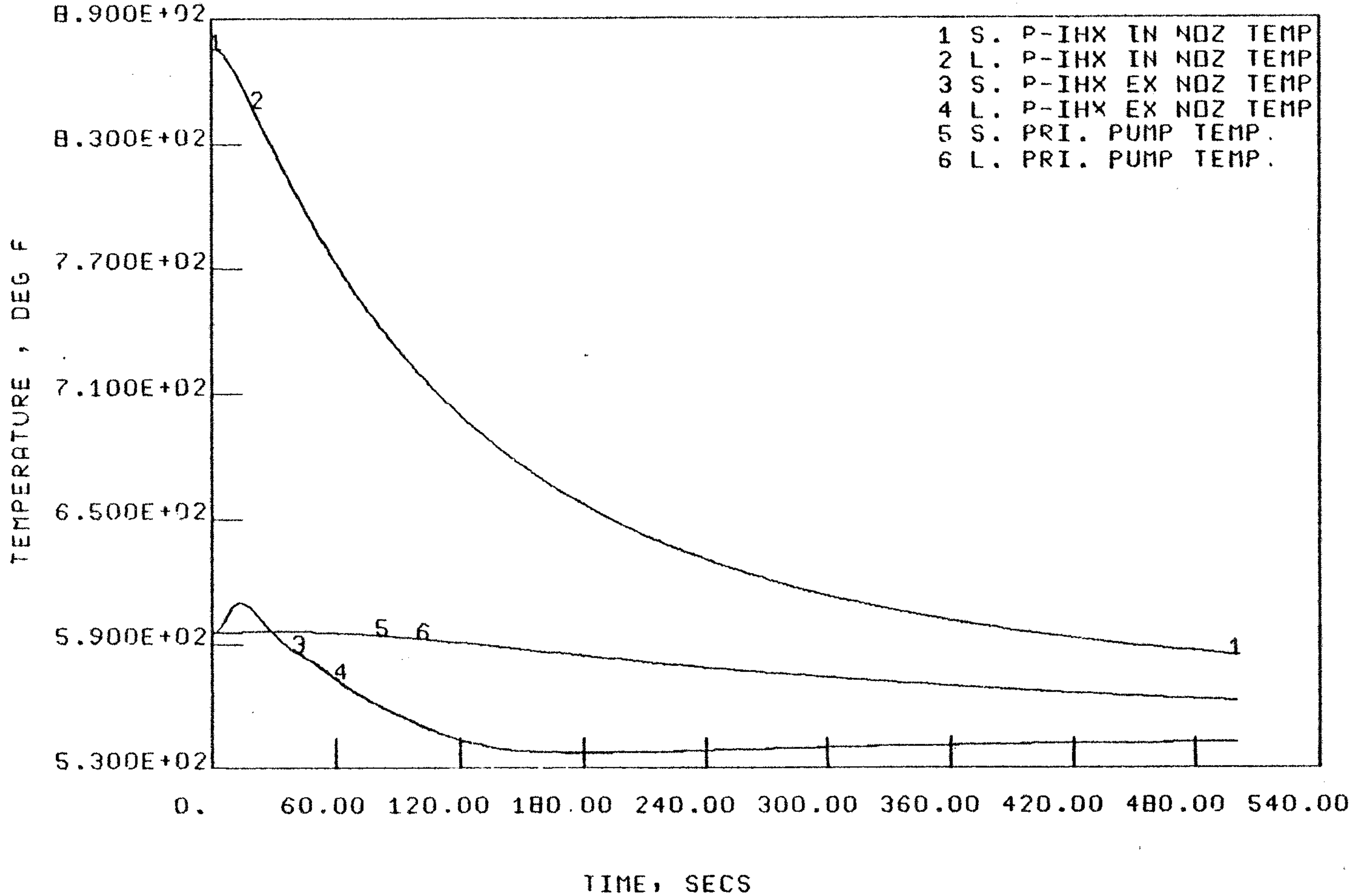

FIGURE 4-5
POOL REACTOR SCRAM FROM FULL POWER WITH NOMINAL DECAY HEAT
RUN DATED 10/04/78
NUMBER PAPGE00

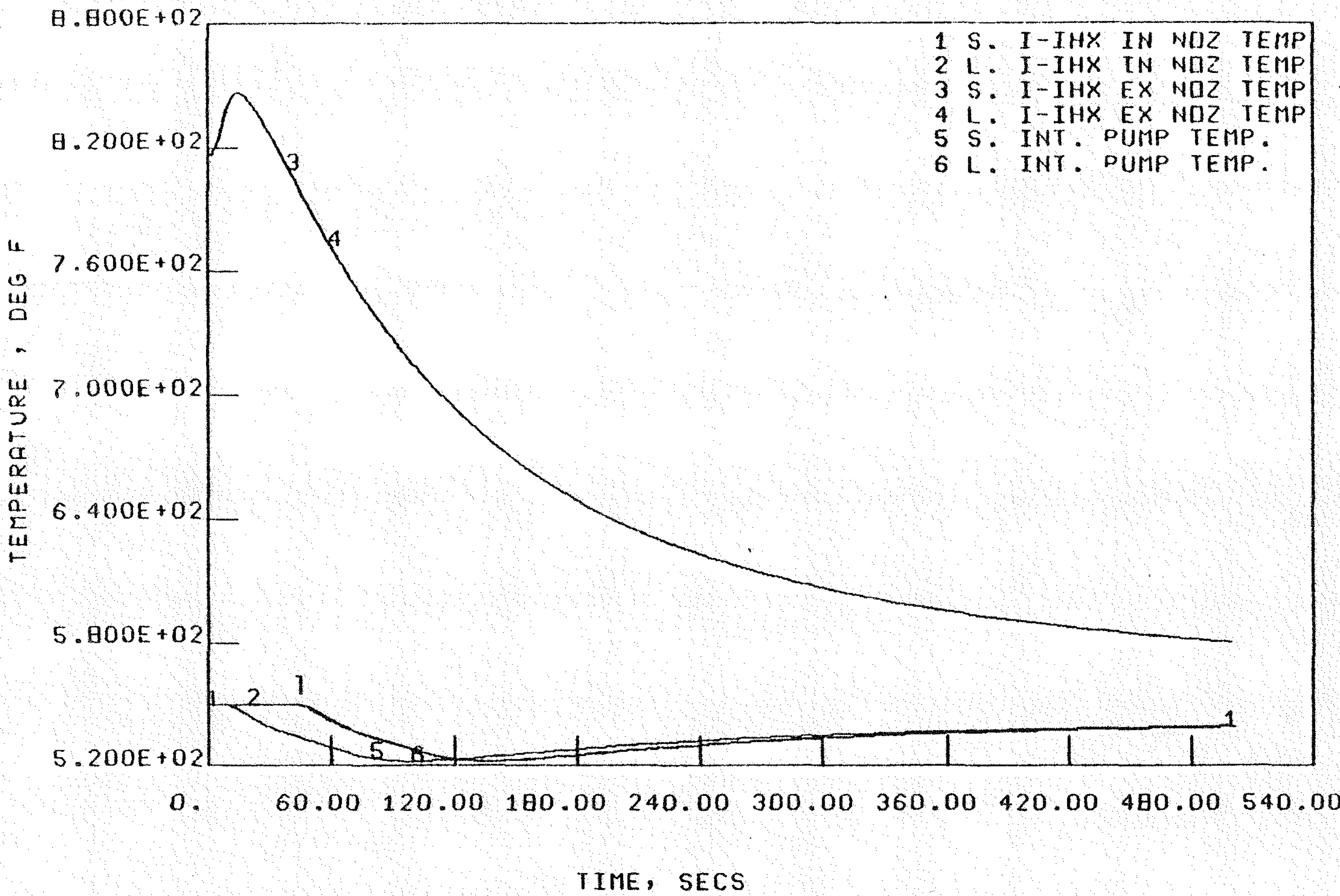

FIGURE 4-6
POOL REACTOR SCRAM FROM FULL POWER WITH NOMINAL DECAY HEAT
RUN DATED 10/04/78
NUMBER PAPGE00

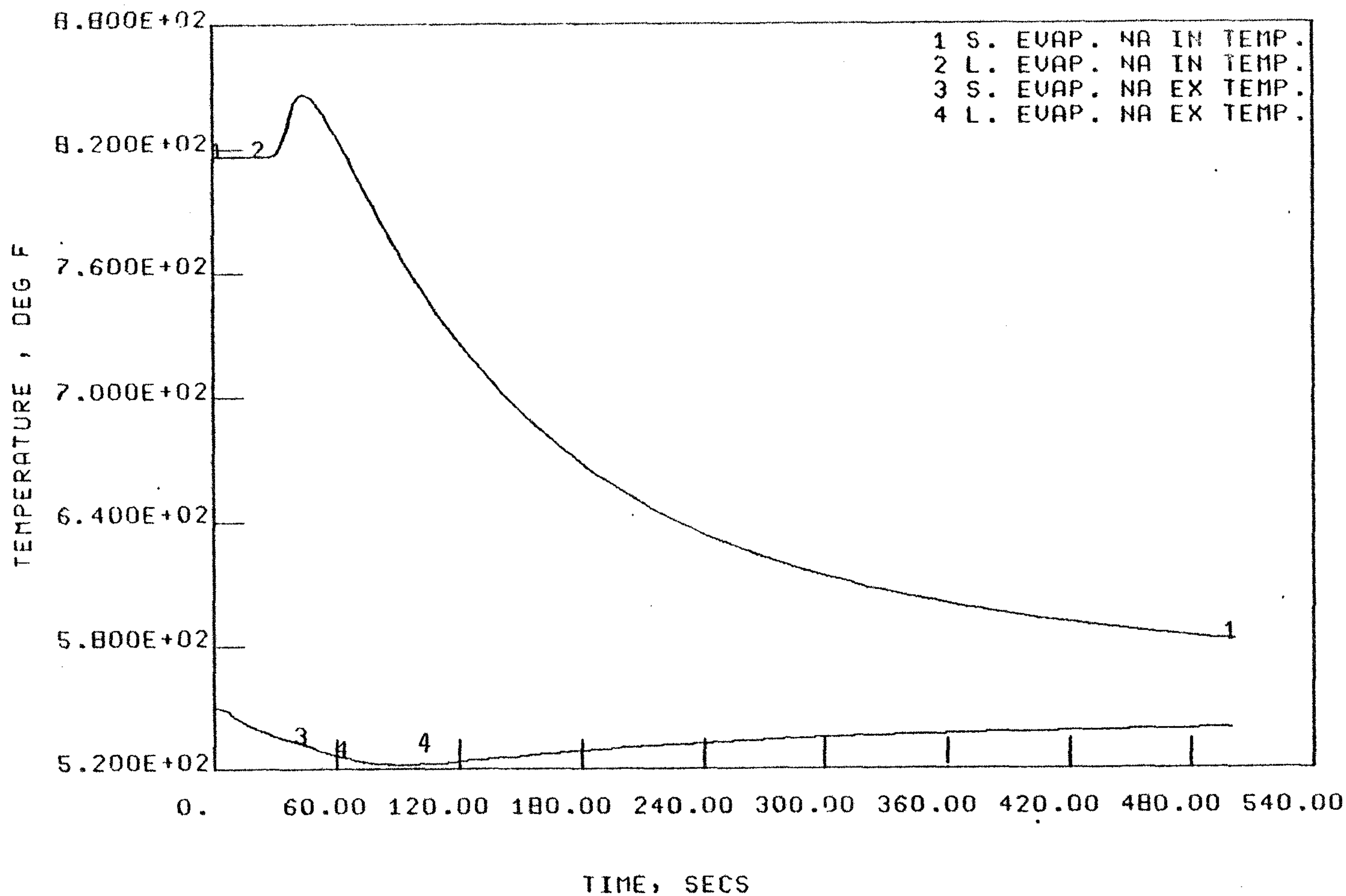

FIGURE 4-7
POOL REACTOR SCRAM FROM FULL POWER WITH NOMINAL DECAY HEAT
RUN DATED 10/04/78
NUMBER PAPGE00

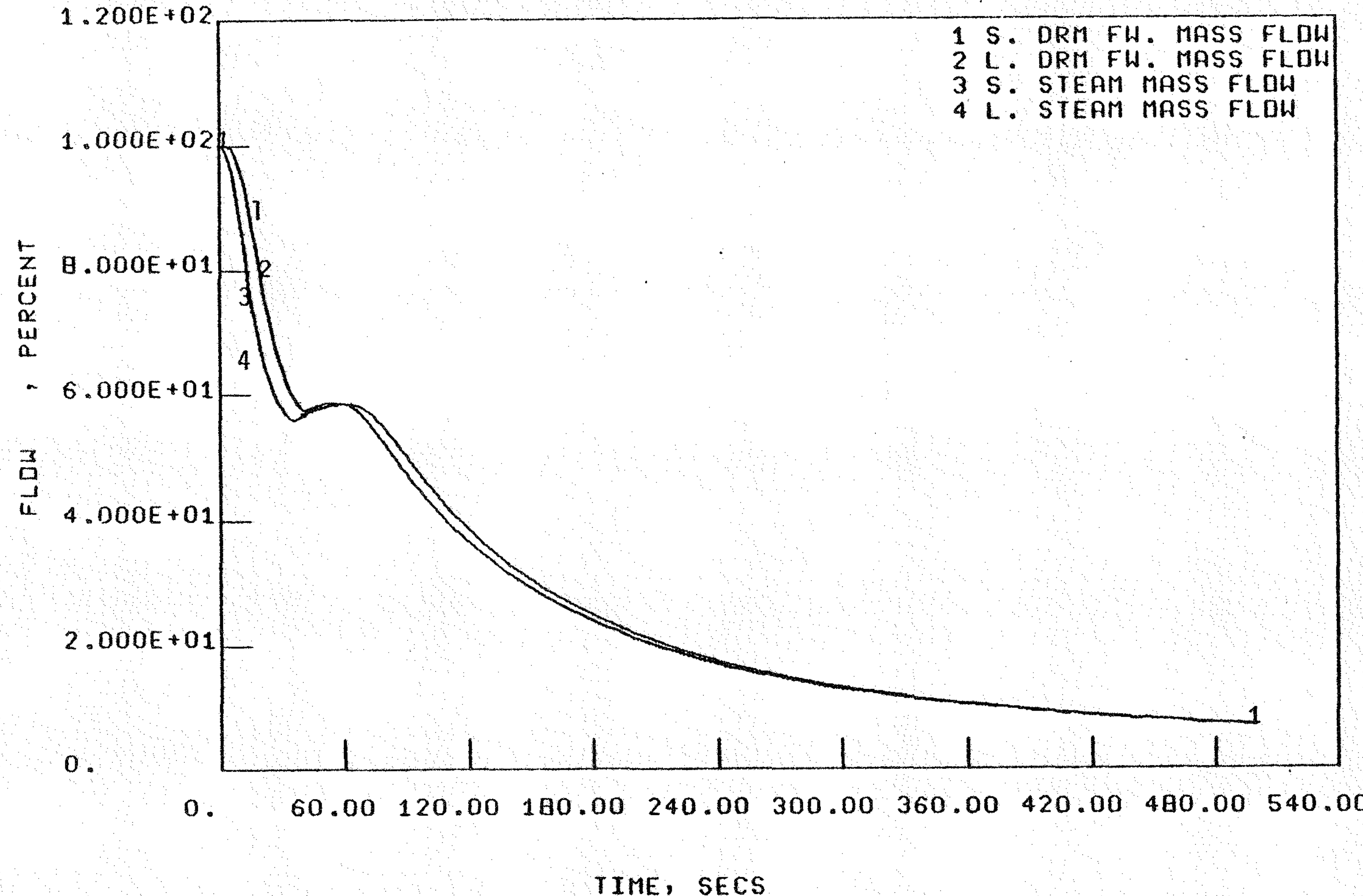

FIGURE 4-8
POOL REACTOR SCRAM FROM FULL POWER WITH NOMINAL DECAY HEAT
RUN DATED 10/04/78
NUMBER PAPGE00

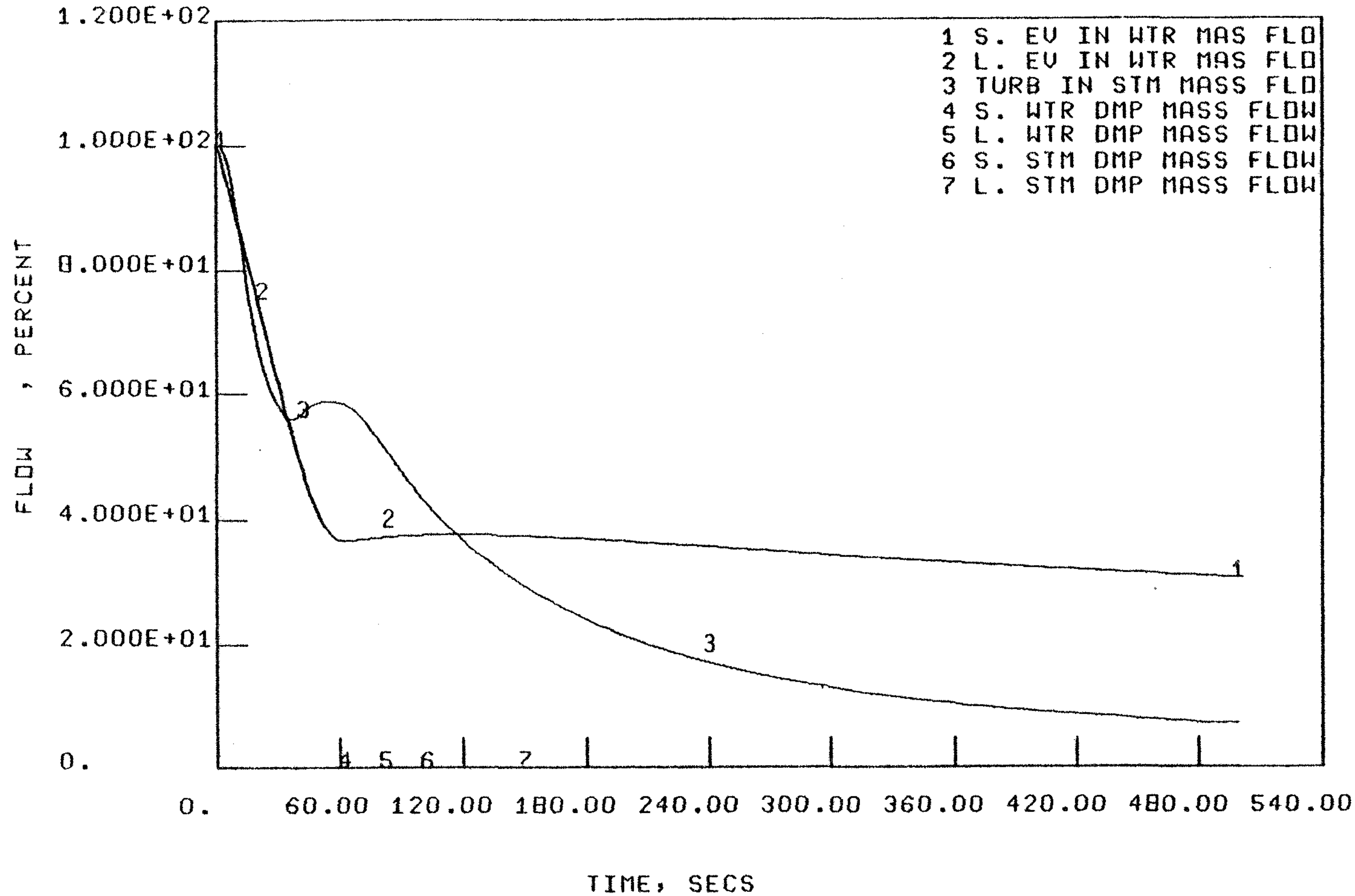

FIGURE 4-9
POOL REACTOR SCRAM FROM FULL POWER WITH NOMINAL DECAY HEAT
RUN DATED 10/04/78
NUMBER PAPGE00

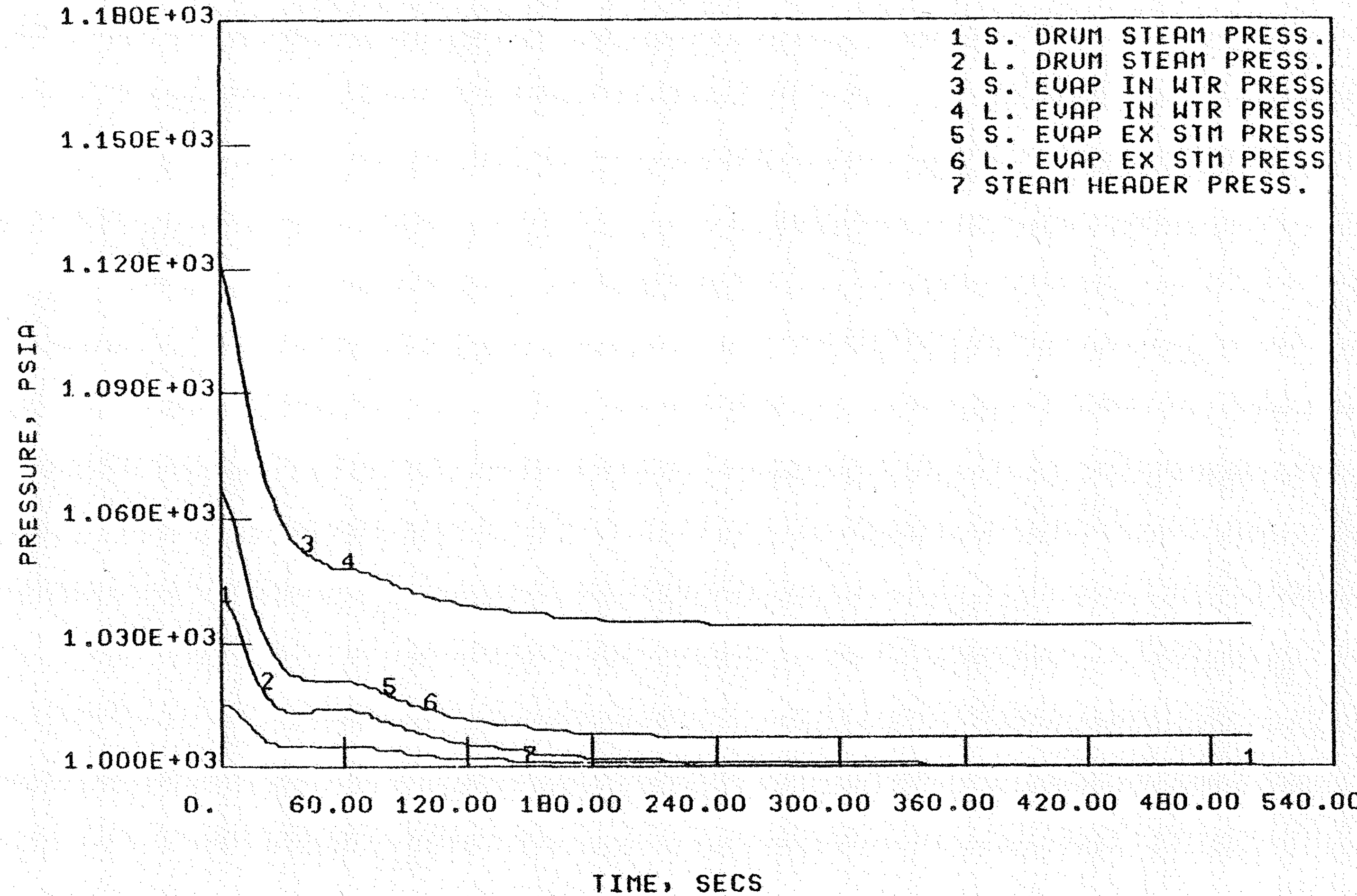

FIGURE 4-10
POOL REACTOR SCRAM FROM FULL POWER WITH NOMINAL DECAY HEAT
RUN DATED 10/04/78
NUMBER PAPGE00

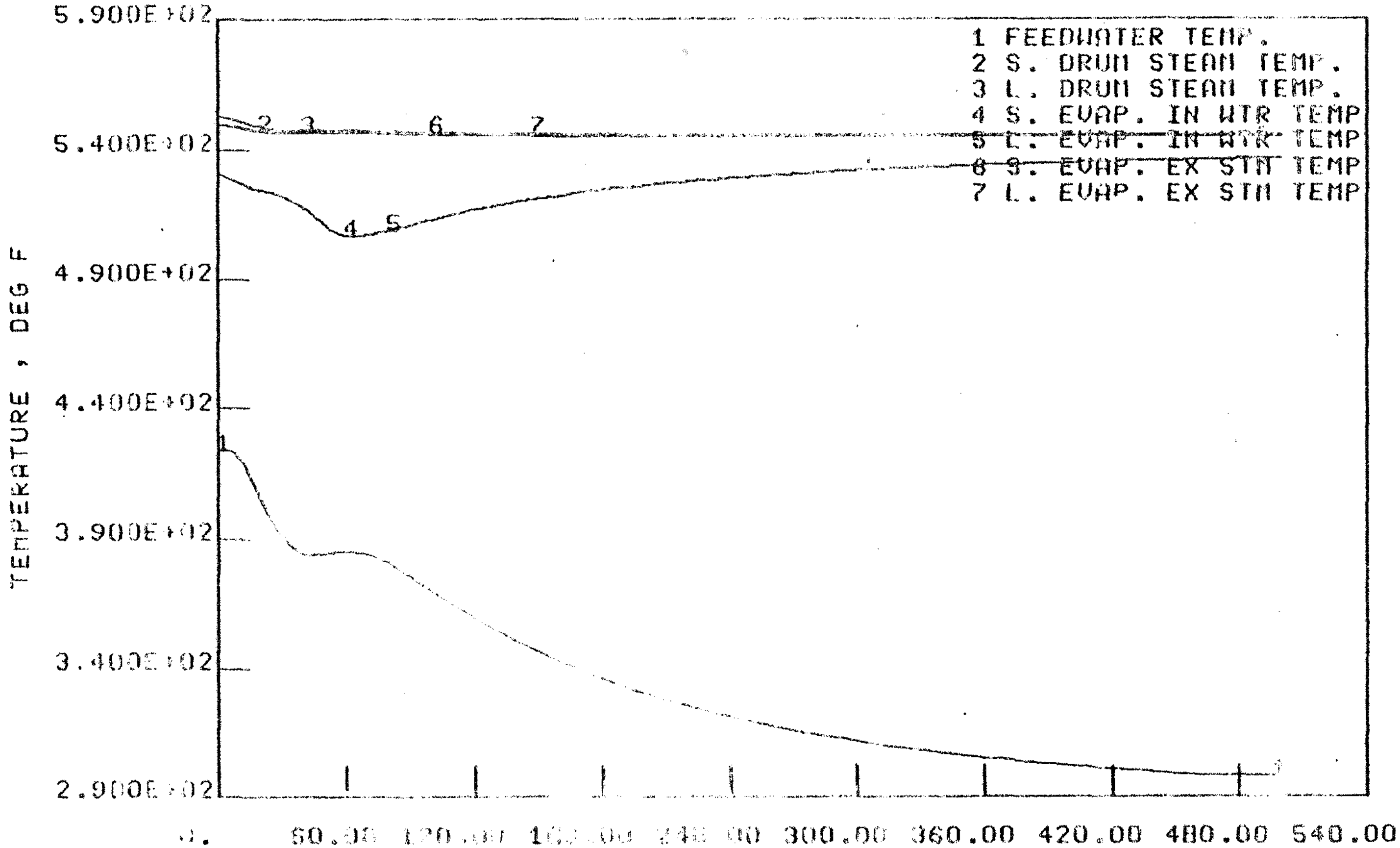

FIGURE 4-11
POOL REACTOR SCRAM FROM FULL POWER WITH NOMINAL DECAY HEAT
RUN DATED 10/04/78
NUMBER PAPGE00

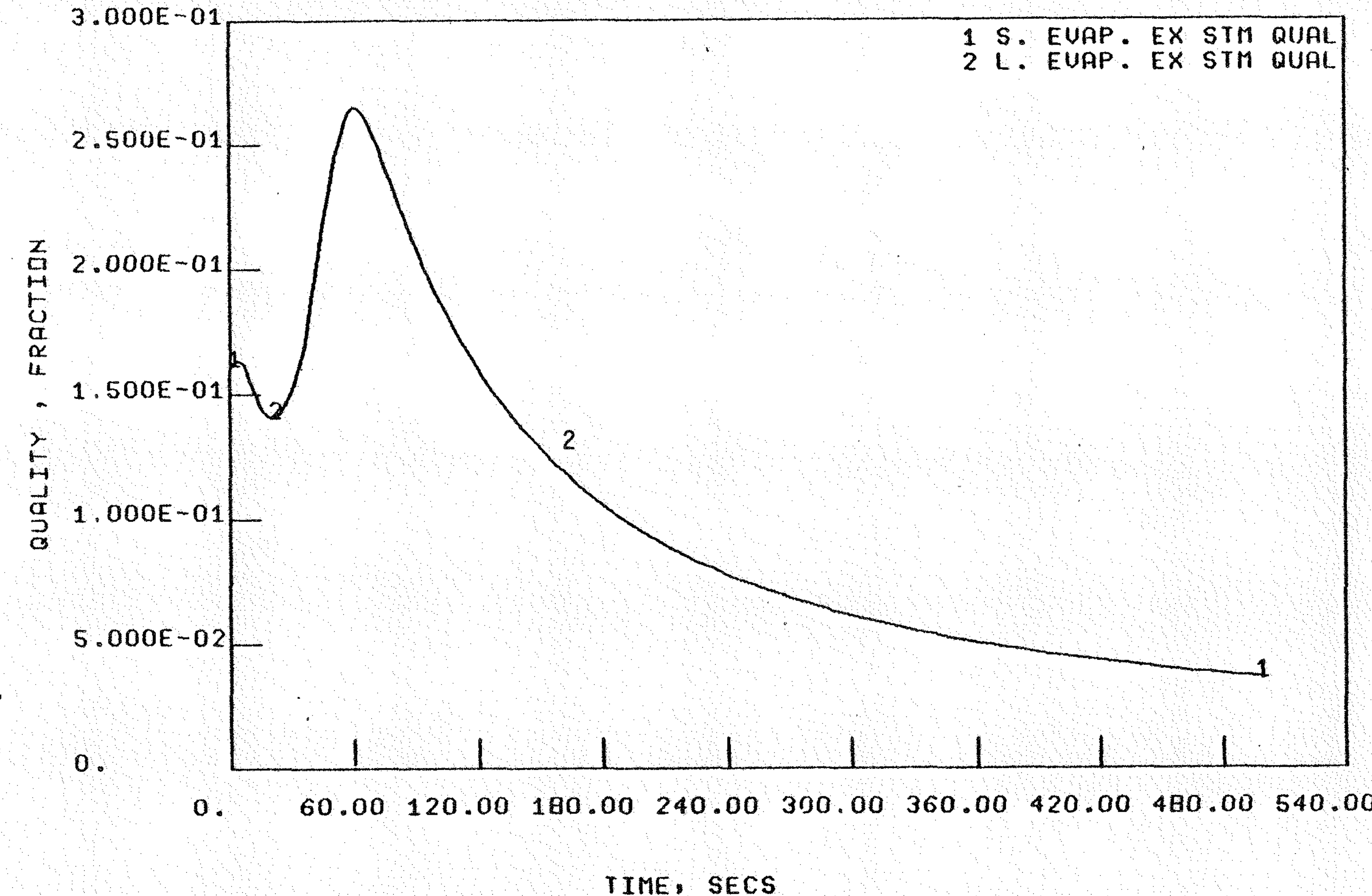

FIGURE 4-12
POOL REACTOR SCRAM FROM FULL POWER WITH NOMINAL DECAY HEAT
RUN DATED 10/04/78
NUMBER PAPGE00

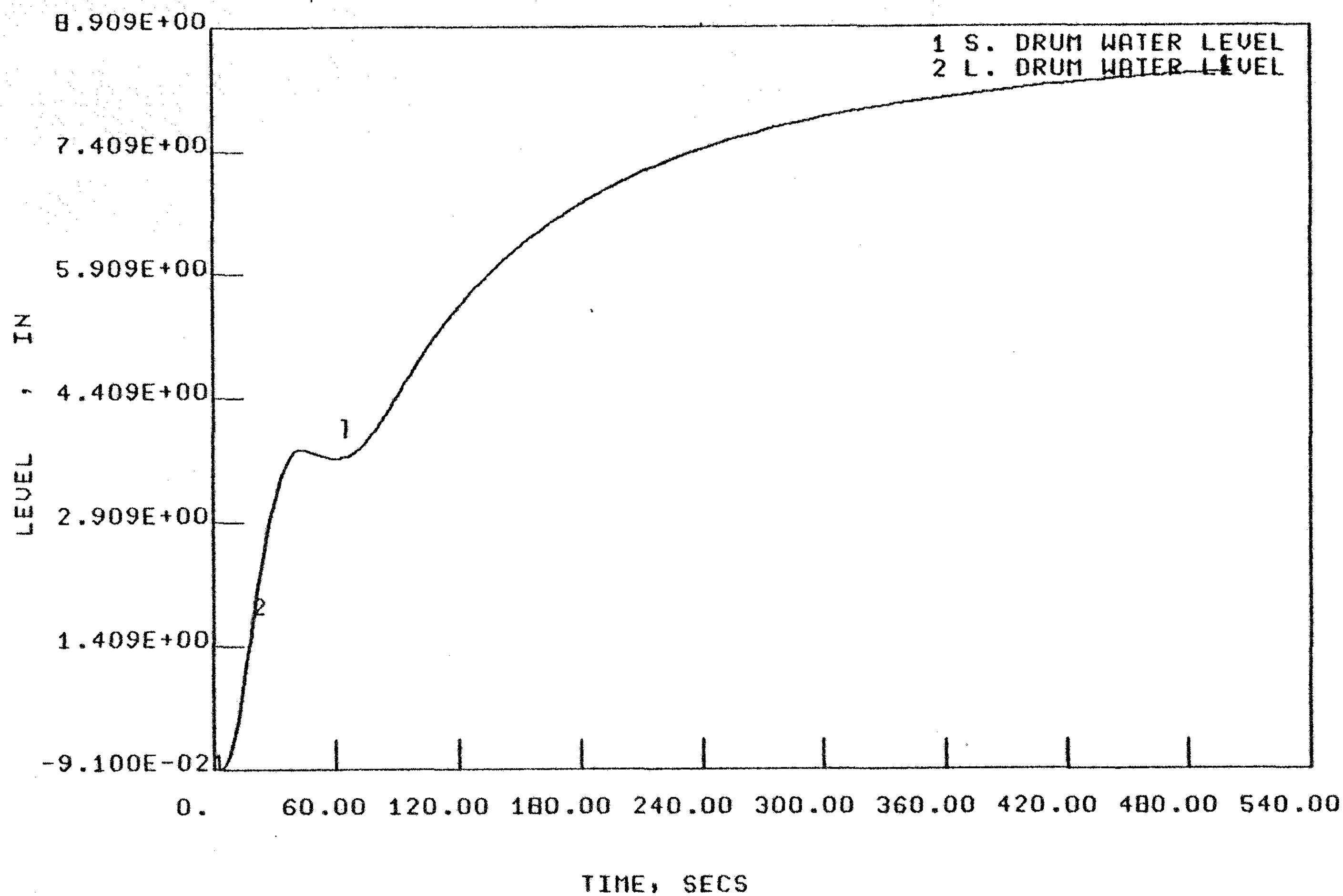

FIGURE 4-13
POOL REACTOR SCRAM WITH 50 PERCENT MIXING AND PUMP TRIP TO HALF SPEED
RUN DATED 04/03/78
NUMBER DEPGEOO

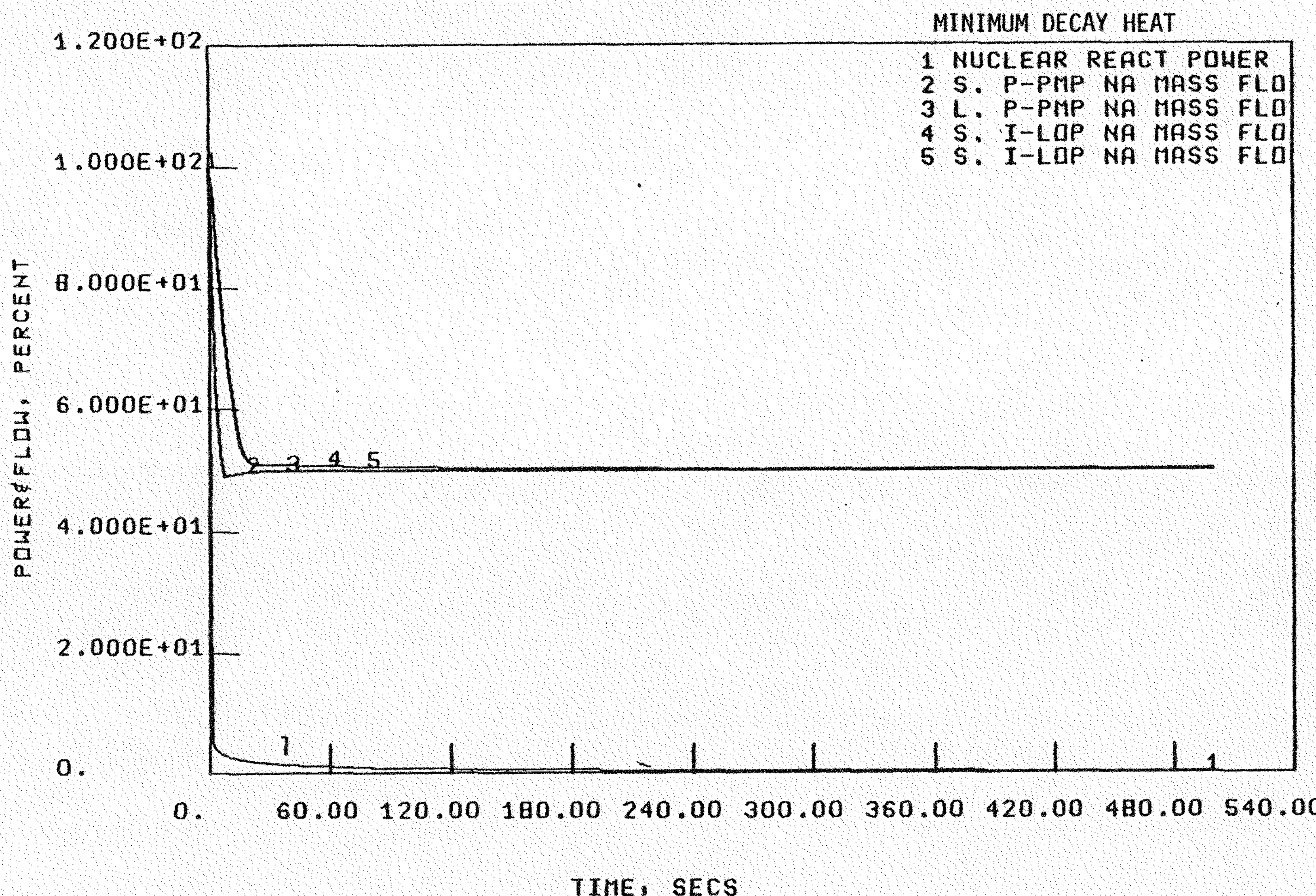

FIGURE 4-14
POOL REACTOR SCRAM WITH 50 PERCENT MIXING AND PUMP TRIP TO HALF SPEED
RUN DATED 04/03/78
NUMBER DEPGE00

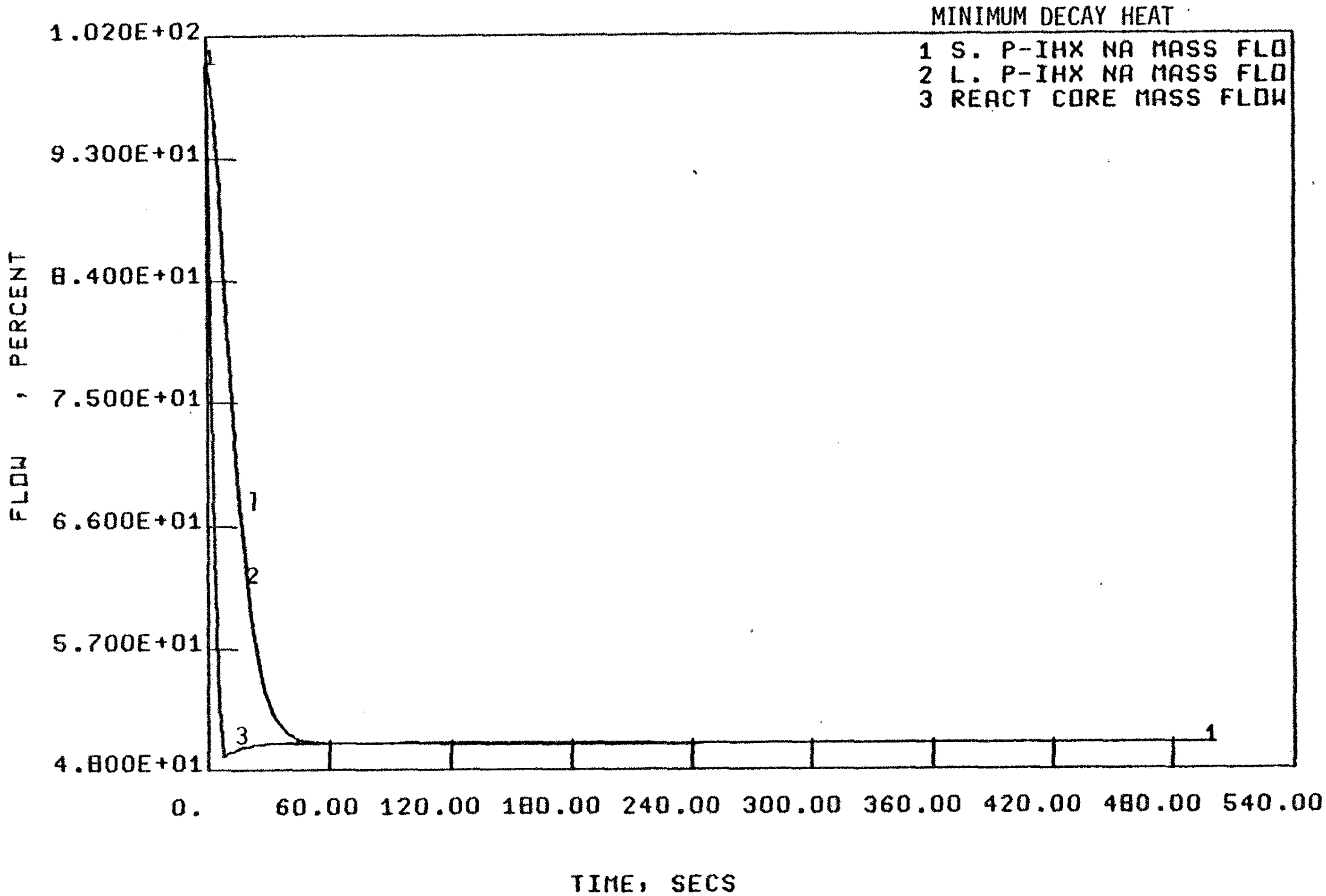

FIGURE 4-15

POOL REACTOR SCRAM WITH 50 PERCENT MIXING AND PUMP TRIP TO HALF SPEED

RUN DATED 04/03/78

NUMBER DEPGEOO

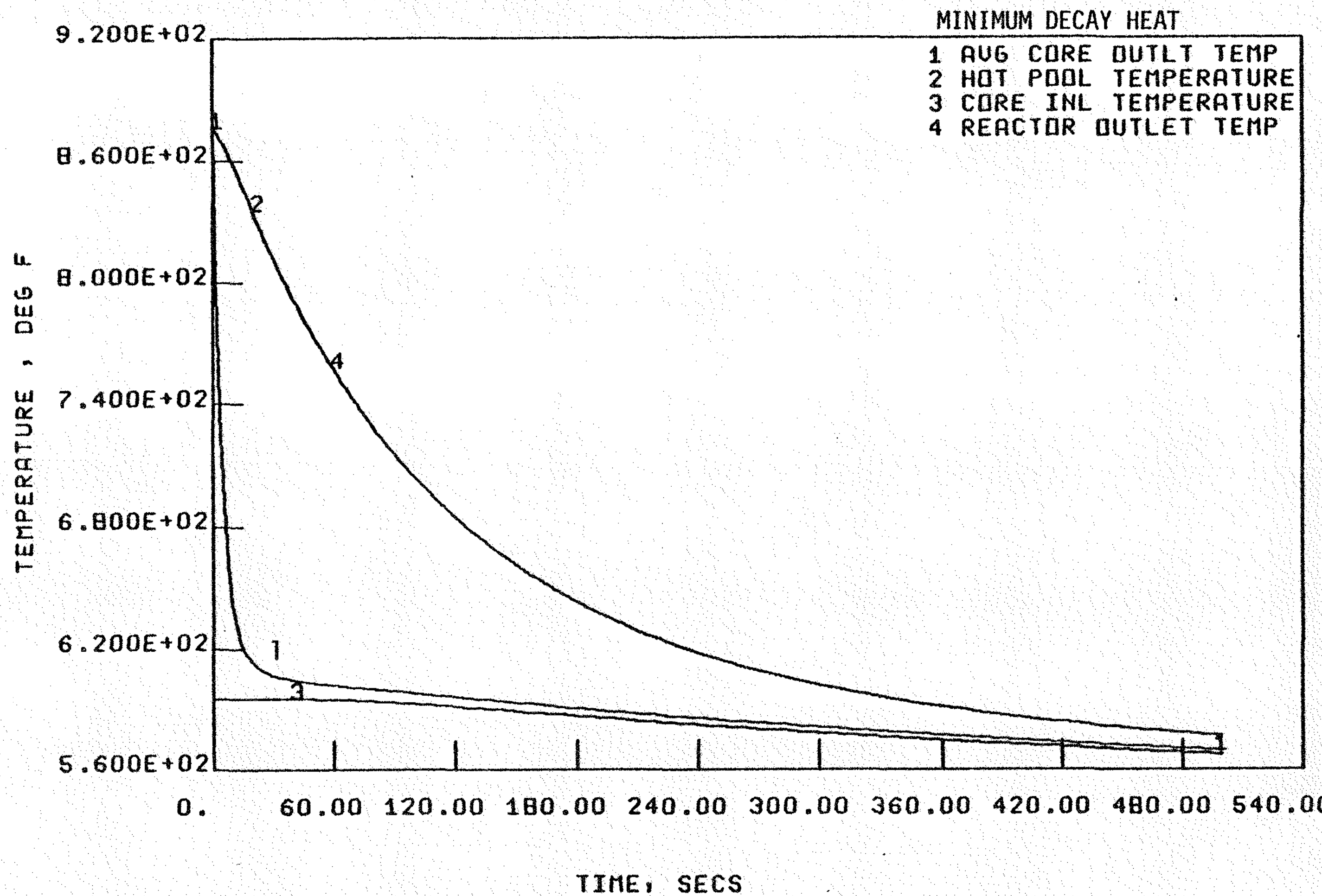

FIGURE 4-16
POOL REACTOR SCRAM WITH 50 PERCENT MIXING AND PUMP TRIP TO HALF SPEED
RUN DATED 04/03/78
NUMBER DEPGEOO

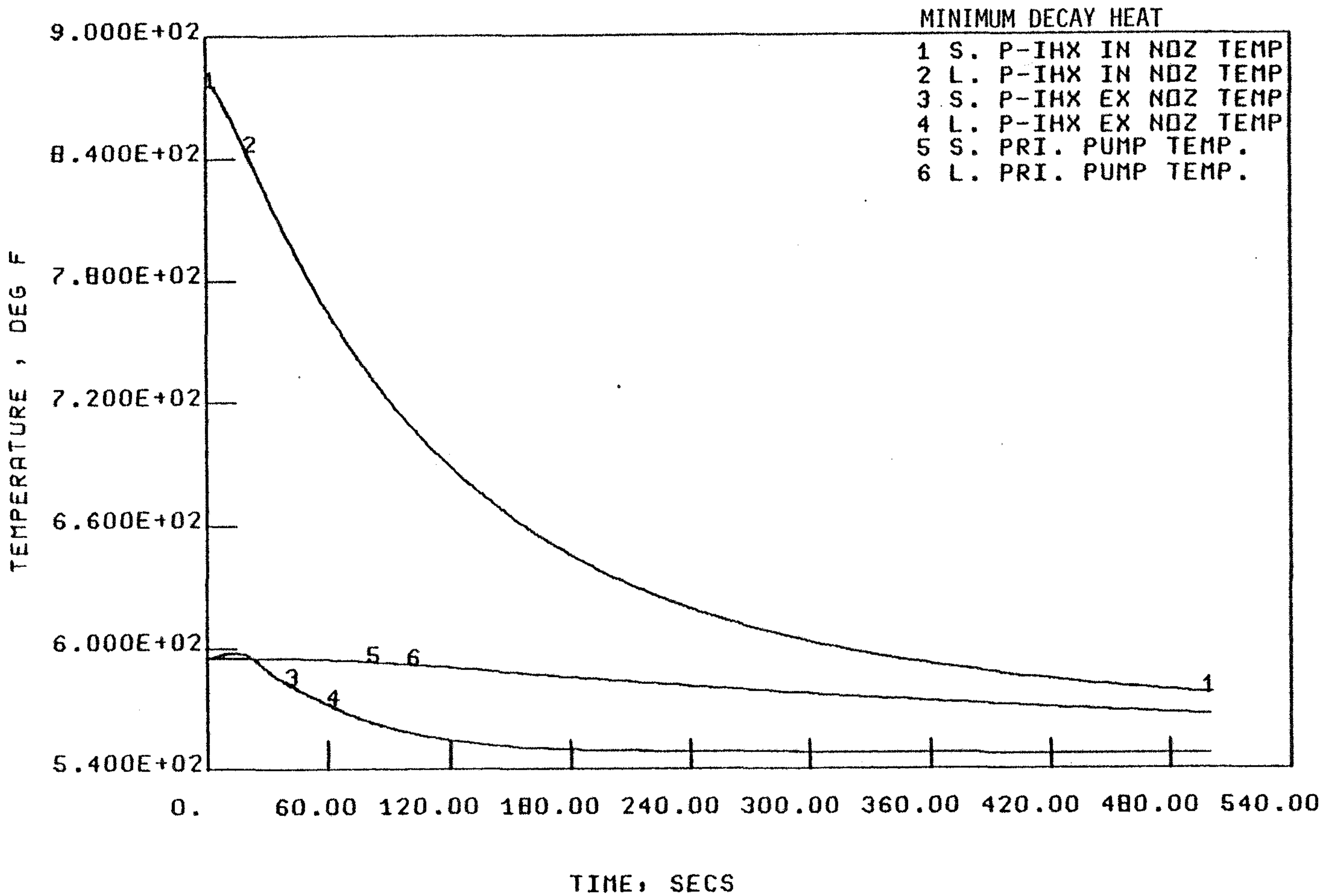

FIGURE 4-17
POOL REACTOR SCRAM WITH 50 PERCENT MIXING AND PUMP TRIP TO HALF SPEED
RUN DATED 04/03/78
NUMBER DEPGE00

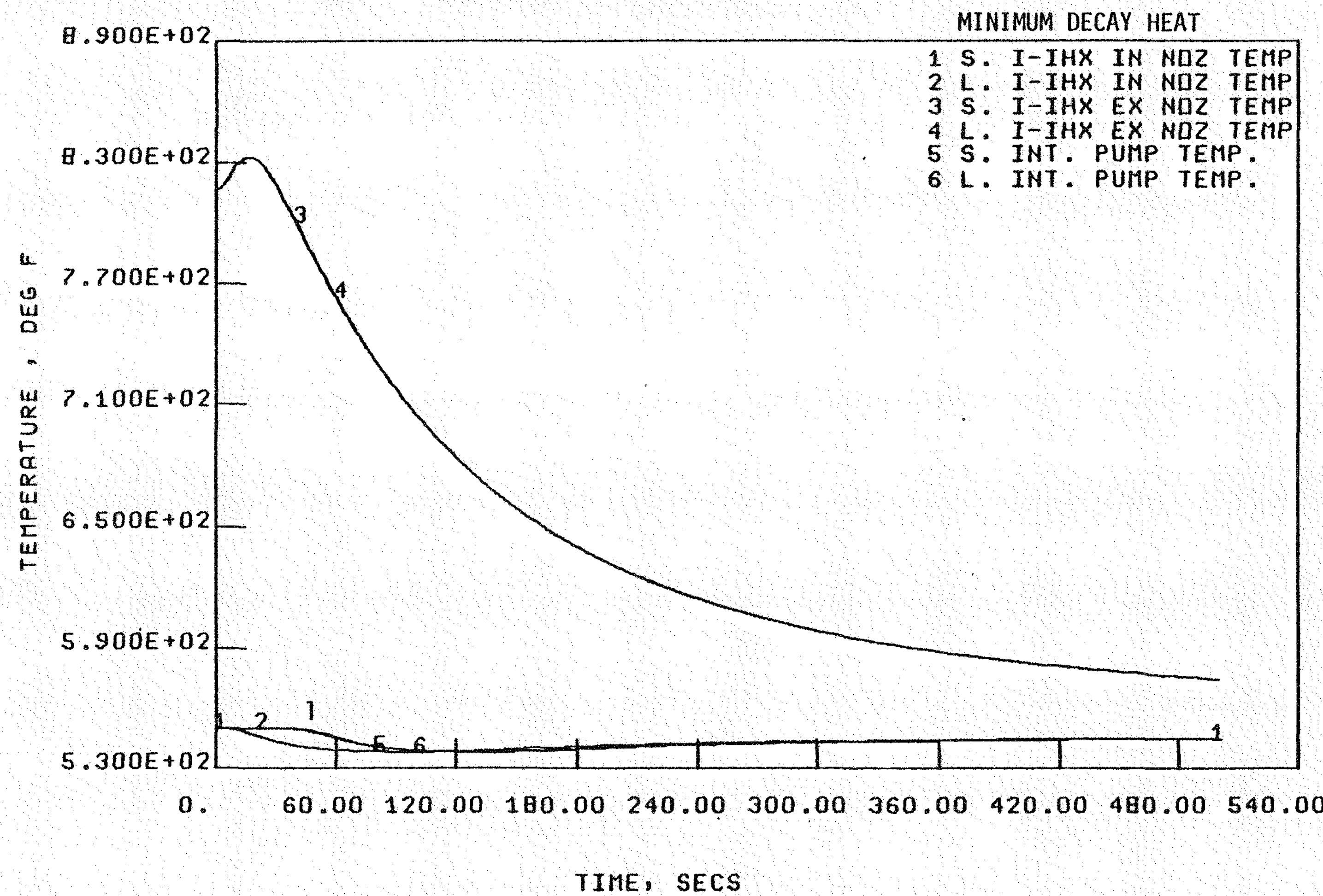

FIGURE 4-18
POOL REACTOR SCRAM WITH 50 PERCENT MIXING AND PUMP TRIP TO HALF SPEED
RUN DATED 04/03/78
NUMBER DEPGE00

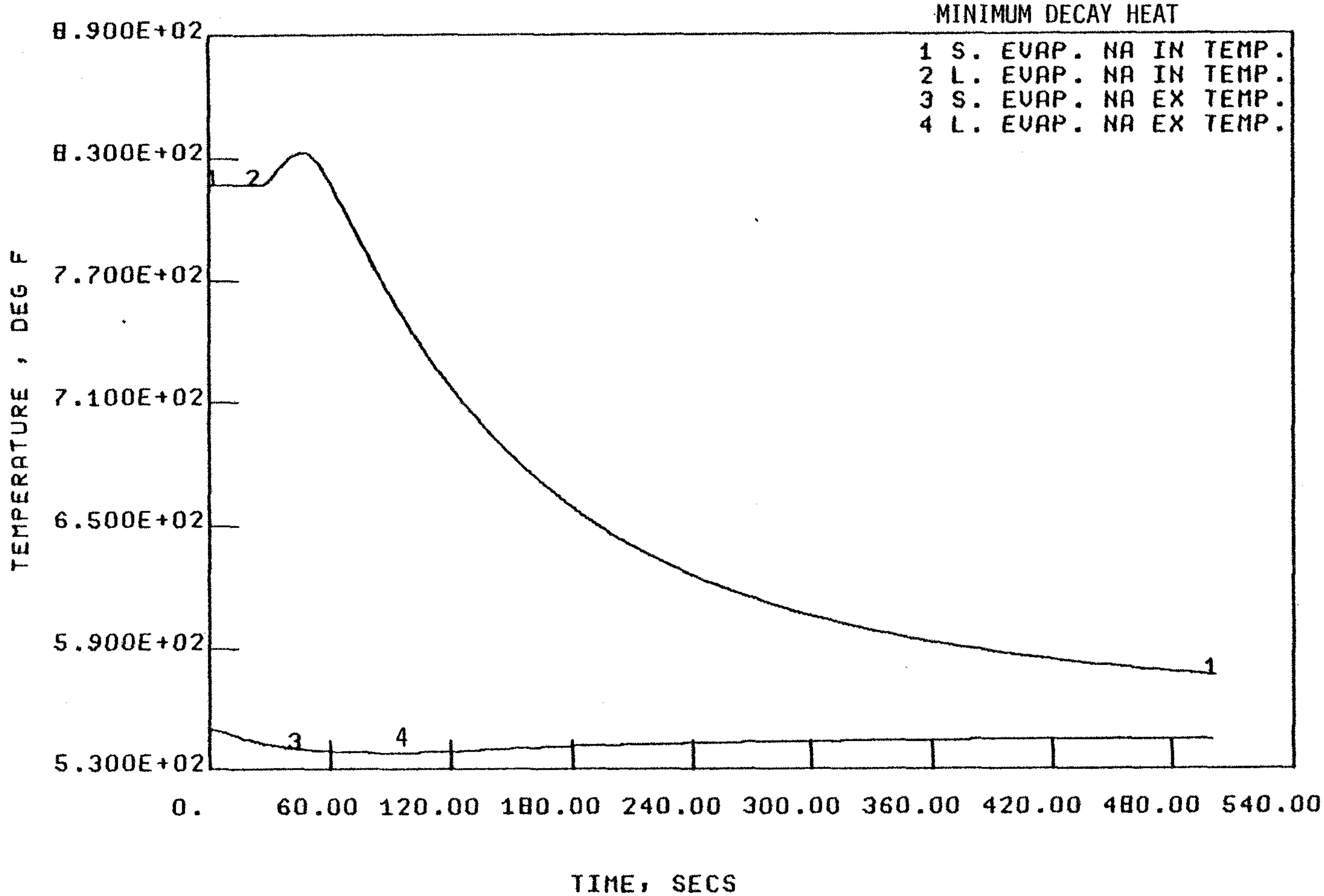

FIGURE 4-19
POOL REACTOR SCRAM WITH 50 PERCENT MIXING AND PUMP TRIP TO HALF SPEED
RUN DATED 04/03/78
NUMBER DEPGEOO

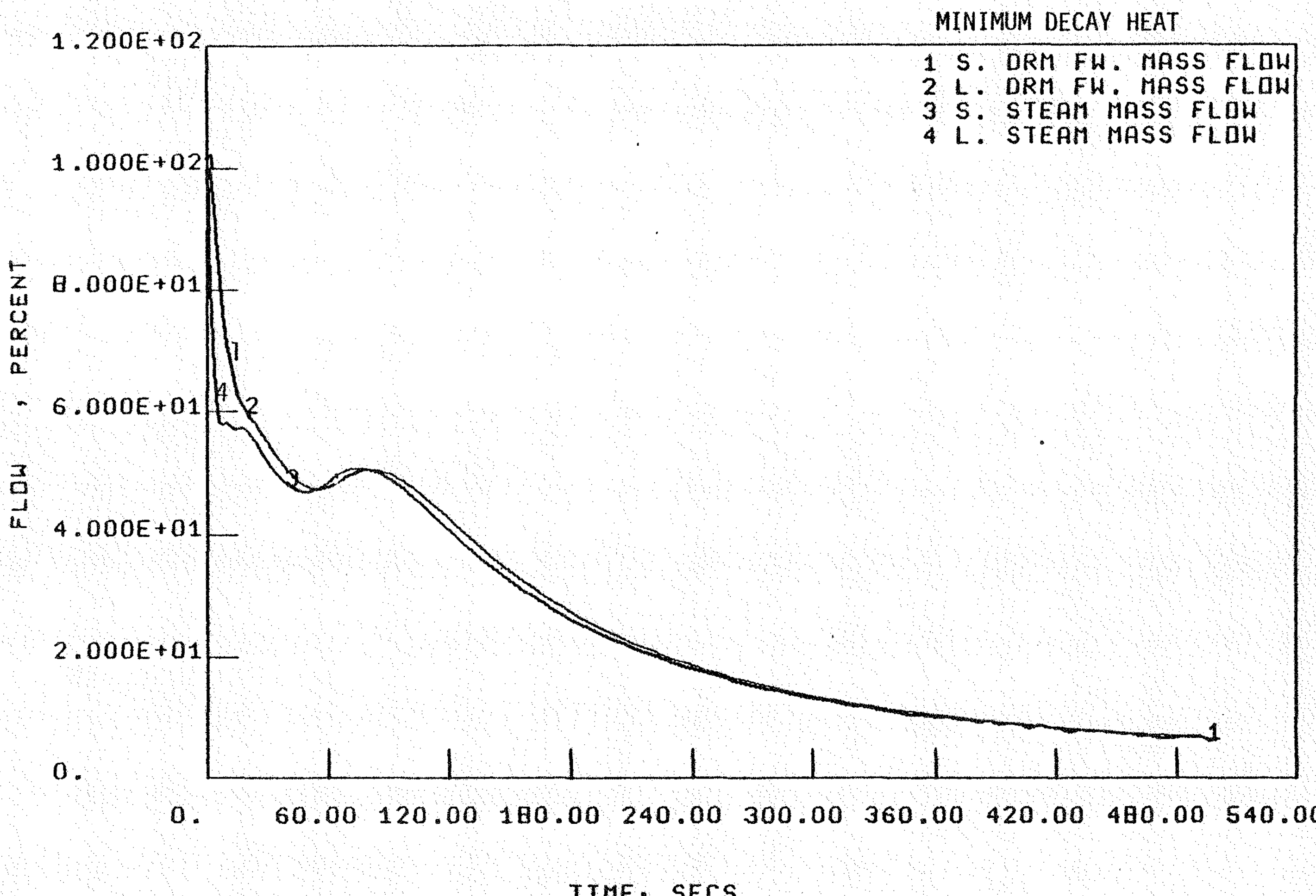

FIGURE 4-20
POOL REACTOR SCRAM WITH 50 PERCENT MIXING AND PUMP TRIP TO HALF SPEED
RUN DATED 04/03/78
NUMBER DEPGE00

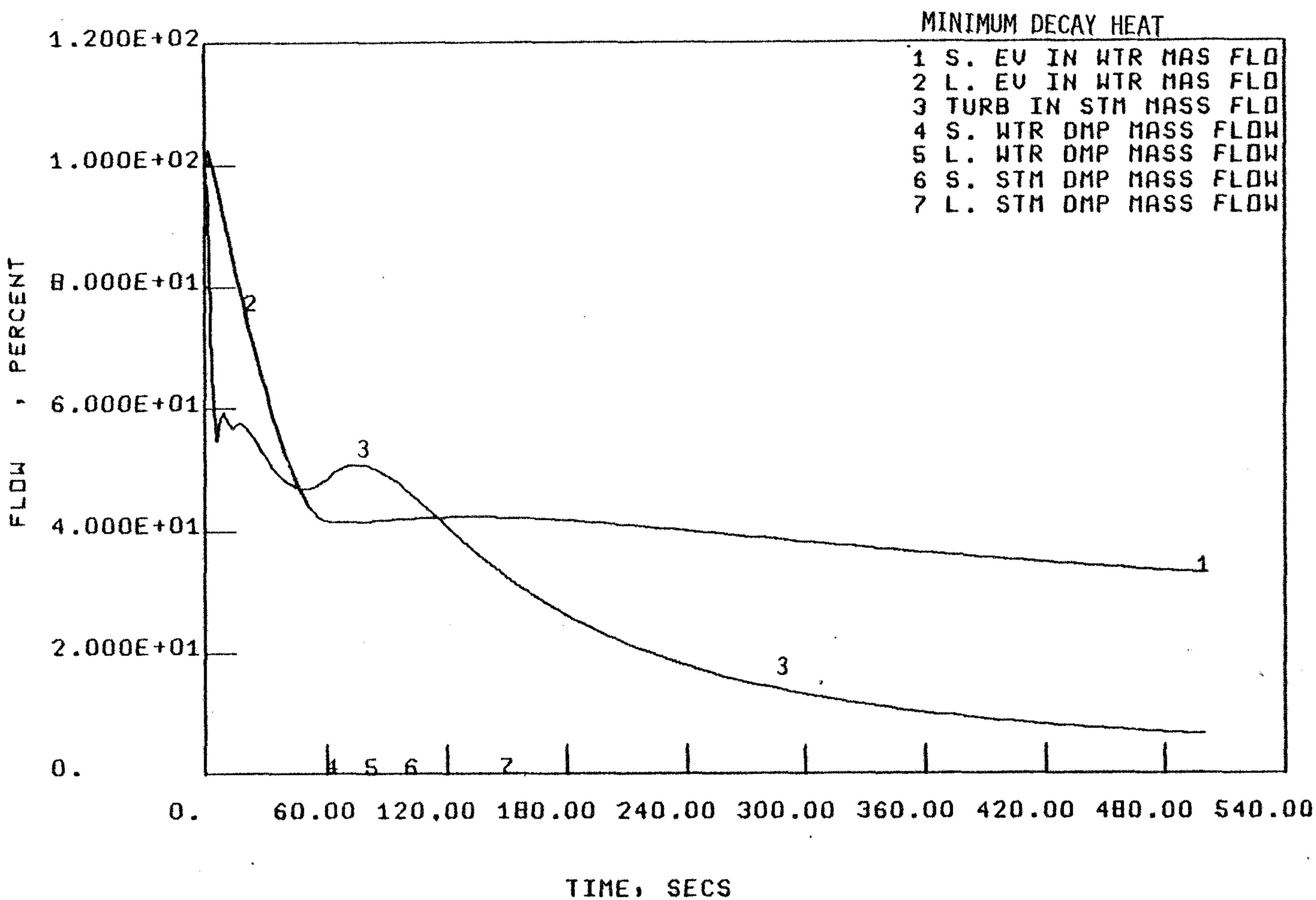

FIGURE 4-21

POOL REACTOR SCRAM WITH 50 PERCENT MIXING AND PUMP TRIP TO HALF SPEED

RUN DATED 04/03/78

NUMBER DEPGEOO

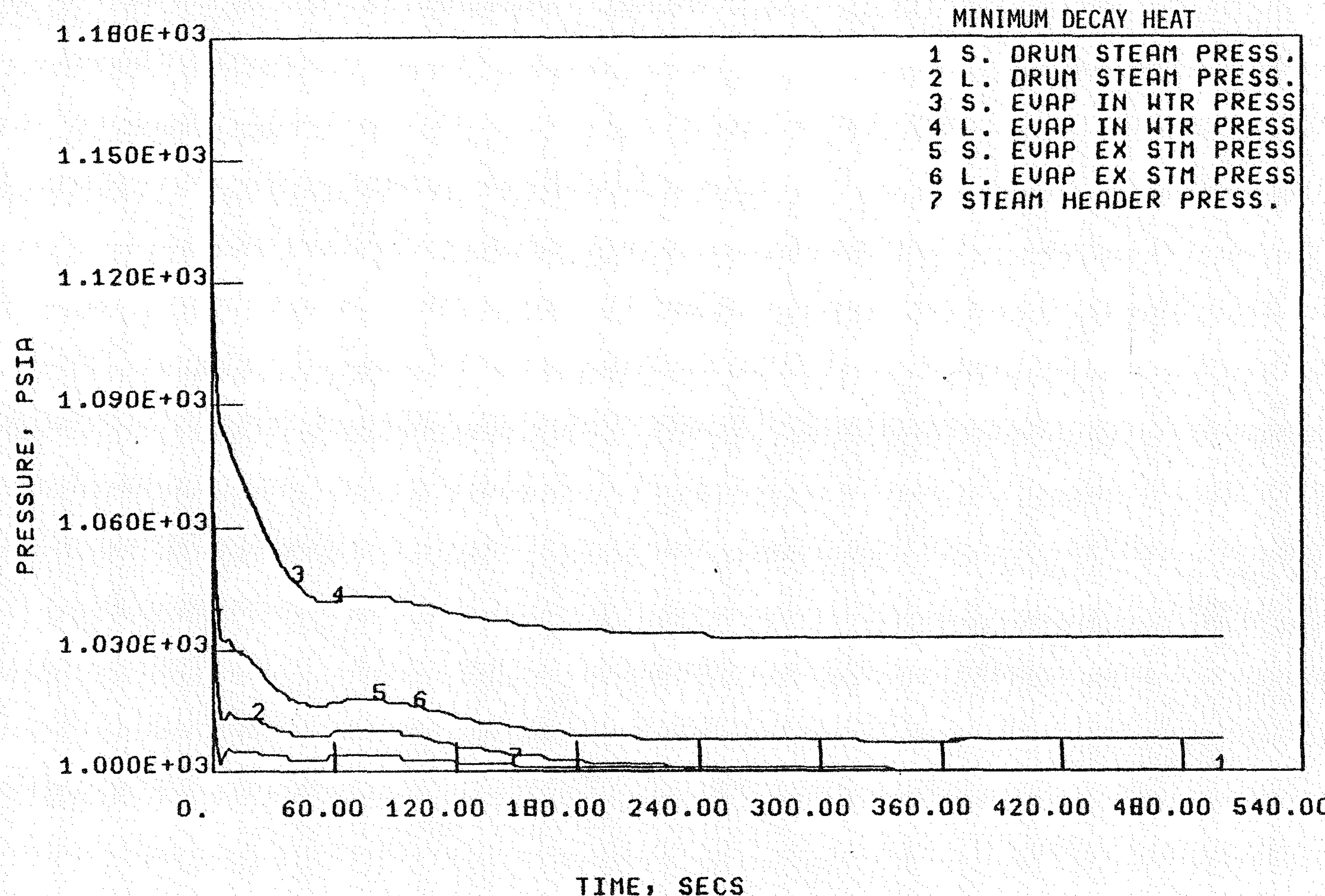

FIGURE 4-22
POOL REACTOR SCRAM WITH 50 PERCENT MIXING AND PUMP TRIP TO HALF SPEED
RUN DATED 04/03/78
NUMBER DEP6E00

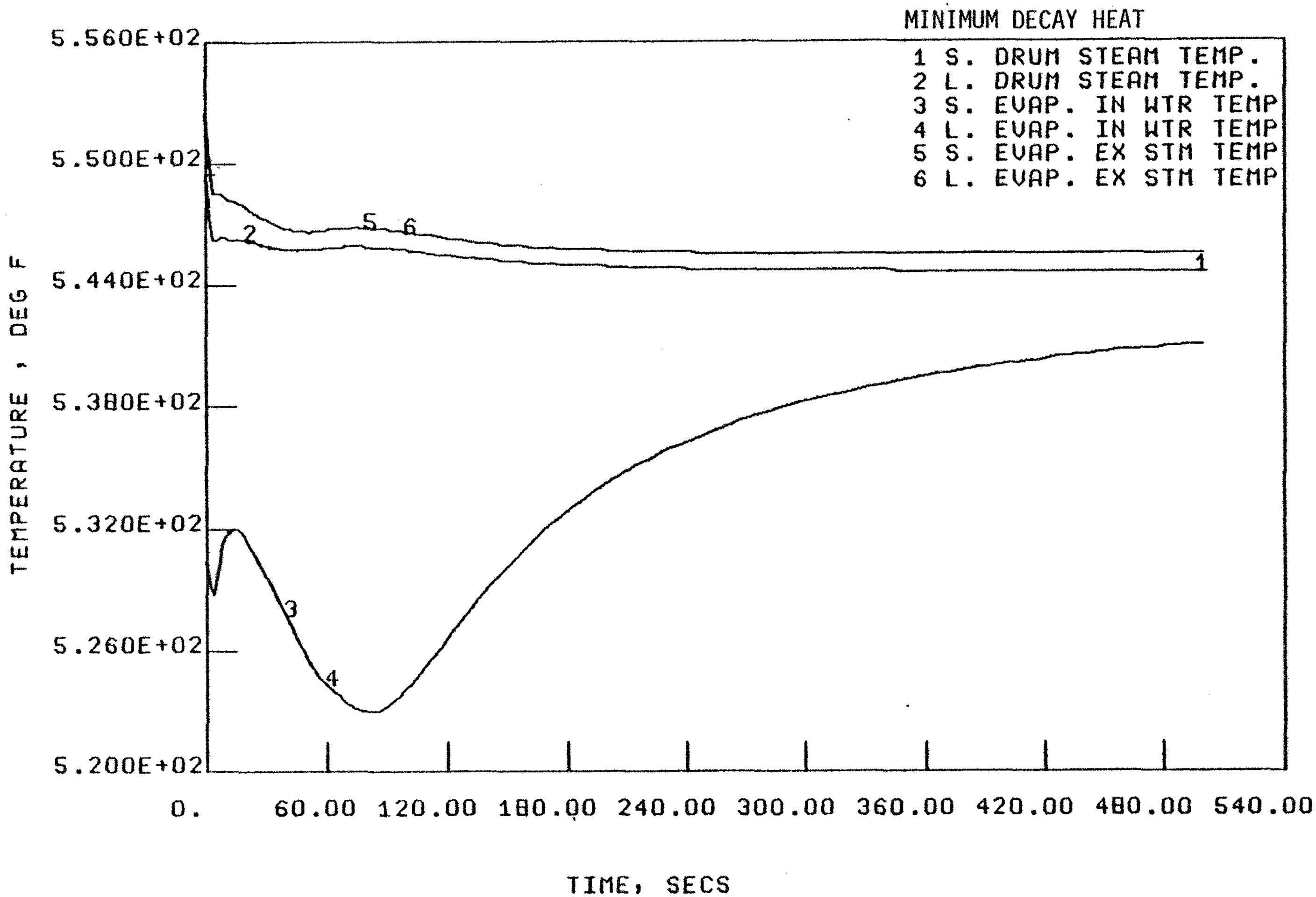

FIGURE 4-23

POOL REACTOR SCRAM WITH 50 PERCENT MIXING AND PUMP TRIP TO HALF SPEED
RUN DATED 04/03/78
NUMBER DEPGEOO

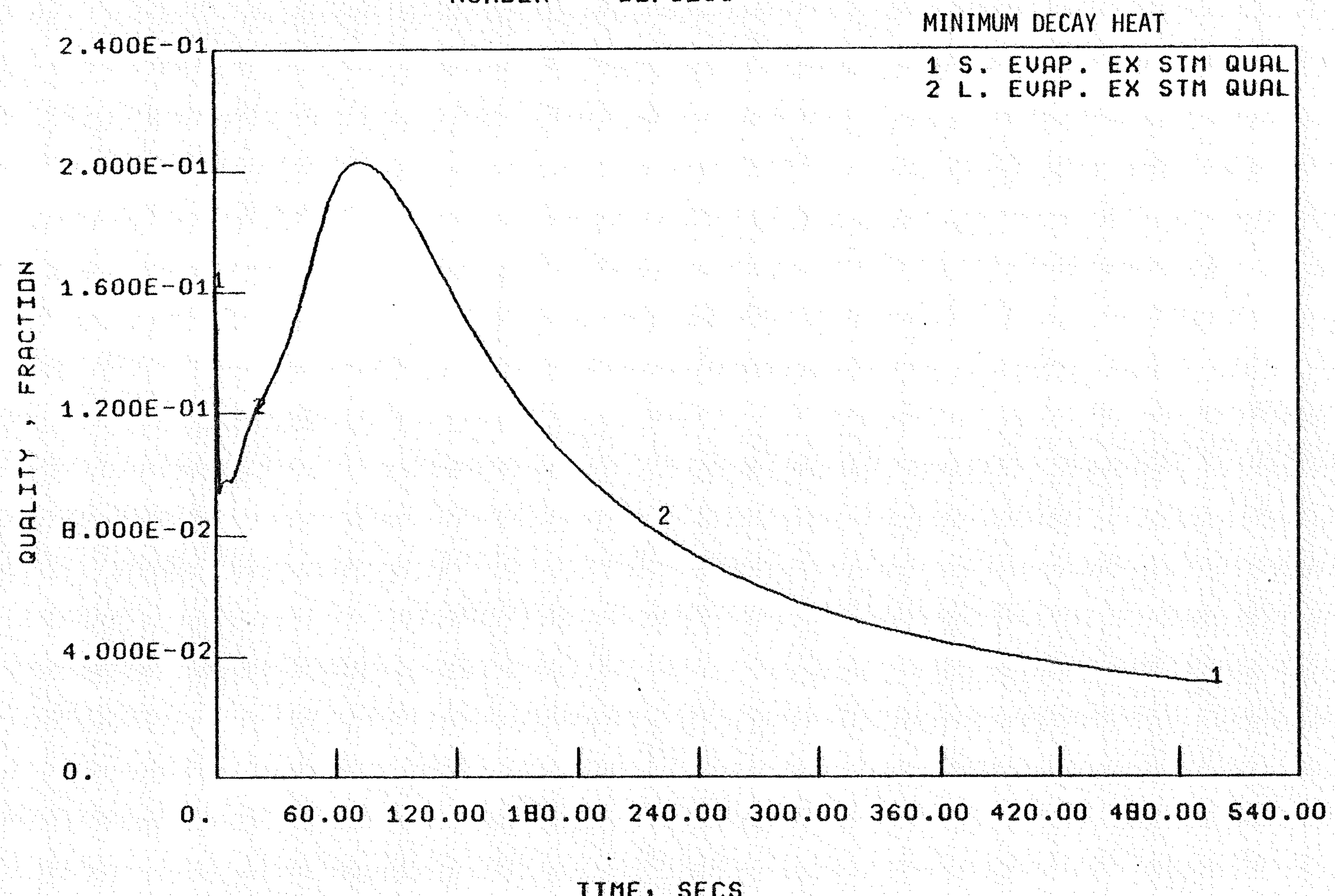

FIGURE 4-24

POOL REACTOR SCRAM WITH 50 PERCENT MIXING AND PUMP TRIP TO HALF SPEED
RUN DATED 04/03/78
NUMBER DEPGE00

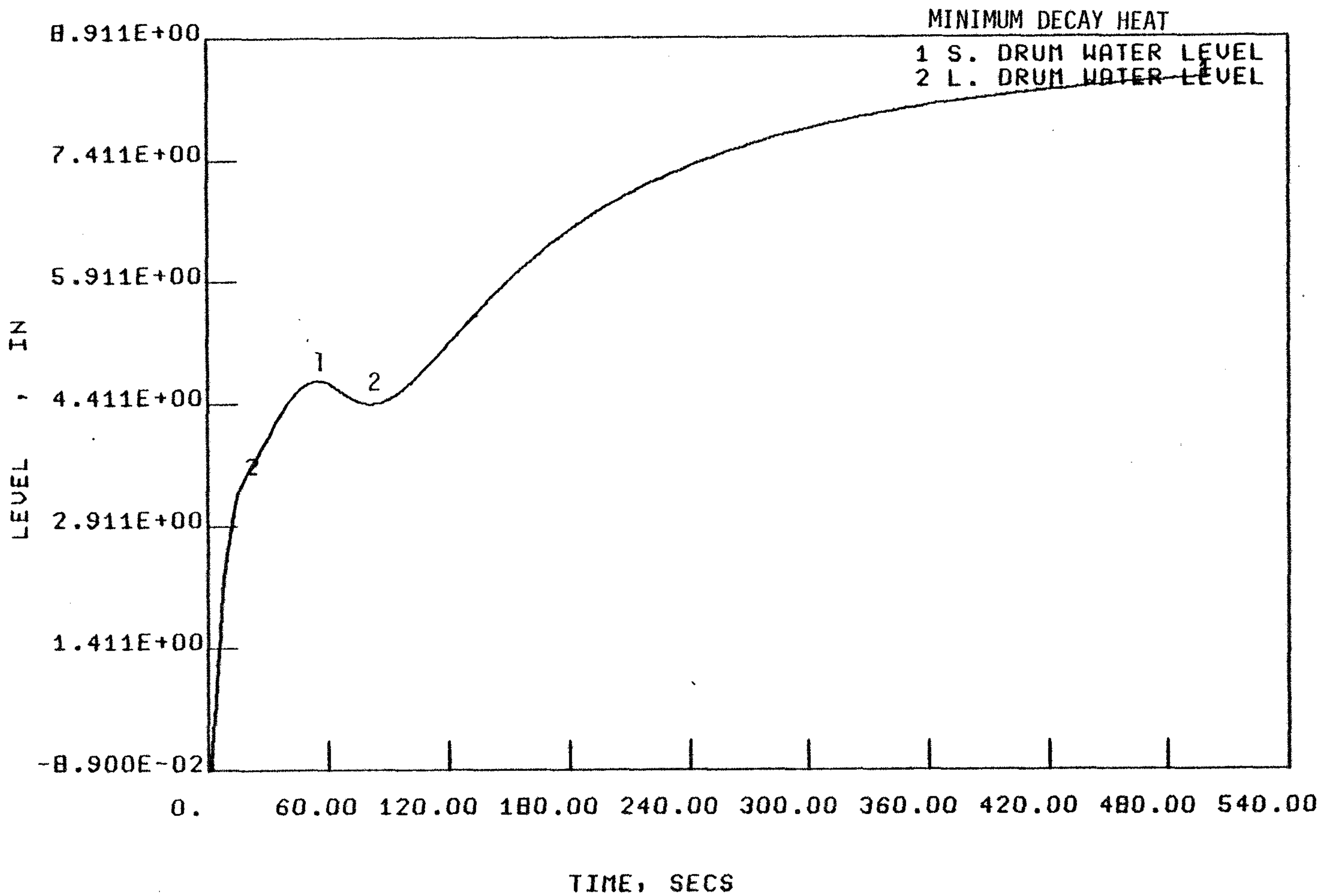

FIGURE 4-25

POOL REACTOR UNCONTROLLED ROD INSERTION WITH DELAYED MANUAL SCRAM
RUN DATED 10/06/78
NUMBER PAPGE05

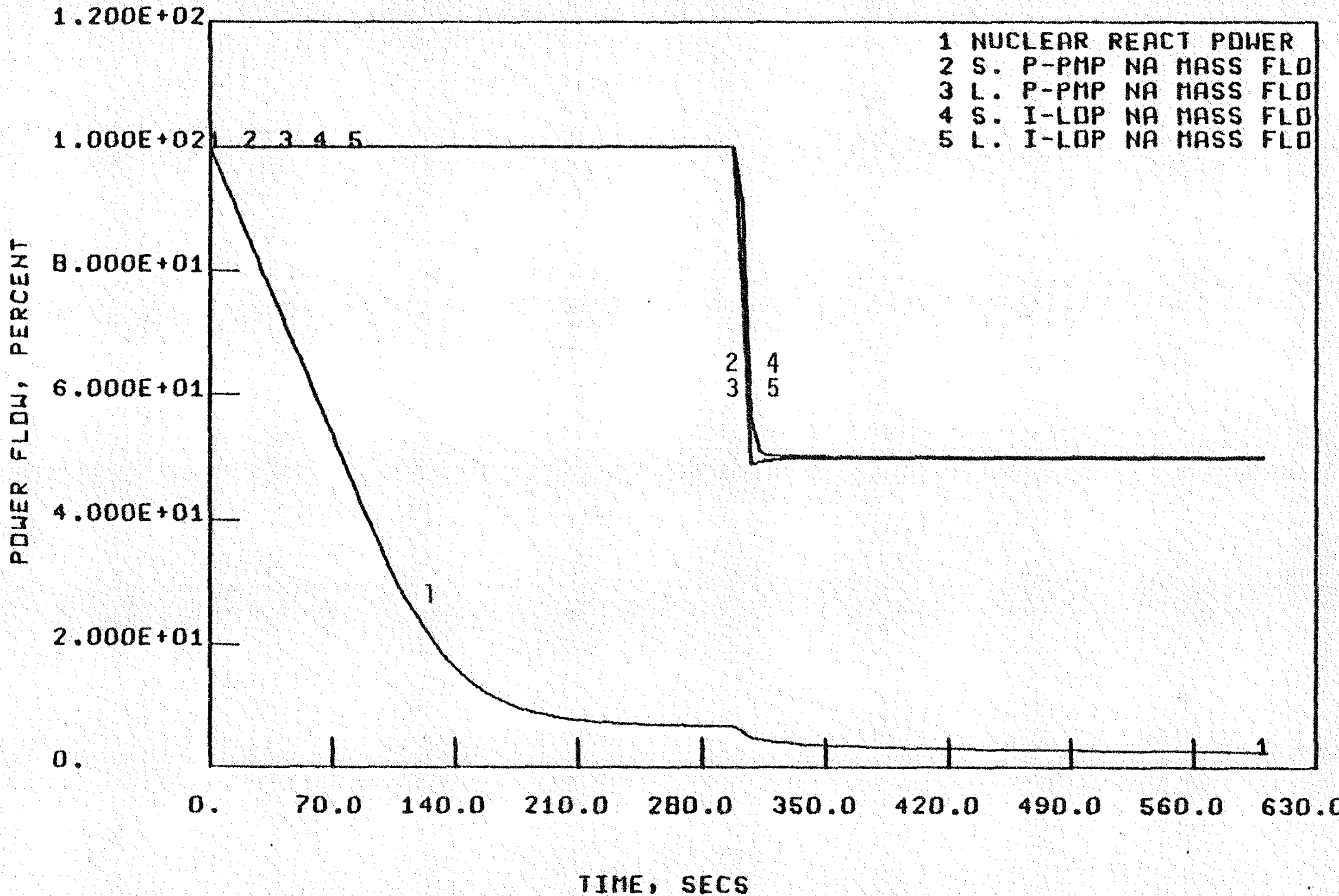

FIGURE 4-26
POOL REACTOR UNCONTROLLED ROD INSERTION WITH DELAYED MANUAL SCRAM
RUN DATED 10/06/78
NUMBER PAPGE05

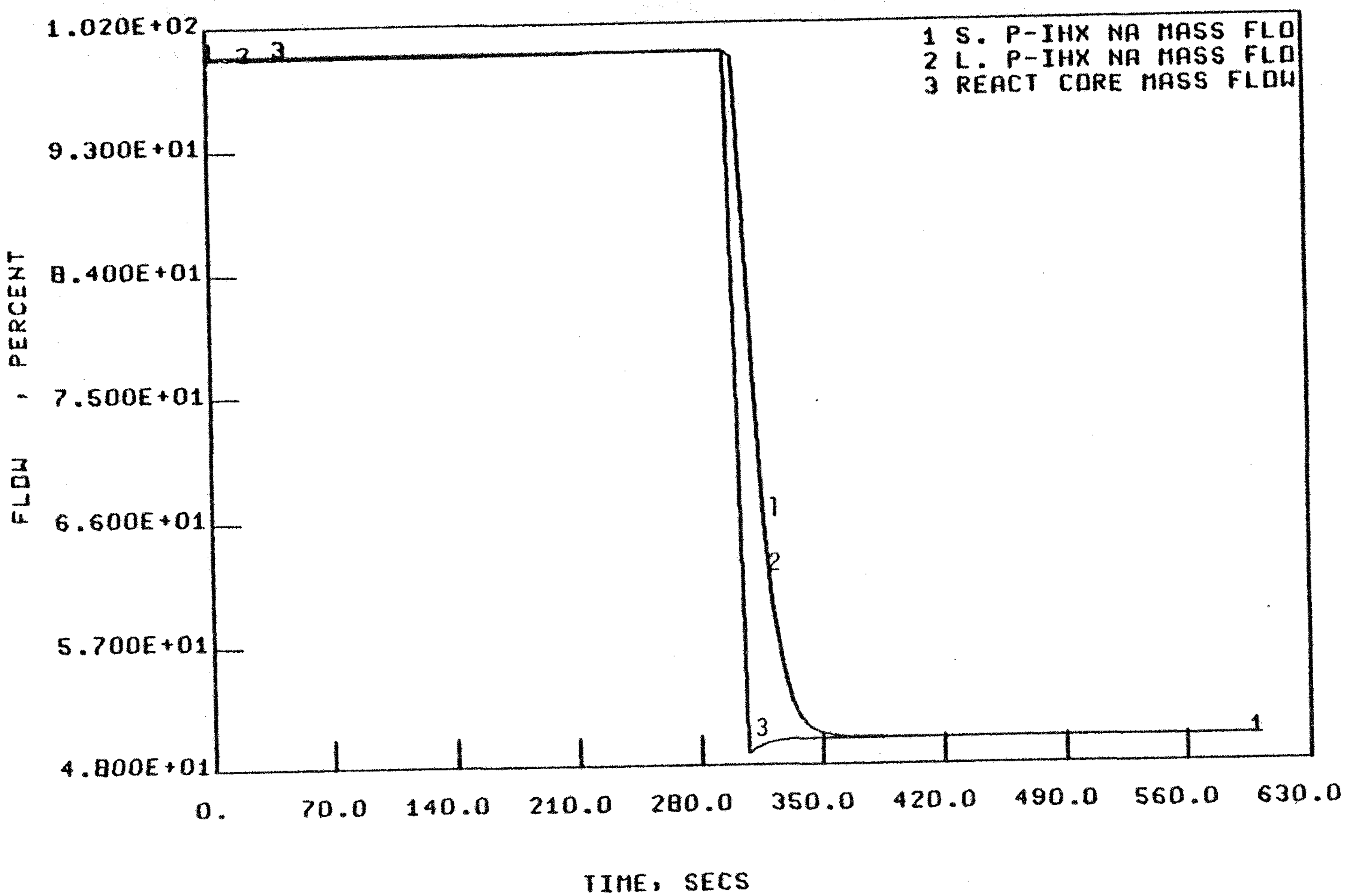

FIGURE 4-27

POOL REACTOR UNCONTROLLED ROD INSERTION WITH DELAYED MANUAL SCRAM

RUN DATED 10/06/78

NUMBER PAPGE05

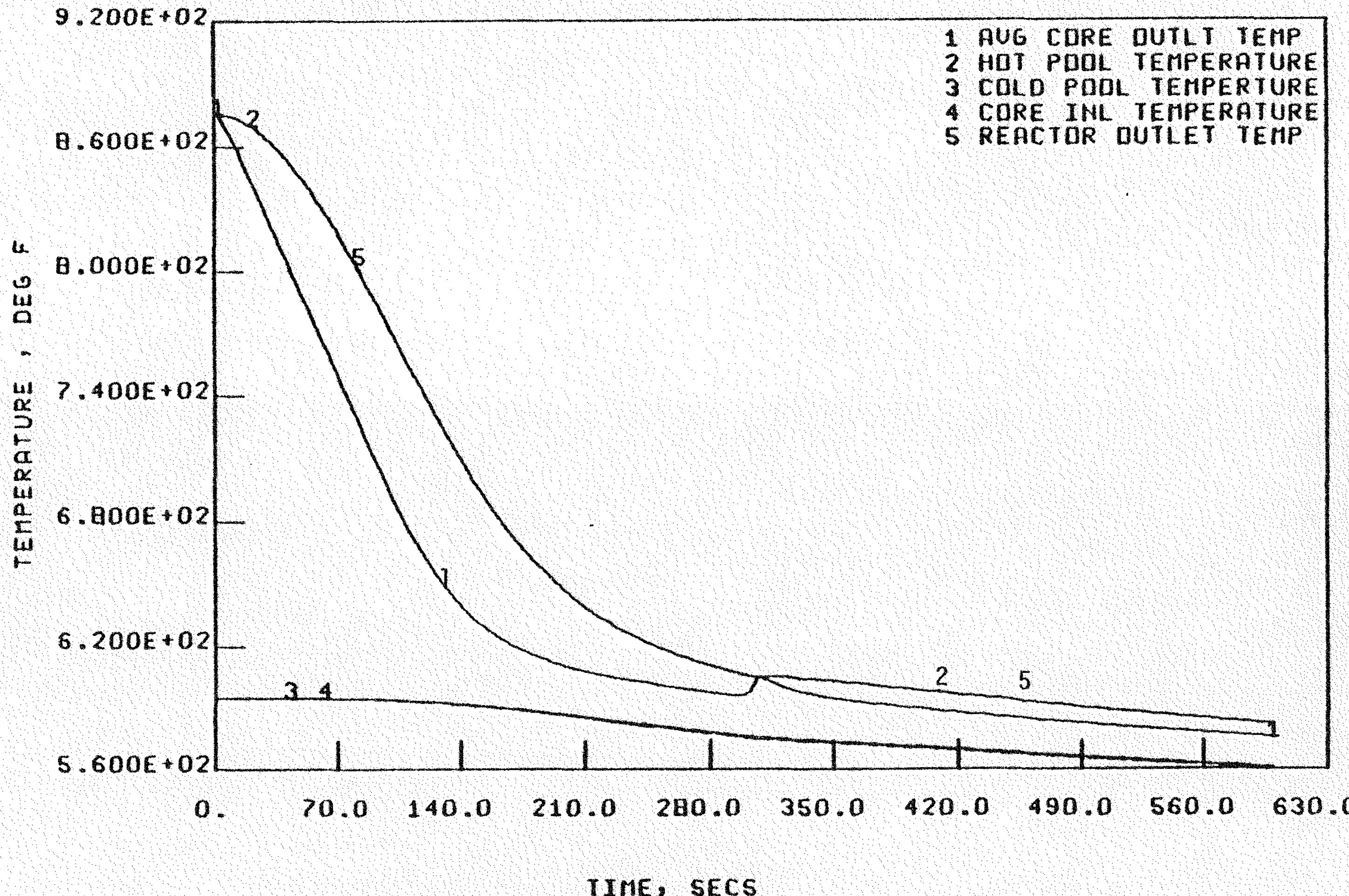

FIGURE 4-28

POOL REACTOR UNCONTROLLED ROD INSERTION WITH DELAYED MANUAL SCRAM
RUN DATED 10/06/78
NUMBER PAPGE05

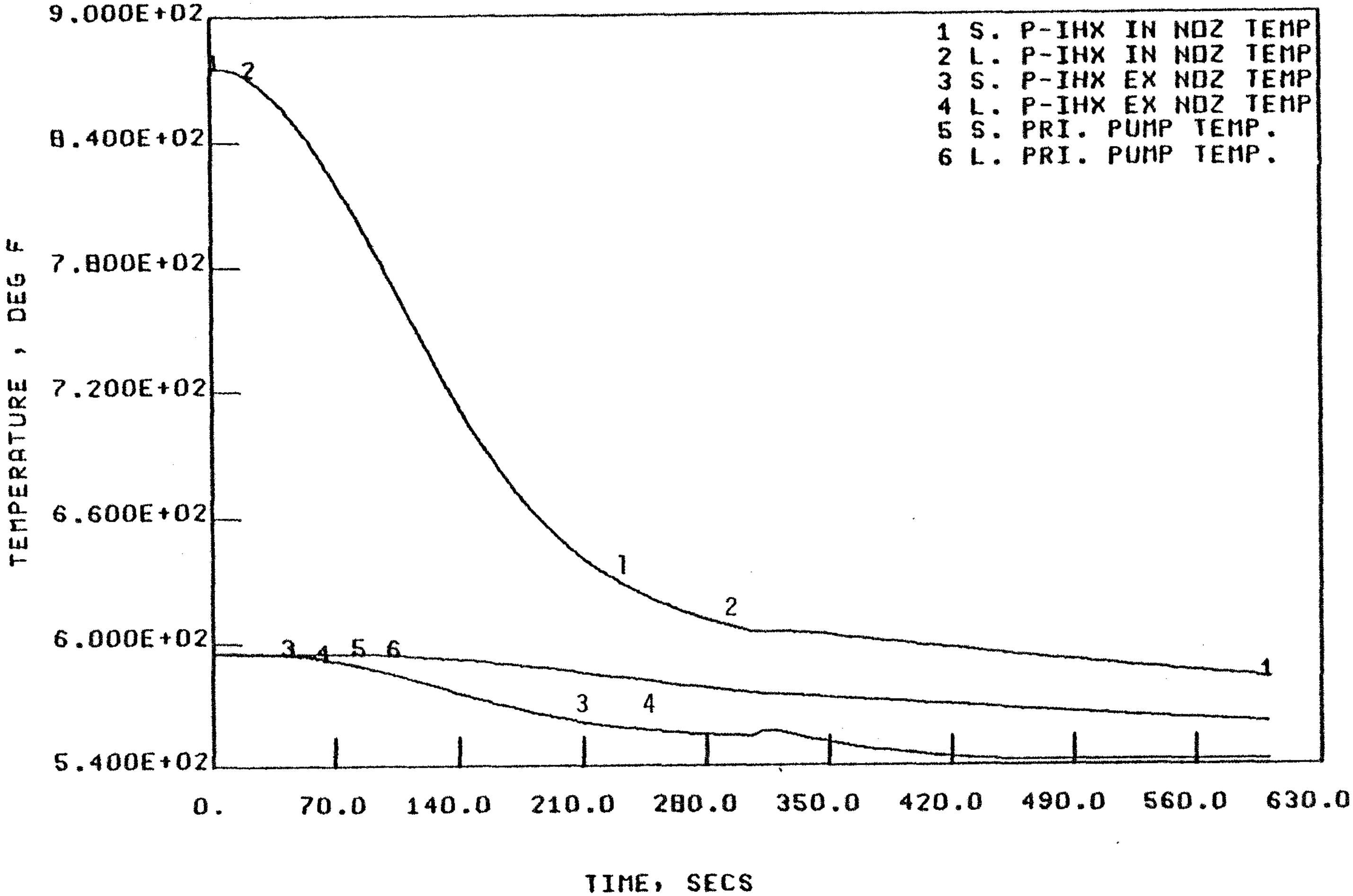

FIGURE 4-29

POOL REACTOR UNCONTROLLED ROD INSERTION WITH DELAYED MANUAL SCRAM

RUN DATED 10/06/78

NUMBER PAPGE05

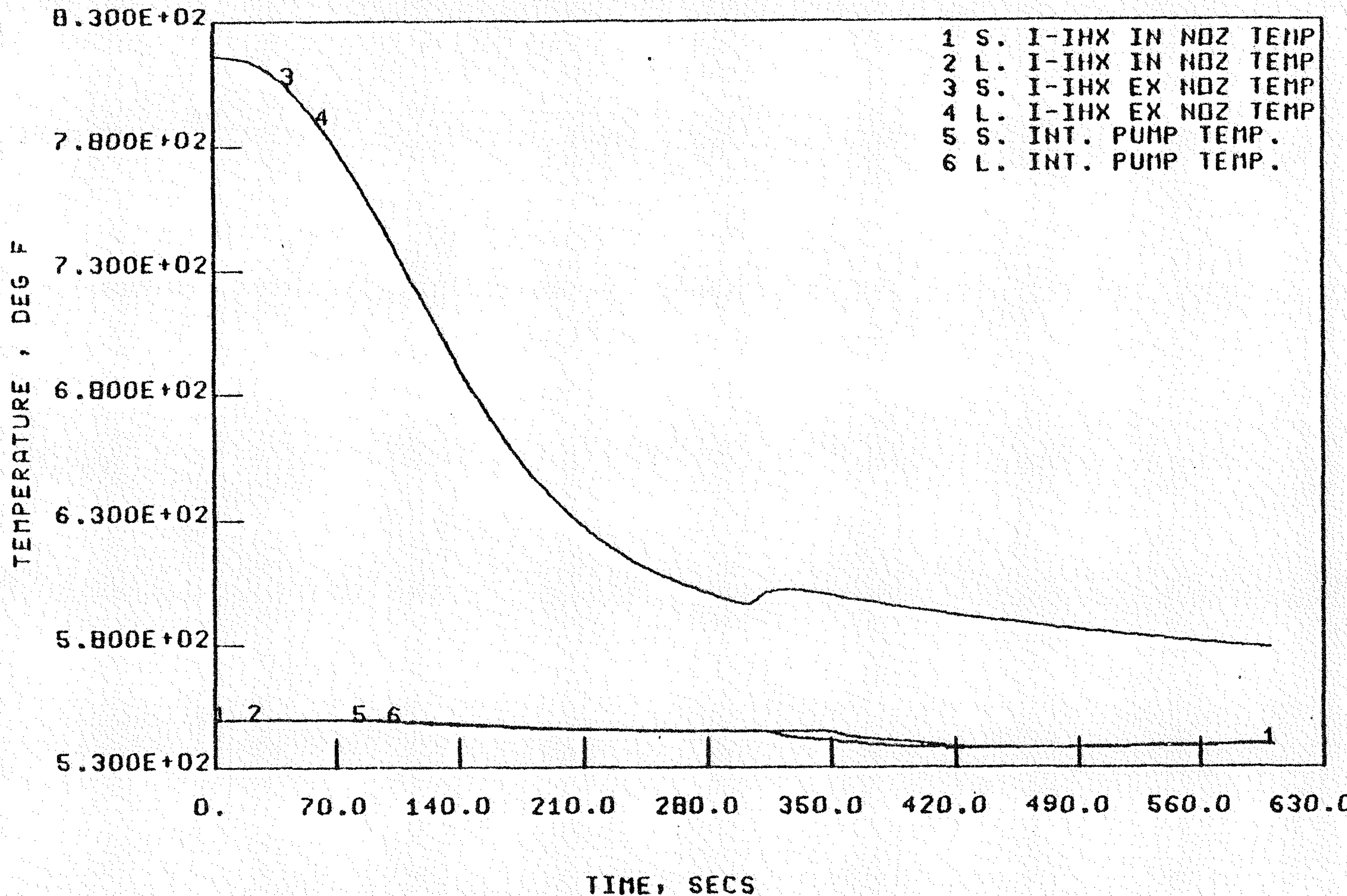

FIGURE 4-30

POOL REACTOR UNCONTROLLED ROD INSERTION WITH DELAYED MANUAL SCRAM
RUN DATED 10/06/78
NUMBER PAPGE05

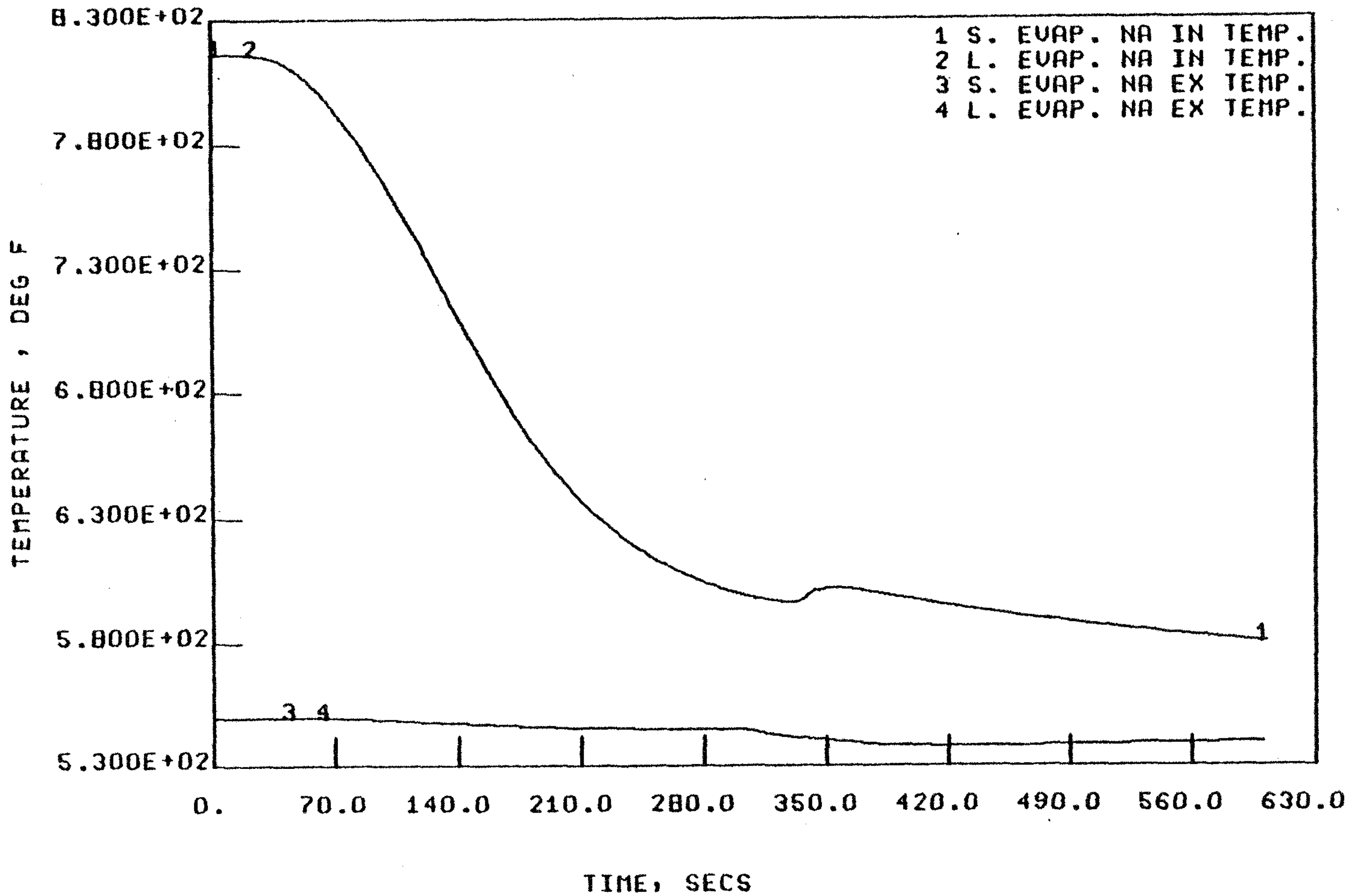

FIGURE 4-31
POOL REACTOR UNCONTROLLED ROD INSERTION WITH DELAYED MANUAL SCRAM
RUN DATED 10/06/78
NUMBER PAP6E05

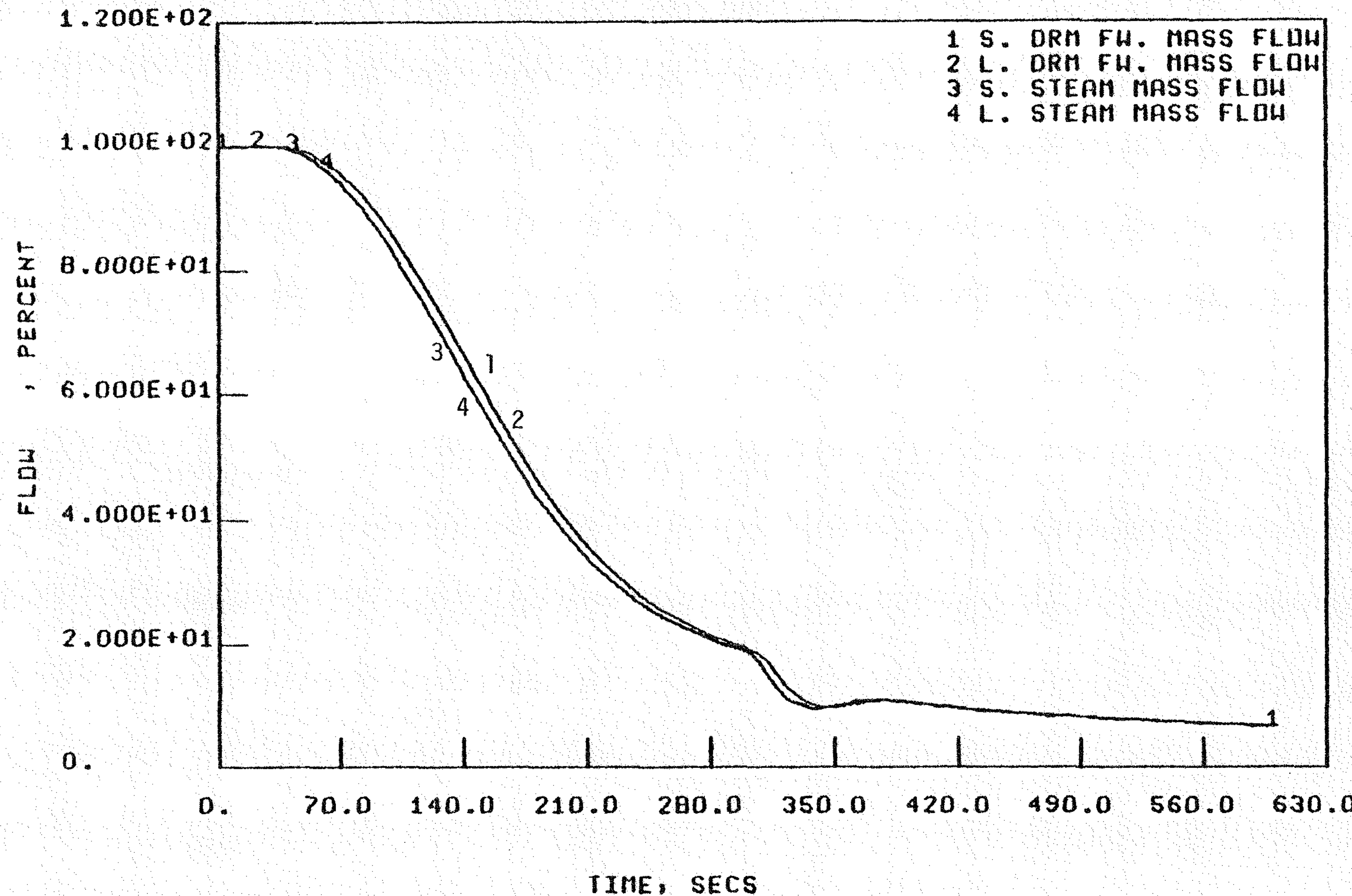

FIGURE 4-32

POOL REACTOR UNCONTROLLED ROD INSERTION WITH DELAYED MANUAL SCRAM

RUN DATED 10/06/78

NUMBER PAPGE05

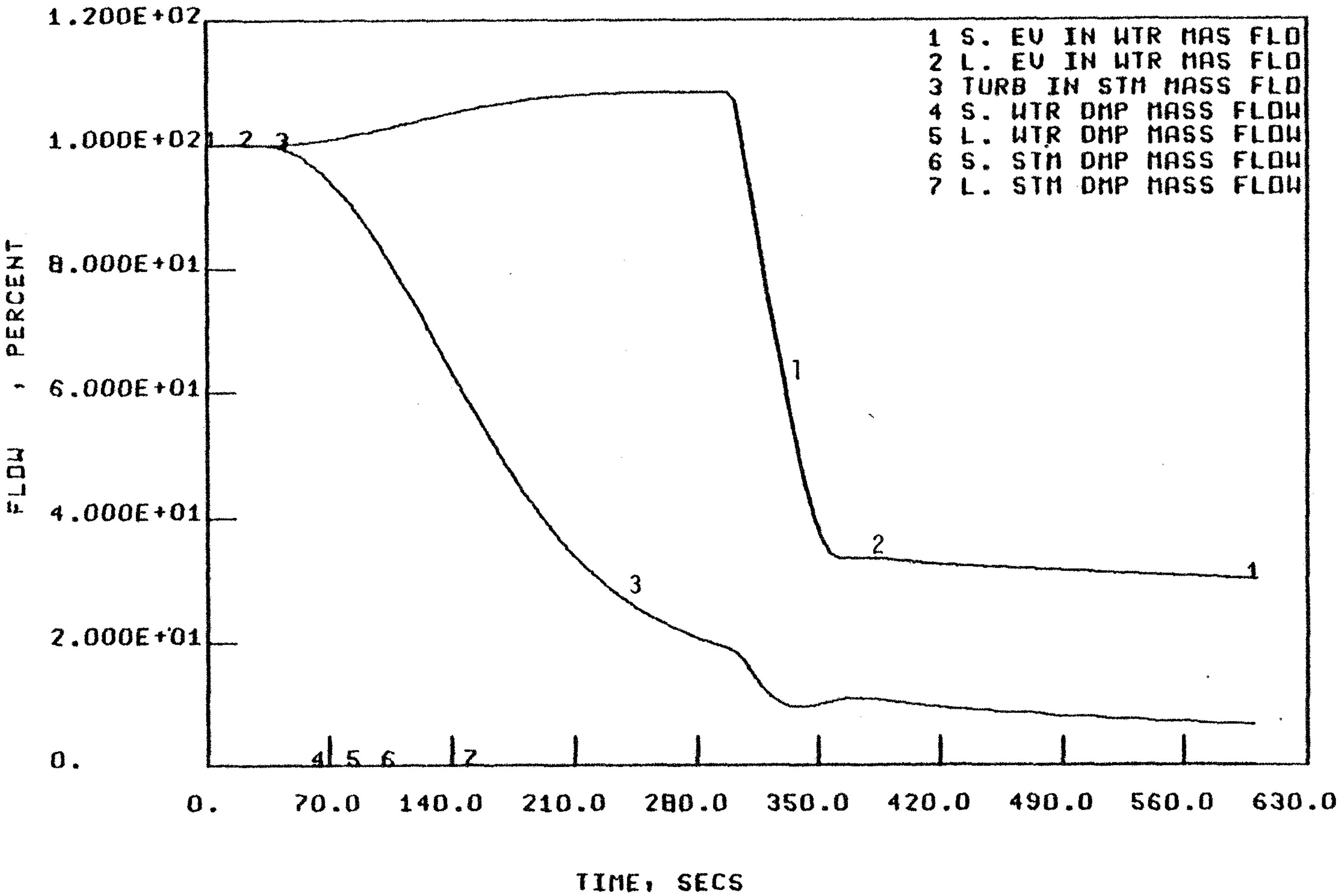

FIGURE 4-33

POOL REACTOR UNCONTROLLED ROD INSERTION WITH DELAYED MANUAL SCRAM

RUN DATED 10/06/78

NUMBER PAPGE05

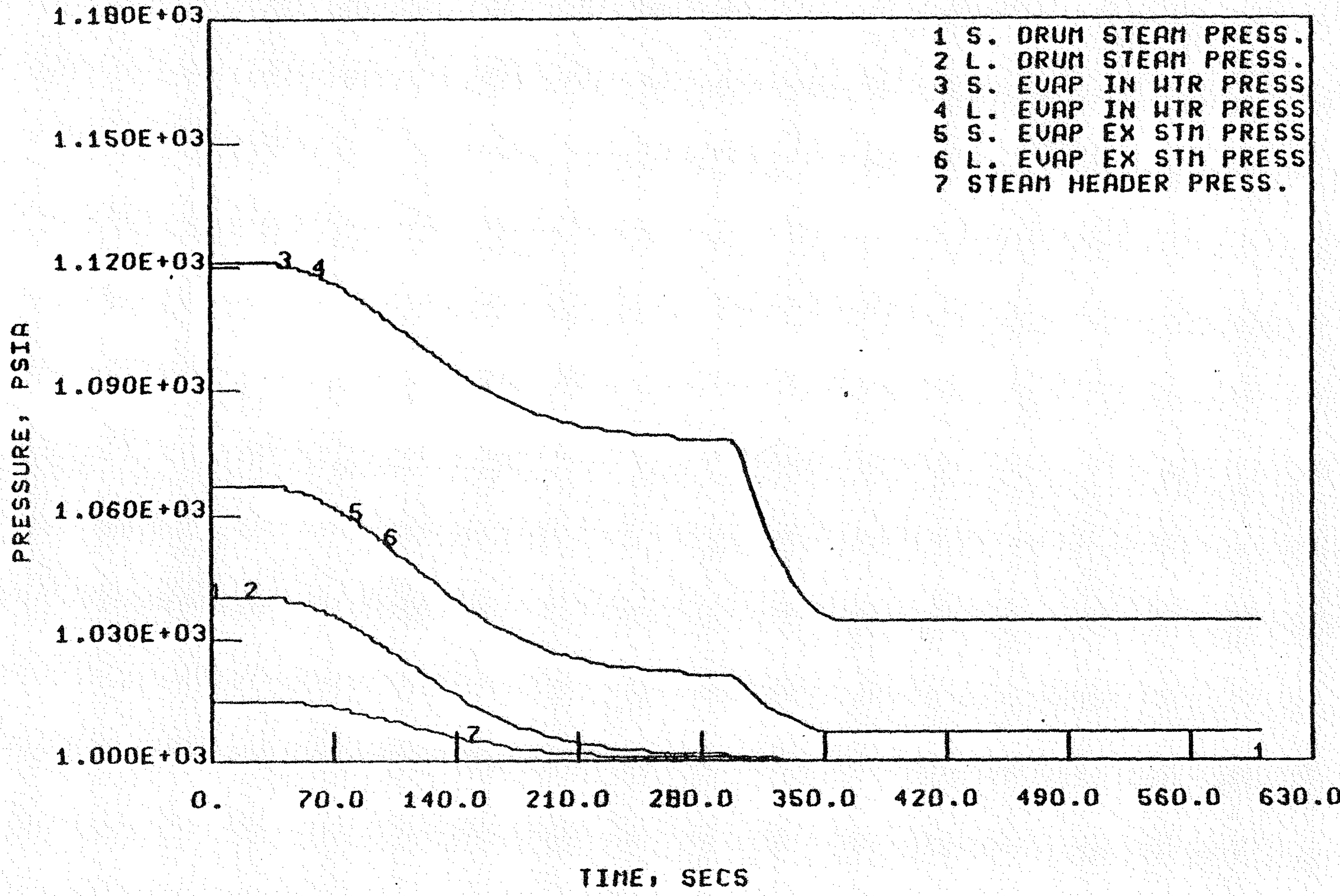

FIGURE 4-34
POOL REACTOR UNCONTROLLED ROD INSERTION WITH DELAYED MANUAL SCRAM
RUN DATED 10/06/78
NUMBER PAPGE06

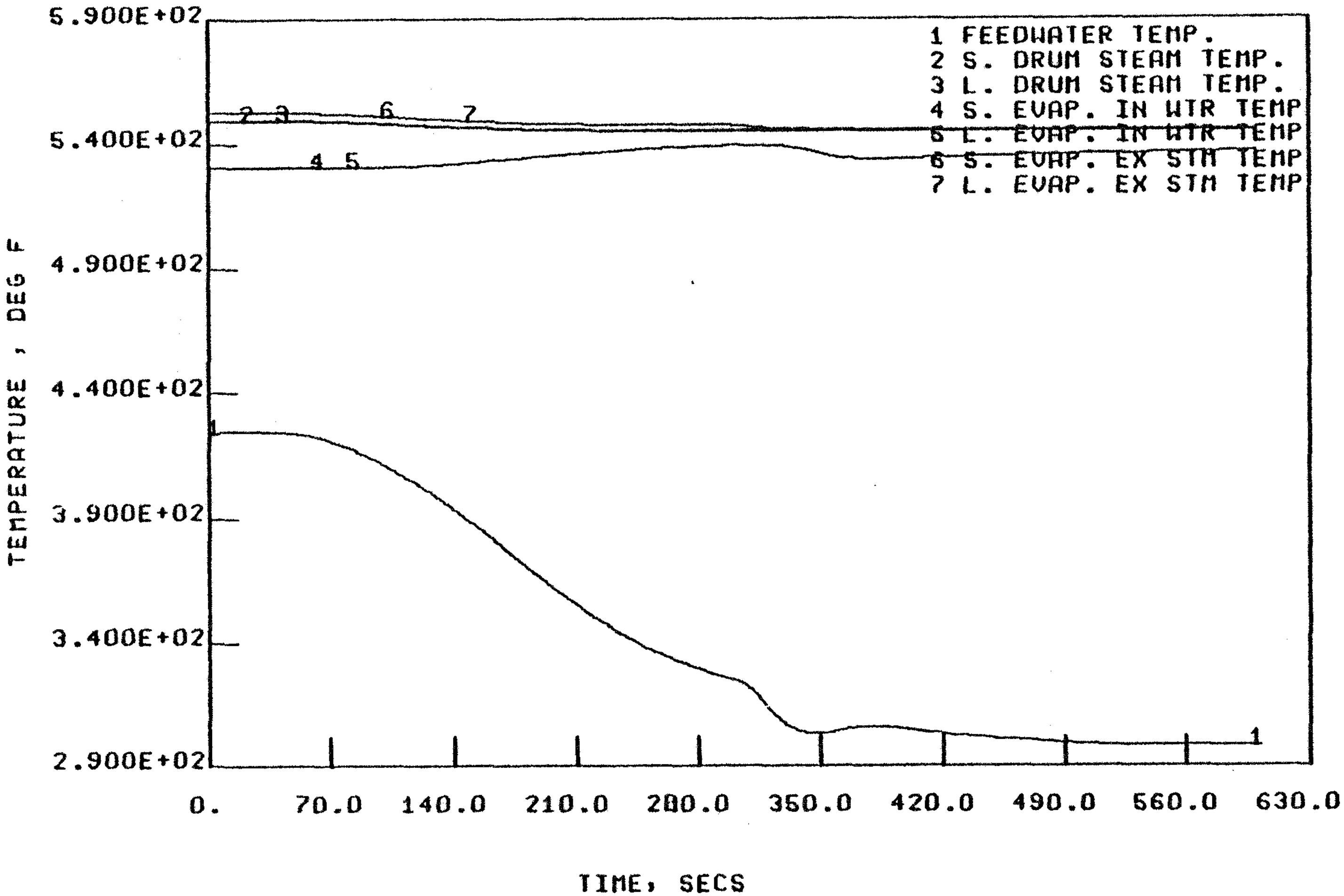

FIGURE 4-35
POOL REACTOR UNCONTROLLED ROD INSERTION WITH DELAYED MANUAL SCRAM
RUN DATED 10/06/78
NUMBER PAPGE06

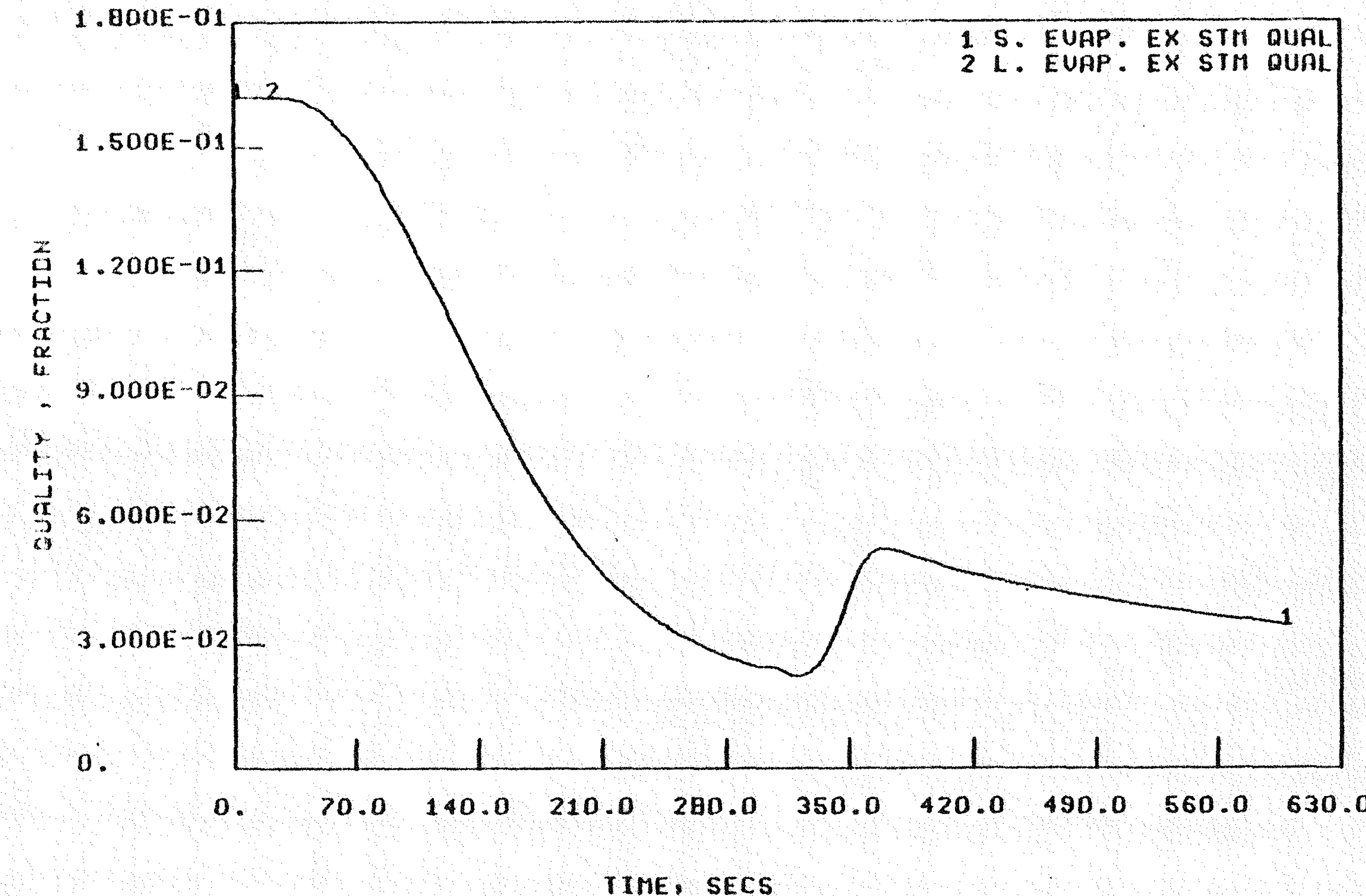

FIGURE 4-36

POOL REACTOR UNCONTROLLED ROD INSERTION WITH DELAYED MANUAL SCRAM
RUN DATED 10/06/78
NUMBER PAPGE05

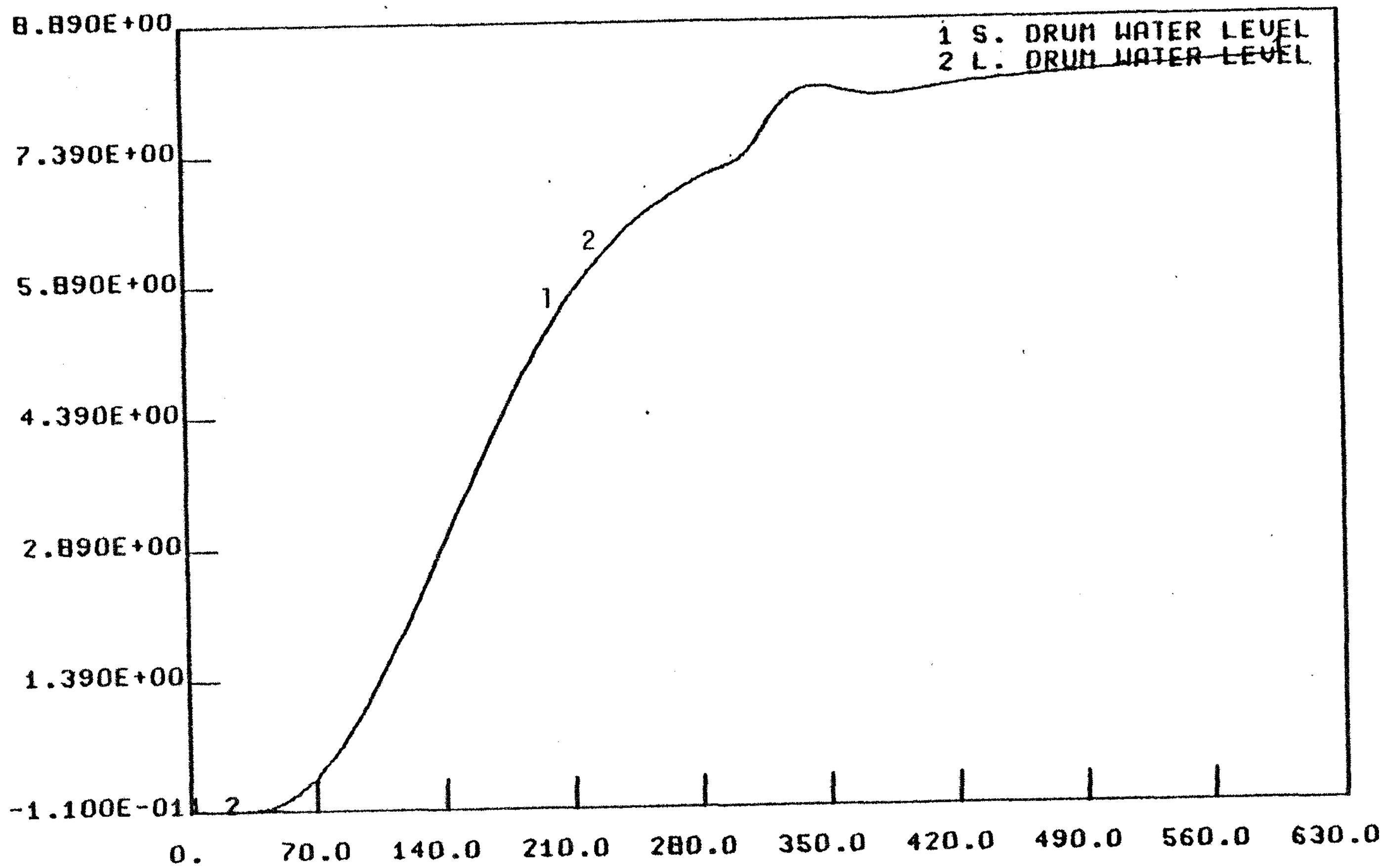

FIGURE 4-37
POOL REACTOR PLANT LOADING AT MAXIMUM RATE (VARIABLE SPEED PUMPS)
RUN DATED 10/18/78
NUMBER TAPGE00

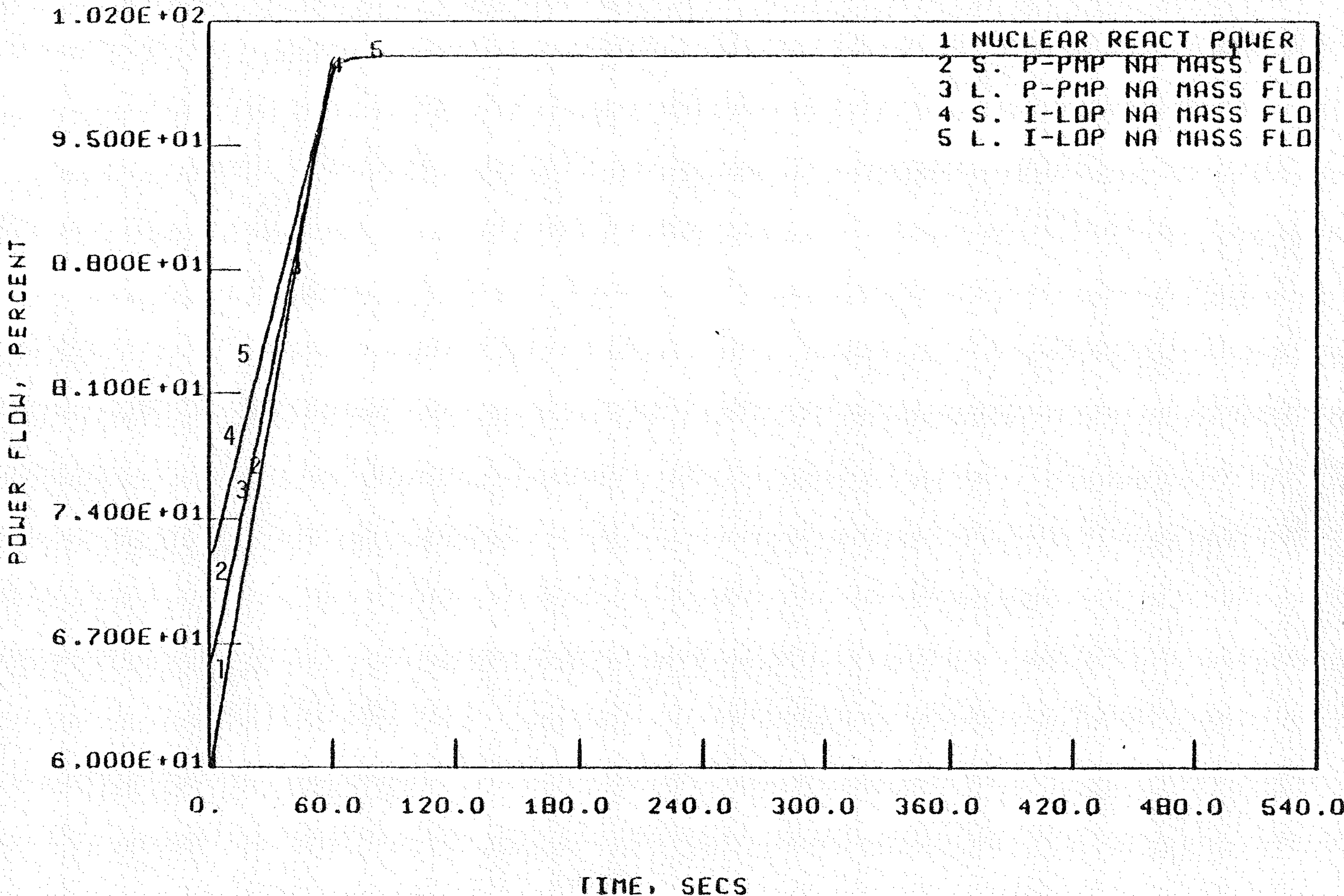

FIGURE 4-38

POOL REACTOR PLANT LOADING AT MAXIMUM RATE (VARIABLE SPEED PUMPS)
RUN DATED 10/19/78
NUMBER TAPGE00

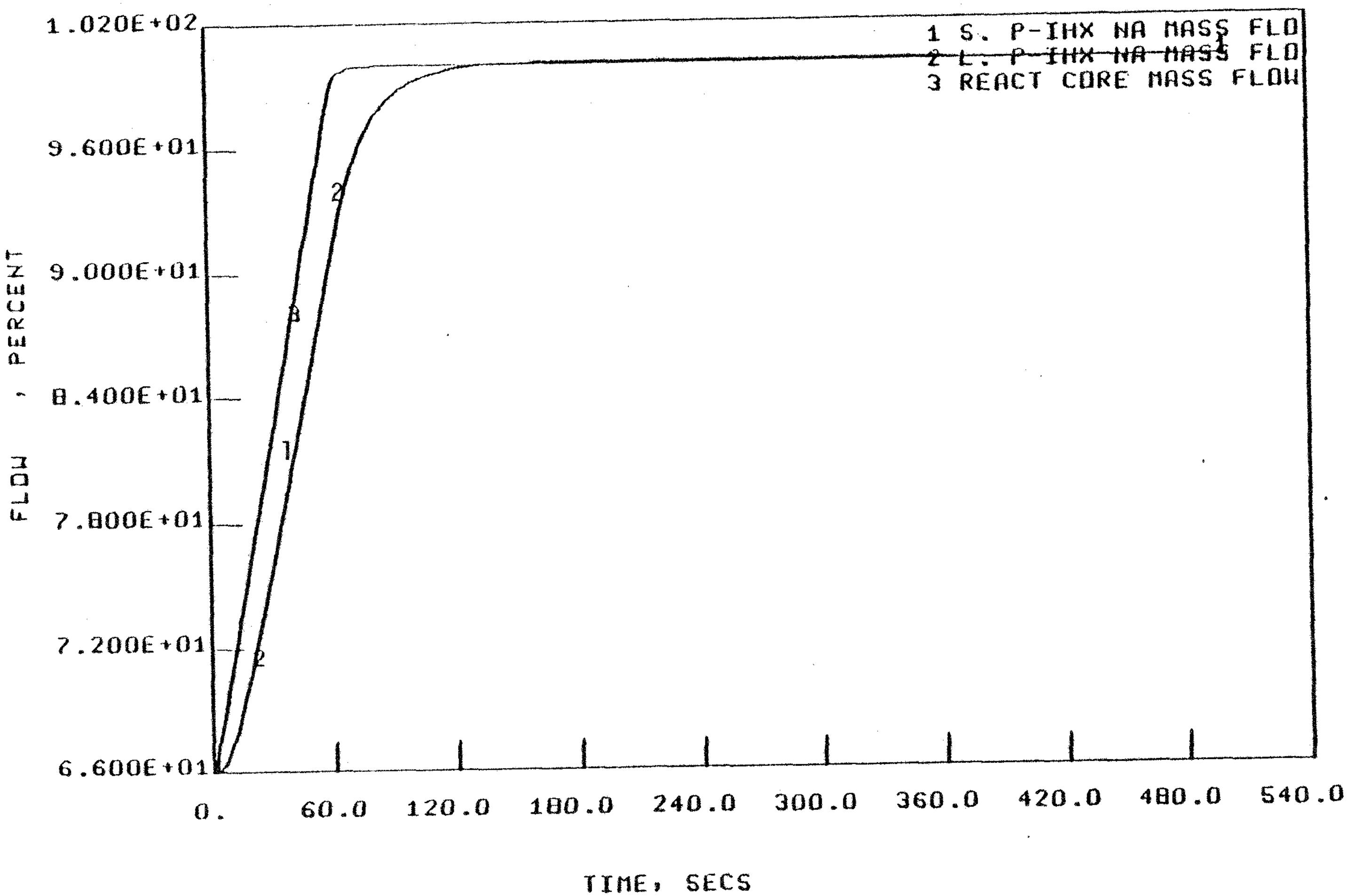

FIGURE 4-39

POOL REACTOR PLANT LOADING AT MAXIMUM RATE (VARIABLE SPEED PUMPS)
RUN DATED 10/18/78
NUMBER TAPGE00

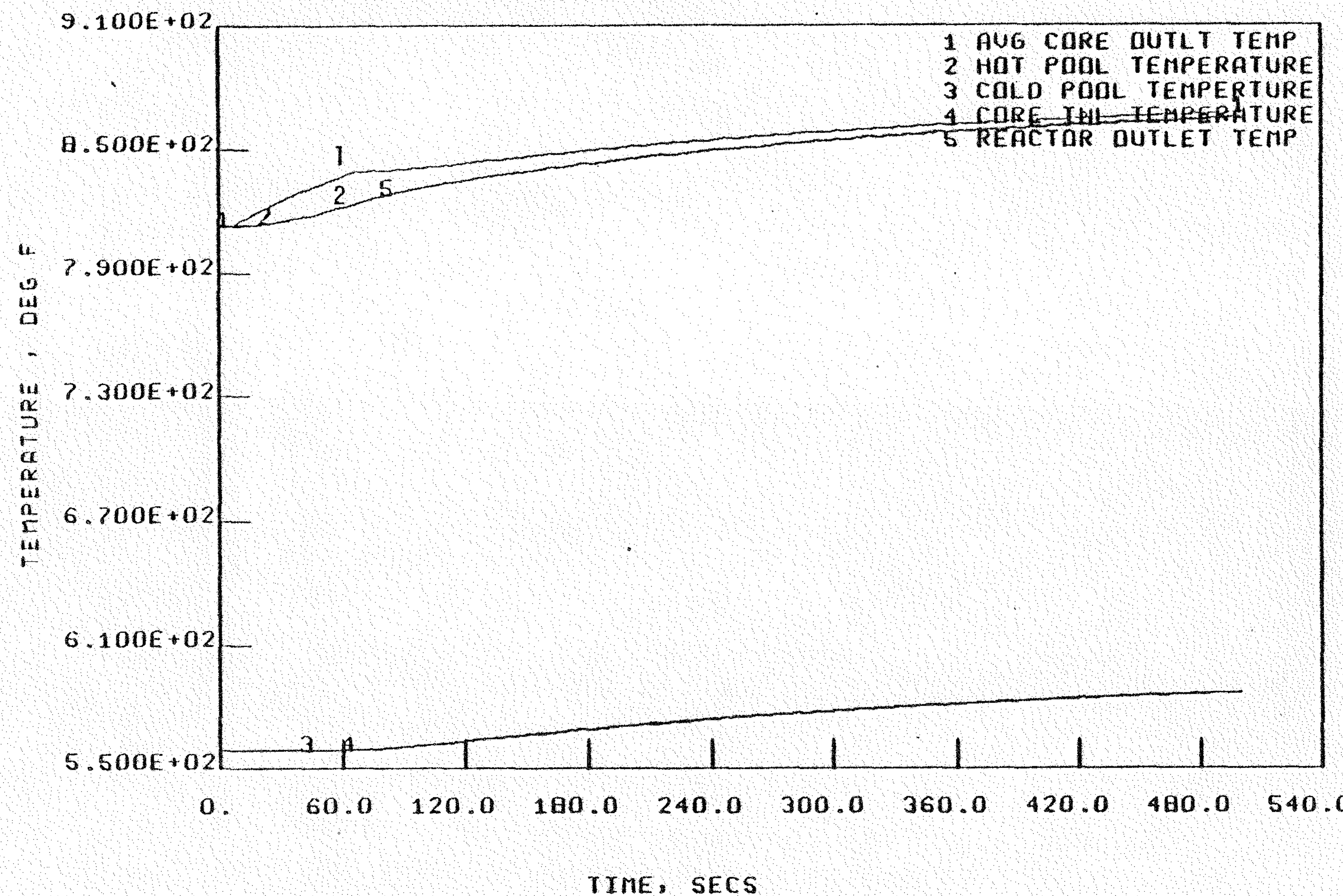

FIGURE 4-40
POOL REACTOR PLANT LOADING AT MAXIMUM RATE (VARIABLE SPEED PUMPS)
RUN DATED 10/18/78
NUMBER TAPGE00

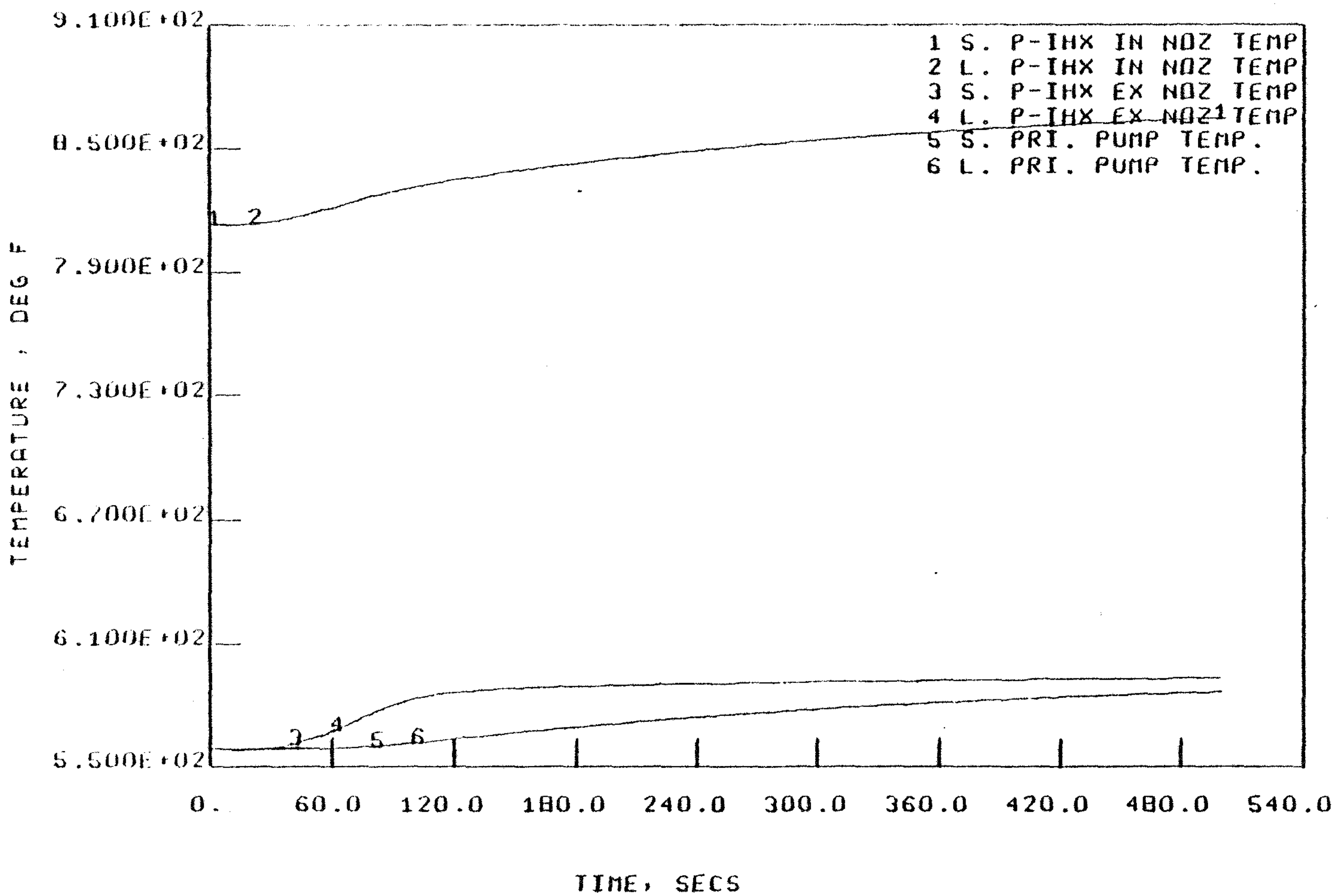

FIGURE 4-41
POOL REACTOR PLANT LOADING AT MAXIMUM RATE (VARIABLE SPEED PUMPS)
RUN DATED 10/18/78
NUMBER TAP6E00

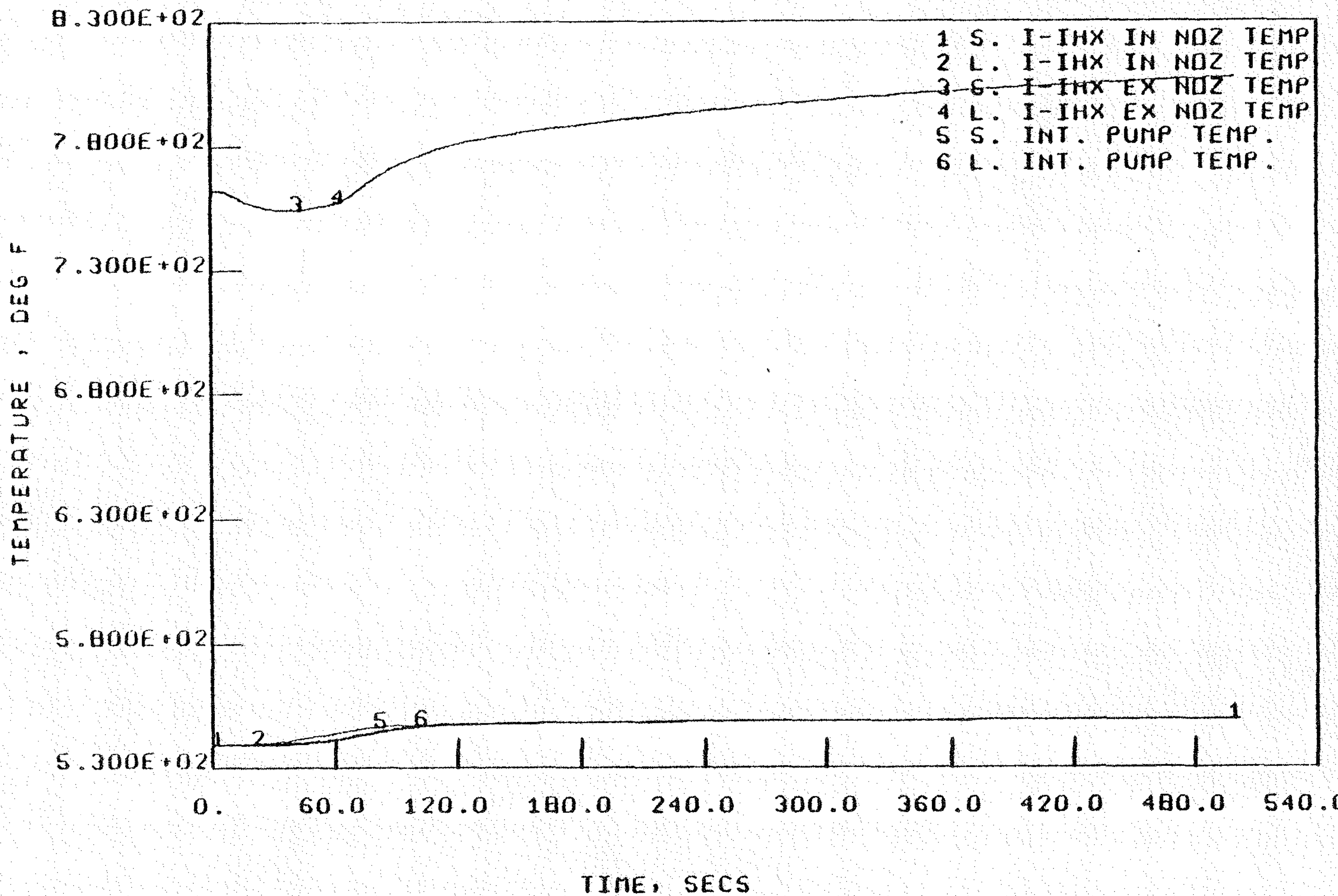

FIGURE 4-42

POOL REACTOR PLANT LOADING AT MAXIMUM RATE (VARIABLE SPEED PUMPS)
RUN DATED 10/18/78
NUMBER TAPGE00

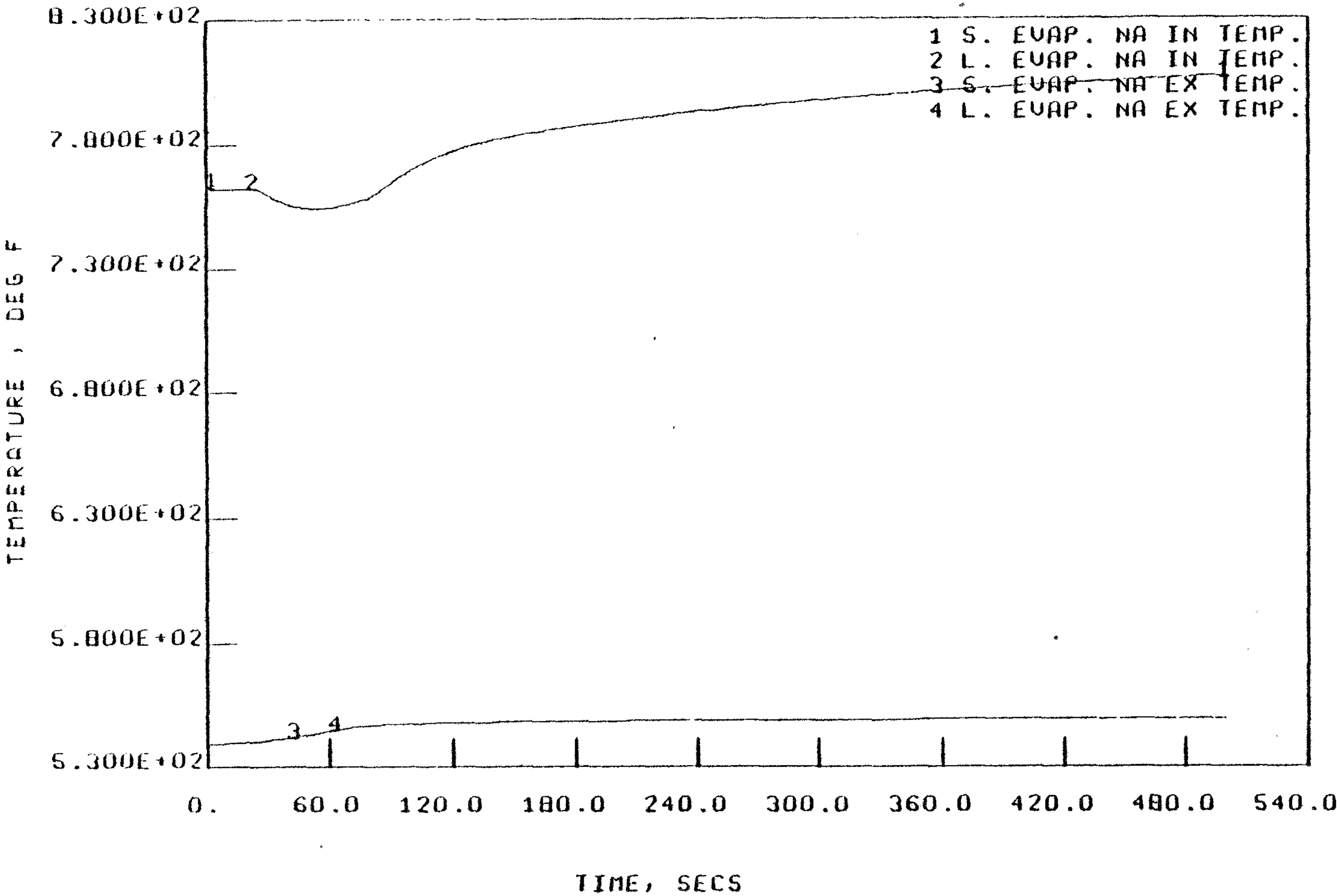

FIGURE 4-43

POOL REACTOR PLANT LOADING AT MAXIMUM RATE (VARIABLE SPEED PUMPS)
RUN DATED 10/18/78
NUMBER TAPGE00

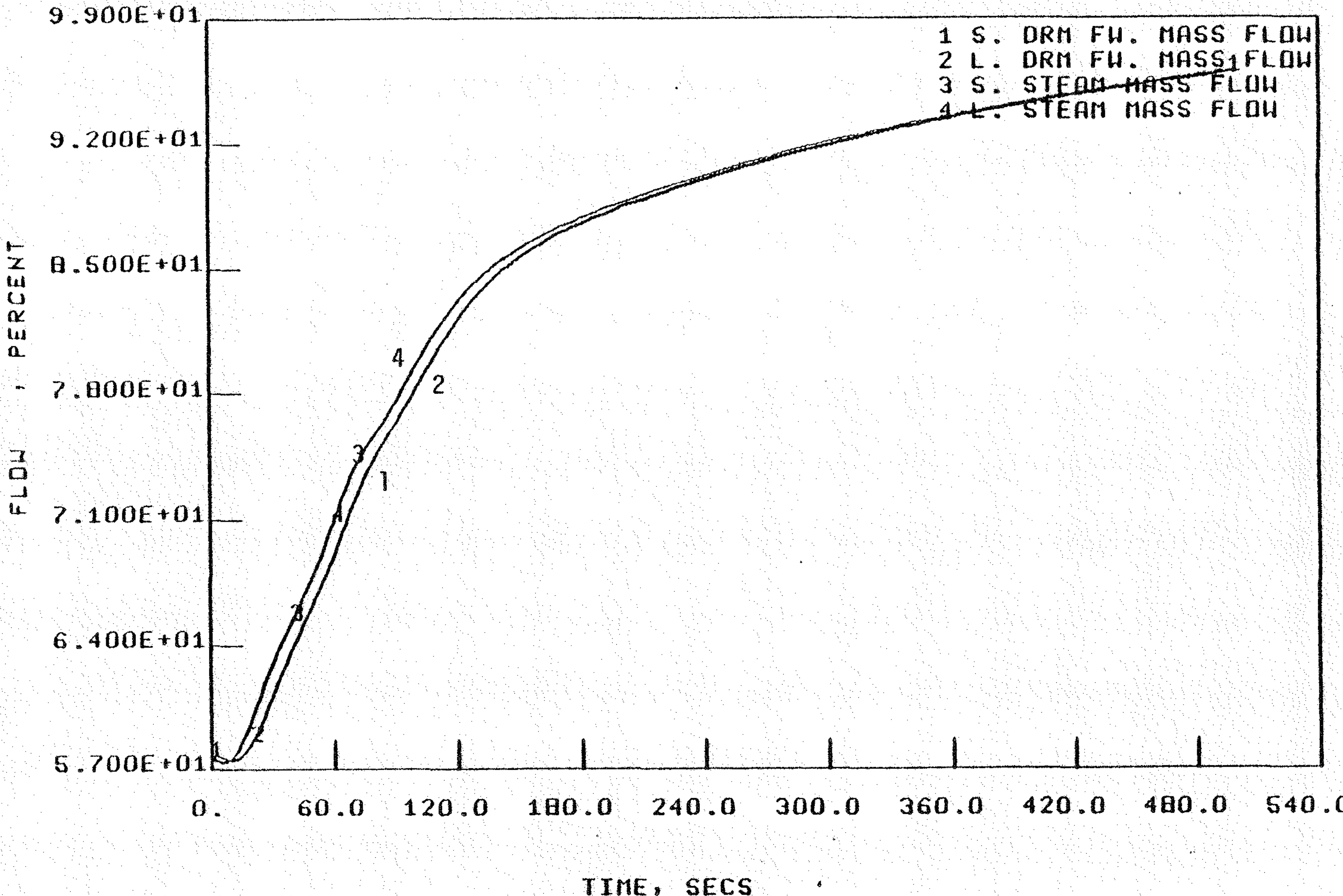

FIGURE 4-44

POOL REACTOR PLANT LOADING AT MAXIMUM RATE (VARIABLE SPEED PUMPS)
RUN DATED 10/18/78
NUMBER TAPGE00

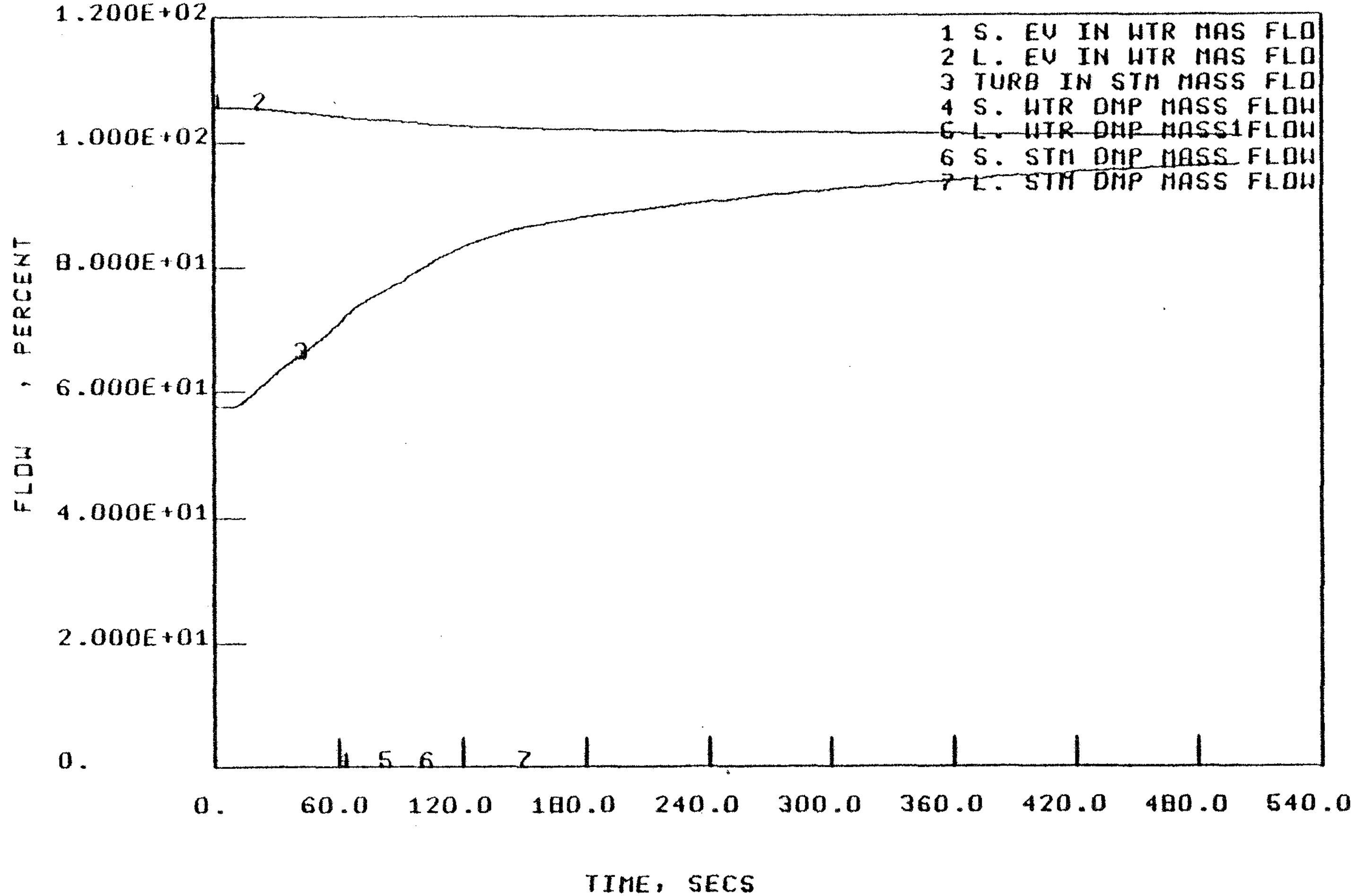

FIGURE 4-45

POOL REACTOR PLANT LOADING AT MAXIMUM RATE (VARIABLE SPEED PUMPS)
RUN DATED 10/18/78
NUMBER TAP6E00

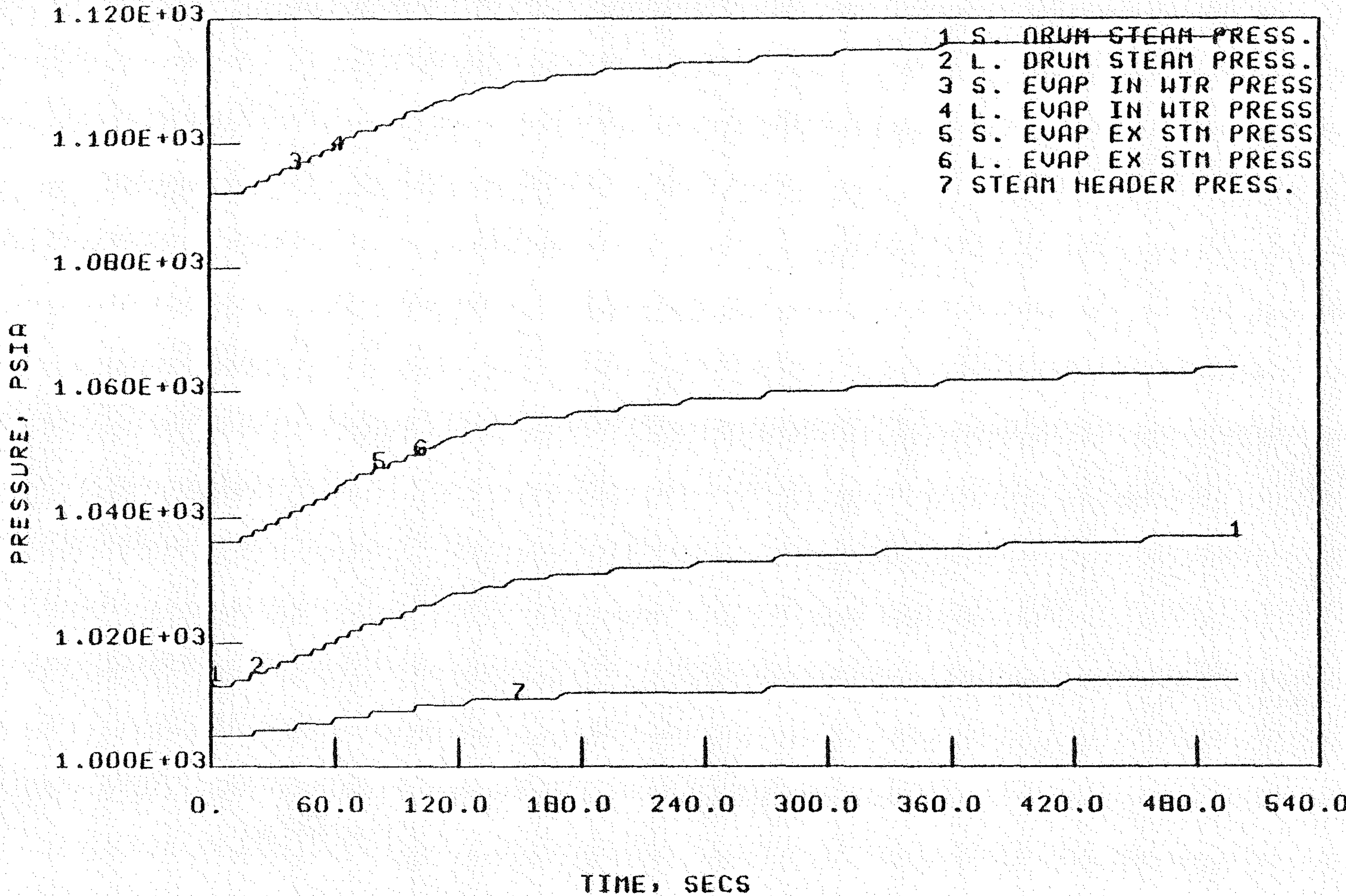

FIGURE 4-46

POOL REACTOR PLANT LOADING AT MAXIMUM RATE (VARIABLE SPEED PUMPS)
RUN DATED 10/18/78
NUMBER TAPGE00

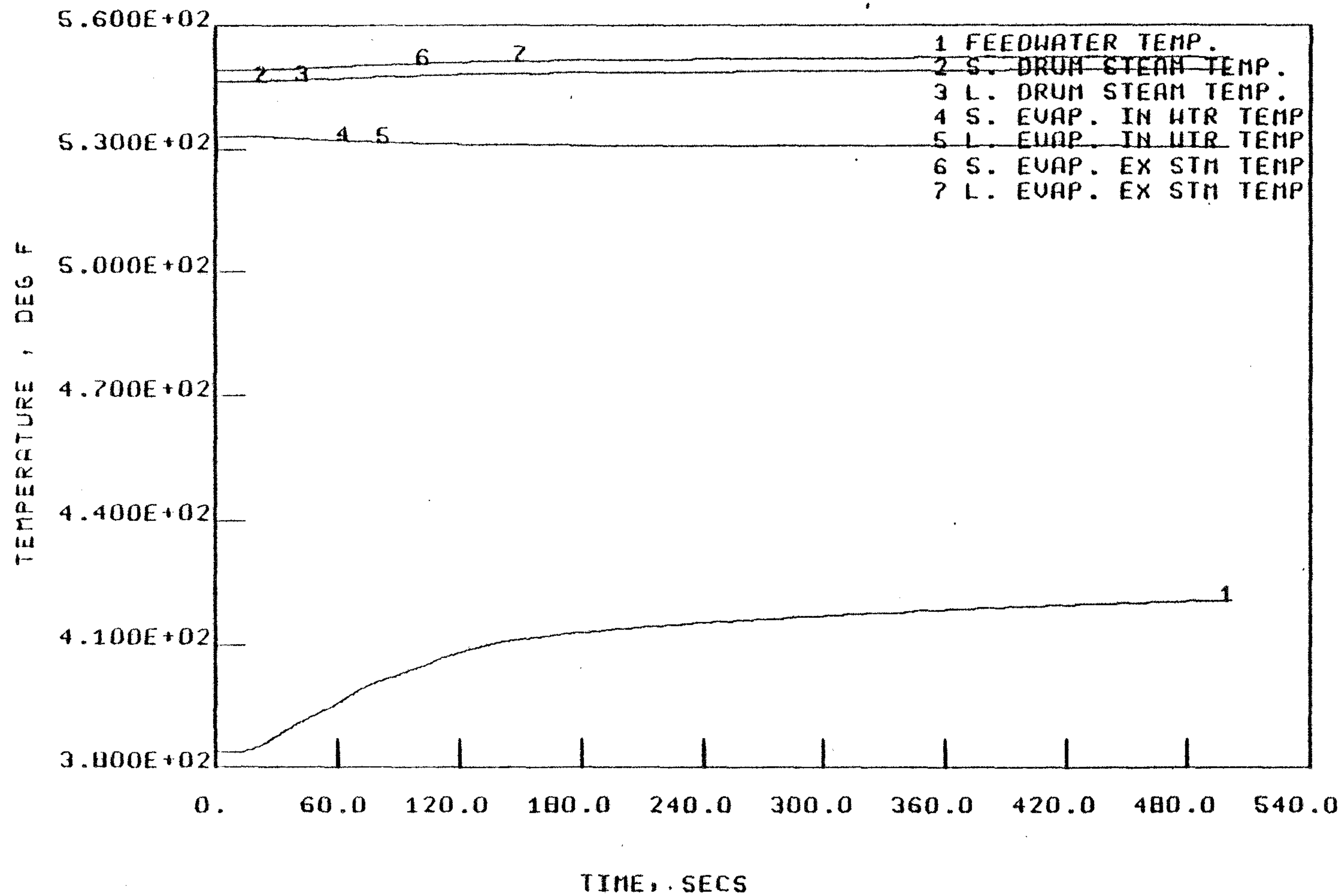

FIGURE 4-47
POOL REACTOR PLANT LOADING AT MAXIMUM RATE (VARIABLE SPEED PUMPS)
RUN DATED 10/18/78
NUMBER TAPGE00

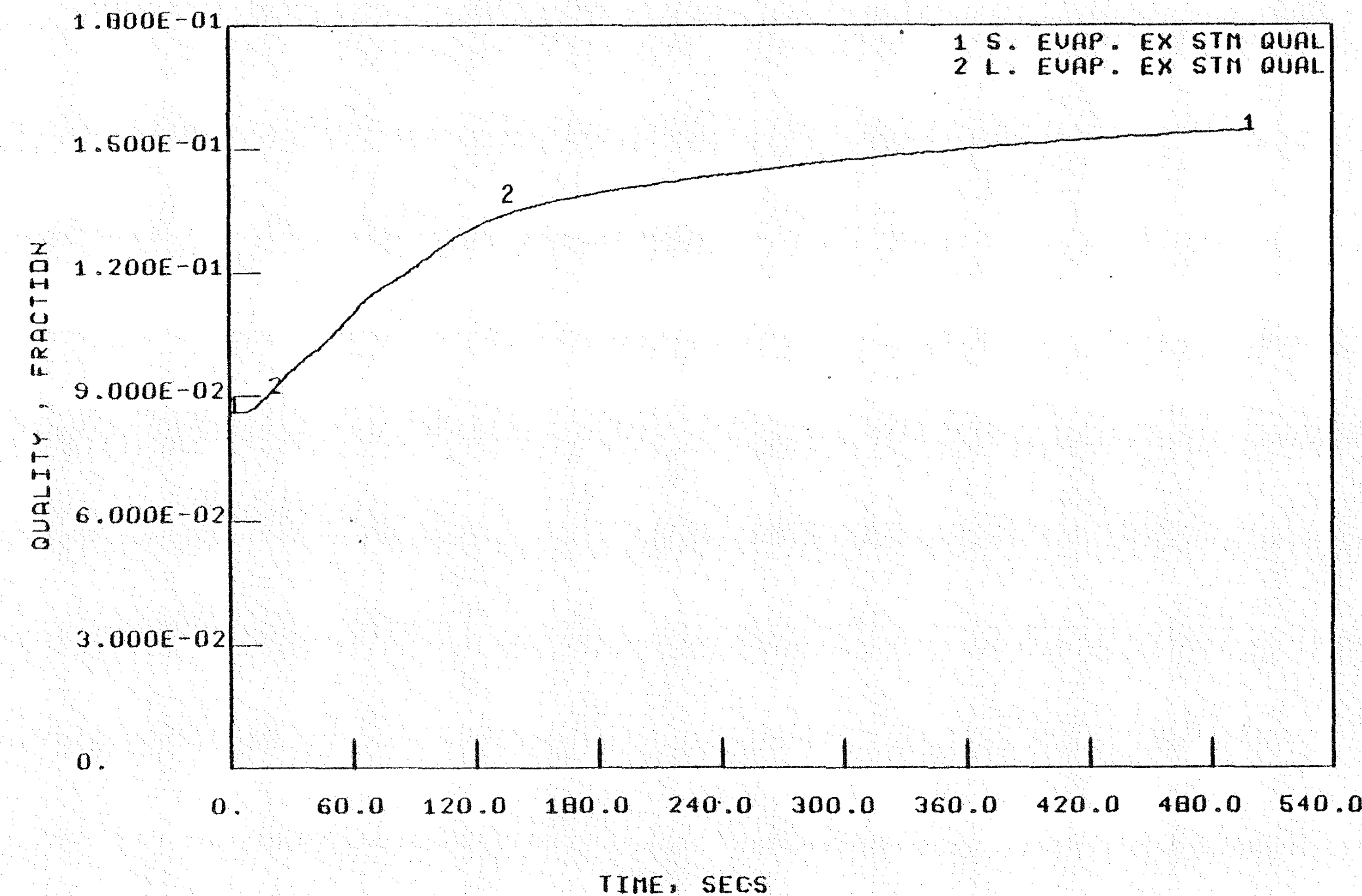

FIGURE 4-48

POOL REACTOR PLANT LOADING AT MAXIMUM RATE (VARIABLE SPEED PUMPS)
RUN DATED 10/18/78
NUMBER TAPGE00

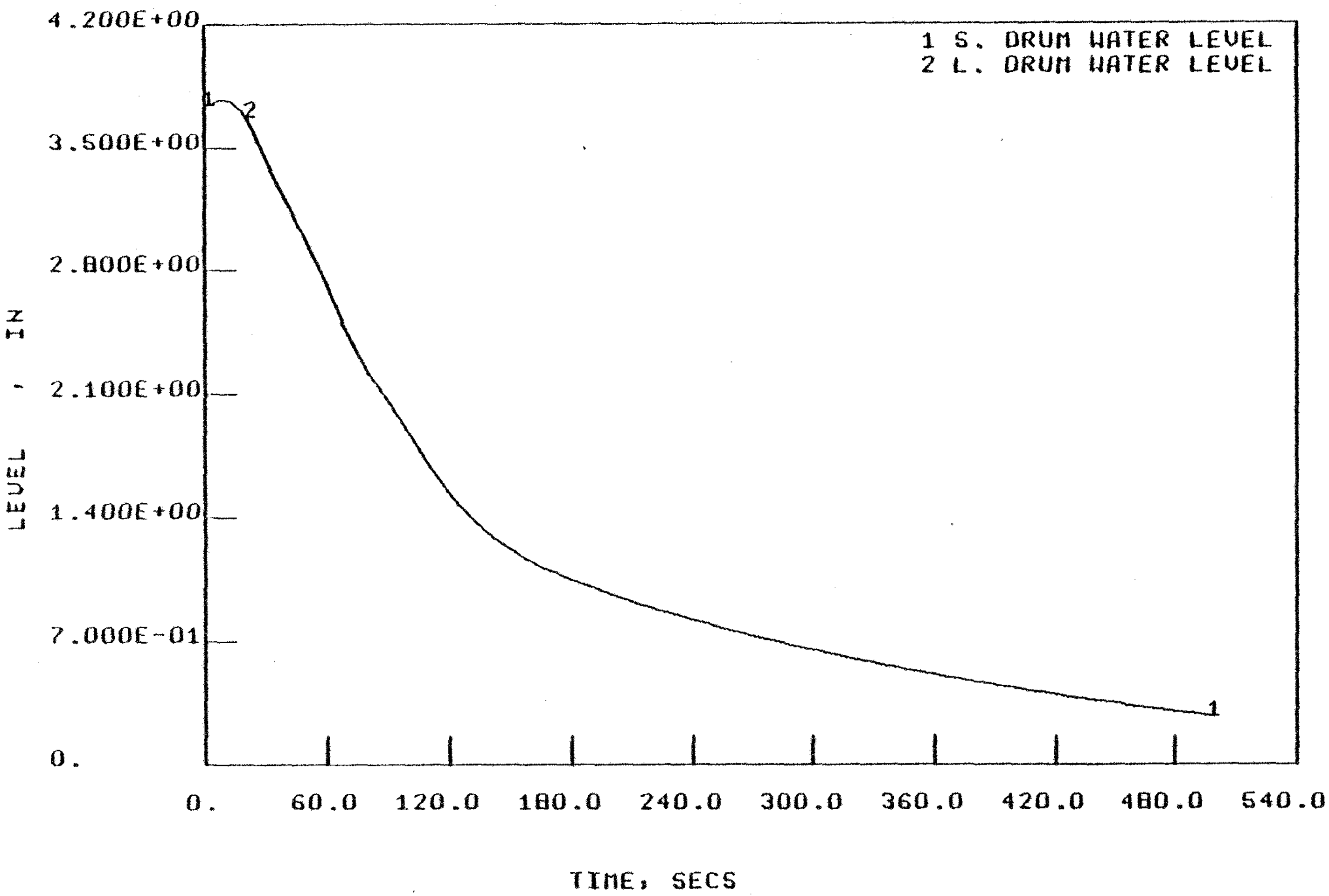

FIGURE 4-49

POOL REACTOR PLANT LOADING AT MAXIMUM RATE (CONSTANT SPEED PUMPS)
RUN DATED 10/13/78
NUMBER XEPGEOO

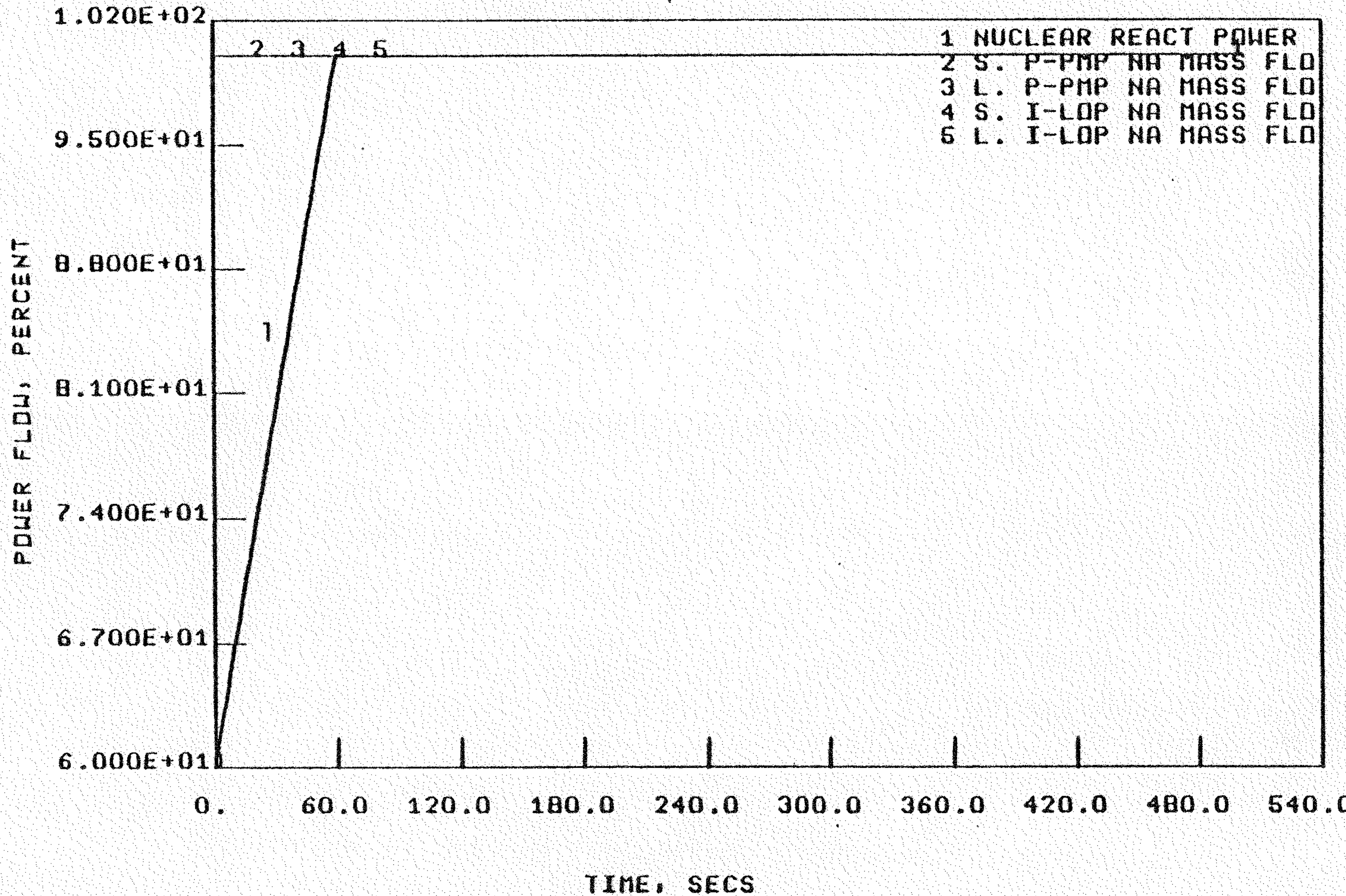

FIGURE 4-50

POOL REACTOR PLANT LOADING AT MAXIMUM RATE (CONSTANT SPEED PUMPS)
RUN DATED 10/13/78
NUMBER XEP6E00

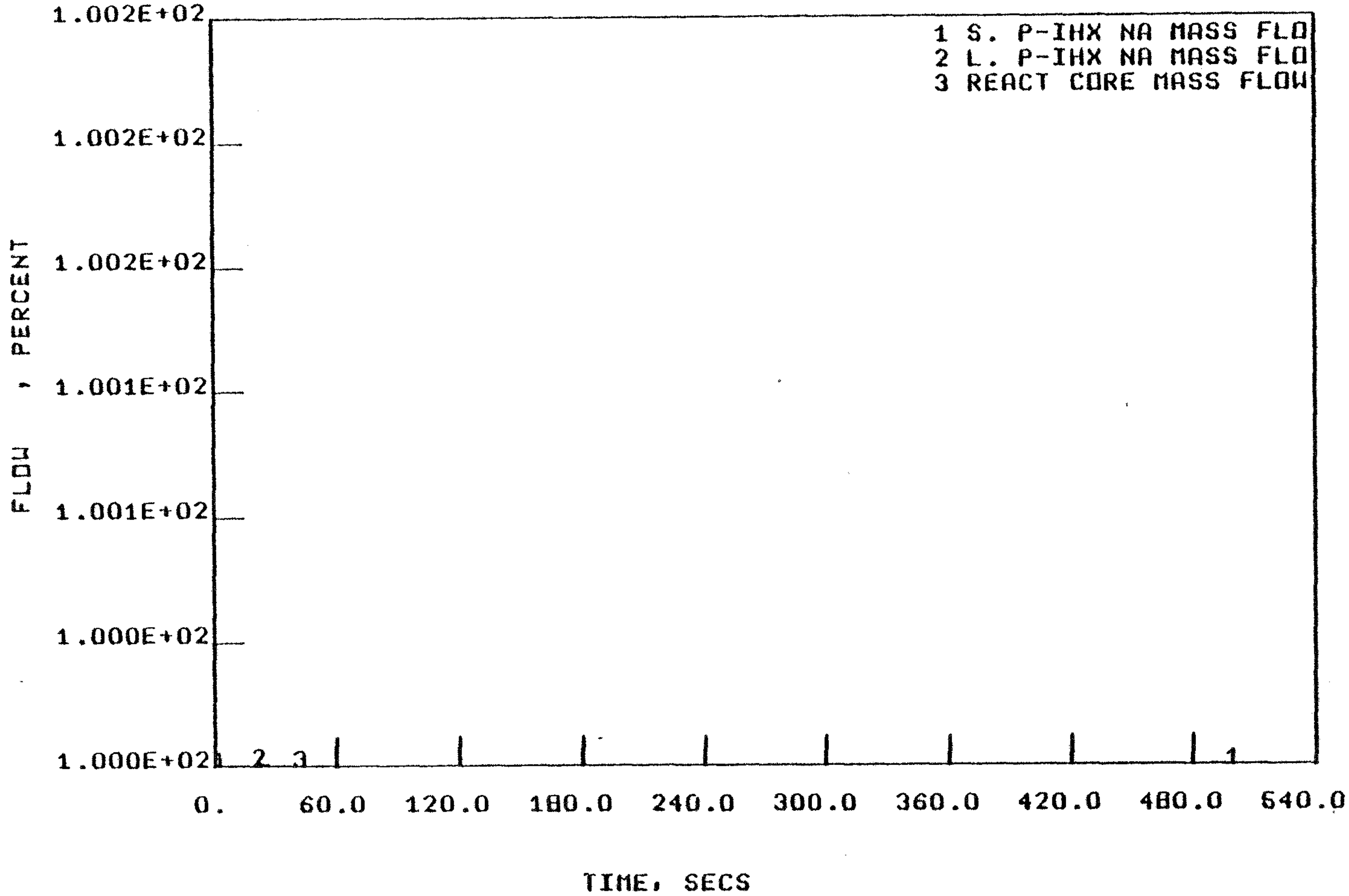

V-2.3-69

FIGURE 4-51

POOL REACTOR PLANT LOADING AT MAXIMUM RATE (CONSTANT SPEED PUMPS)
RUN DATED 10/13/78
NUMBER XEP6E00

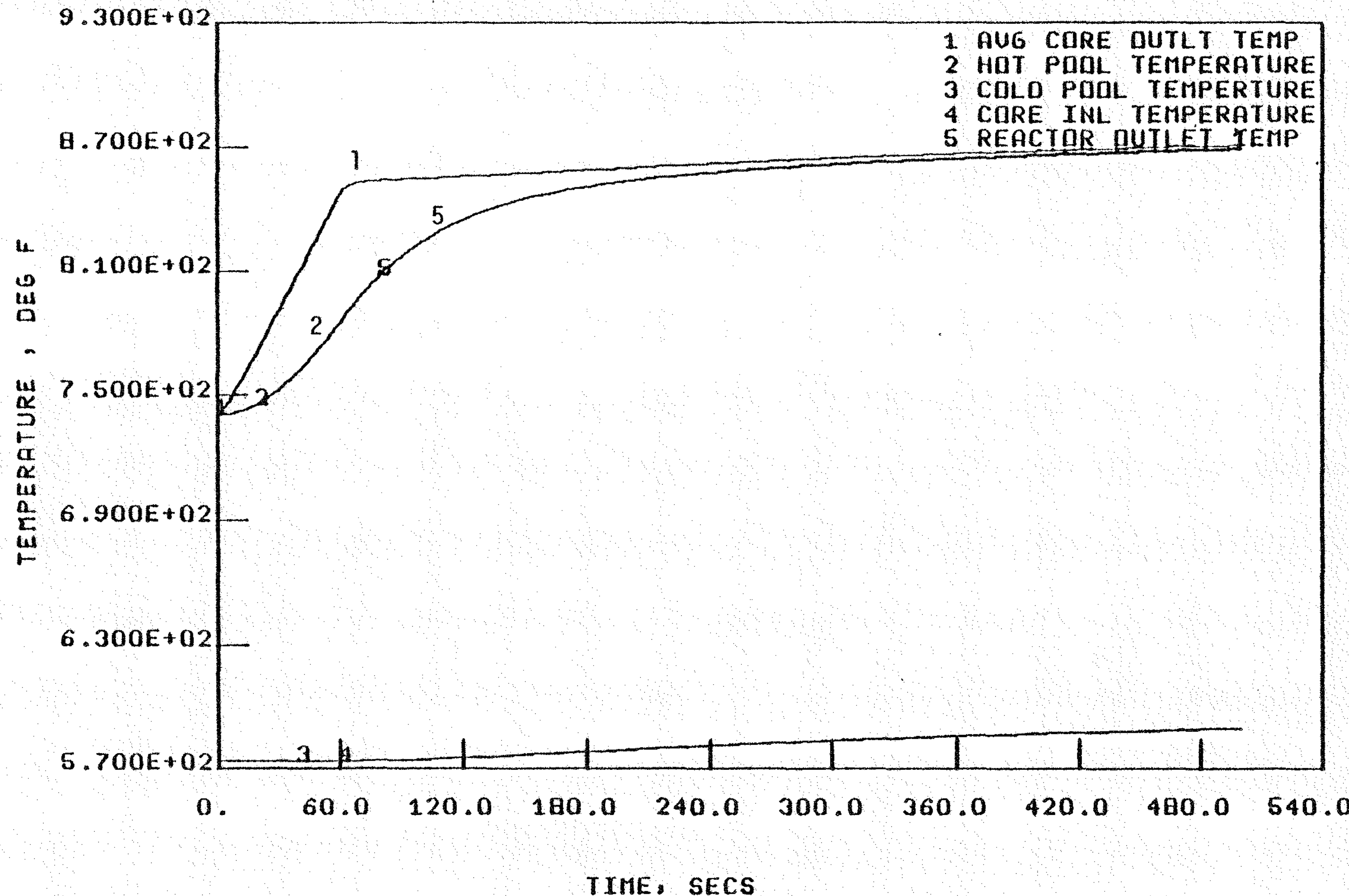

FIGURE 4-52

POOL REACTOR PLANT LOADING AT MAXIMUM RATE (CONSTANT SPEED PUMPS)
RUN DATED 10/13/78
NUMBER XEPGEOO

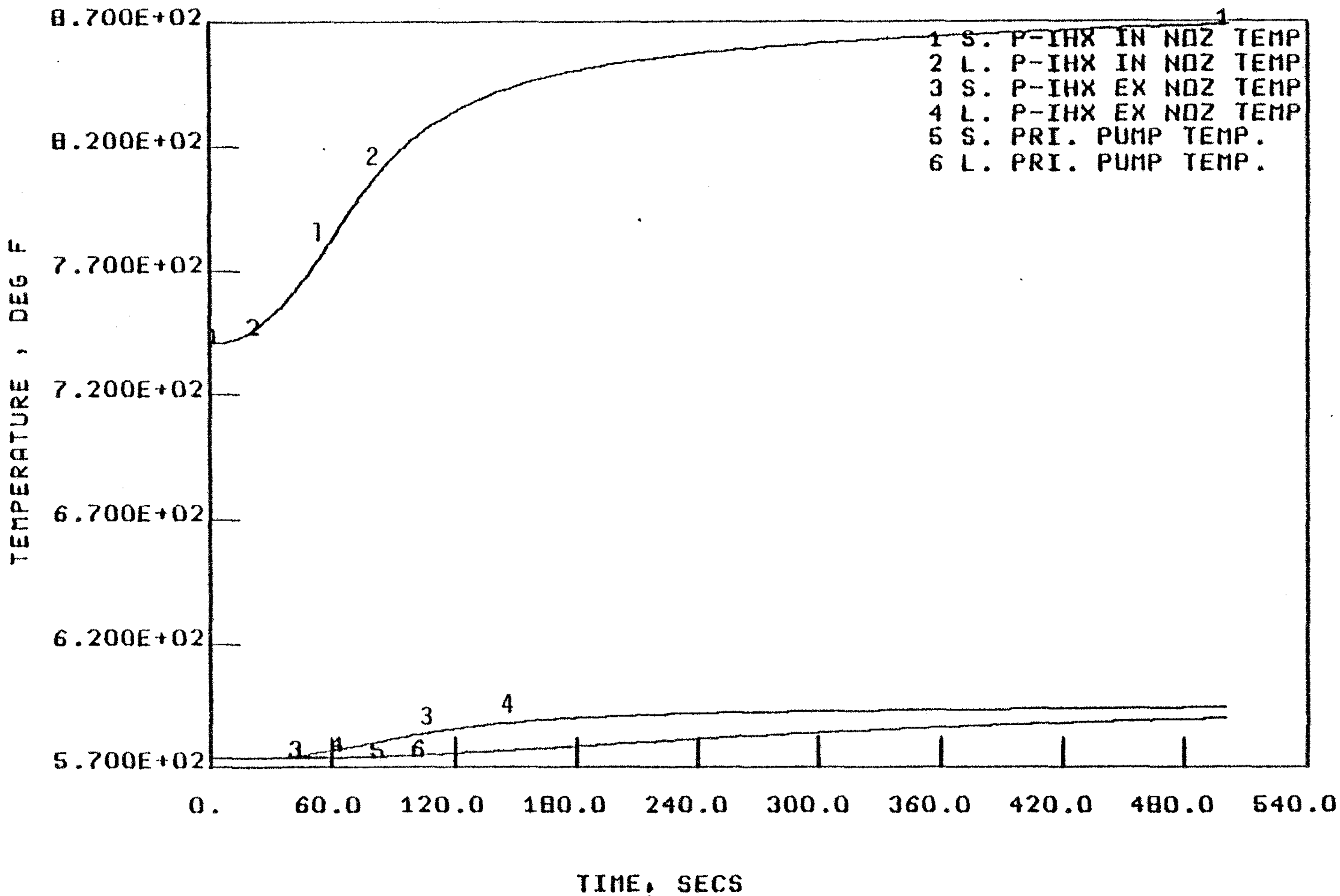

FIGURE 4-53

POOL REACTOR PLANT LOADING AT MAXIMUM RATE (CONSTANT SPEED PUMPS)
RUN DATED 10/13/78
NUMBER XEPGEOO

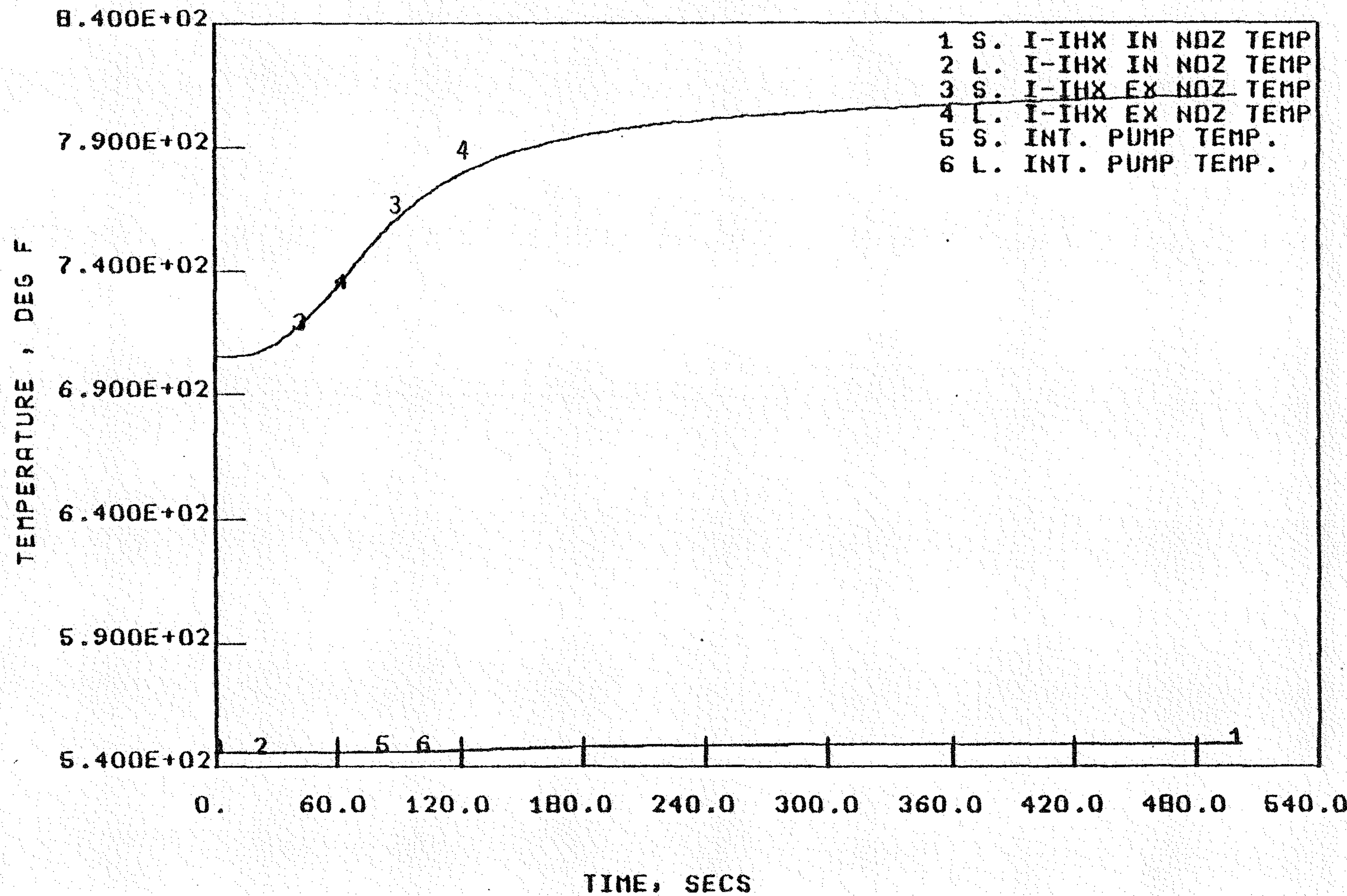

FIGURE 4-54

POOL REACTOR PLANT LOADING AT MAXIMUM RATE (CONSTANT SPEED PUMPS)
RUN DATED 10/13/78
NUMBER XEP6E00

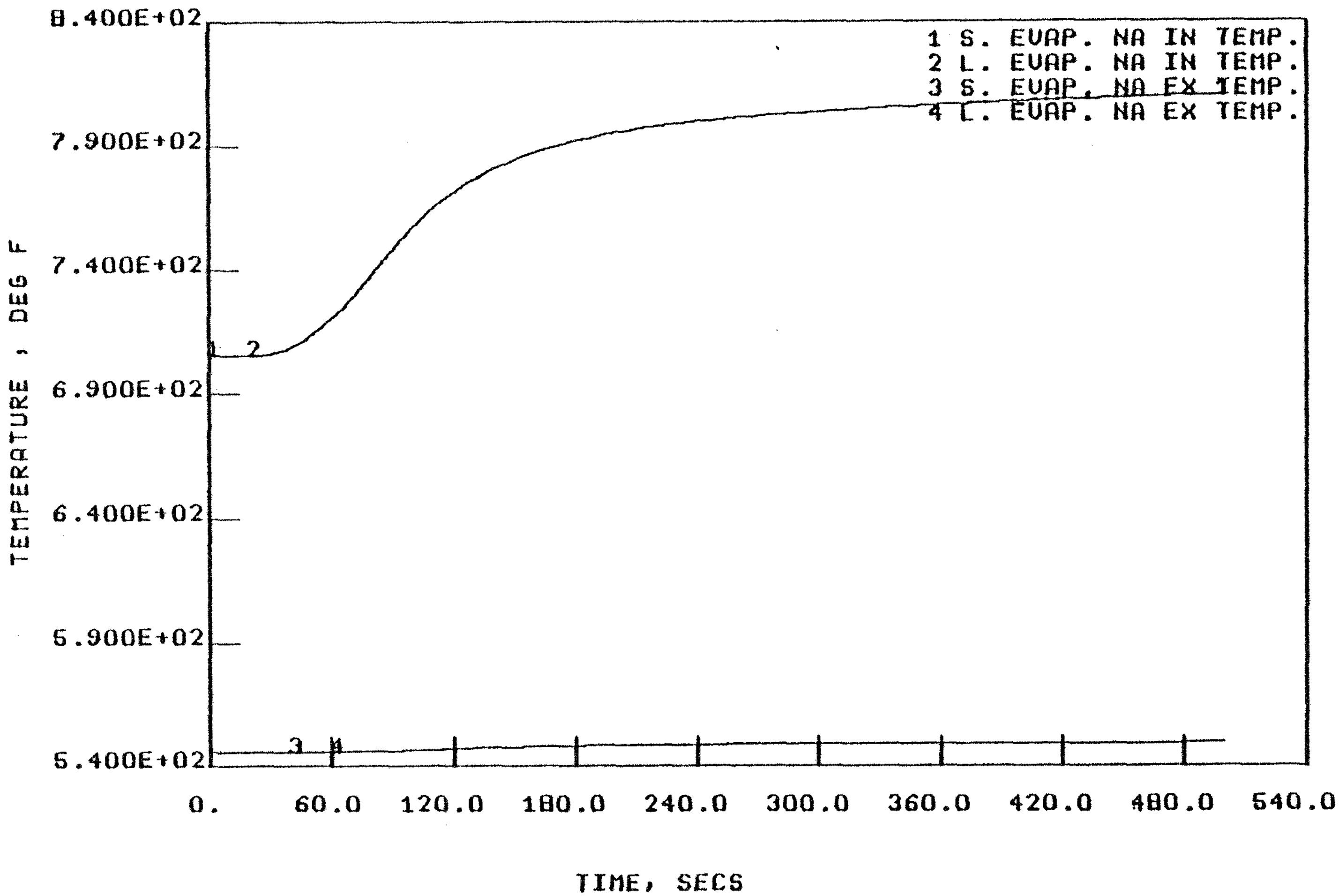

FIGURE 4-55
POOL REACTOR PLANT LOADING AT MAXIMUM RATE (CONSTANT SPEED PUMPS)
RUN DATED 10/13/78
NUMBER XEP6E00

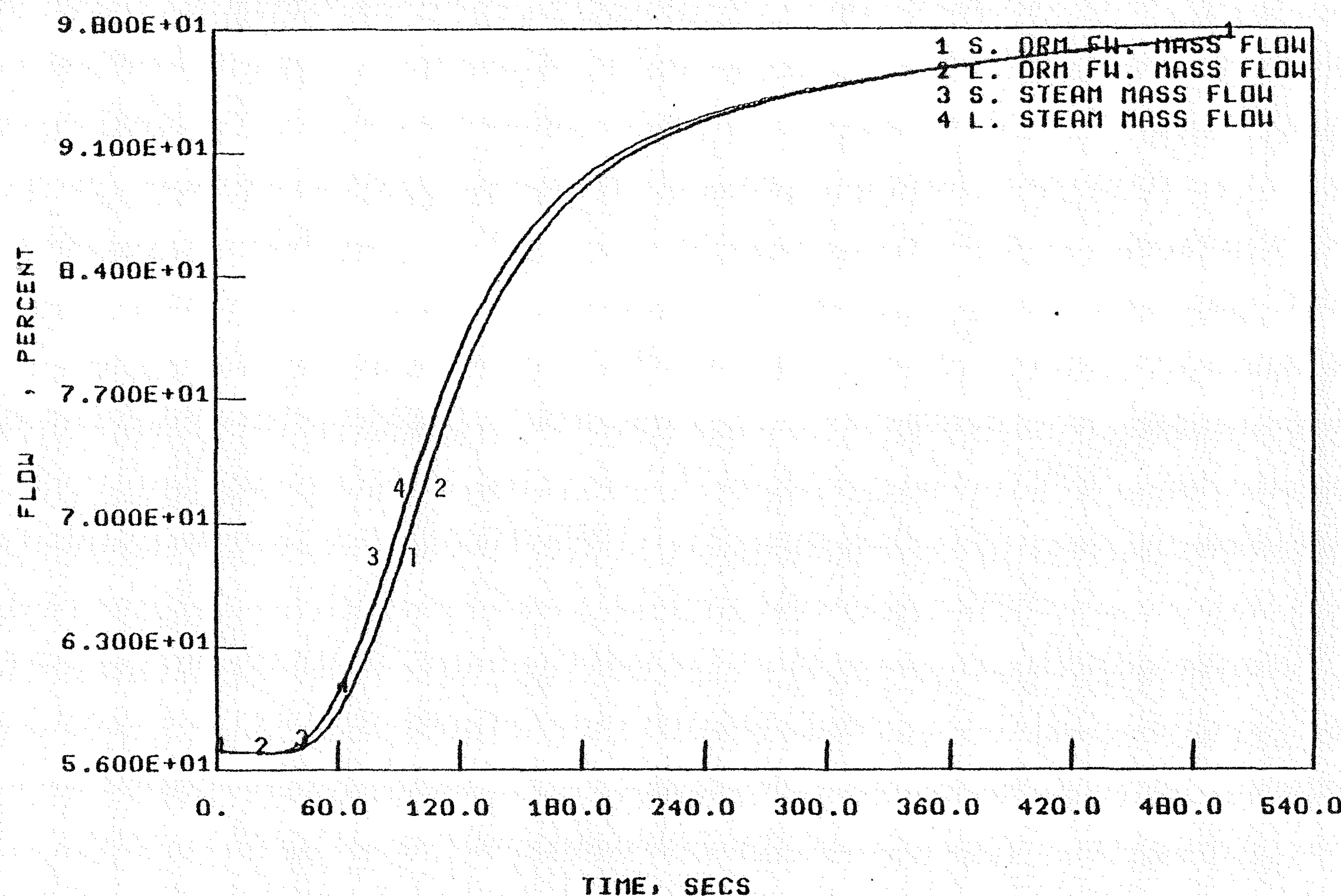

FIGURE 4-56

POOL REACTOR PLANT LOADING AT MAXIMUM RATE (CONSTANT SPEED PUMPS)
RUN DATED 10/13/78
NUMBER XEPGE00

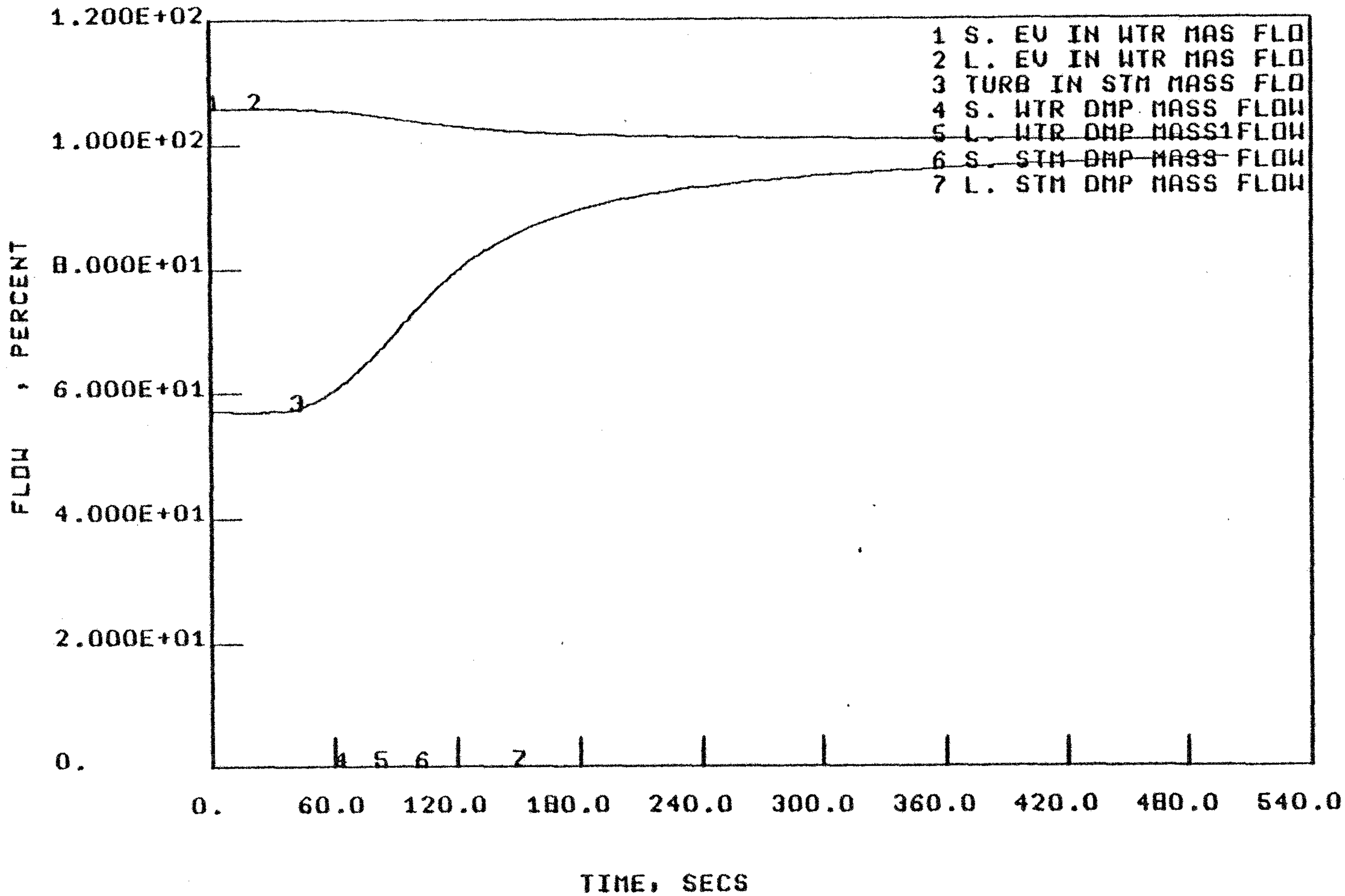

FIGURE 4-57
POOL REACTOR PLANT LOADING AT MAXIMUM RATE (CONSTANT SPEED PUMPS)
RUN DATED 10/13/78
NUMBER XEP6E00

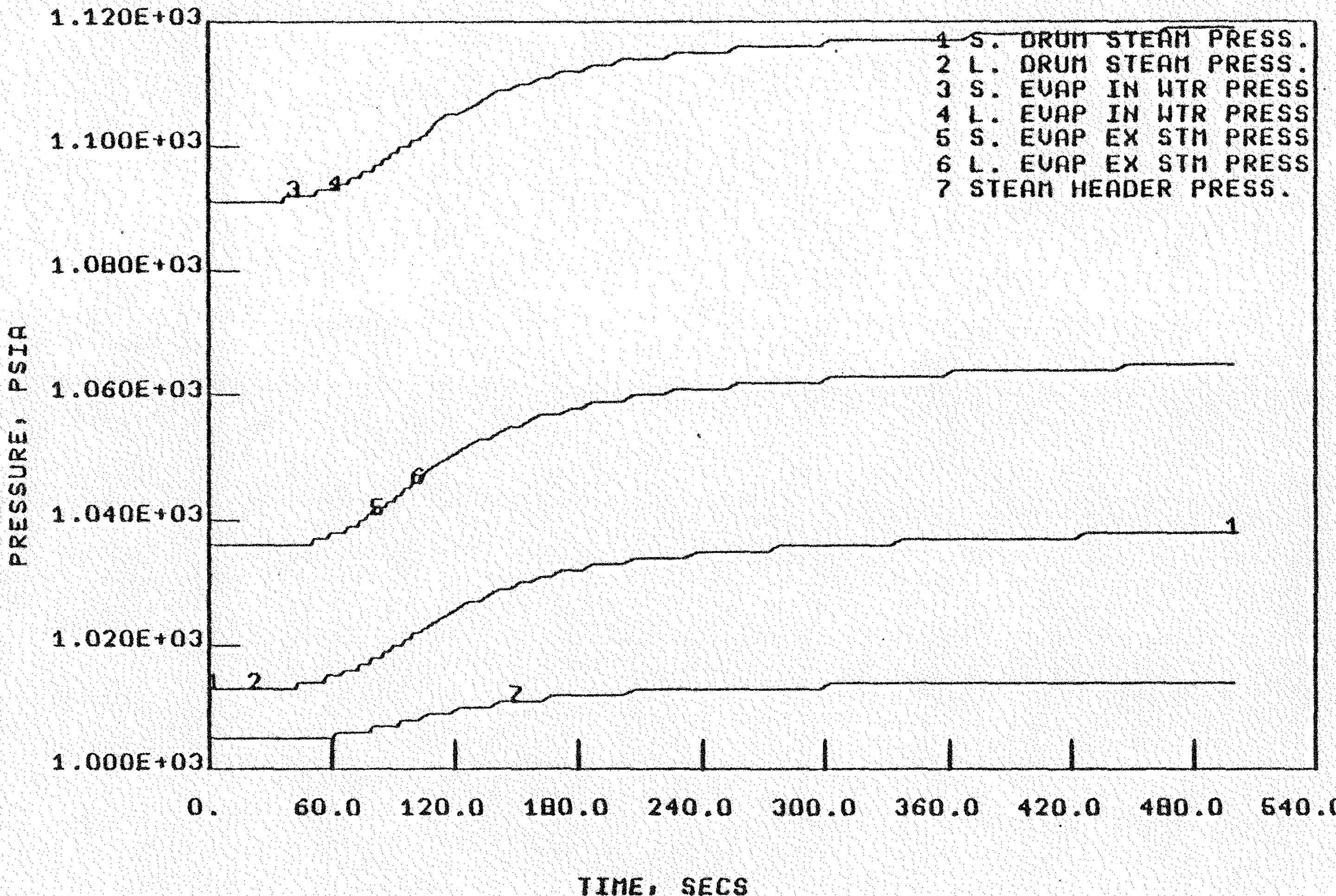

FIGURE 4-58
POOL REACTOR PLANT LOADING AT MAXIMUM RATE (CONSTANT SPEED PUMPS)
RUN DATED 10/13/78
NUMBER XEP6E00

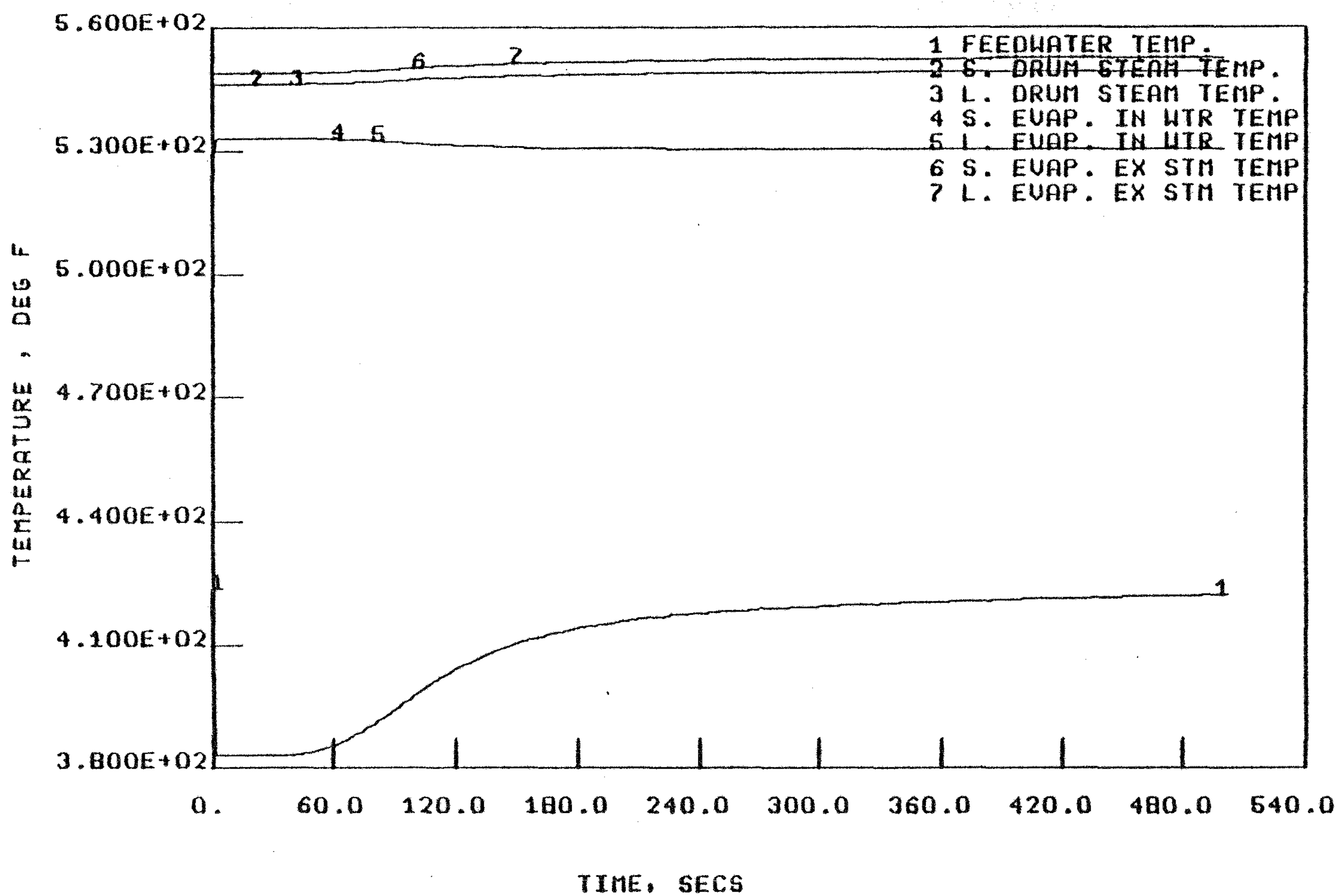

FIGURE 4-59

POOL REACTOR PLANT LOADING AT MAXIMUM RATE (CONSTANT SPEED PUMPS)
RUN DATED 10/13/78
NUMBER XEP6E00

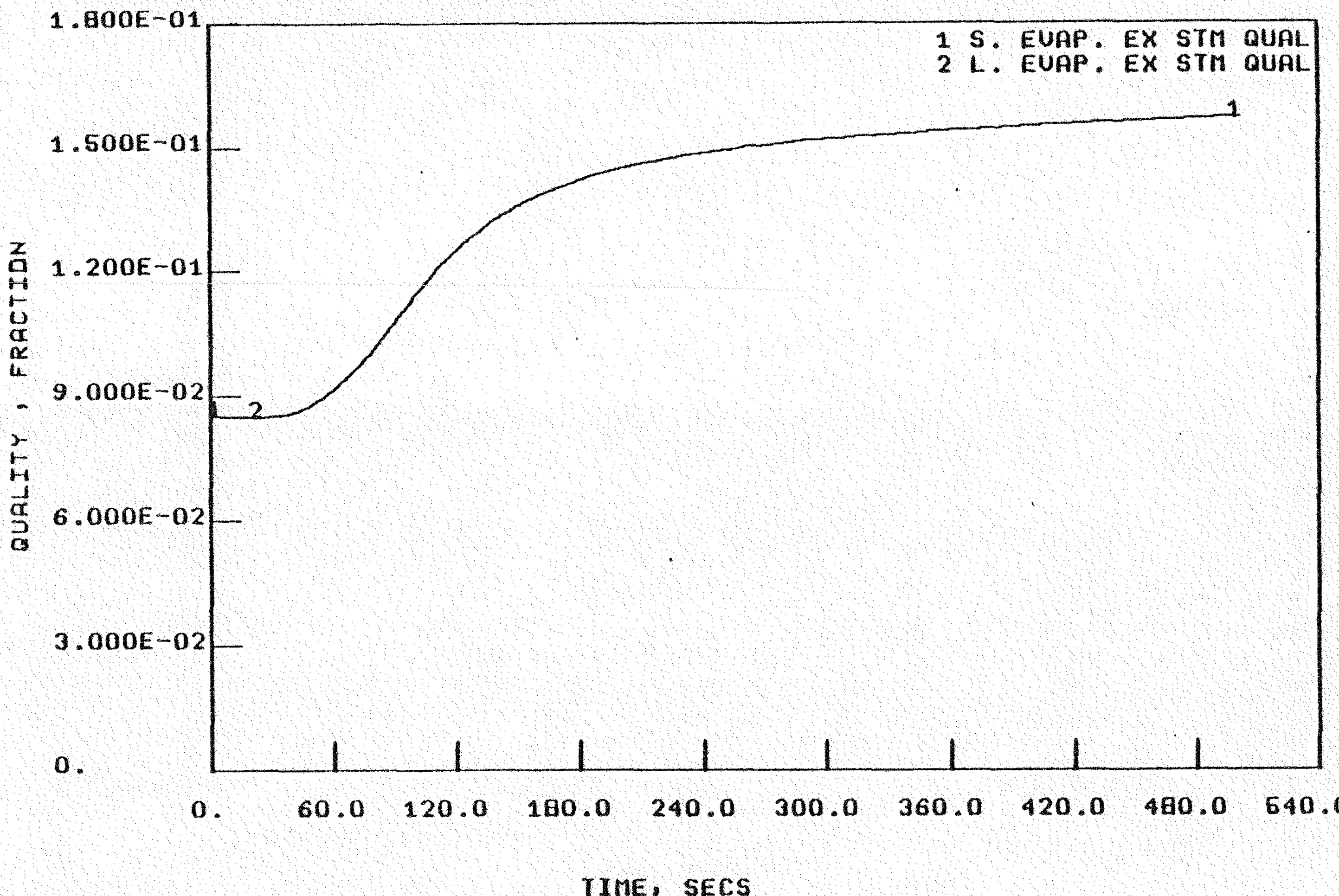

FIGURE 4-60
POOL REACTOR PLANT LOADING AT MAXIMUM RATE (CONSTANT SPEED PUMPS)
RUN DATED 10/13/78
NUMBER XEP6E00

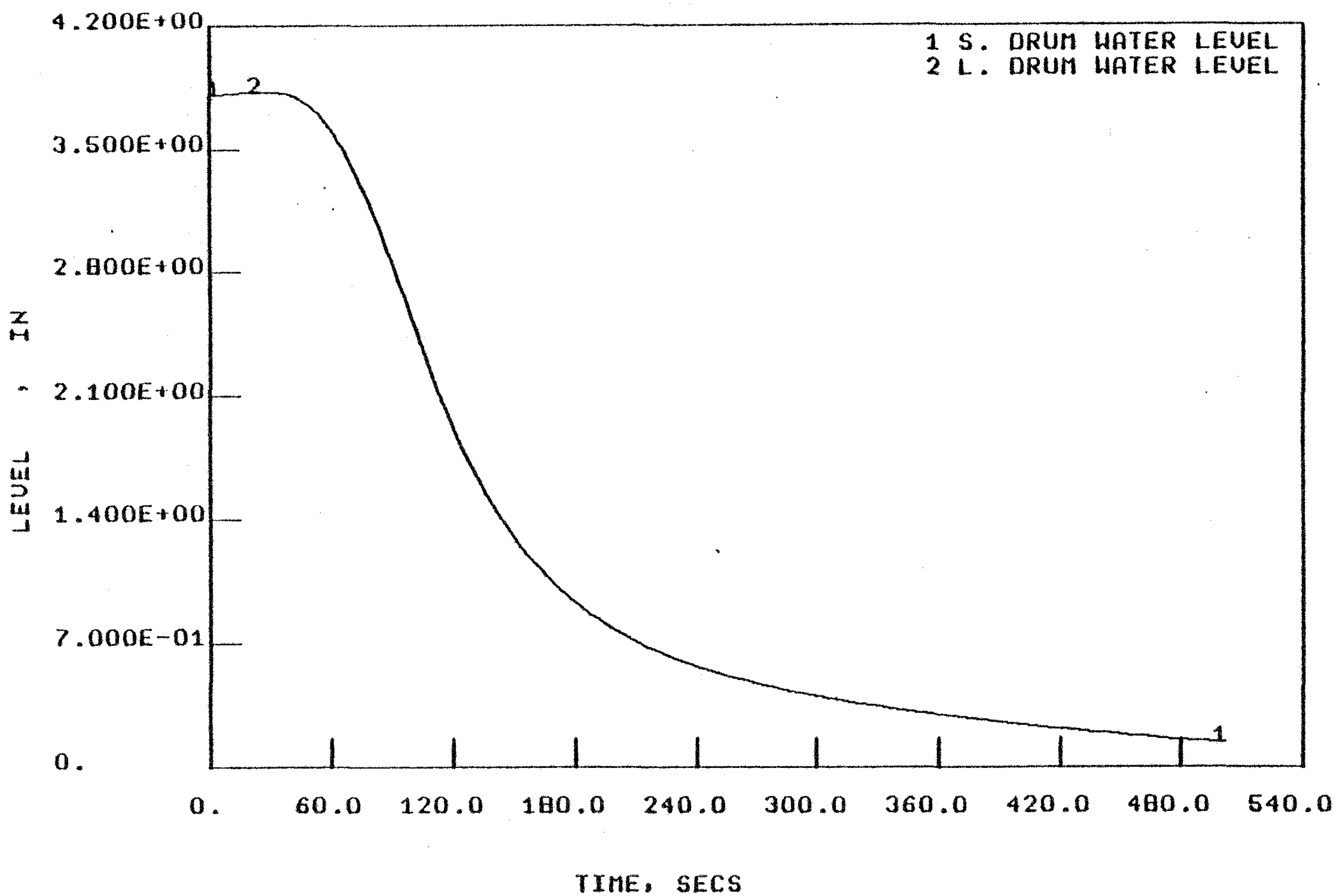

FIGURE 4-61
POOL REACTOR ISOLATION AND BLOWDOWN OF ONE STEAM GENERATOR
RUN DATED 10/04/78
NUMBER SUPGE01

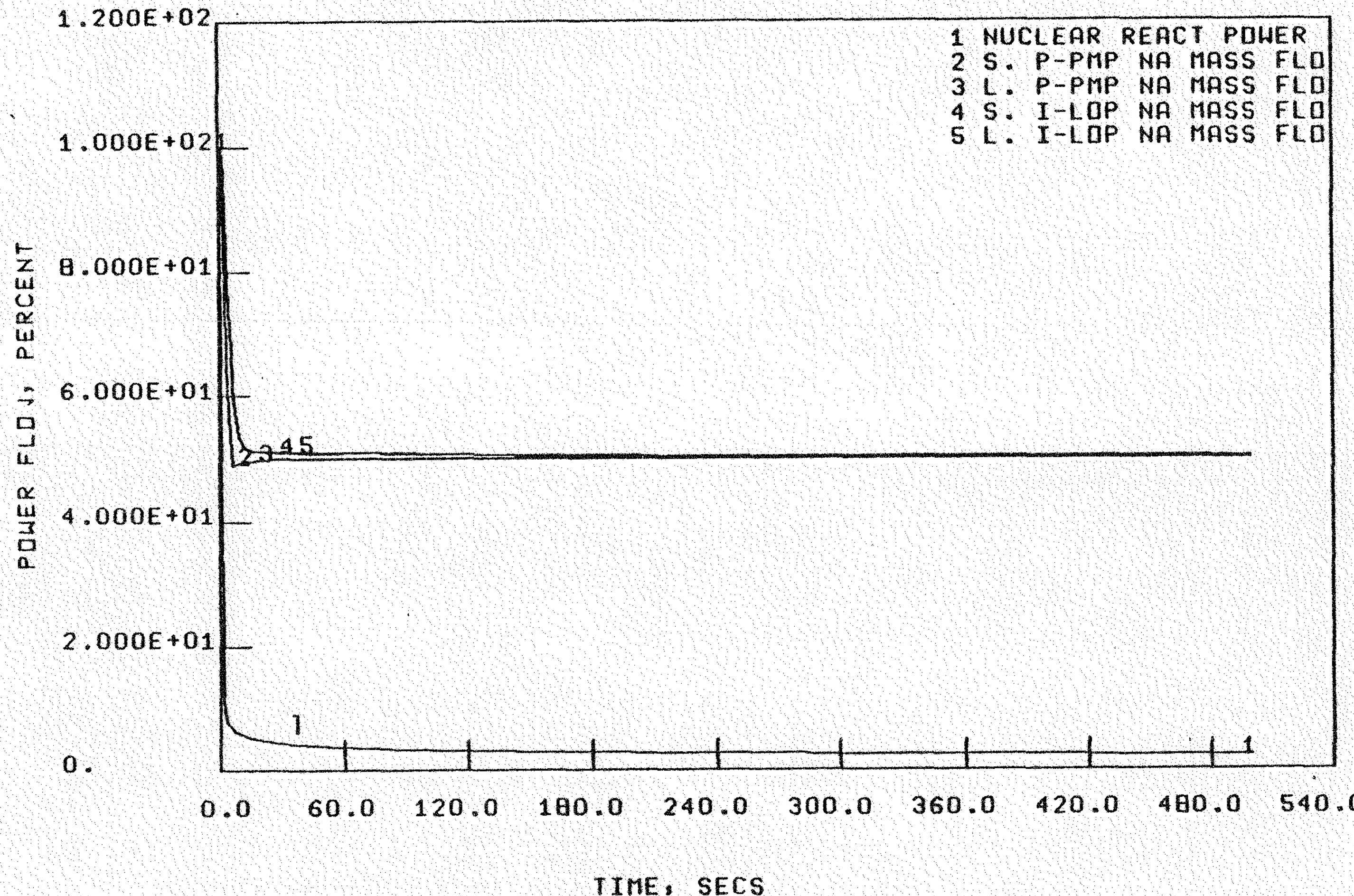

FIGURE 4-62

POOL REACTOR ISOLATION AND BLOWDOWN OF ONE STEAM GENERATOR
RUN DATED 10/04/78
NUMBER SUPGE01

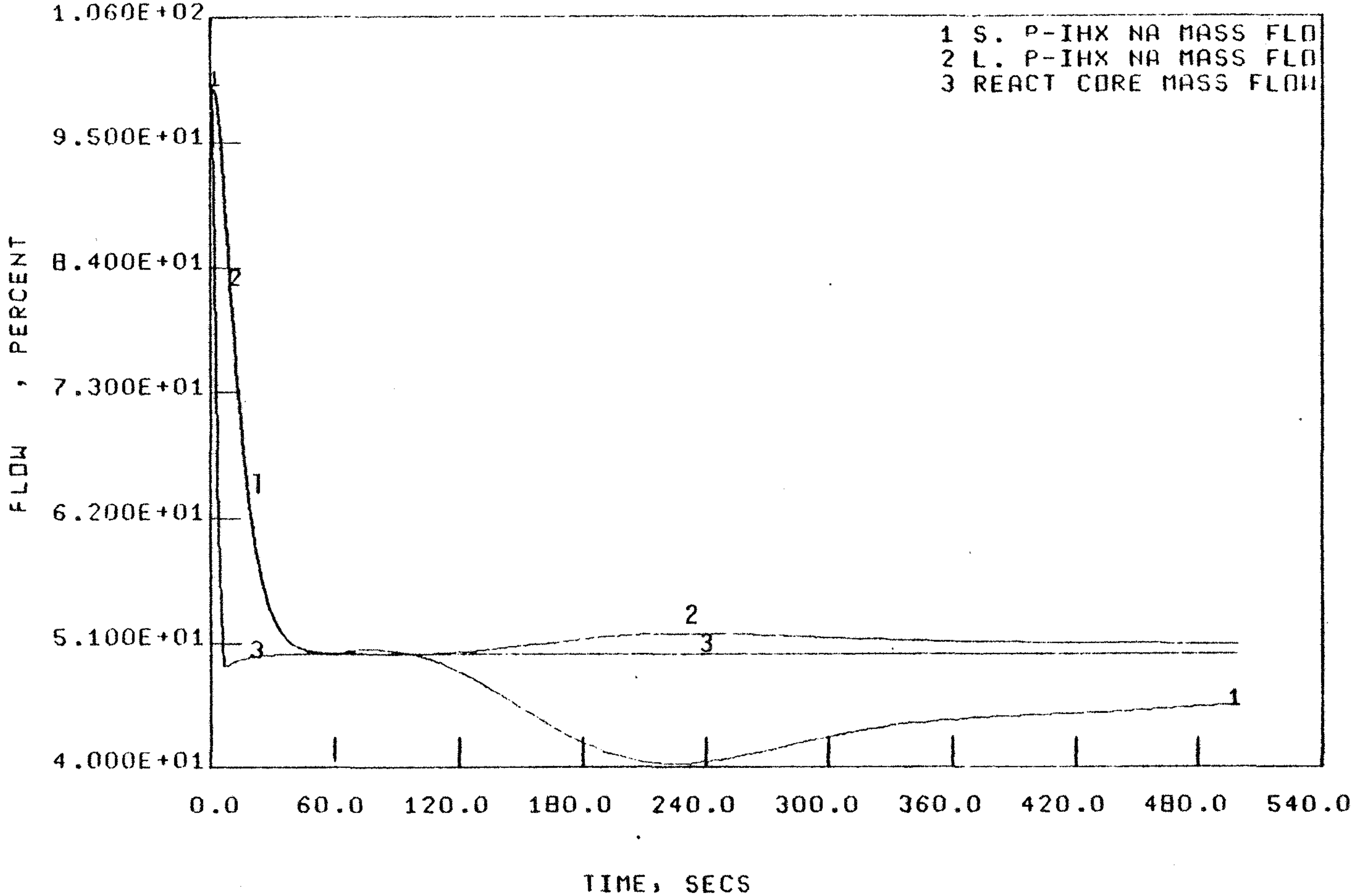

FIGURE 4-63
POOL REACTOR ISOLATION AND BLOWDOWN OF ONE STEAM GENERATOR
RUN DATED 10/04/78
NUMBER SUPGE01

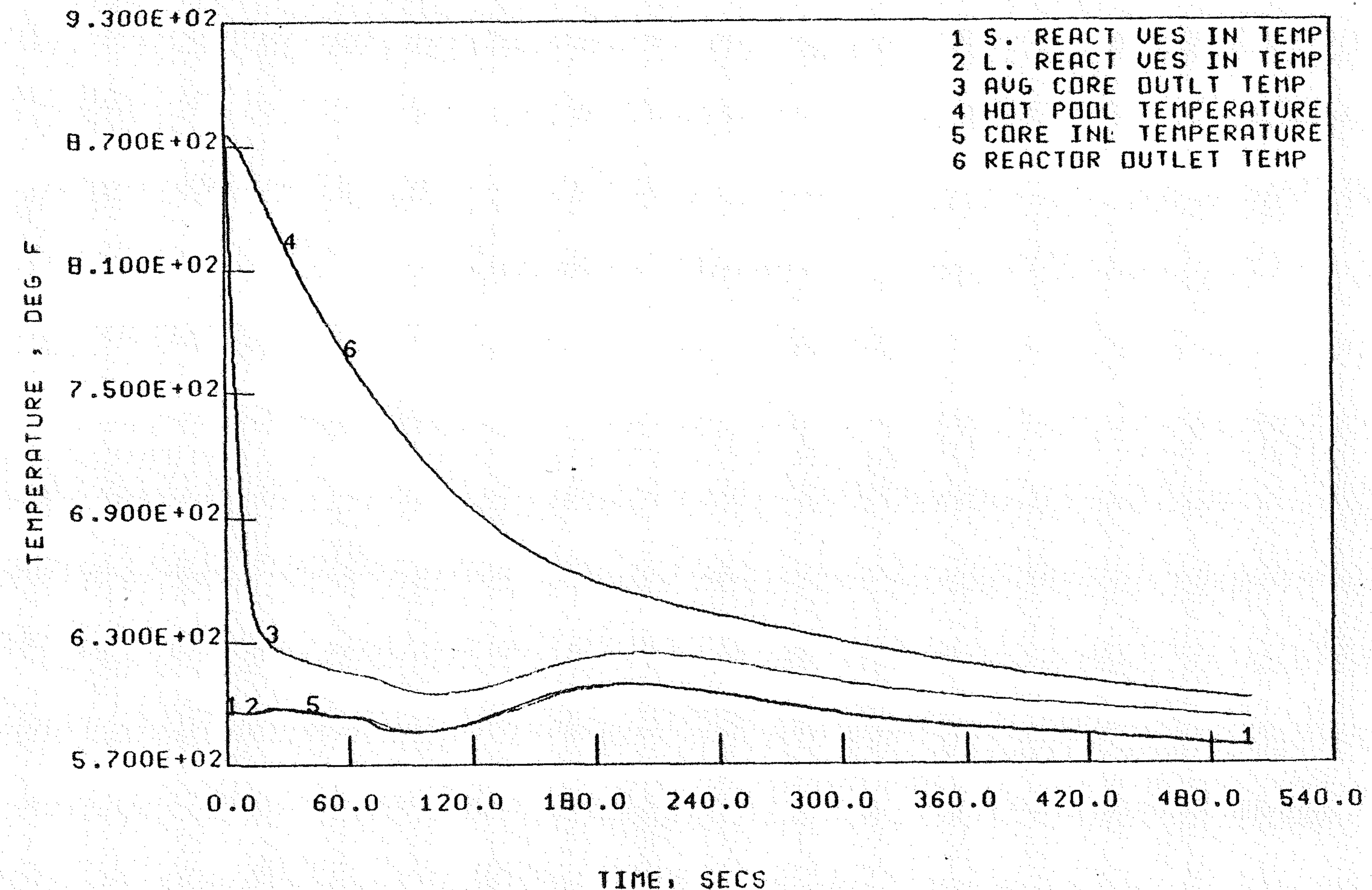

FIGURE 4-64

POOL REACTOR ISOLATION AND BLOWDOWN OF ONE STEAM GENERATOR
RUN DATED 10/04/78
NUMBER SUPGE01

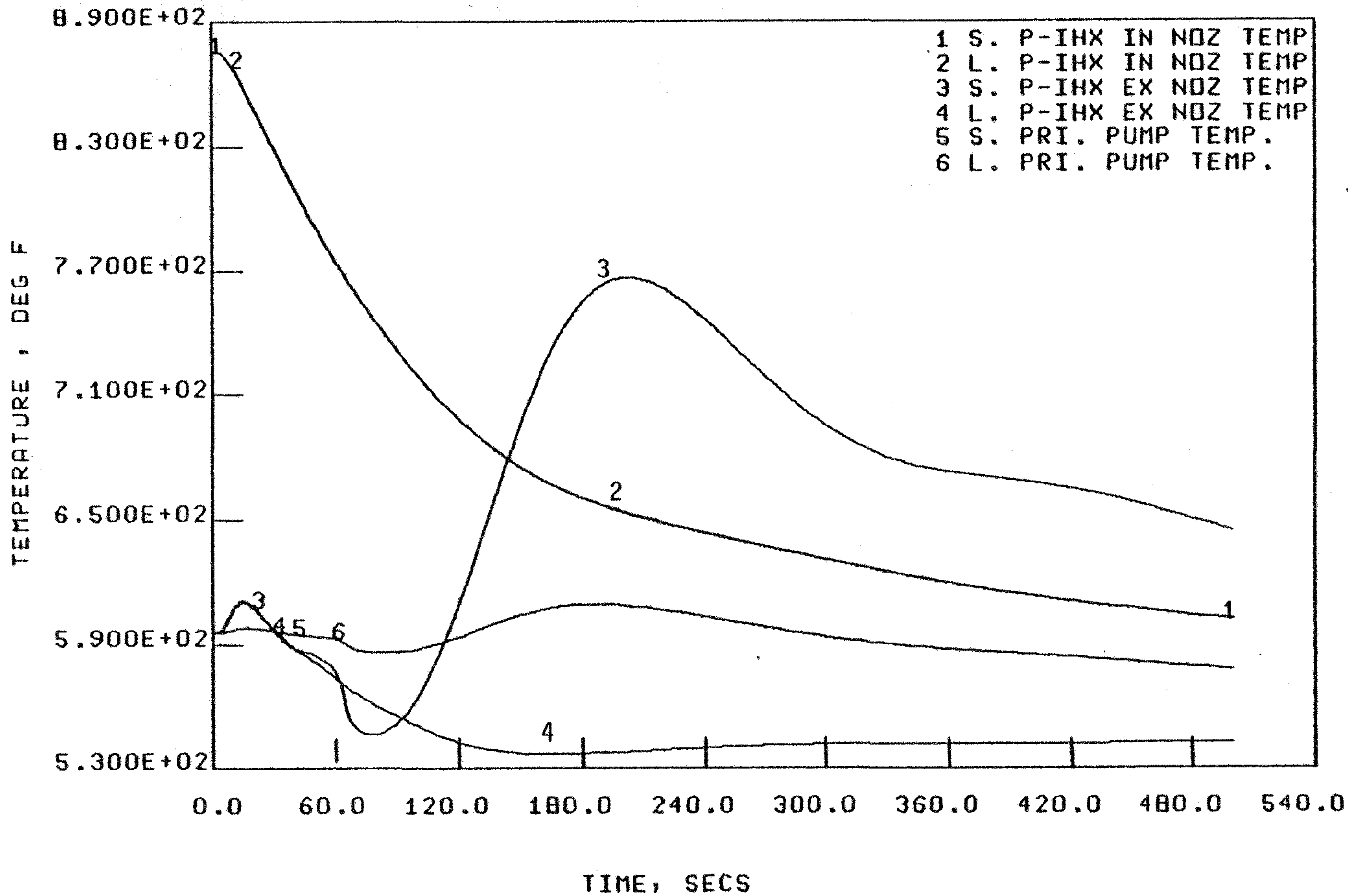

FIGURE 6-65

POOL REACTOR ISOLATION AND BLOWDOWN OF ONE STEAM GENERATOR
RUN DATED 10/04/78
NUMBER SUPGE01

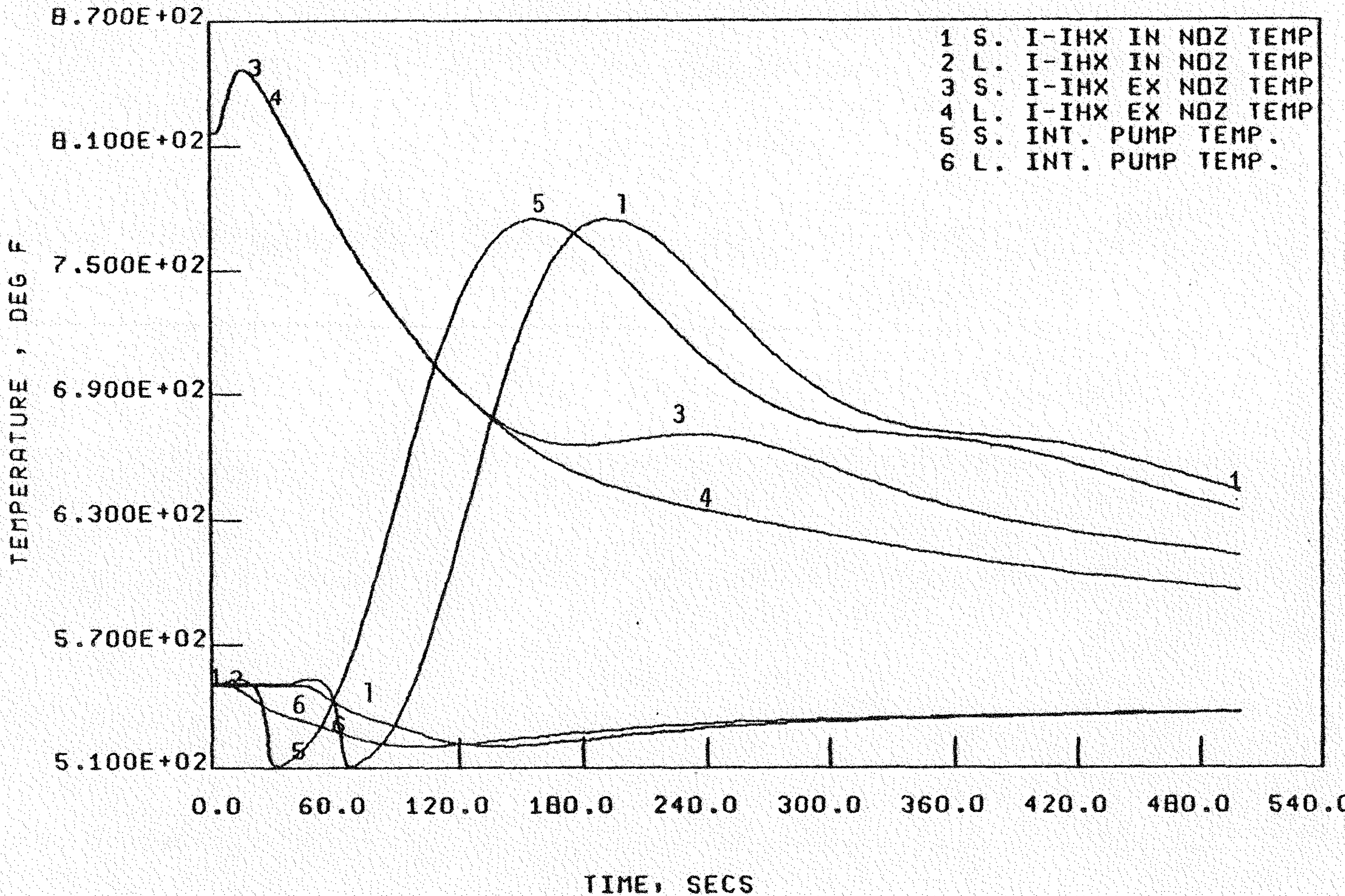

FIGURE 4-66

POOL REACTOR ISOLATION AND BLOWDOWN OF ONE STEAM GENERATOR
RUN DATED 10/04/78
NUMBER SUPGE01

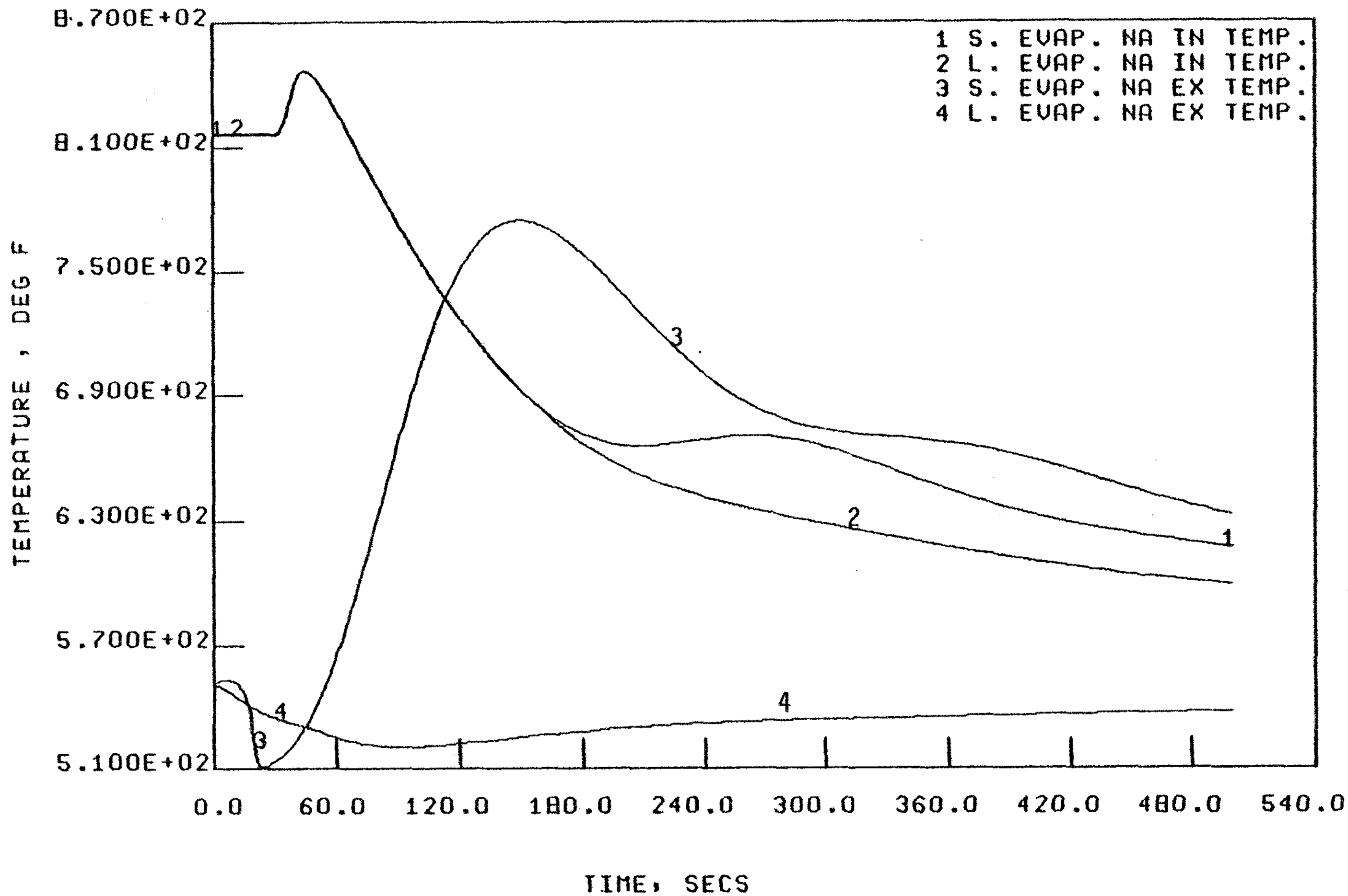

FIGURE 4-67
POOL REACTOR ISOLATION AND BLOWDOWN OF ONE STEAM GENERATOR
RUN DATED 10/04/78
NUMBER SUPGE01

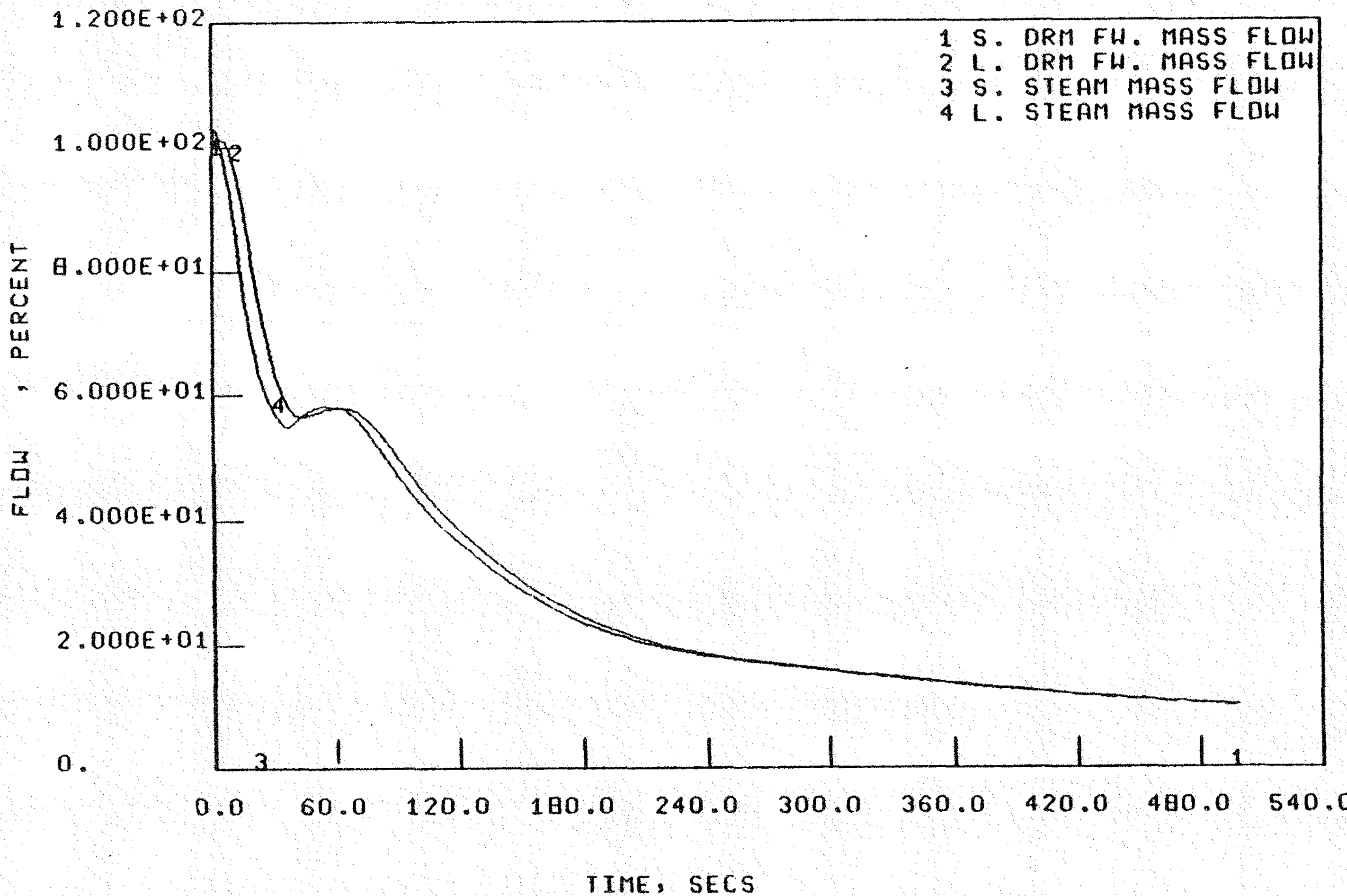

FIGURE 4-68
POOL REACTOR ISOLATION AND BLOWDOWN OF ONE STEAM GENERATOR
RUN DATED 10/04/78
NUMBER SUPGE01

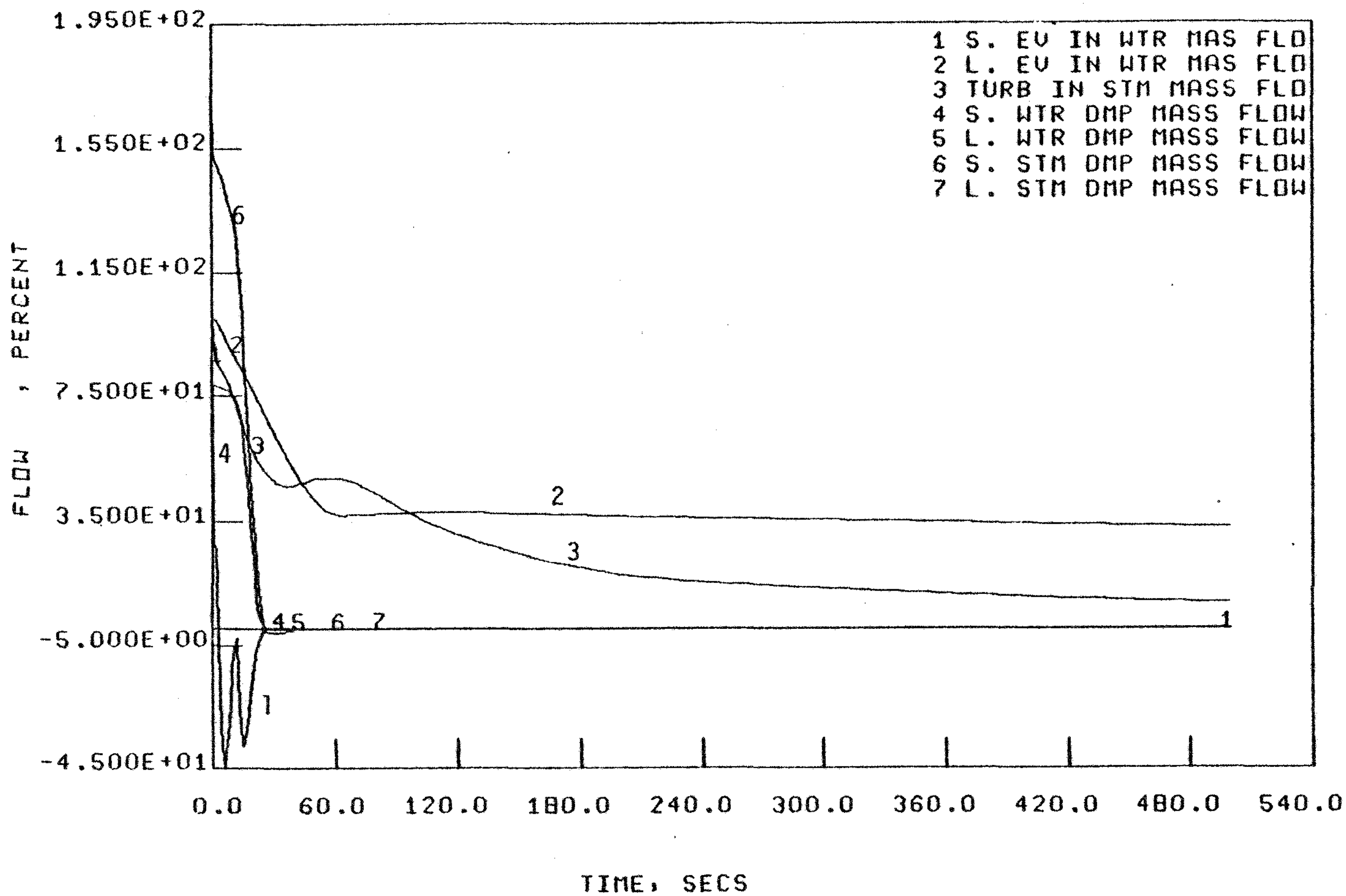

FIGURE 4-69

POOL REACTOR ISOLATION AND BLOWDOWN OF ONE STEAM GENERATOR
RUN DATED 10/04/78
NUMBER SUPGE01

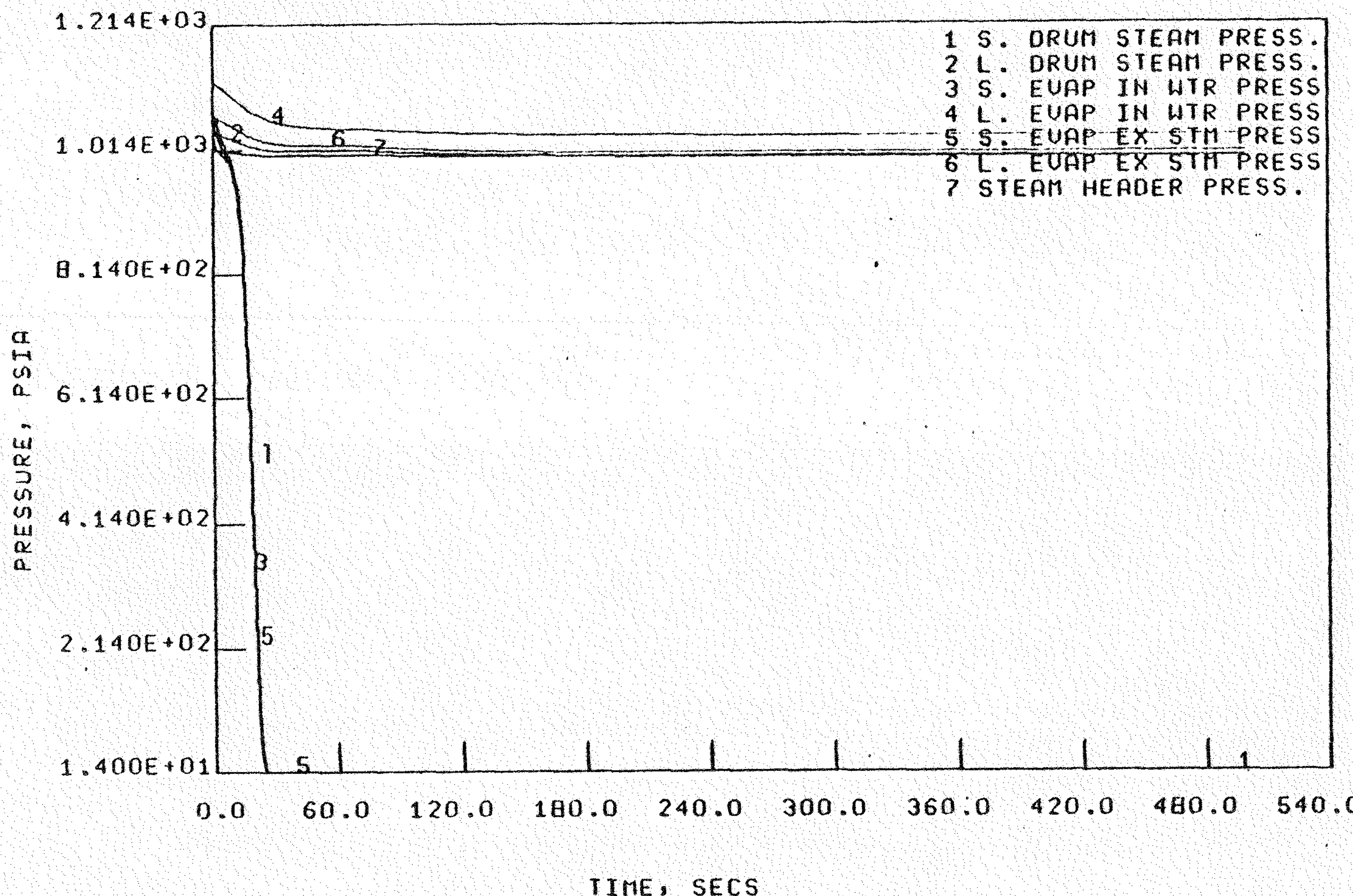

FIGURE 4-70

POOL REACTOR ISOLATION AND BLOWDOWN OF ONE STEAM GENERATOR

RUN DATED 10/04/78

NUMBER SUPGE01

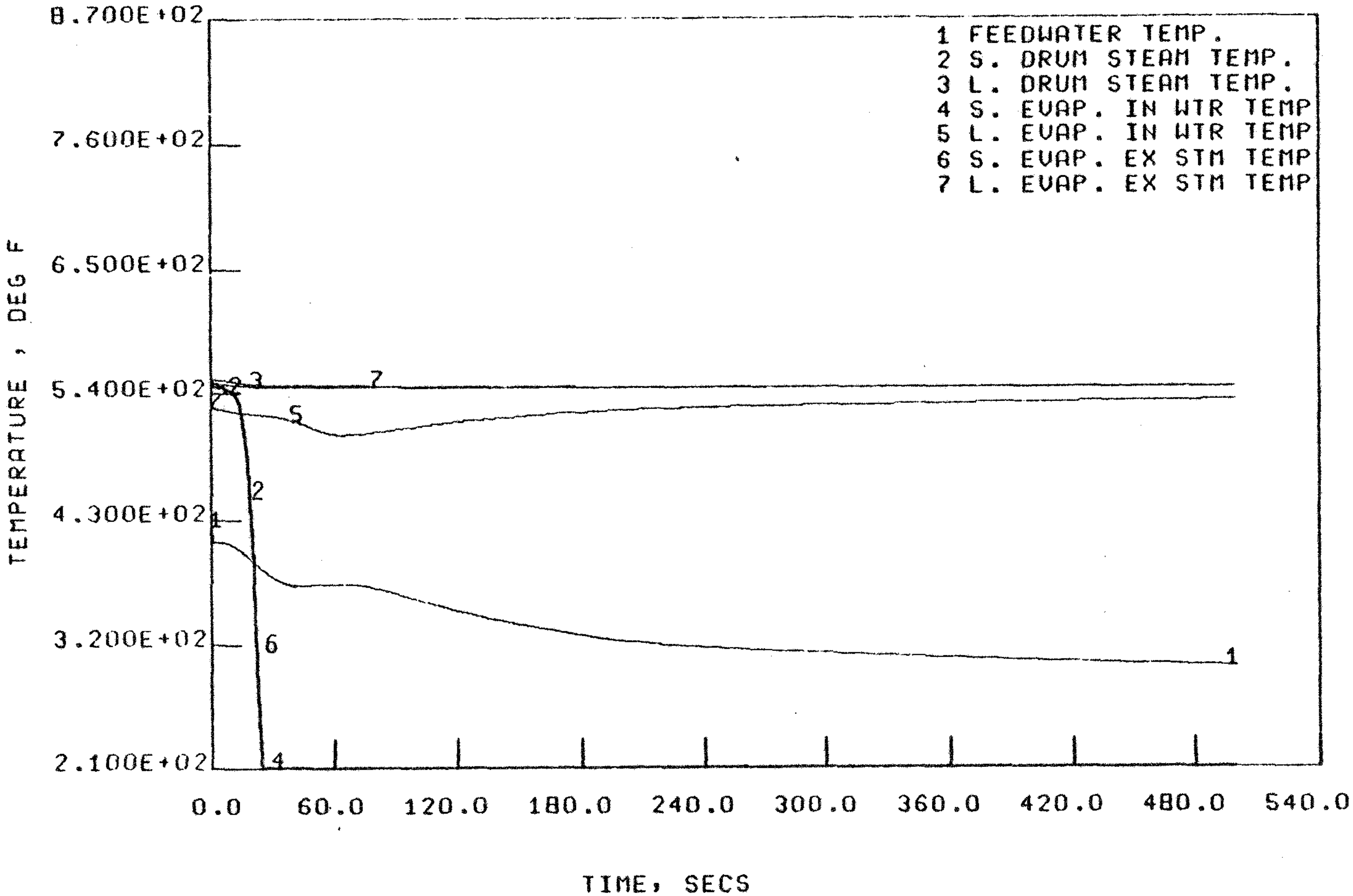

FIGURE 4-71
POOL REACTOR ISOLATION AND BLOWDOWN OF ONE STEAM GENERATOR
RUN DATED 10/04/78
NUMBER SUPGE01

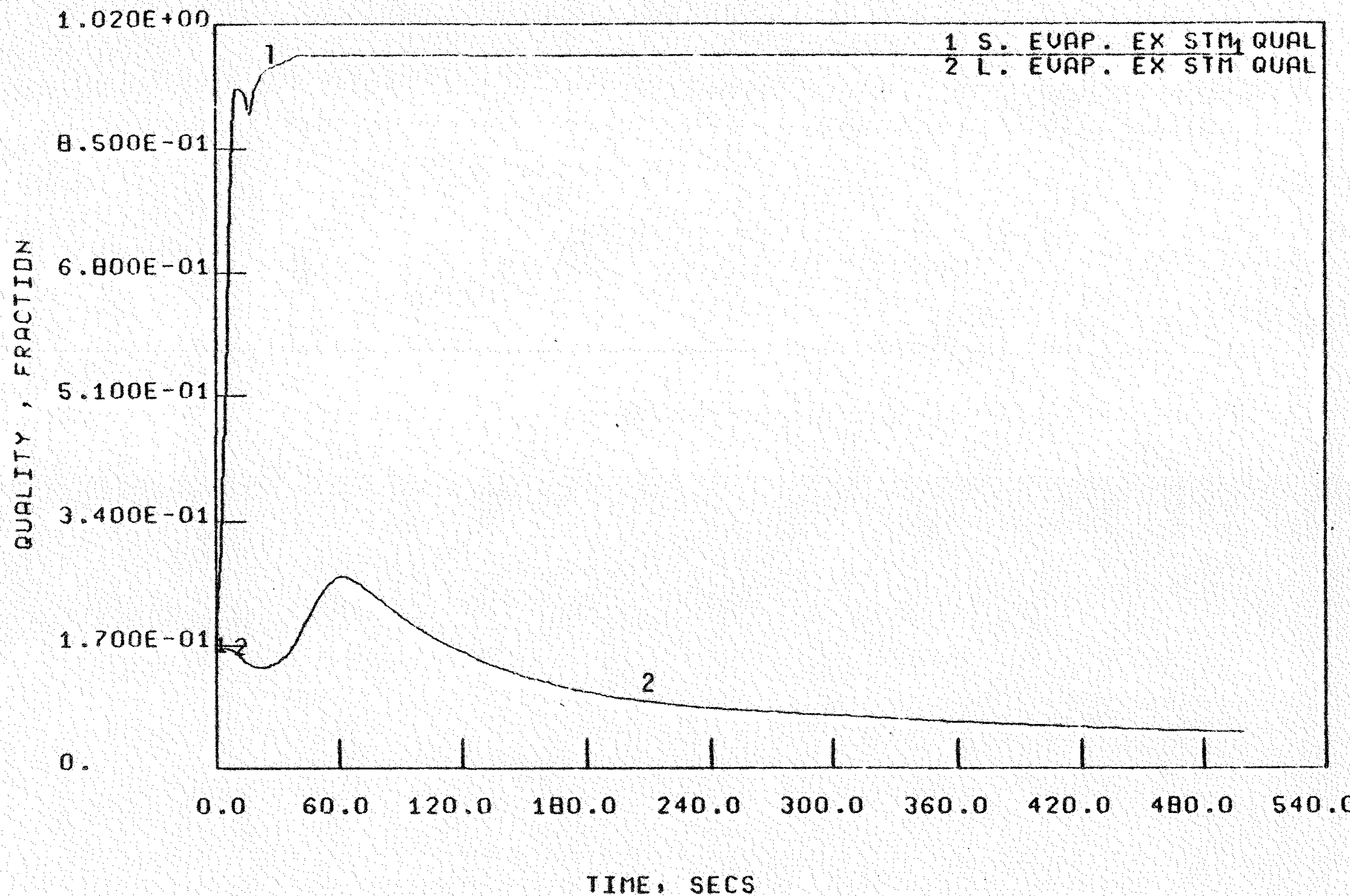

FIGURE 4-72
POOL REACTOR ISOLATION AND BLOWDOWN OF ONE STEAM GENERATOR
RUN DATED 10/04/78
NUMBER SUPGE01

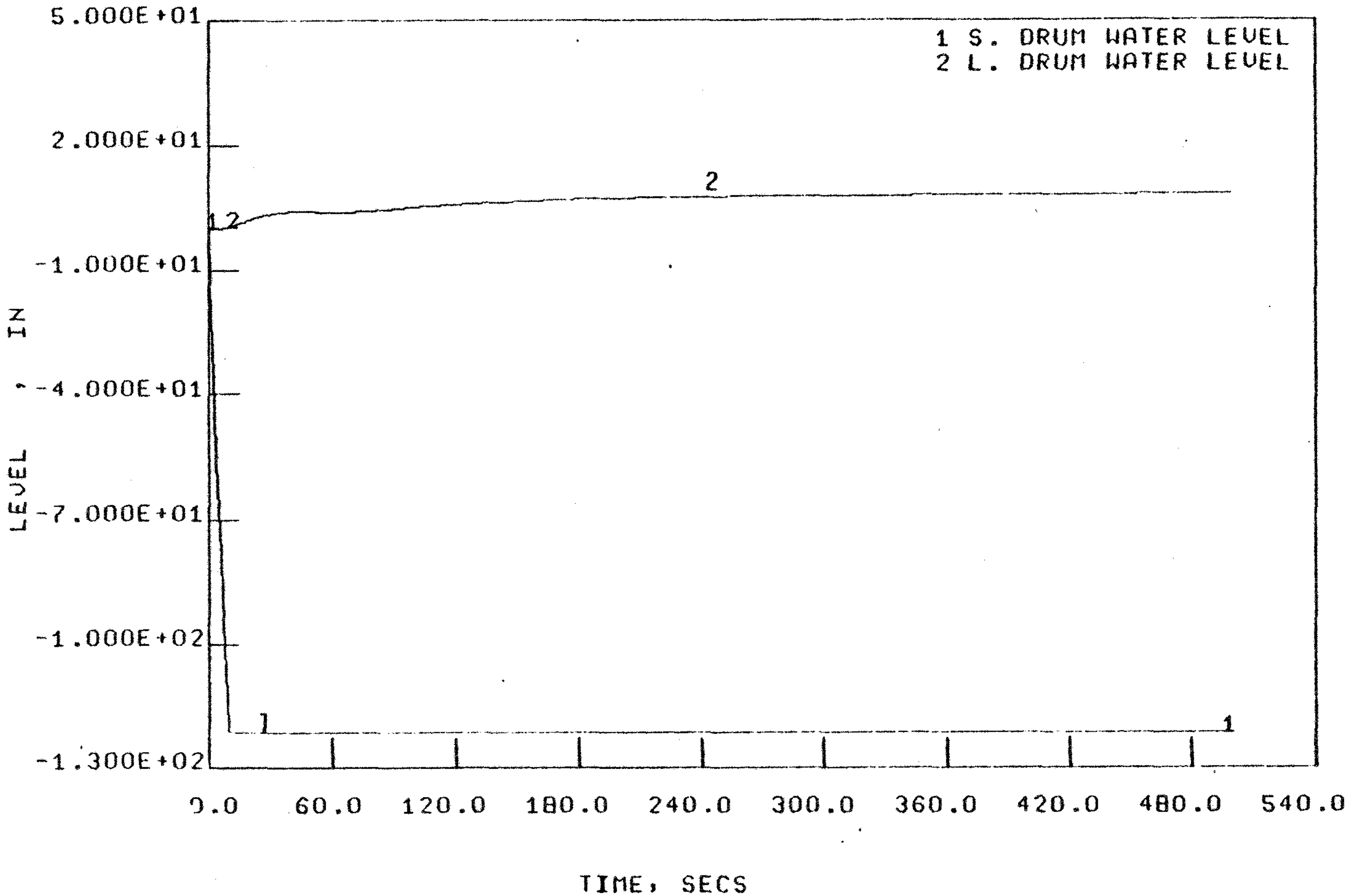

FIGURE 4-73
POOL REACTOR ISOLATION AND BLOWDOWN OF ONE STEAM GENERATOR
RUN DATED 11/20/78
NUMBER SUPGE00

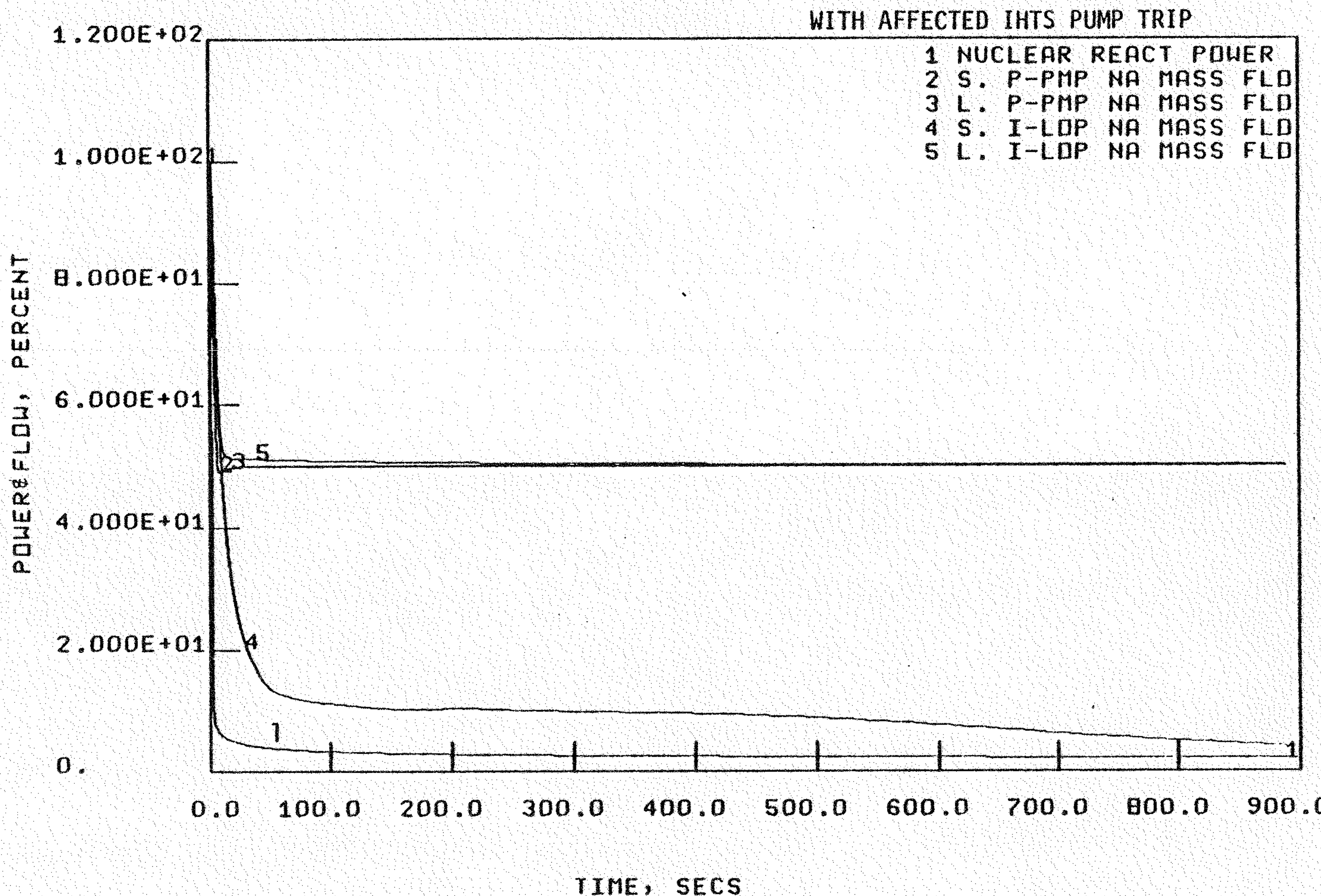

FIGURE 4-74

POOL REACTOR ISOLATION AND FL... STEAM GENERATO...

RUN DATED 11/20/78

NUMBER SUPGEOU

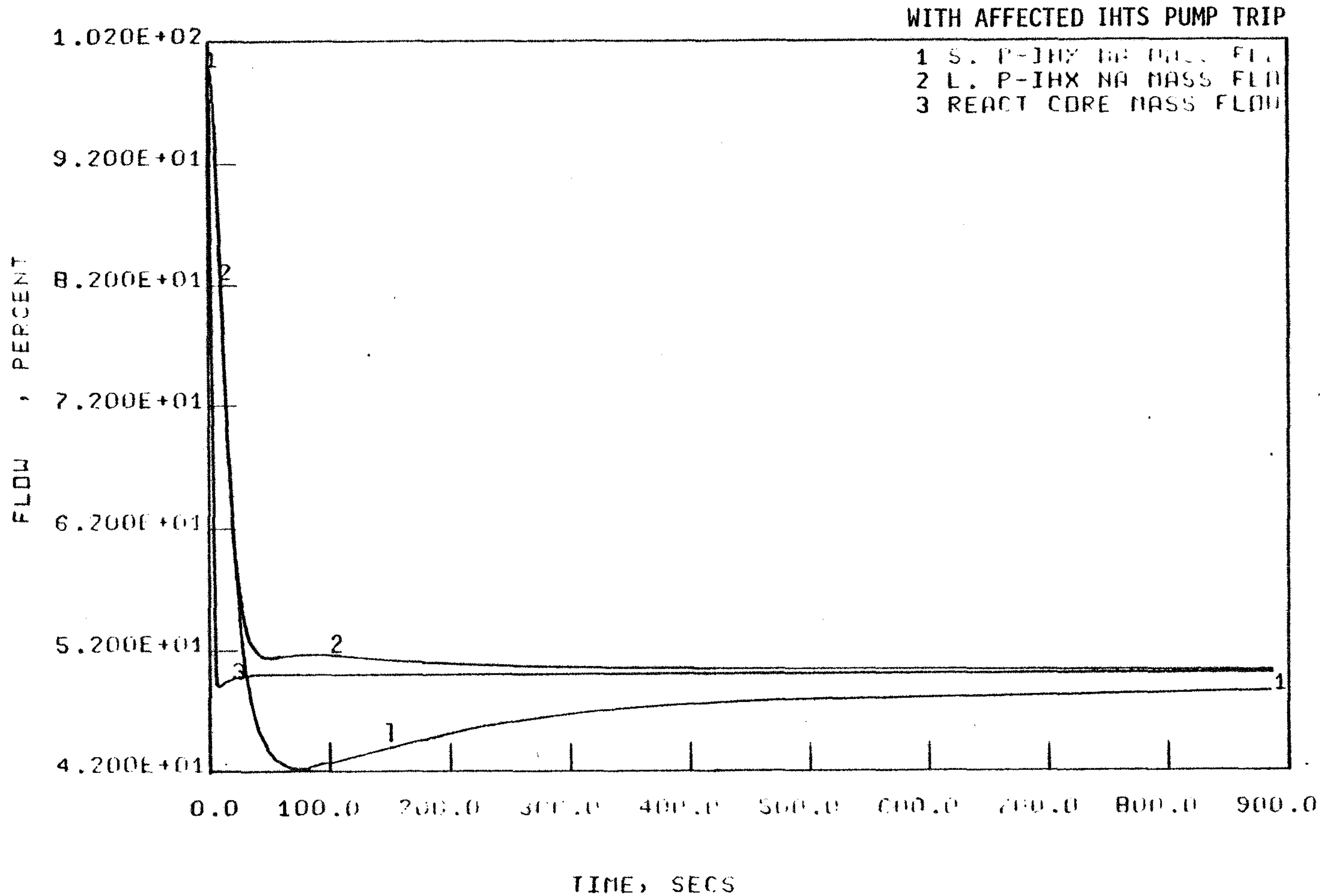

V-2.3-93

FIGURE 4-75

POOL REACTOR ISOLATION AND BLOWDOWN OF ONE STEAM GENERATOR
RUN DATED 11/20/78
NUMBER SURGE00

WITH AFFECTED IHTS PUMP TRIP

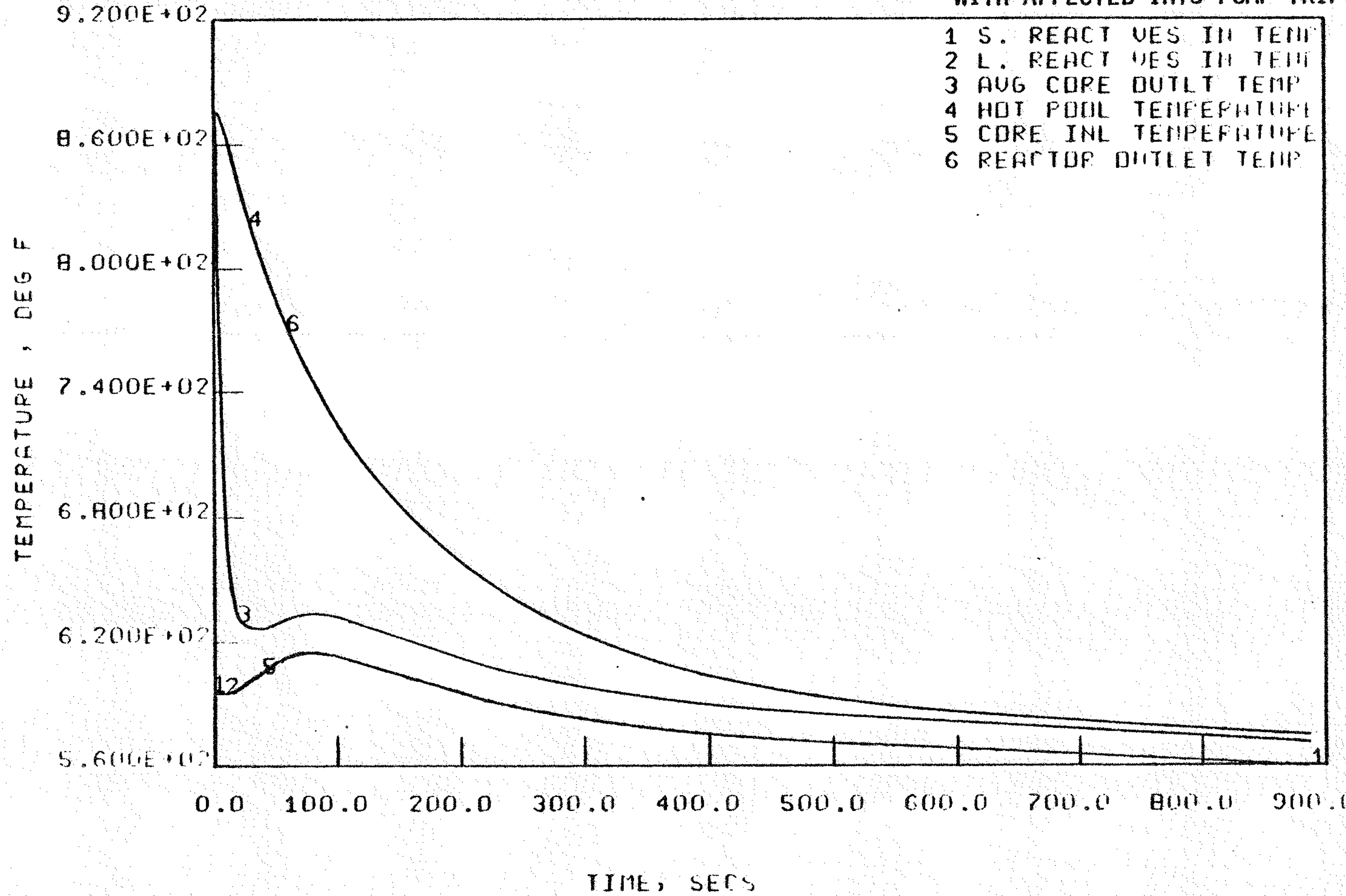

FIGURE 4-76
POOL REACTOR ISOLATION AND BLOWDOWN OF ONE STEAM GENERATOR
RUN DATED 11/20/78
NUMBER SUPGE00

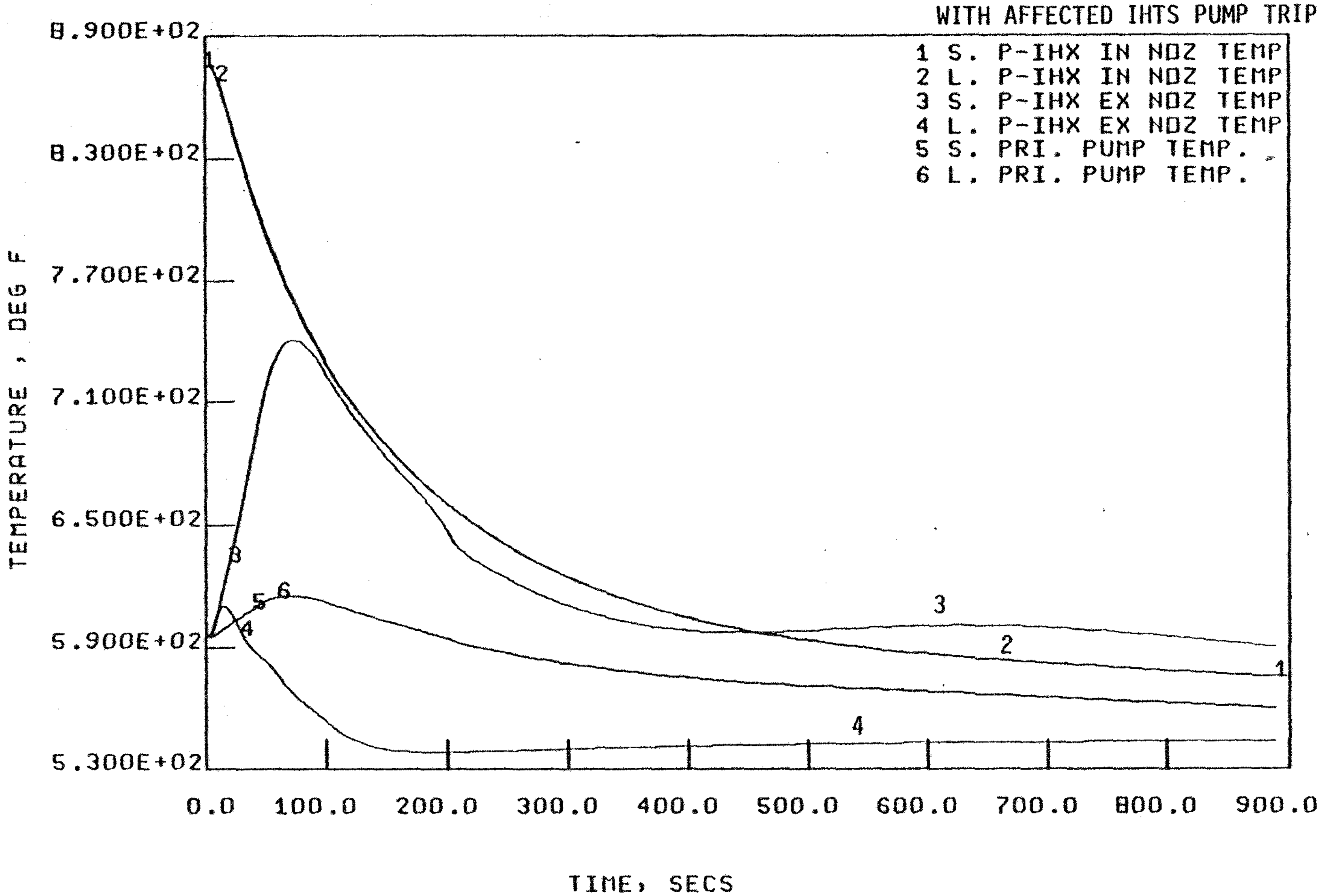

FIGURE 4-77
POOL REACTOR ISOLATION AND BLOWDOWN OF ONE STEAM GENERATOR
RUN DATED 11/20/78
NUMBER SUPGE00

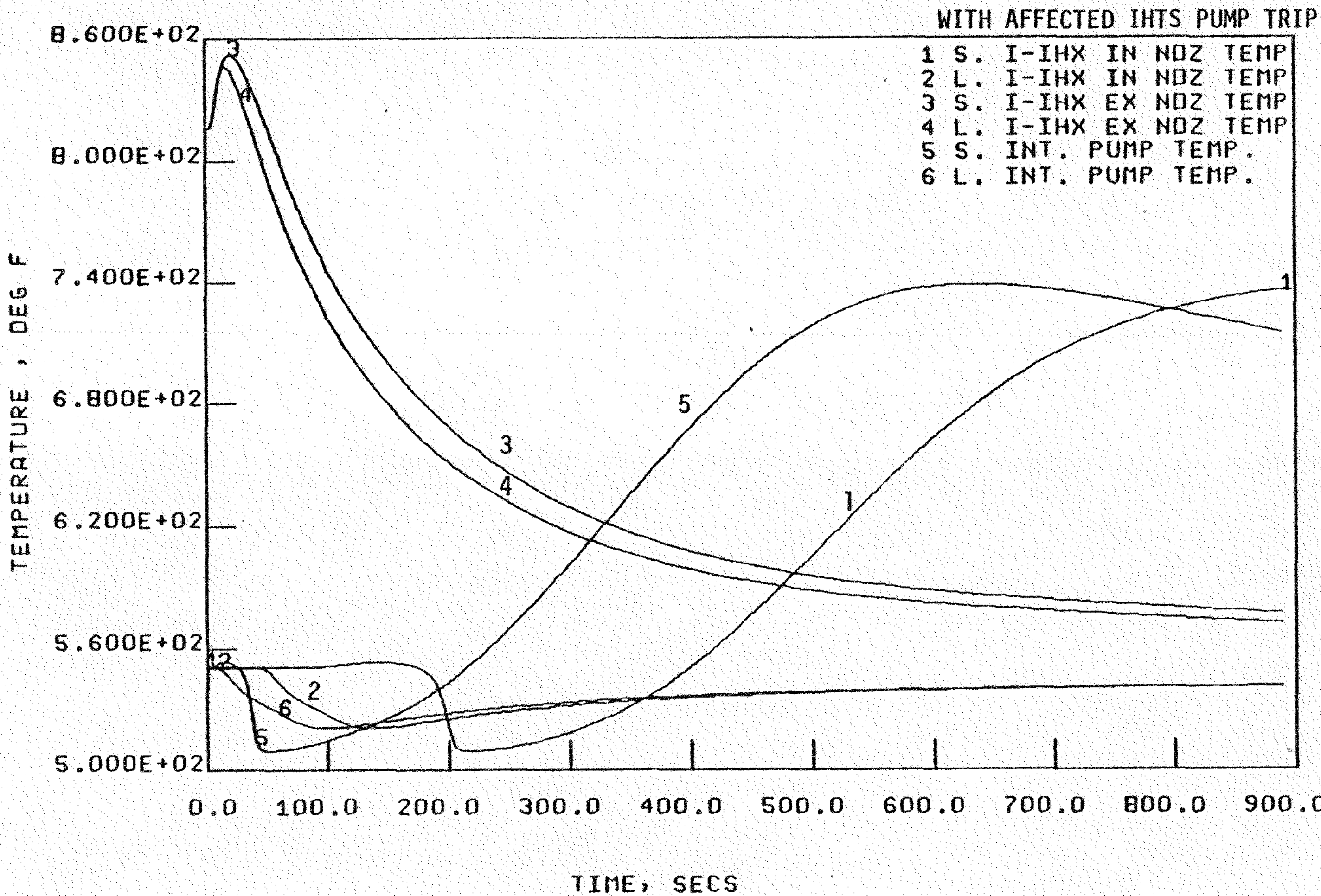

FIGURE 4-78
POOL REACTOR ISOLATION AND BLOWDOWN OF ONE STEAM GENERATOR
RUN DATED 11/20/78
NUMBER SUPGE00

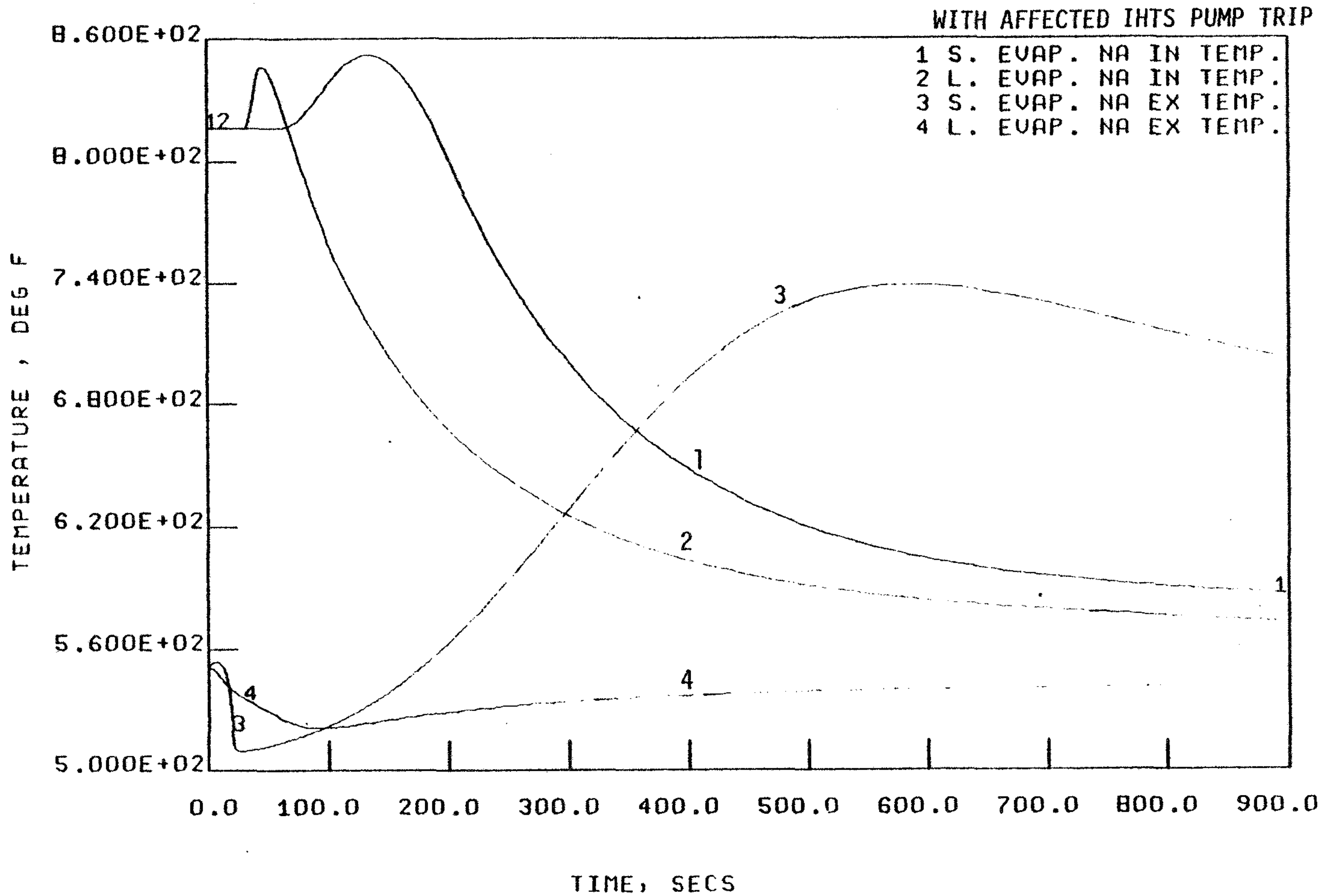

FIGURE 4-79
POOL REACTOR ISOLATION AND BLOWDOWN OF ONE STEAM GENERATOR
RUN DATED 11/20/78
NUMBER SUPGE00

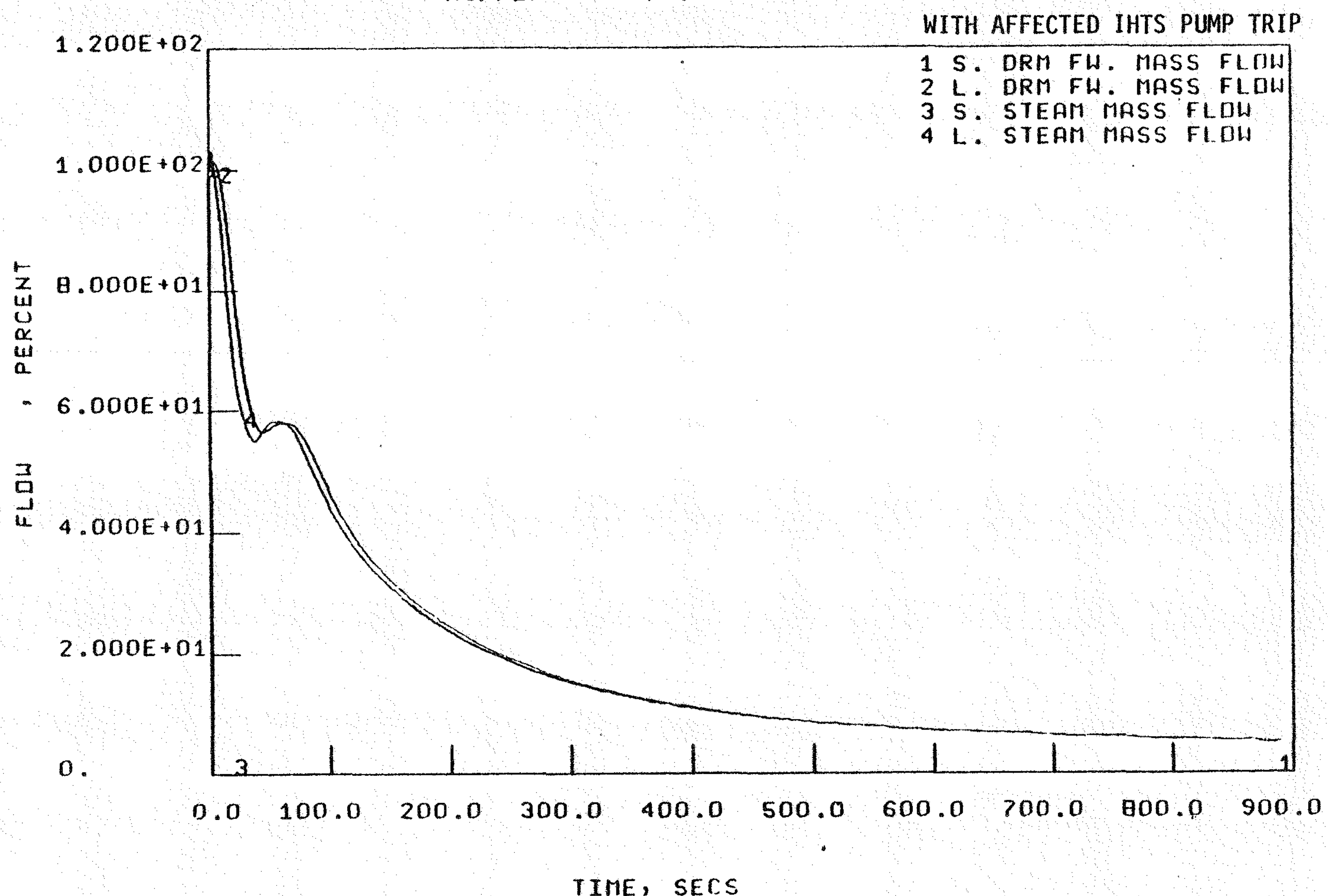

FIGURE 4-80
POOL REACTOR ISOLATION AND BLOWDOWN OF ONE STEAM GENERATOR
RUN DATED 11/20/78
NUMBER SUPGEO0

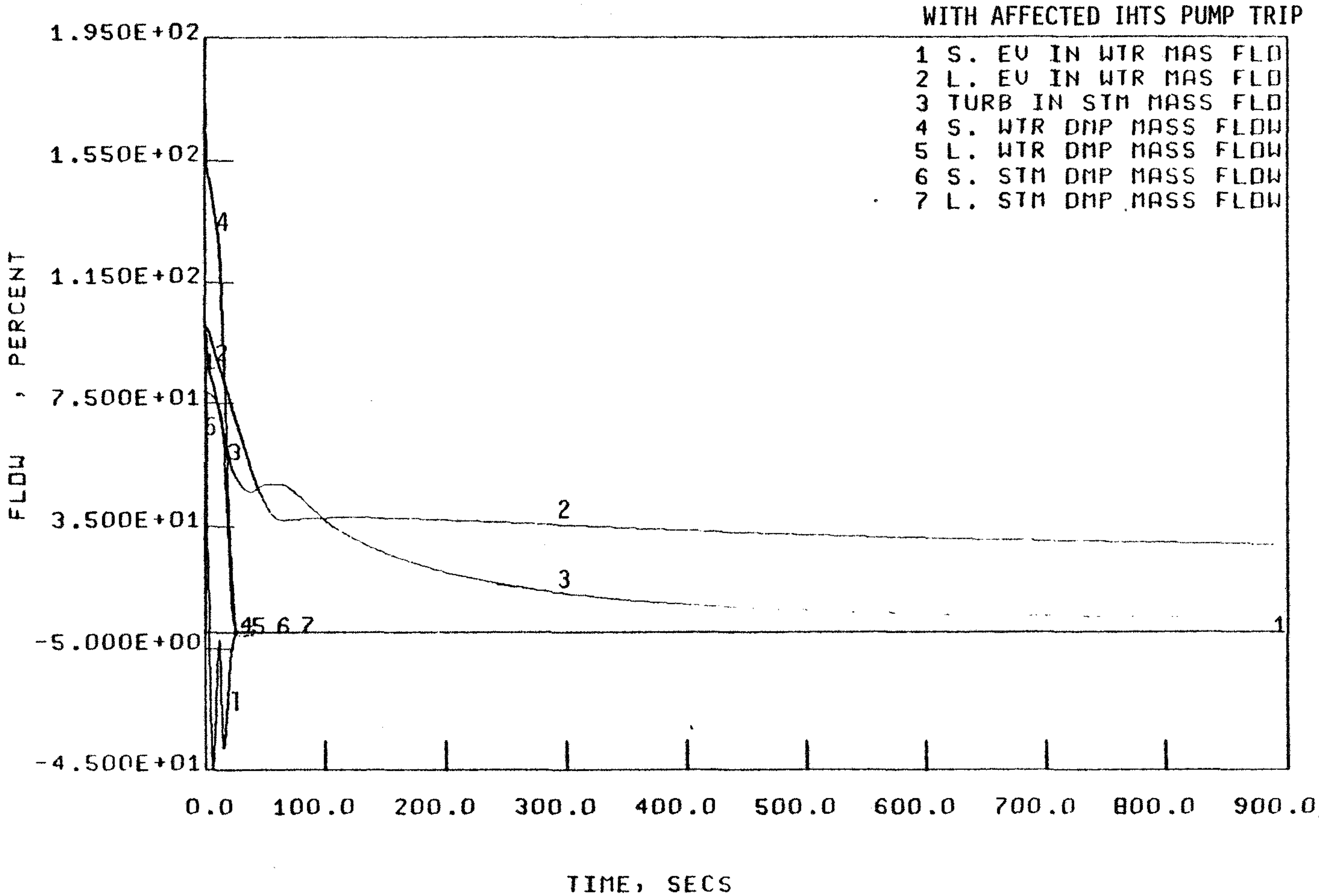

FIGURE 4-81
POOL REACTOR ISOLATION AND BLOWDOWN OF ONE STEAM GENERATOR
RUN DATED 11/20/78
NUMBER SUPGE00

WITH AFFECTED IHTS PUMP TRIP

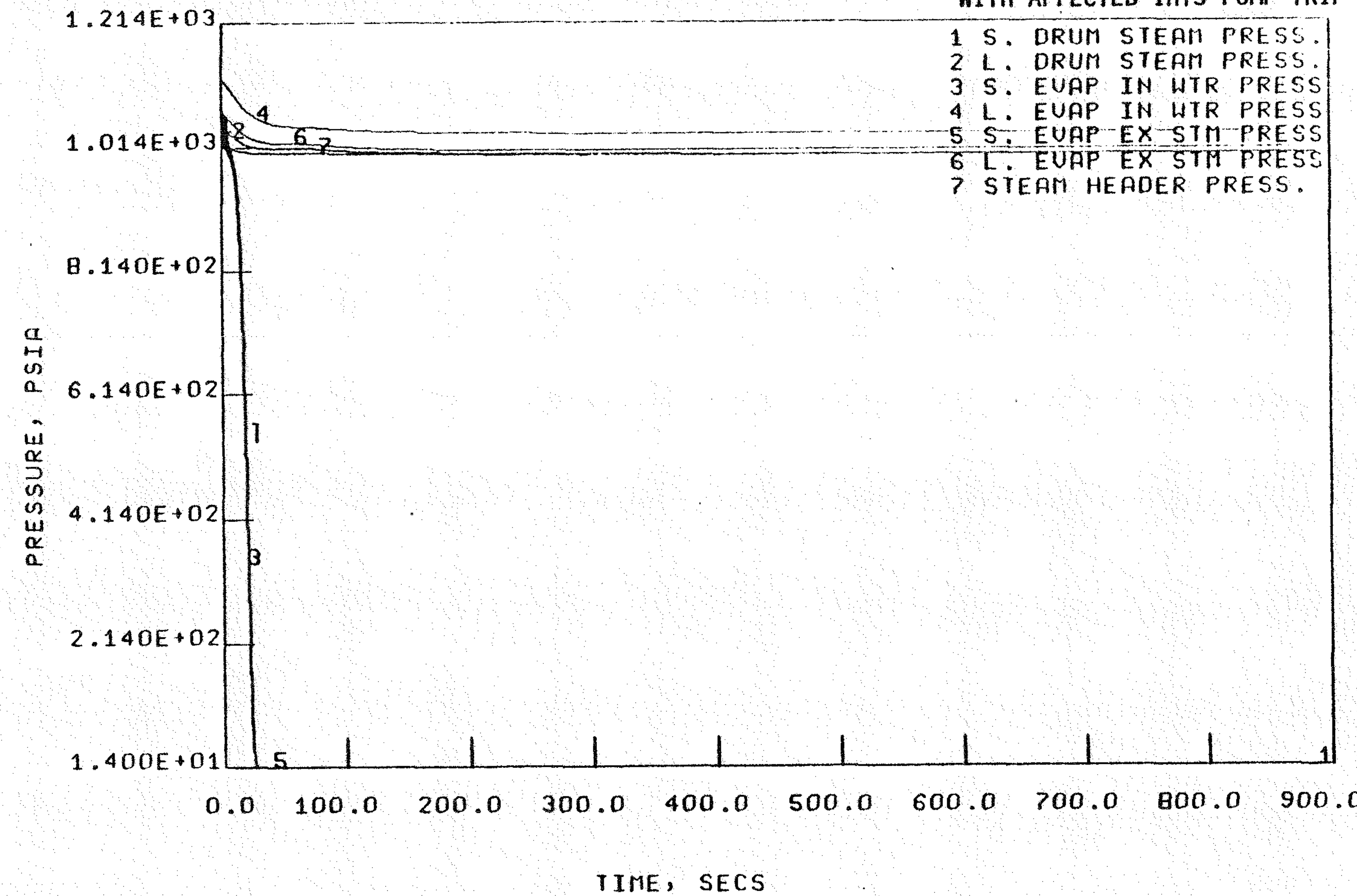

FIGURE 4-82
POOL REACTOR ISOLATION AND BLOWDOWN OF ONE STEAM GENERATOR
RUN DATED 11/20/78
NUMBER SUPGE00

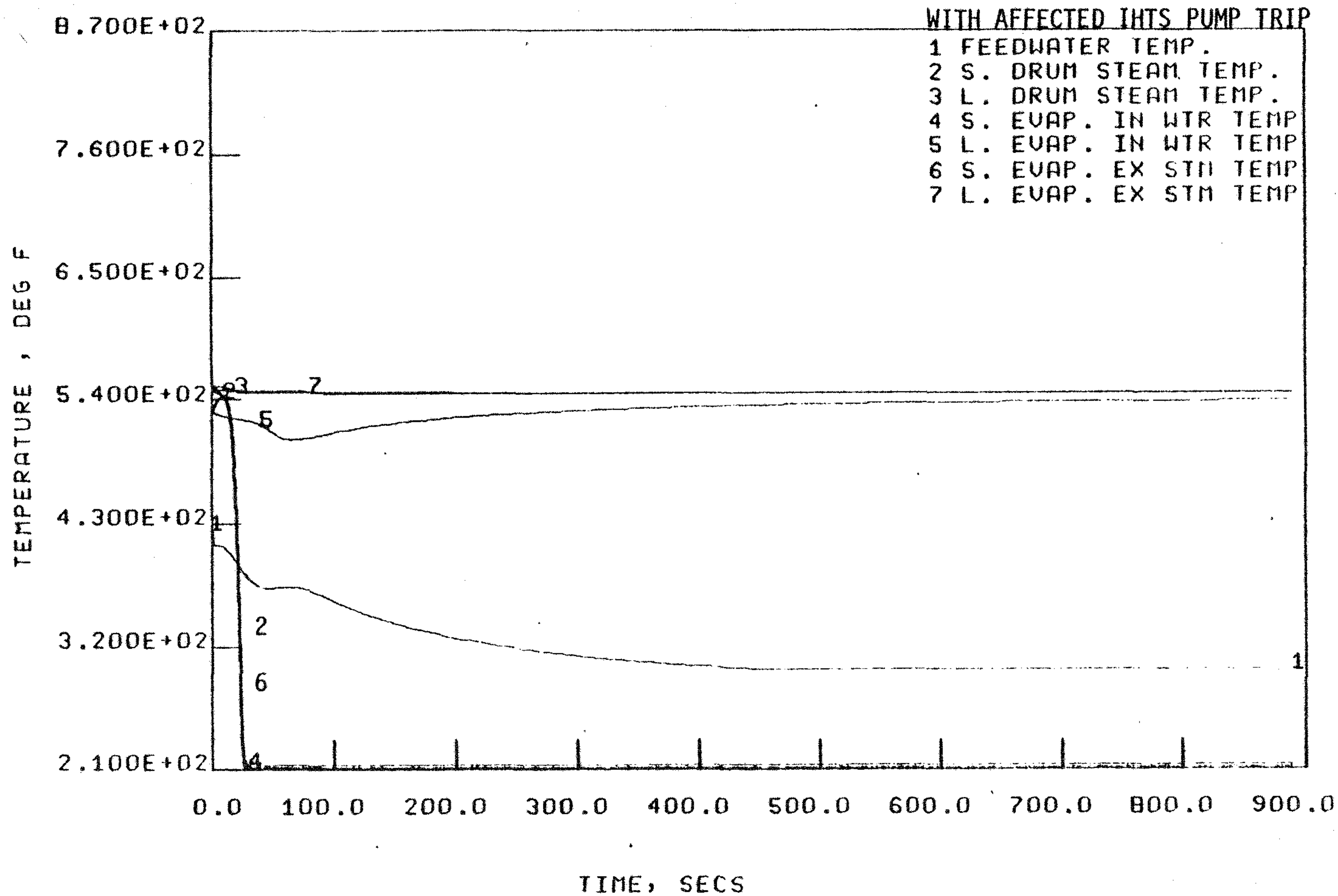

FIGURE 4-83
POOL REACTOR ISOLATION AND BLOWDOWN OF ONE STEAM GENERATOR
RUN DATED 11/20/78
NUMBER SUPGE00

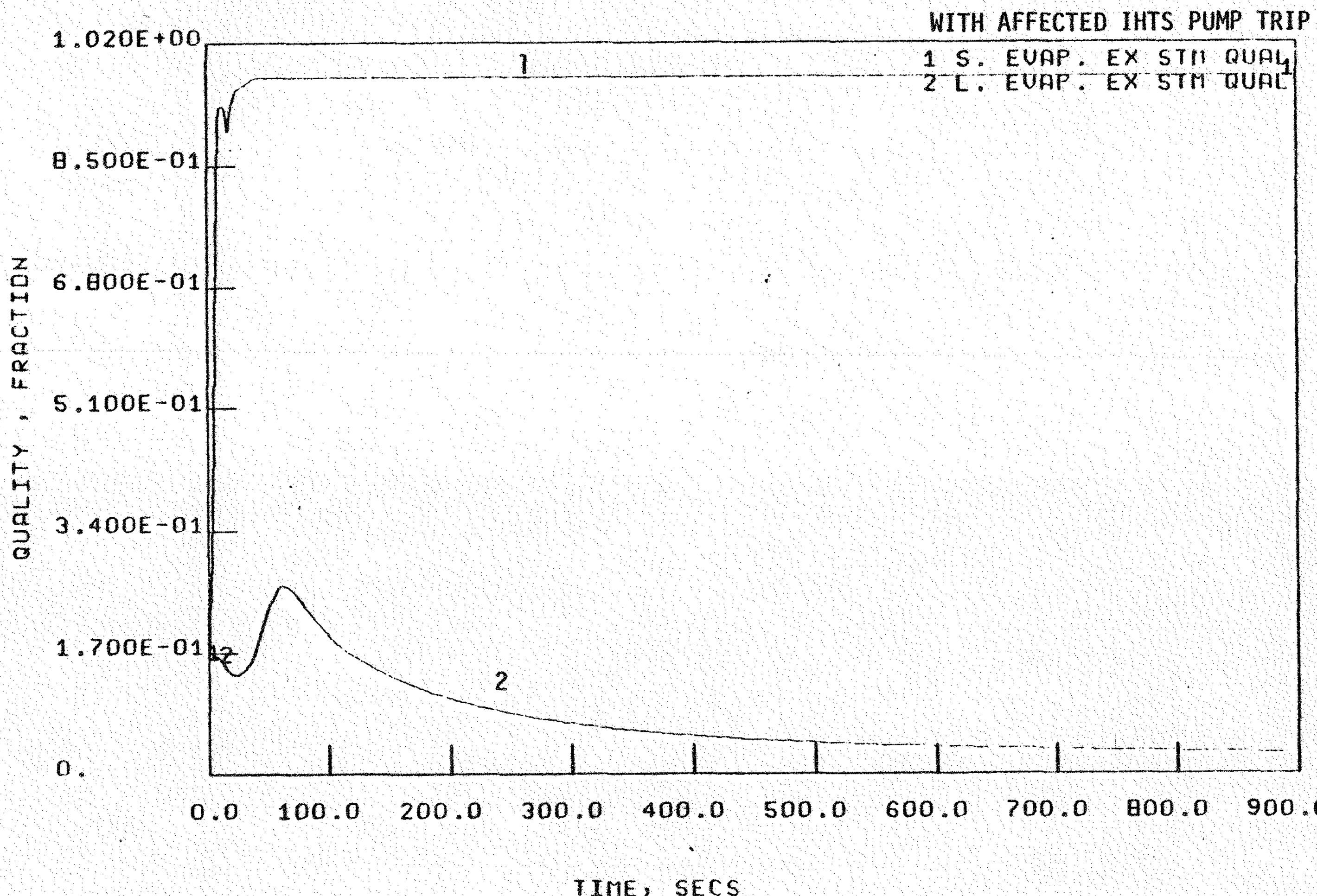

FIGURE 4-84

POOL REACTOR ISOLATION AND BLOWDOWN OF ONE STEAM GENERATOR

RUN DATED 11/20/78

NUMBER SUPGE00

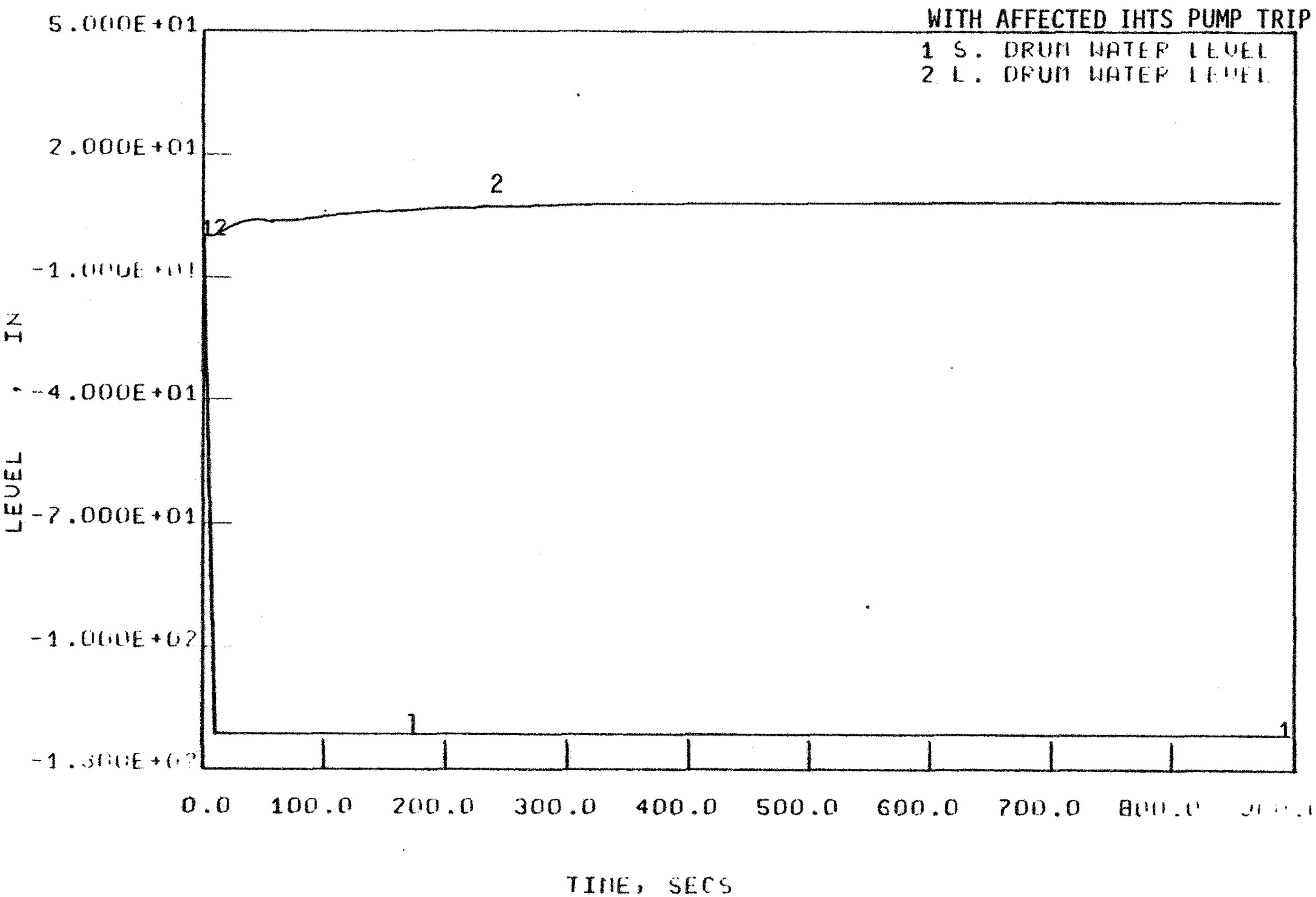

FIGURE 4-85
POOL REACTOR LOSS OF FEEDWATER TO ONE STEAM GENERATOR
RUN DATED 10/06/78
NUMBER PAPGE03

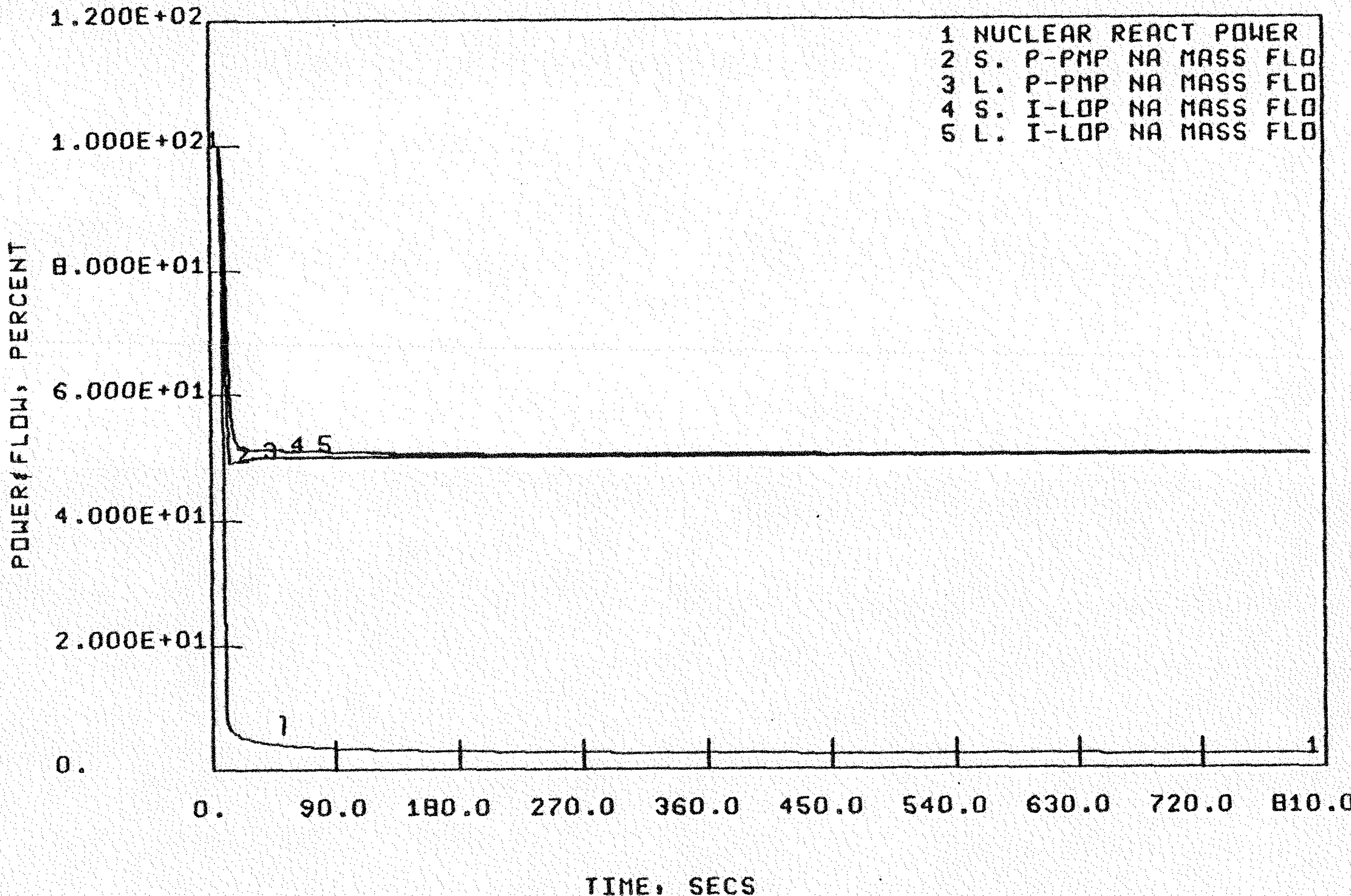

FIGURE 4-86
POOL REACTOR LOSS OF FEEDWATER TO ONE STEAM GENERATOR
RUN DATED 10/06/78
NUMBER PAPGE03

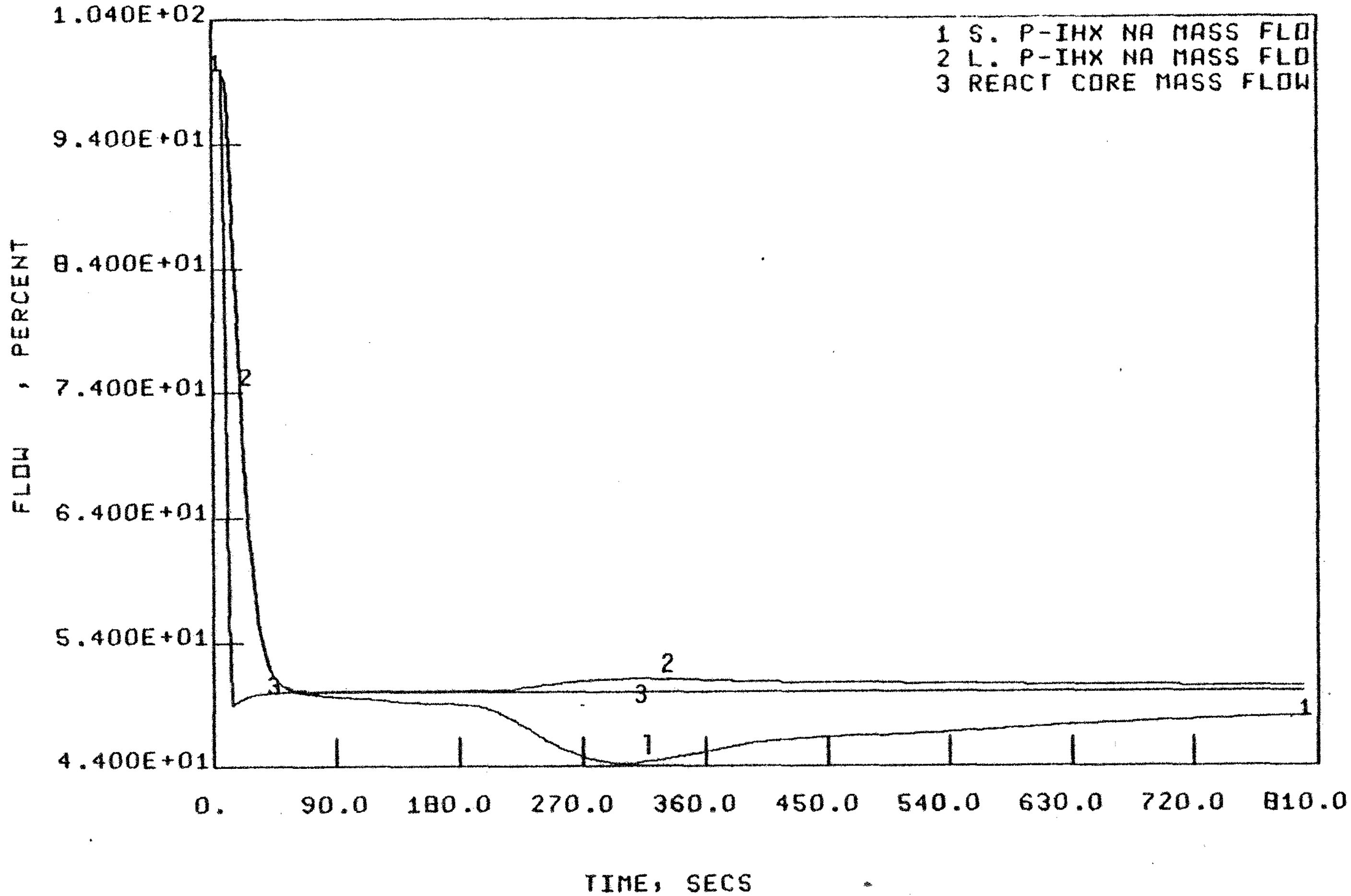

FIGURE 4-87
POOL REACTOR LOSS OF FEEDWATER TO ONE STEAM GENERATOR
RUN DATED 10/06/78
NUMBER PAPGE03

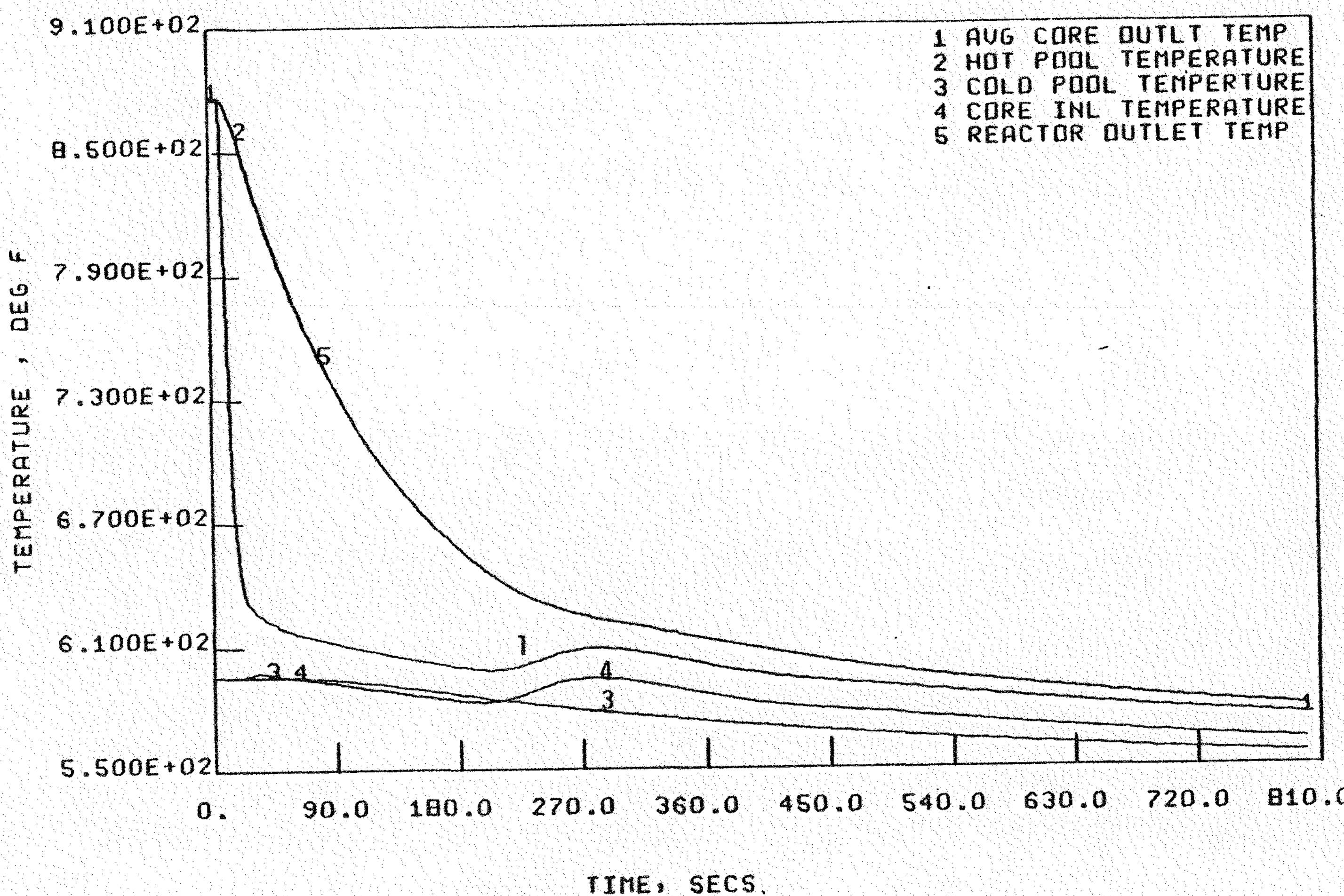

V-2.3-106

FIGURE 4-88
POOL REACTOR LOSS OF FEEDWATER TO ONE STEAM GENERATOR
RUN DATED 10/06/78
NUMBER PAPGE03

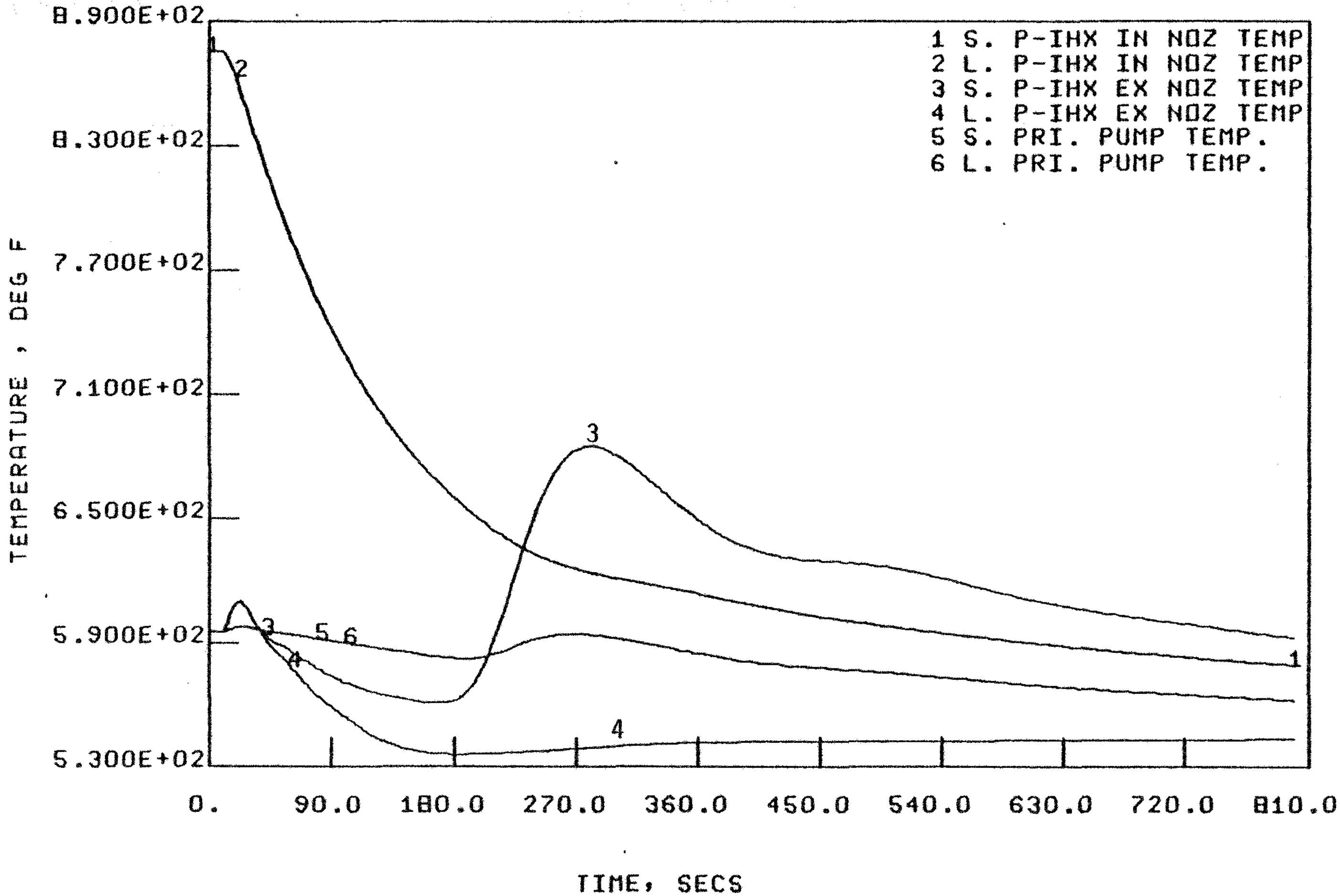

FIGURE 4-89

POOL REACTOR LOSS OF FEEDWATER TO ONE STEAM GENERATOR
RUN DATED 10/06/78
NUMBER PAPGE03

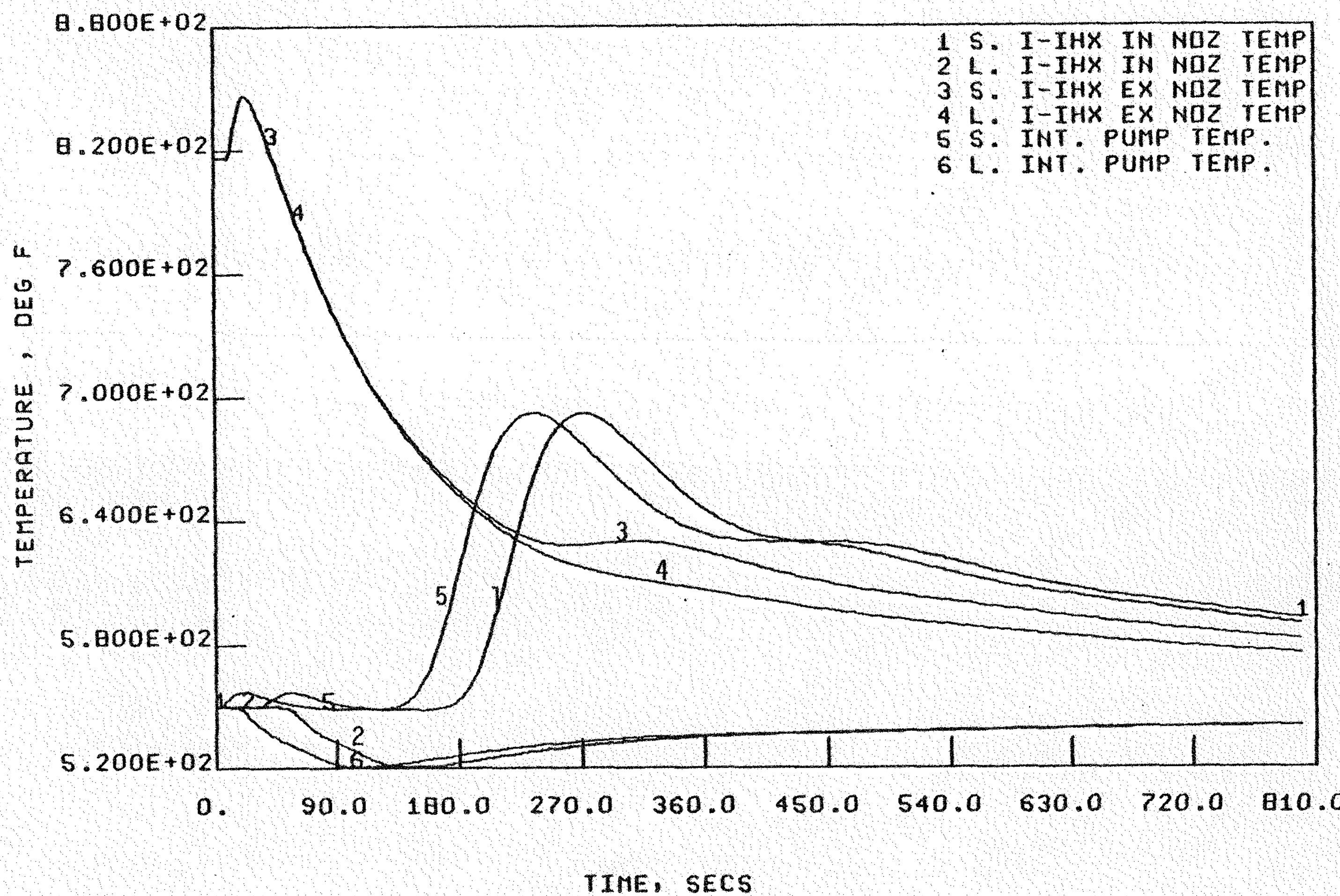

FIGURE 4-90
POOL REACTOR LOSS OF FEEDWATER TO ONE STEAM GENERATOR
RUN DATED 10/06/78
NUMBER PAPGE03

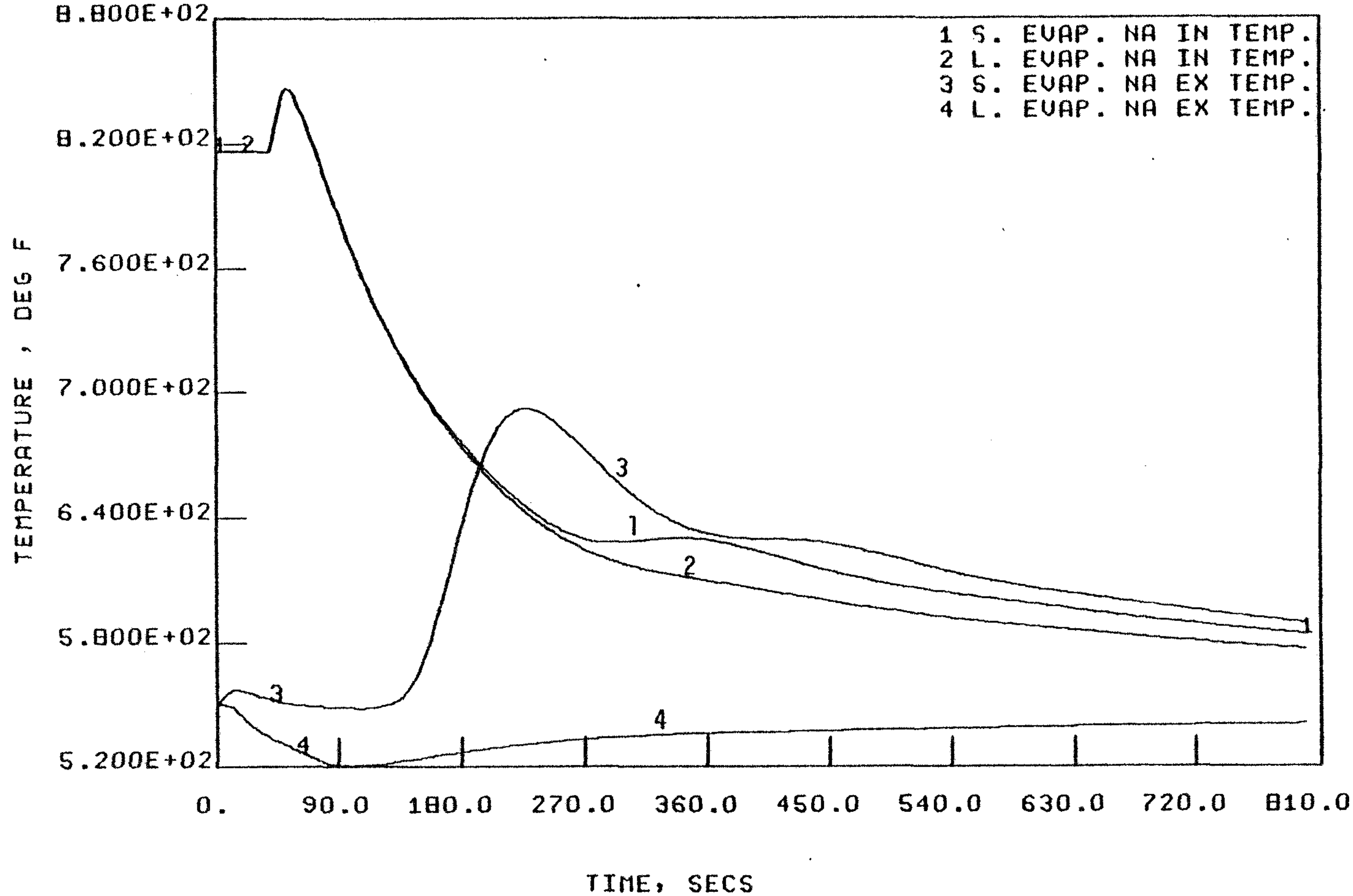

FIGURE 4-91

POOL REACTOR LOSS OF FEEDWATER TO ONE STEAM GENERATOR
RUN DATED 10/06/78
NUMBER PAPGE03

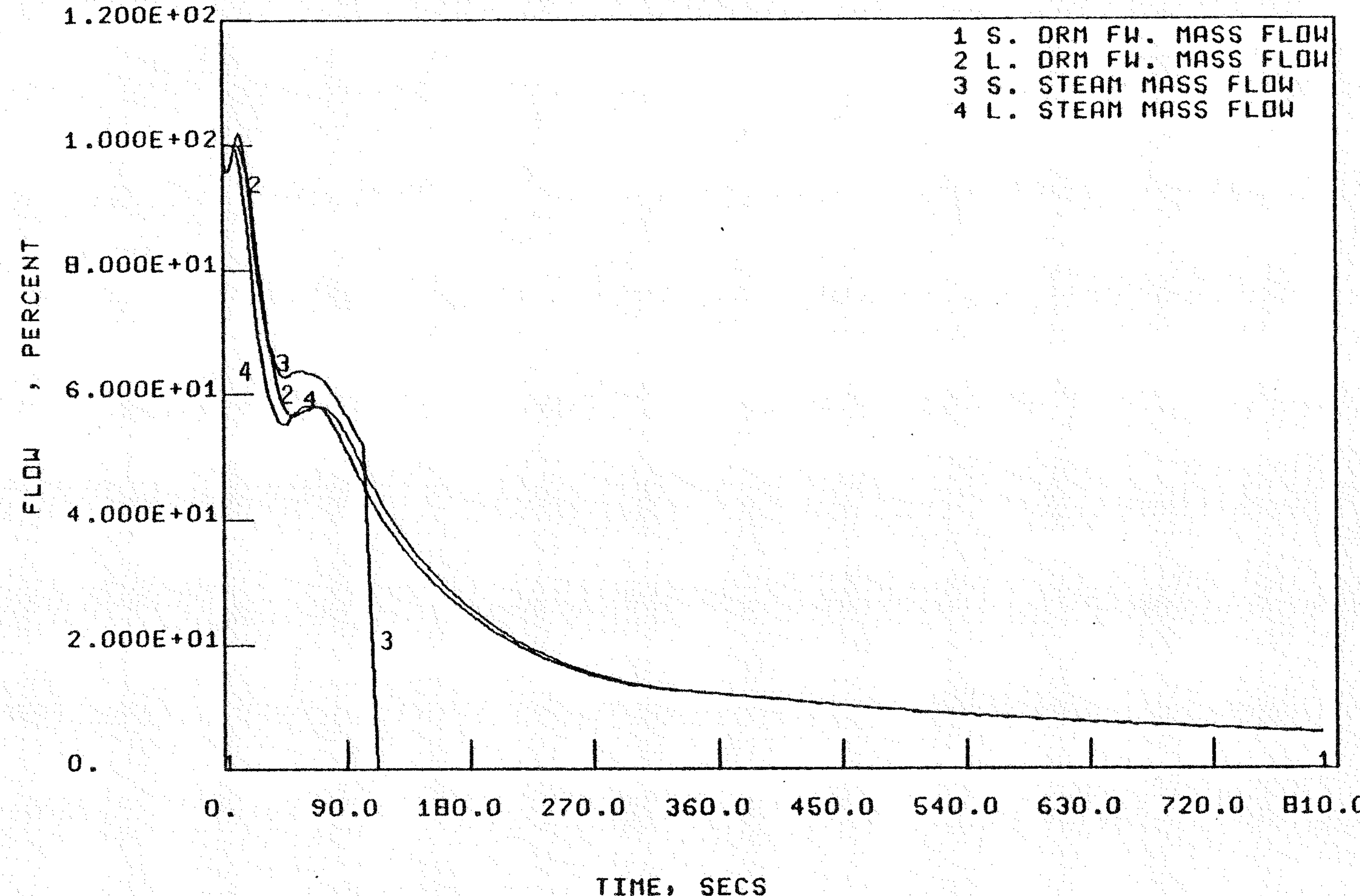

FIGURE 4-92

POOL REACTOR LOSS OF FEEDWATER TO ONE STEAM GENERATOR
RUN DATED 10/06/78
NUMBER PAPGE03

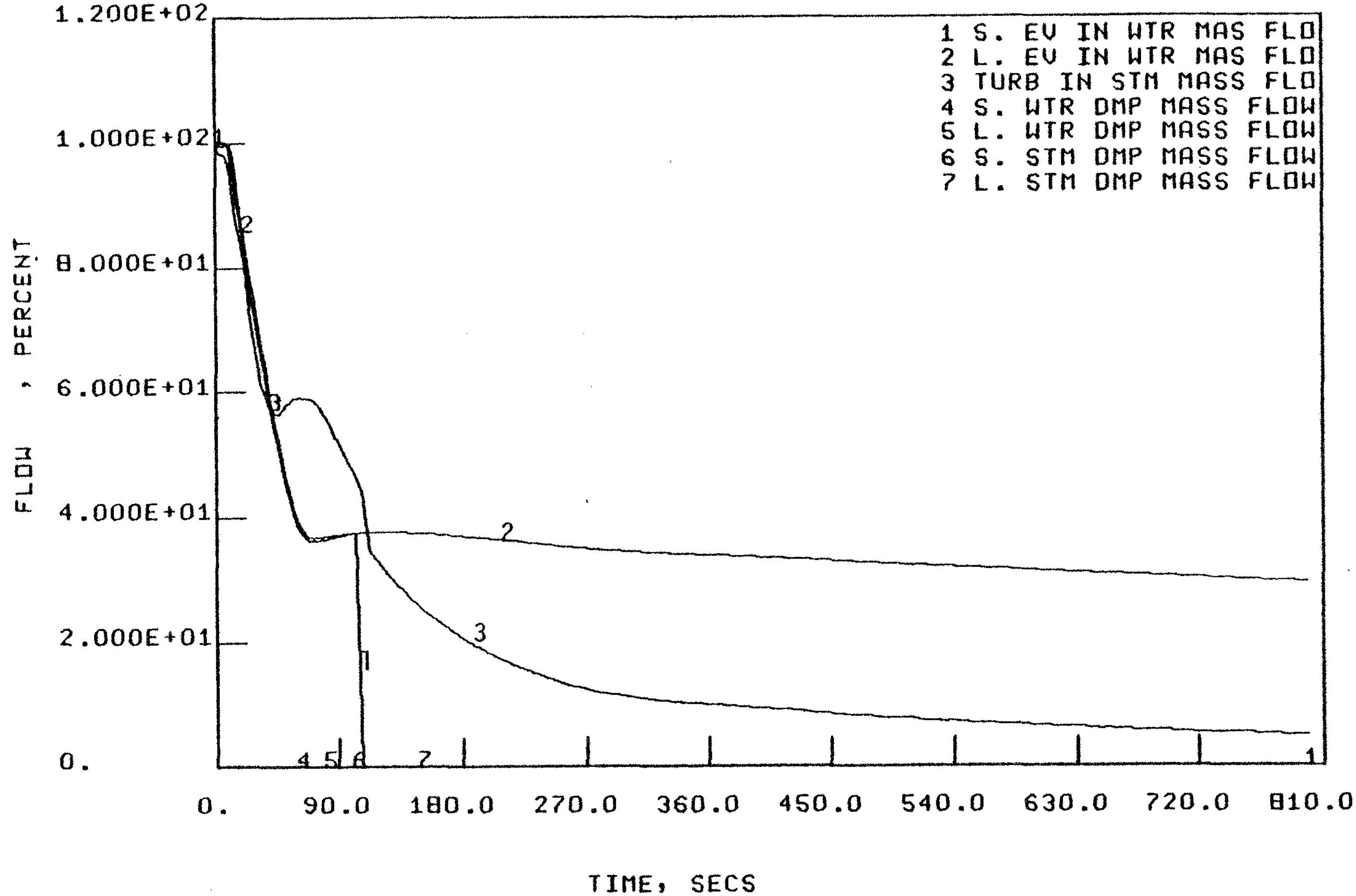

FIGURE 4-93

POOL REACTOR LOSS OF FEEDWATER TO ONE STEAM GENERATOR
RUN DATED 10/06/78
NUMBER PAPGE03

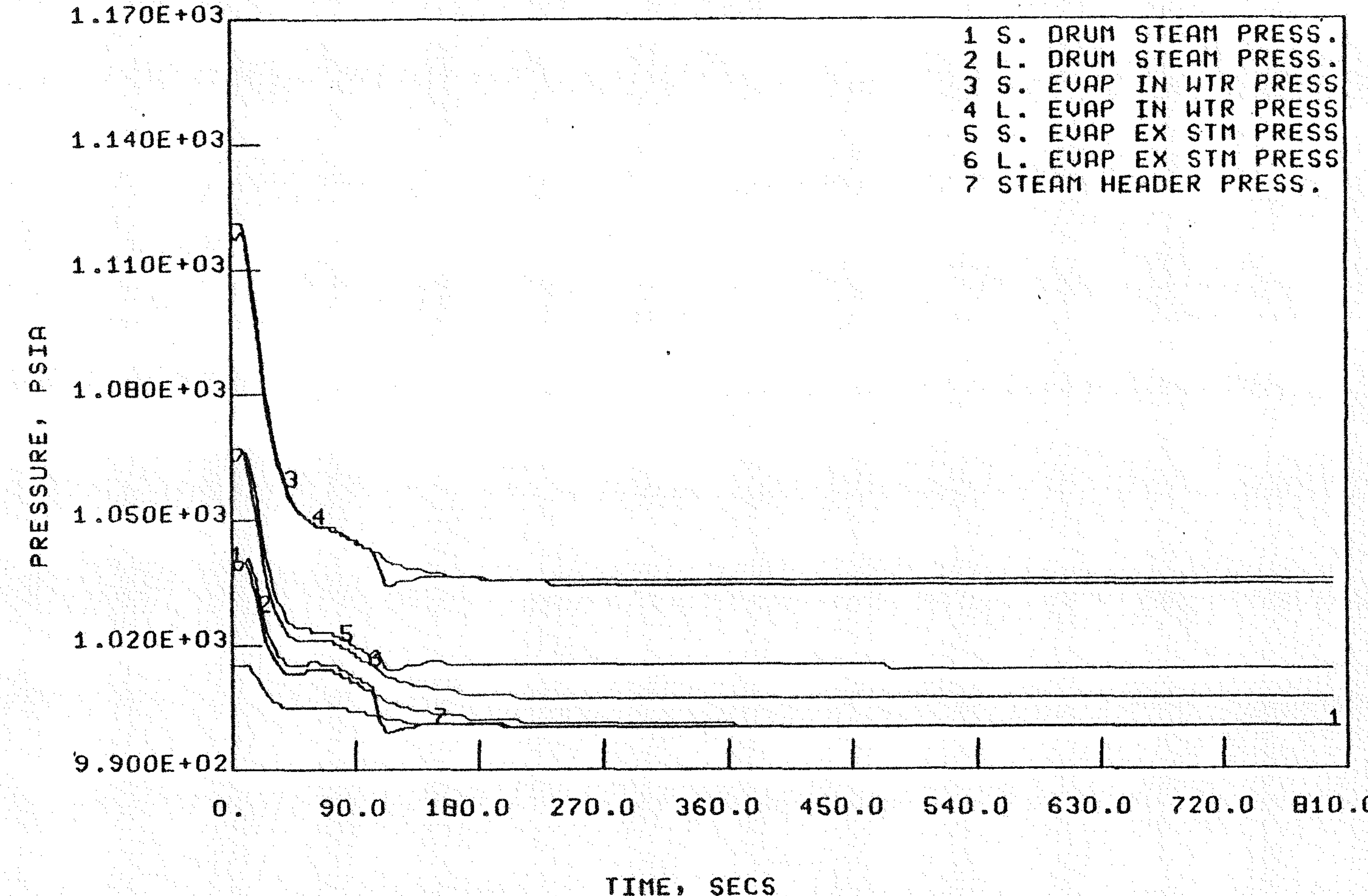

FIGURE 4-94
POOL REACTOR LOSS OF FEEDWATER TO ONE STEAM GENERATOR
RUN DATED 10/06/78
NUMBER PAPGE03

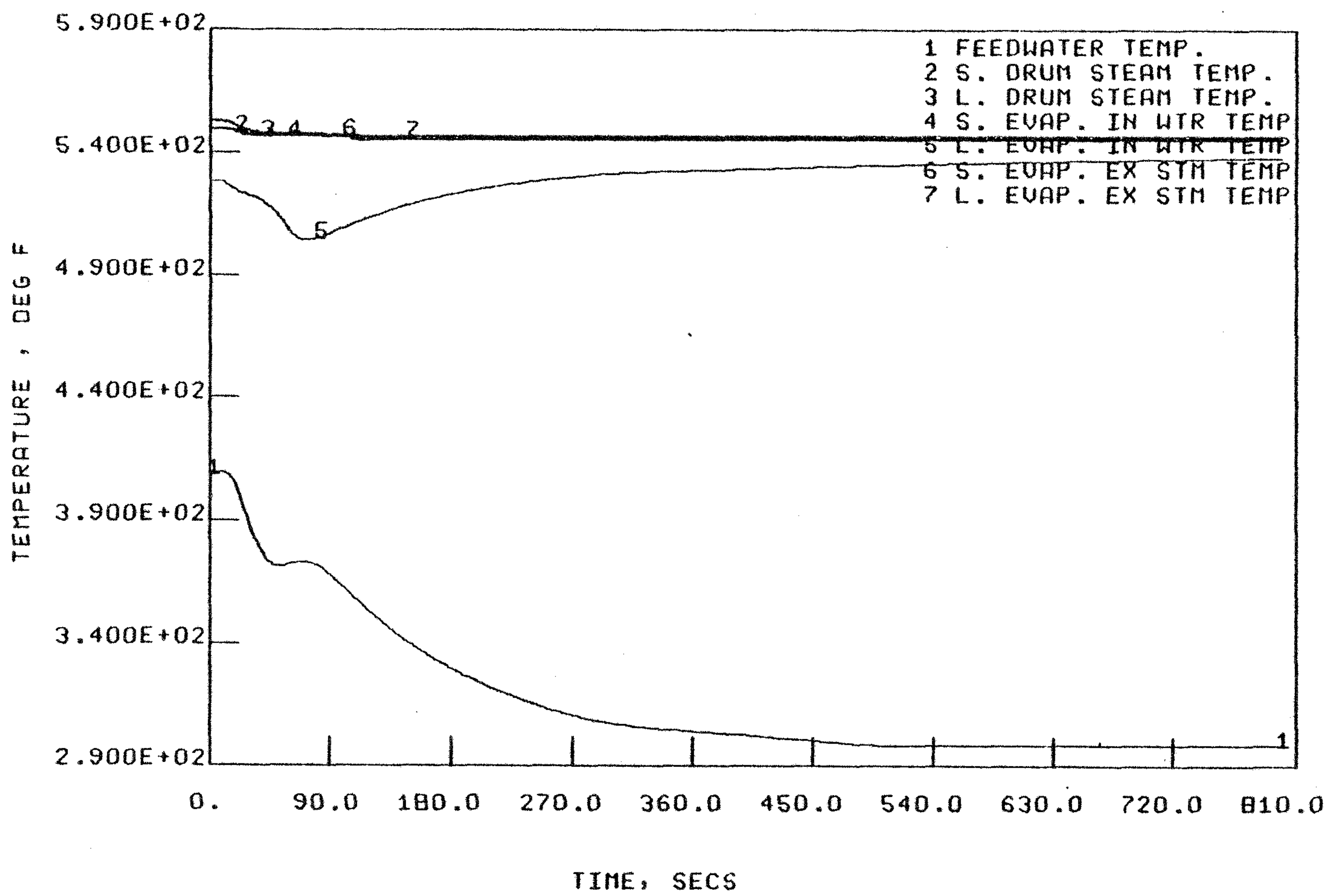

FIGURE 4-95
POOL REACTOR LOSS OF FEEDWATER TO ONE STEAM GENERATOR
RUN DATED 10/06/78
NUMBER PAPGE03

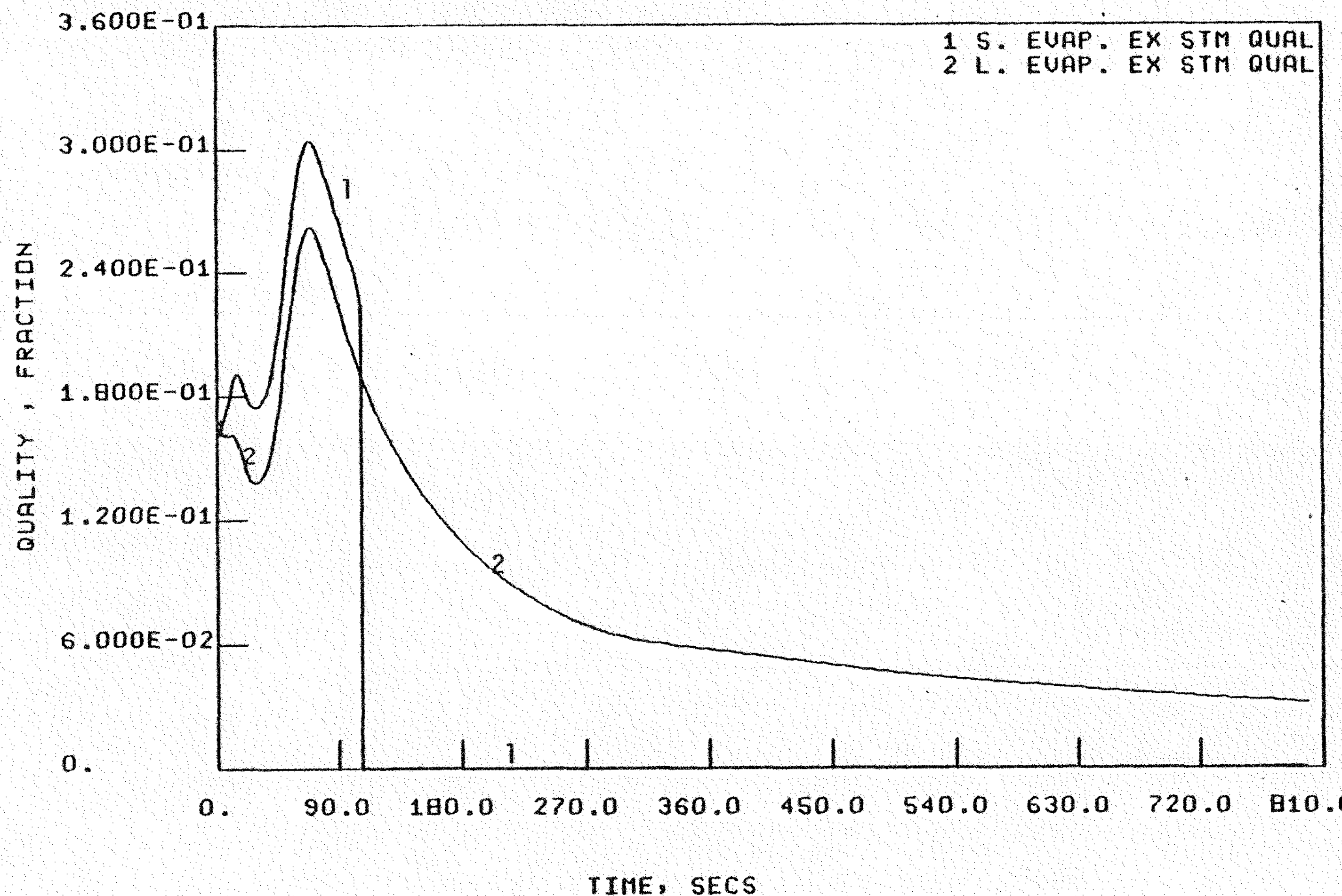

FIGURE 4-96
POOL REACTOR LOSS OF FEEDWATER TO ONE STEAM GENERATOR
RUN DATED 10/06/78
NUMBER PAPGE03

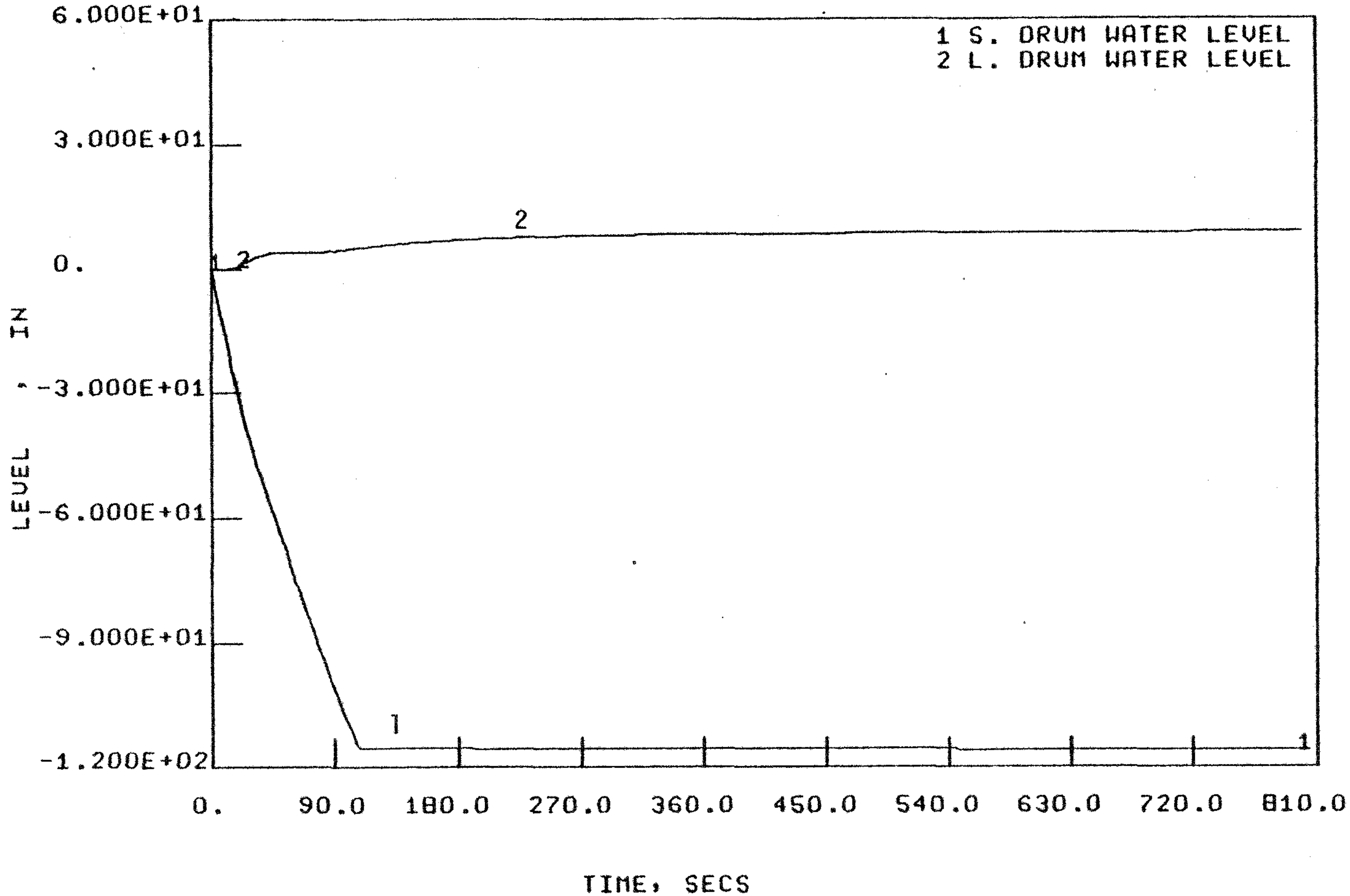

FIGURE 4-97
REACTOR LOSS OF OFF-SITE POWER WITH MINIMUM DECAY HEAT
RUN DATED 11/03/78
NUMBER PAPGE04

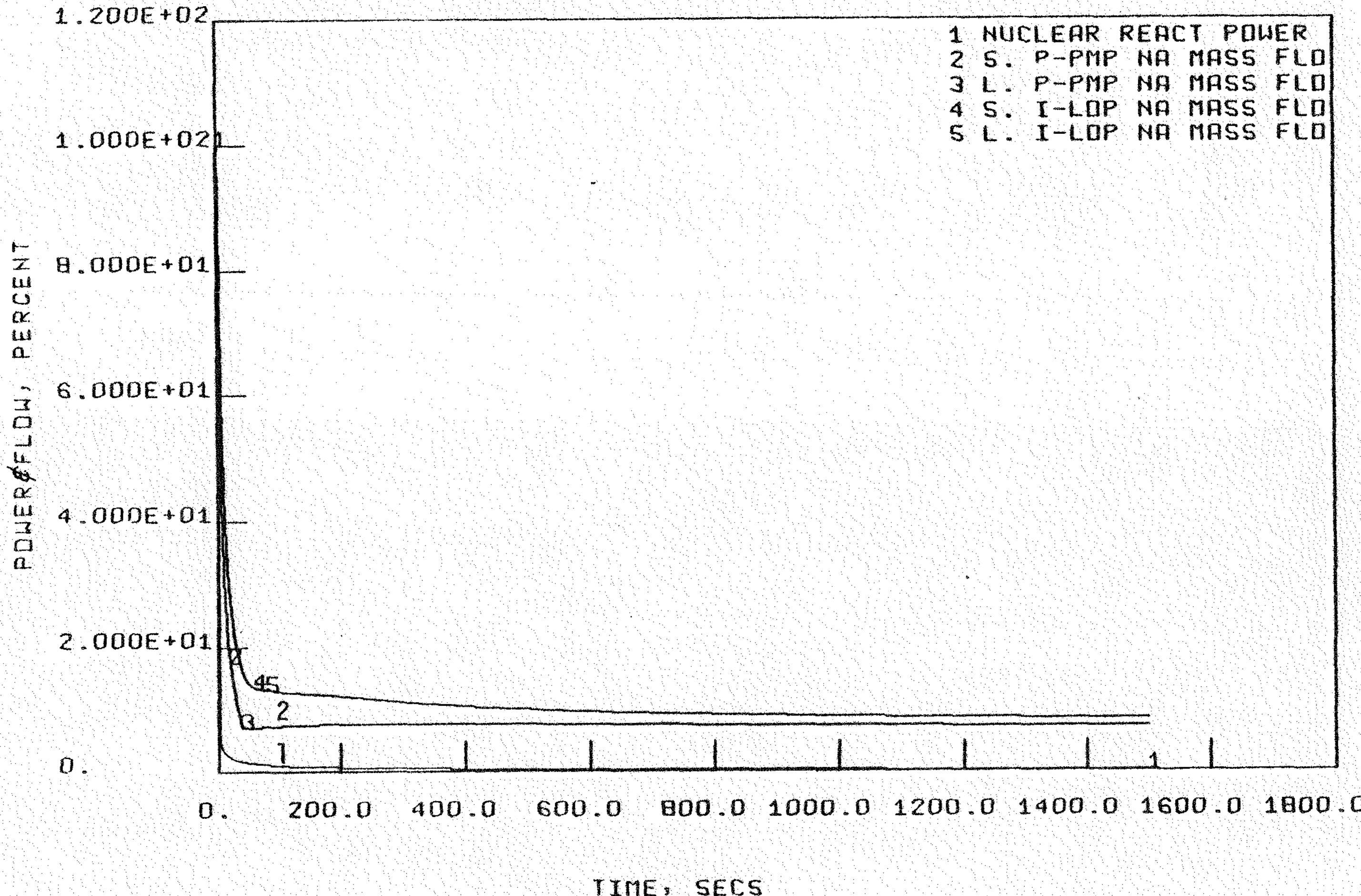

FIGURE 4-98

REACTOR LOSS OF OFF-SITE POWER WITH MINIMUM DECAY HEAT
RUN DATED 11/03/78
NUMBER PAPGE04

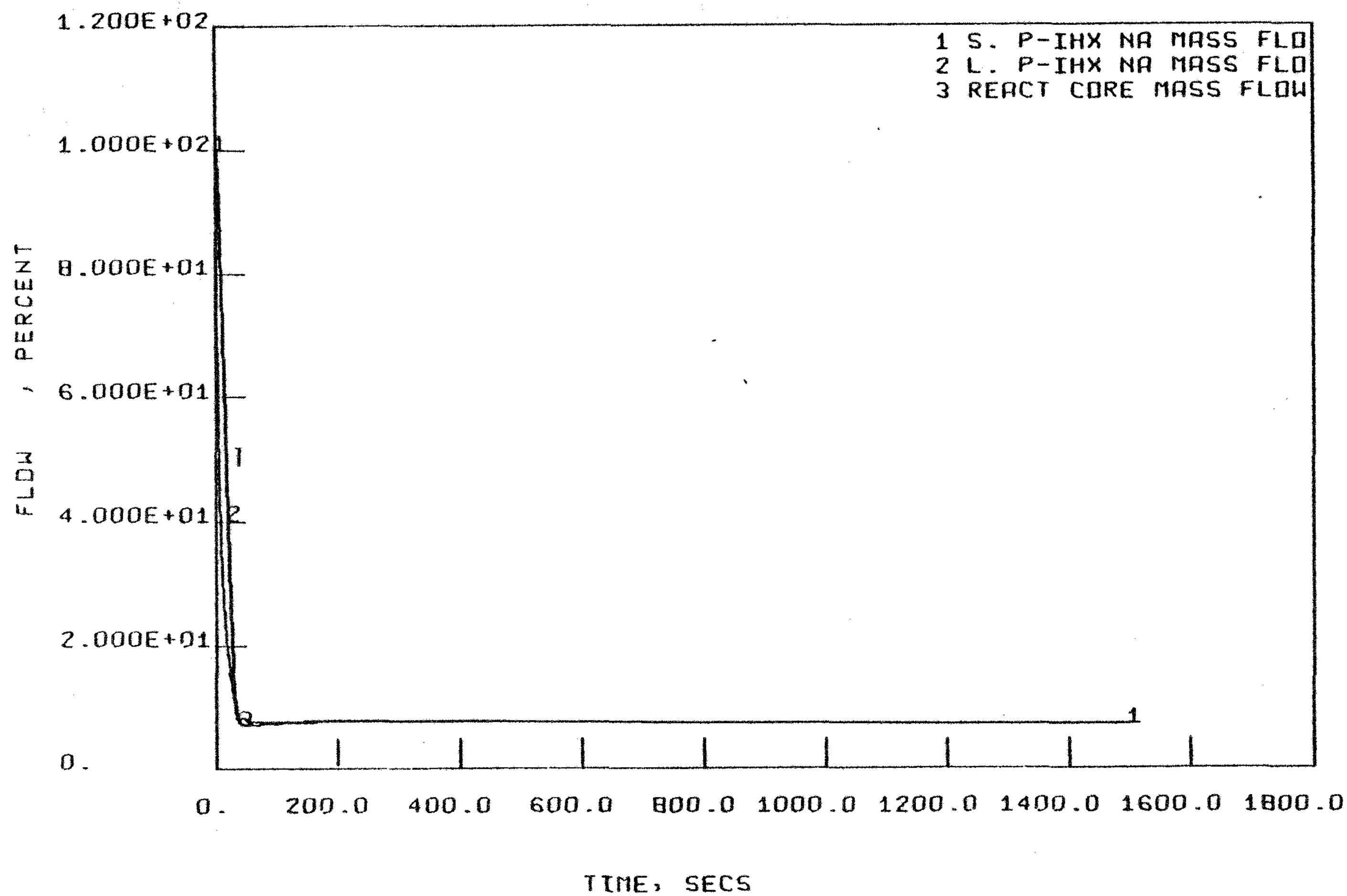

FIGURE 4-99

REACTOR LOSS OF OFF-SITE POWER WITH MINIMUM DECAY HEAT
RUN DATED 11/03/78
NUMBER PAPGE04

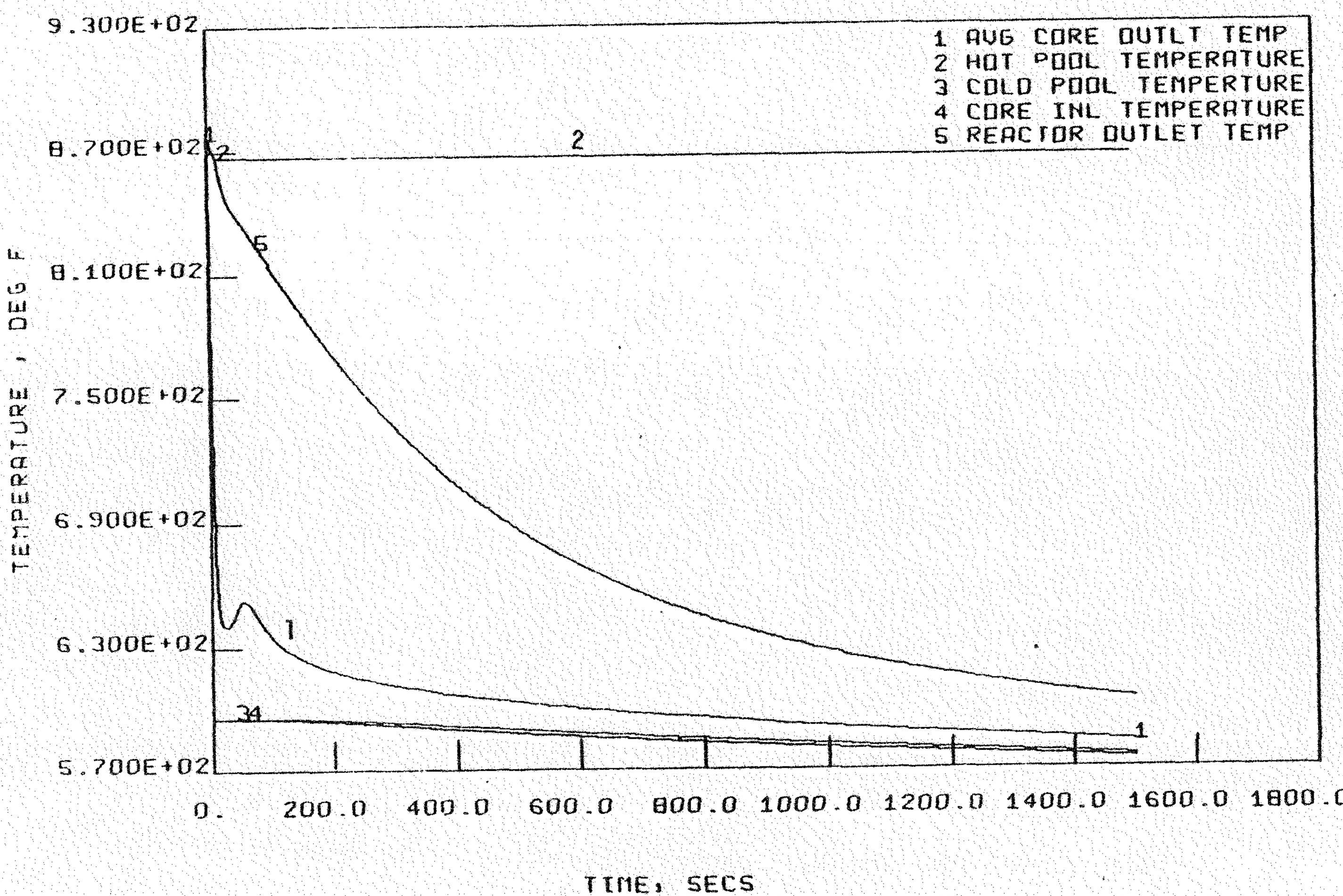

FIGURE 4-100

REACTOR LOSS OF OFF-SITE POWER WITH MINIMUM DECAY HEAT

RUN DATED 11/03/78

NUMBER PAPGE04

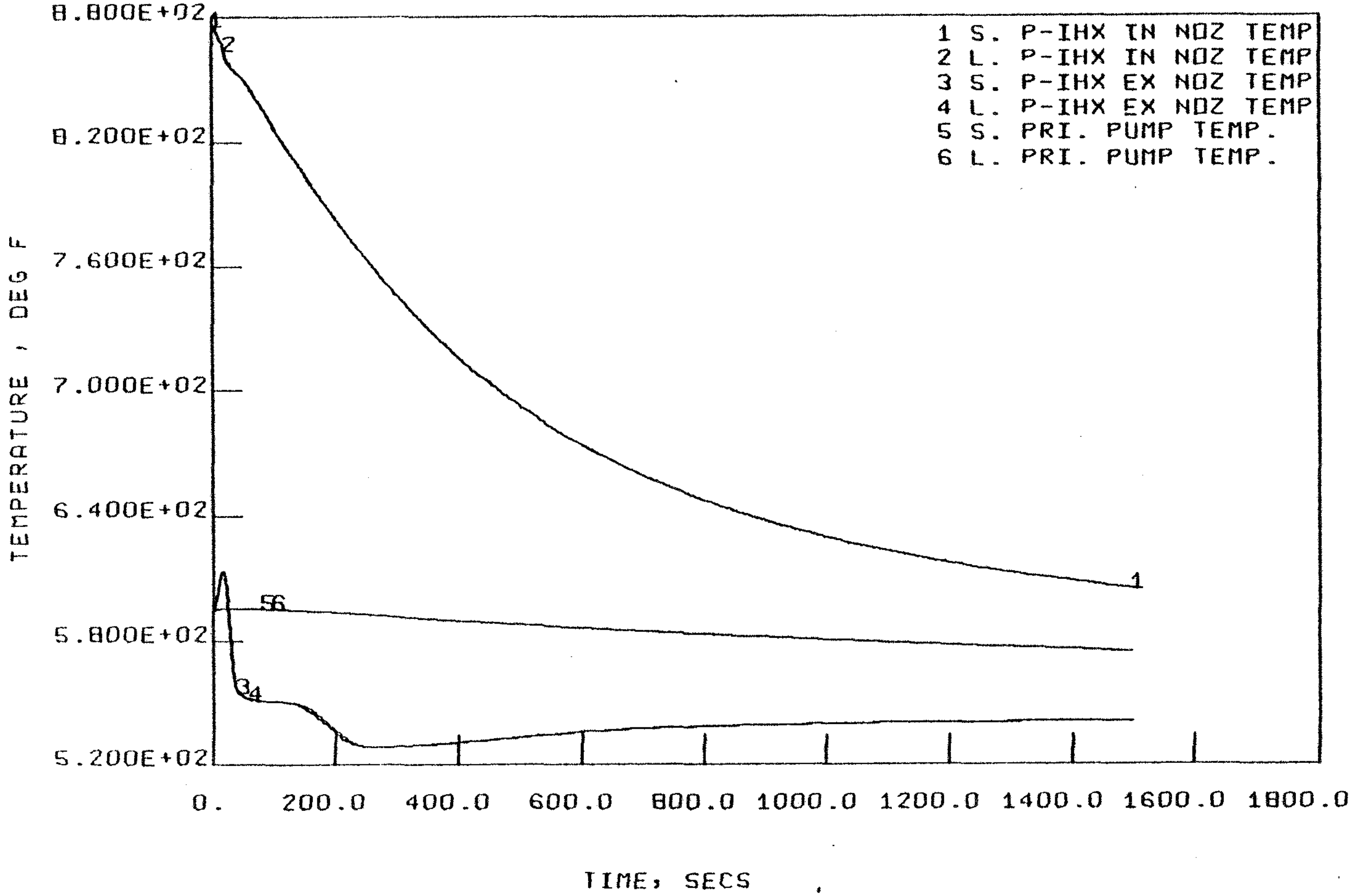

FIGURE 4-101

REACTOR LOSS OF OFF-SITE POWER WITH MINIMUM DECAY HEAT
RUN DATED 11/03/78
NUMBER PAPGE04

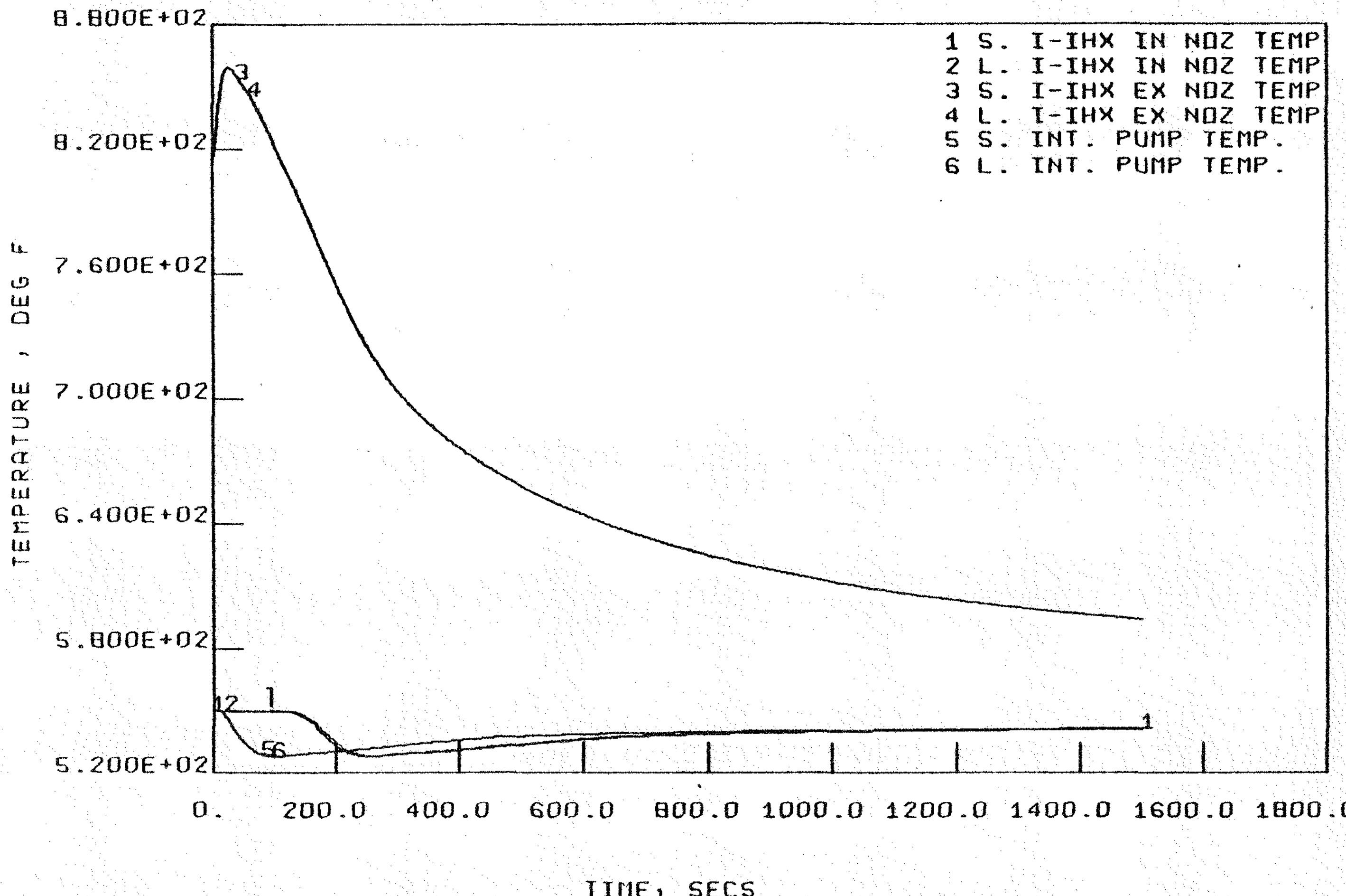

FIGURE 4-102

REACTOR LOSS OF OFF-SITE POWER WITH MINIMUM DECAY HEAT
RUN DATED 11/03/78
NUMBER PAPGE04

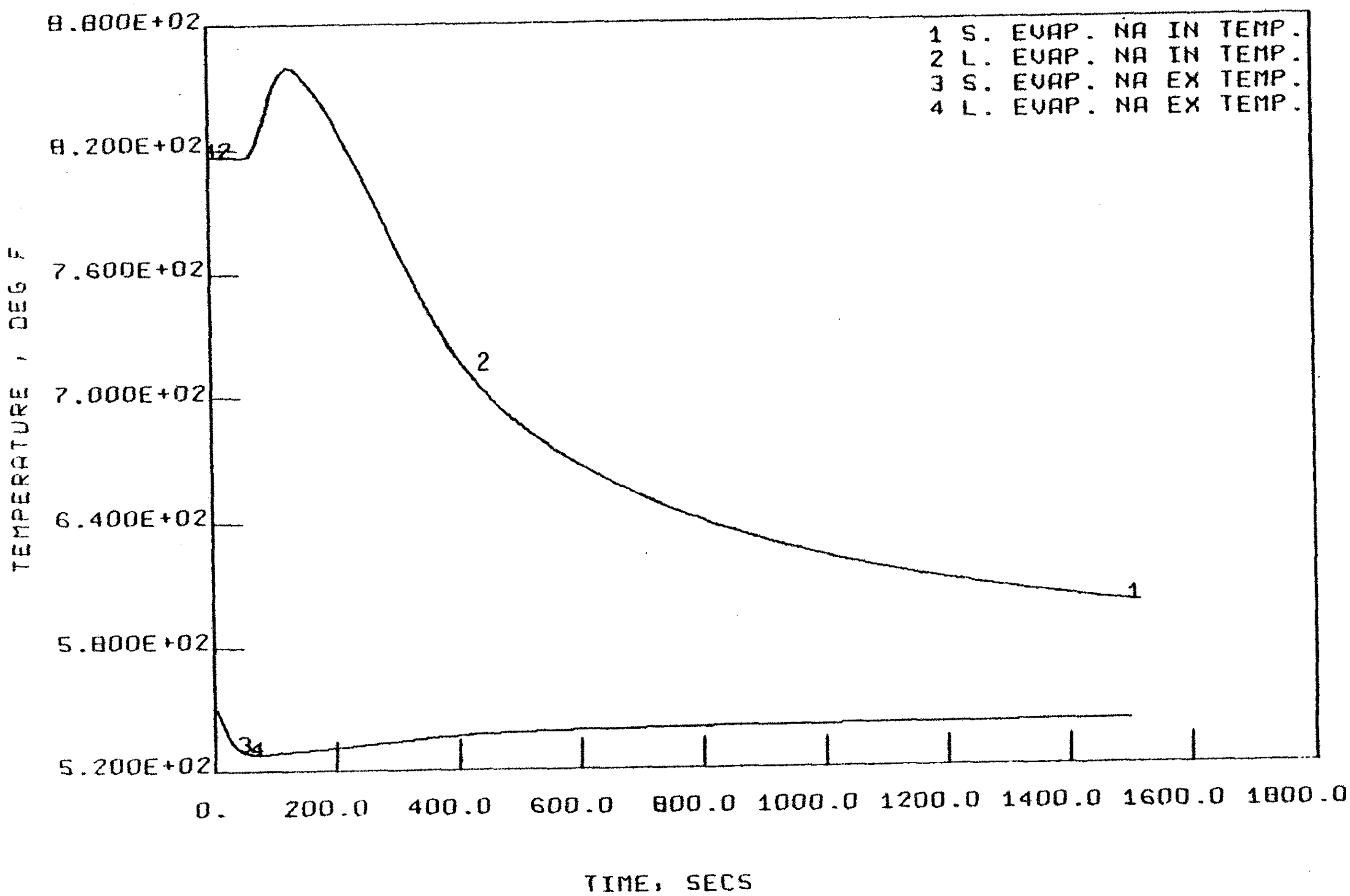

FIGURE 4-103

REACTOR LOSS OF OFF-SITE POWER WITH MINIMUM DECAY HEAT
RUN DATED 11/03/78
NUMBER PAPGE04

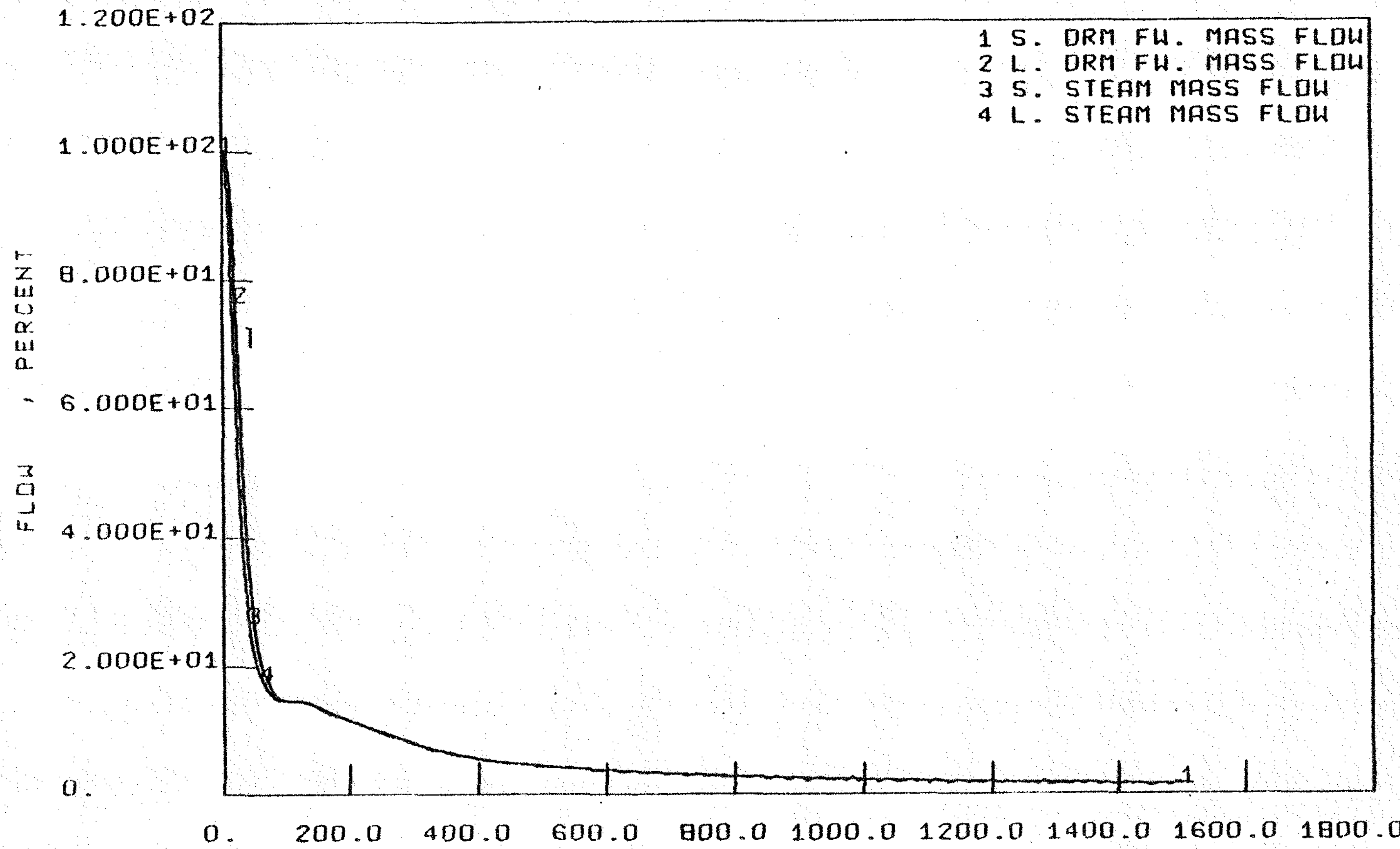

FIGURE 4-104

REACTOR LOSS OF OFF-SITE POWER WITH MINIMUM DECAY HEAT
RUN DATED 11/03/78
NUMBER PAPGE04

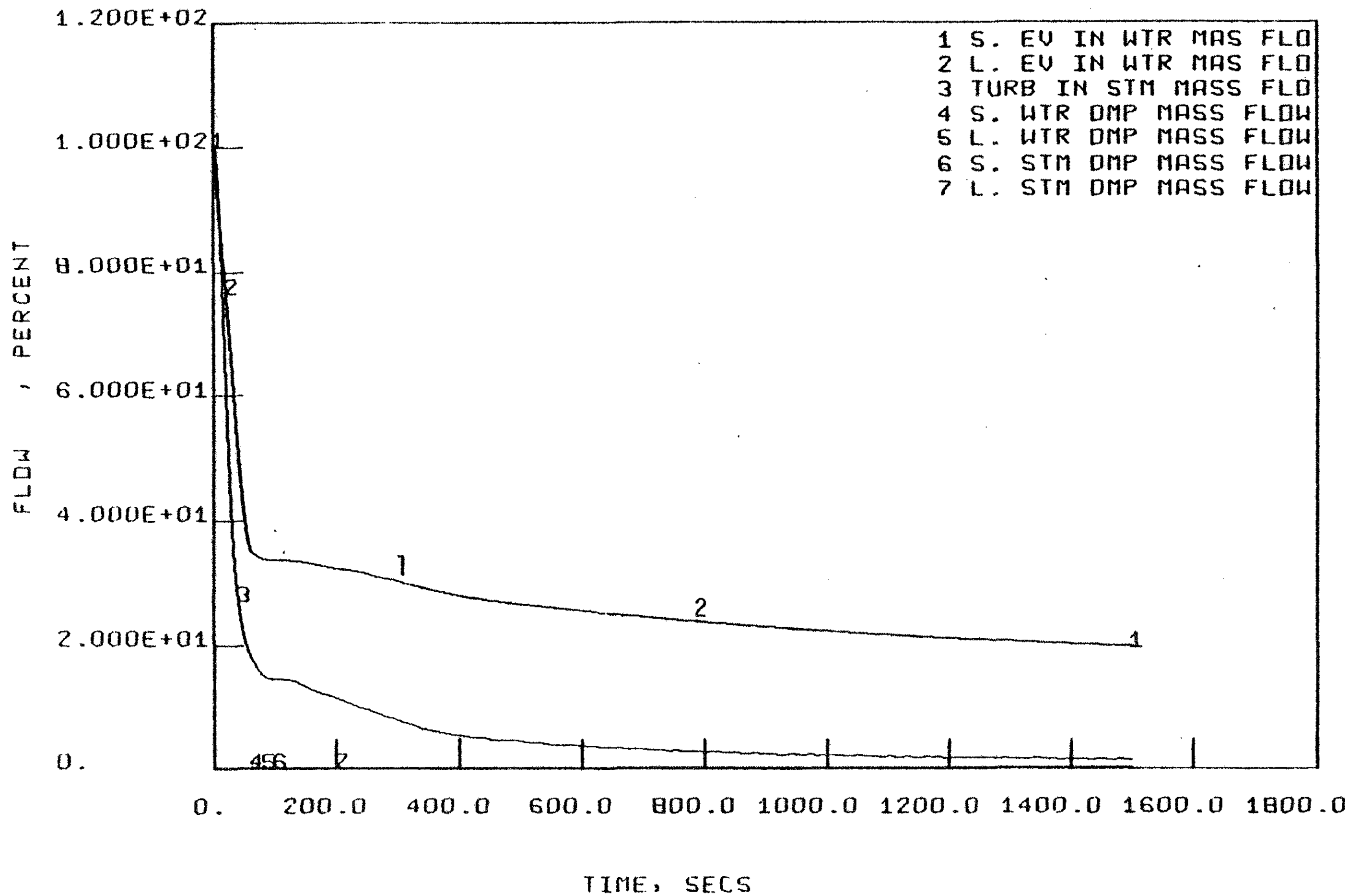

FIGURE 4-105

REACTOR LOSS OF OFF-SITE POWER WITH MINIMUM DECAY HEAT
RUN DATED 11/03/78
NUMBER PAPGE04

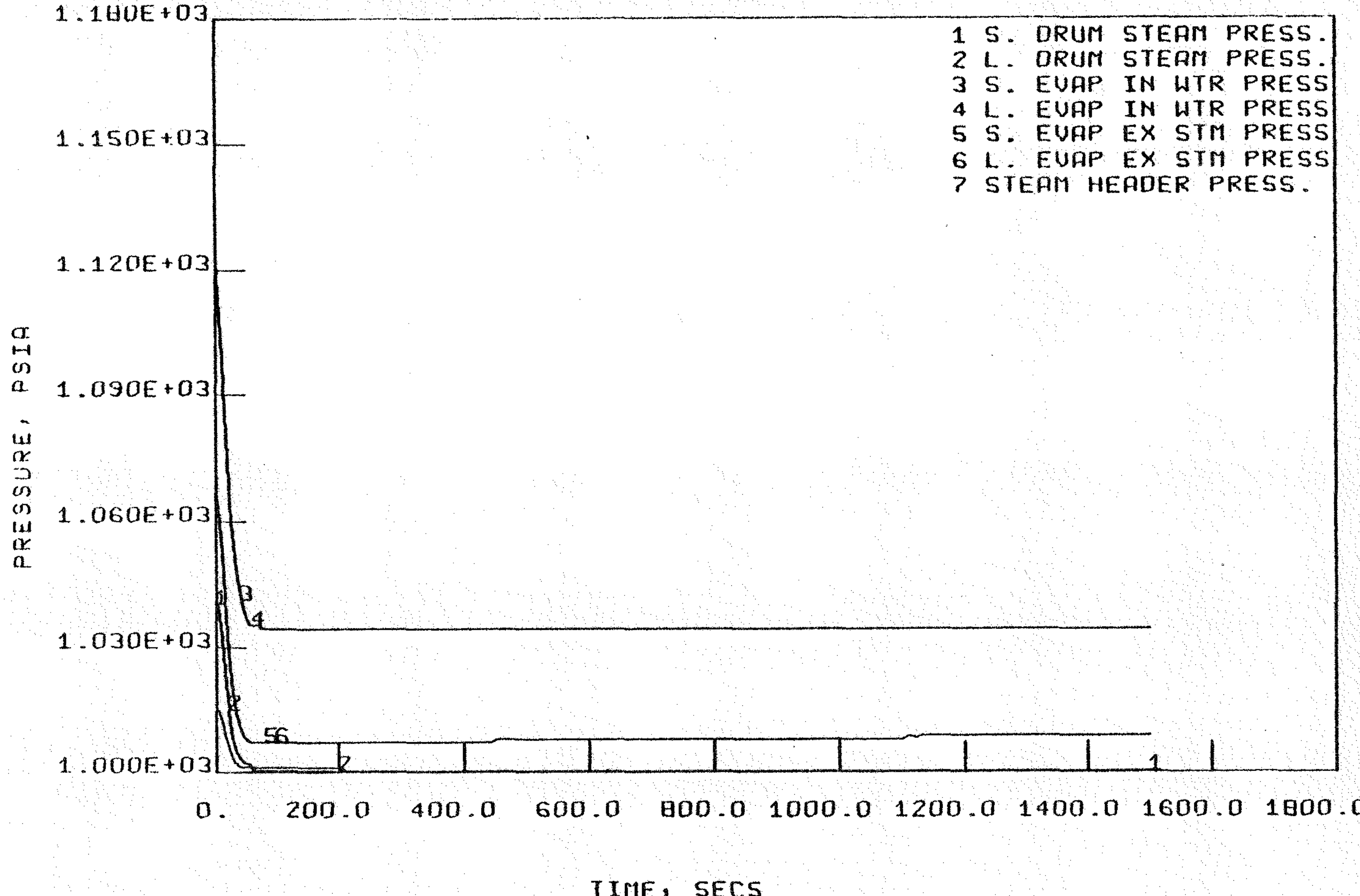

FIGURE 4-106

REACTOR LOSS OF OFF-SITE POWER WITH MINIMUM DECAY HEAT
RUN DATED 11/03/78
NUMBER PAPGE04

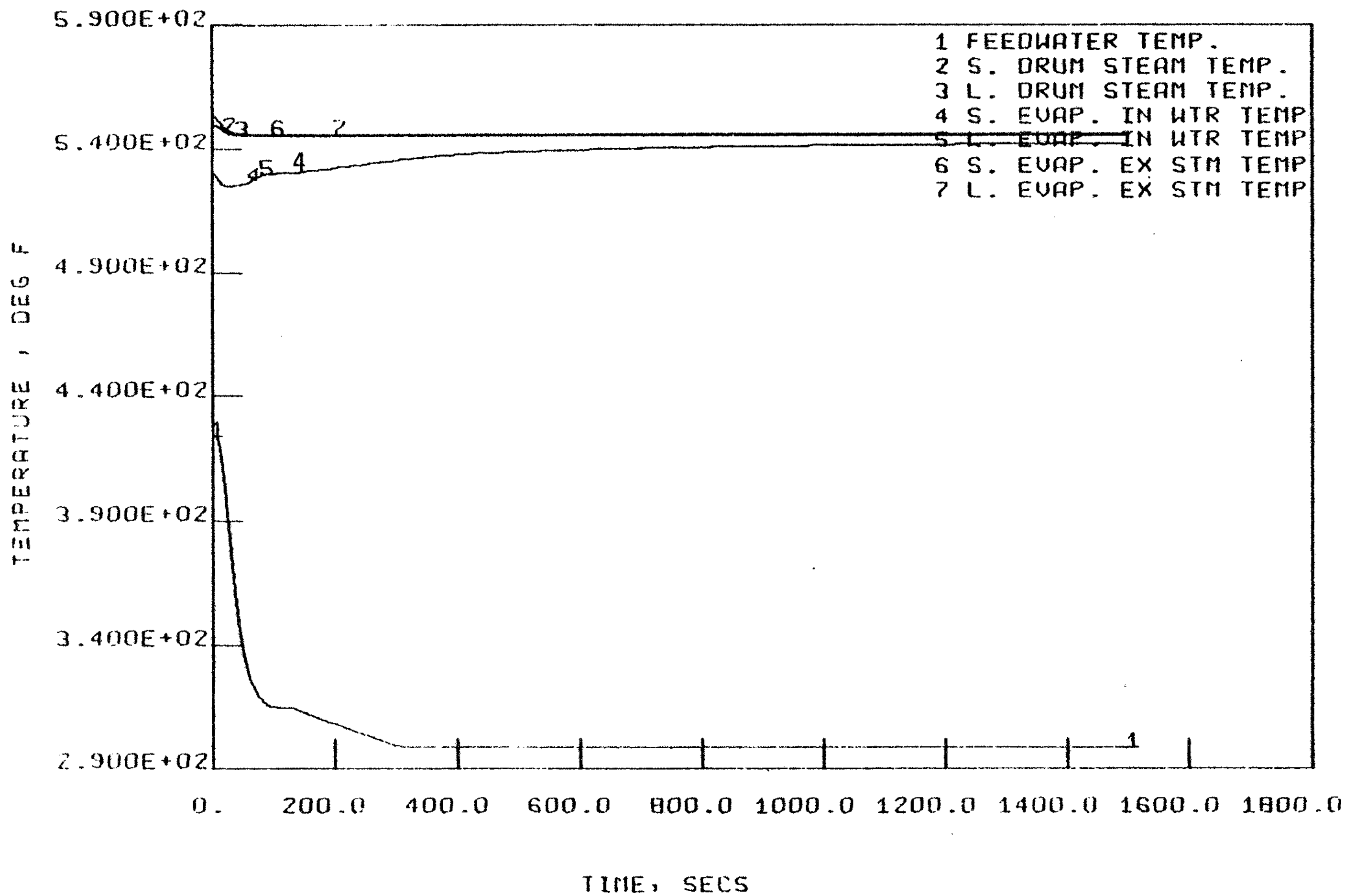

FIGURE 4-107

REACTOR LOSS OF OFF-SITE POWER WITH MINIMUM DECAY HEAT
RUN DATED 11/03/78
NUMBER RAPGE04

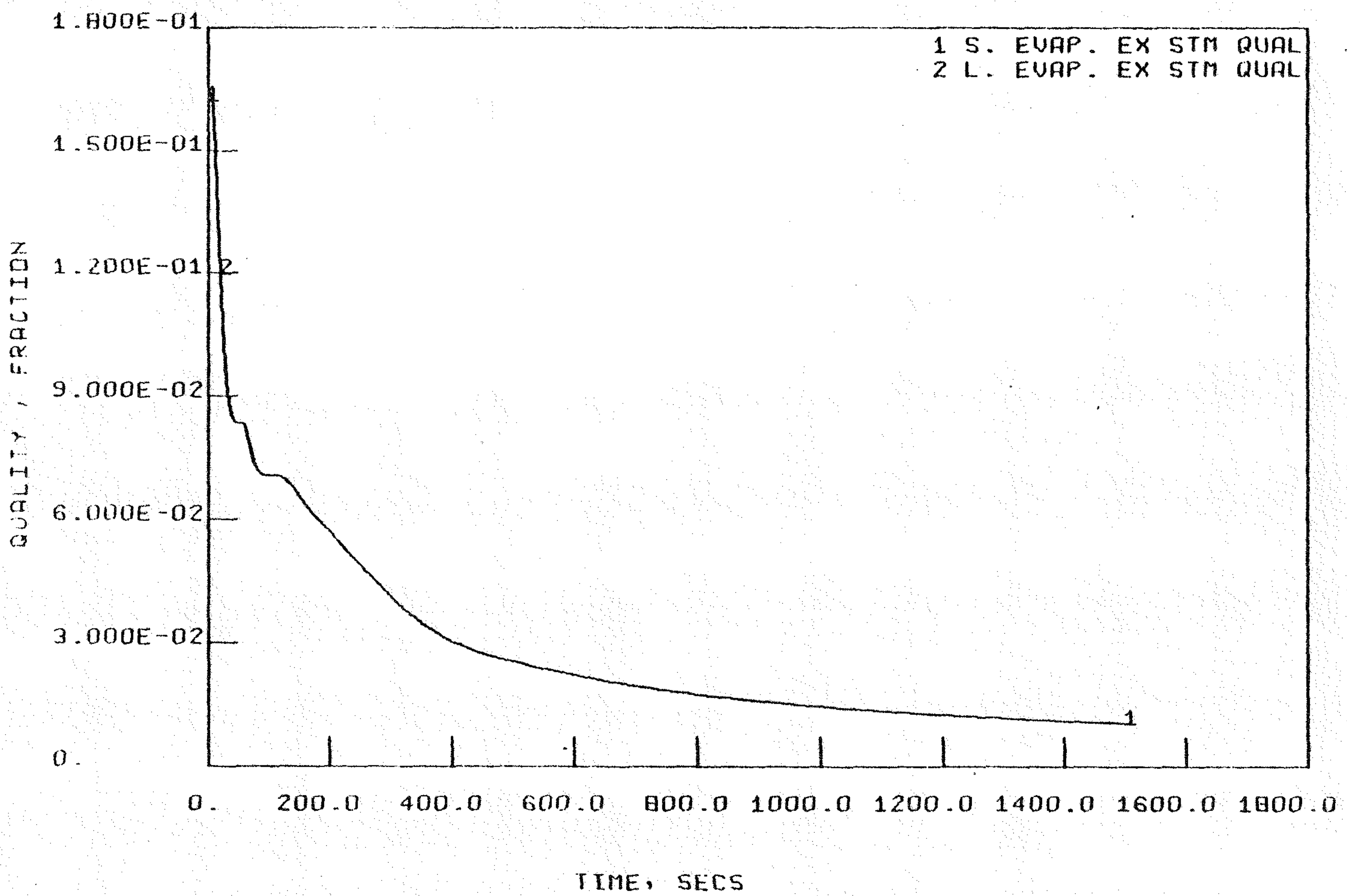

FIGURE 4-108
REACTOR LOSS OF OFF-SITE POWER WITH MINIMUM DECAY HEAT
RUN DATED 11/03/78
NUMBER PAPGE04

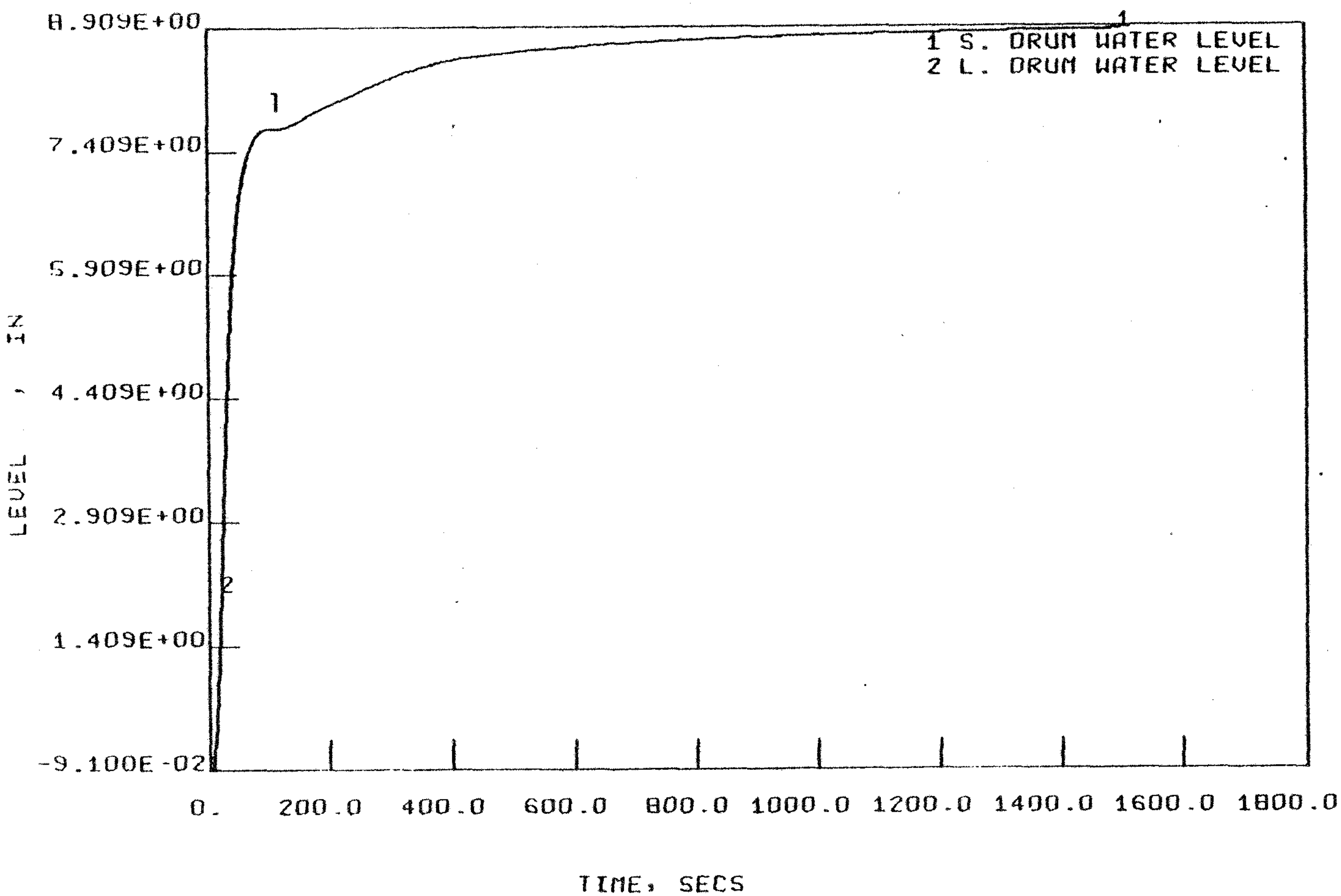

FIGURE 4-109

POOL REACTOR OPENING OF STEAM LINE SAFETY VALVE WITH DELAYED SCRAM
RUN DATED 10/06/78
NUMBER TEPGE03

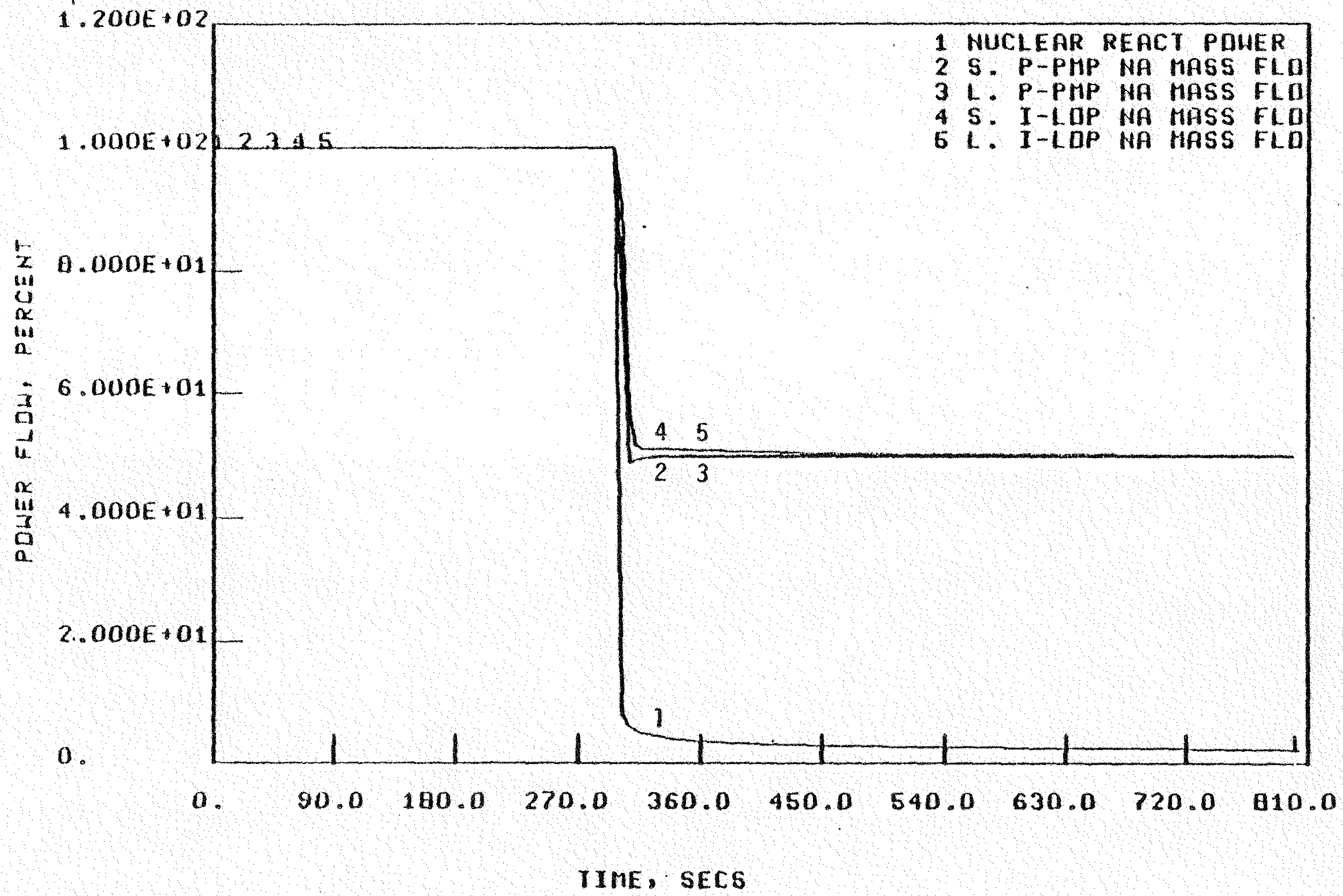

FIGURE 4-110

POOL REACTOR OPENING OF STEAM LINE SAFETY VALVE WITH DELAYED SCRAM
RUN DATED 10/06/78
NUMBER TEPGE03

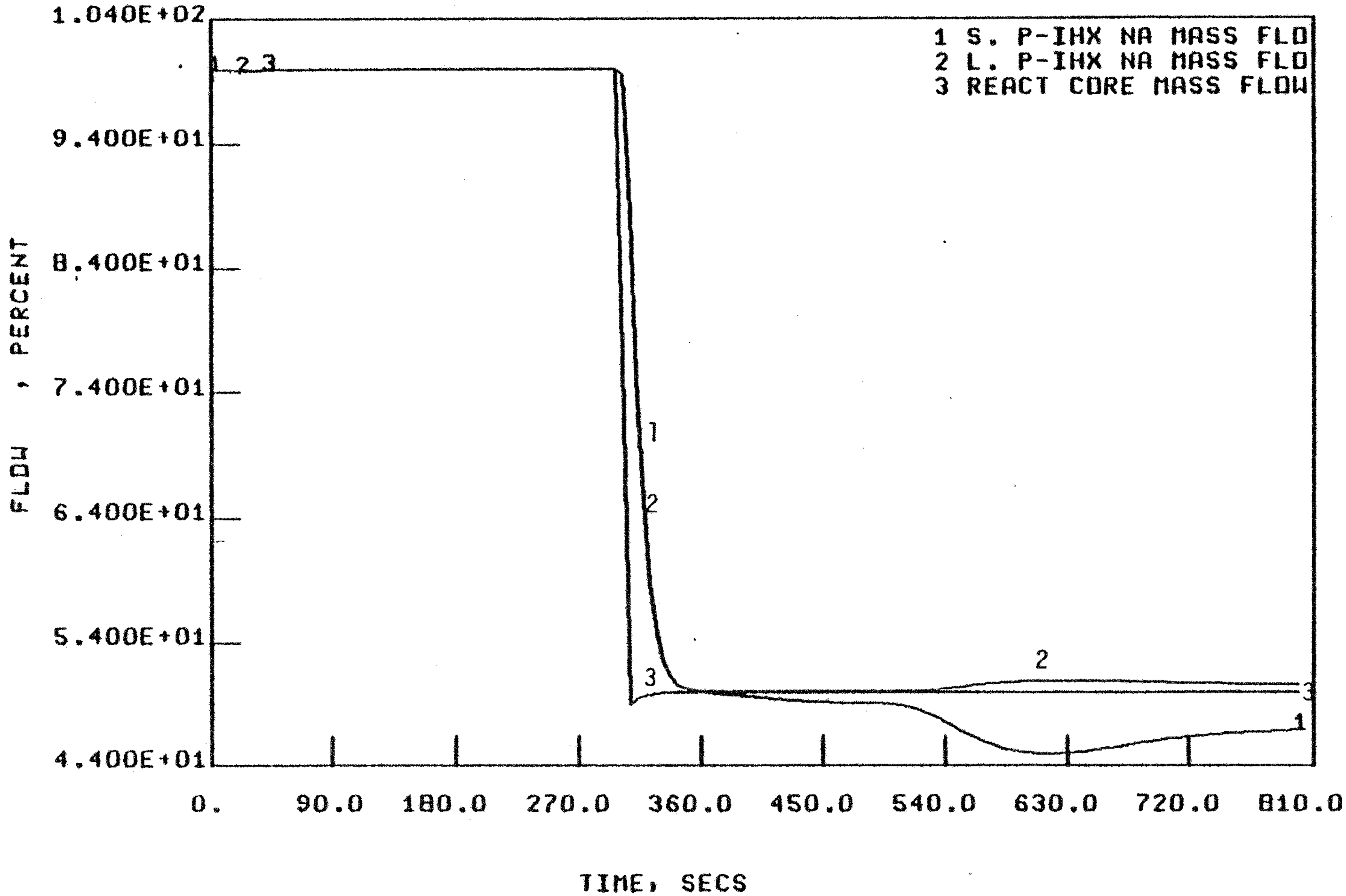

FIGURE 4-111
POOL REACTOR OPENING OF STEAM LINE SAFETY VALVE WITH DELAYED SCRAM
RUN DATED 10/06/78
NUMBER TEPGE03

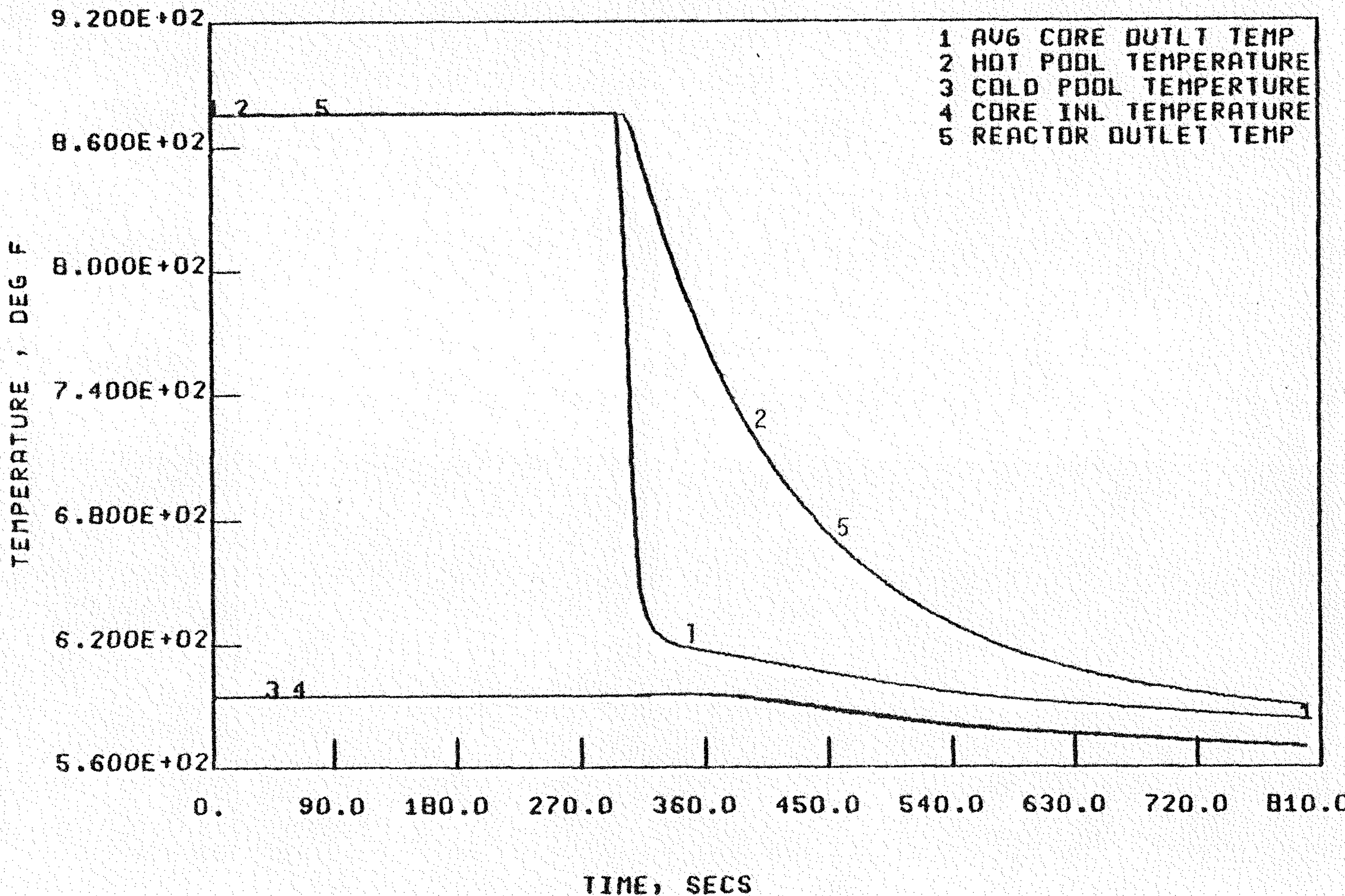

FIGURE 4-112

POOL REACTOR OPENING OF STEAM LINE SAFETY VALVE WITH DELAYED SCRAM
RUN DATED 10/06/78
NUMBER TEPGE03

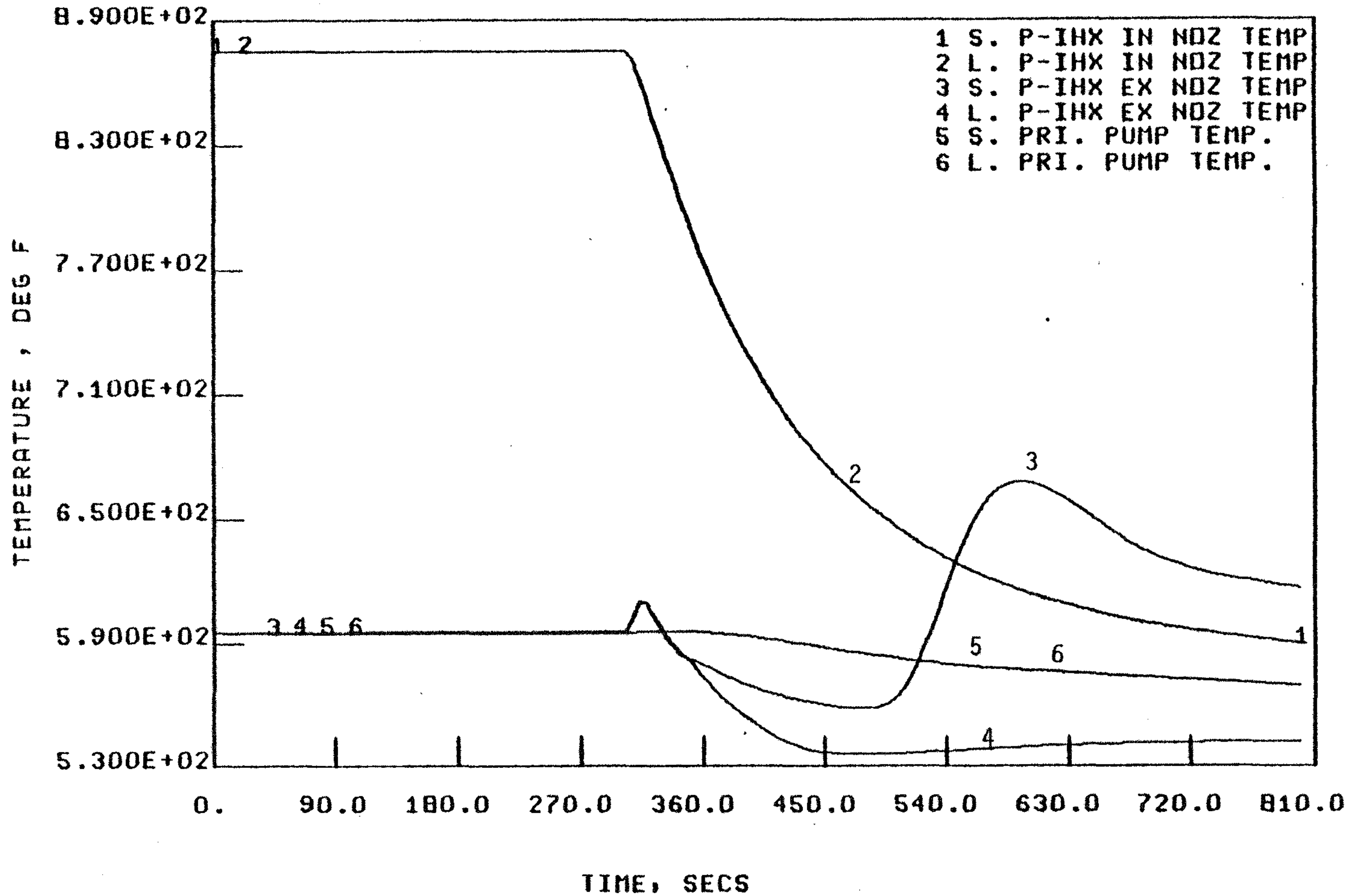

FIGURE 4-113

POOL REACTOR OPENING OF STEAM LINE SAFETY VALVE WITH DELAYED SCRAM
RUN DATED 10/06/78
NUMBER TEPGE03

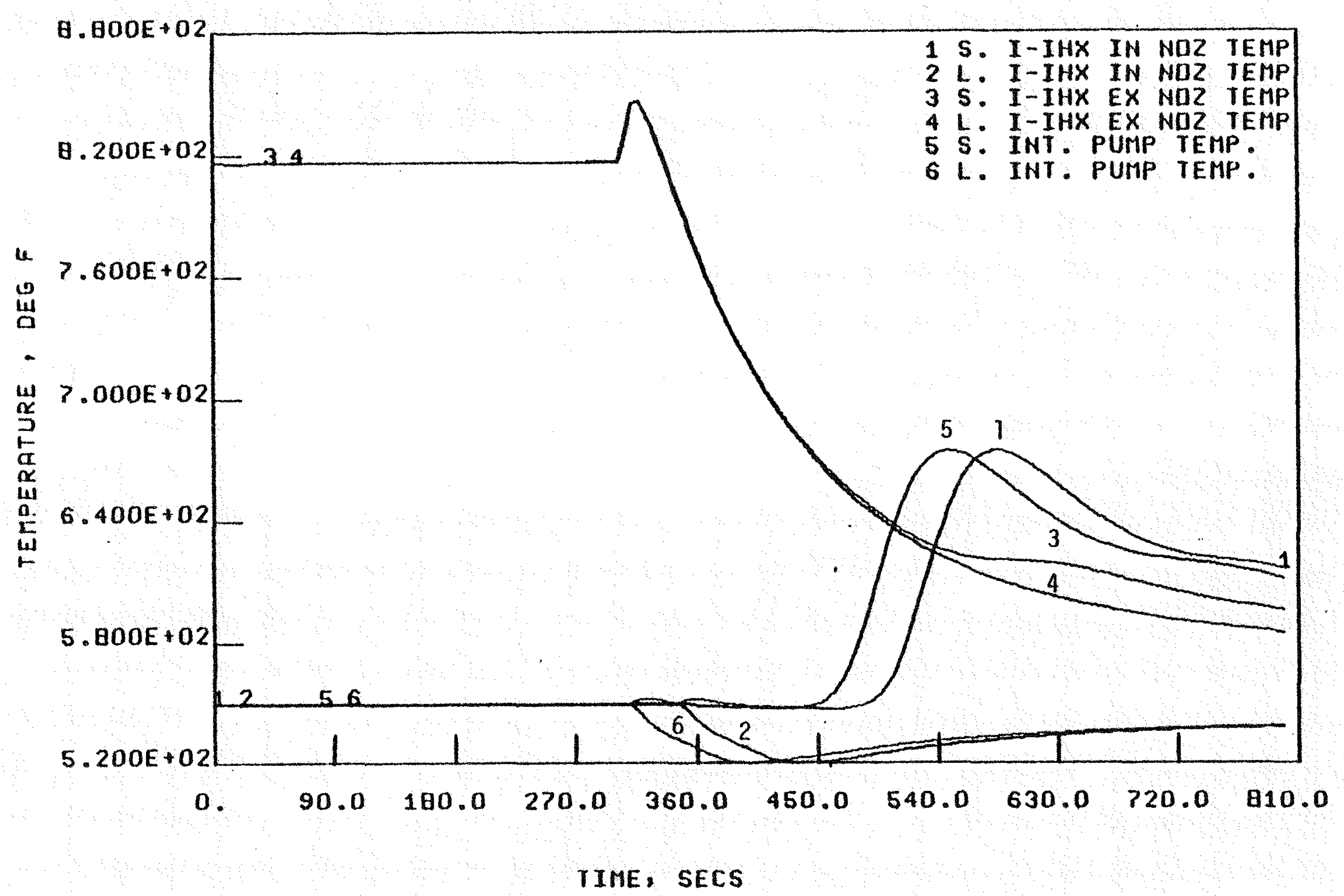

FIGURE 4-114

POOL REACTOR OPENING OF STEAM LINE SAFETY VALVE WITH DELAYED SCRAM
RUN DATED 10/06/78
NUMBER TEP6E03

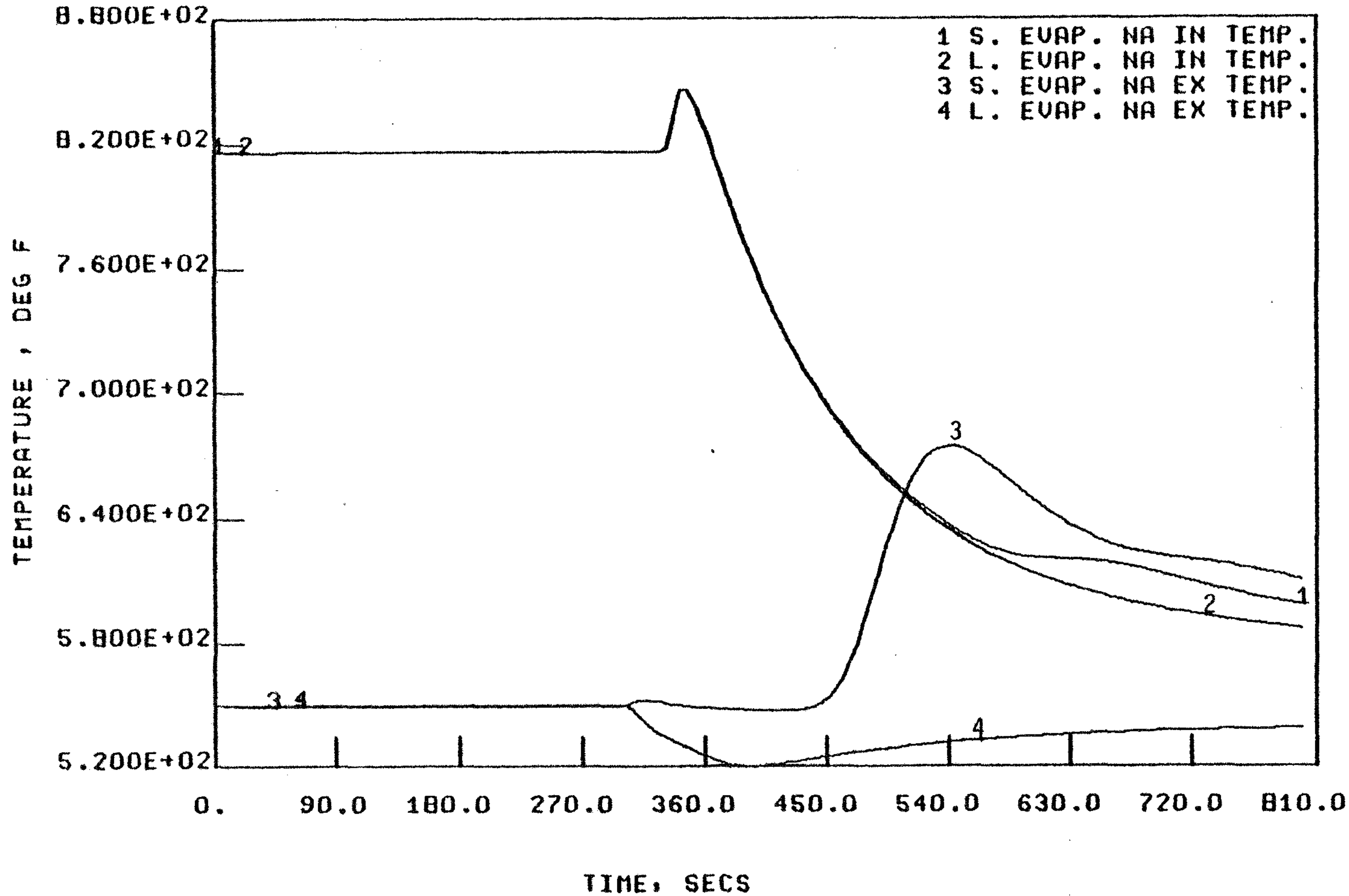

FIGURE 4-115

POOL REACTOR OPENING OF STEAM LINE SAFETY VALVE WITH DELAYED SCRAM
RUN DATED 10/06/78
NUMBER TEPGE03

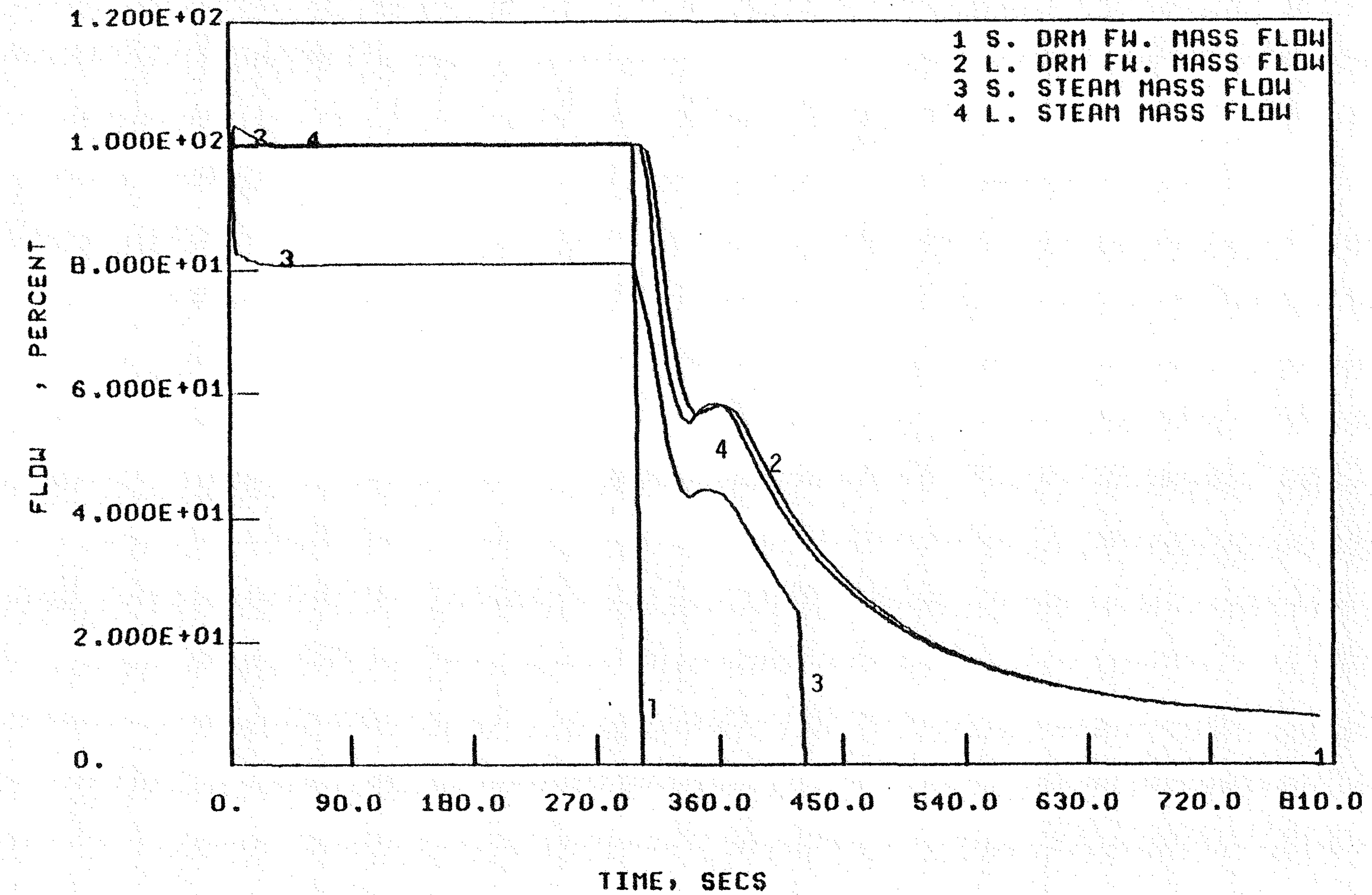

FIGURE 4-116

POOL REACTOR OPENING OF STEAM LINE SAFETY VALVE WITH DELAYED SCRAM
RUN DATED 10/06/78
NUMBER TEPGE03

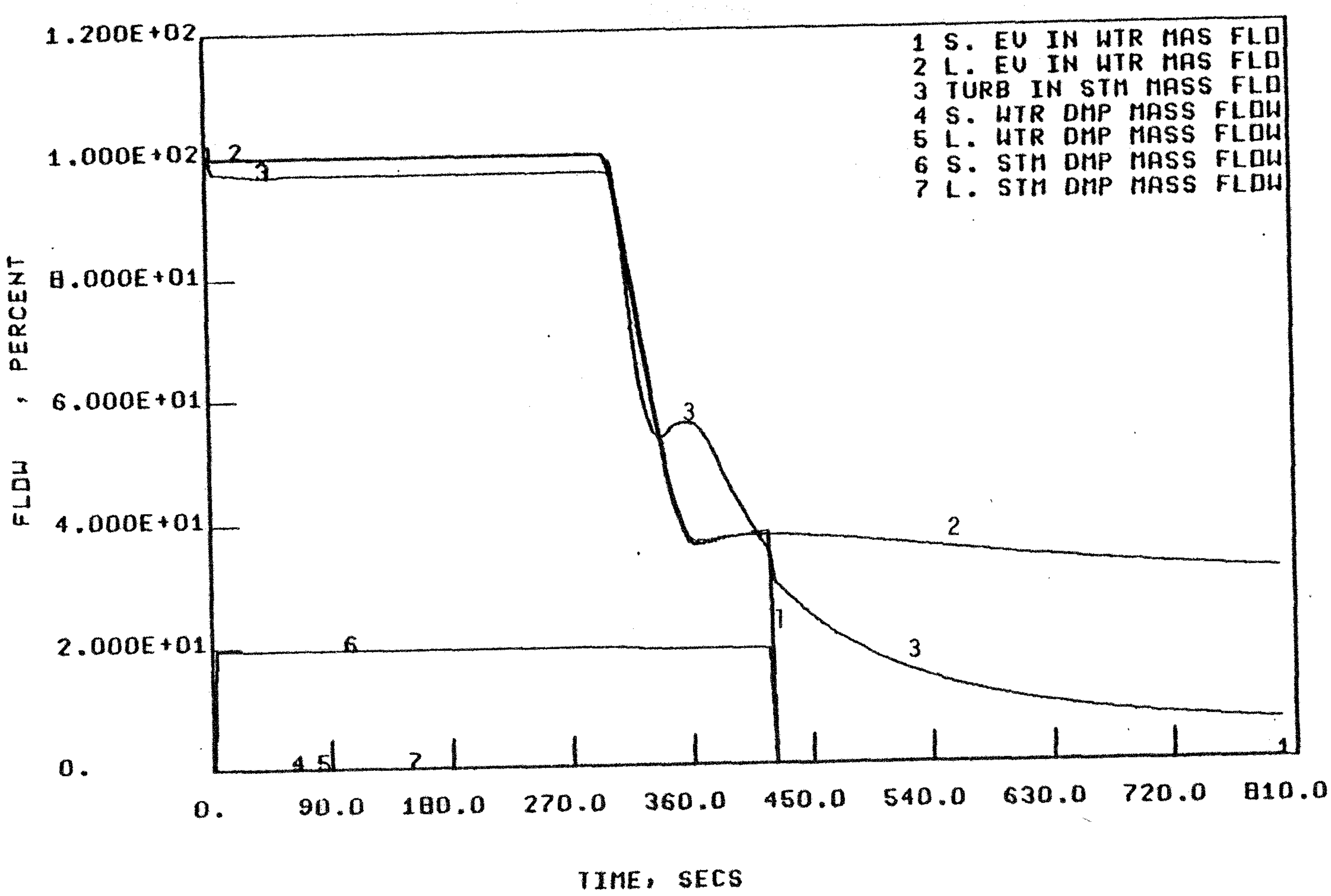

FIGURE 4-117
POOL REACTOR OPENING OF STEAM LINE SAFETY VALVE WITH DELAYED SCRAM
RUN DATED 10/06/78
NUMBER TEPGE03

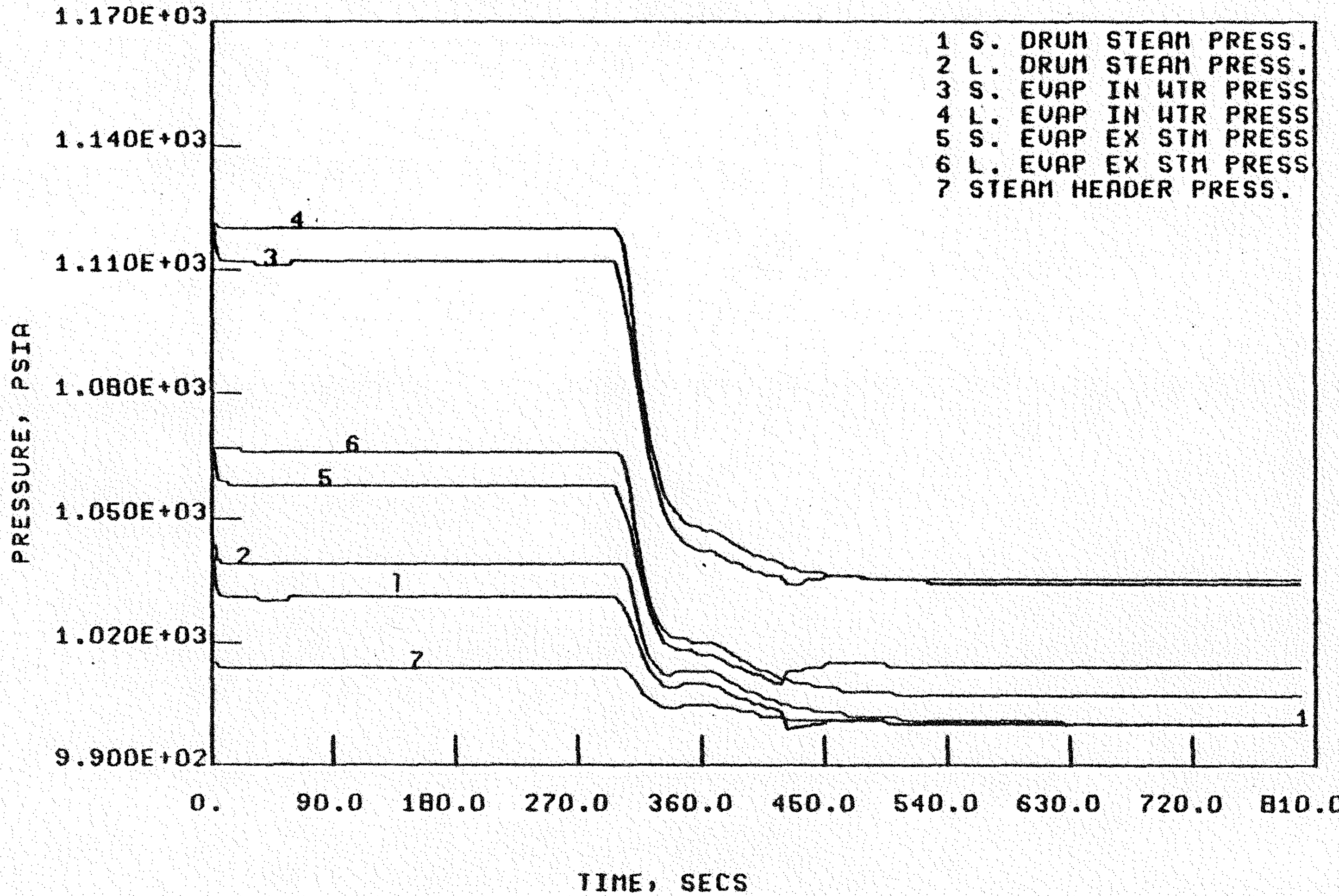

FIGURE 4-118

POOL REACTOR OPENING OF STEAM LINE SAFETY VALVE WITH DELAYED SCRAM
RUN DATED 10/06/78
NUMBER TEP6E03

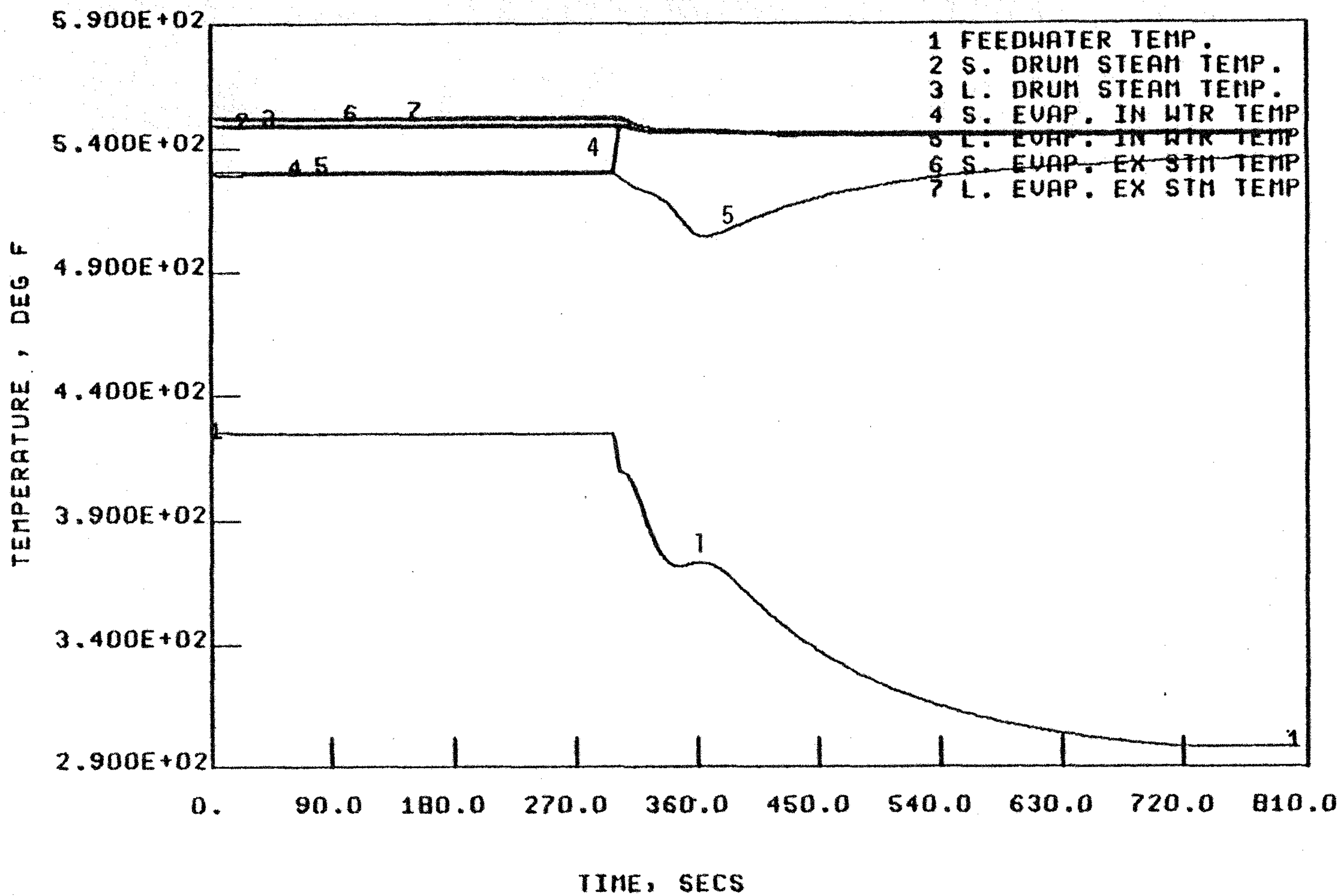

FIGURE 4-119

POOL REACTOR OPENING OF STEAM LINE SAFETY VALVE WITH DELAYED SCRAM
RUN DATED 10/06/78
NUMBER TEPGE03

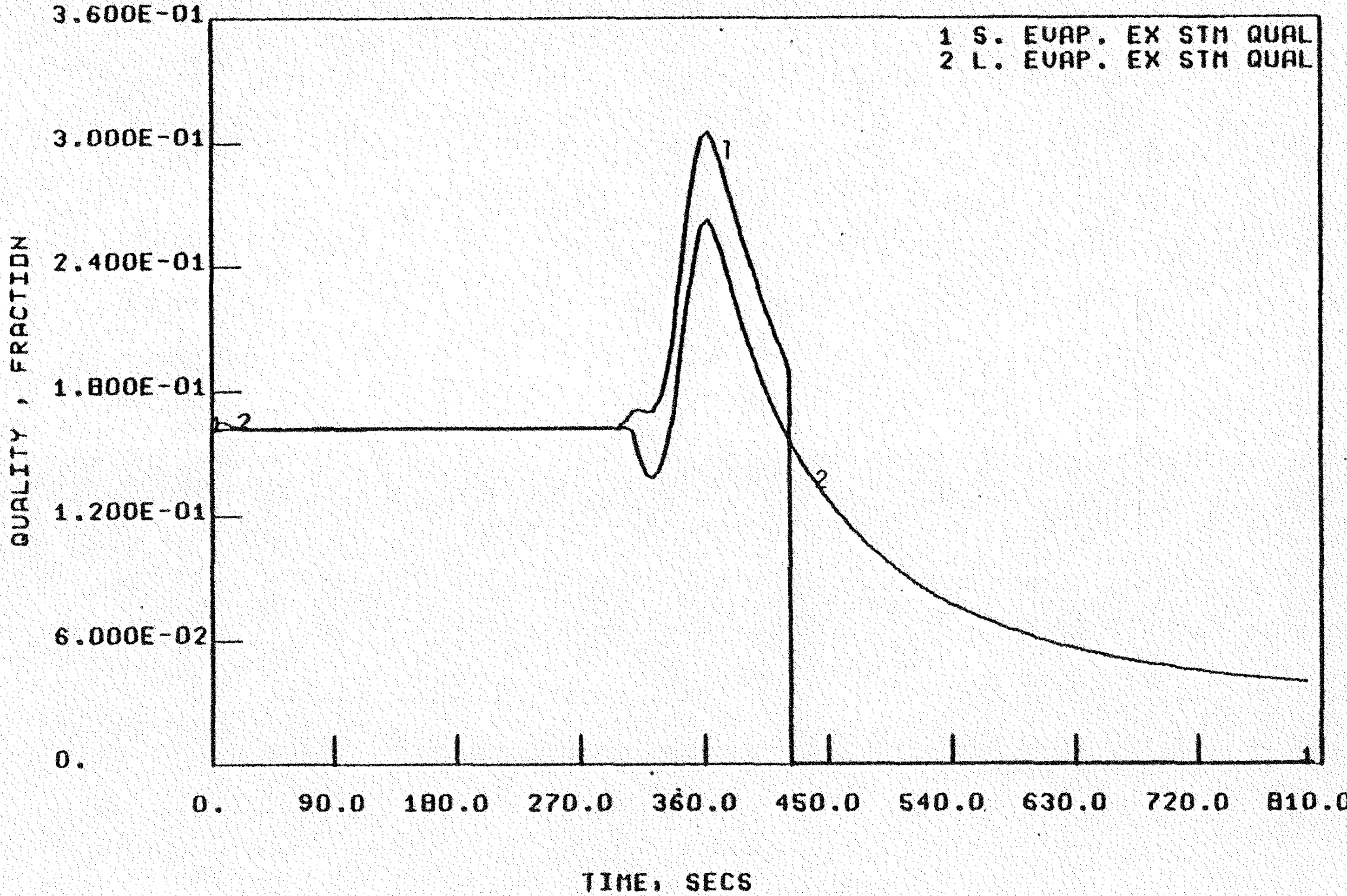

FIGURE 4-120

POOL REACTOR OPENING OF STEAM LINE SAFETY VALVE WITH DELAYED SCRAM
RUN DATED 10/06/78
NUMBER TEPGE03

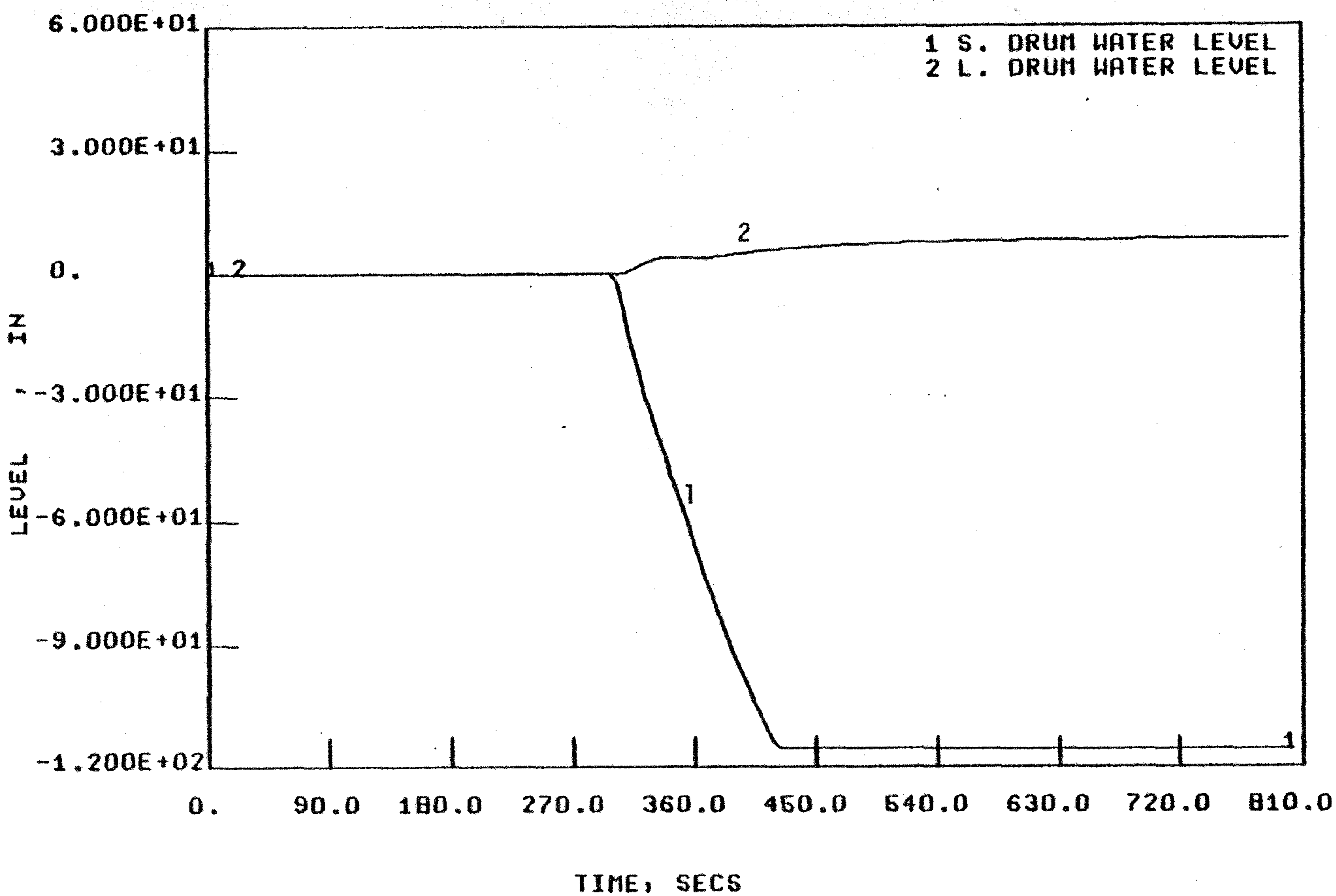

FIGURE 4-121

POOL REACTOR CONTROL ROD WITHDRAWL WITH DELAYED MANUAL SCRAM
RUN DATED 10/05/78
NUMBER PAPGE04

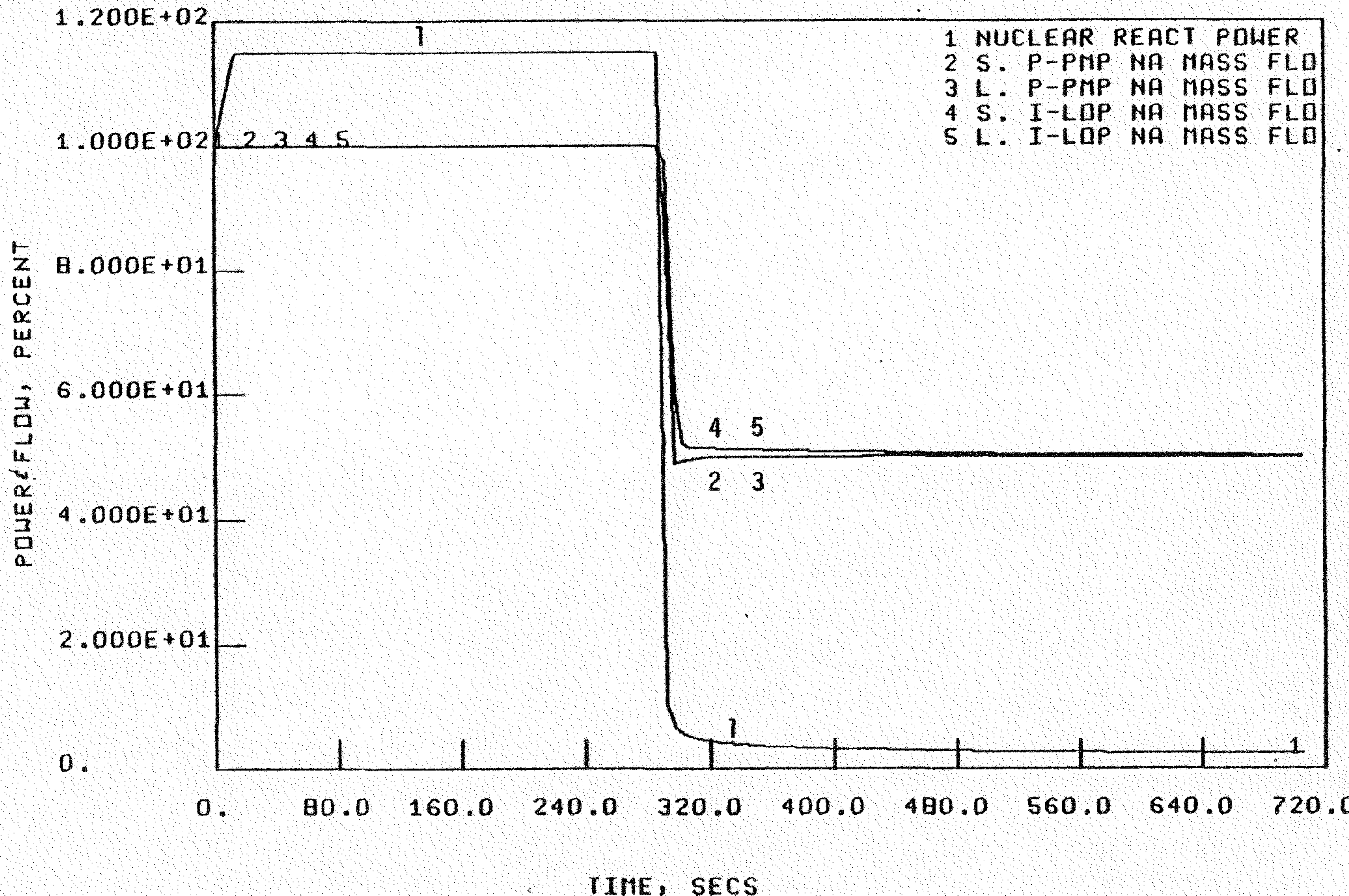

FIGURE 4-122

POOL REACTOR CONTROL ROD WITHDRAWL WITH DELAYED MANUAL SCRAM

RUN DATED 10/05/78

NUMBER PAPGE04

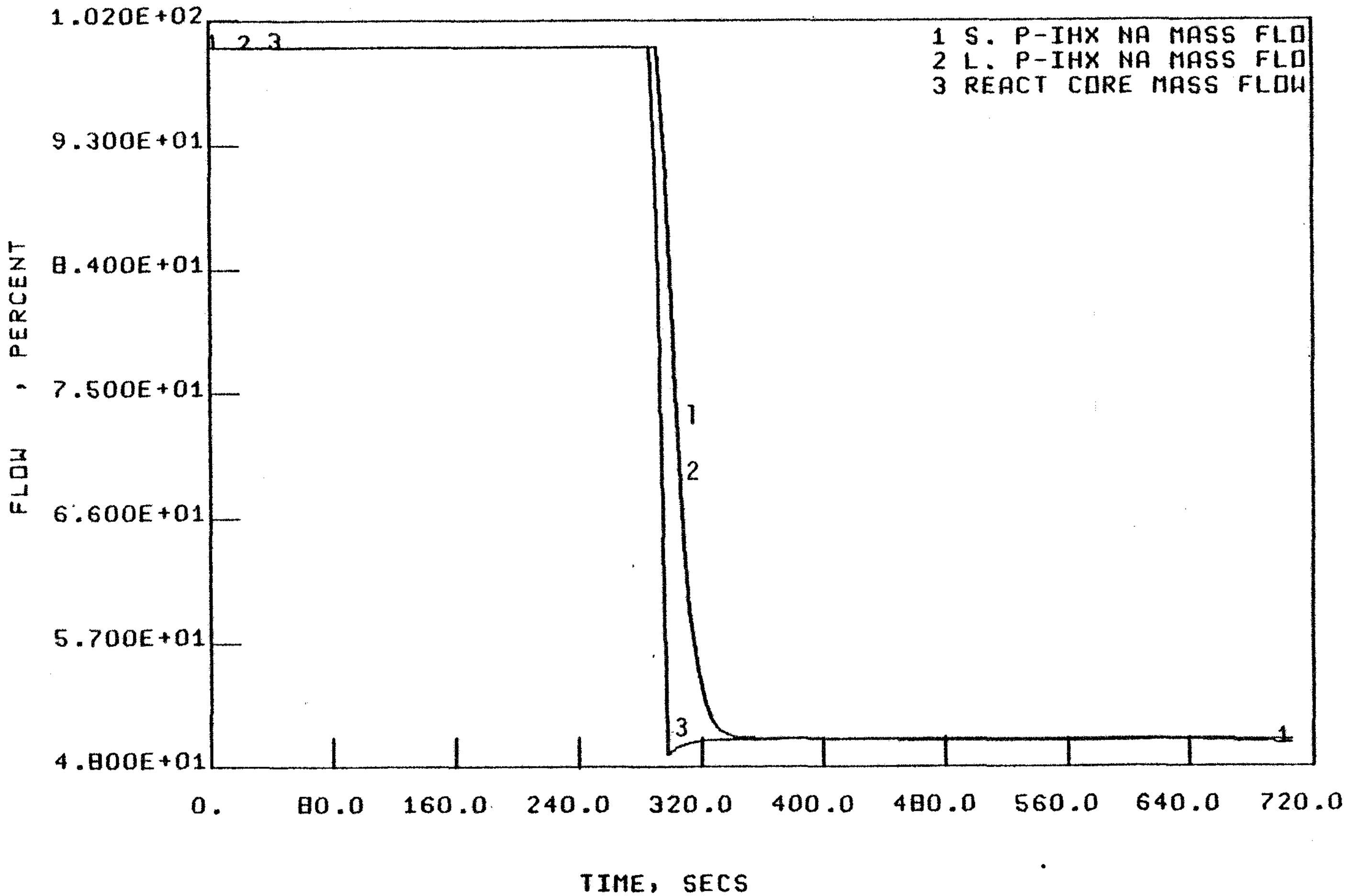

FIGURE 4-123
POOL REACTOR CONTROL ROD WITHDRAWL WITH DELAYED MANUAL SCRAM
RUN DATED 10/05/78
NUMBER PAPGE04

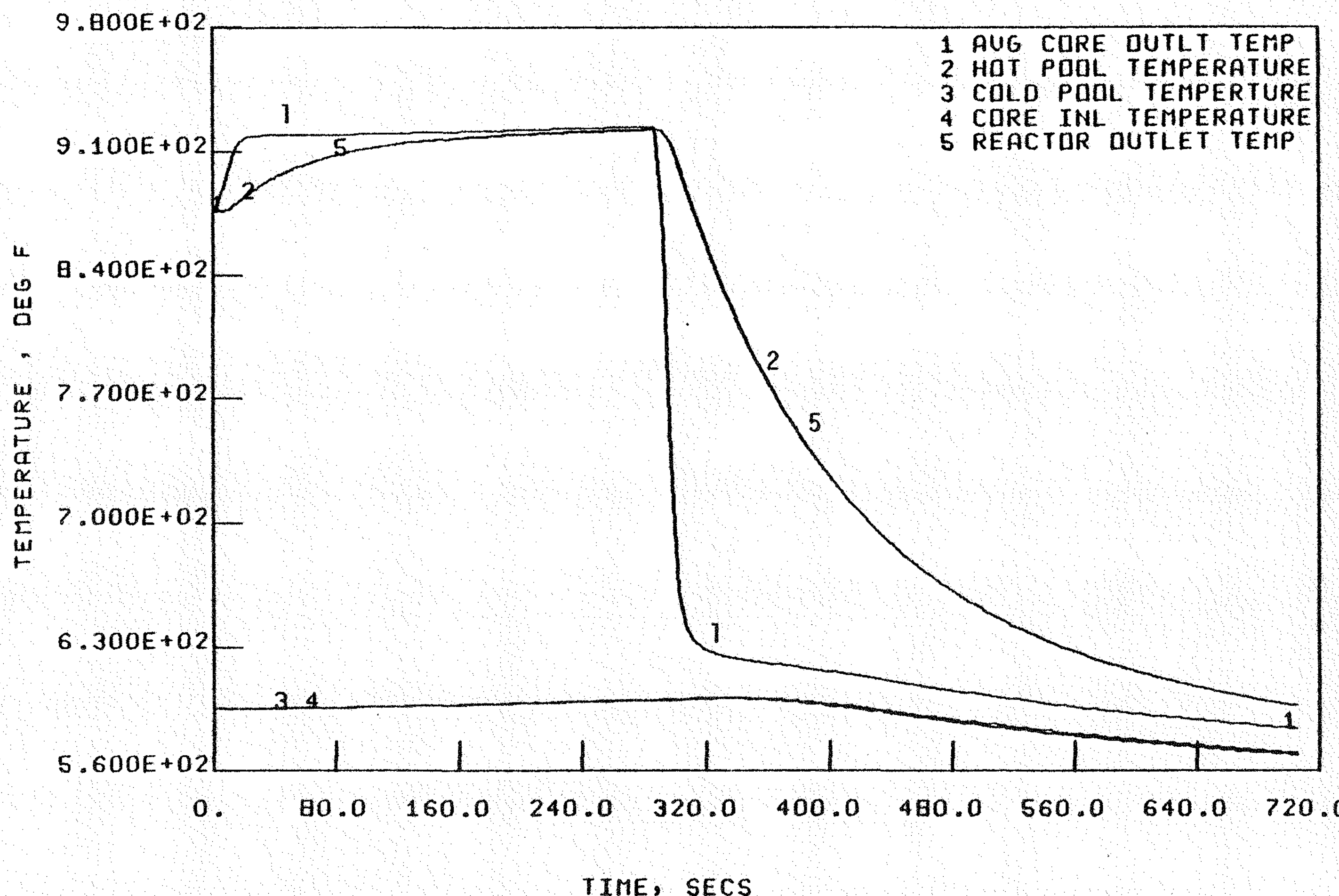

FIGURE 4-124
POOL REACTOR CONTROL ROD WITHDRAWL WITH DELAYED MANUAL SCRAM
RUN DATED 10/05/78
NUMBER PAPGE04

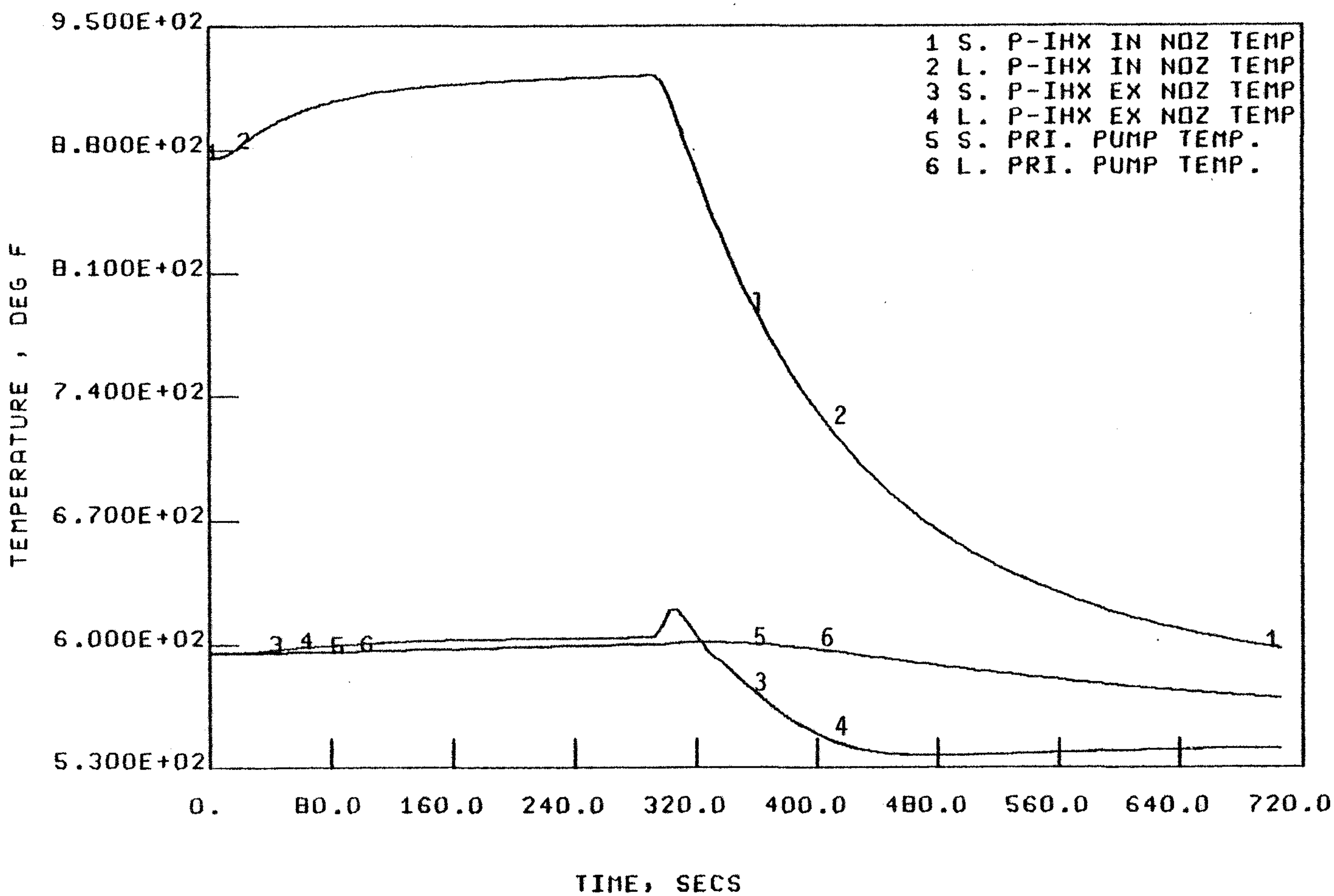

FIGURE 4-125

POOL REACTOR CONTROL ROD WITHDRAWL WITH DELAYED MANUAL SCRAM
RUN DATED 10/05/78
NUMBER PAPGE04

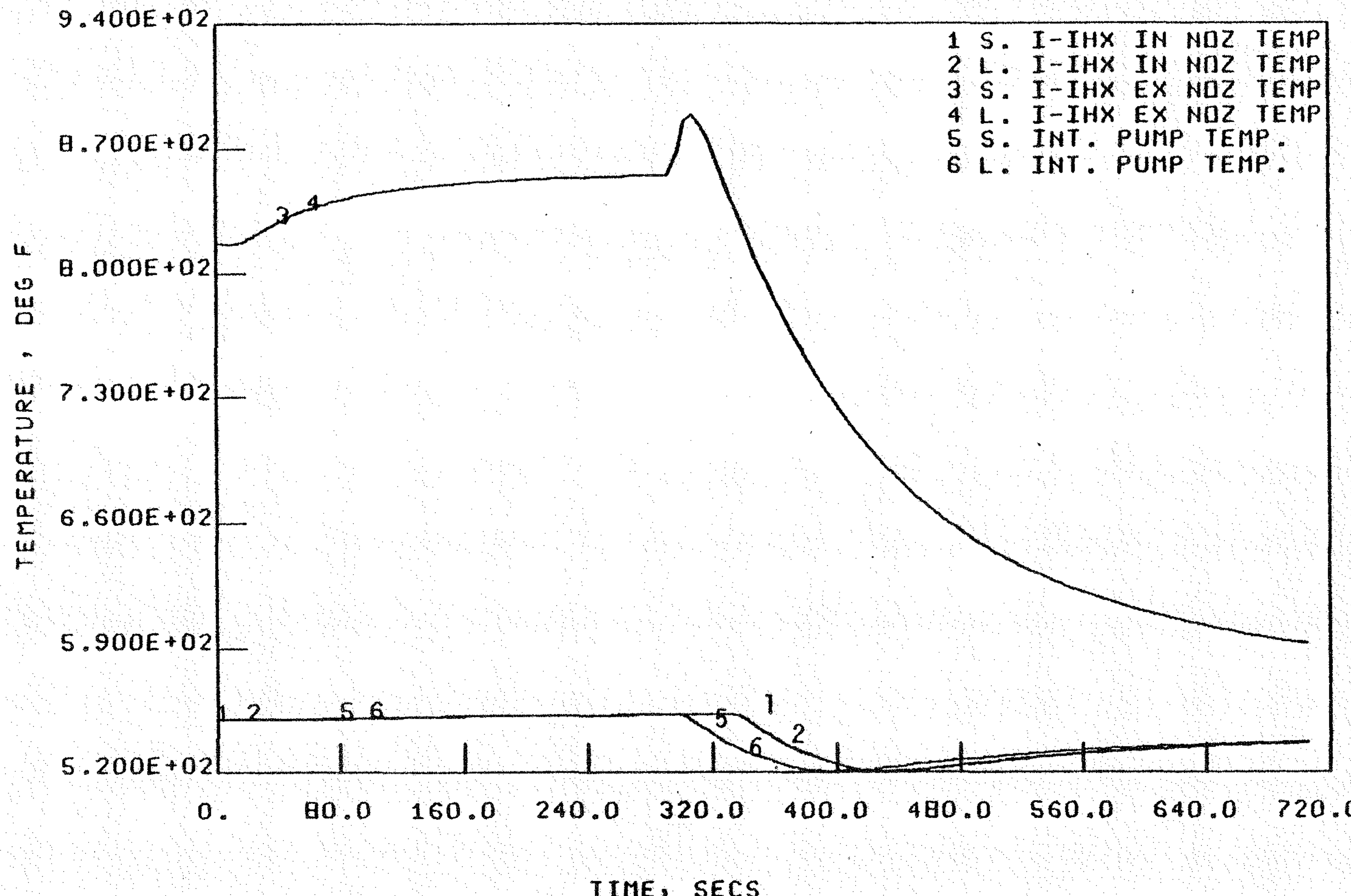

FIGURE 4-126

POOL REACTOR CONTROL ROD WITHDRAWL WITH DELAYED MANUAL SCRAM
RUN DATED 10/05/78
NUMBER PAPGE04

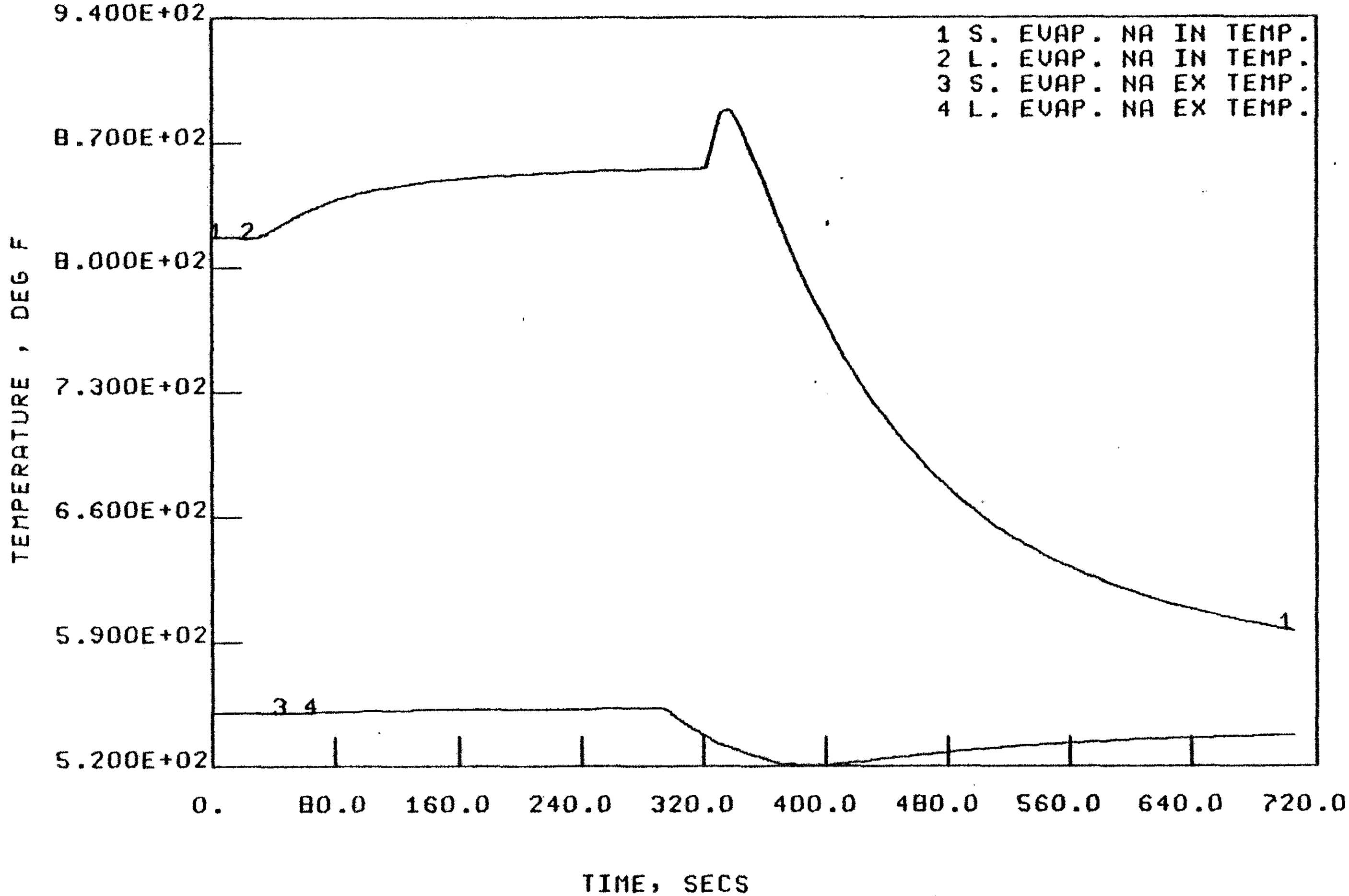

FIGURE 4-127
POOL REACTOR CONTROL ROD WITHDRAWL WITH DELAYED MANUAL SCRAM
RUN DATED 10/05/78
NUMBER PAPGE04

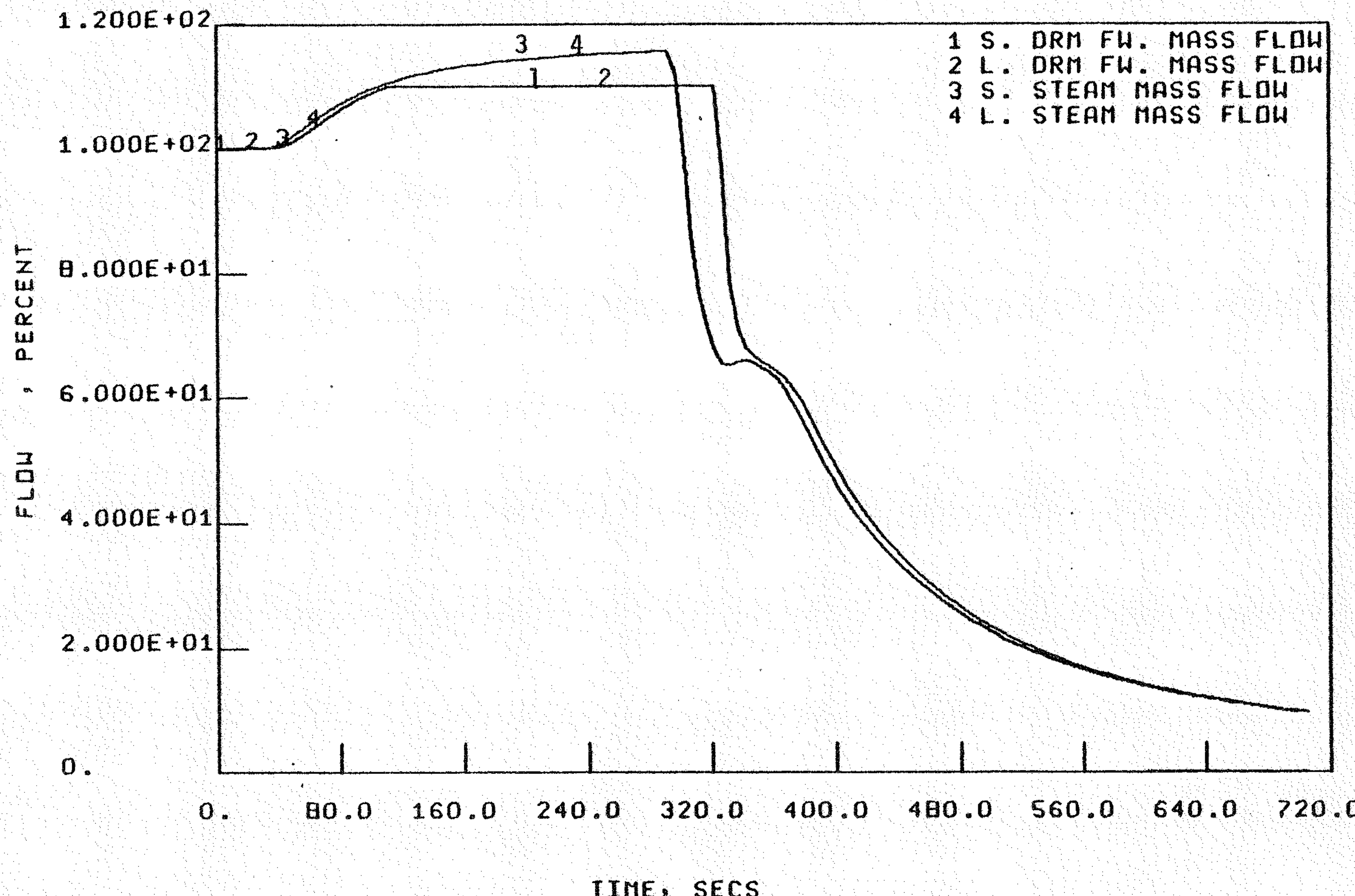

FIGURE 4-128

POOL REACTOR CONTROL ROD WITHDRAWL WITH DELAYED MANUAL SCRAM
RUN DATED 10/05/78
NUMBER PAPGE04

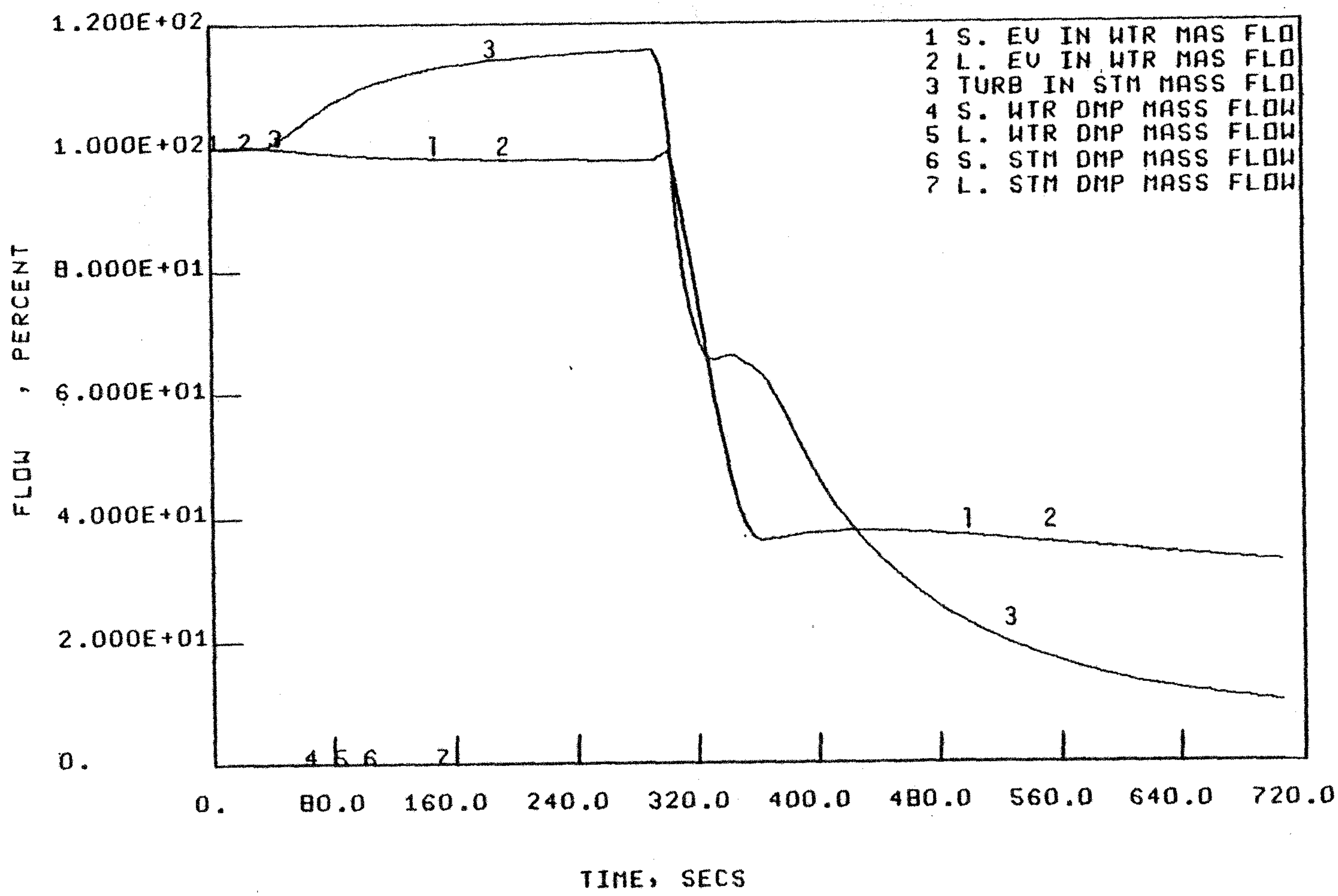

FIGURE 4-129
POOL REACTOR CONTROL ROD WITHDRAWL WITH DELAYED MANUAL SCRAM
RUN DATED 10/05/78
NUMBER PAPGE04

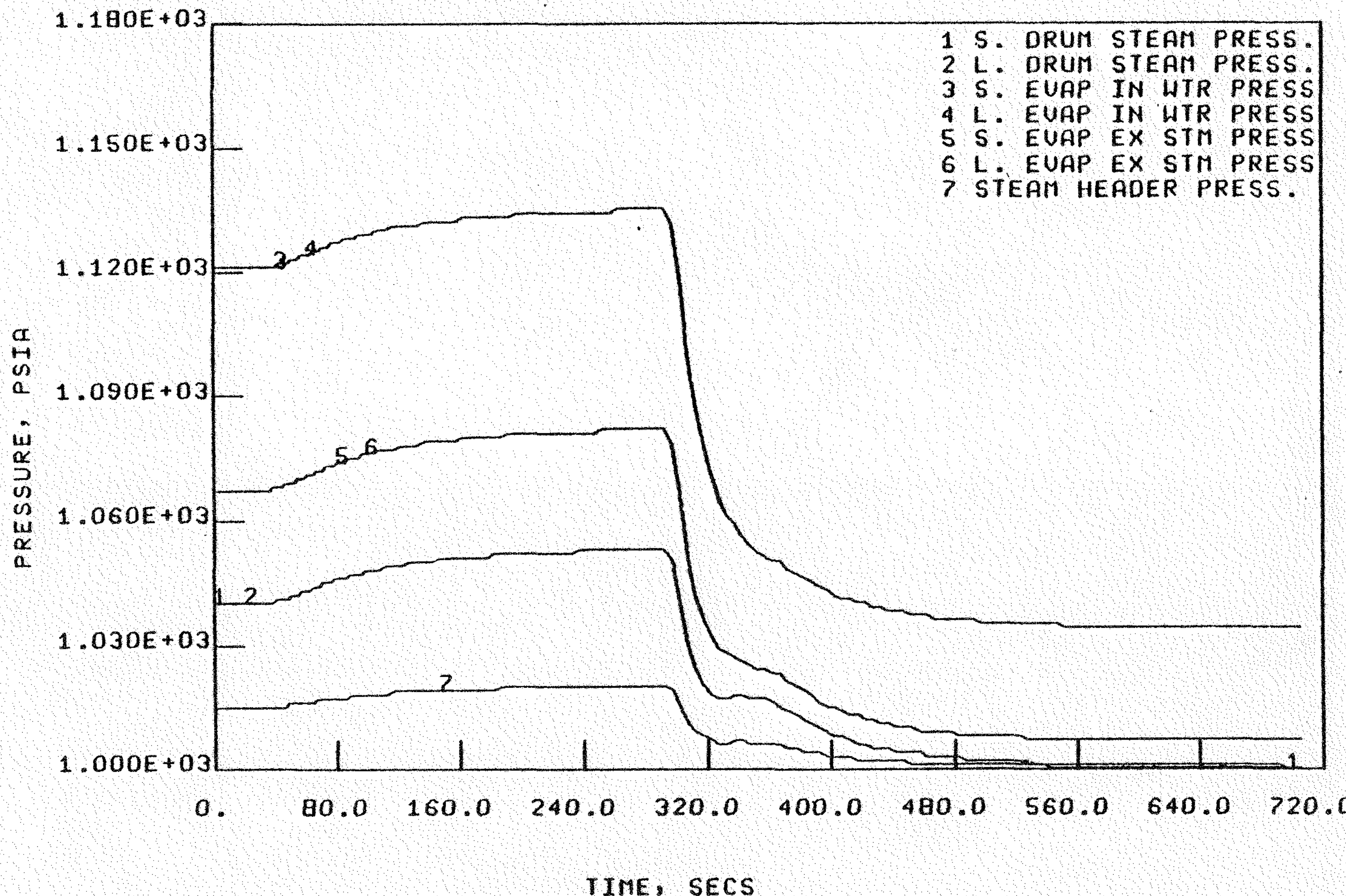

FIGURE 4-130
POOL REACTOR CONTROL ROD WITHDRAWL WITH DELAYED MANUAL SCRAM
RUN DATED 10/05/78
NUMBER PAPGE04

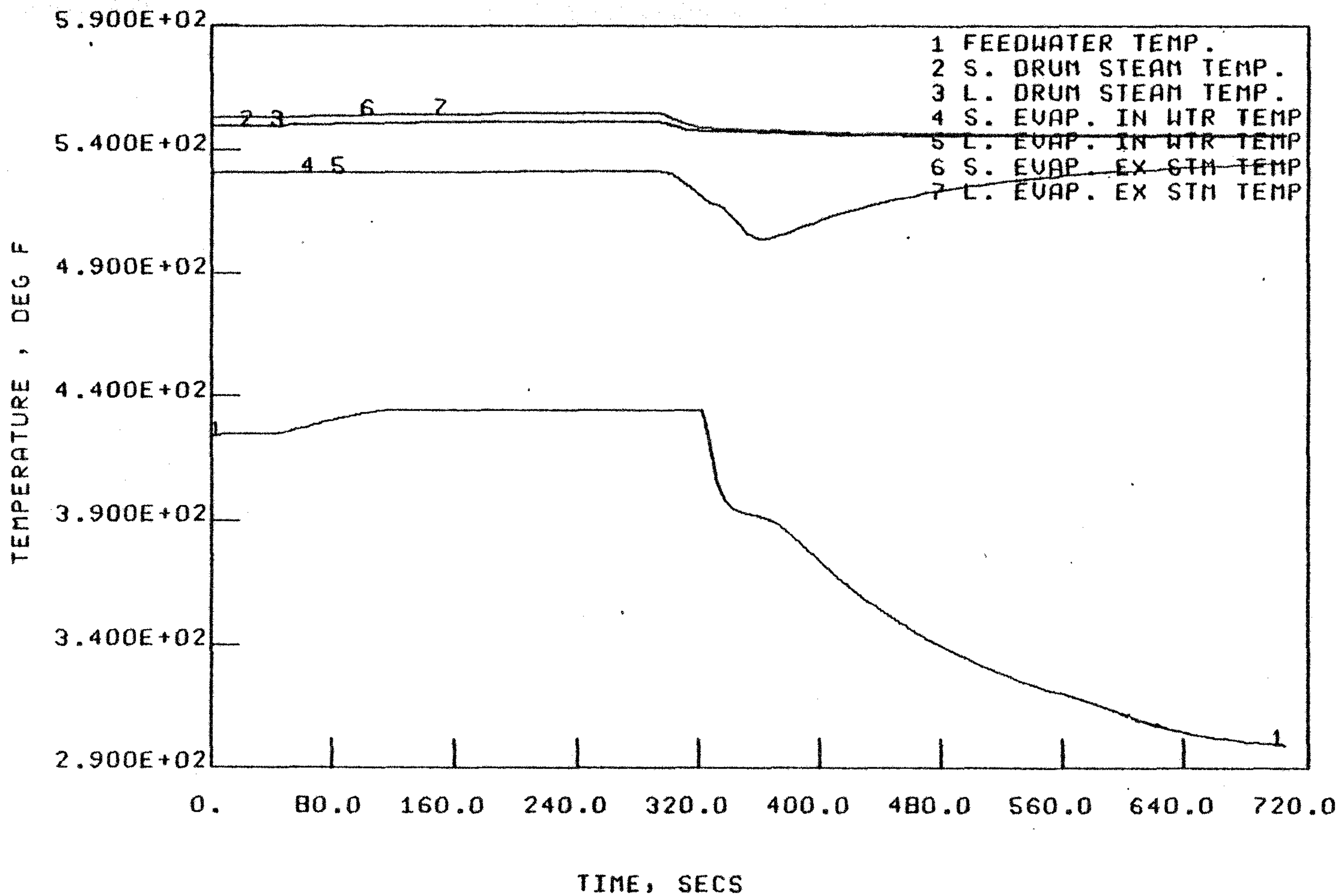

FIGURE 4-131
POOL REACTOR CONTROL ROD WITHDRAWL WITH DELAYED MANUAL SCRAM
RUN DATED 10/05/78
NUMBER PAPGE04

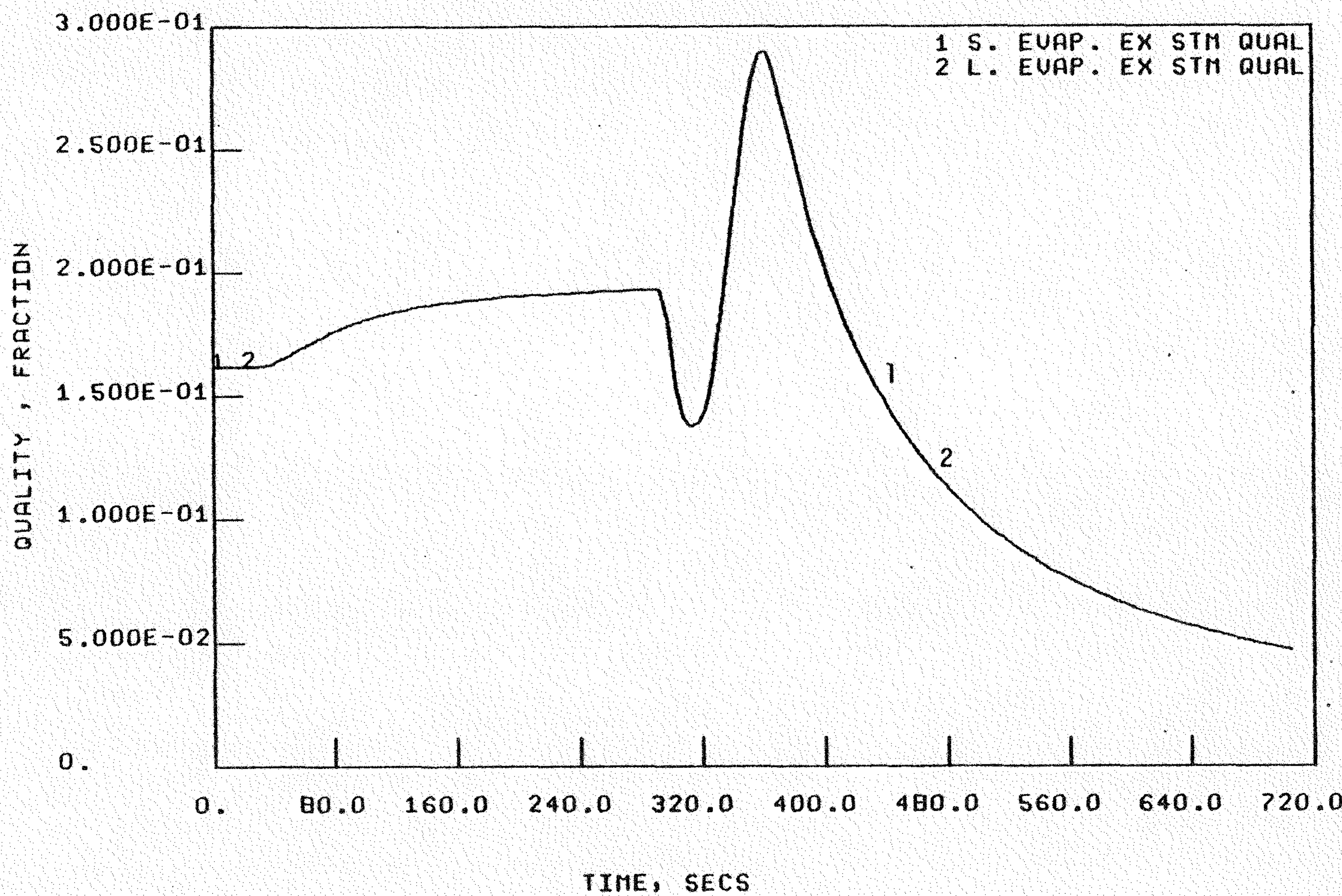

FIGURE 4-132
POOL REACTOR CONTROL ROD WITHDRAWL WITH DELAYED MANUAL SCRAM
RUN DATED 10/05/78
NUMBER PAPGE04

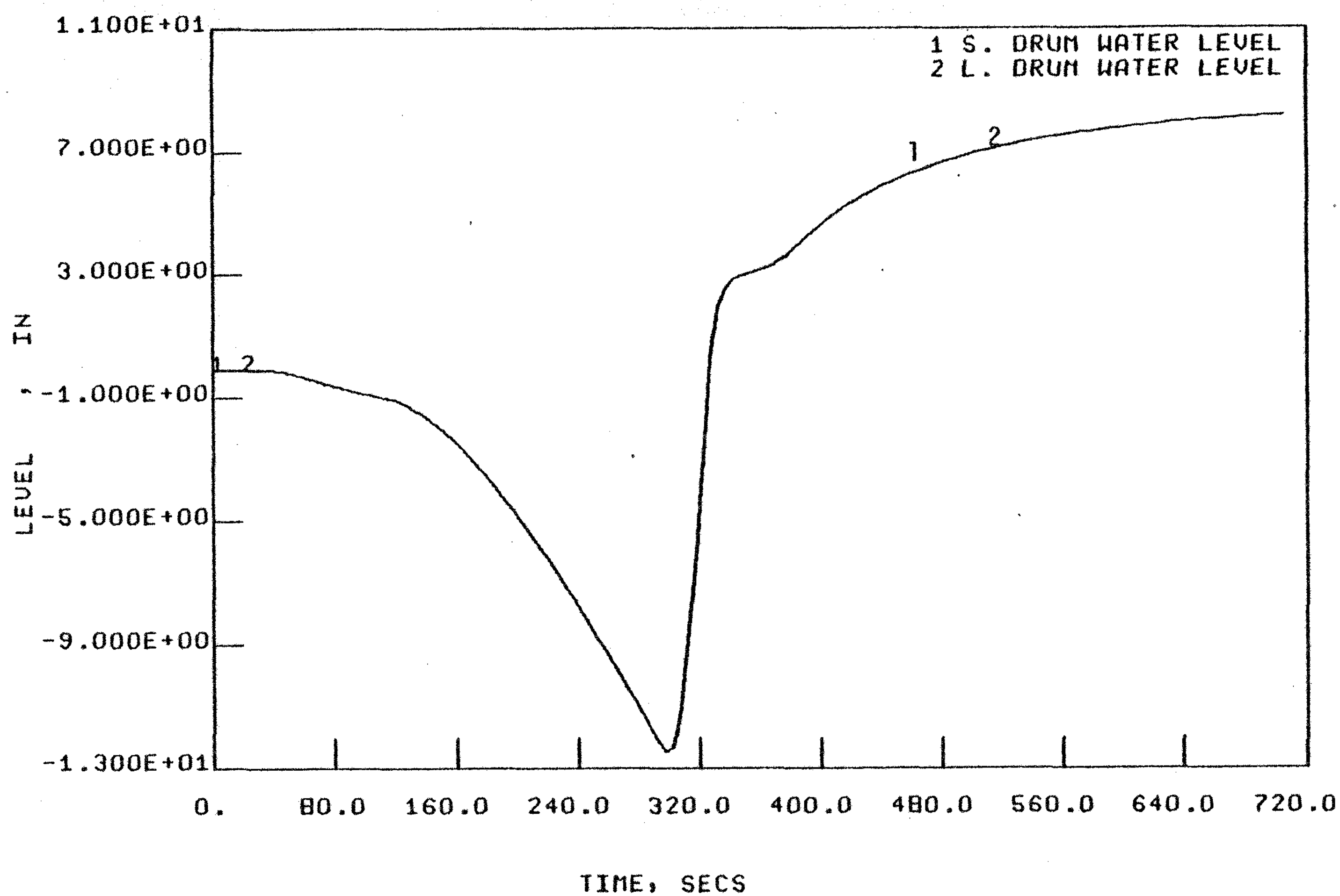

FIGURE 4-133
POOL REACTOR ISOLATION OF ONE STEAM GENERATOR AND DUMP VALVE FAILURE
RUN DATED 10/06/78
NUMBER TEPGE01

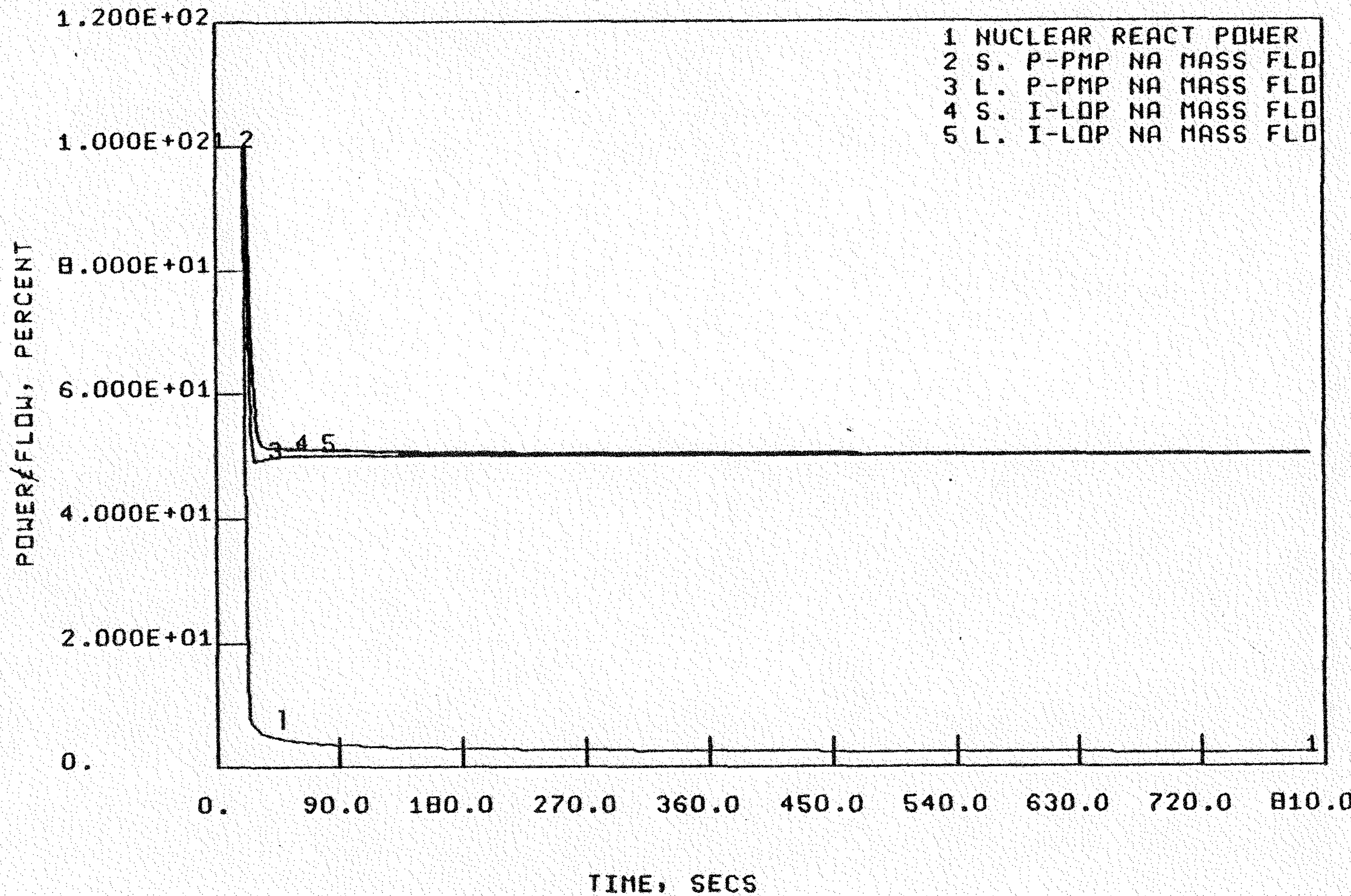

FIGURE 4-134
POOL REACTOR ISOLATION OF ONE STEAM GENERATOR AND DUMP VALVE FAILURE
RUN DATED 10/06/78
NUMBER TEP6E01

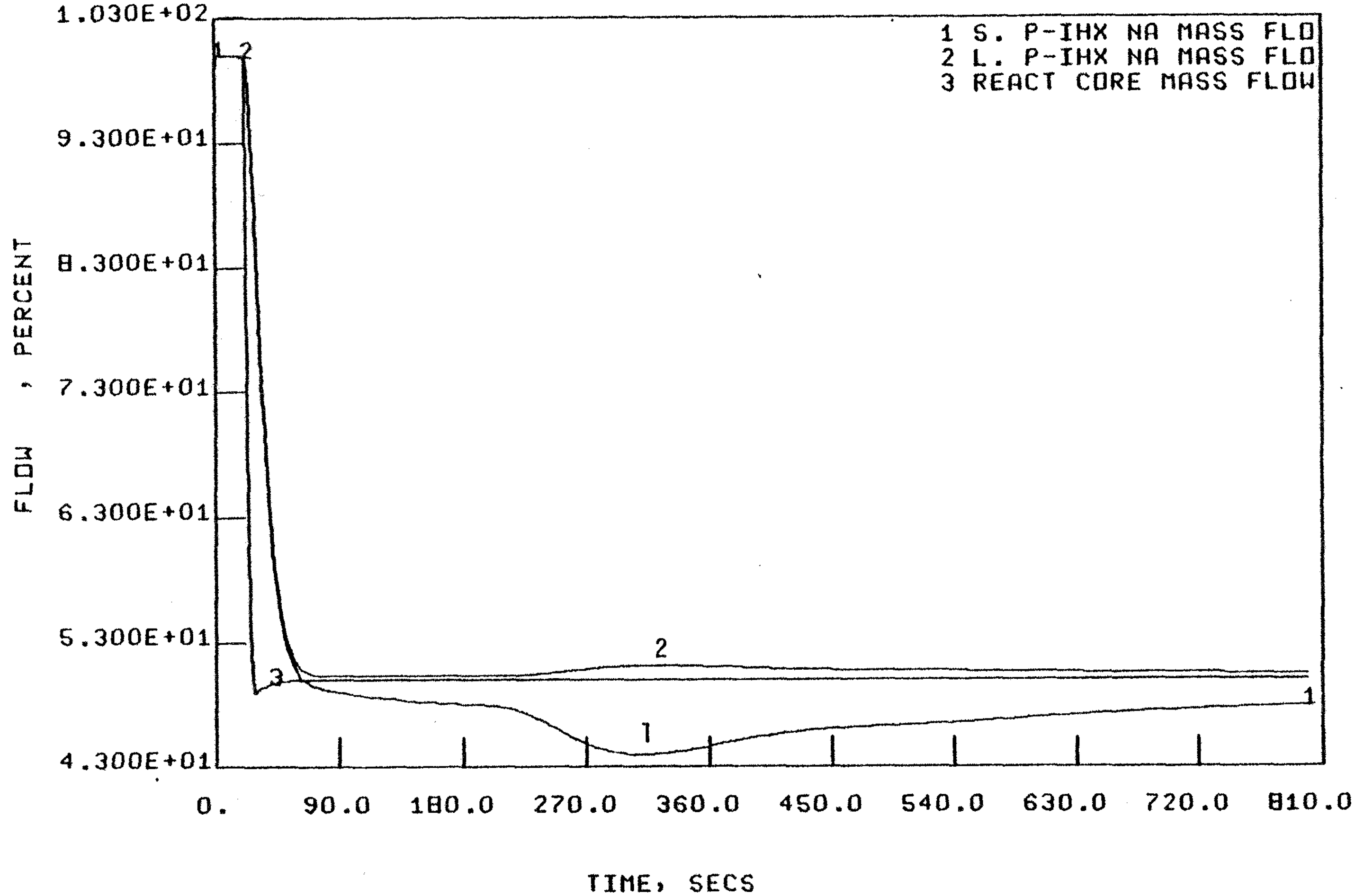

FIGURE 4-135
POOL REACTOR ISOLATION OF ONE STEAM GENERATOR AND DUMP VALVE FAILURE
RUN DATED 10/06/78
NUMBER TEPGE01

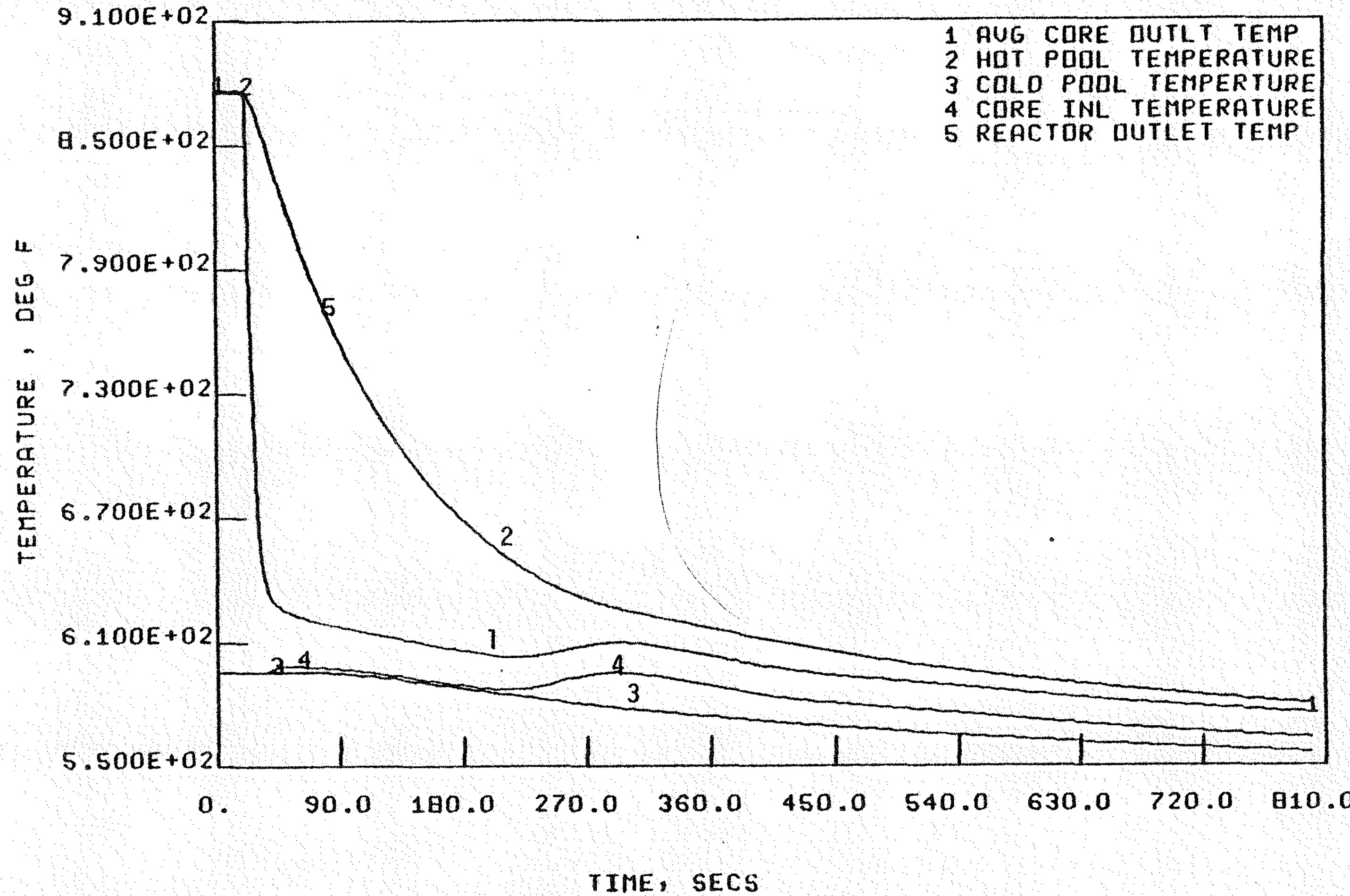

FIGURE 4-136

POOL REACTOR ISOLATION OF ONE STEAM GENERATOR AND DUMP VALVE FAILURE
RUN DATED 10/06/78
NUMBER TEPGE01

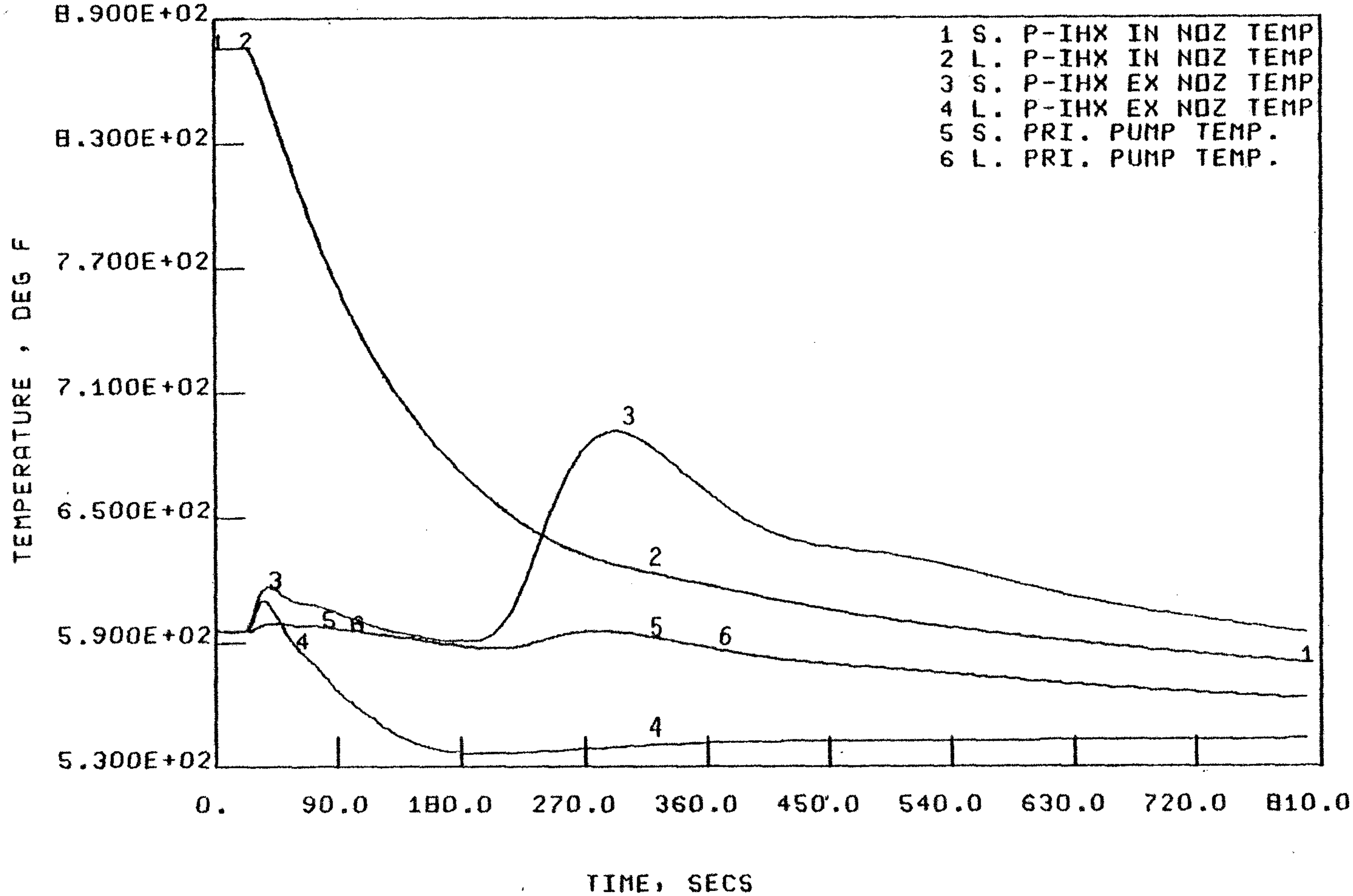

FIGURE 4-137
POOL REACTOR ISOLATION OF ONE STEAM GENERATOR AND DUMP VALVE FAILURE
RUN DATED 10/06/78
NUMBER TEPGE01

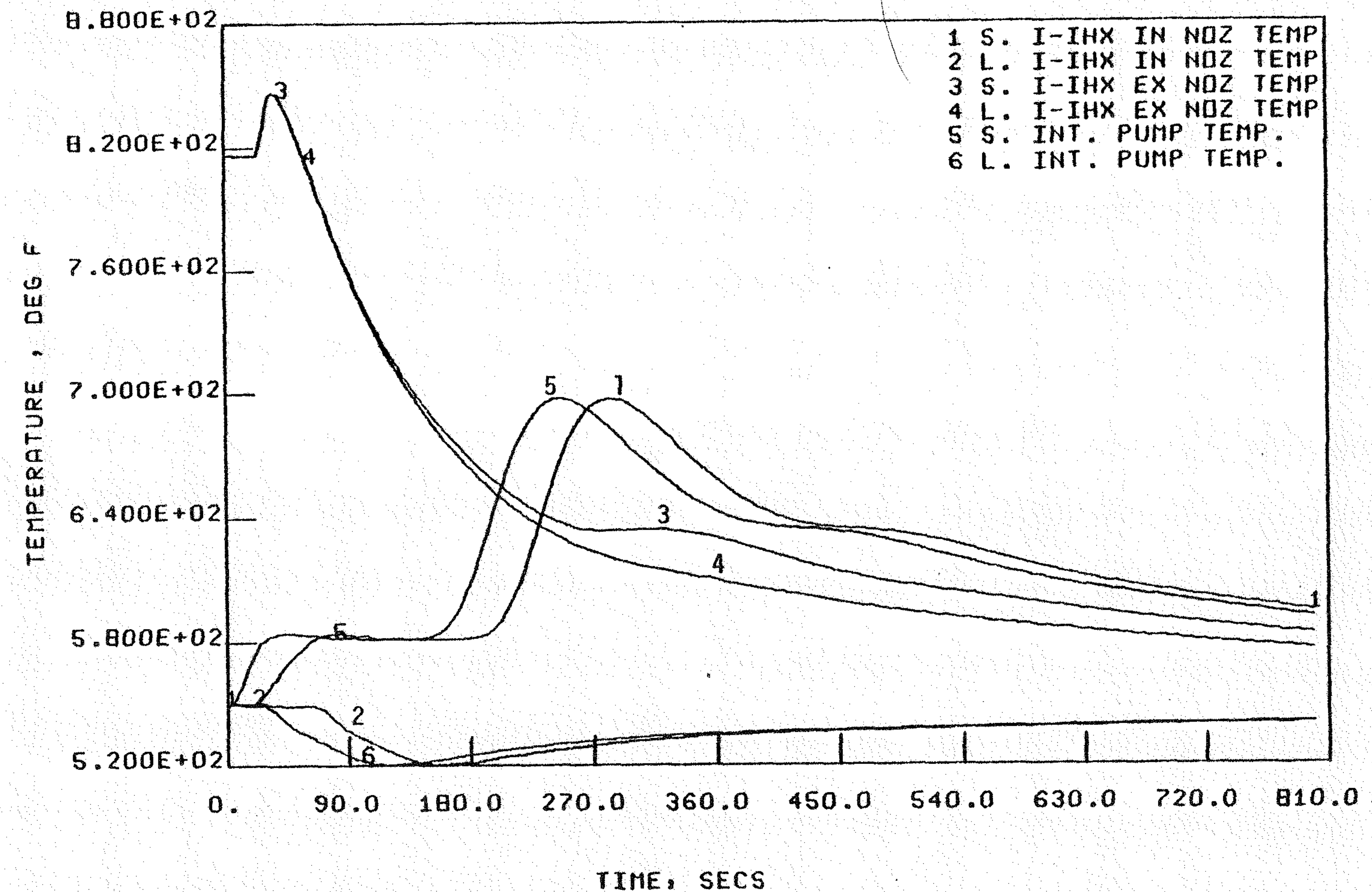

FIGURE 4-138

POOL REACTOR ISOLATION OF ONE STEAM GENERATOR AND DUMP VALVE FAILURE

RUN DATED 10/06/78

NUMBER TEPGE01

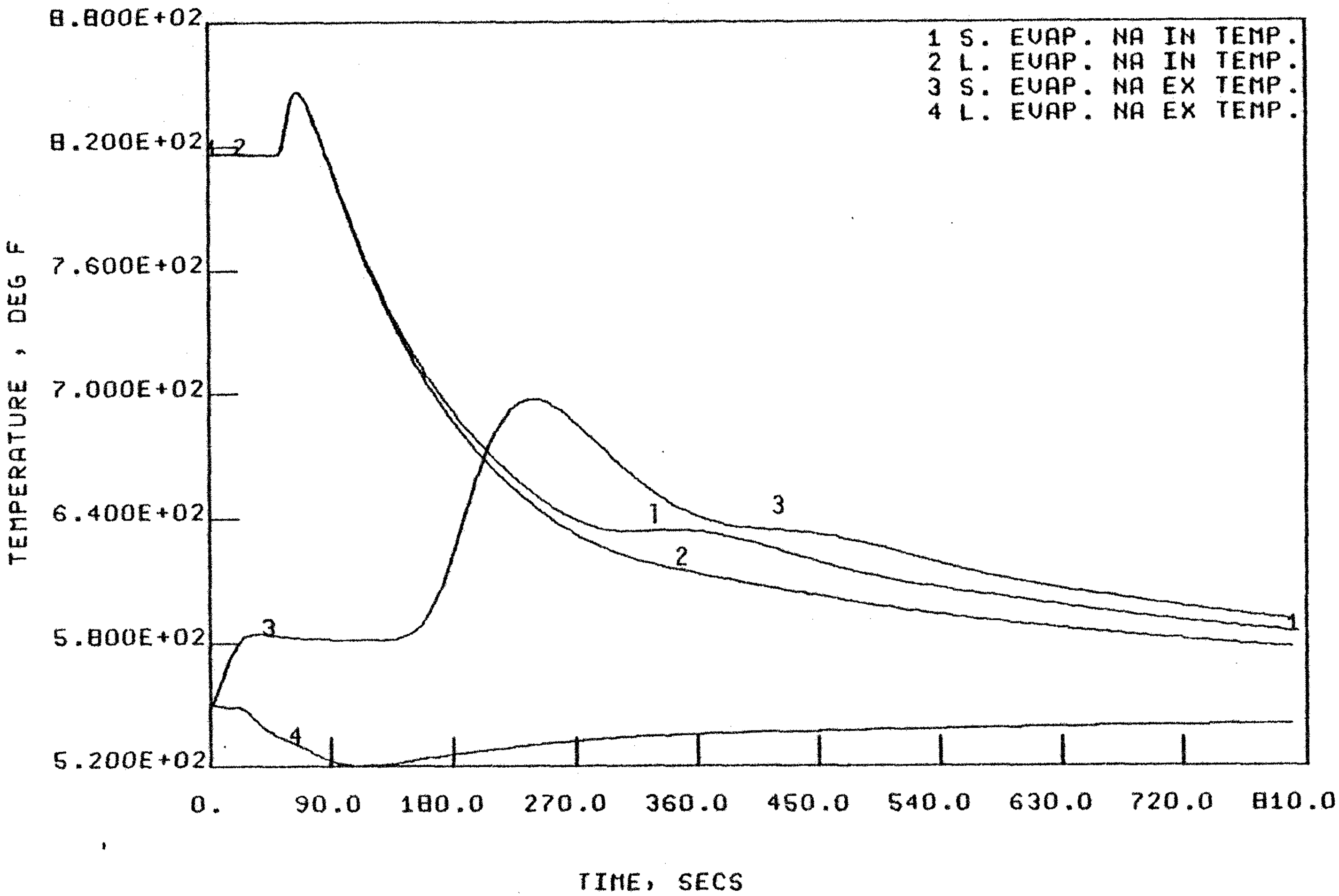

FIGURE 4-139

POOL REACTOR ISOLATION OF ONE STEAM GENERATOR AND DUMP VALVE FAILURE
RUN DATED 10/06/78
NUMBER TEPGE01

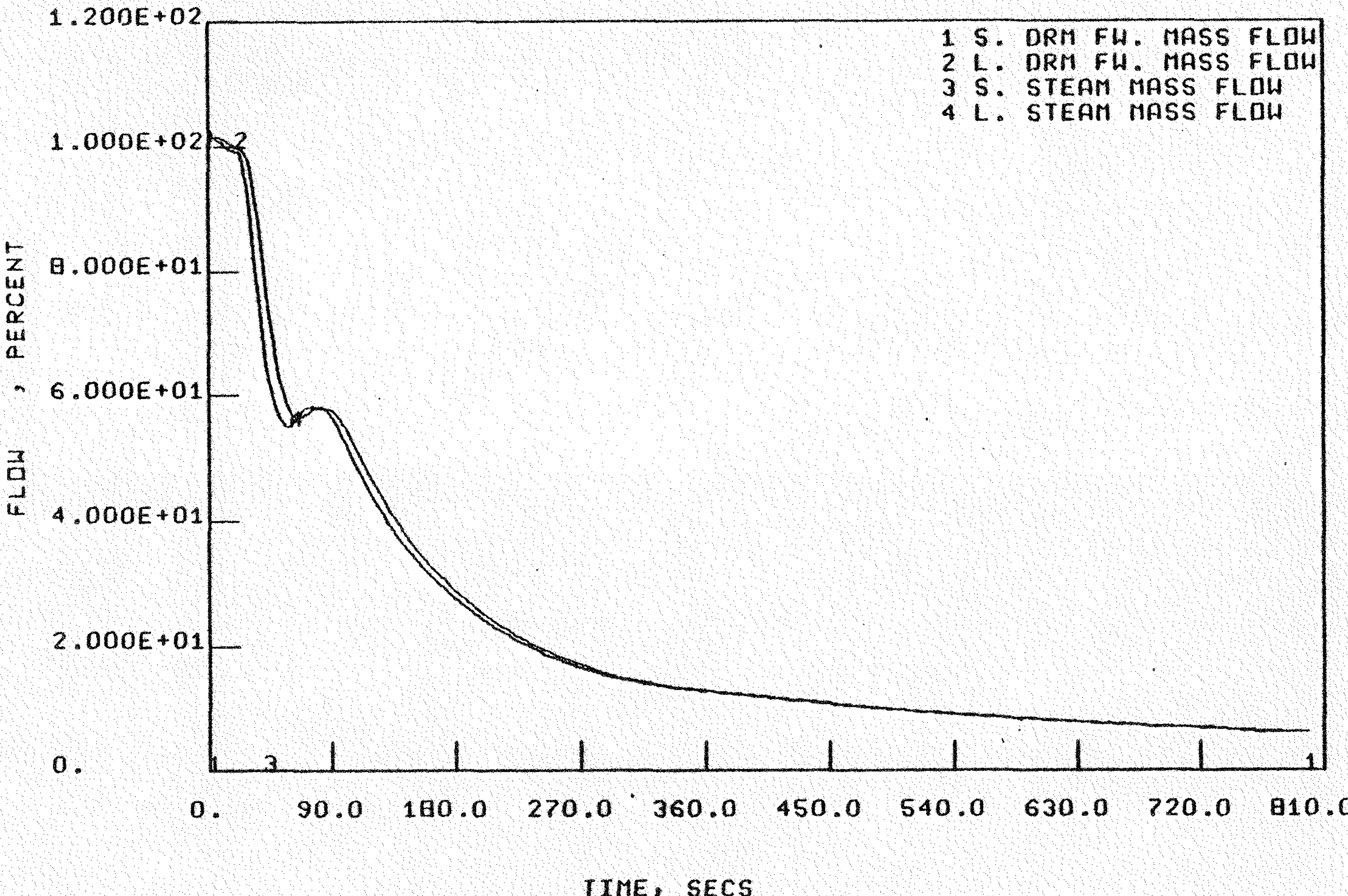

FIGURE 4-140
POOL REACTOR ISOLATION OF ONE STEAM GENERATOR AND DUMP VALVE FAILURE
RUN DATED 10/06/78
NUMBER TEPGE01

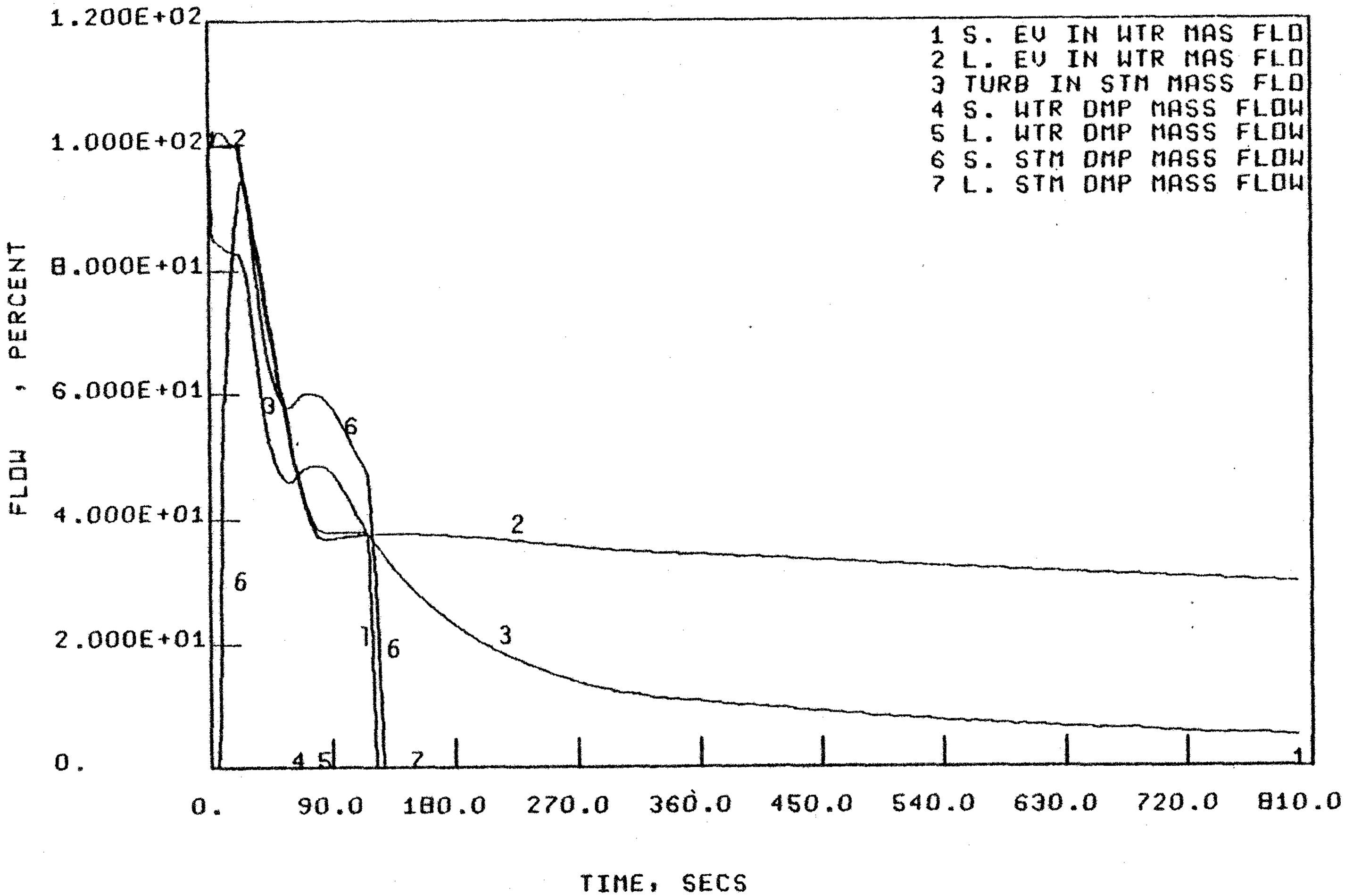

FIGURE 4-141
POOL REACTOR ISOLATION OF ONE STEAM GENERATOR AND DUMP VALVE FAILURE
RUN DATED 10/06/78
NUMBER TEPGE01

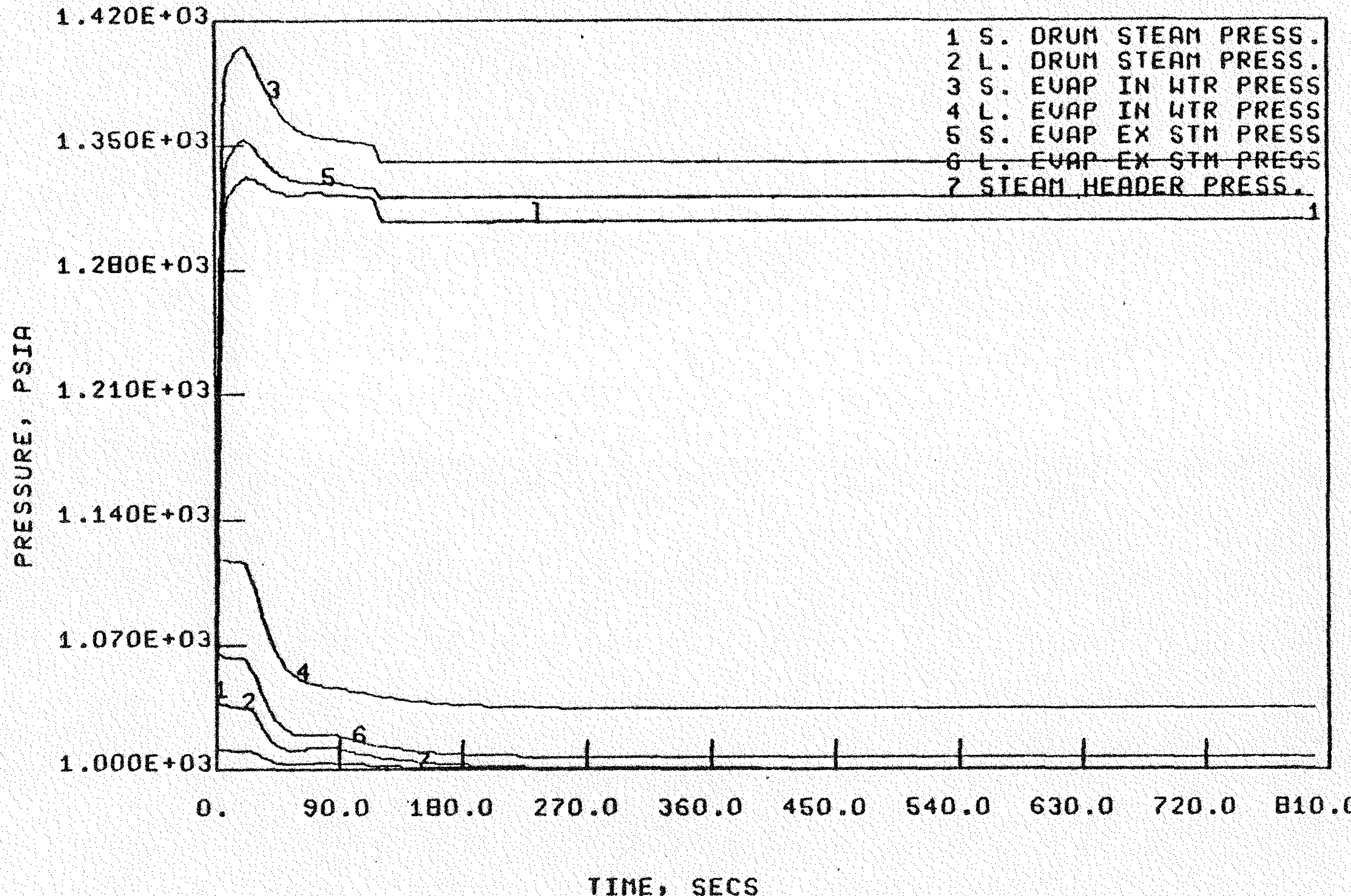

FIGURE 4-142
POOL REACTOR ISOLATION OF ONE STEAM GENERATOR AND DUMP VALVE FAILURE
RUN DATED 10/06/78
NUMBER TEPGE01

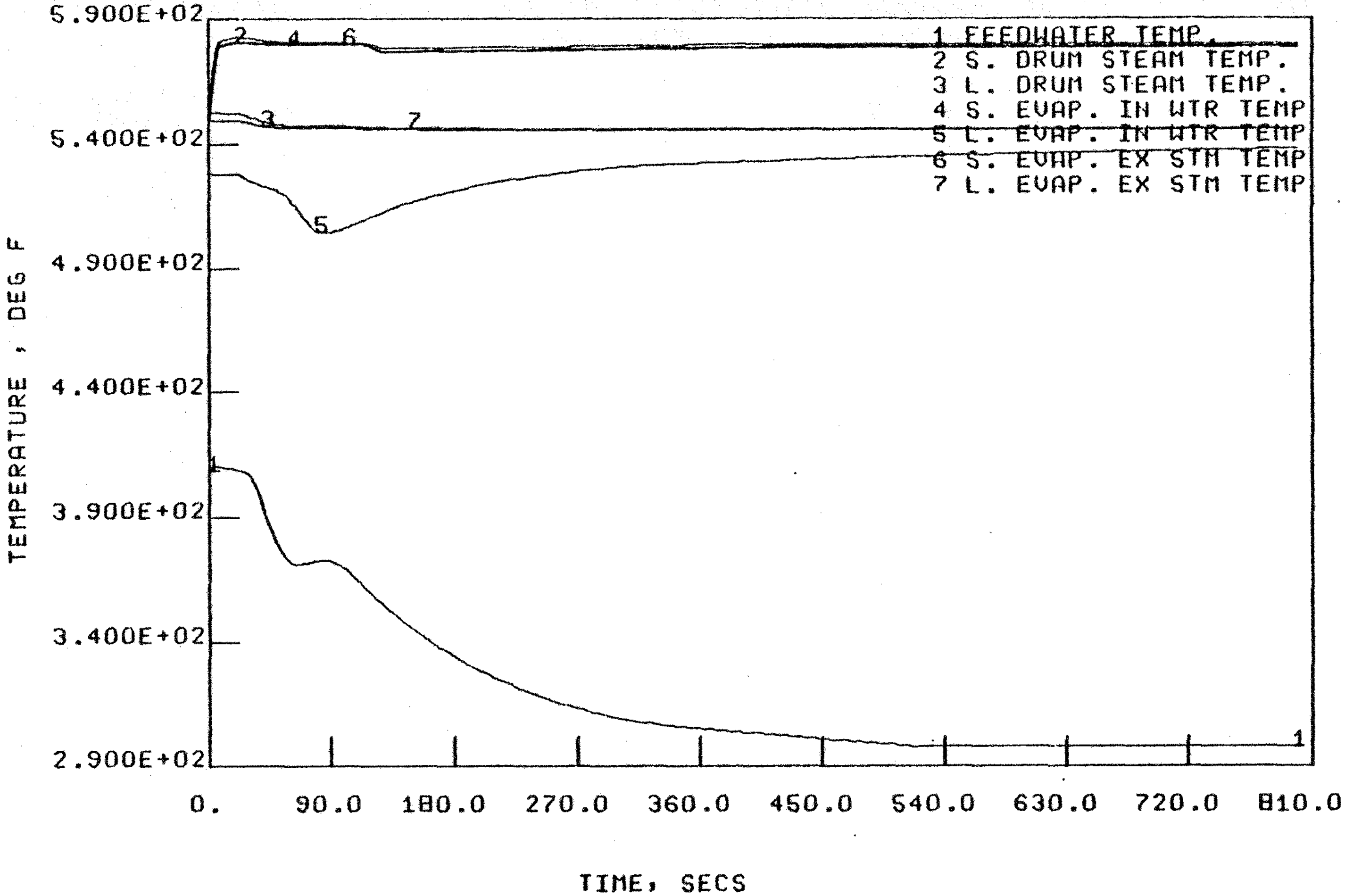

FIGURE 4-143
POOL REACTOR ISOLATION OF ONE STEAM GENERATOR AND DUMP VALVE FAILURE
RUN DATED 10/06/78
NUMBER TEPGE01

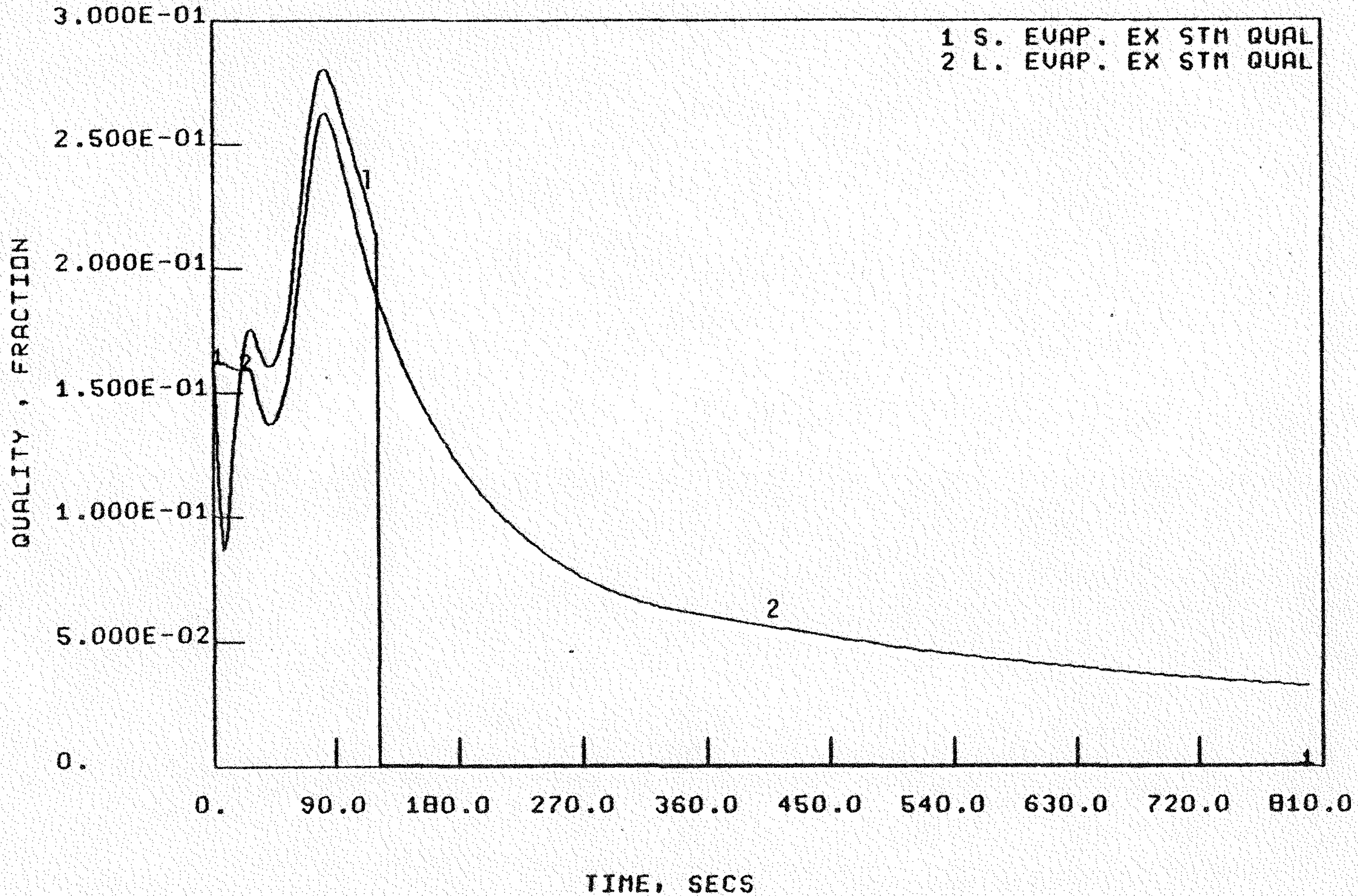

FIGURE 4-144
POOL REACTOR ISOLATION OF ONE STEAM GENERATOR AND DUMP VALVE FAILURE
RUN DATED 10/06/78
NUMBER TEPGE01

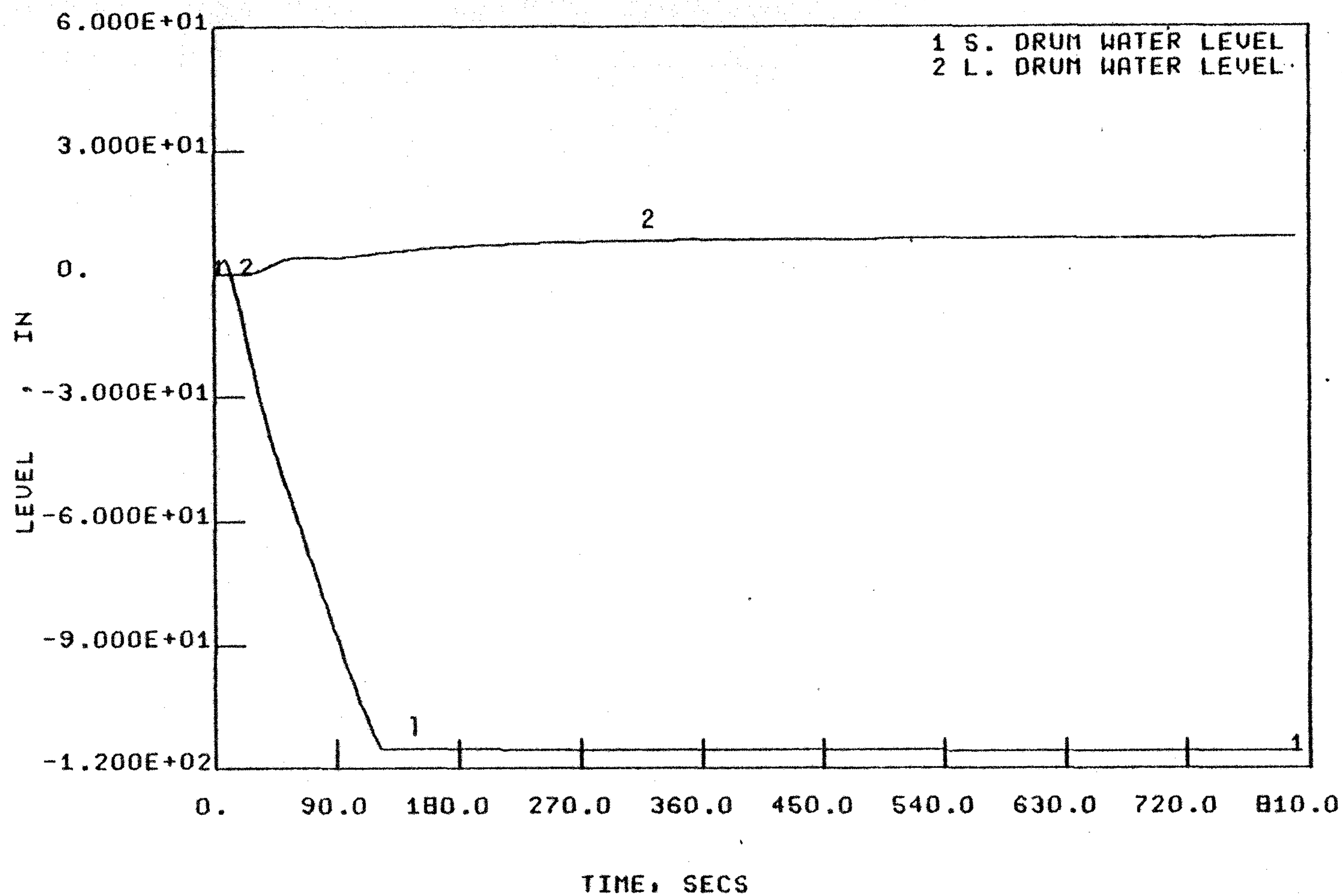

V-2.3-163

FIGURE 5-1

POOL IHTS PUMP PWR LOSS WITH SCRAM AND NO PUMP TRIP(MAX DECAY HT)
RUN DATED 10/31/78
NUMBER PAPGEOO

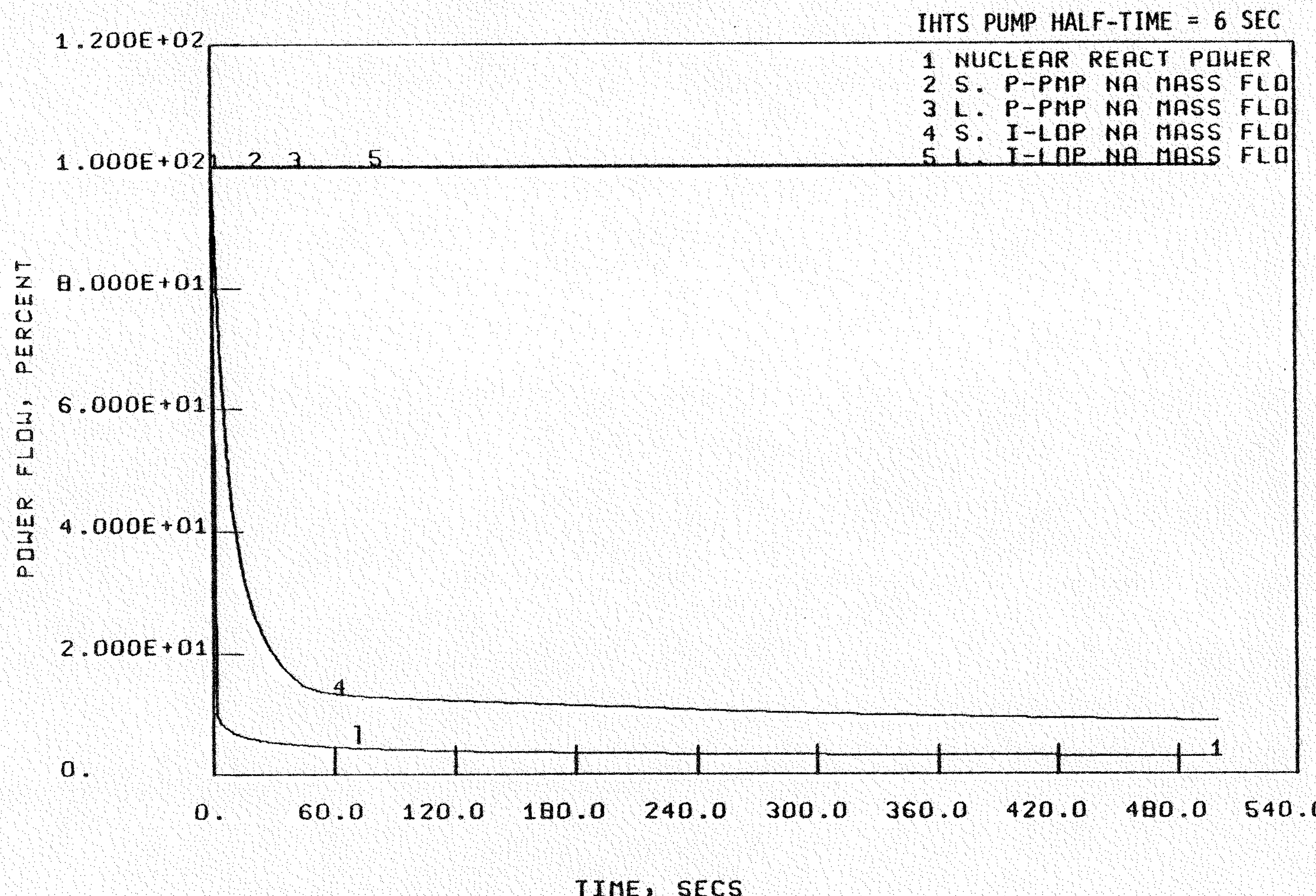

FIGURE 5-2
POOL IHTS PUMP PWR LOSS WITH SCRAM AND NO PUMP TRIP(MAX DECAY HT)
RUN DATED 10/31/78
NUMBER PAPGEOO

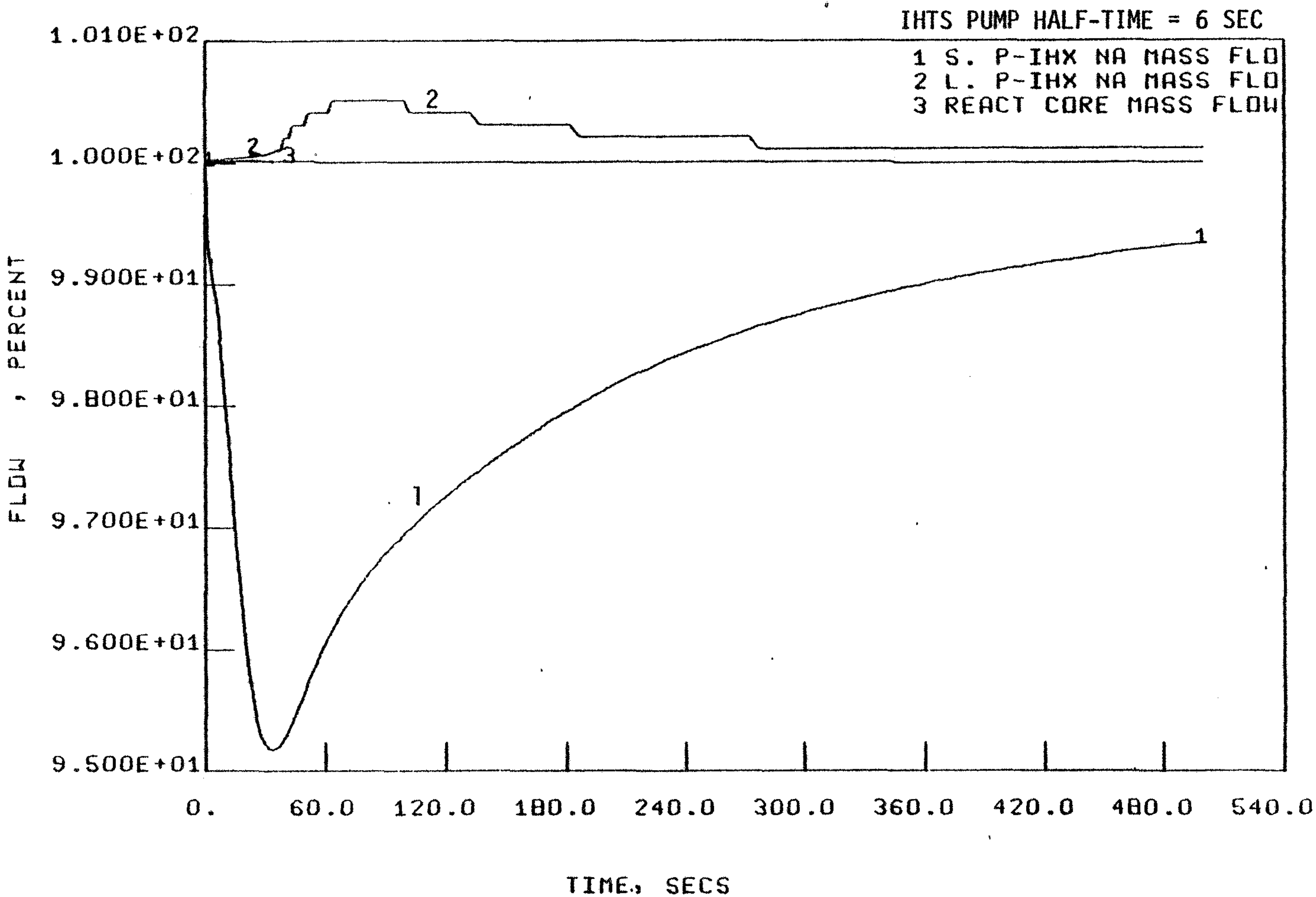

FIGURE 5-3

POOL IHTS PUMP PWR LOSS WITH SCRAM AND NO PUMP TRIP(MAX DECAY HT)
RUN DATED 10/31/78
NUMBER PAPGEOO

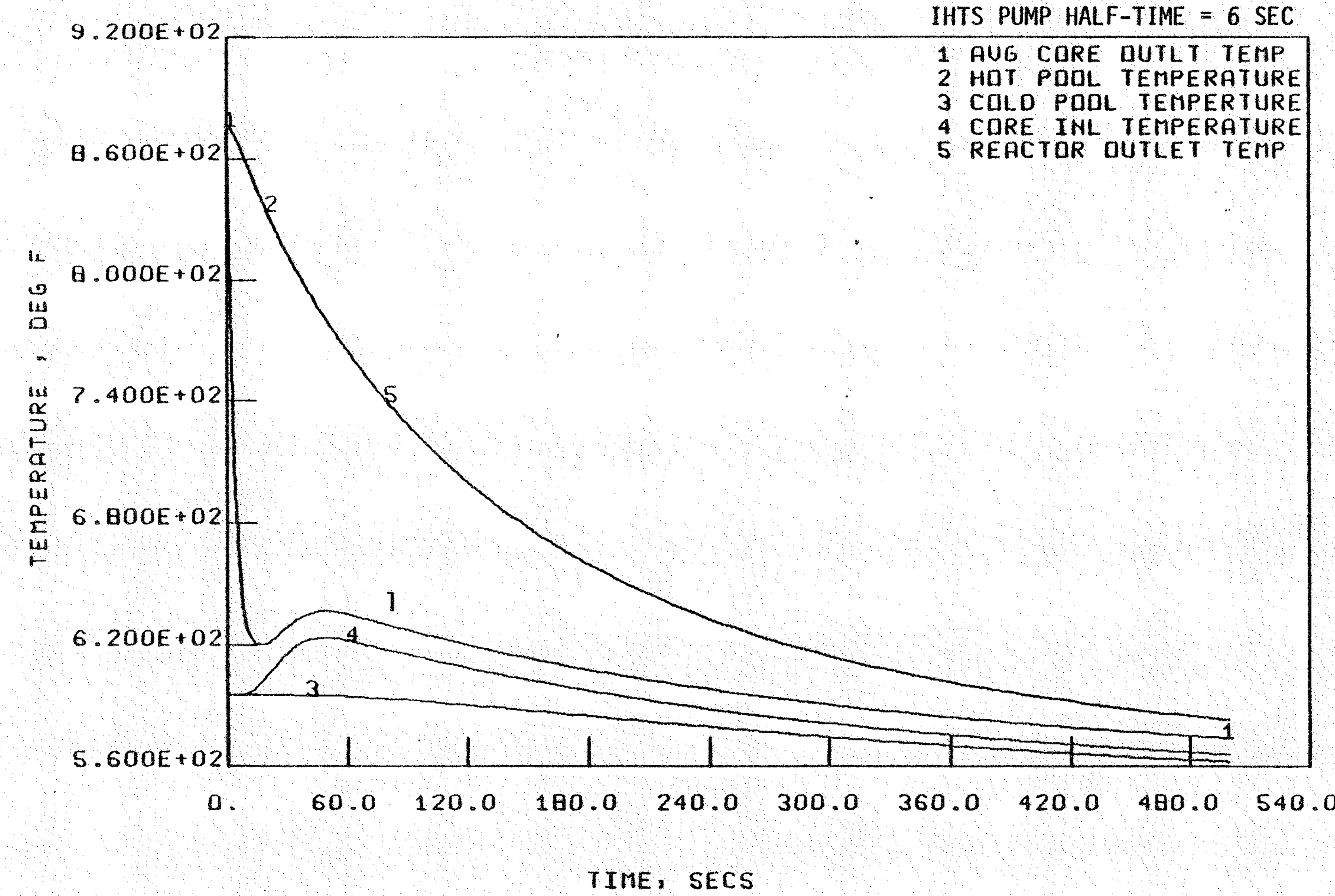

FIGURE 5-4
POOL IHTS PUMP PWR LOSS WITH SCRAM AND NO PUMP TRIP(MAX DECAY HT)
RUN DATED 10/31/78
NUMBER PAPGEOO

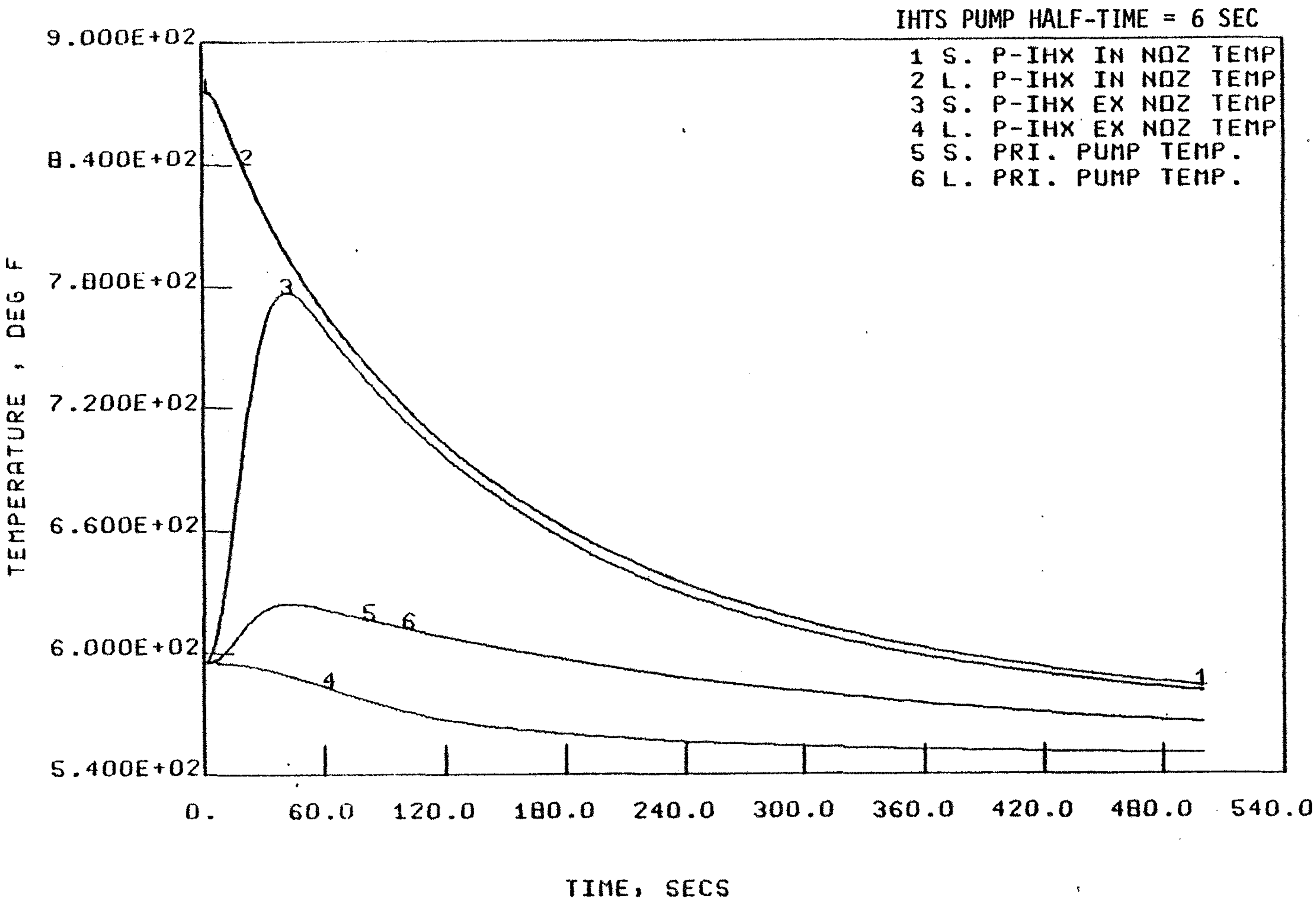

FIGURE 5-5

POOL IHTS PUMP PWR LOSS WITH SCRAM AND NO PUMP TRIP(MAX DECAY HT)

RUN DATED 10/31/78

NUMBER PAPGEOO

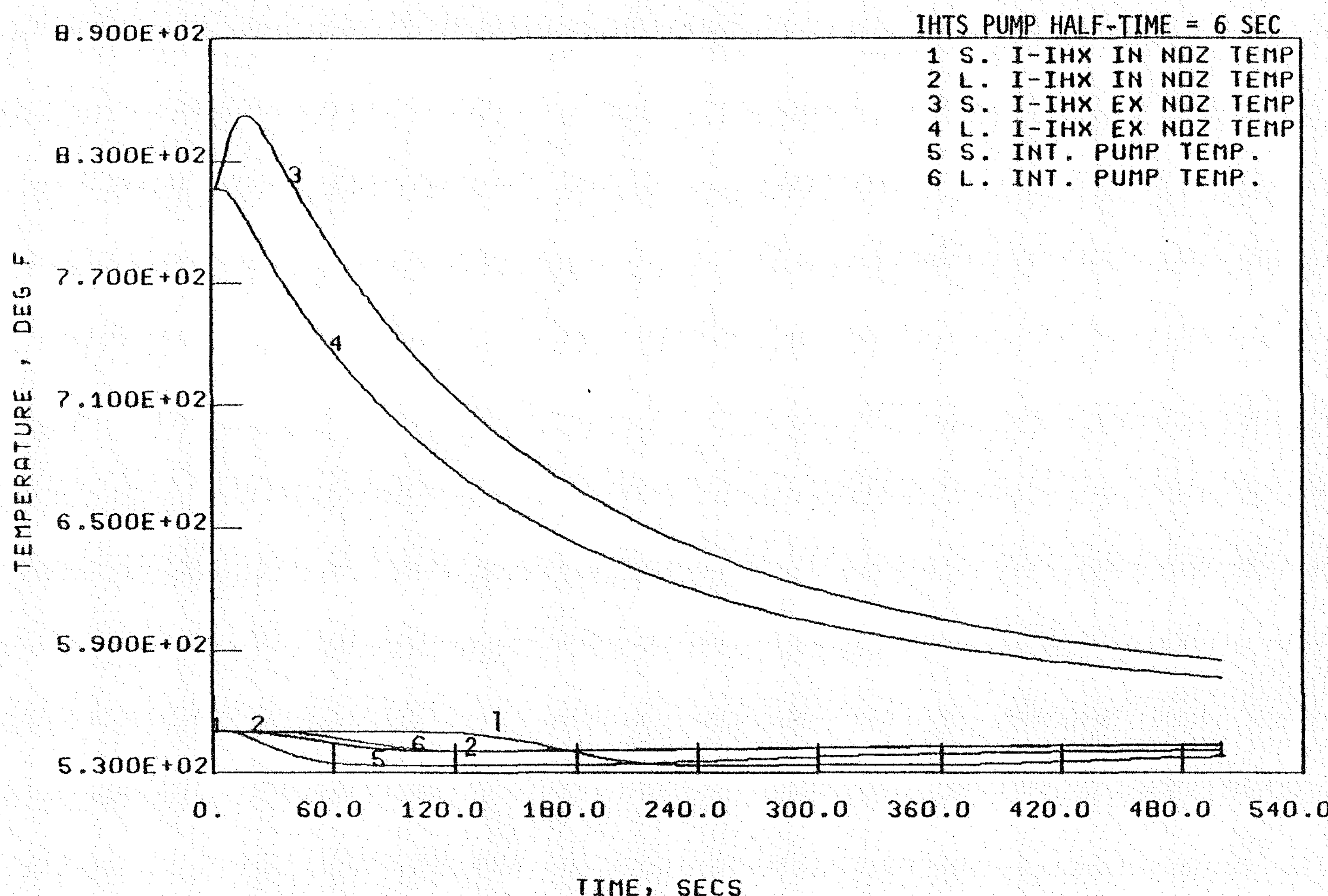

FIGURE 5-6

POOL IHTS PUMP PWR LOSS WITH SCRAM AND NO PUMP TRIP(MAX DECAY HT)
RUN DATED 10/31/78
NUMBER PAPGE00

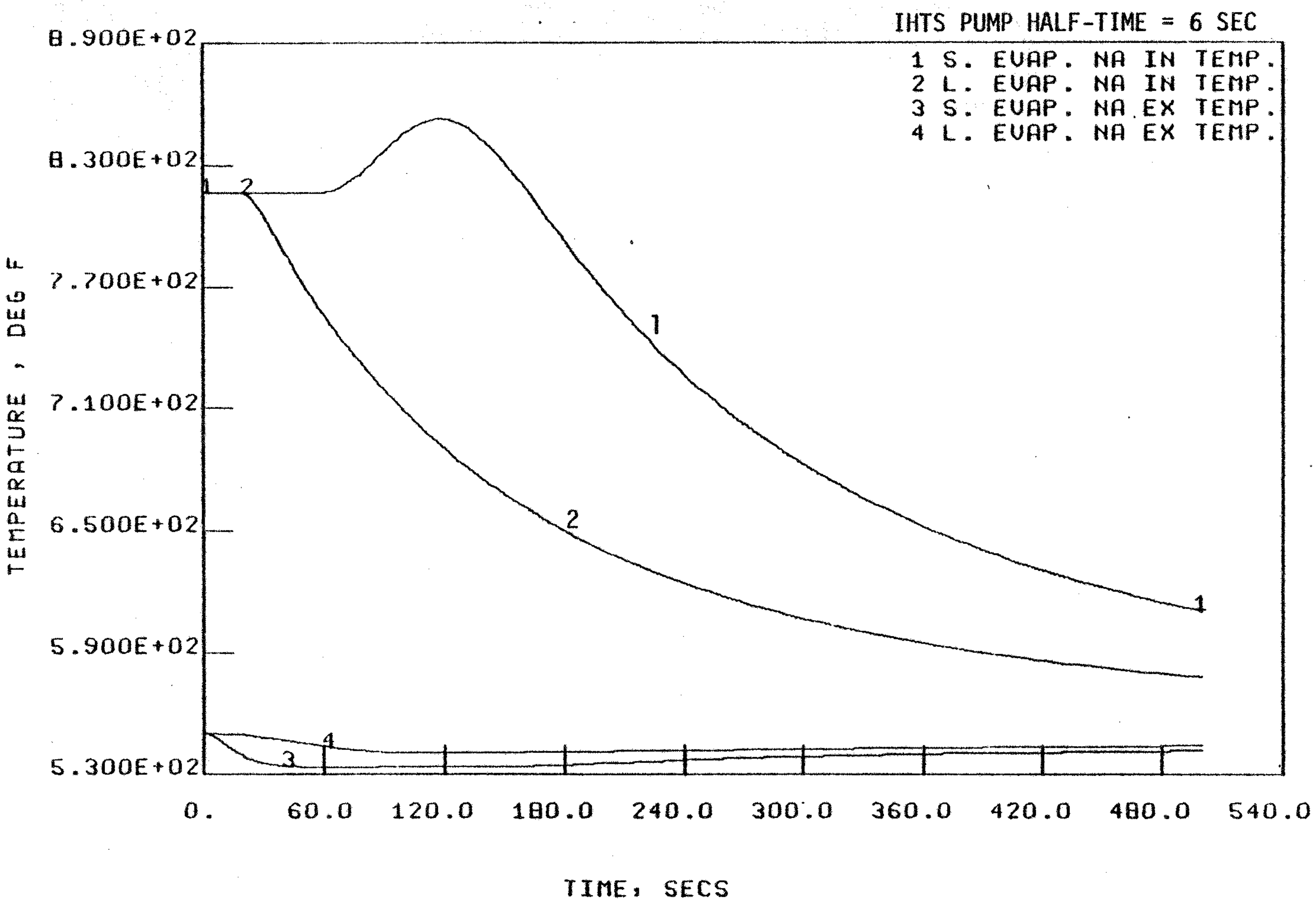

FIGURE 5-7

POOL IHTS PUMP PWR LOSS WITH SCRAM AND NO PUMP TRIP(MAX DECAY HT)

RUN DATED 10/31/78

NUMBER PAPGEOO

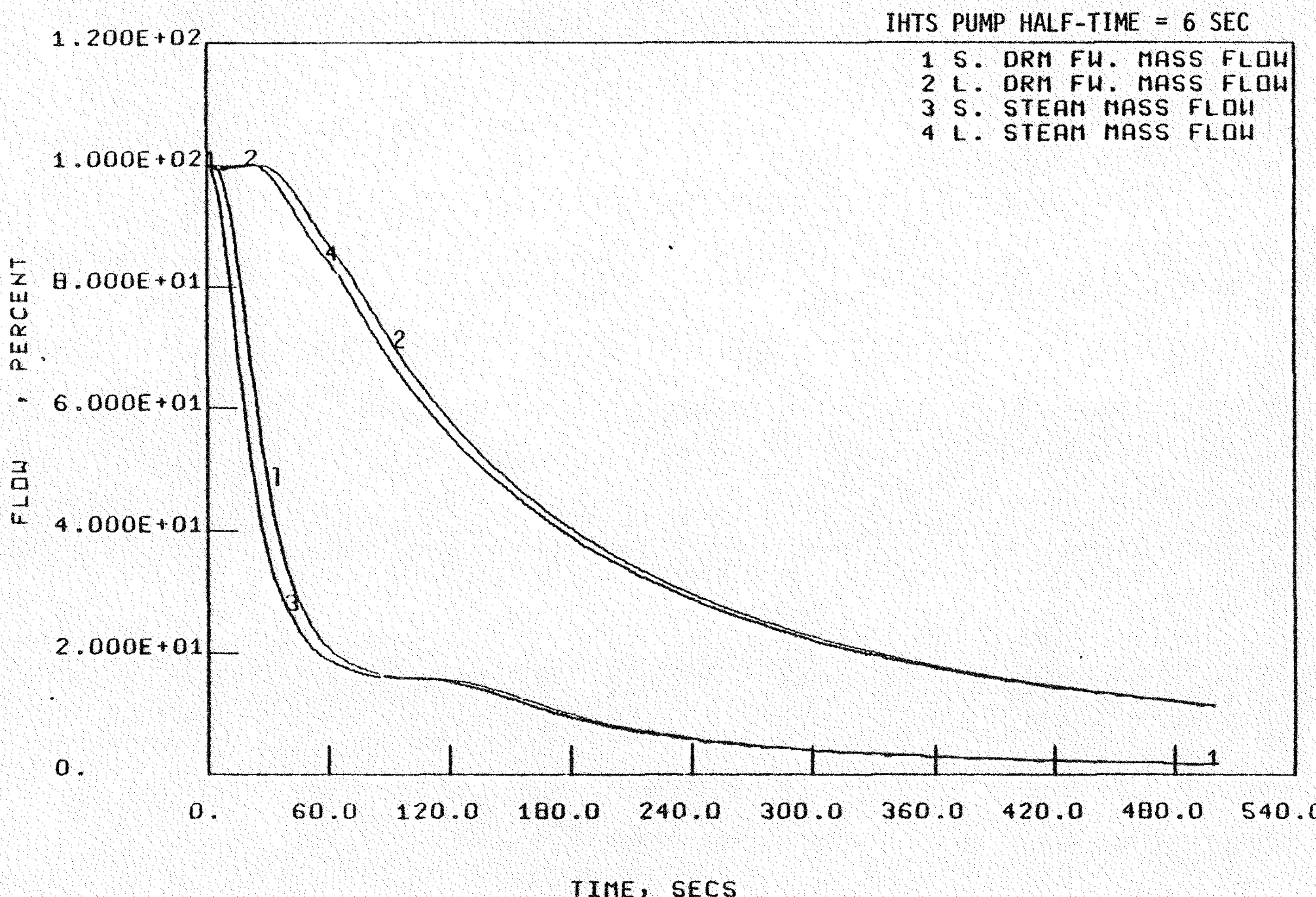

FIGURE 5-8
POOL IHTS PUMP PWR LOSS WITH SCRAM AND NO PUMP TRIP(MAX DECAY HT)
RUN DATED 10/31/78
NUMBER PAPGE00

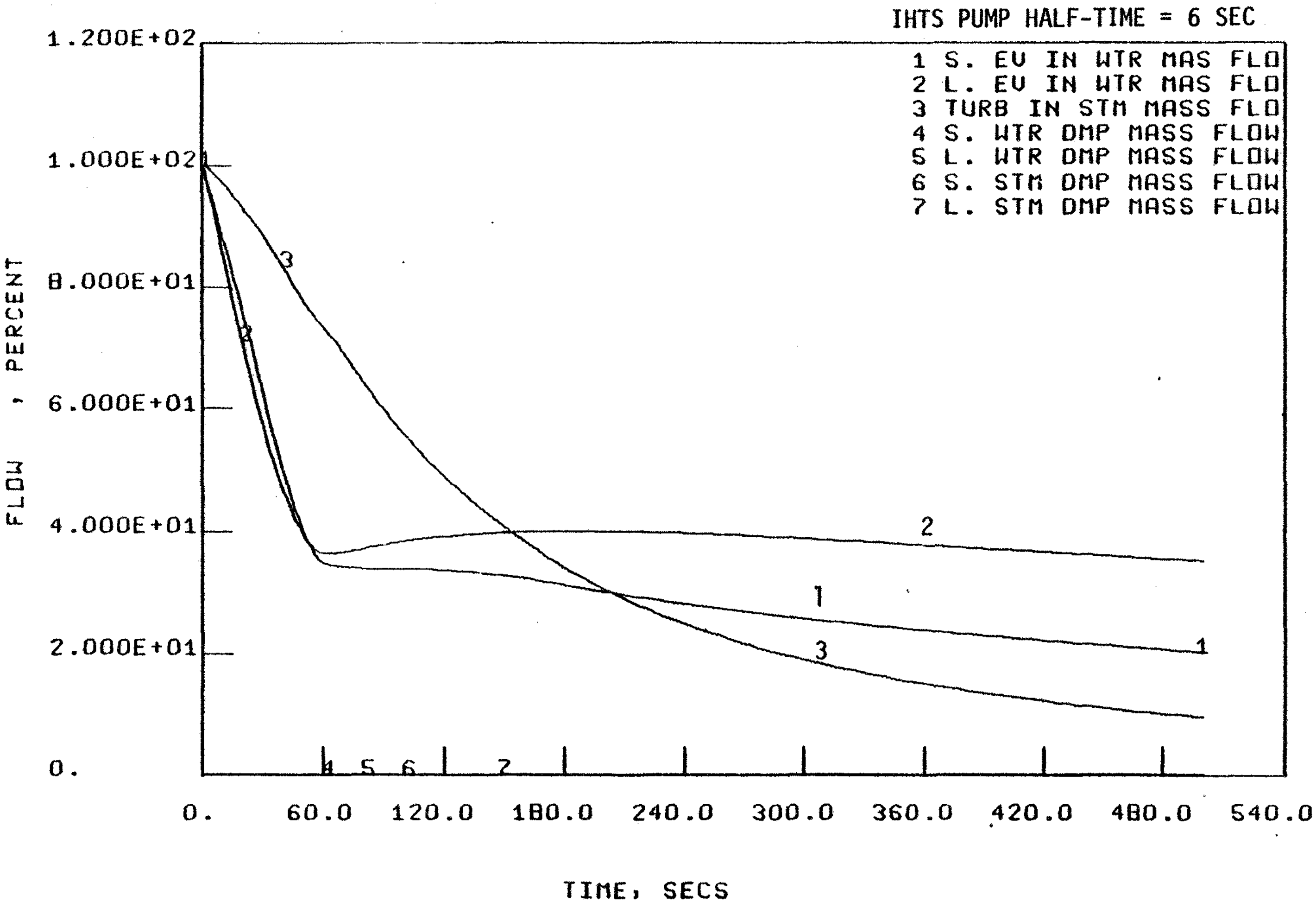

FIGURE 5-9
POOL IHTS PUMP PWR LOSS WITH SCRAM AND NO PUMP TRIP(MAX DECAY HT)
RUN DATED 10/31/78
NUMBER PAPGEOO

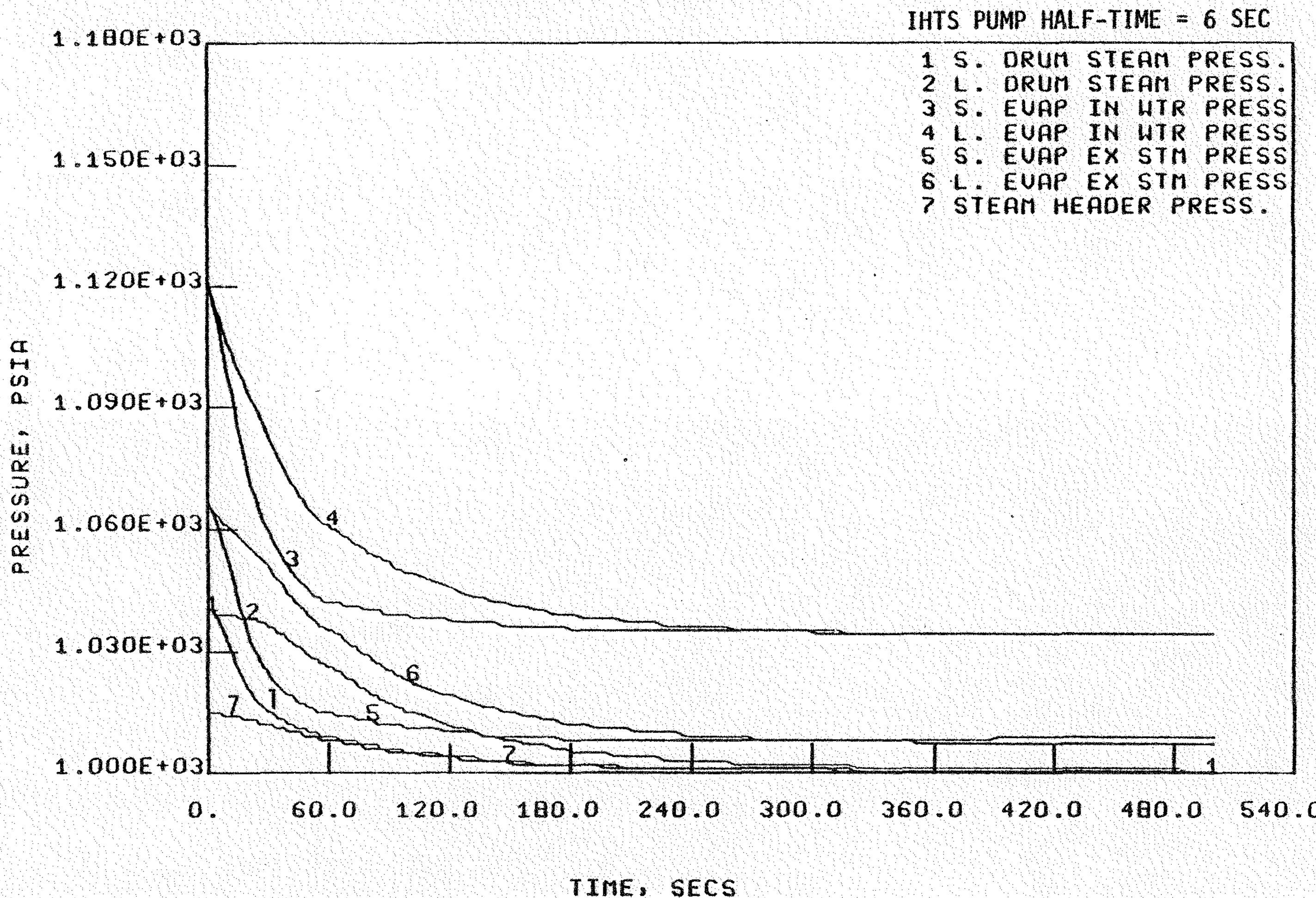

FIGURE 5-10
POOL IHTS PUMP PWR LOSS WITH SCRAM AND NO PUMP TRIP(MAX DECAY HT)
RUN DATED 10/31/78
NUMBER PAPGE00

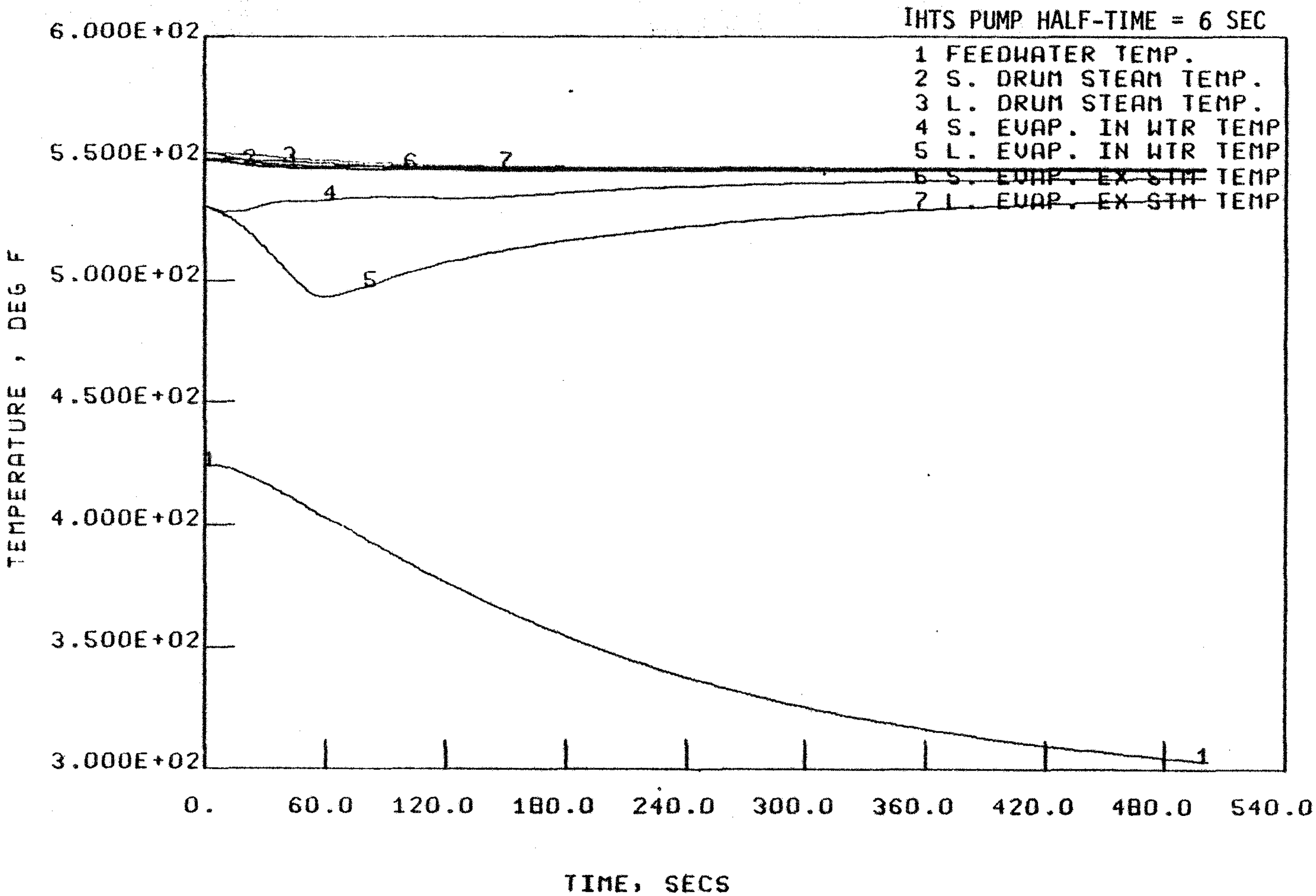

FIGURE 5-11
POOL IHTS PUMP PWR LOSS WITH SCRAM AND NO PUMP TRIP(MAX DECAY HT)
RUN DATED 10/31/78
NUMBER PAP6E00

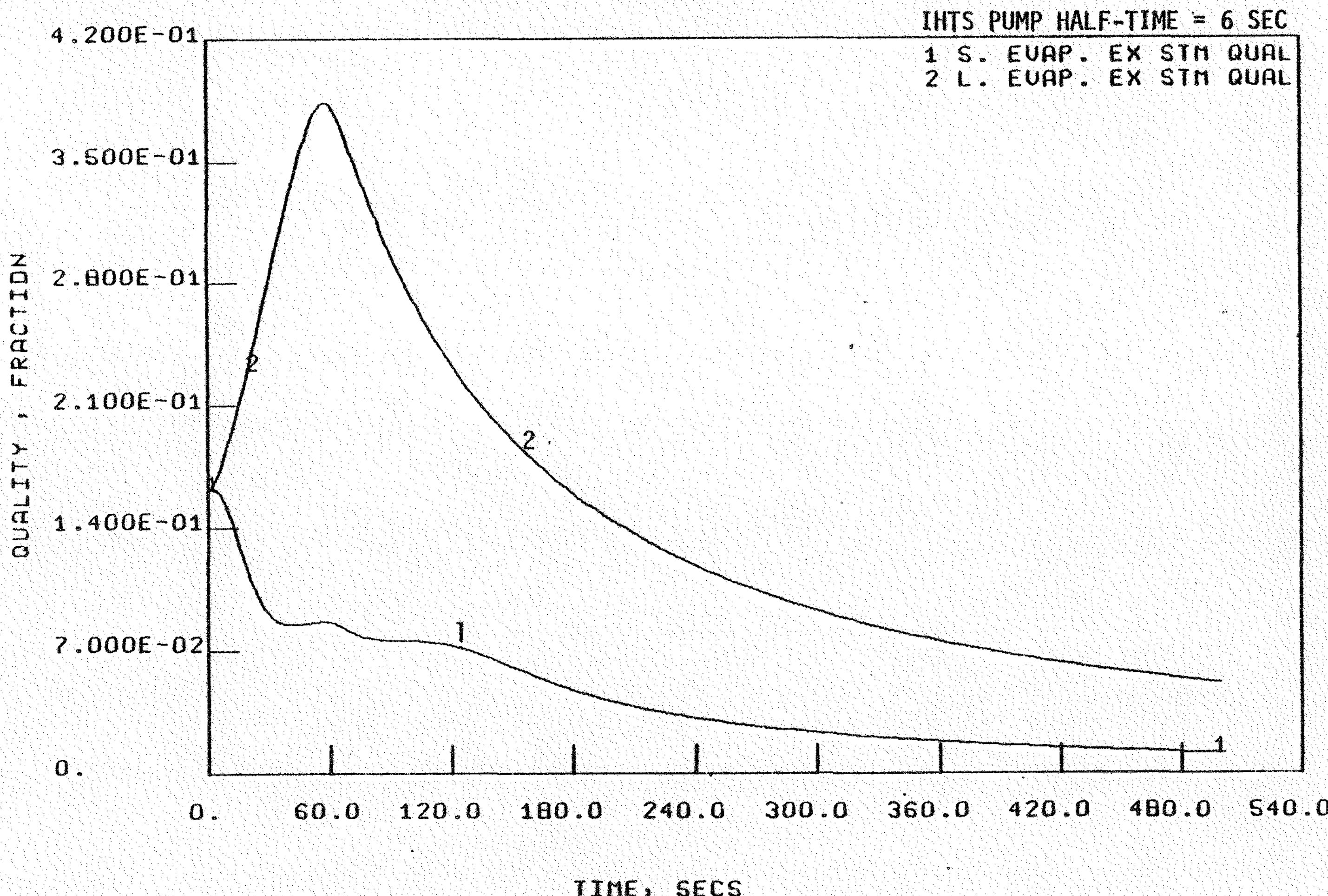

FIGURE 5-12

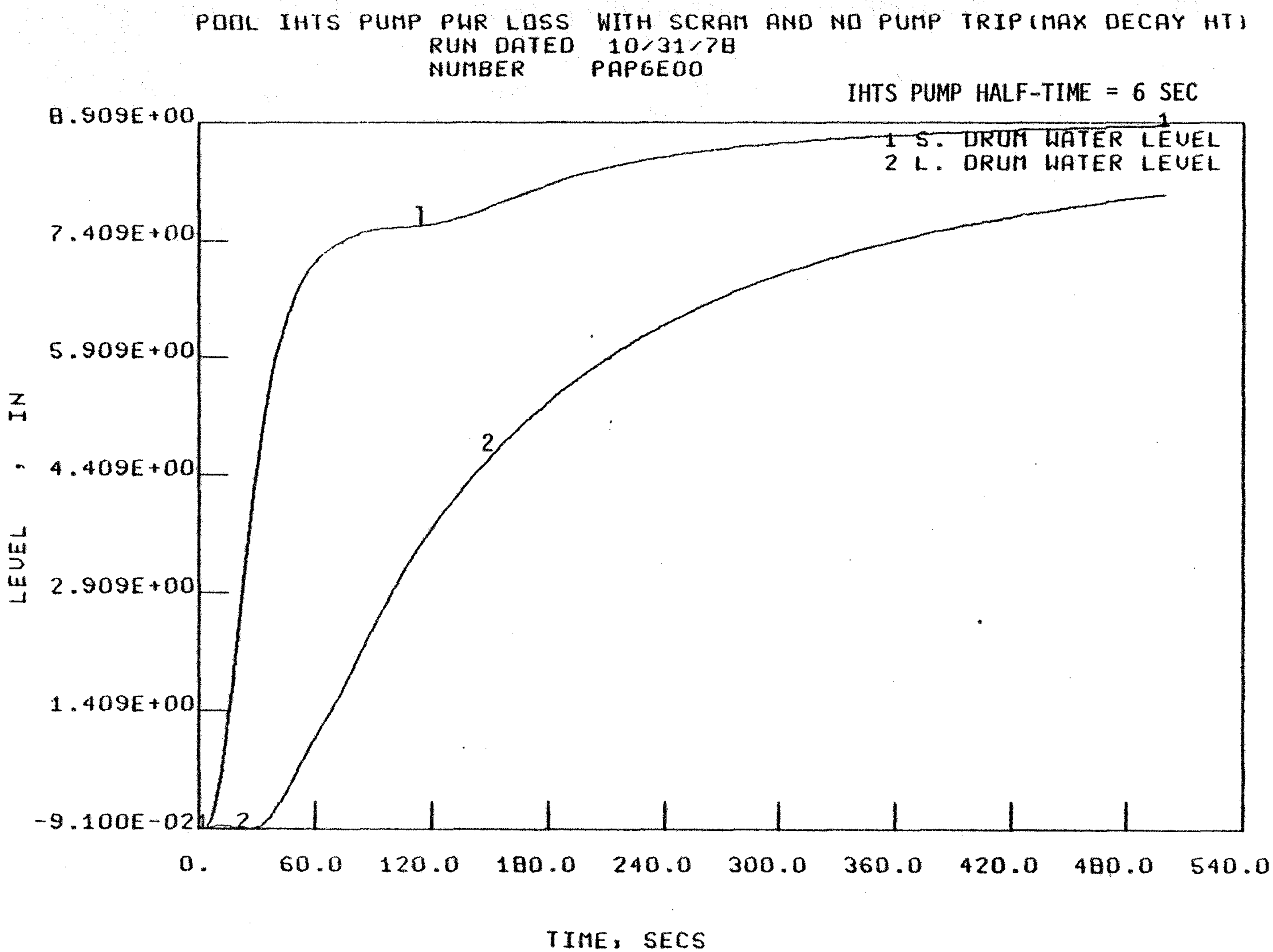
POOL IHTS PUMP PWR LOSS WITH SCRAM AND NO PUMP TRIP(MAX DECAY HT)
RUN DATED 10/31/78
NUMBER PAP6E00
IHTS PUMP HALF-TIME = 6 SEC
1 S. DRUM WATER LEVEL
2 L. DRUM WATER LEVEL
8.909E+00
7.409E+00
5.909E+00
4.409E+00
2.909E+00
1.409E+00
-9.100E-02
LEVEL , IN
0.
60.0
120.0
180.0
240.0
300.0
360.0
420.0
480.0
540.0
TIME, SECS
1
2

FIGURE 5-13
POOL IHTS PUMP PWR LOSS WITH SCRAM AND NO PUMP TRIP (MAX DECAY HT)
RUN DATED 11/01/78
NUMBER PAP6E01

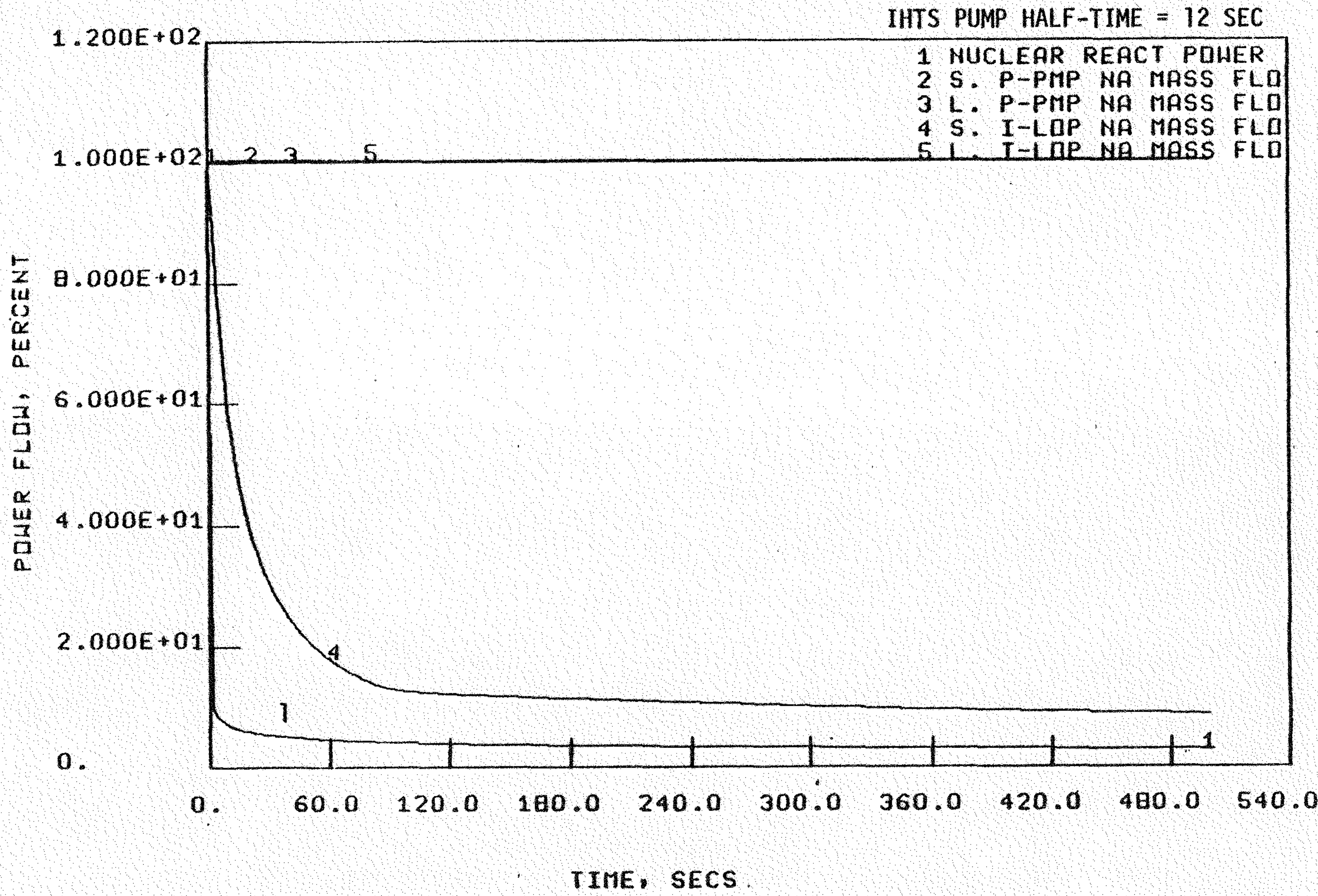

FIGURE 5-14

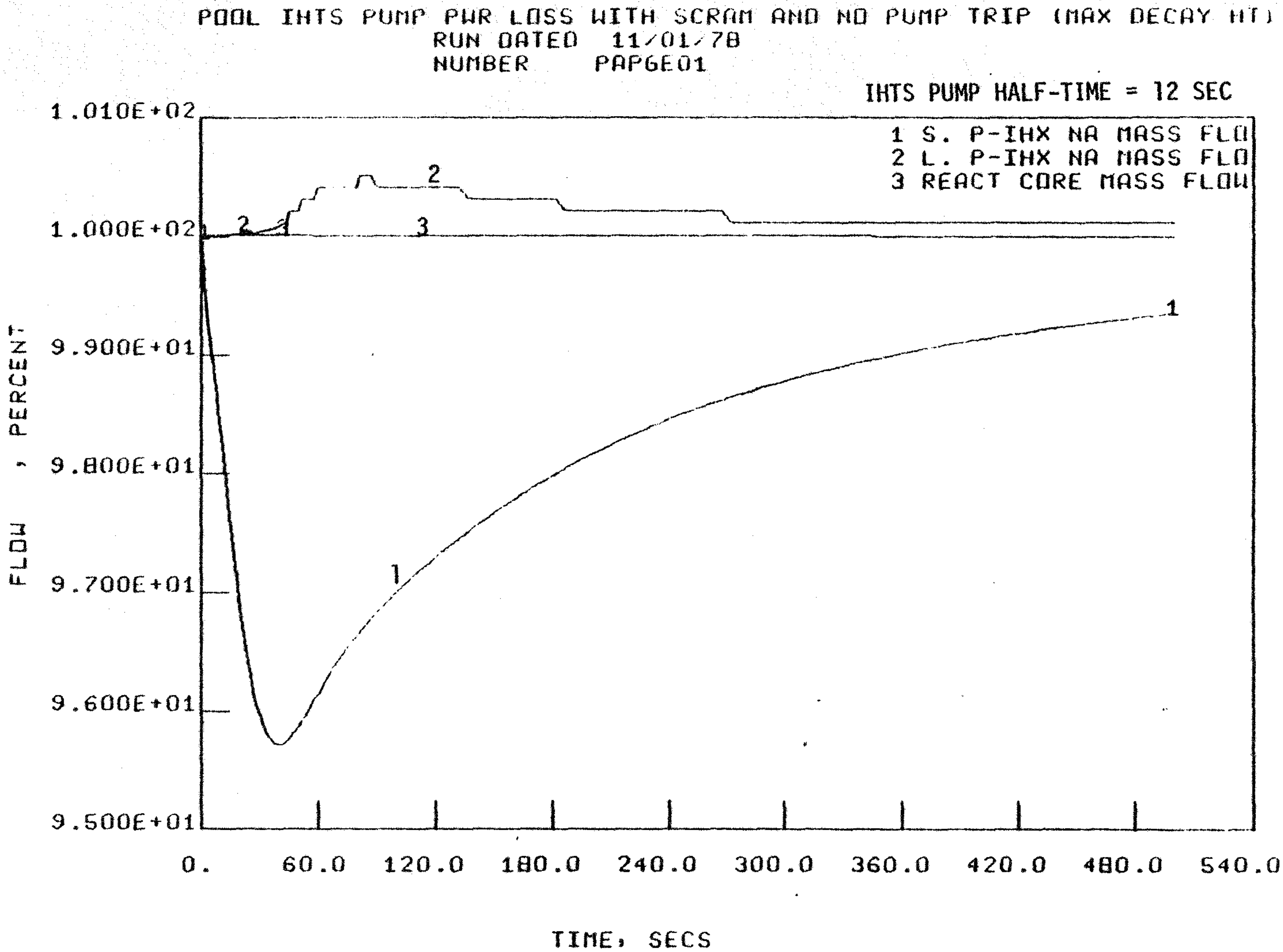

POOL IHTS PUMP PWR LOSS WITH SCRAM AND NO PUMP TRIP (MAX DECAY HT)
RUN DATED 11/01/78
NUMBER PAPGE01
IHTS PUMP HALF-TIME = 12 SEC
1 S. P-IHX NA MASS FLO
2 L. P-IHX NA MASS FLO
3 REACT CORE MASS FLOW
FLOW , PERCENT
1.010E+02
1.000E+02
9.900E+01
9.800E+01
9.700E+01
9.600E+01
9.500E+01
0.
60.0
120.0
180.0
240.0
300.0
360.0
420.0
480.0
540.0
TIME, SECS

FIGURE 5-15
POOL IHTS PUMP PWR LOSS WITH SCRAM AND NO PUMP TRIP (MAX DECAY HT)
RUN DATED 11/01/78
NUMBER PAPGE01

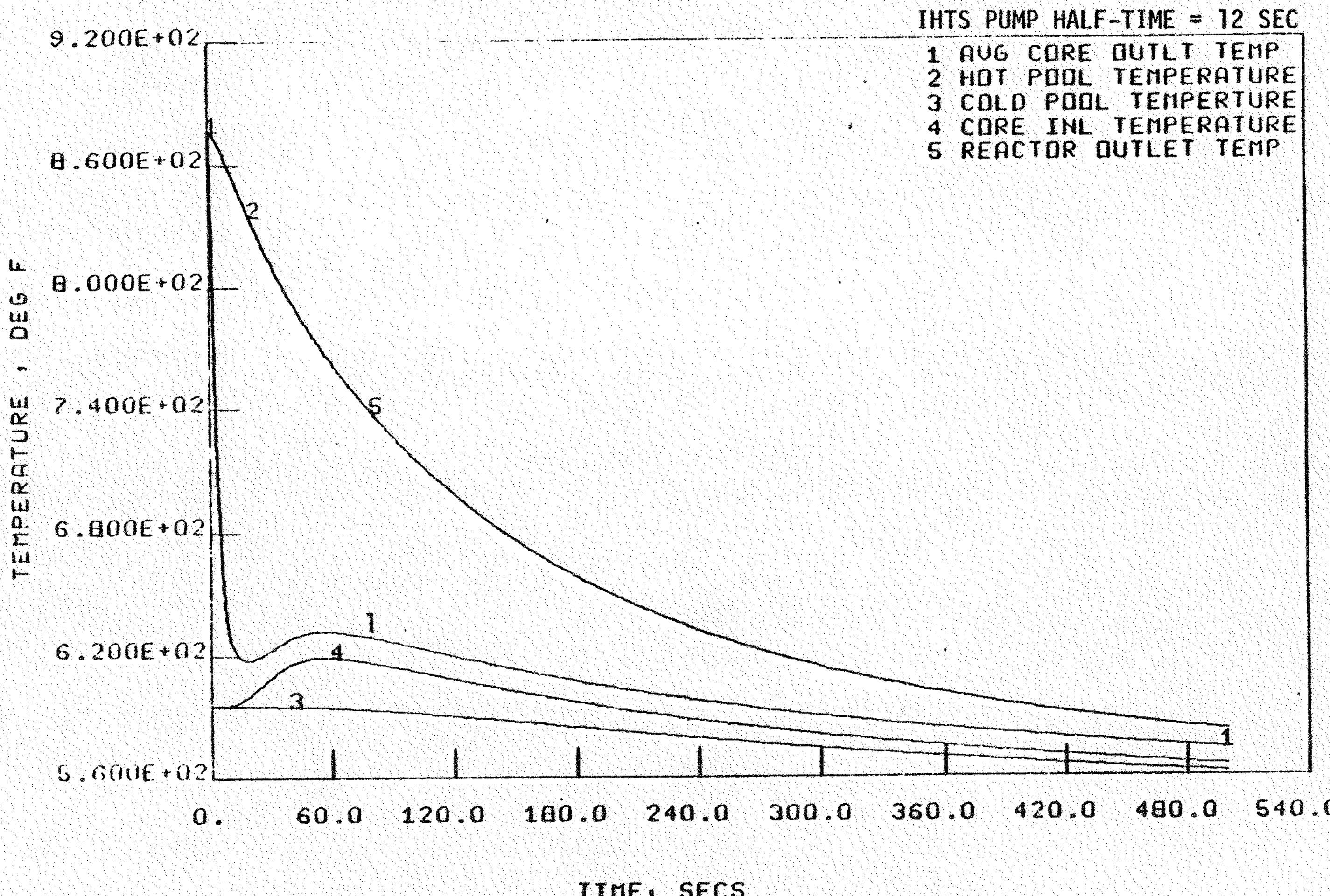

FIGURE 5-16

POOL IHTS PUMP PWR LOSS WITH SCRAM AND NO PUMP TRIP (MAX DECAY HT)
RUN DATED 11/01/78
NUMBER PAPGE01

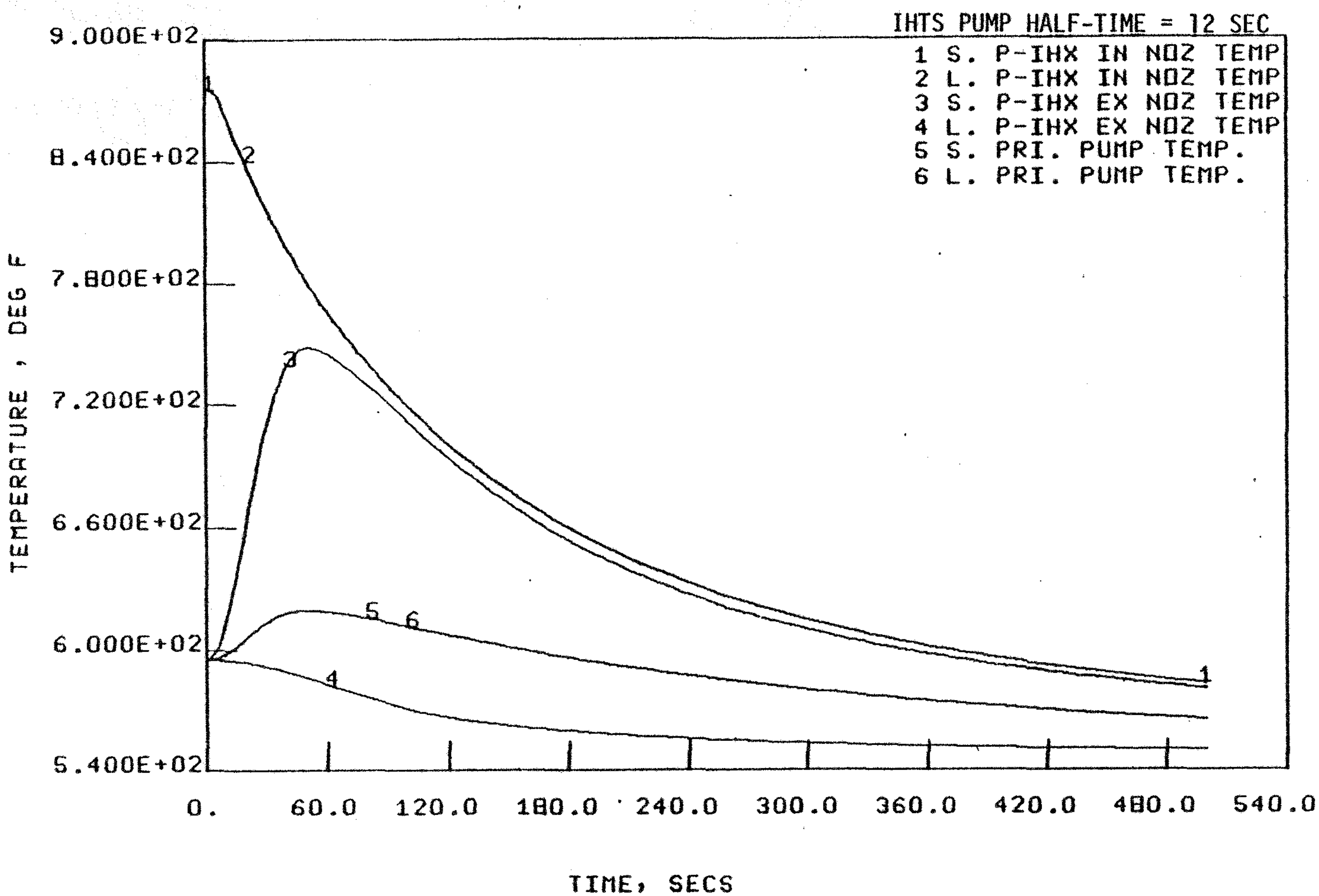

FIGURE 5-17

POOL IHTS PUMP PWR LOSS WITH SCRAM AND NO PUMP TRIP (MAX DECAY HT)
RUN DATED 11/01/78
NUMBER PAPGE01

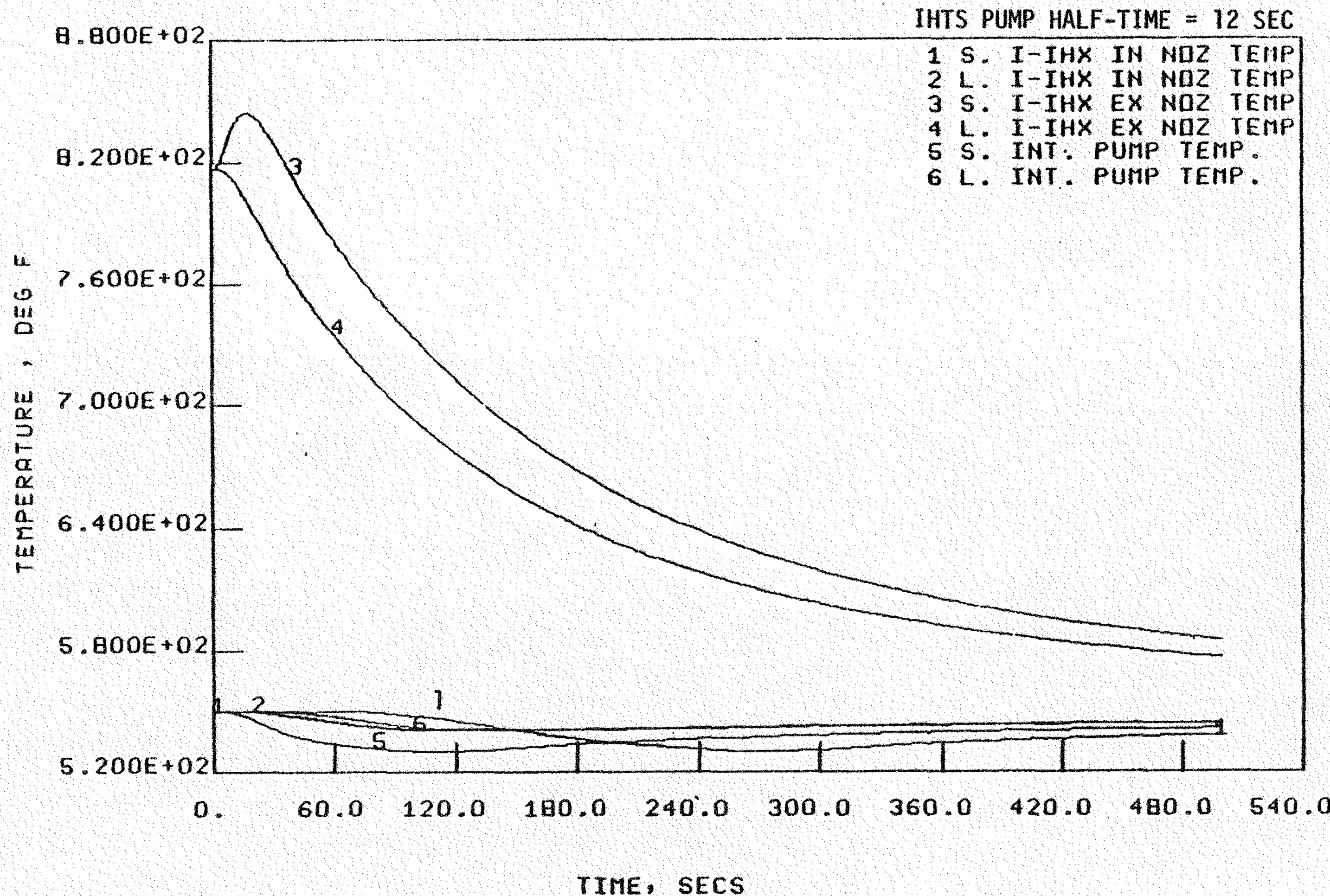

FIGURE 5-18
POOL IHTS PUMP PWR LOSS WITH SCRAM AND NO PUMP TRIP (MAX DECAY HT)
RUN DATED 11/01/78
NUMBER PAP6E01

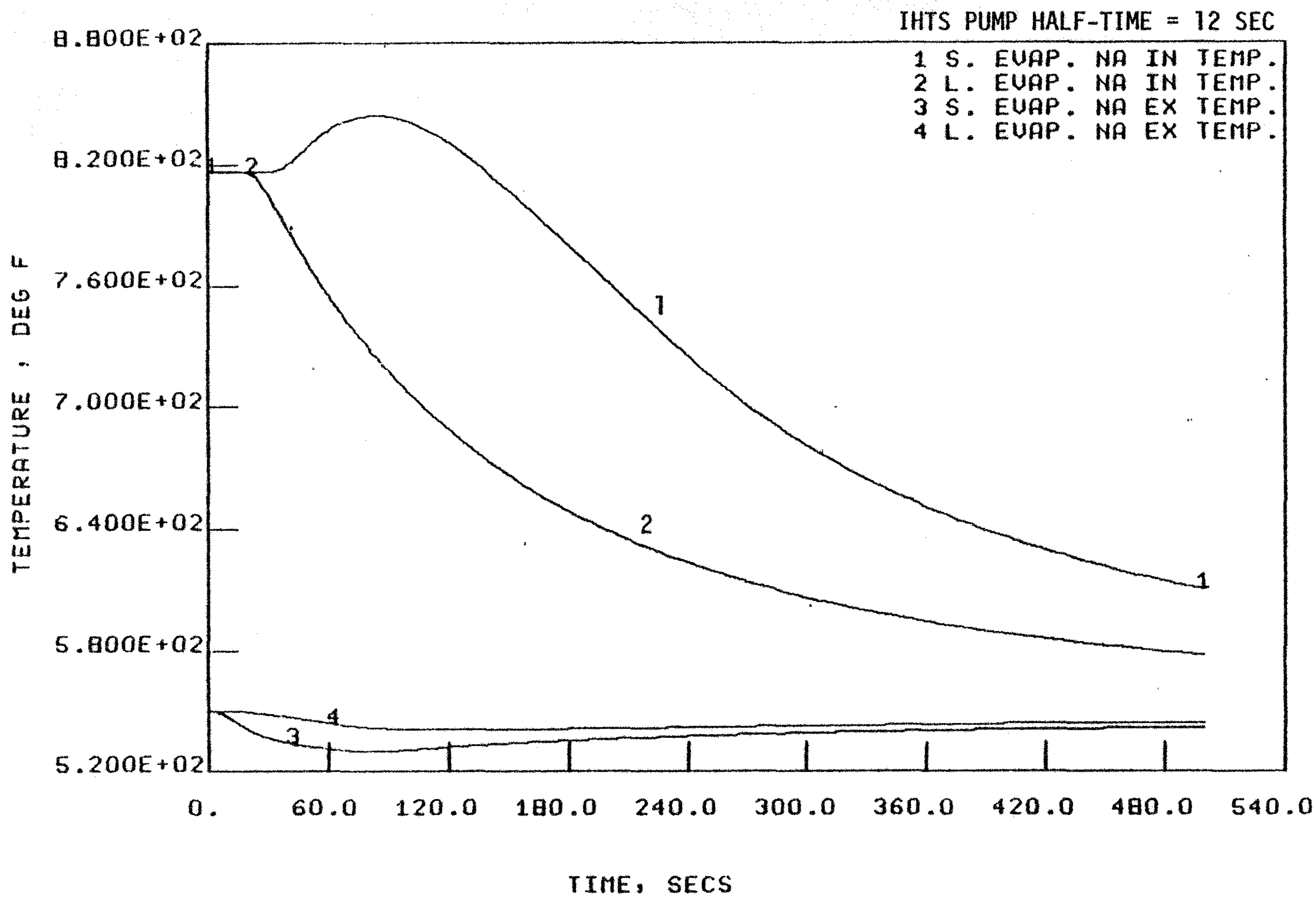

FIGURE 5-19

POOL IHTS PUMP PWR LOSS WITH SCRAM AND NO PUMP TRIP (MAX DECAY HT)
RUN DATED 11/01/78
NUMBER PAPGE01

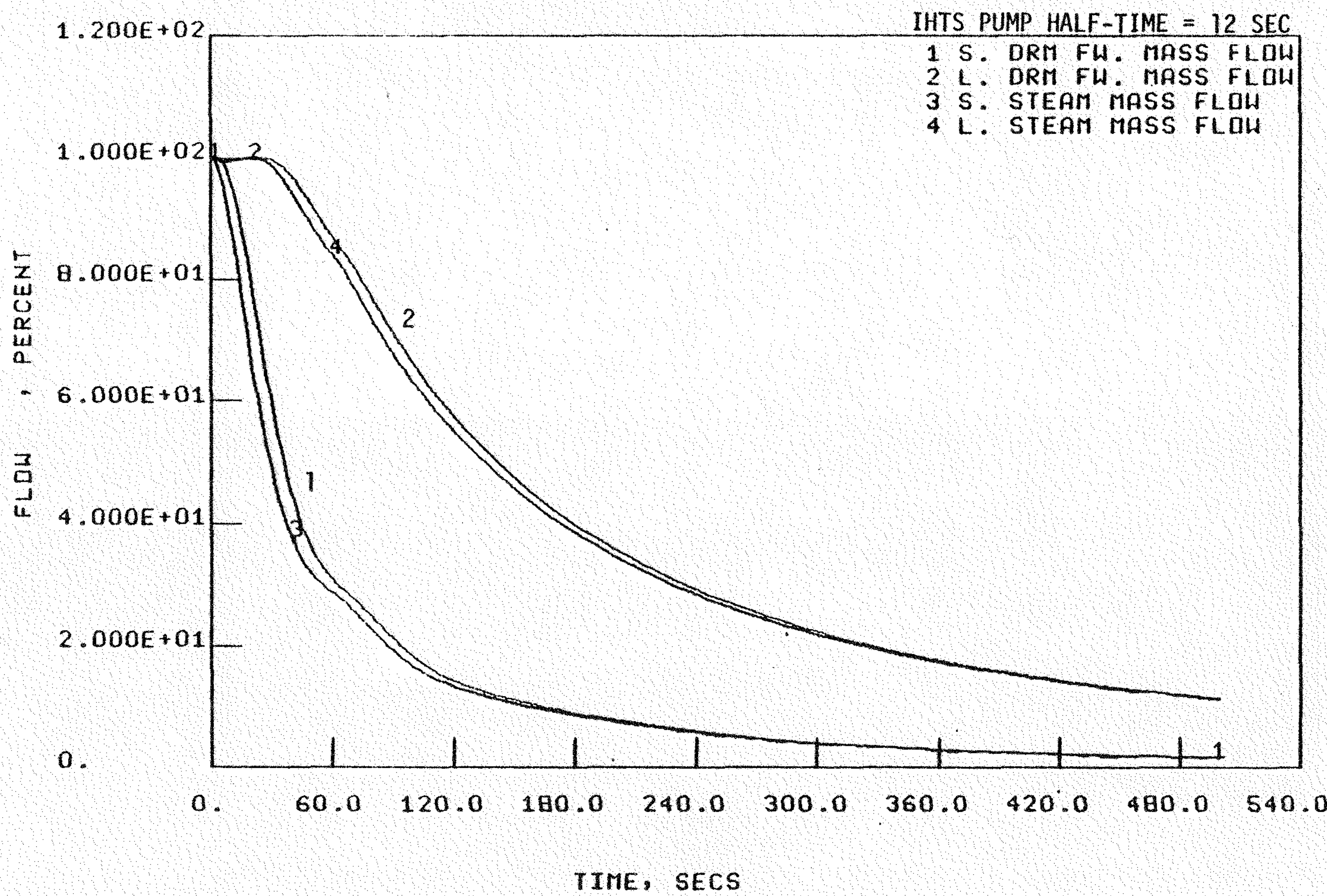

FIGURE 5-20
POOL IHTS PUMP PWR LOSS WITH SCRAM AND NO PUMP TRIP (MAX DECAY HT)
RUN DATED 11/01/78
NUMBER PAPGE01

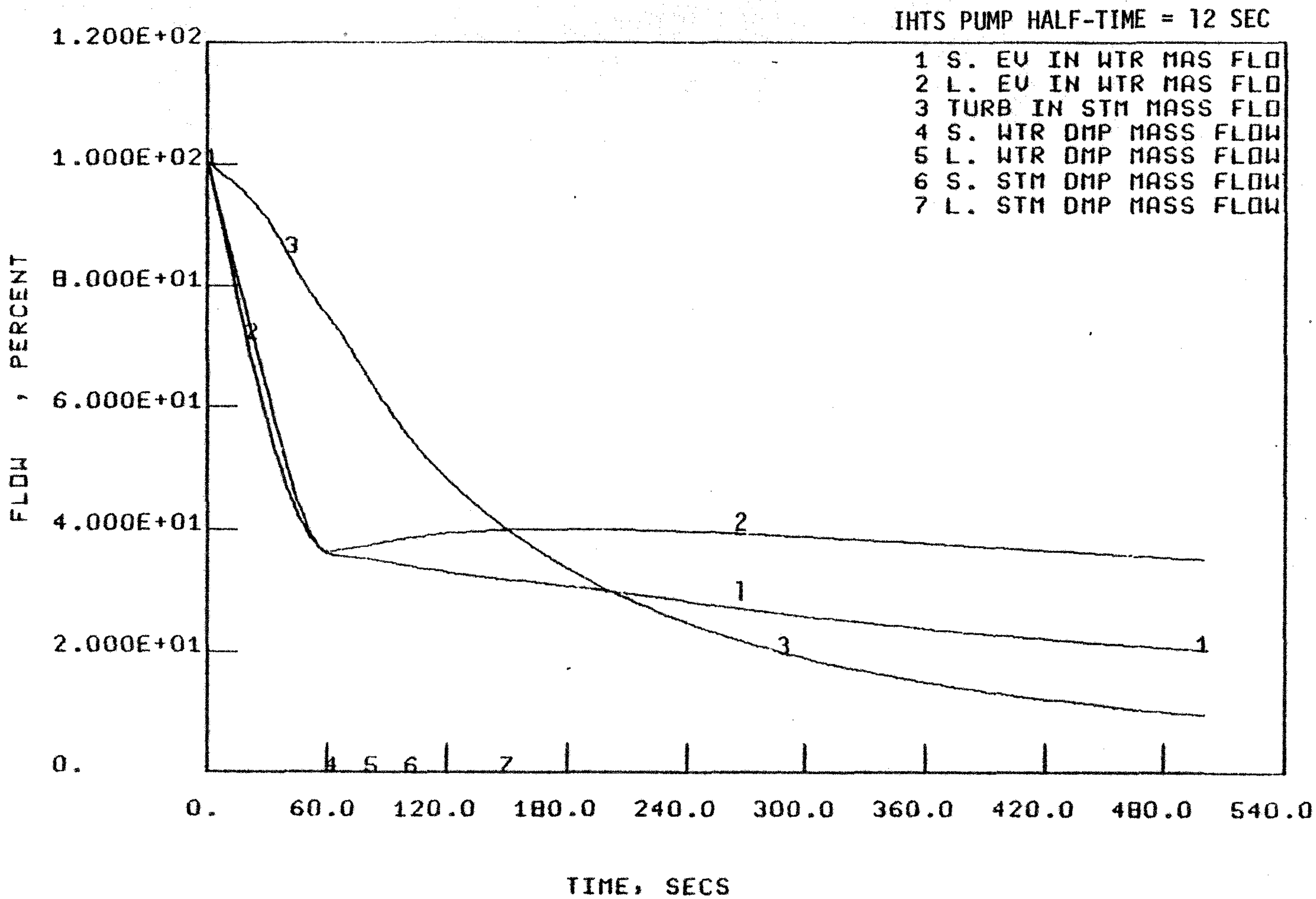

FIGURE 5-21
POOL IHTS PUMP PWR LOSS WITH SCRAM AND NO PUMP TRIP (MAX DECAY HT)
RUN DATED 11/01/78
NUMBER PAPGE01

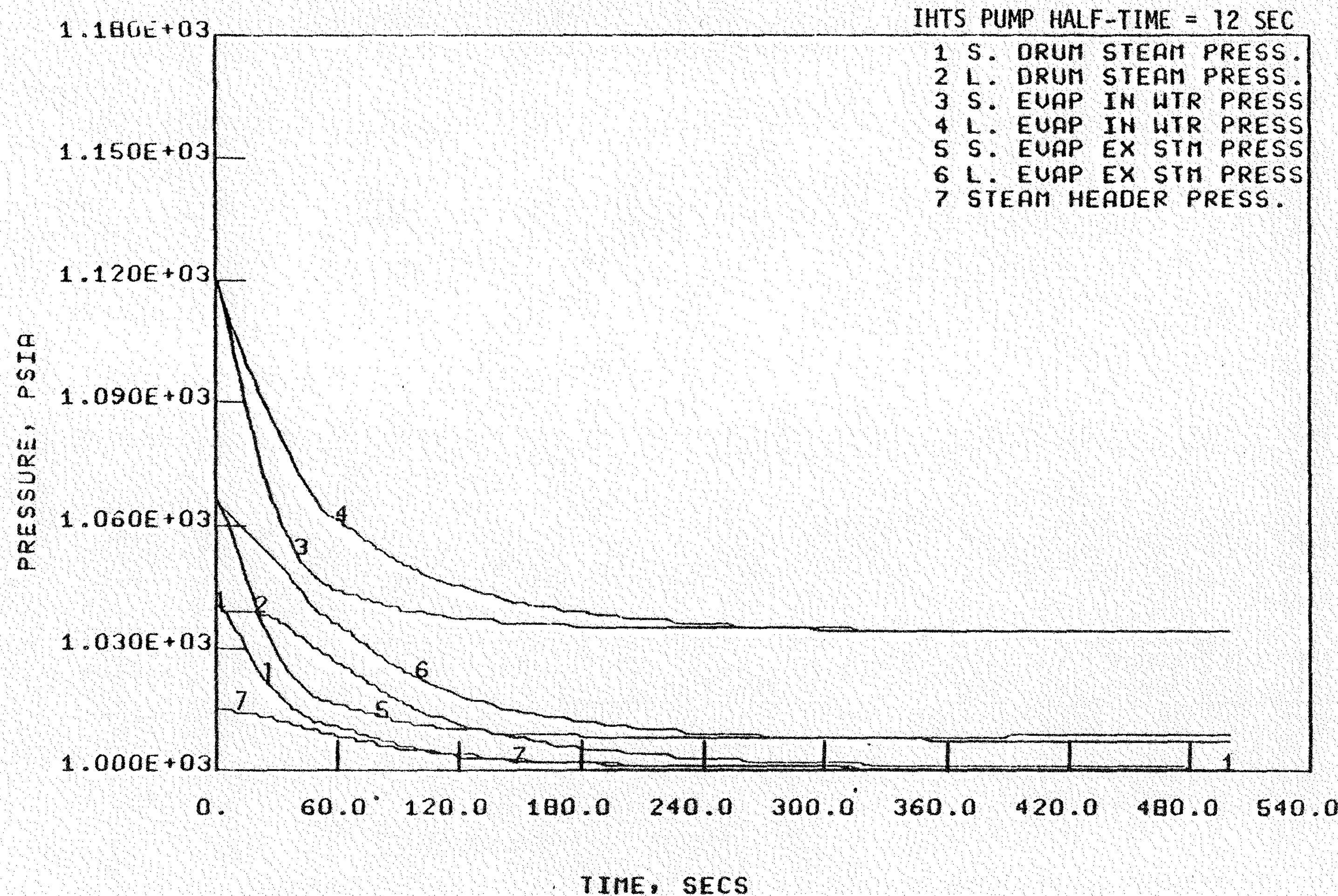

FIGURE 5-22
POOL IHTS PUMP PWR LOSS WITH SCRAM AND NO PUMP TRIP (MAX DECAY HT)
RUN DATED 11/01/78
NUMBER PAPGE01

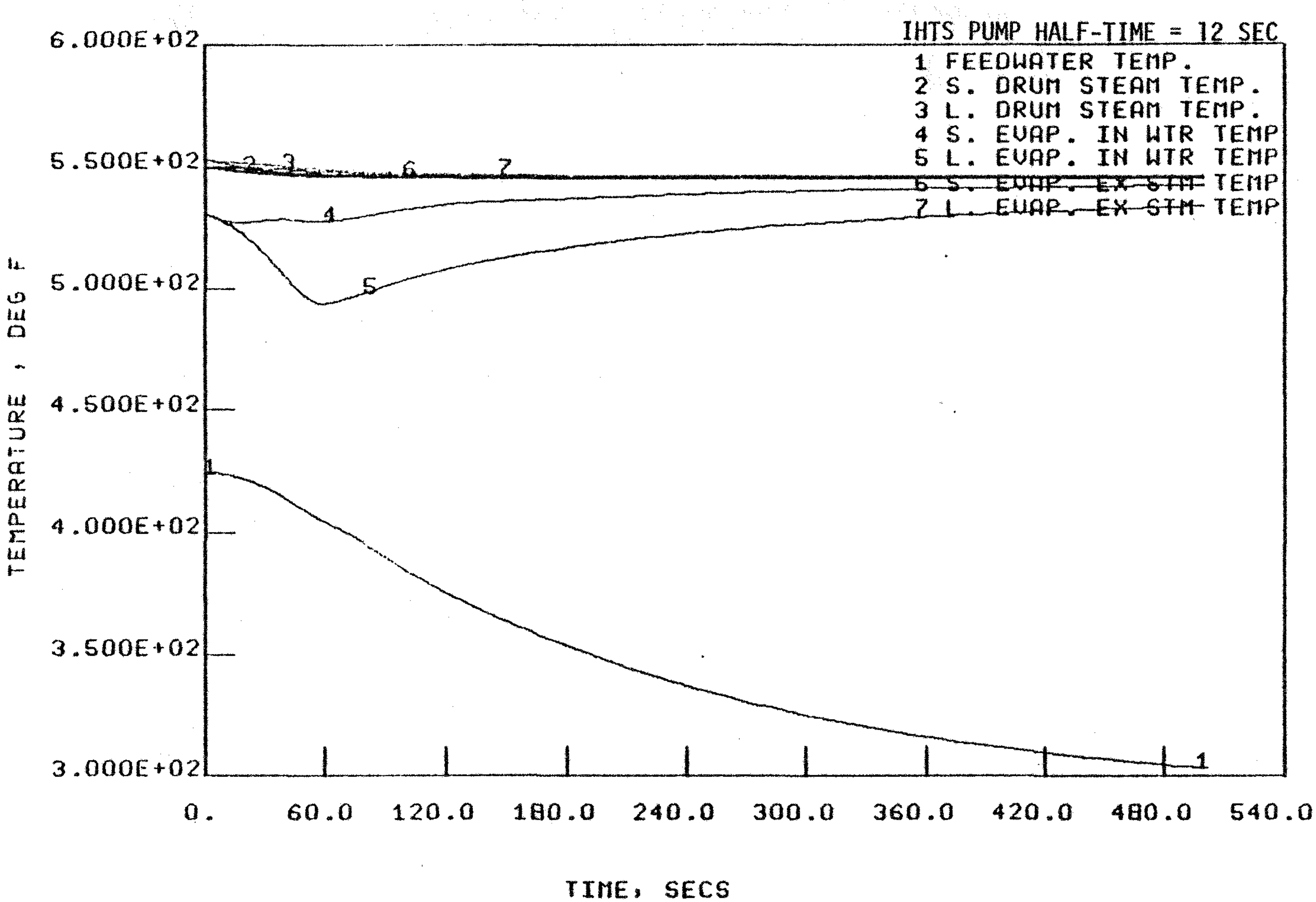

FIGURE 5-23
POOL IHTS PUMP PWR LOSS WITH SCRAM AND NO PUMP TRIP (MAX DECAY HT)
RUN DATED 11/01/78
NUMBER PAP6E01

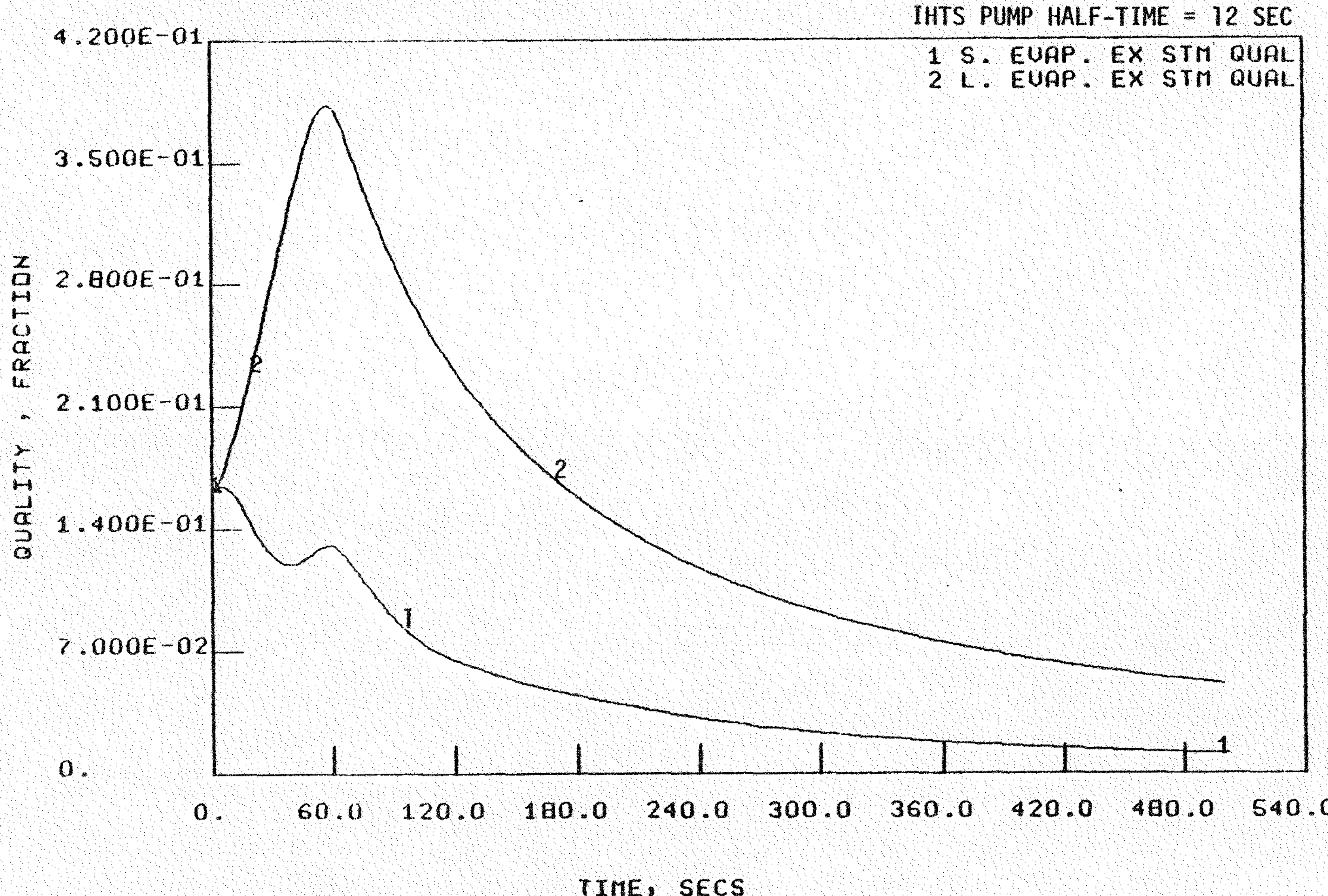

FIGURE 5-24

POOL IHTS PUMP PWR LOSS WITH SCRAM AND NO PUMP TRIP (MAX DECAY HT)

RUN DATED 11/01/78

NUMBER PAPGE01

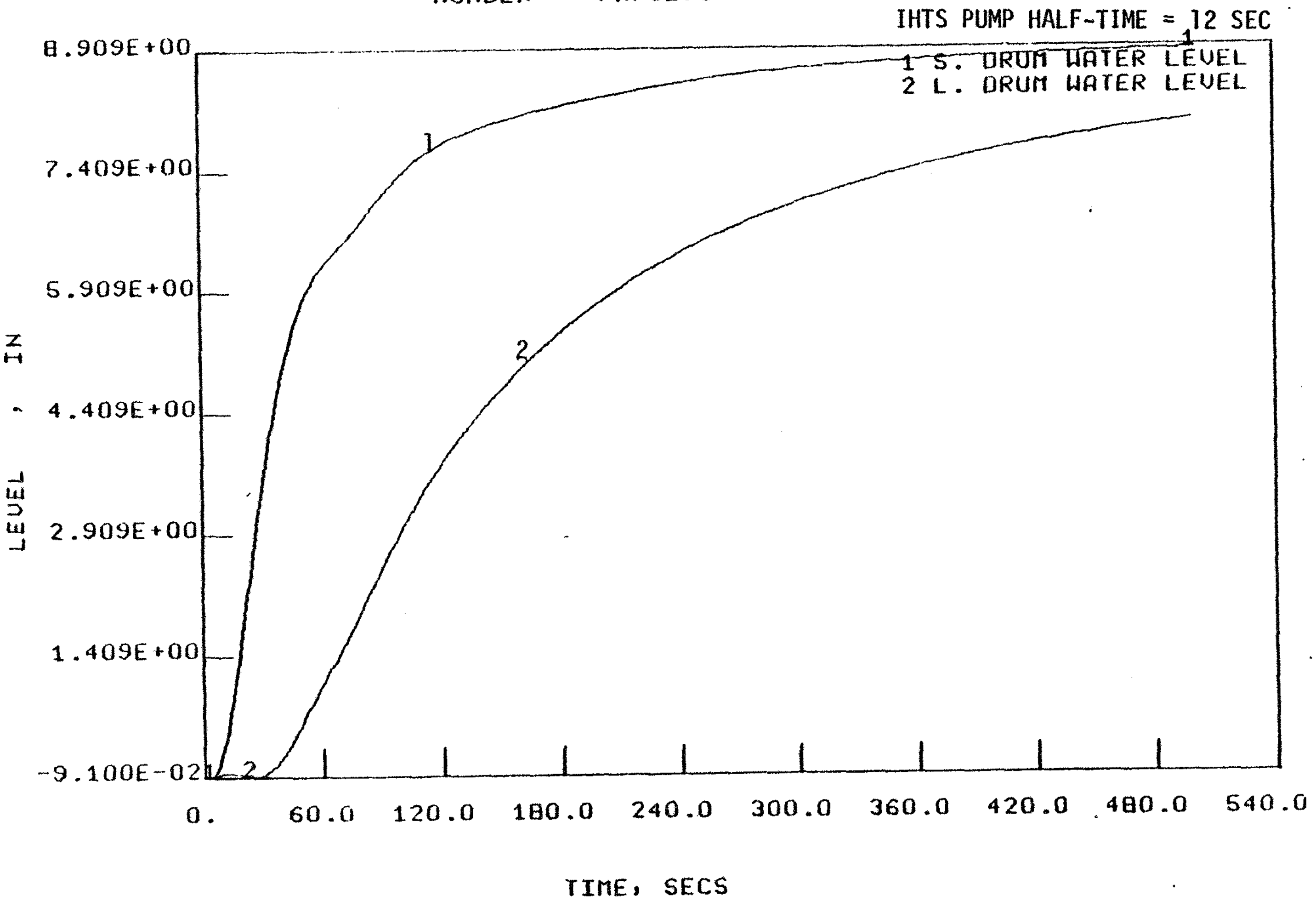

FIGURE 5-25
POOL IHTS PUMP PWR LOSS WITH SCRAM AND NO PUMP TRIP (MAX DECAY HT)
RUN DATED 11/01/78
NUMBER PAPGE02

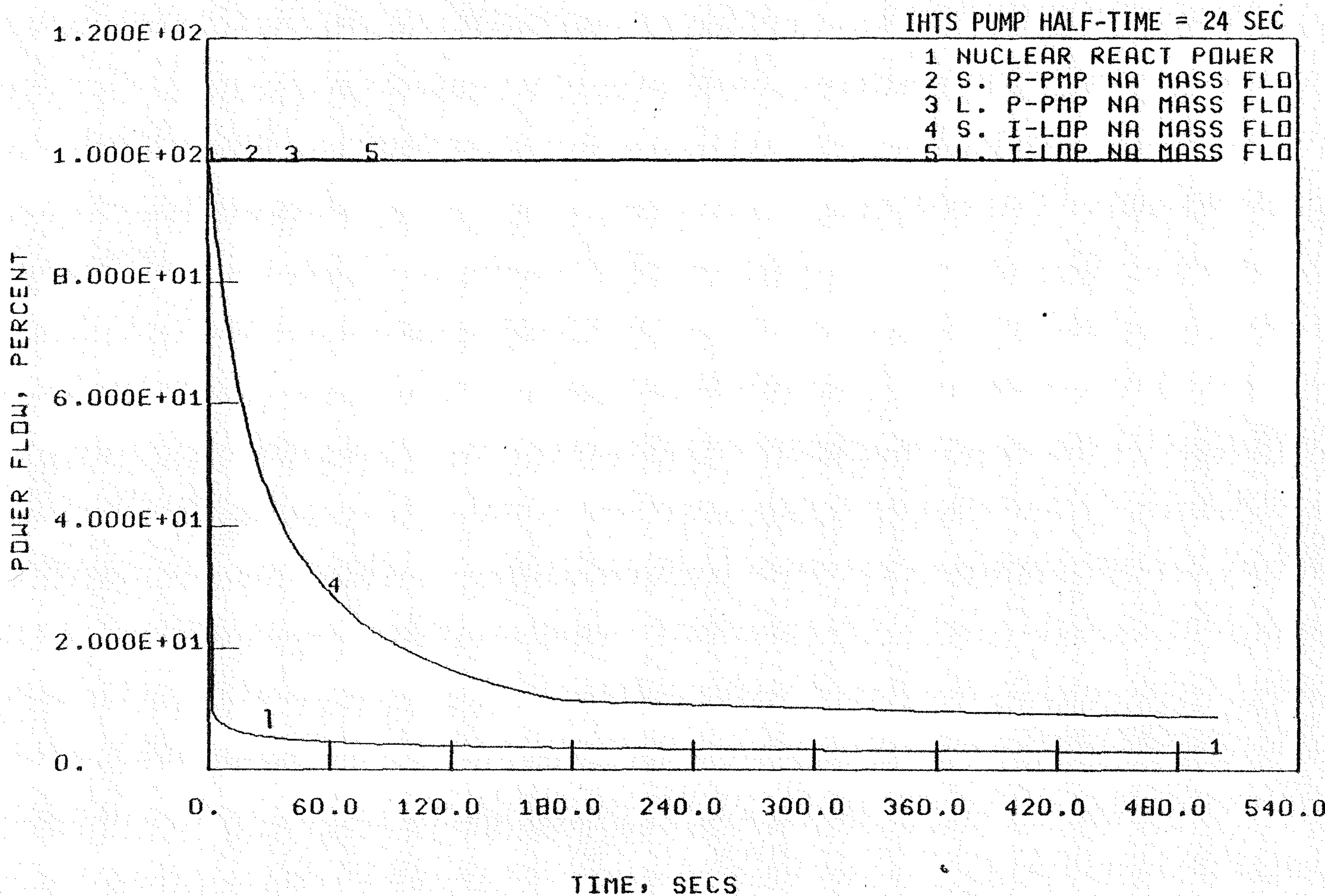

FIGURE 5-26

POOL IHTS PUMP PWR LOSS WITH SCRAM AND NO PUMP TRIP (MAX DECAY HT)
RUN DATED 11/01/78
NUMBER PAPGE02

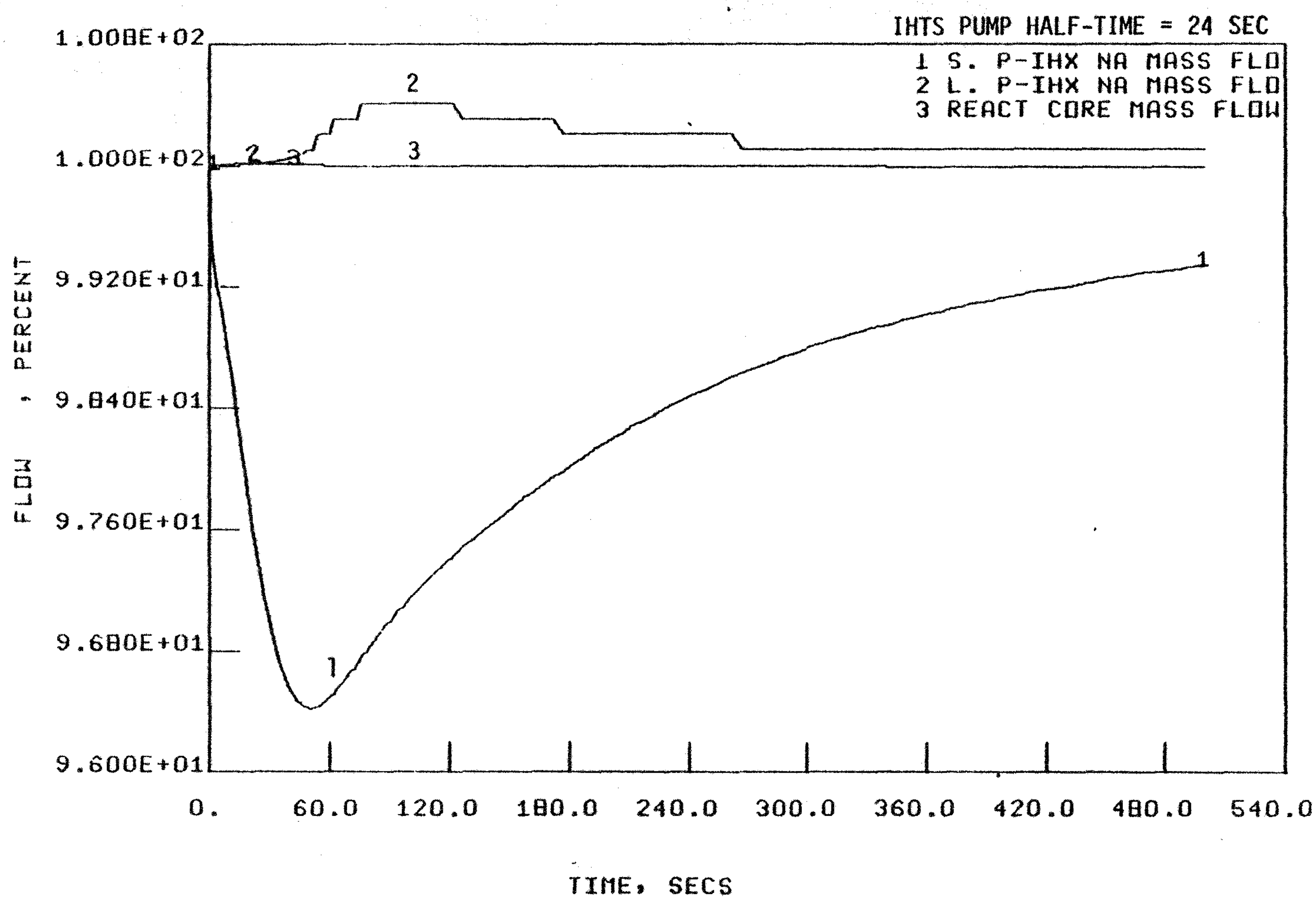

FIGURE 5-27

POOL IHTS PUMP PWR LOSS WITH SCRAM AND NO PUMP TRIP (MAX DECAY HT)
RUN DATED 11/01/78
NUMBER PAPGE02

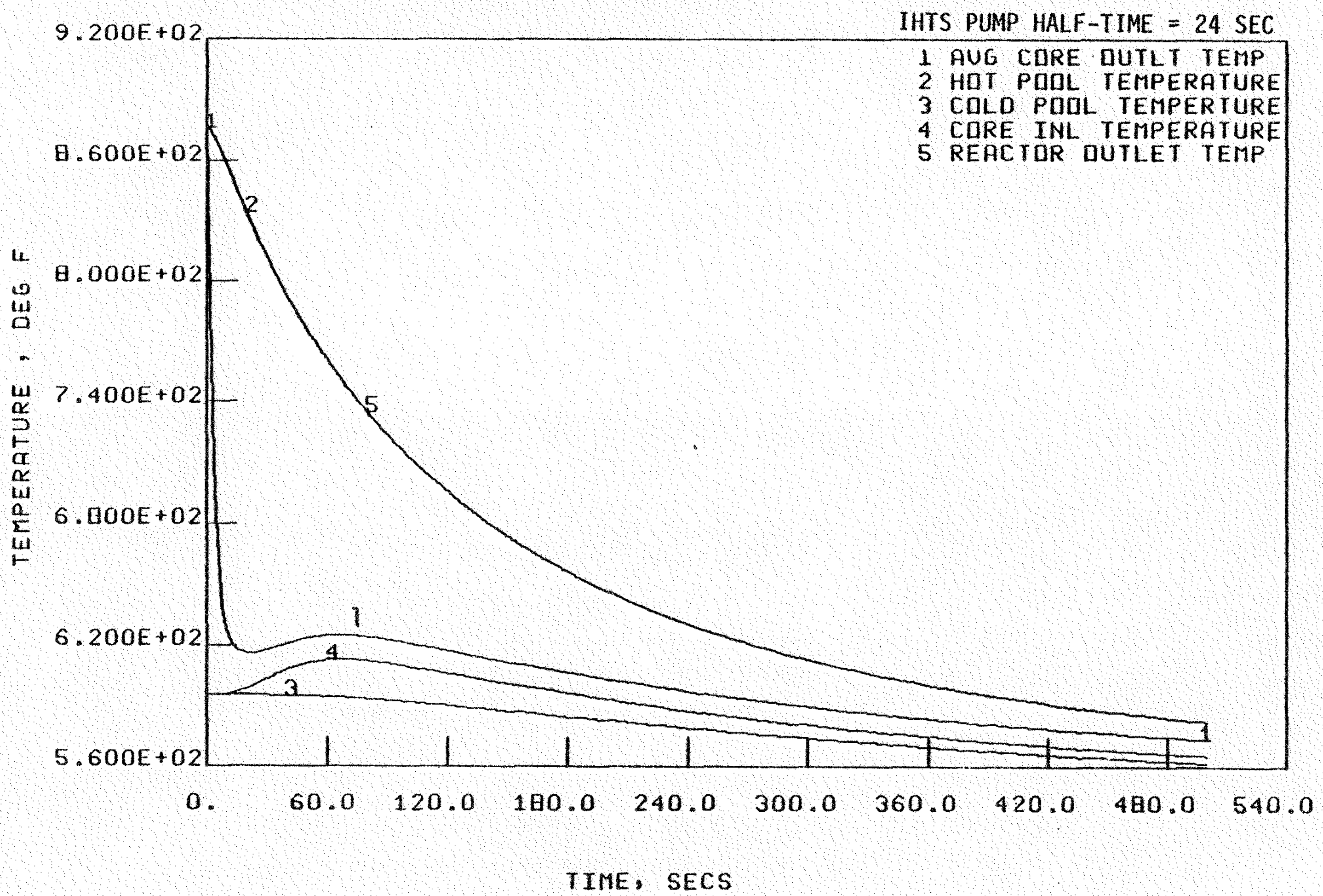

FIGURE 5-28

POOL IHTS PUMP PWR LOSS WITH SCRAM AND NO PUMP TRIP (MAX DECAY HT)
RUN DATED 11/01/78
NUMBER PAPGE02

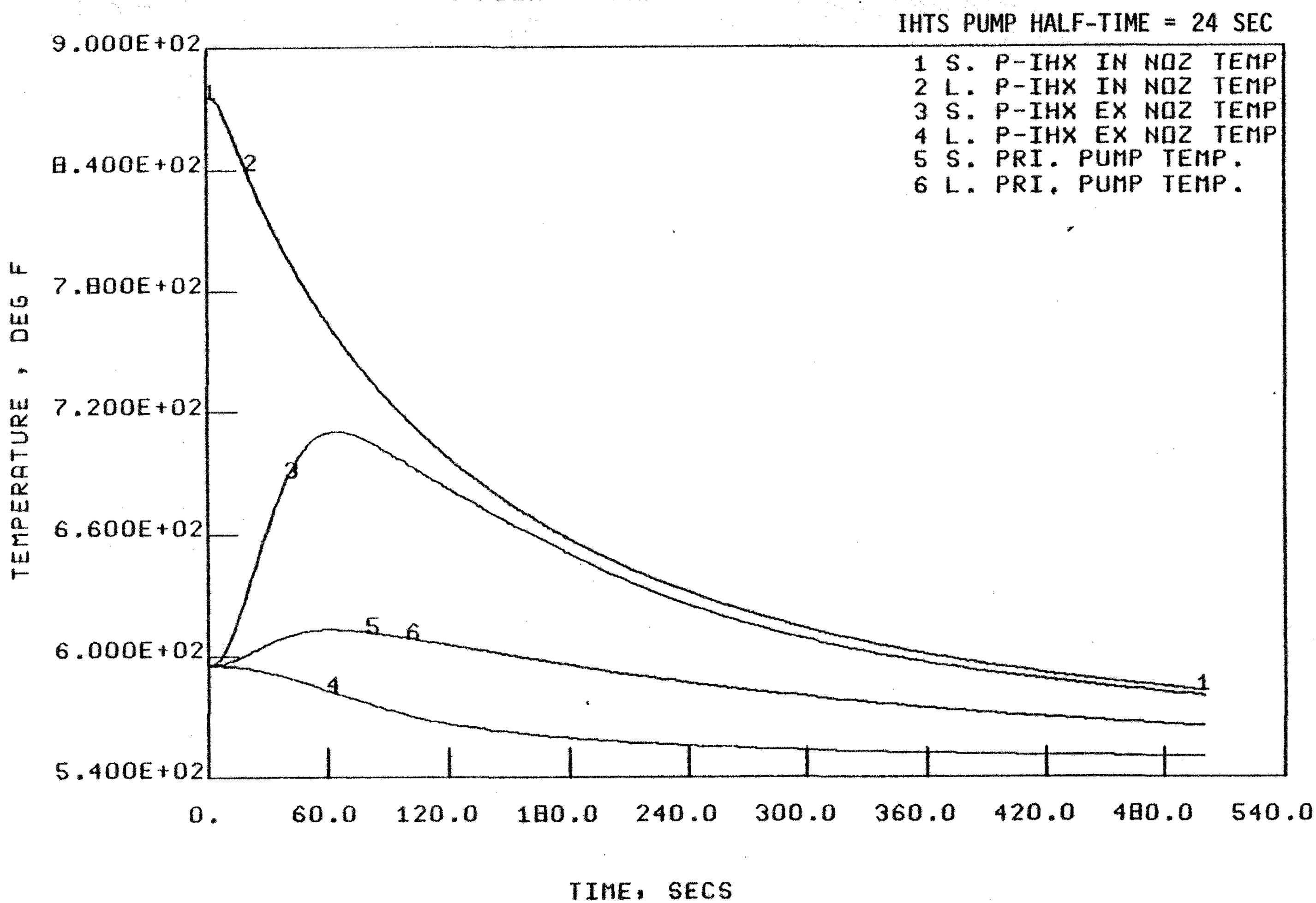

FIGURE 5-29

POOL IHTS PUMP PWR LOSS WITH SCRAM AND NO PUMP TRIP (MAX DECAY HT)
RUN DATED 11/01/78
NUMBER PAPGE02

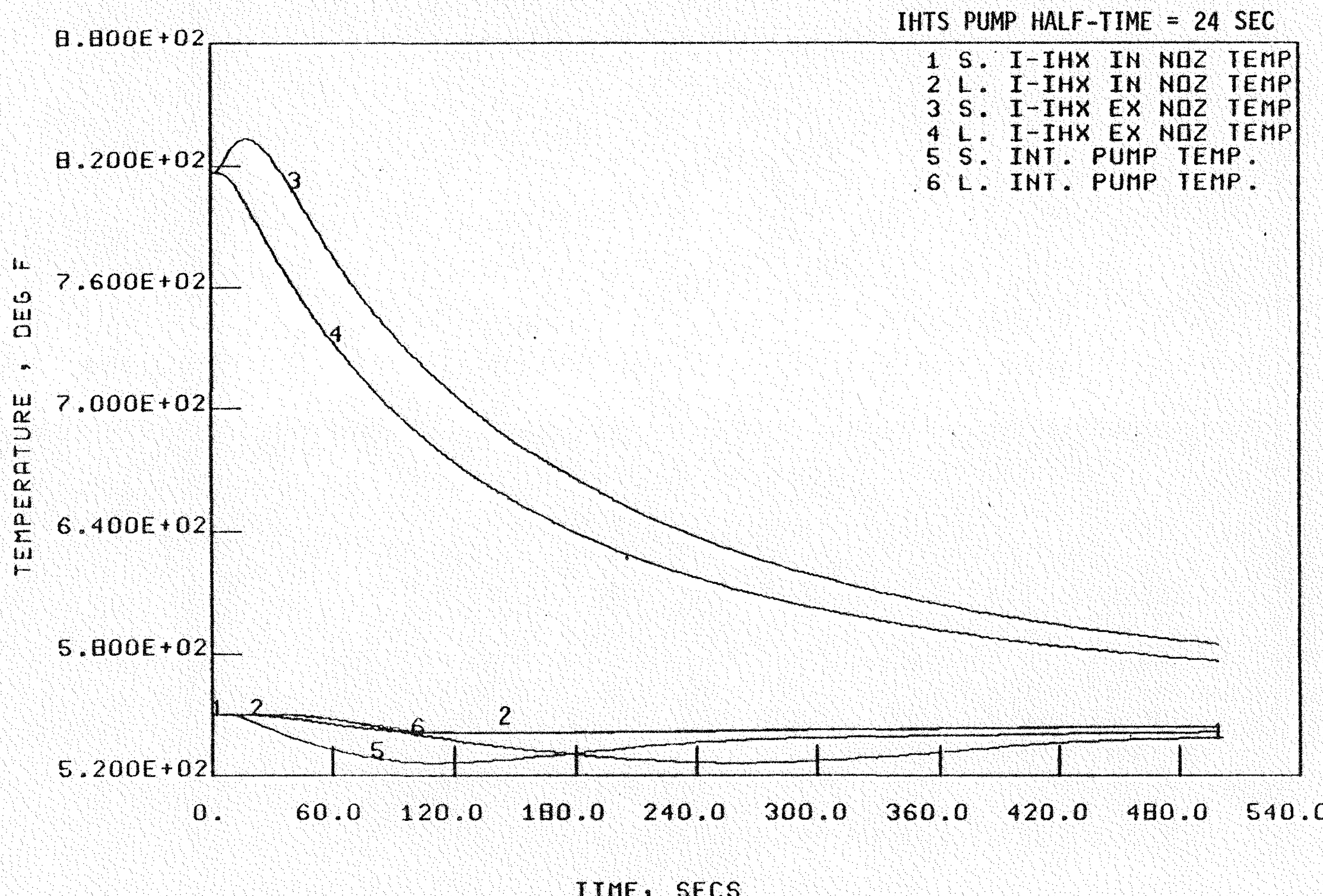

FIGURE 5-30
POOL IHTS PUMP PWR LOSS WITH SCRAM AND NO PUMP TRIP (MAX DECAY HT)
RUN DATED 11/01/78
NUMBER PAPGE02

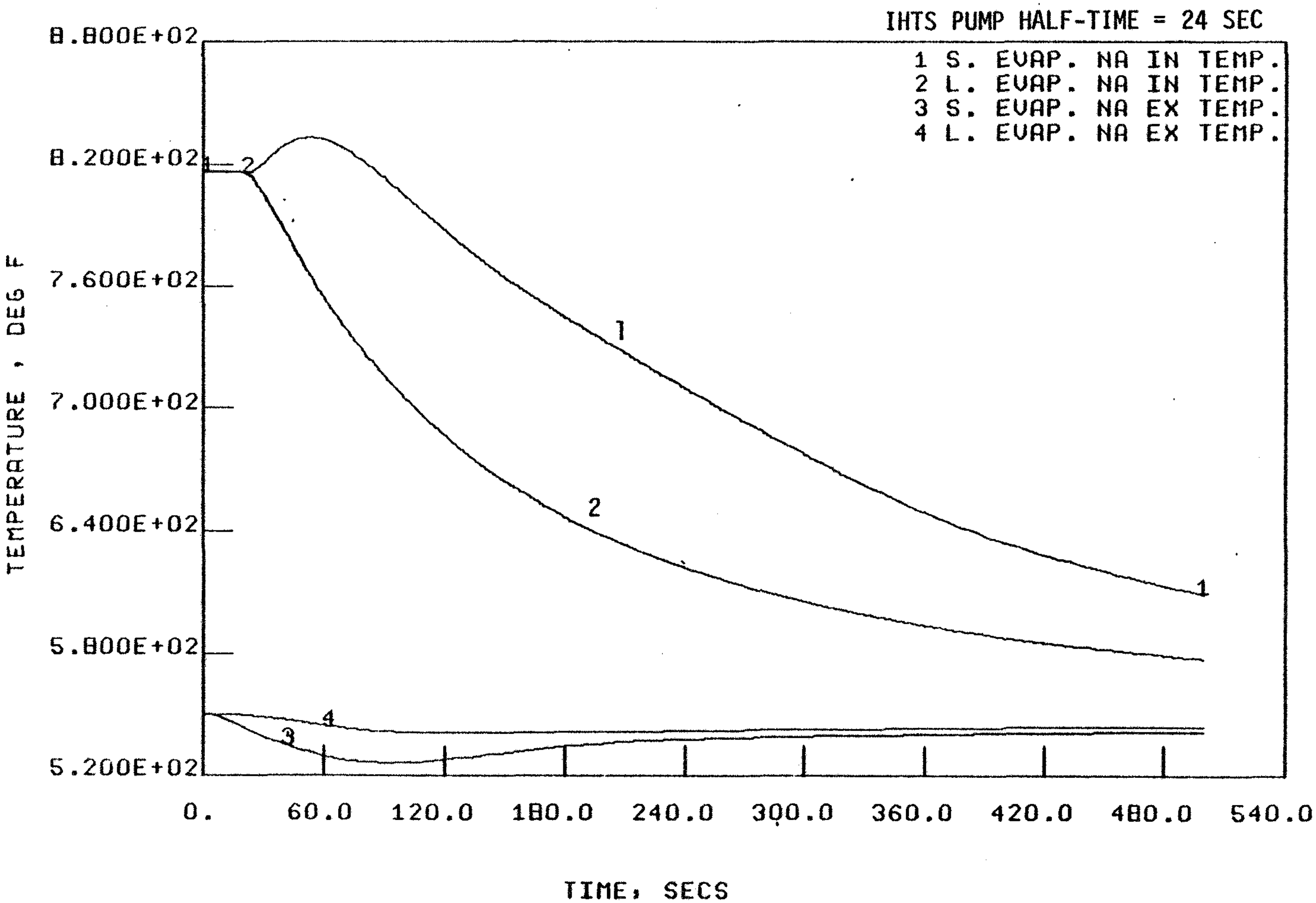

FIGURE 5-31
POOL IHTS PUMP PWR LOSS WITH SCRAM AND NO PUMP TRIP (MAX DECAY HT)
RUN DATED 11/01/78
NUMBER PAPGE02

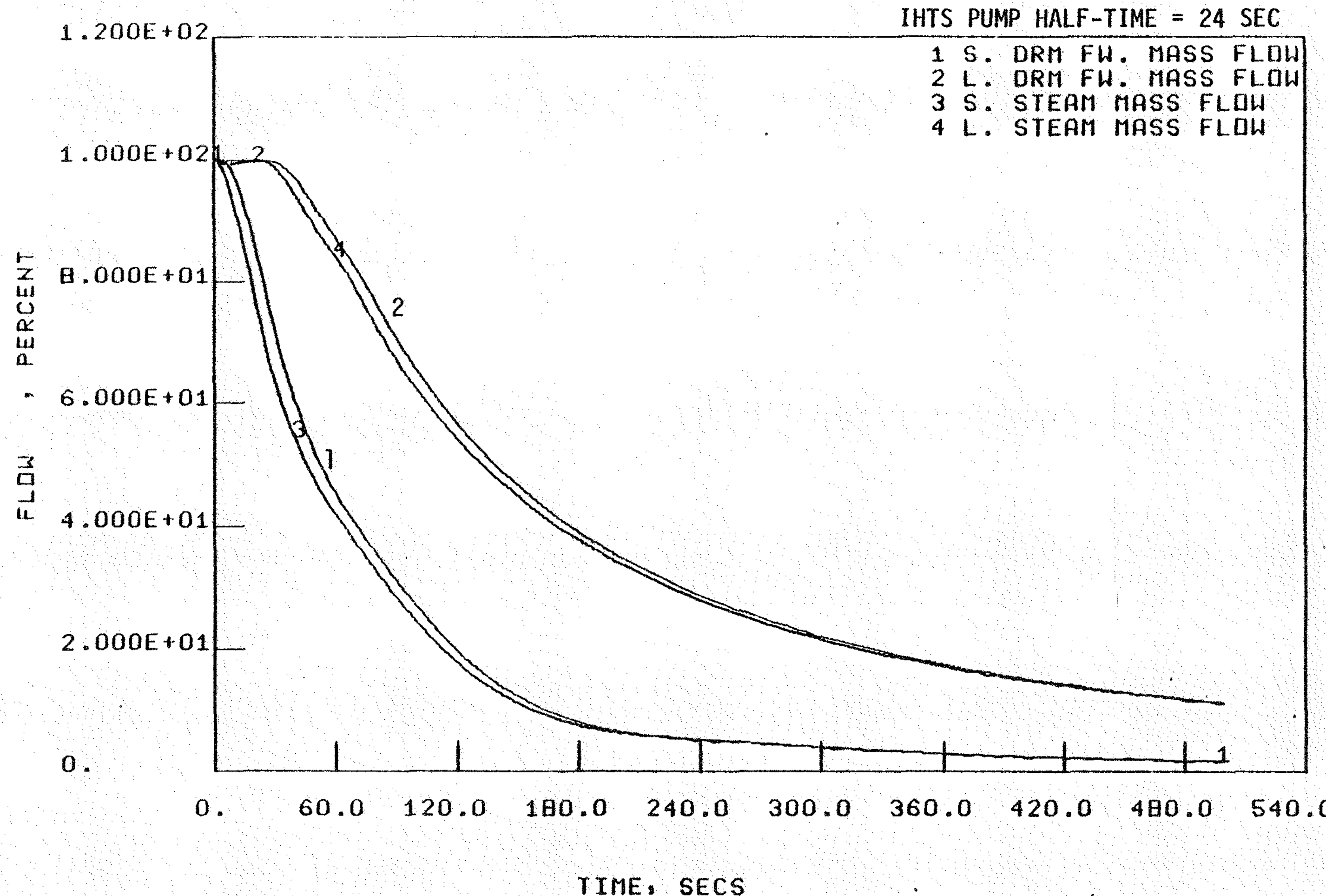

FIGURE 5-32

POOL IHTS PUMP PWR LOSS WITH SCRAM AND NO PUMP TRIP (MAX DECAY HT)
RUN DATED 11/01/78
NUMBER PAPGE02

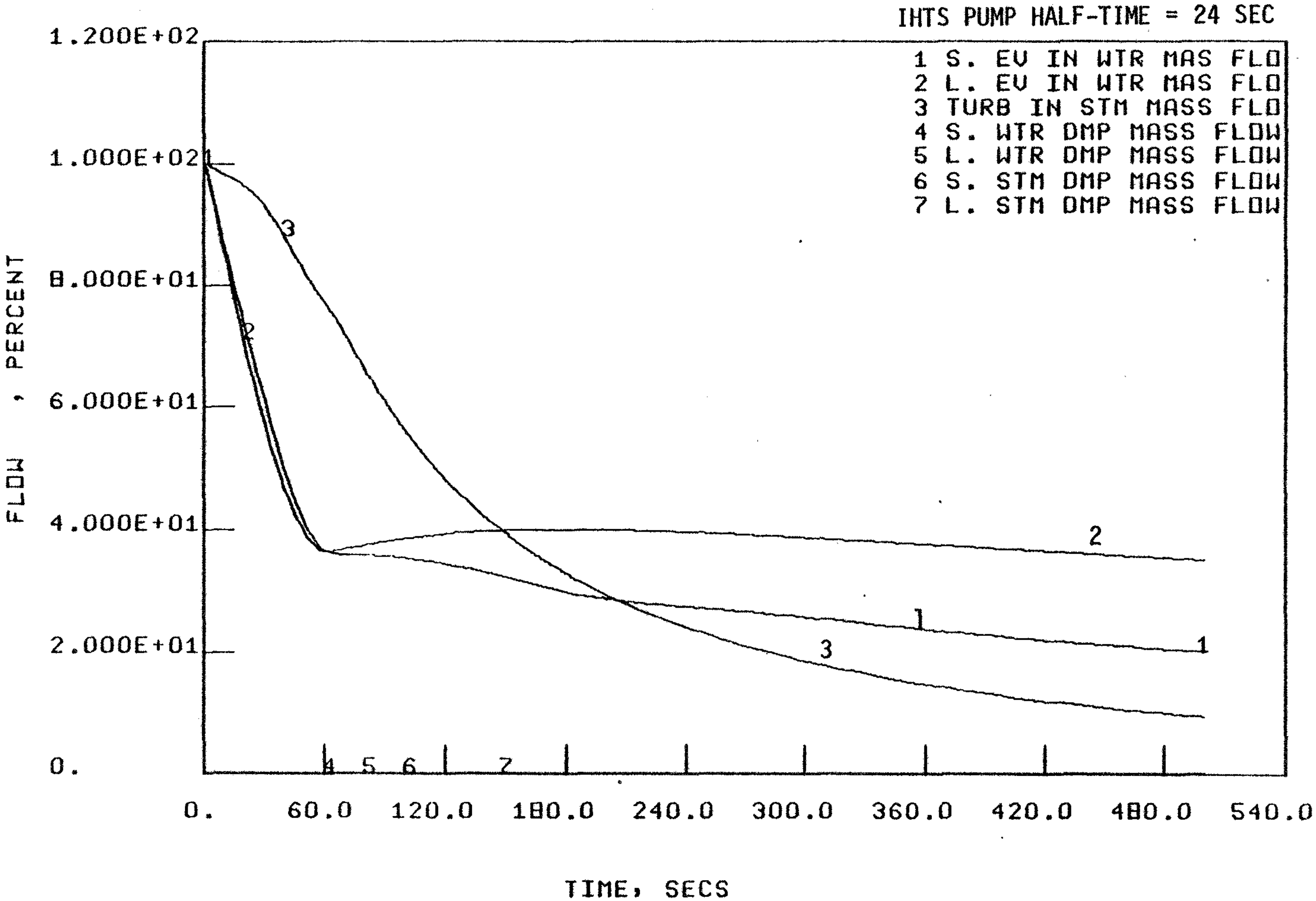

V-2.3-195

FIGURE 5-33

POOL IHTS PUMP PWR LOSS WITH SCRAM AND NO PUMP TRIP (MAX DECAY HT)
RUN DATED 11/01/78
NUMBER PAPGE02

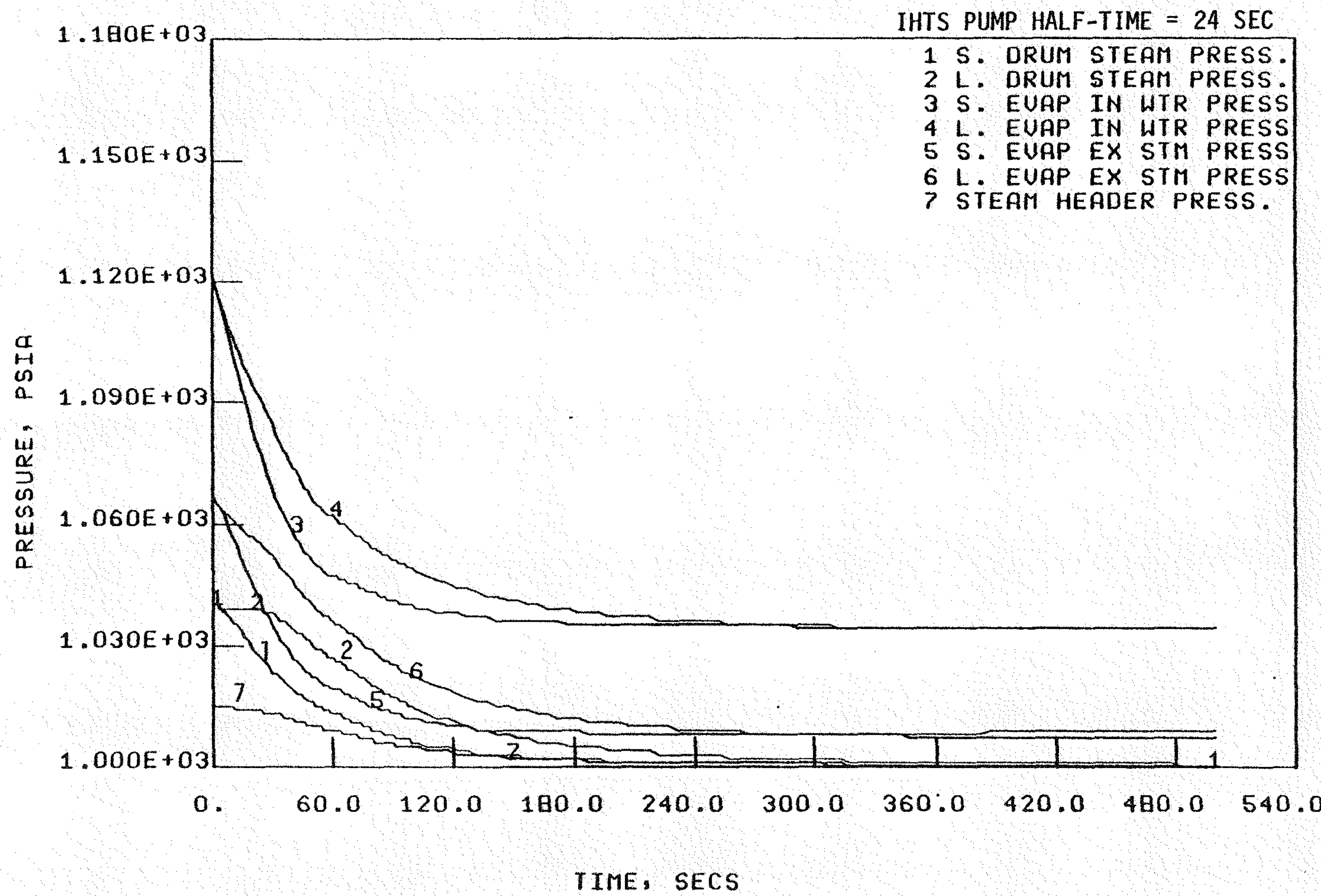

FIGURE 5-34
POOL IHTS PUMP PWR LOSS WITH SCRAM AND NO PUMP TRIP (MAX DECAY HT)
RUN DATED 11/01/78
NUMBER PAPGE02

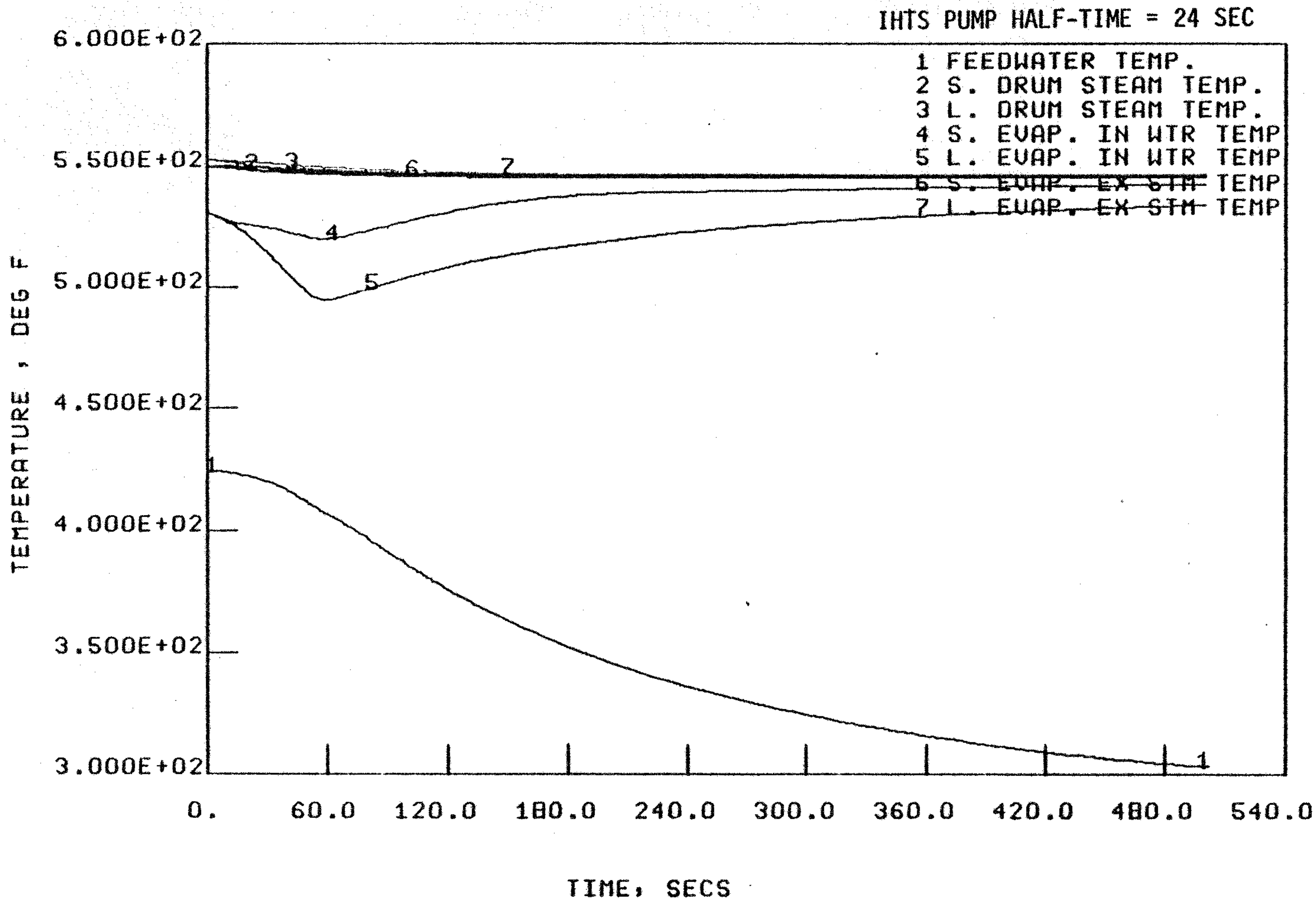

FIGURE 5-35
POOL IHTS PUMP PWR LOSS WITH SCRAM AND NO PUMP TRIP (MAX DECAY HT)
RUN DATED 11/01/78
NUMBER PAPGE02

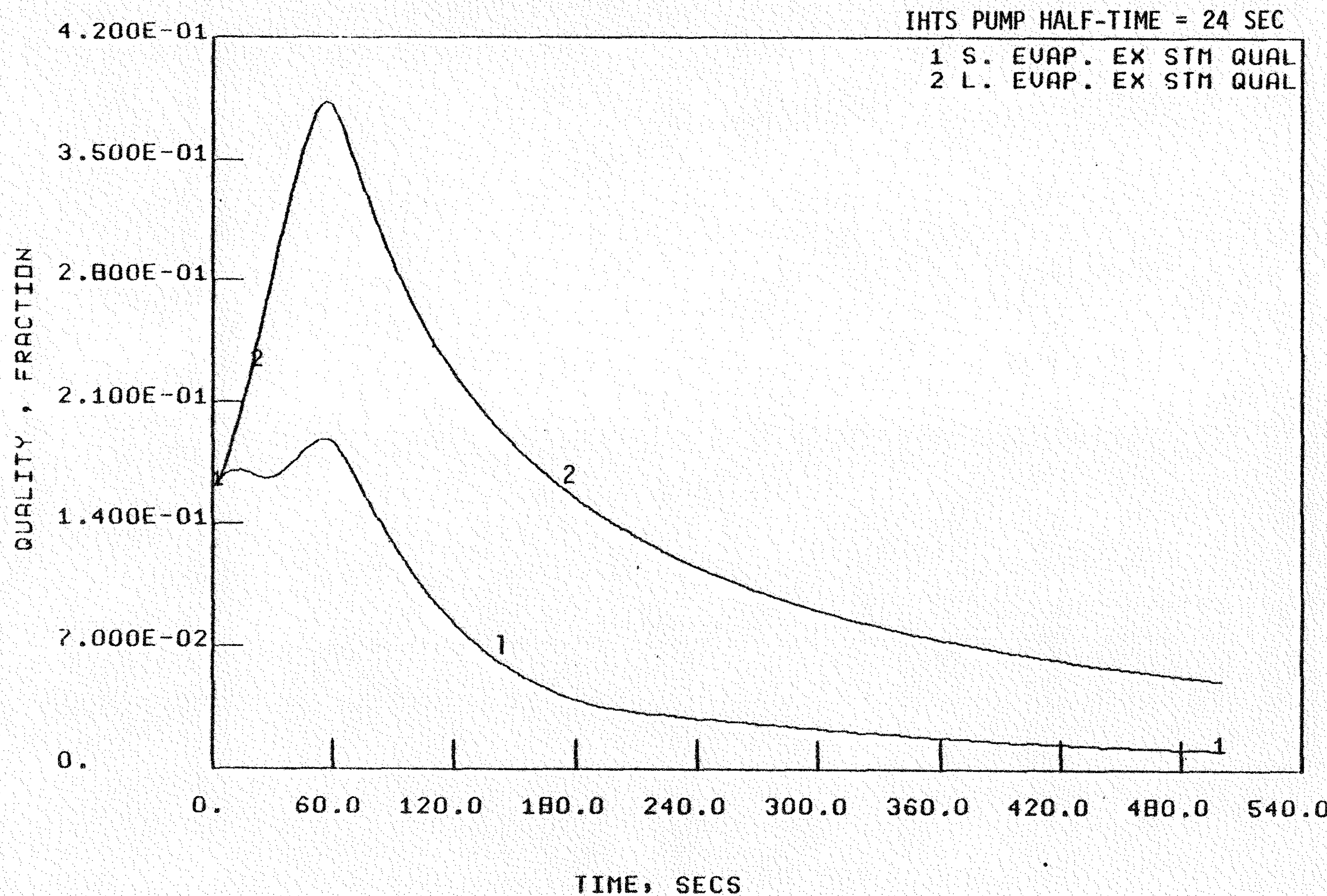

FIGURE 5-36

POOL IHTS PUMP PWR LOSS WITH SCRAM AND NO PUMP TRIP (MAX DECAY HT)
RUN DATED 11/01/78
NUMBER PAPGE02

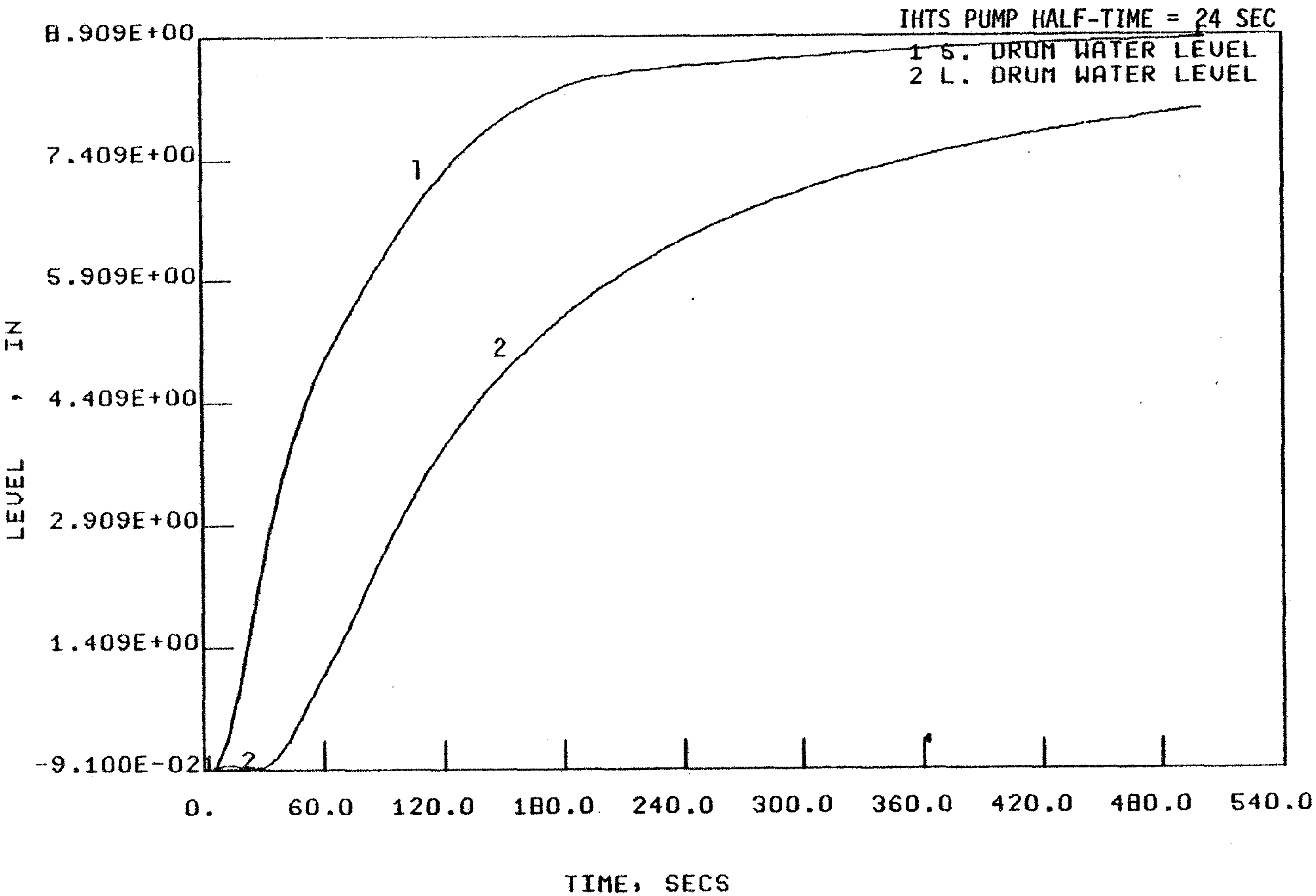

FIGURE 5-37

POOL REACTOR ISOLATION AND BLOWDOWN OF ONE STEAM GENERATOR
RUN DATED 11/03/78
NUMBER SUPGEOO

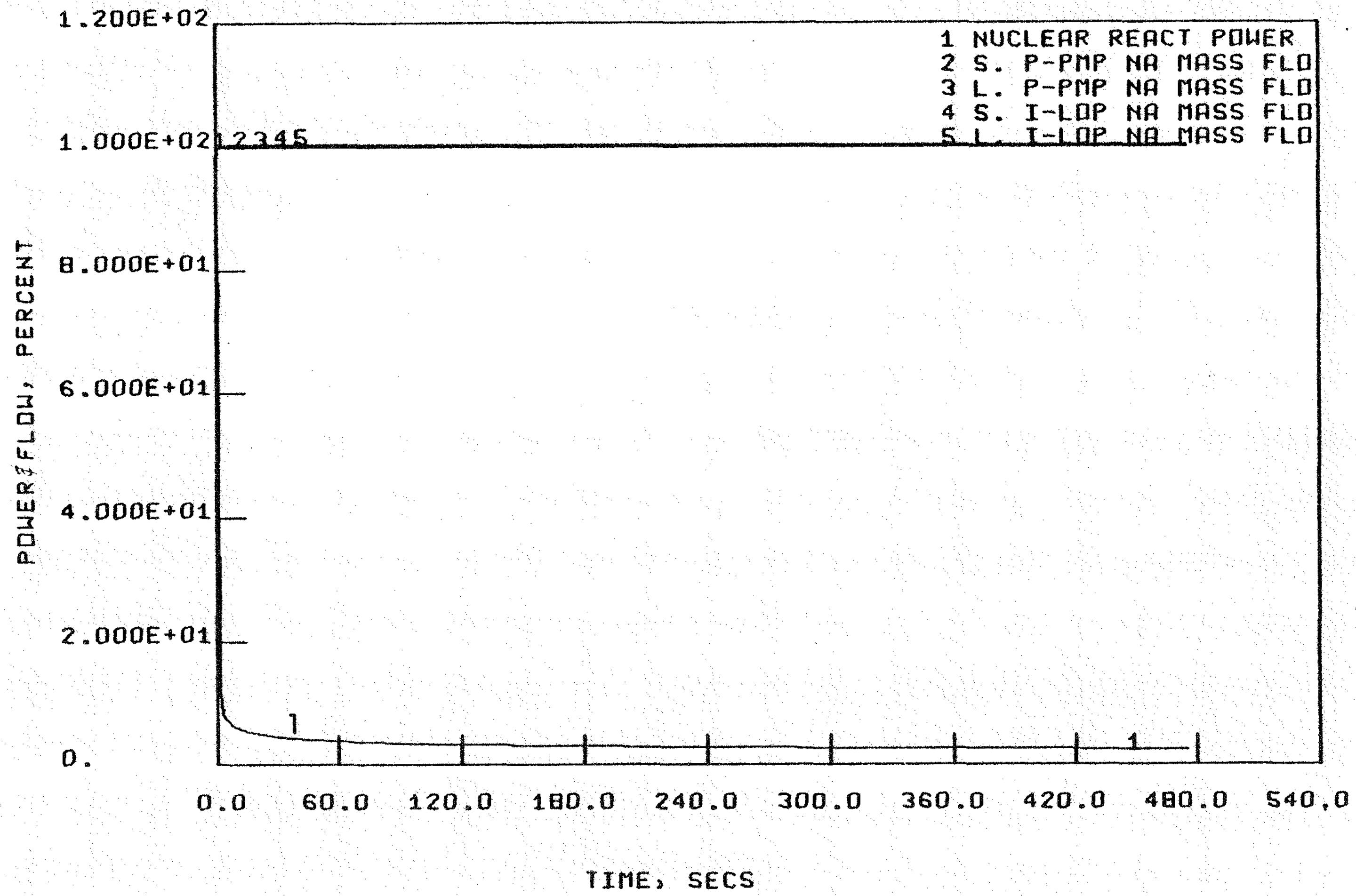

FIGURE 5-38

POOL REACTOR ISOLATION AND BLOWDOWN OF ONE STEAM GENERATOR
RUN DATED 11/03/78
NUMBER SUPGE00

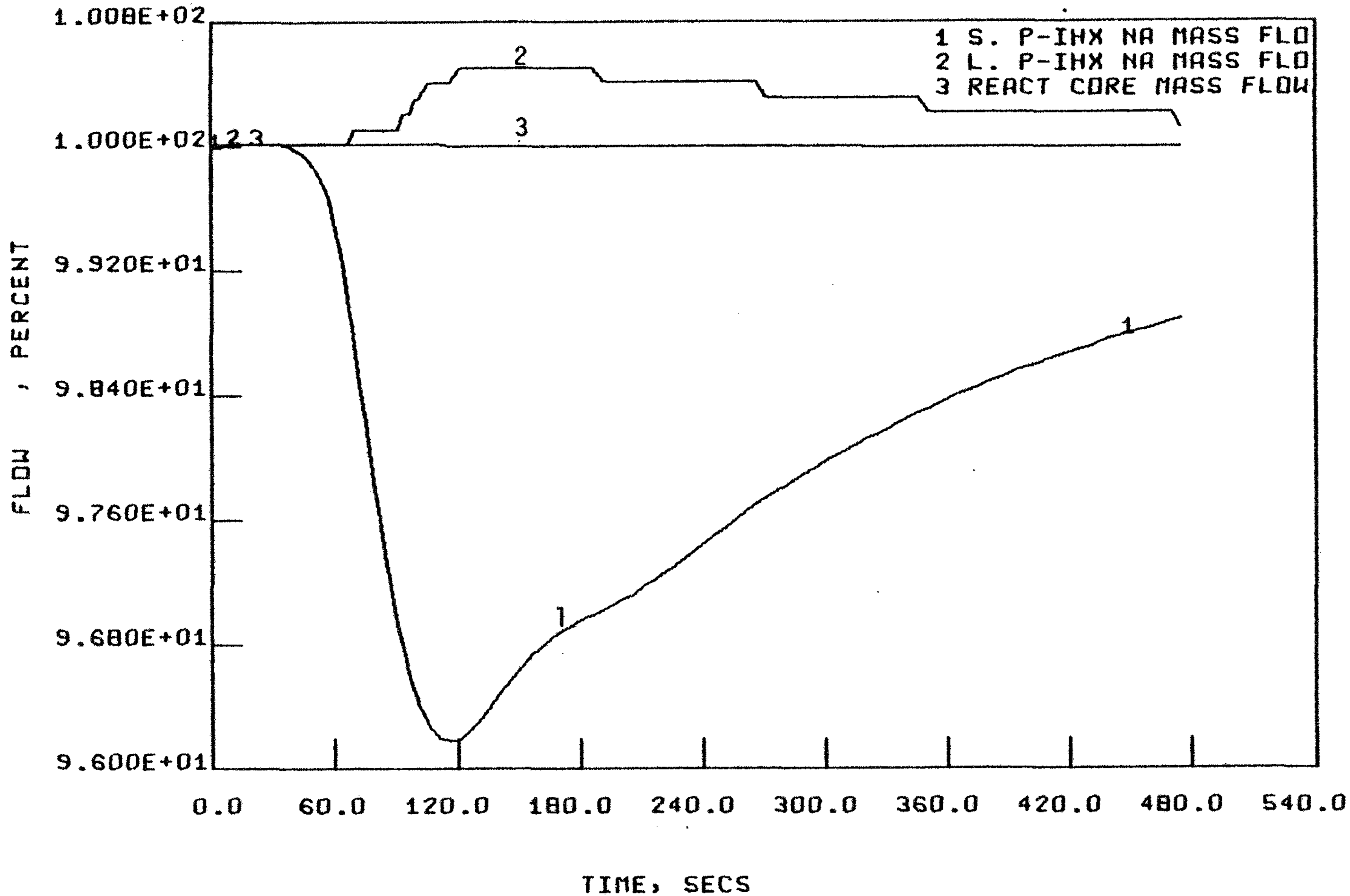

FIGURE 5-39

POOL REACTOR ISOLATION AND BLOWDOWN OF ONE STEAM GENERATOR

RUN DATED 11/03/78

NUMBER SUPGEOO

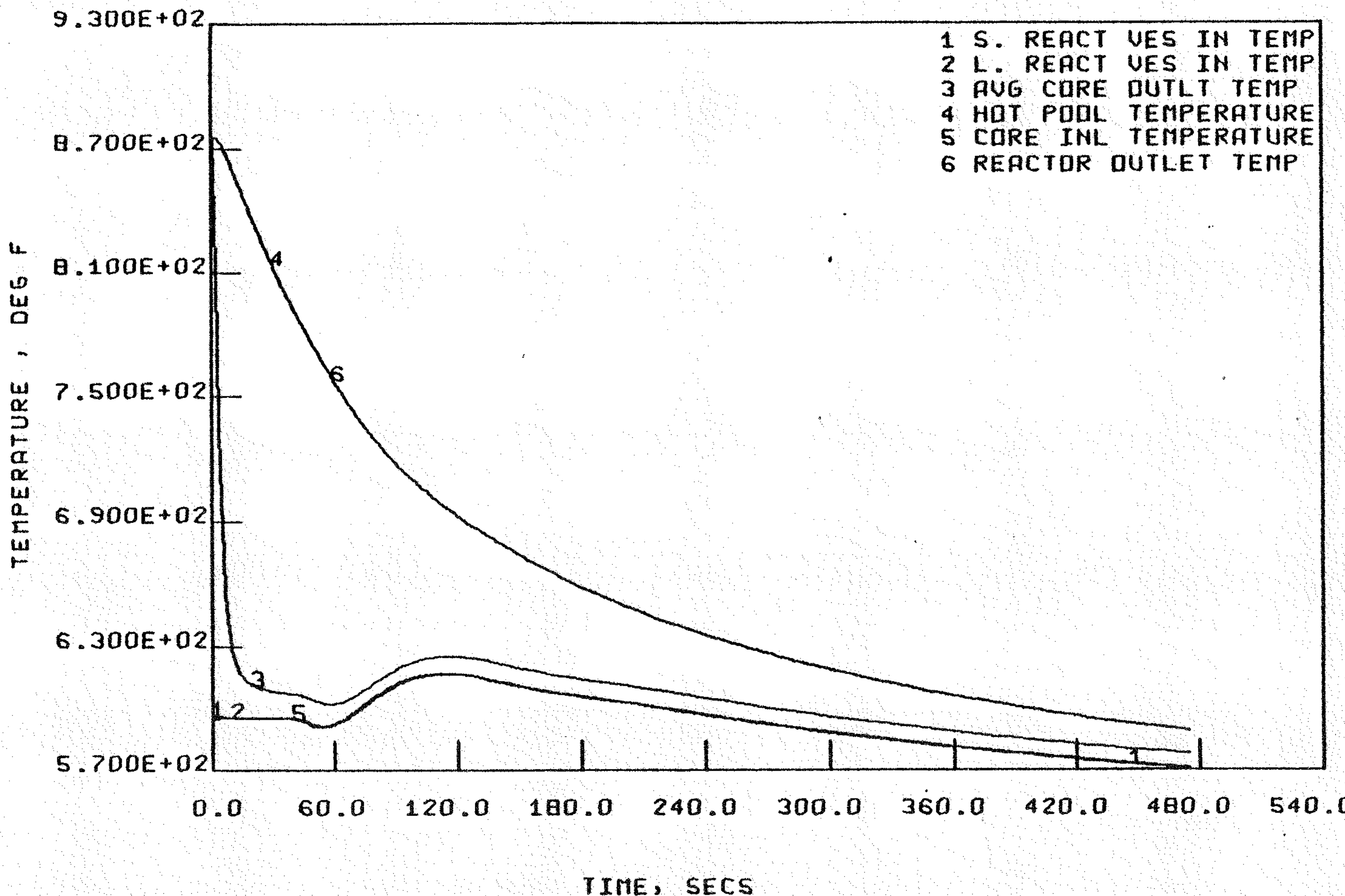

FIGURE 5-40

POOL REACTOR ISOLATION AND BLOWDOWN OF ONE STEAM GENERATOR

RUN DATED 11/03/78

NUMBER SUPGE00

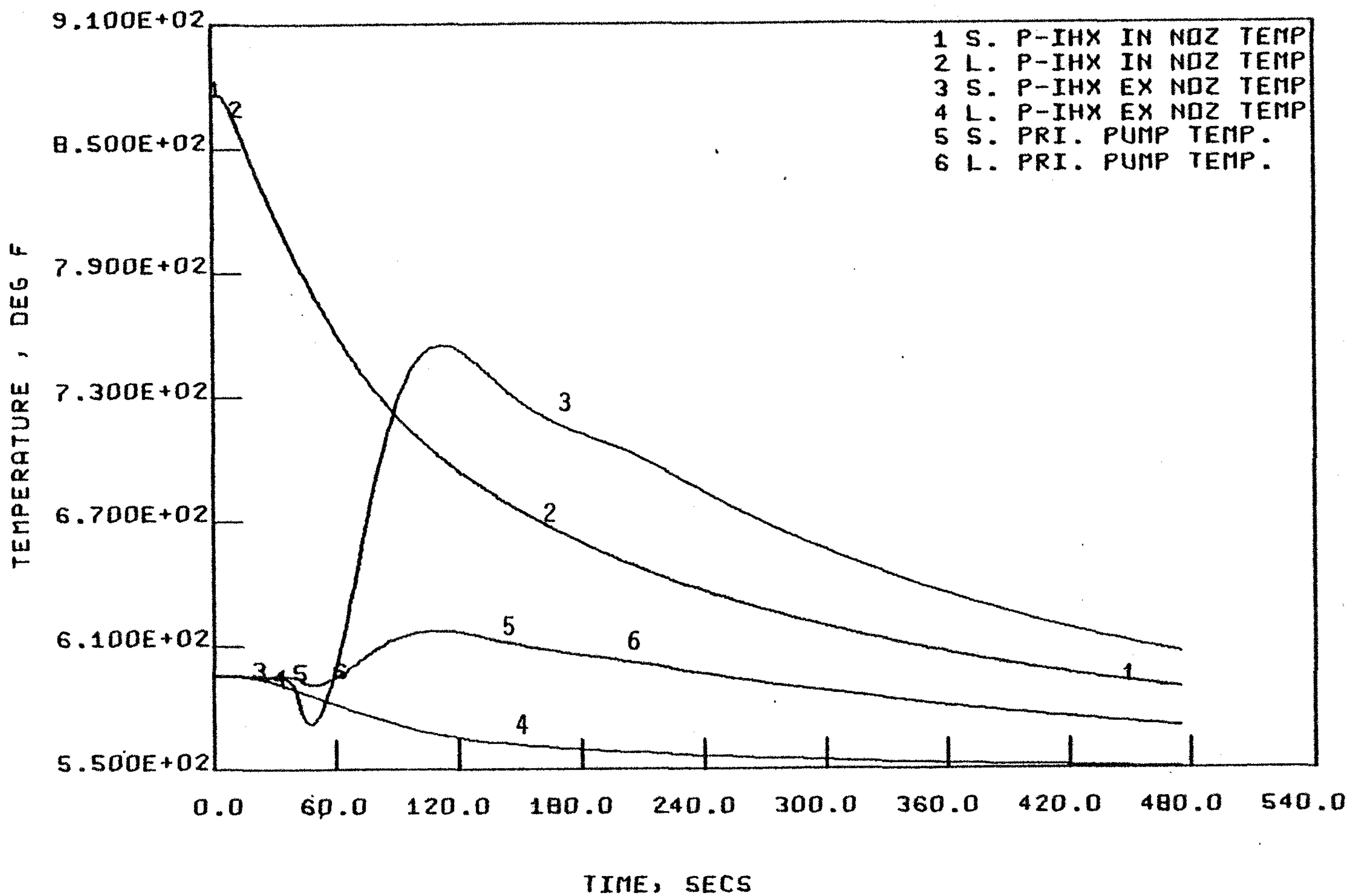

FIGURE 5-41

POOL REACTOR ISOLATION AND BLOWDOWN OF ONE STEAM GENERATOR
RUN DATED 11/03/78
NUMBER SUPGE00

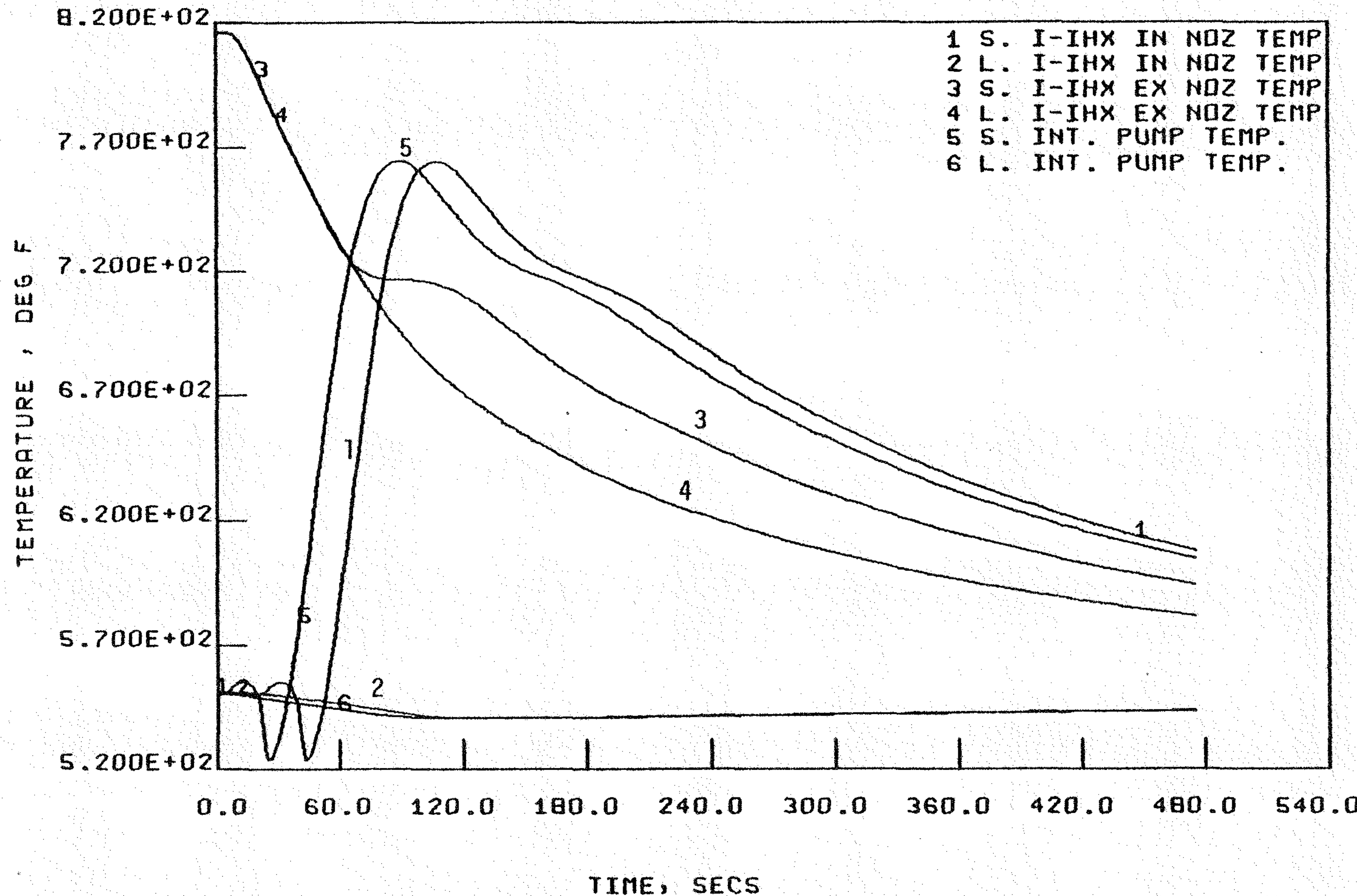

FIGURE 5-42
POOL REACTOR ISOLATION AND BLOWDOWN OF ONE STEAM GENERATOR
RUN DATED 11/03/78
NUMBER SUPGE00

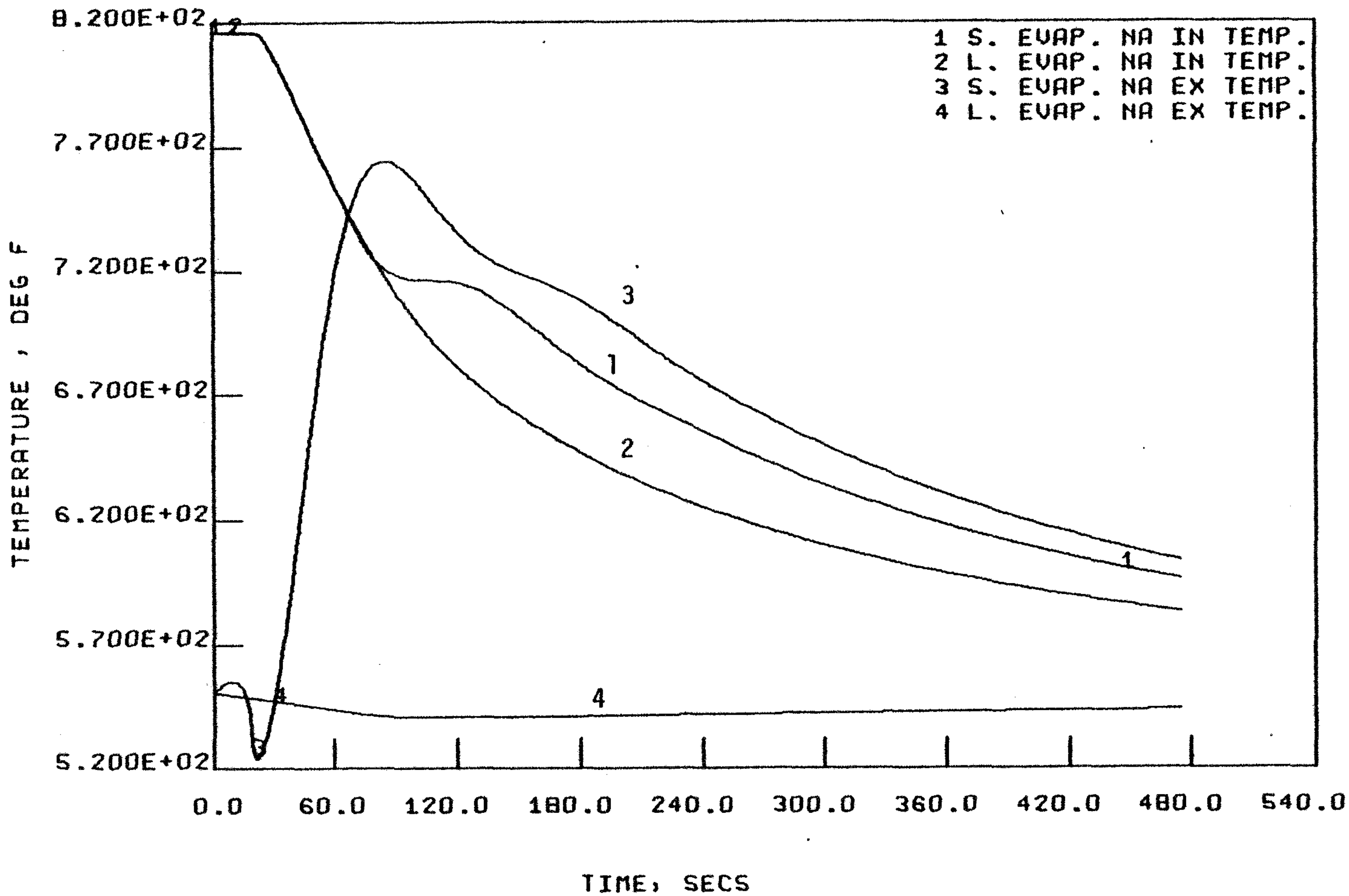

FIGURE 5-43
POOL REACTOR ISOLATION AND BLOWDOWN OF ONE STEAM GENERATOR
RUN DATED 11/03/78
NUMBER SUPGE00

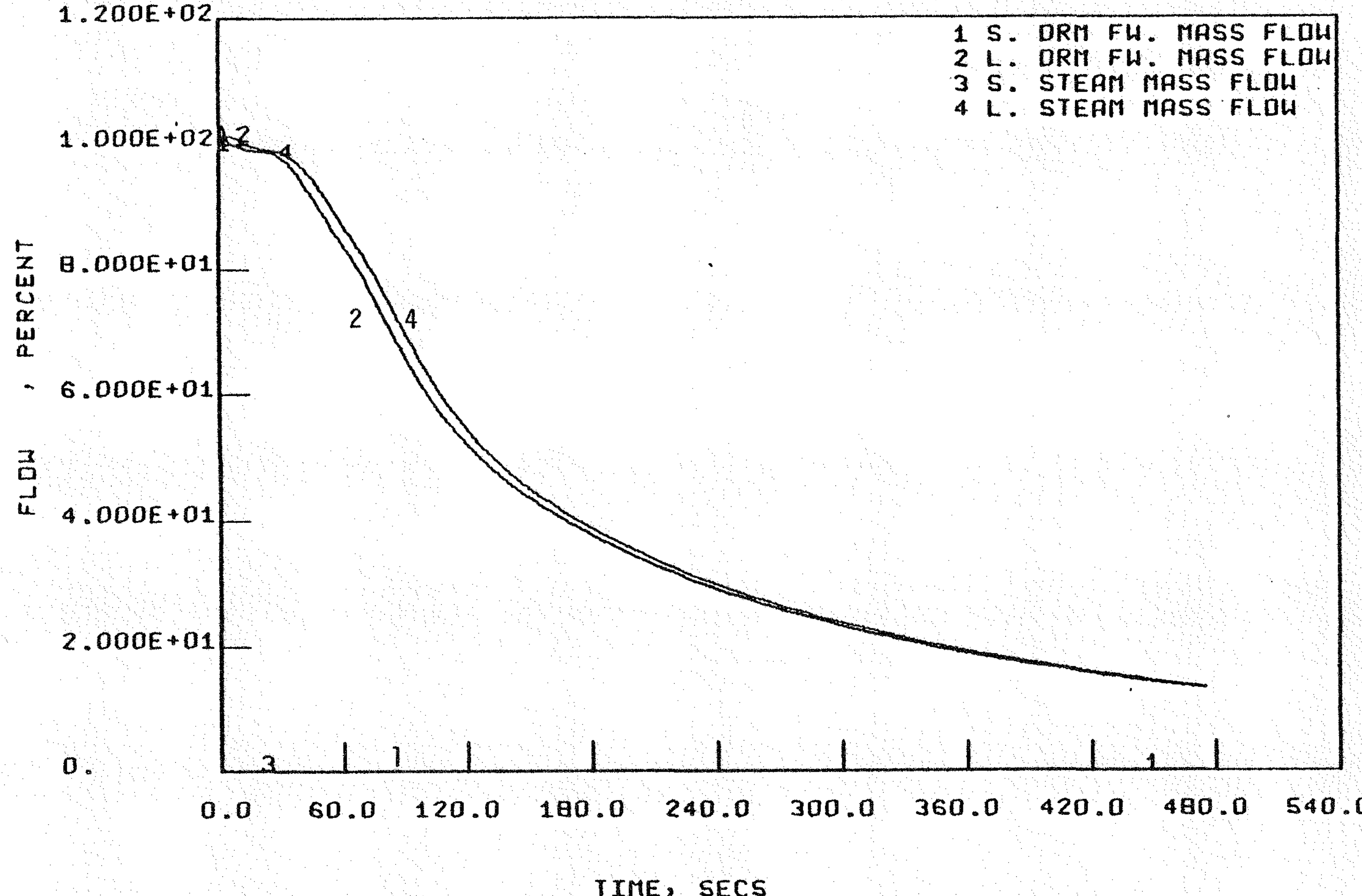

FIGURE 5-44

POOL REACTOR ISOLATION AND BLOWDOWN OF ONE STEAM GENERATOR
RUN DATED 11/03/78
NUMBER SUPGE00

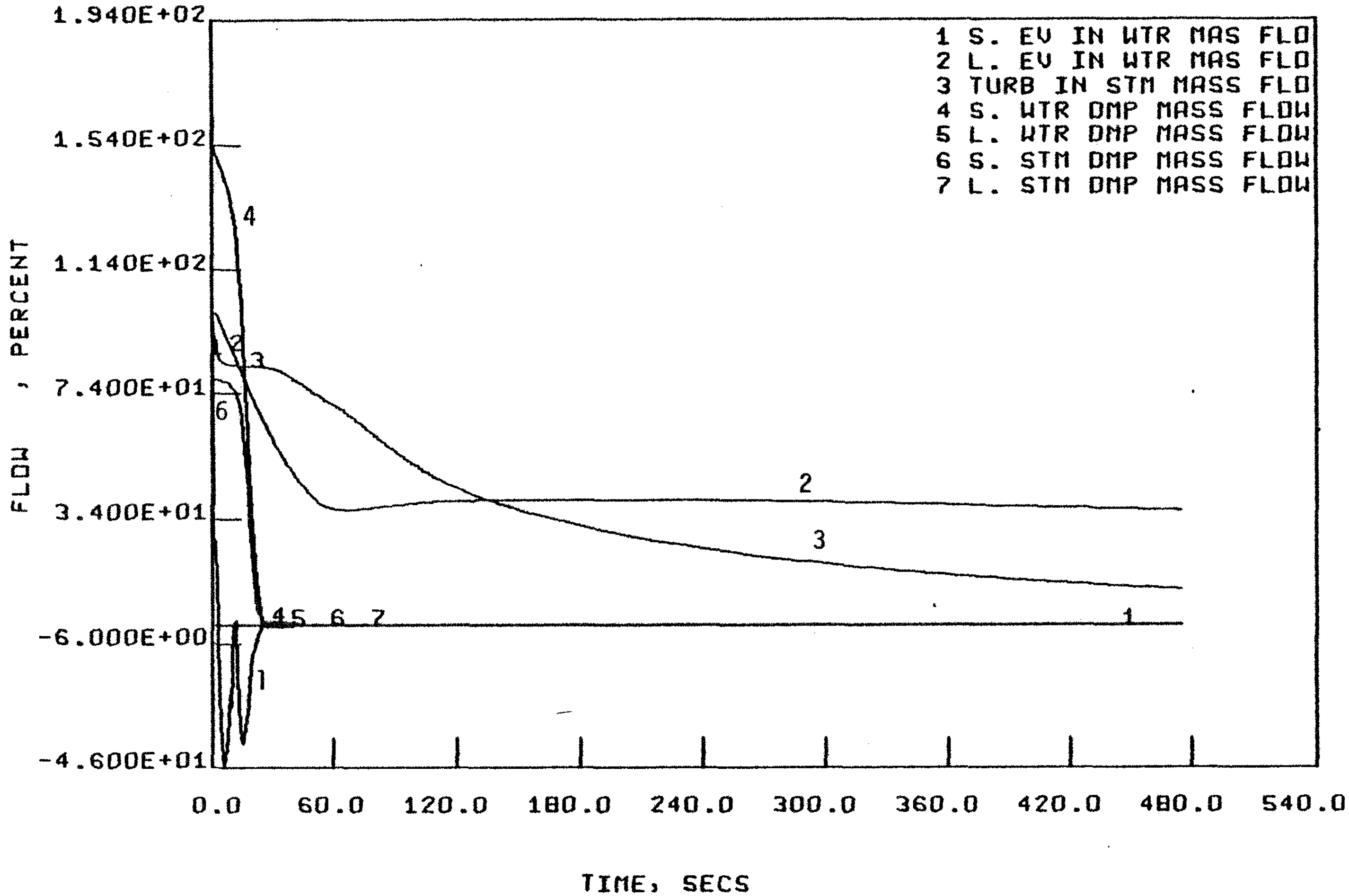

FIGURE 5-45

POOL REACTOR ISOLATION AND BLOWDOWN OF ONE STEAM GENERATOR
RUN DATED 11/03/78
NUMBER SUPGE00

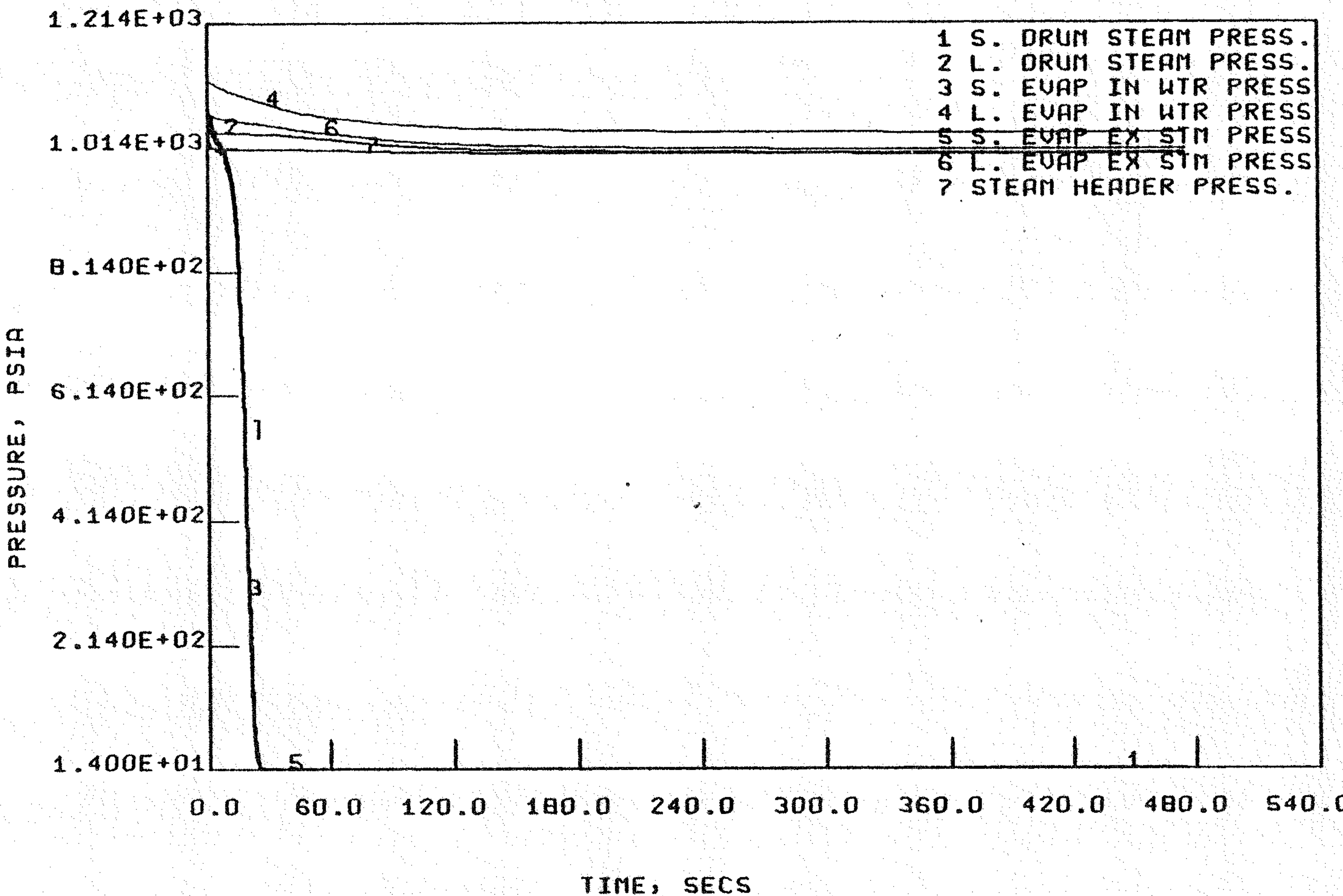

FIGURE 5-46

POOL REACTOR ISOLATION AND BLOWDOWN OF ONE STEAM GENERATOR

RUN DATED 11/03/78

NUMBER SUPGE00

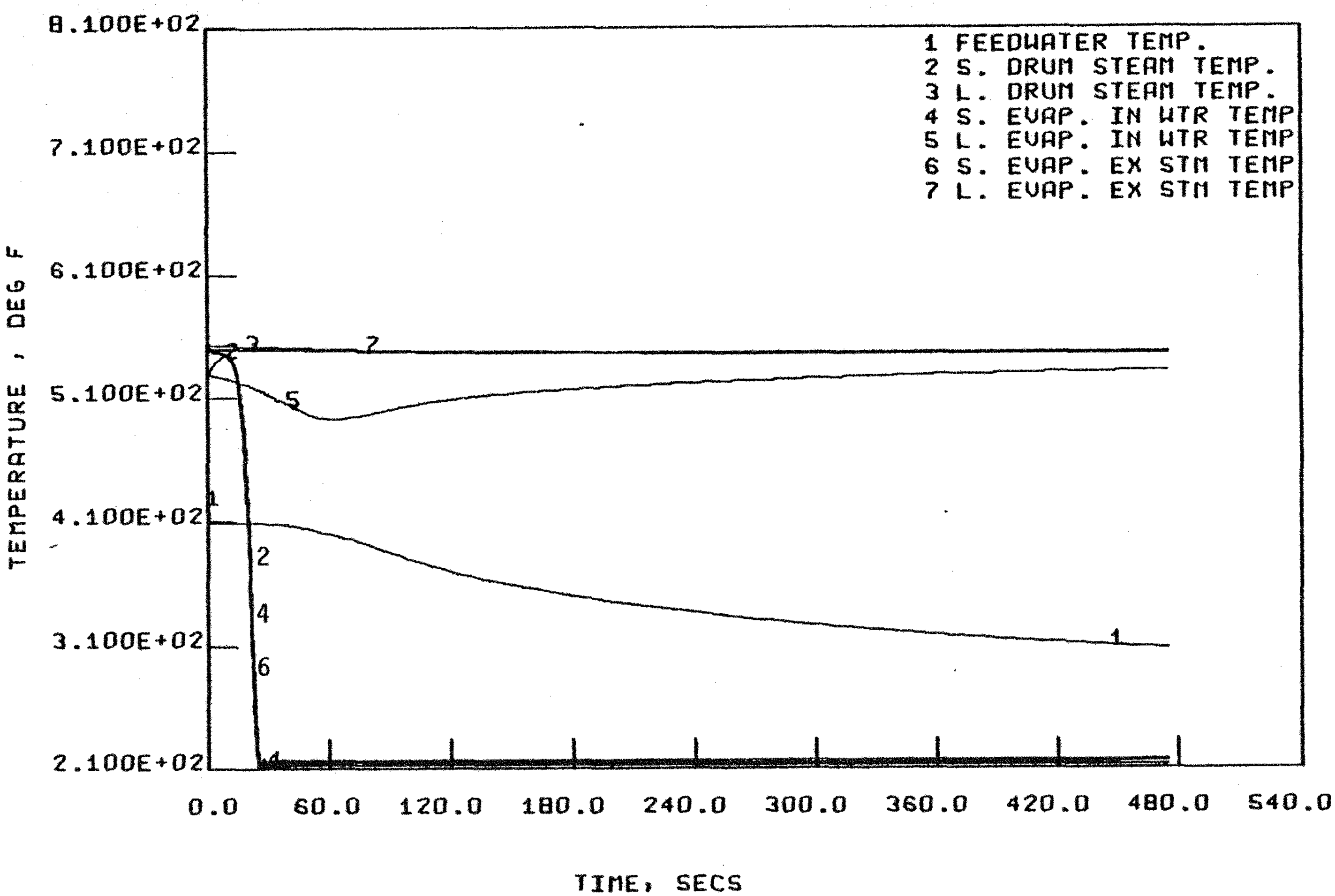

FIGURE 5-47

POOL REACTOR ISOLATION AND BLOWDOWN OF ONE STEAM GENERATOR
RUN DATED 11/03/78
NUMBER SUPGEOO

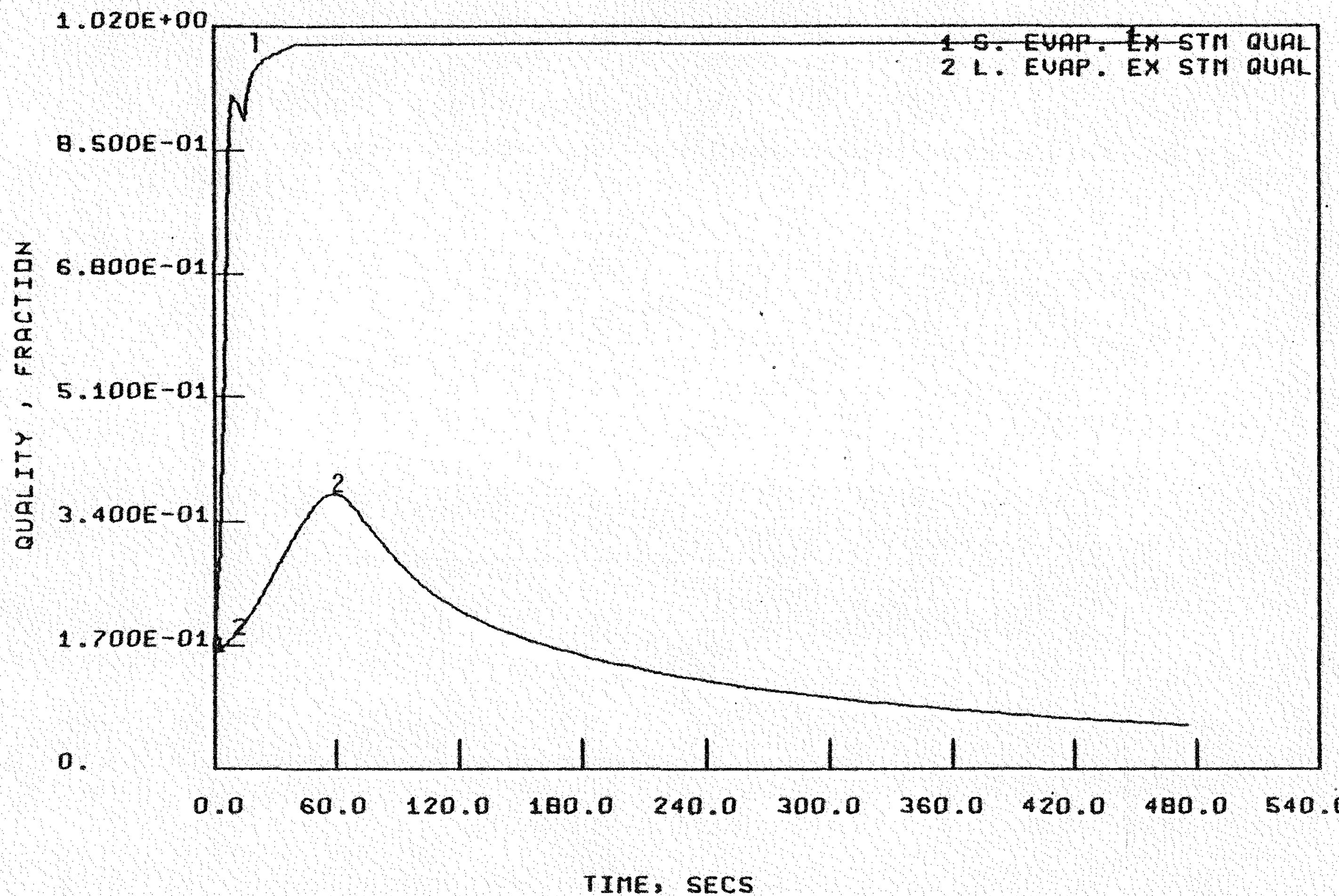

FIGURE 5-48

POOL REACTOR ISOLATION AND BLOWDOWN OF ONE STEAM GENERATOR
RUN DATED 11/03/78
NUMBER SUPGE00

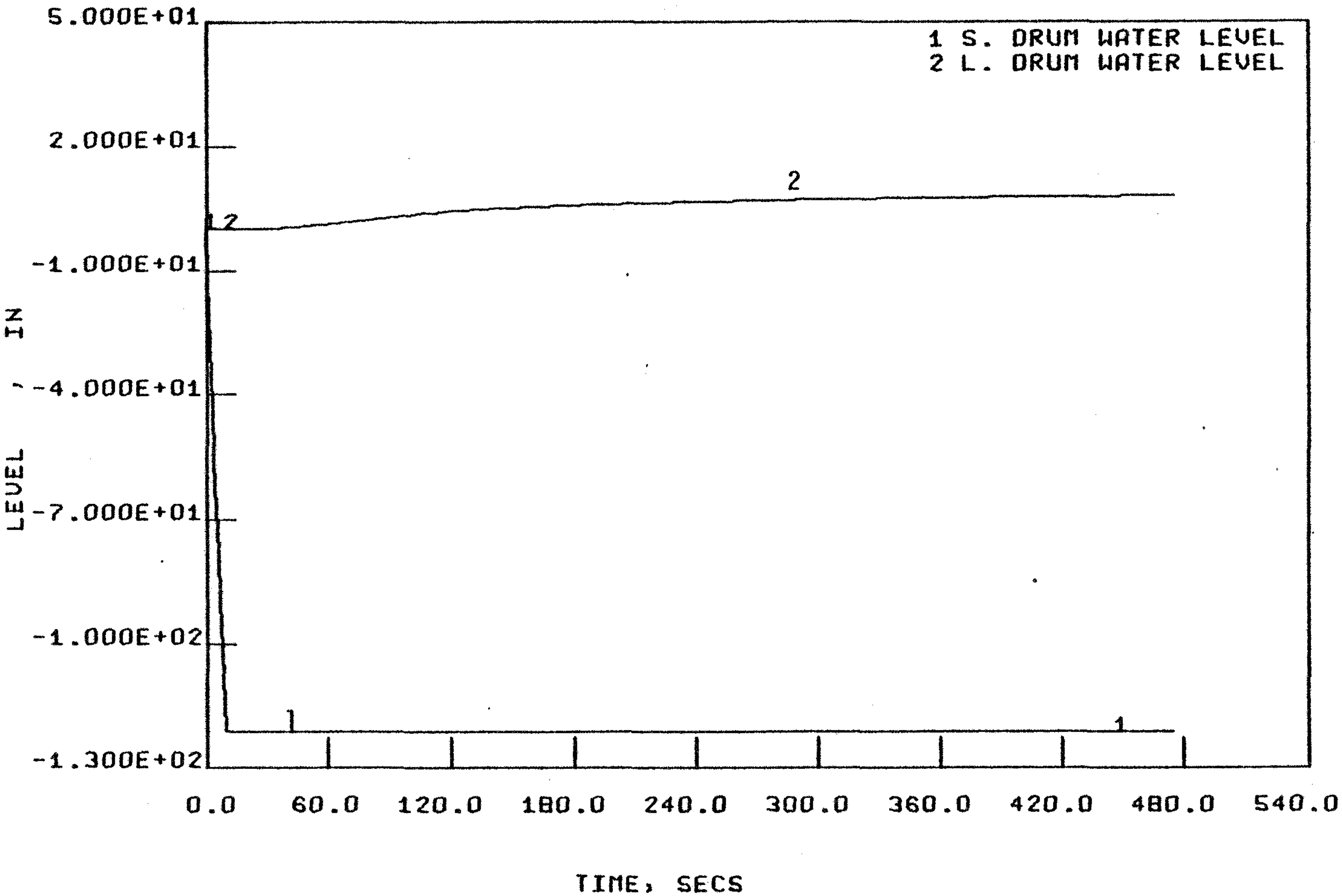

FIGURE 5-49
REACTOR LOSS OF OFF-SITE POWER WITH MINIMUM DECAY HEAT
RUN DATED 11/02/78
NUMBER PAPGE03

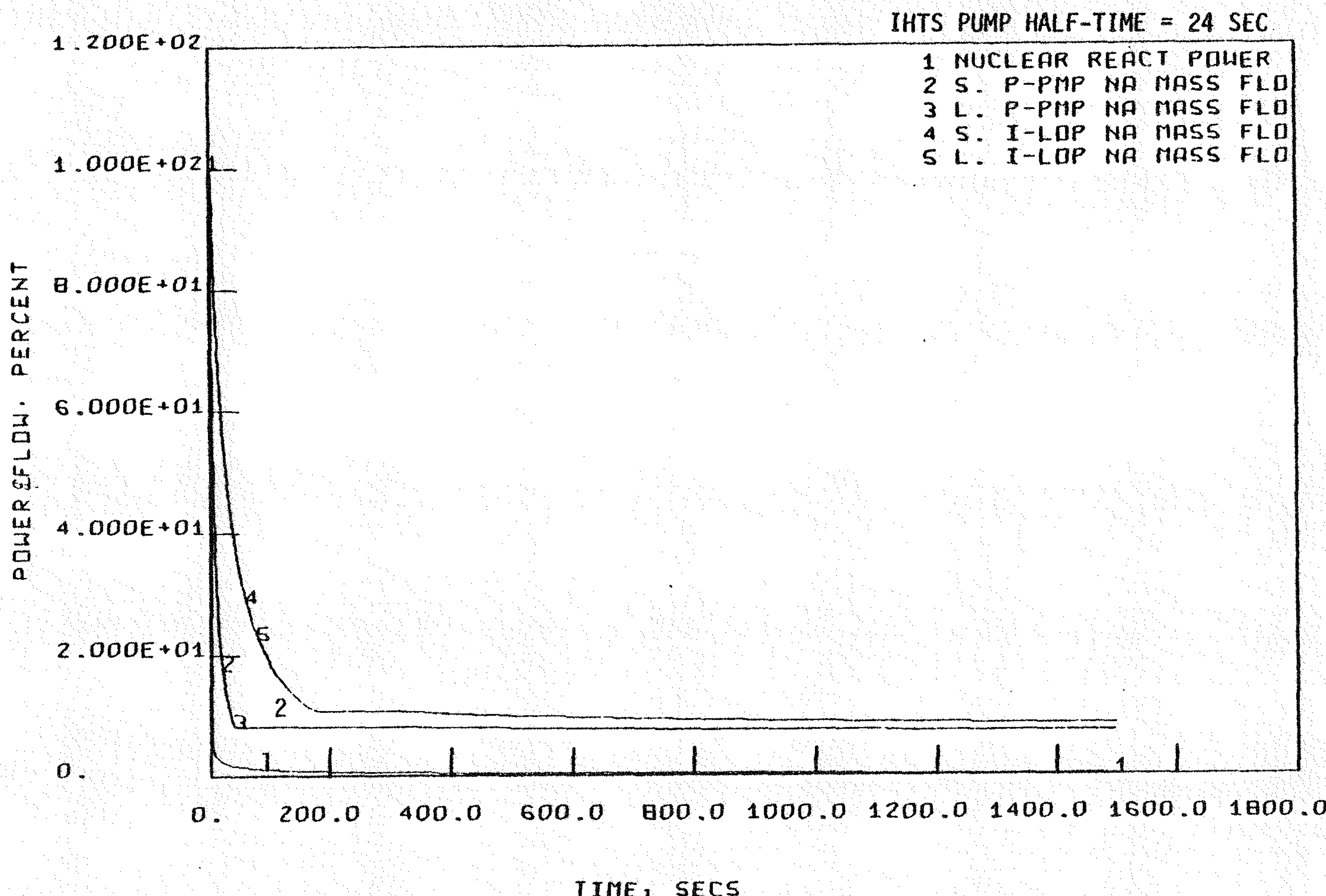

FIGURE 5-50

REACTOR LOSS OF OFF-SITE POWER WITH MINIMUM DECAY HEAT
RUN DATED 11/02/78
NUMBER PAPDE03

IHTS PUMP HALF-TIME = 24 SEC

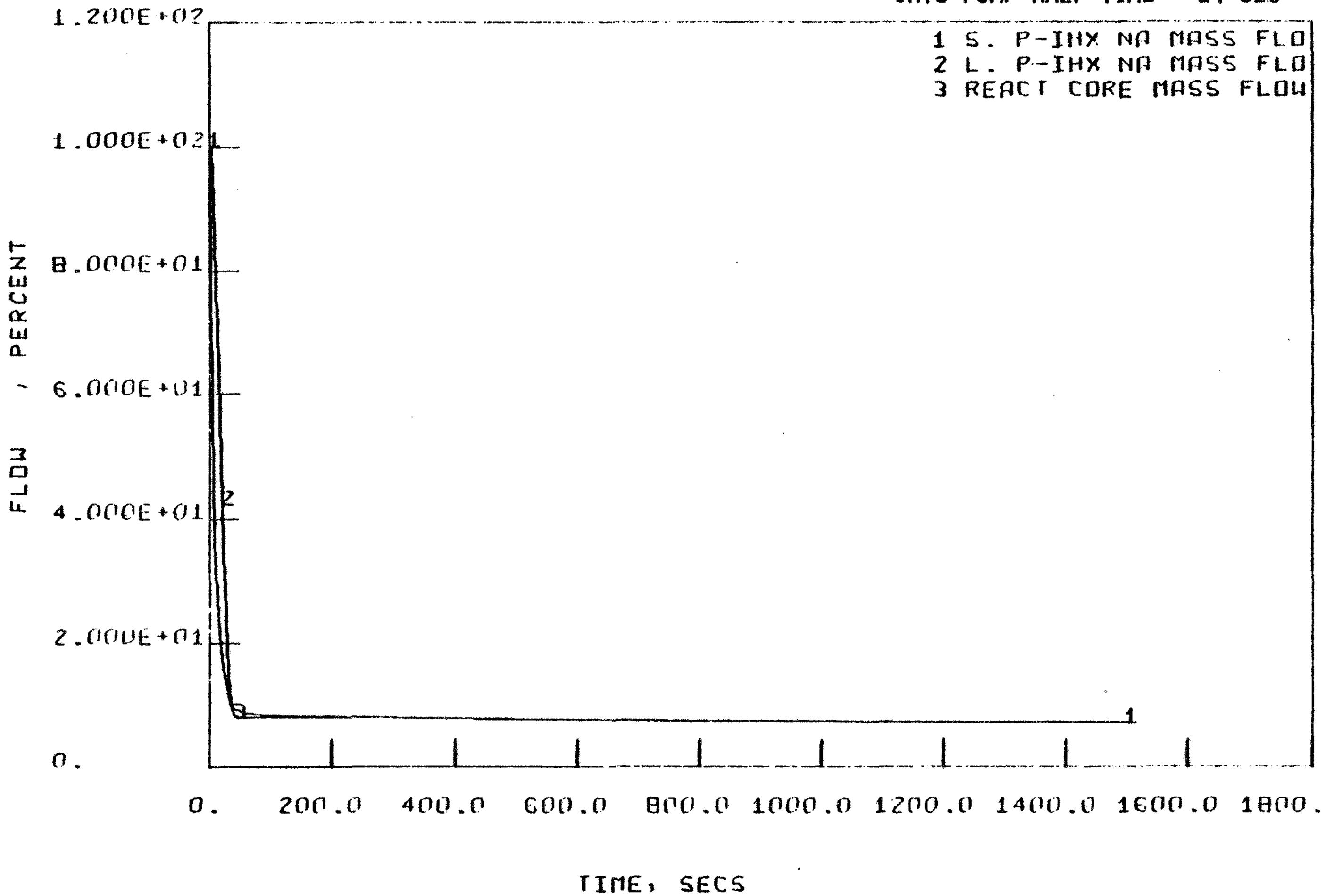

FIGURE 5-51
REACTOR LOSS OF OFF-SITE POWER WITH MINIMUM DECAY HEAT
RUN DATED 11/02/78
NUMBER PAPGE03

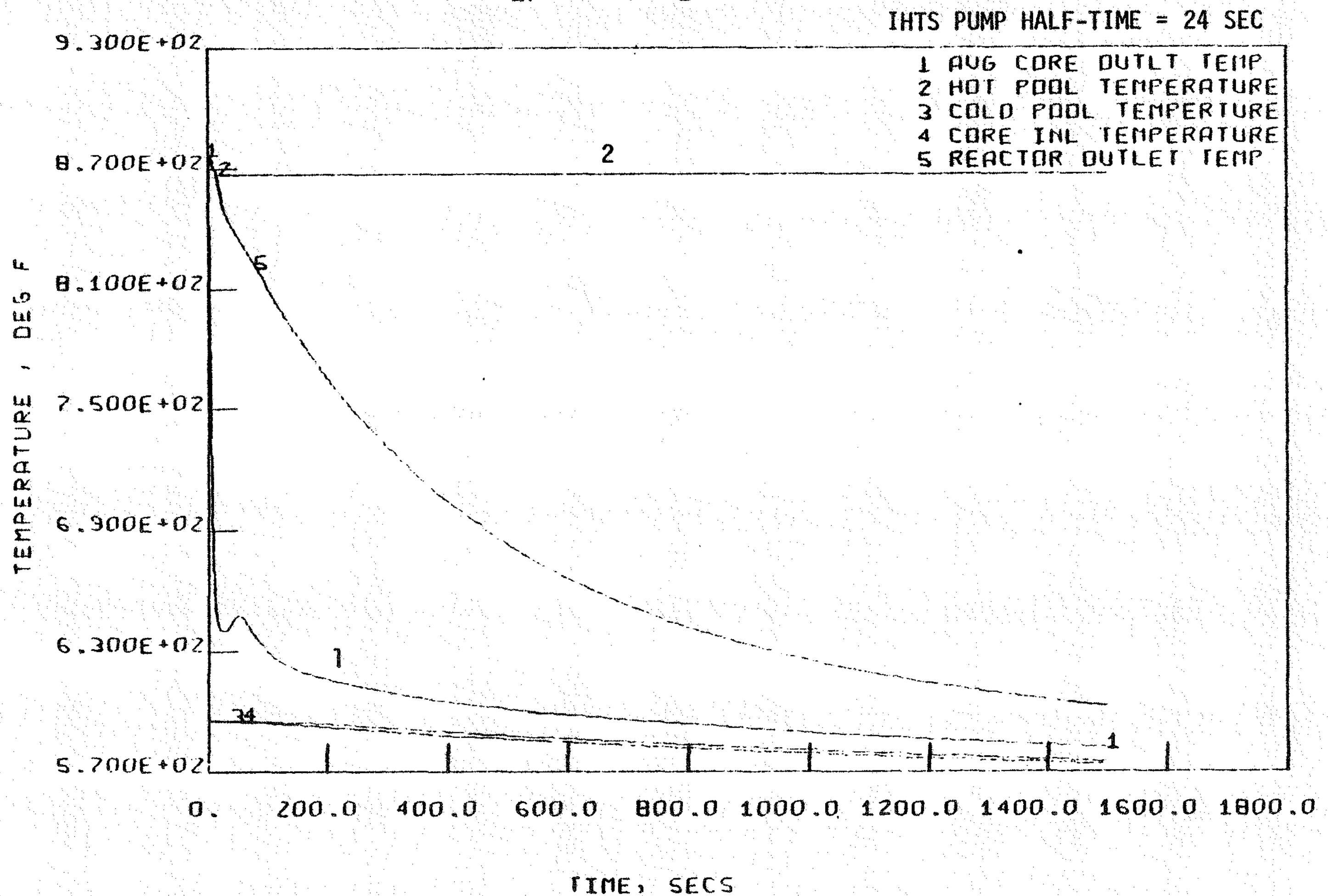

FIGURE 5-52

REACTOR LOSS OF OFF-SITE POWER WITH MINIMUM DECAY HEAT
RUN DATED 11/02/78
NUMBER PAPGE03

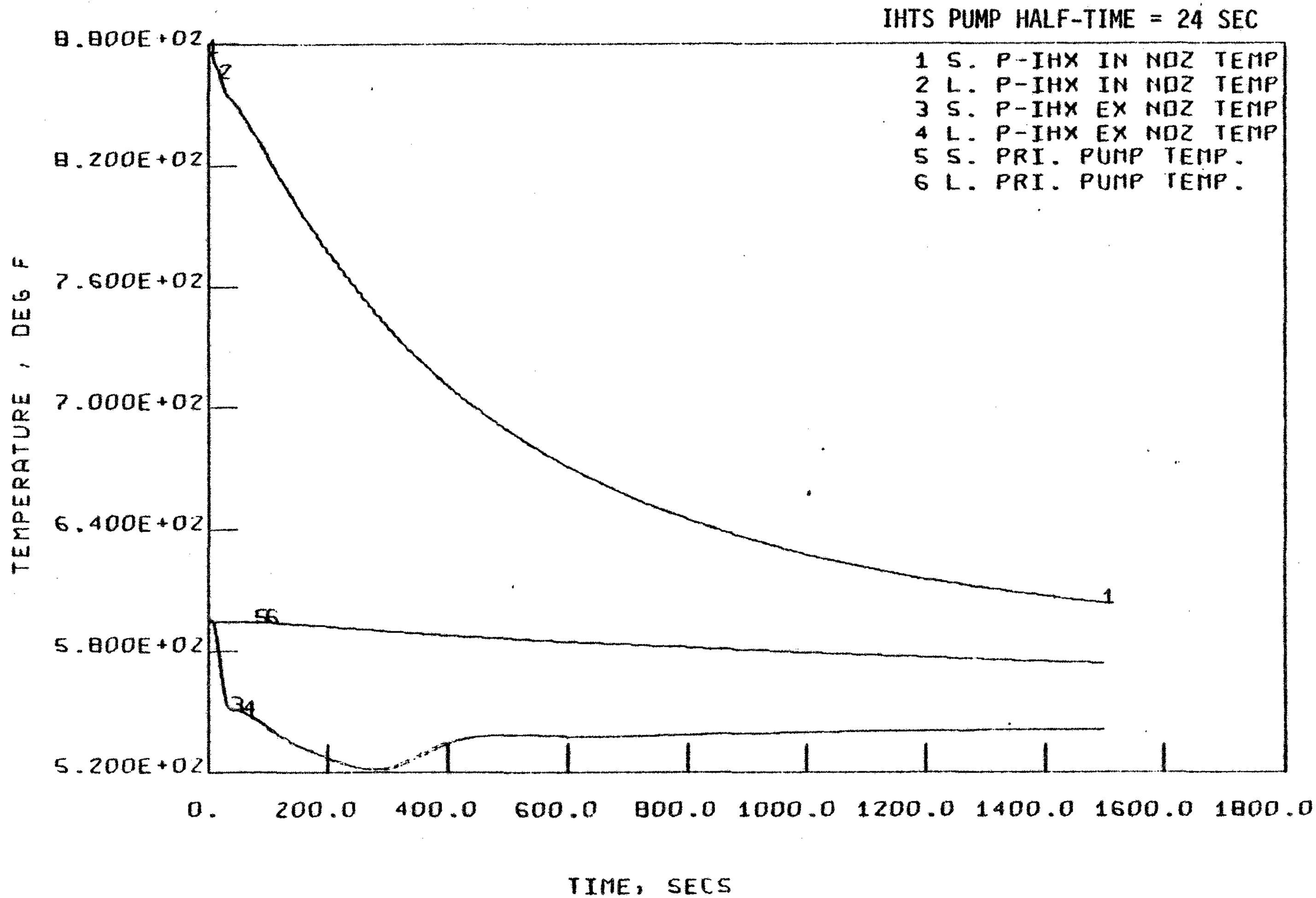

FIGURE 5-53

REACTOR LOSS OF OFF-SITE POWER WITH MINIMUM DECAY HEAT
RUN DATED 11/02/78
NUMBER PAPGE03

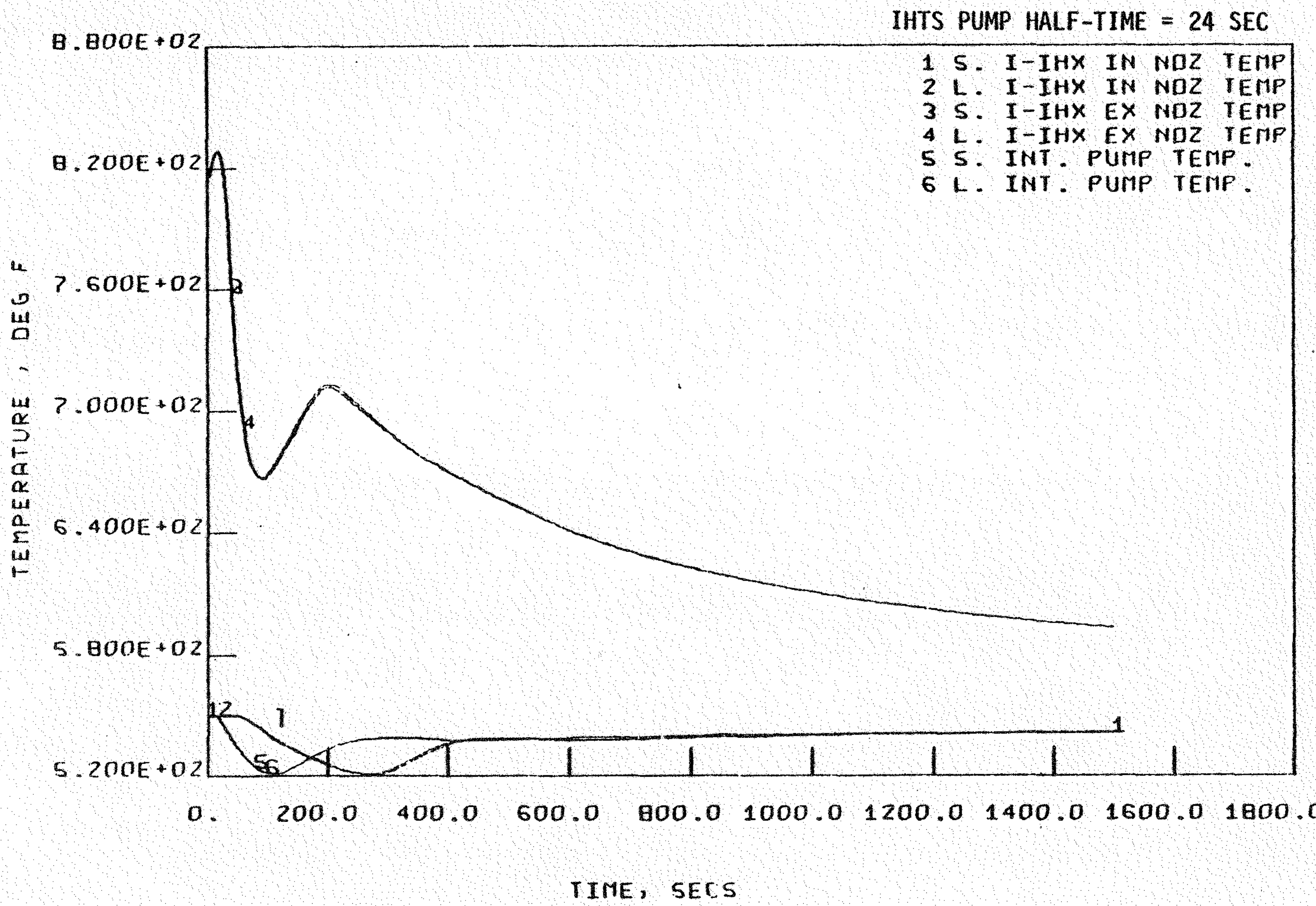

FIGURE 5-54

REACTOR LOSS OF OFF-SITE POWER WITH MINIMUM DECAY HEAT
RUN DATED 11/02/78
NUMBER PAPGE03

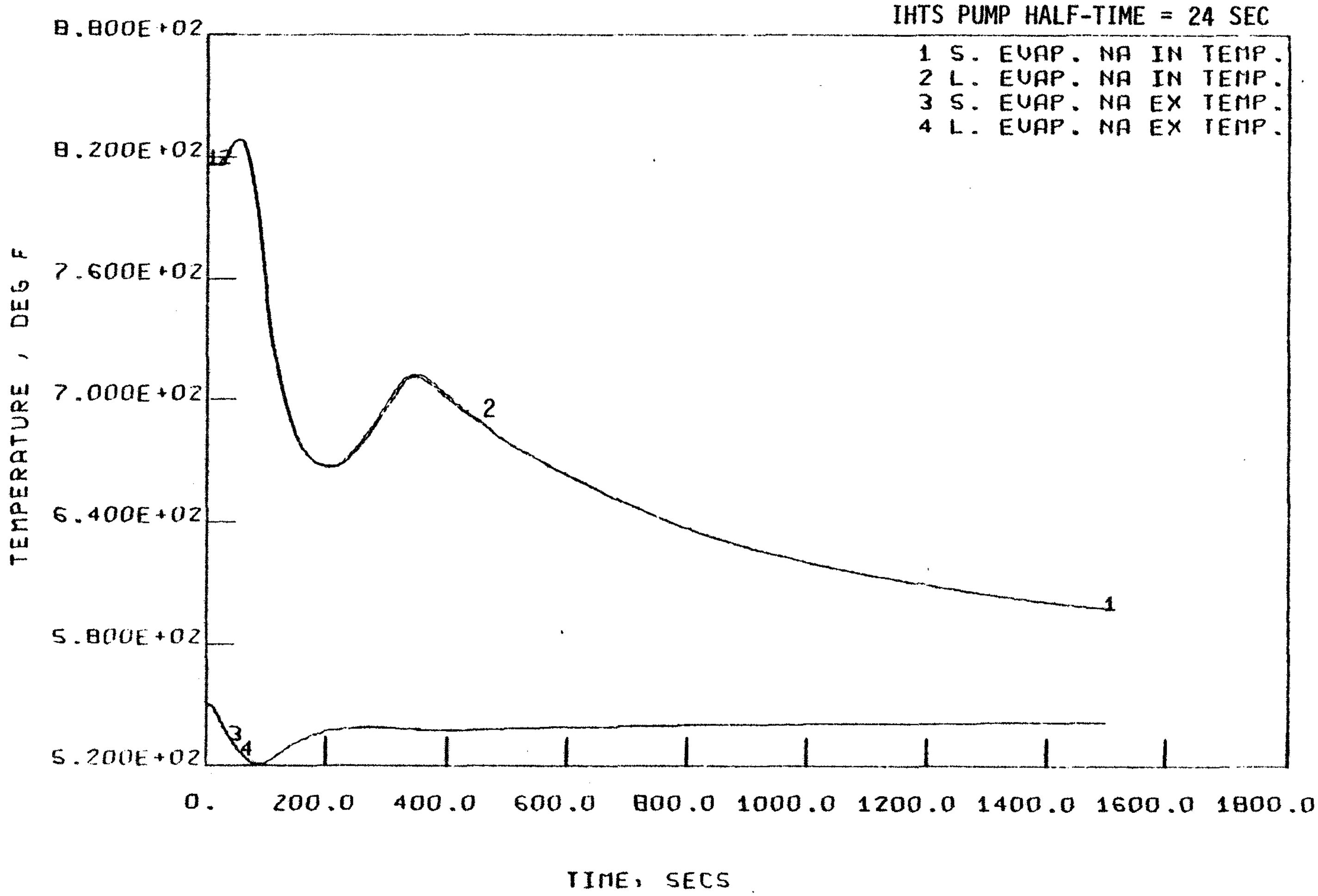

FIGURE 5-55

REACTOR LOSS OF OFF-SITE POWER WITH MINIMUM DECAY HEAT
RUN DATED 11/02/78
NUMBER PAPGE03

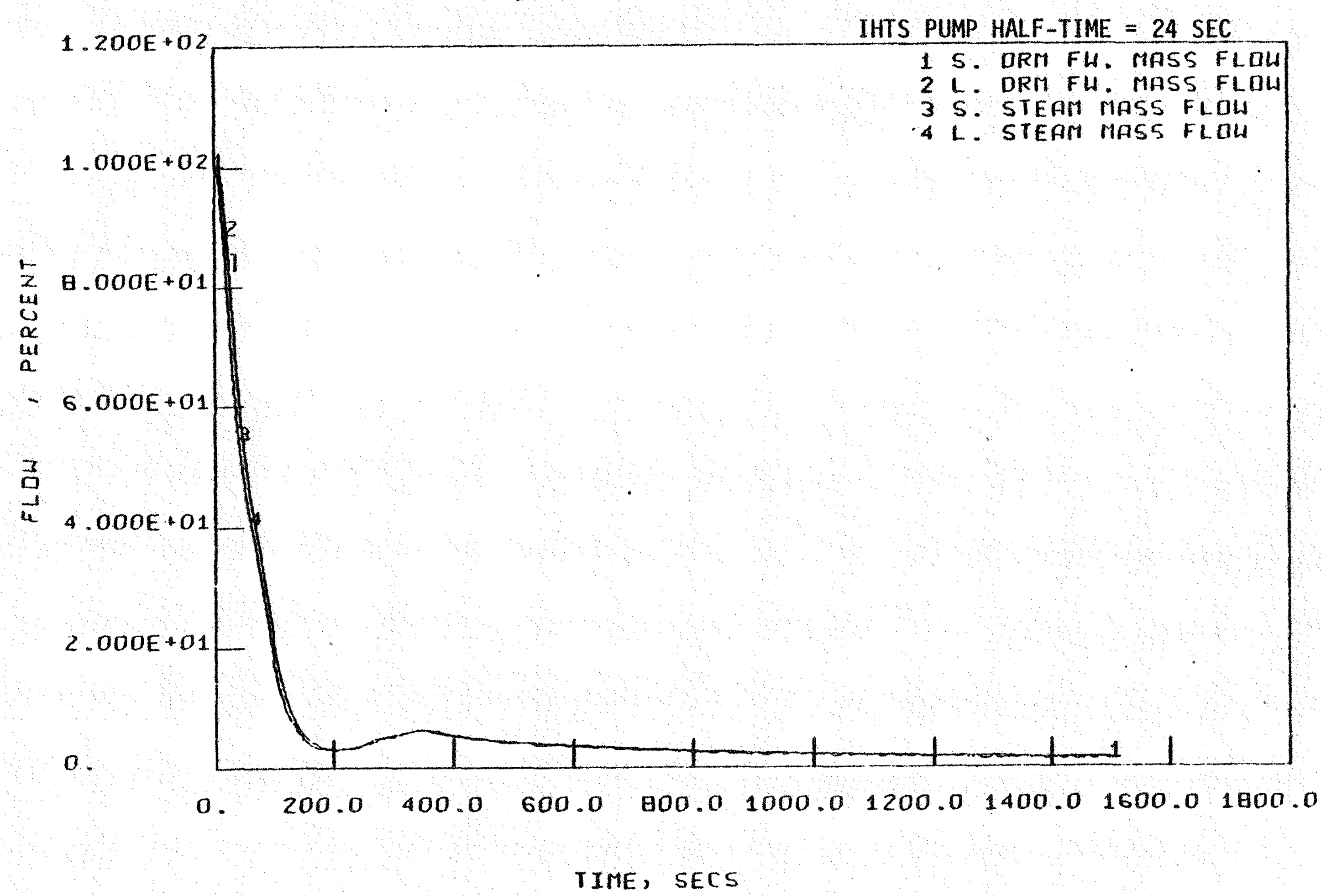

FIGURE 5-56

REACTOR LOSS OF OFF-SITE POWER WITH MINIMUM DECAY HEAT
RUN DATED 11/02/78
NUMBER PAPGE03

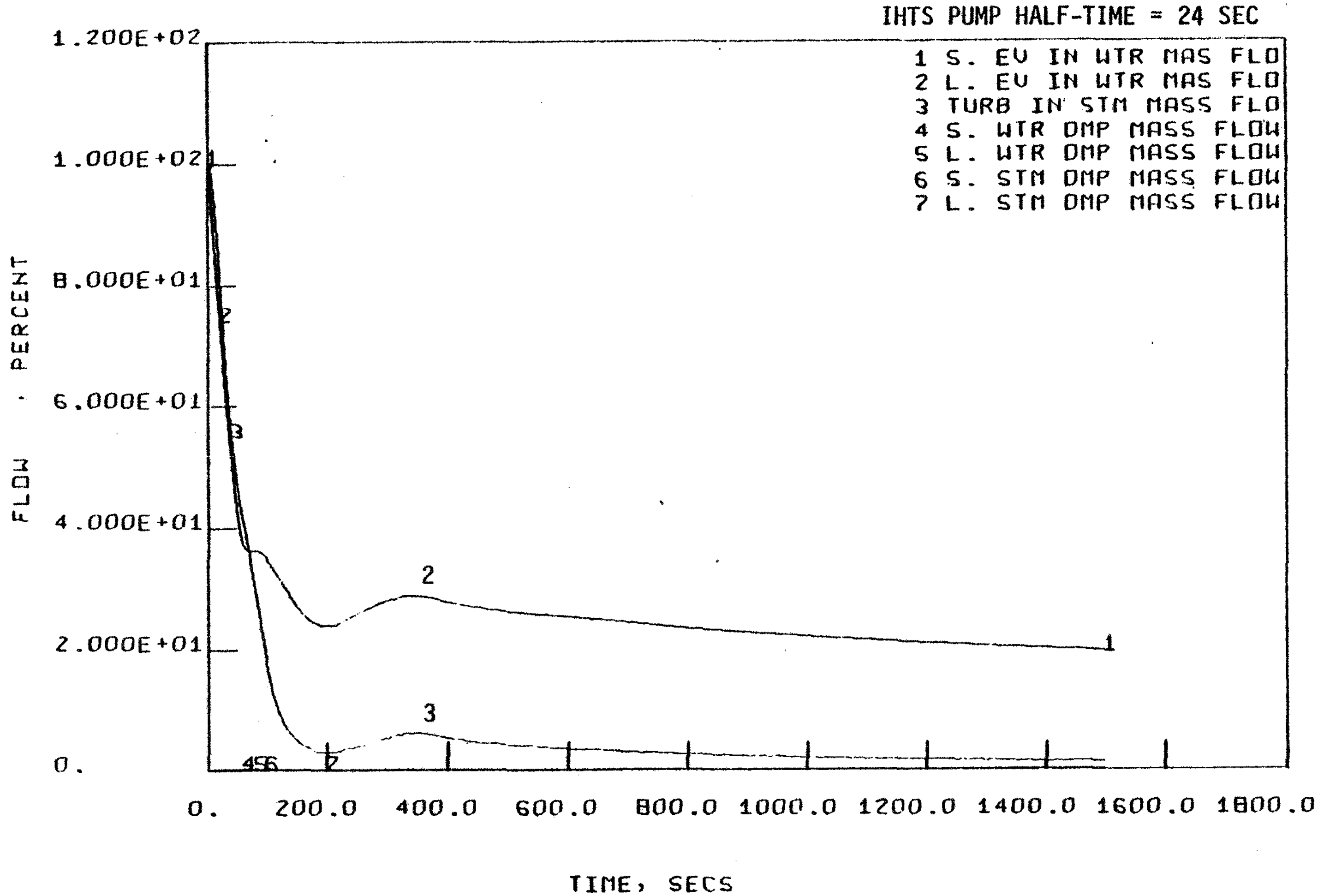

FIGURE 5-57
REACTOR LOSS OF OFF-SITE POWER WITH MINIMUM DECAY HEAT
RUN DATED 11/02/78
NUMBER PAPGE03

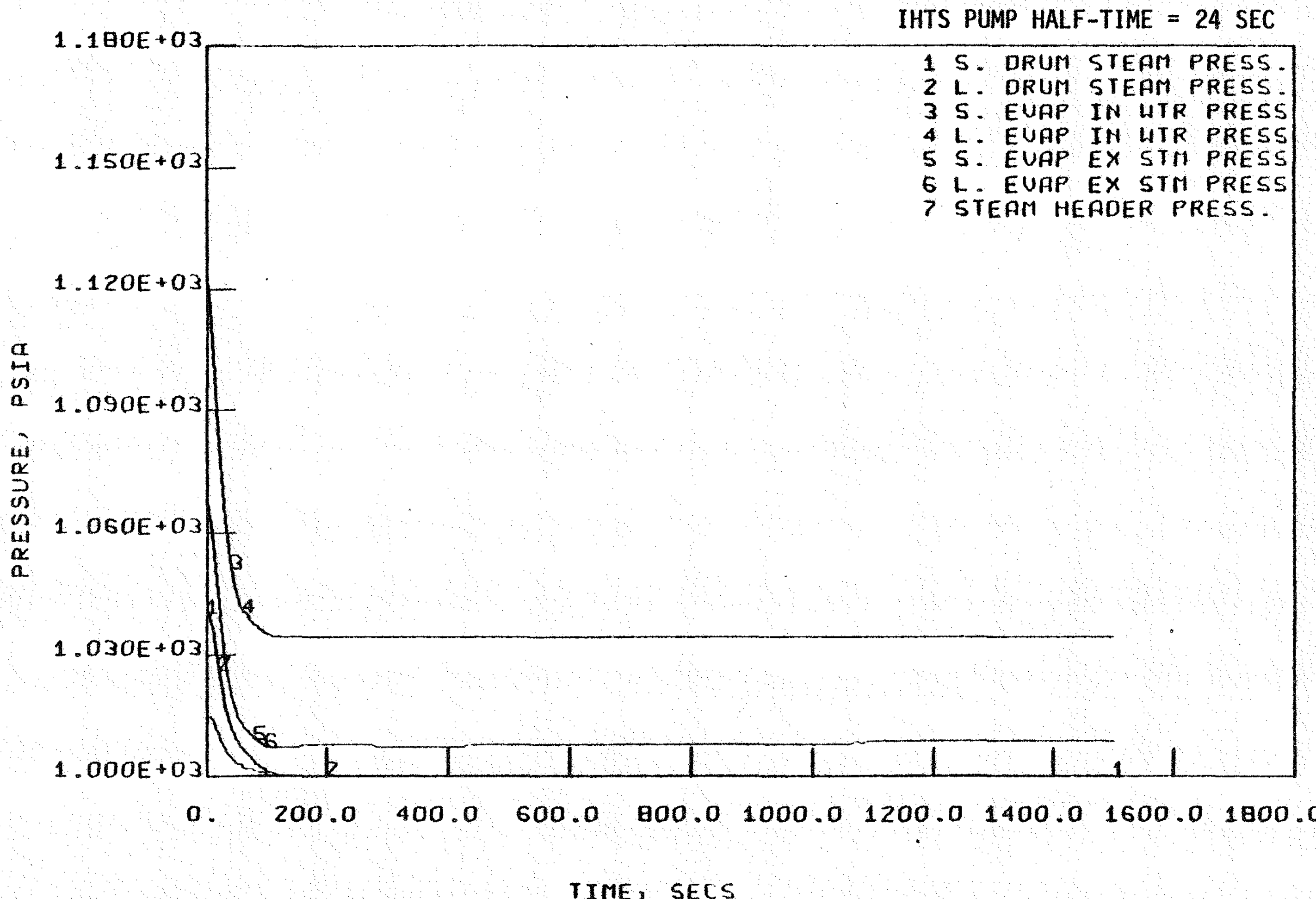

FIGURE 5-58
REACTOR LOSS OF OFF-SITE POWER WITH MINIMUM DECAY HEAT
RUN DATED 11/02/78
NUMBER PAPGE03

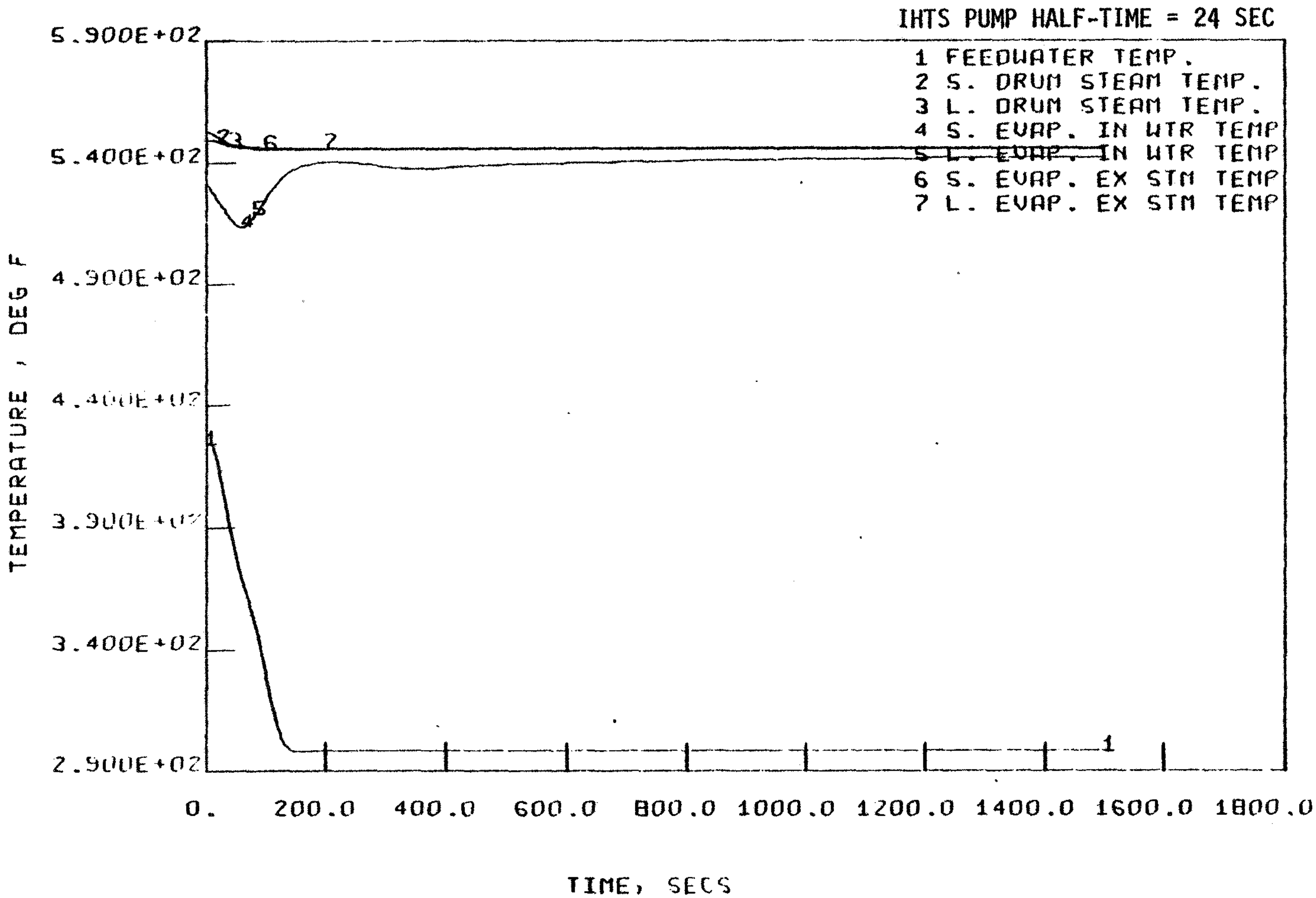

FIGURE 5-59

REACTOR LOSS OF OFF-SITE POWER WITH MINIMUM DECAY HEAT

RUN DATED 11/02/78

NUMBER PAPGE03

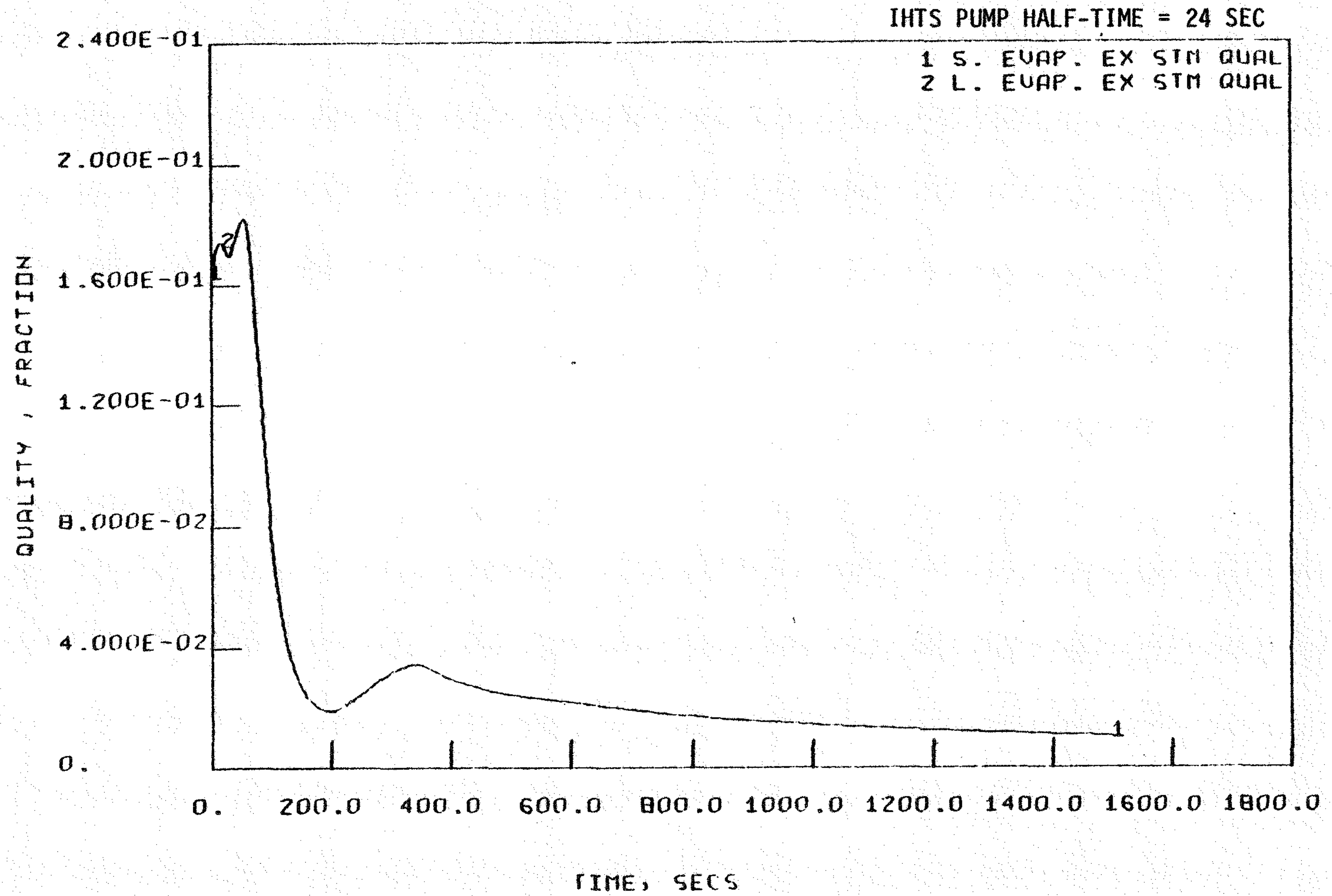

FIGURE 5-60
REACTOR LOSS OF OFF-SITE POWER WITH MINIMUM DECAY HEAT
RUN DATED 11/02/78
NUMBER PAPGE03

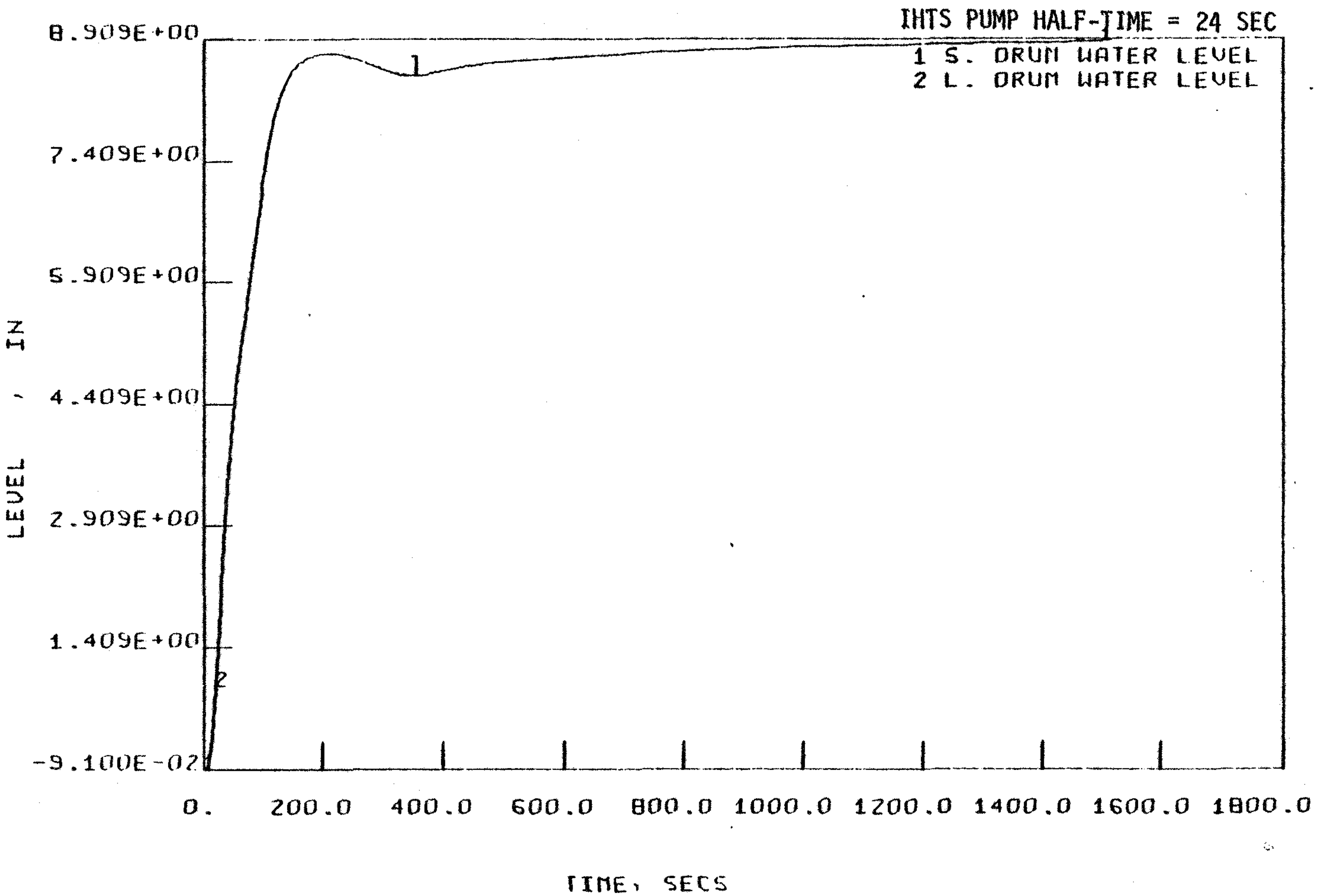

Part V: Heat Transport Systems

Section 2: Work Performed During Extension 2

Subsection 2.4: Fixed Speed Pump Effects

CONTENTS

TABLES

FIGURES

1. INTRODUCTION AND SUMMARY

The combination of a saturated steam cycle and a pool-type LMFBR offers the possibility of a plant control scheme using constant speed pumps. The saturated steam cycle allows part-load operation at low reactor outlet temperature, and the pool configuration does not require balanced primary pump flow to equalize the thermal load of the IHX's. The feasibility and practicality of using constant speed pumps for the EPRI pool design are discussed in this subsection.

Constant speed pump systems are less expensive and more reliable than variable speed pump systems. In general, constant speed pumps do not impose major component design changes or plant cperational limitations, although they do not provide the range of operating flexibility that may be an important requirement for a first-of-a-kind plant. Within the range of component design uncertainties, the actual full load plant temperatures are within the established design limits. Under part-load operations, constant speed pumps result in reduced load change rate to minimize core thermal transients. As compared to variable speed pumps, constant speed pumps do not impose additional risk to plant operation or penalize the plant operation or penalize the plant energy availability due to components out of service. Nevertheless, analysis of operation with one primary pump out of service suggests that the NPSH designed into the pumps should be increased. The pump runout characteristics also require three primary pumps be started simultaneously.

The conclusions of this study are as follows:

1. It is feasible to use constant speed pumps for the pool-type LMFBR.
2. The use of constant speed pumps will have little adverse effect on other component designs.
3. Since the actual plant temperatures under normal plant operation are likely to be lower than the design conditions, the use of constant speed pumps will not affect the safe operation of the plant.
4. Part load operation should be accomplished with a lower power change rate to minimize plant temperature transients. The capabilities of the constant speed and the variable speed pump system are similar with respect to most transient conditions.
5. With the Phase A pump design, pump NPSH is the limiting factor for constant speed pump operation with one primary pump out of service.

6. Power output levels for constant speed pump operation with components out of service are essentially the same as those for variable speed pump operation.

However, considering the EPRI-pool design as a first-of-a-kind LMFBR, EPRI has chosen to retain the variable speed pump concept as the reference design, and consider the constant speed pump as an alternate option. Pump design changes and pump impeller elevation in the reactor vessel are now being explored to improve pump NPSH characteristics. (See Appendix VB)

2. APPROACH

A systemmatic approach shown in Table 2-1 was used to identify cause-effect relationships between component designs and plant conditions in constant speed pump operation. Analyses were then planned and performed to determine the plant operation effects.

A computer code PARTCON was developed for the parametric study. The analysis basically consists of two parts. The first part is a component design sensitivity analysis which calculates the plant conditions under various component design conditions and design uncertainties. The second part is a plant performance analysis under part load operation and with components out of service. The results of the study are presented in Appendix A.

TABLE 2-1

Constant Speed Pump Effect Matrix*

Variable / Design	Flow			Plant Temperature						Pool Level	
	PHTS	IHTS	RFW	T_{PH}	T_{PC}	T_{IH}	T_{IC}	T_{WH}	T_{WC}	Hot Pool	Cold Pool
IHX ΔP_{pri}	X	–	–	X	X	–	–	–	–	X	X
Core ΔP_{pri}	X	–	–	X	X	–	–	–	–	X	X
IHX H.T.*** Coeff.	–	–	–	X	X	–	–	–	–	–	–
Pump NPSH	X	–	–	–	–	–	–	–	–	–	X
Pri. Pump Speed	X	–	–	X	X	–	–	–	–	X	X
IHX ΔP_{int}	–	X	–	X	X	X	X	–	–	–	–
SG ΔP_{int}	–	X	–	X	X	X	X	X	X	–	–
SG H.T.*** Coeff.	–	–	–	X	X	X	X	X	X	–	–
SG ΔP_{fw}	–	–	X	–	–	–	–	X	X	–	–
(N-1)** Loop	X	–	–	X	X	X	X	–	–	X	X
(N-2)**** Loop	X	–	–	X	X	X	X	–	–	X	X
(N-1)** Pump	X	–	–	X	X	X	X	–	–	X	X
Core Power	–	–	–	X	X	X	X	–	–	–	–
Startup	X	–	–	–	–	–	–	–	–	–	–

* X possible cause-effect relationship.

** (N-1): one IHTS loop or one primary pump out of service.

*** Heat transfer coefficient is a junction of the coolant flows in the tube side and the shell side dictated by component design. For normal constant speed pump operation, circuit flow is affected only by head change.

**** (N-2) loop: two IHTS loops out of service.

3. CONSTANT SPEED PUMP DRIVE ALTERNATES

Both single speed and two speed drives may be considered for a pool-type LMFBR plant. They impose similar constraints on plant starting and load changing. Upset transients following a scram appear to be more severe for a single speed drive than for a two speed drive. See Part V, Subsection 2.3 for details of plant thermal transients. Nevertheless single speed drives are still attractive if sufficient steam by-pass capacity is provided to reduce the number of scrams resulting from turbine trips.

Except for starting the pump drives, plant startup procedure is similar to that for the variable speed drives. Because the discharge flow of the primary pumps passes through a common reactor core hydraulic impedance, the flow for a pump increases when one or more pumps are not available for service. The pump runout characteristics require that three pumps must be running to assure operation without cavitation.

As an alternate to starting three pumps simultaneously, it is possible to design a position controlled valve instead of an isolation valve on the current pump assembly. This valve could be partially closed when starting each pump one at a time to prevent pump runout. Large throttling valves for the BWR recirculation loops have been designed but they have presented some challenging vibration problems. However, it would be easier to cope with these problems if the valves were mainly used for throttling only during the startup. The vibration could be a more serious problem than load impulses on the deck structure due to starting three pumps concurrently. In practice, auto-transformers would be used to prevent full voltage starting and minimize load impulses on the deck structure.

Consequently, common feeders and starters of the primary pump motors must be sized for synchronized starting of any three primary pumps simultaneously. The requirements for starting two speed motors are similar to those for single speed drives. The main difference is that the reduced speed state may be used in lieu of auto transformer starting. Pump motors may be started sequentially from pony motor speed to the intermediate speed (about 50% full speed). To avoid cavitation the speed of three pumps must increase simultaneously from the intermediate speed to full speed. This is true even if all four pumps are operating at intermediate speed.

When increasing or decreasing the load of a plant having constant speed pump drives, the temperature difference across the reactor and heat exchanger components also increase or decrease. Heavy structures such as heat exchanger nozzles and tubesheets, and the reactor support structure are subject to considerable internal stresses if the temperature of the sodium that wets their surface is changing too fast. CRBRP is being designed to accommodate a power change of 3% per minute maximum which in the present design requires that the primary sodium temperature change at about 4°F/minute.

For the large commercial LMFBR, it is proposed to limit the rate of change in temperature to about 3°F/minute. For constant speed pump operation, core outlet temperature is proportional to power and the corresponding power change rate will be about 1%/minute.

A more detailed treatment of constant speed pump drive systems is given in Part VII, Subsection 2.1.

4. COST COMPARISON OF SOME PUMP DRIVE SYSTEMS

Table 4-1 shows the estimated cost of five different pump drive systems. These systems are arranged sequentially from the lowest cost system to the highest cost system. The first column identifies the drive systems. The total estimated cost shown in column 5 consists of the cost of the drive motor and all auxiliaries (column 2), the power supplies, controls and their installation (column 3), and the building space for the power supplies and controls (column 4). Building space cost is based upon $200/ft^2. Estimated cost data are for 16 pump drives.

It is apparent that the single speed drives offer a savings over the rectifier-inverter variable speed drives of about 17 million dollars. Two speed systems also offer a savings of 11 to 13 million dollars over the variable speed drive system. The liquid rheostat, variable speed drive system offers a savings of about 5 million dollars over the rectifier-inverter system but it has several deficiencies if it were used for the primary pump drives. These deficiencies and the pump characteristics are discussed in detail in Part VII, Subsection 2.1.

TABLE 4-1

Cost Comparison of Pump Motor Drive Systems*

Type of Drive	Motor & Auxiliaries Cost	Power Supply, Controls & Installation Cost	Building Cost	Estimated Total Cost
Single Speed Induction Motor	9000K	1500K	320K ($1600\ ft^2$)	10820K
Two Speed Drive Single Winding	9000K	5100K	800K ($4000\ ft^2$)	14900K
Two Speed Drive Two Winding	14000K	2000K	500K ($2500\ ft^2$)	16500K
Liquid Rheostat Variable Speed Drive	14800K	6000K	1600K ($4000\ ft^2$)	22400K
Rectifier-Inverter Variable Speed Drive	9600K	16200K	2400K ($12000\ ft^2$)	28200K

*K refers to thousands of dollars.

The estimated cost data in this table are for 16 pump drive systems, 4 primary pump drives, 6 intermediate pump drives, and 6 steam generator recirculation pump drives. Drive systems data and more detail cost breakdown is given in Part VII,Subsection 2.1.

5. COMPONENT DESIGN SENSITIVITY UNDER FULL LOAD OPERATION

Without variable pump speed control capability, plant temperatures become a function of the system pressure drops and the heat exchanger performance. At full load with four primary pump and six IHTS loops, the actual plant temperatures will be lower than the design limits provided that the pumps are designed with margins. For instance, if the design pump head margin is 17%, the hot pool temperature which is the most critical and limiting condition for plant operation will not exceed the designed 875°F even if pressure drop in the primary loops, intermediate loops and feedwater loops are 30% underestimated.

Similarly, for the present IHXs and steam generator designs, a 25% reduction in heat transfer performance (H.T. Area or H.T. coefficient) should not adversely affect the overall plant conditions. Figure 5-1 shows the combined effects of the system pressure drops and heat exchanger performance on core outlet temperature at a steady state full power condition. The expected core outlet temperature is about 850°F and it is very unlikely that the temperature would exceed the design 875°F even with pessimistic assumptions.

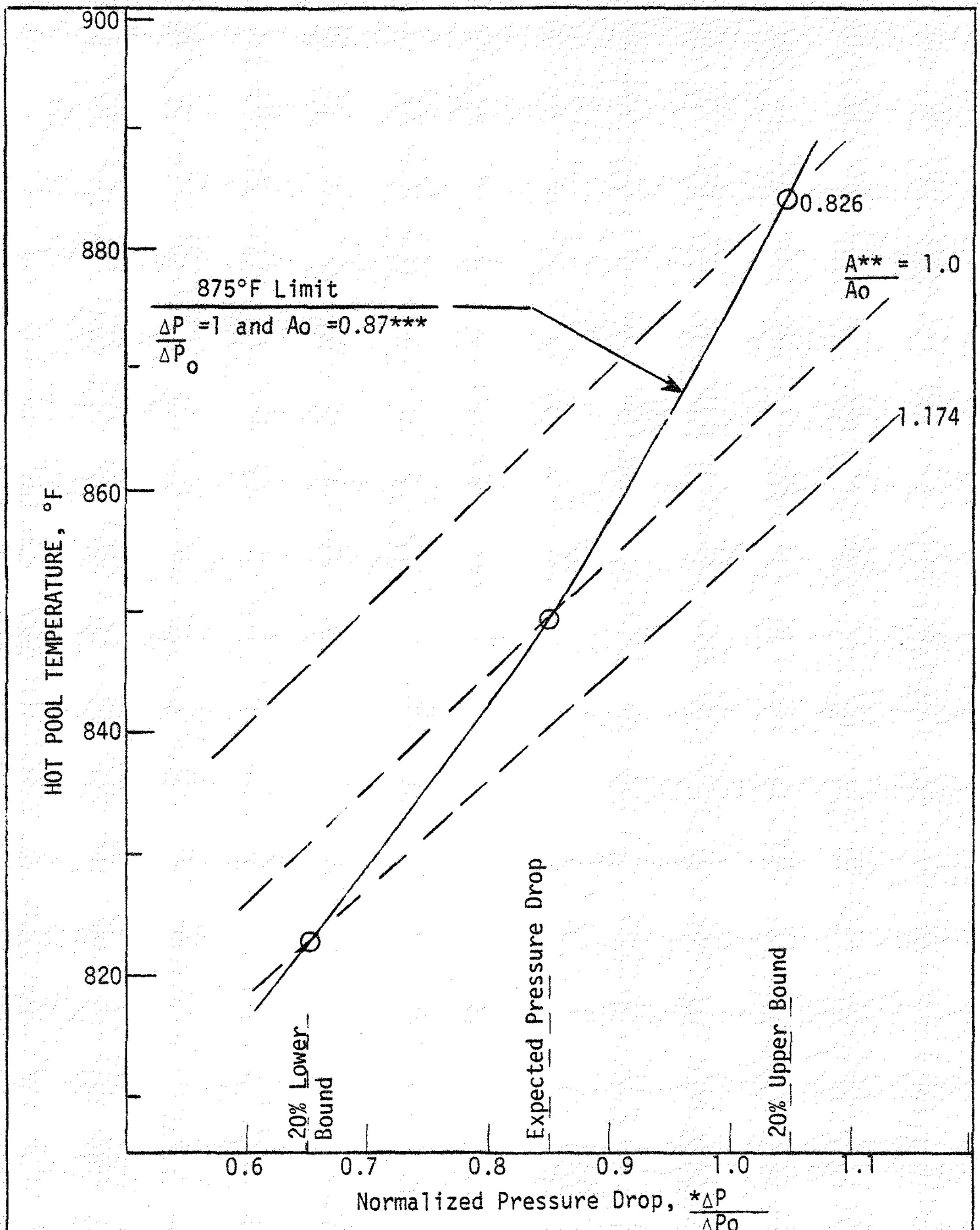

*For the primary, intermediation and recirculation loops.
**Heat Transfer Performance (H.T. Area and H.T. Coefficient) of IHX's and Steam Generators.

$***\frac{A}{Ao} = \frac{100\%}{115\%} = 0.87$

FIGURE 5-1 EFFECTS OF COMPONENT ΔP AND HEAT TRANSFER PERFORMANCE

6. PLANT CONTROL UNDER PART LOAD OPERATION

With constant speed pump operation and high feedwater recirculation (6 to 1 ratio) in the steam generators, the primary and the intermediate sodium cold leg temperature will be very stable. Consequently, the core outlet temperature and the intermediate hot leg temperature are proportional to the core power. Between 60% and full load change the resulting core temperature swing is about 130°F which is considerably greater than the 50°F swing for the variable speed pump system. One way to reduce core flow to minimize the core outlet temperature swing is to use two speed pumps. The lower speed reduces the possibility of pump cavitation and helps to minimize the core temperature swing to about 65°F.

The effects on plant operation from thermal transients are similar for the single speed and variable speed pump systems. Figure 6-1 shows the core outlet temperature at part load operation for the three systems. Between 60% and full load operation, the core temperature change is 50°F for the variable speed pump, $\sim$ 65°F for the two speed pump and 130°F for the single speed pump. The maximum load change rate for the variable speed pump is 3%/minute under normal plant operations. At this rate, the corresponding core temperature transient is 3.75°F/minute. If one assumes that the operating risk due to core thermal transients is proportional to the core step temeprature change and the temperature transient rate, then for similar degree of risk, the load change rate for the two speed and single speed pump system will be 0.9%/minute and 0.45%/minute, respectively. The difference in load change time between the single speed and the variable speed system is 1.25 hours but the difference is less than 36 minutes between the two speed and the variable speed system. For a base-load plant, the load change flexibility between the constant speed pump and the variable speed pump system is not significantly different.

During load change, core power will increase or decrease at a pre-determined rate. The plant temperature transient usually will be very low for all three pump systems. Incase of upset, faulted or emergency conditions, the reactor will scram and the pumps will remain at 100% speed, trip to 50% speed or trip to pony motor speed depending on the post-scram system chosen. However, the maximum core temperature drop is still $\sim$320°F (from 860°F to 540°F) no matter which post-scram operating mode is selected (of course single speed pump cannot operate at 50% speed). The plant must be designed for this severe transient whichever pump system is adoped. The only condition that makes some difference is an uncontrolled rod insertion event. For instance, the worst case is when core power drops rapidly from full load to 60% load. Core outlet temperature will drop 50°F for the variable speed, 65°F for the two speed, and 130°F for the single speed pump system. These rapid core temperature changes do represent some degree of plant operating risks. However, the likelihood of an uncontrolled rod insertion event is very low. The plant duty cycle analysis shows that the frequency of an uncontrolled rod insertion event is 10 out of 763 total level B type services during 40 years of plant life.

During part load operations, a decrease in power will result in both bowing reactivity and Doppler reactivity additions. Alternately, increasing core power produces negative bowing reactivity and Dopper reactivity. However, the core power (change by control rods) is the dominant factor which dictates the net core power output. For a low load change rate such as 1%/minute (1.5°F/minute core outlet temperature change) the bowing reactivity and Doppler effect will not be significant.

Considering the plant thermal transients during design and off-design conditions and plant control flexibilities, selection of either pump system should not affect the safe operation of the plant.

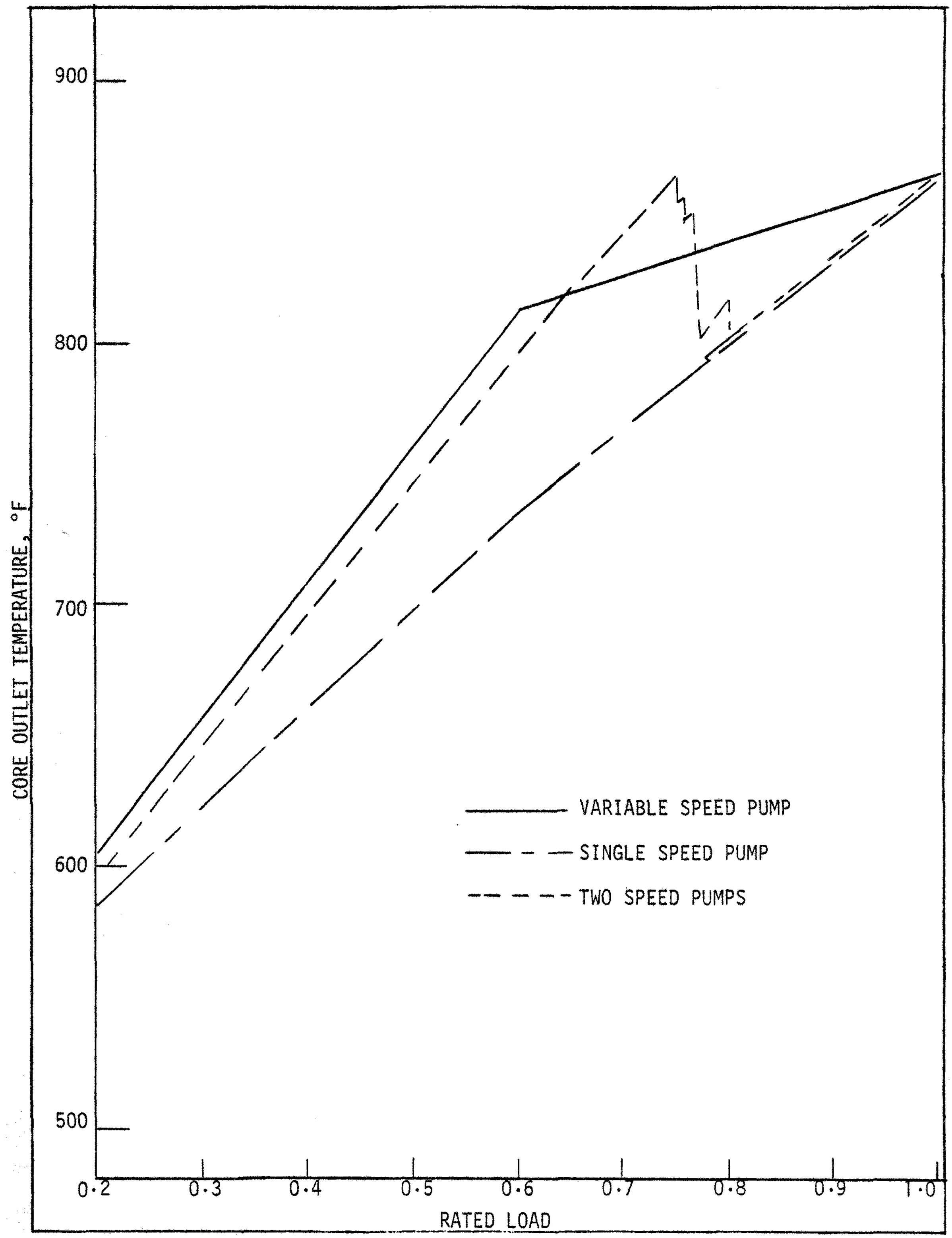

FIGURE 6-1 CORE OUTLET TEMPERATURE AT PARTLOAD OPERATION

7. COMPONENTS OUT OF SERVICE

Plant operation with component outage is a means to improve plant availability. In this report, single and double component failures were considered for the constant speed pump operation. These include the failure of:

(1) One IHTS loop
(2) One primary pump
(3) Two IHTS loops
and (4) One primary pump and one IHTS loop.

Generally, constant speed pumps would not impose major restrictions on plant operation with component outages. Figure 7-1 shows that the intermediate hot leg temperature is a more restrictive limitation for maximum power level operation than the core outlet temperature. The power output level of the plant with one component out of service is a respectable 90% average. (95% for one pump out and 85% for one IHX out). For case 3 and case 4 above, the power levels are 68% and 85% resepctively. These power output levels for constant speed pump operations are essentially the same as those for the variable speed pumps with similar plant operating conditions.

With the present design, pump cavitation is a potential problem if the plant operates with one primary pump out of service. In this condition, pump flow increases about 16%. The required pump NPSH will increase from 39 ft. to about 47 ft. of sodium. For double failure with one IHTS loop also out, the available pump NPSH is about 47 ft. which is only marginal. There is potential for pump cavitation to develop. Pump NPSH, therefore, prohibits the operation of any two primary pumps alone and requires startup of three primary pumps simultaneously to prevent pump cavitation. Effort is being made to improve pump NPSH characteristics and explore the possibility of lowering the pump impeller into the cold pool to improve the reliability of the primary pump operation. (See Section 2.2 and Appendix (VB).

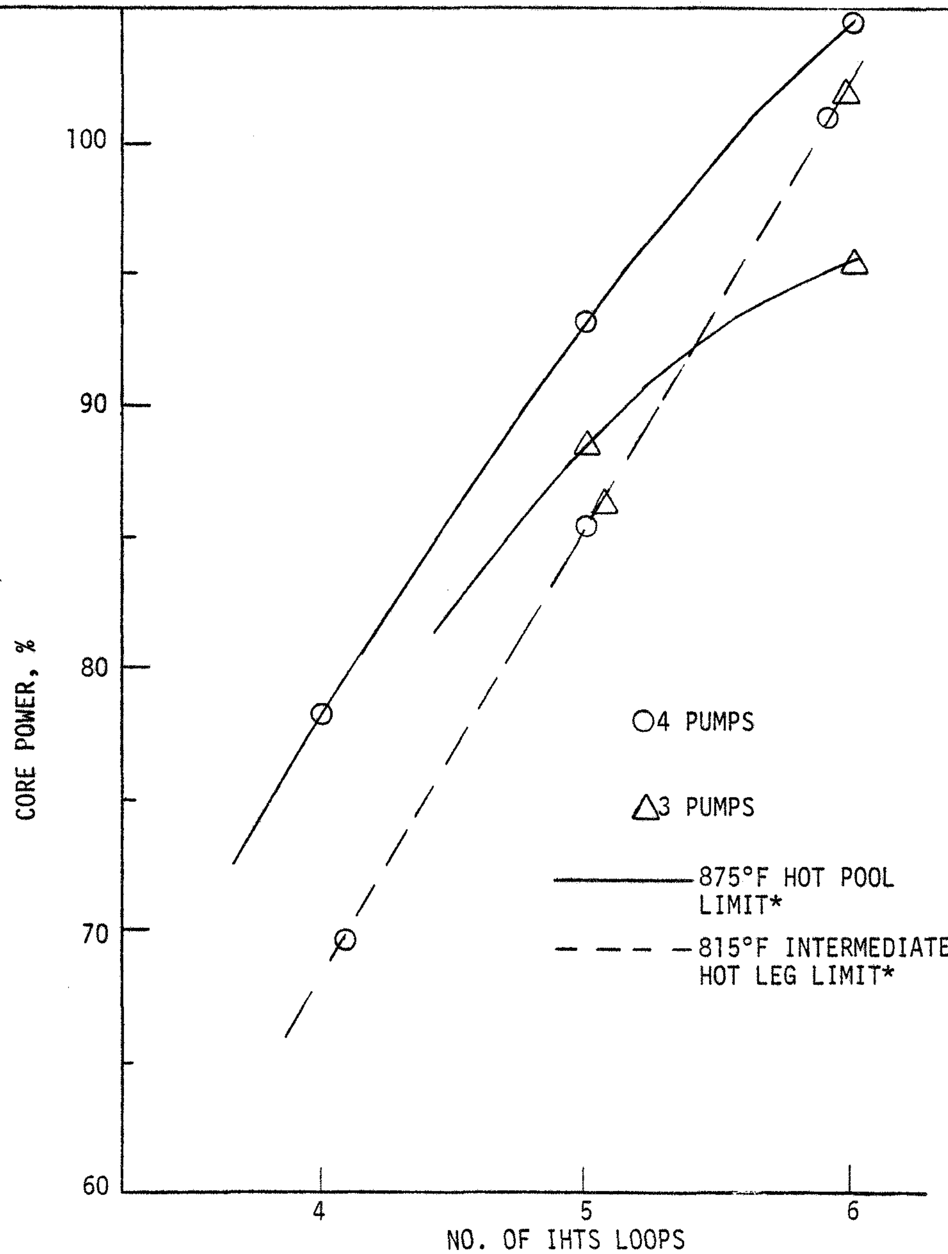

*Maximum CORE POWER allowed to operate without exceeding this limit.

FIGURE 7-1 POWER LIMITATION WITH COMPONENTS OUT OF SERVICE

8. CONSTANT SPEEP PUMP VS VARIABLE SPEED PUMP

Apparently, for a base-load plant, constant speed pumps can perform adequately and impose no major limitations on plant control and operation. Economics is the strongest incentive to use constant speed pumps, particularly for the fifth-of-a-kind design. The economics and reliability aspects of constant speed pump-operation are discussed in Part VII,Section 2.1.

However, for a first-of-a-kind LMFBR design, one must consider the uncertainties involved in the early stage of the plant development and operation. The capability of fine-tuning the plant flows may be considered desirable to research, test, and verify any off-design conditions. Furthermore, variable speed pumps can verify the applicability of constant speed pump operation for subsequent design. The use of variable or constant speed pumps for the EPRI-pool design, however, is an operator/owner choice.

APPENDIX A: CONSTANT SPEED PUMP CALCULATIONS

The constant speed primary pump being considered for the pool design is a two-stage double suction type. At full load, the pump operates at 870 RPM and delivers 65,800 GPM of sodium at a design head of 120 psi. Under part load operations, constant speed pumps maintain good flow mixing and flow distribution in the primary vessel while minimizing the effects of sodium stratification. It also assures adequate sodium flow through an active thermal barrier for reactor vessel protection. (See Part III Section 2.4). Figure A-1 shows the phase A pump characteristics operating at constant speed. The required pump NPSH as a function of pump flow is also shown in the figure. It was assumed the intermediate pumps and the recirculation pumps have similar characteristics.

The pool plant design conditions are presented in Table A-1. At rated conditions the plant operates with 4 primary pumps and 6 IHTS loops. The primary pumps are arranged in parallel so that loss of one primary pump does not directly affect the IHTS function. The design hot pool temperature is 875°F. For a core ΔT of 280°F, the cold pool temperature will be 595°F. The corresponding hot leg and cold leg temperature of the intermediate loops are 815°F and 550°F respectively. The steam turbine throttle pressure is 1000 psig and the turbine throttle temperature is 545°F. The expected plant conditions under constant speed pump operations are also shown in Table A-1.

A.1 Component Design Sensitivity

With adequate design margin, the use of constant speed pumps is not expected to affect other component designs. For instance, the calculated pressure drop of the primary system is about 102 psi. For a margin of 17%, the pressure head specified for the pump design will be 120 psi. However, for constant speed pump operation, the actual system pressure drop, which is the calculated $\Delta P \pm$ the calculation uncertainties, determines the pump flows and eventually the final temperature profiles of the plant. To avoid complication by the different pumps, it was assumed that the primary pumps, the intermediate pumps and the feedwater pumps have similar design margin and design uncertainties. A $\pm$ 20% design uncertainty was used in the study.

A similar parametric analysis was performed for the IHX's and steam generators. It was assumed that the heat exchangers have a surface area design margin of 15% for tube fouling and tube plugging, and the uncertainty for heat exchanger performance is $\pm$ 20% of the required heat transfer area. Thus, the upper and the lower bounds of the effective heat transfer area of the IHX and the steam generators are 117.4% and 82.6% of the reference design.

The results of the component design sensitivity study are presented in Figure A-2. Apparently the cold leg temperatures are not sensitive to the flow conditions. But, the sodium flows will affect the hot leg temperatures which are more critical to normal plant operation. The primary sodium temperatures are also more sensitive to the IHX performance than the intermediate sodium temperature to the steam generators. Due to the high feedwater recirculation, the steam generator inlet water temperature will not vary appreciably.

The hot pool temperature is the most critical design parameter for the safe operation of the plant. Figure A-3 shows how the pump designs and the heat exchanger performance can affect the hot pool temperature. Based on the assumptions discussed earlier, the expected hot pool temperature is about 850°F which is about 25°F below the design temperature. For extreme conditions, the temperature can be 53°F below or 9°F above the design condition. However, since the probability of having the hot pool temperature above 875°F is low, the use of constant speed pump should not impose additional plant operation risk due to elevated pool temperatures.

Figure A-4 also shows that the cold pool temperature will be lower than the design condition. The expected temperature during normal operation is about 585°F. The expected sodium flow as a function of system pressure drop is shown in Figure A-5.

A.2 Part Load Operation

Partload operation is essentially an important part of normal plant operations. Figure A-6 shows the plant conditions of the pool design with constant speed pump as a function of plant load. The primary and the intermediate cold sodium temperatures and the feedwater temperatures virtually are not affected by the load condition. The hot pool and the intermediate hot leg temperature, however, are proportional to the core power. A normal load change between 60% and 100% for instance, can result in a core temperature swing of more than 125°F.

One possible option to control core temperature is to reduce core flow. Figure A-7 shows the resulting core temperature as a function of core power with 4, 3, 2 or 1 pump operating. Apparently, lower core flow such as 66% of rated flow can have the core temperature swing from 125°F to about 65°F. But, the two pump operation induces a core temperature jump of 65°F when pump operation switched from 3 to 2 pumps or vice versa. As the flow increases about 32% in each pump, the required pump NPSH will be so high that pump cavitation will develop. The pump flow and the core flow for different pump operating modes are tabulated in Figure A-7. For single speed pump, therefore, the viable control option is to change load at a moderate rate to minimize core thermal transients.

Use two speed pump is a more practical option to control core flow and reduce core temperature change. For example, at full pump speed, core power can reduce to about 80% while core outlet temperature drops from 865°F to about 800°F; then the pumps will change to the lower speed, but the resulting core outlet temperature will not rise above 865°F. As core power reduces to about 60%, the corresponding core outlet temperature at the lower pump speed is 806°F. Thus, the core temperature change is reduced from 125°F to 65°F. Figure A-8 shows the core temperature profiles for the single speed, two speeds and the variable speed pump system at various load conditions.

A.3 Components Out of Service

To maximize plant availability during plant life, the plant must be able to operate with major components out of service. Two types of failures were considered:

1. Loss of IHTS loop due to the failure of the IHX, intermediate pump or steam generator and,
2. Loss of primary sodium pump.

In this report, plant operation with one or two IHTS loops out of service is referred to as (N-1) loop or (N-2) loop operation. Similarly, (N-1) pump refers to plant operation with one primary pump out of service.

Figure A-9 shows the core outlet temperature under various plant operations with different combinations of component failure. Since the limiting core outlet temperature is 875°F, it becomes one of the limitations for the operation of the plant. Similarly, the intermediate hot leg temperature profiles are shown in Figure A-10. Since the IHTS loops in a pool design are not directly coupled to any primary pumps, the 3 pump or 4 pump operation has no effect on the intermediate hot leg temperature.

Both the design core outlet temperature and the intermediate hot leg temperature impose core operating restrictions as shown in Figure A-11. In general, the intermediate hot leg temperature is more restrictive than the core outlet temperature. It tends to reduce the power level of the plant. The maximum power output can be achieved if the steam generators are designed for higher temperature (860°F maximum) limits.

Pump NPSH is another limitation on plant operation with one primary pump out of service. As shown in Figure A-12, for the (N-2) loop case, the available pump NPSH is higher than the required pump NPSH provided that all 4 primary pumps are operating. However, pump NPSH margin diminished rapidly as one primary pump is out of service. Consequently, operation of two primary pumps is prohibitive.

Even under (N-2) loop operation, the hot pool level will rise about 1-1/2 ft. which should have no effect on plant operation. The cold pool level, however, will drop appreciably reducing the pump available NPSH as shown in Figure A-12.

TABLE A-1

PLBR - Pool Plant Operation

	Design Conditions	Expected Conditions
Power Output, MWe	1000	1000
, %	100	100
Turbine Conditions, psia	1000	1000
, °F	545	549
FW Recirculation Ratio	6	6
Number of Primary Piping	4	4
Number of IHTS loops	6	6
Primary Sodium Condition =		
Hot Leg, °F	875	850
Cold Leg, °F	595	584
Total Flow, lb/hr.	115.4×10^6	122.9×10^6
NPSH Available, ft.	46	47
NPSH Required, ft.	39	40
Total Pressure Drop, psi	120	102
Intermediate Sodium Condition =		
Hot Leg, °F	815	797
Cold Leg, °F	550	547
Total Flow, lb/hr.	121.7×10^6	129.6×10^6

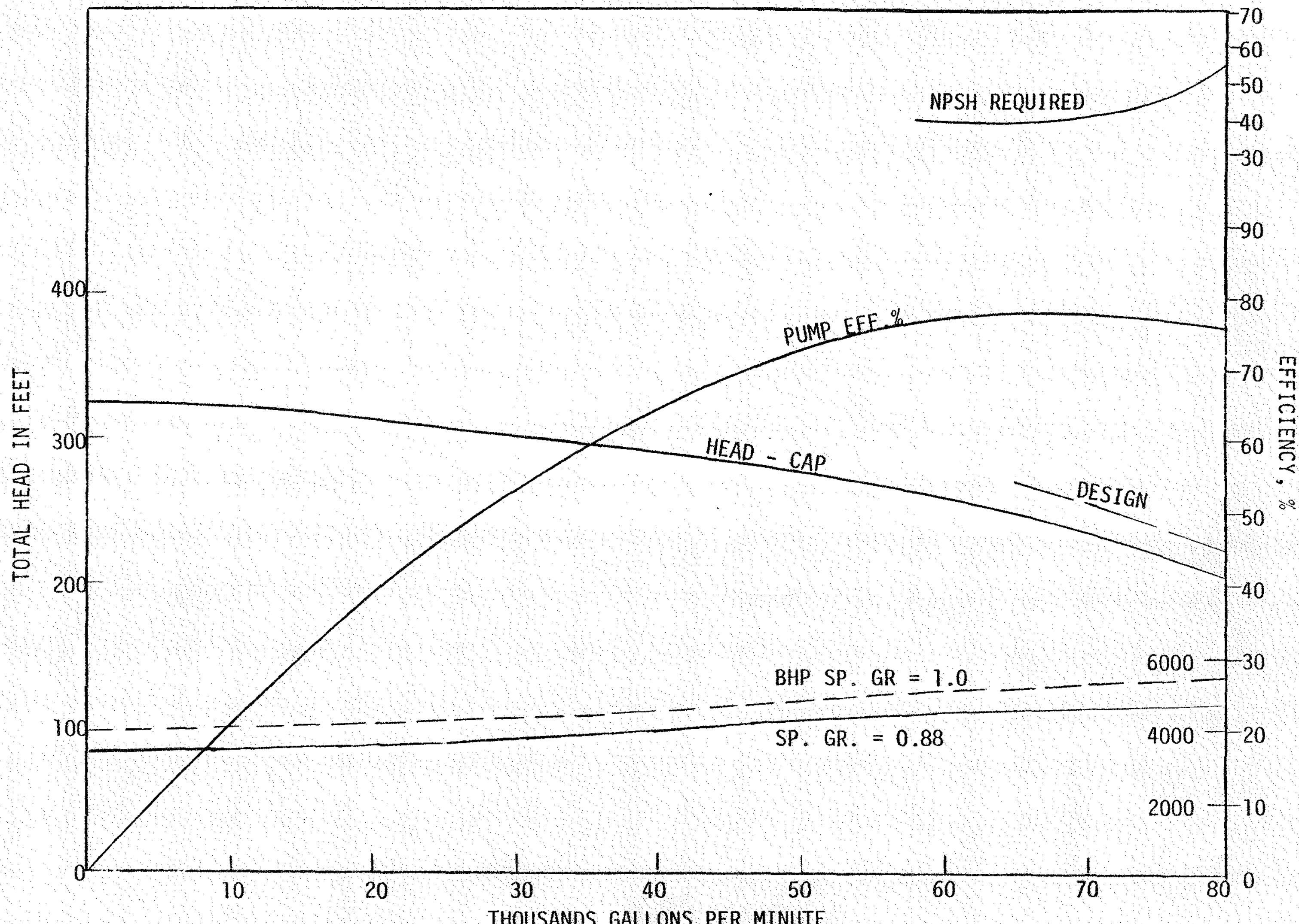

POOL TYPE PUMP - TWO STG. - DBL. SUCTION (EXTENSION 1 DESIGN)

FIGURE A-1 PRIMARY PUMP CHARACTERISTICS

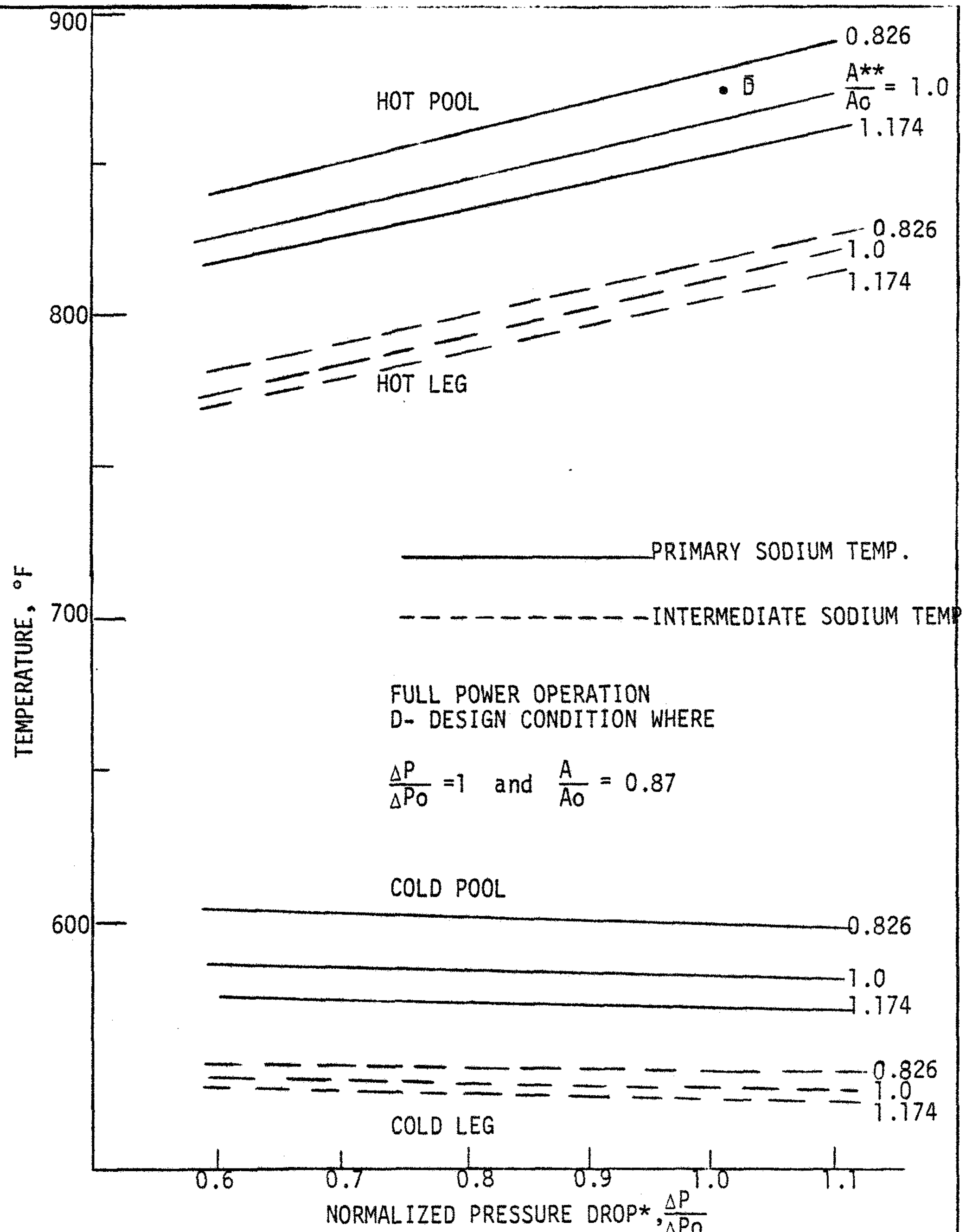

*For the primary intermediate and recirculation loops.
**For IHX and steam generator heat transfer performance.

FIGURE A-2 COMPONENT DESIGN SENSITIVITY

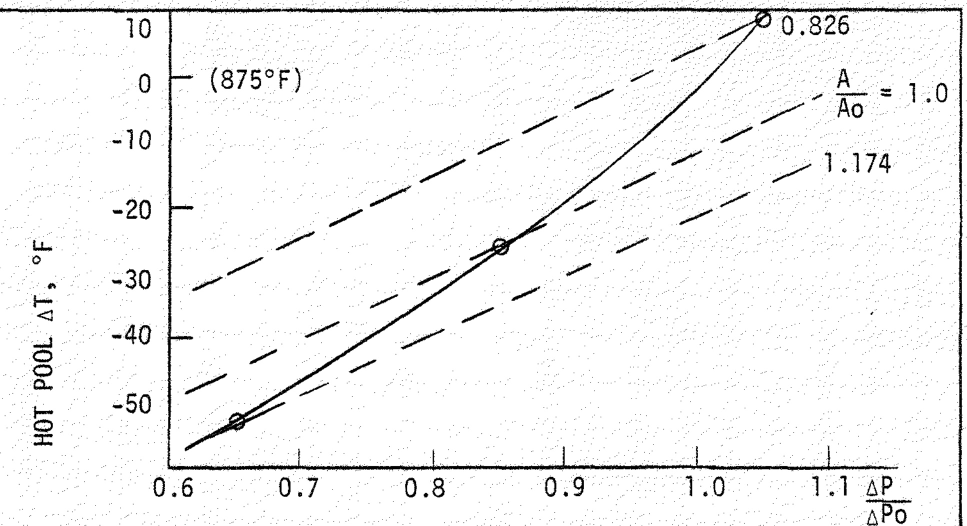

FIGURE A-3 EFFECT OF ΔP AND HEAT TRANSFER AREA ON PRIMARY HOT SODIUM

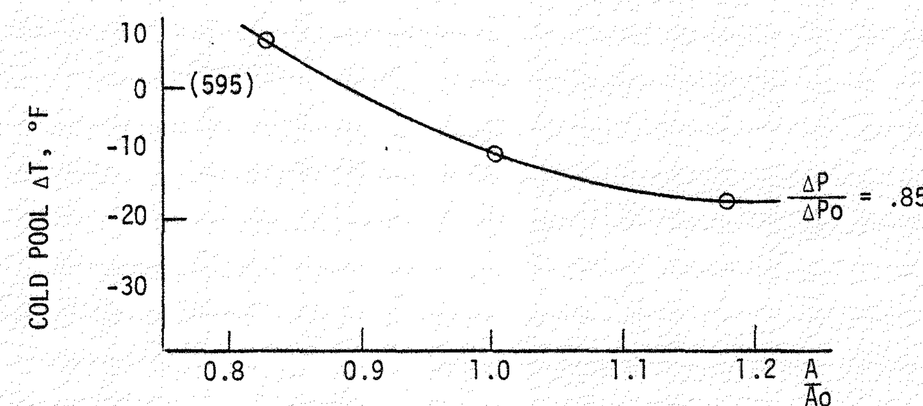

FIGURE A-4 EFFECT OF COMPONENT HEAT TRANSFER PERFORMANCE ON PRIMARY COLD SODIUM

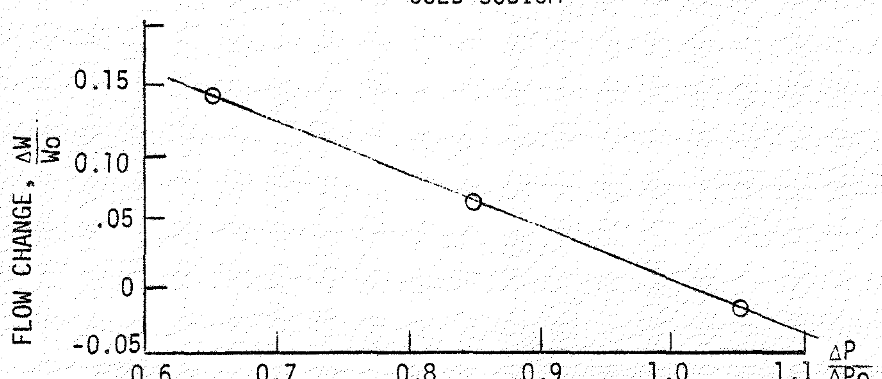

FIGURE A-5 EFFECT OF PRESSURE DROP ON PRIMARY & INTERMEDIATE SODIUM FLOW

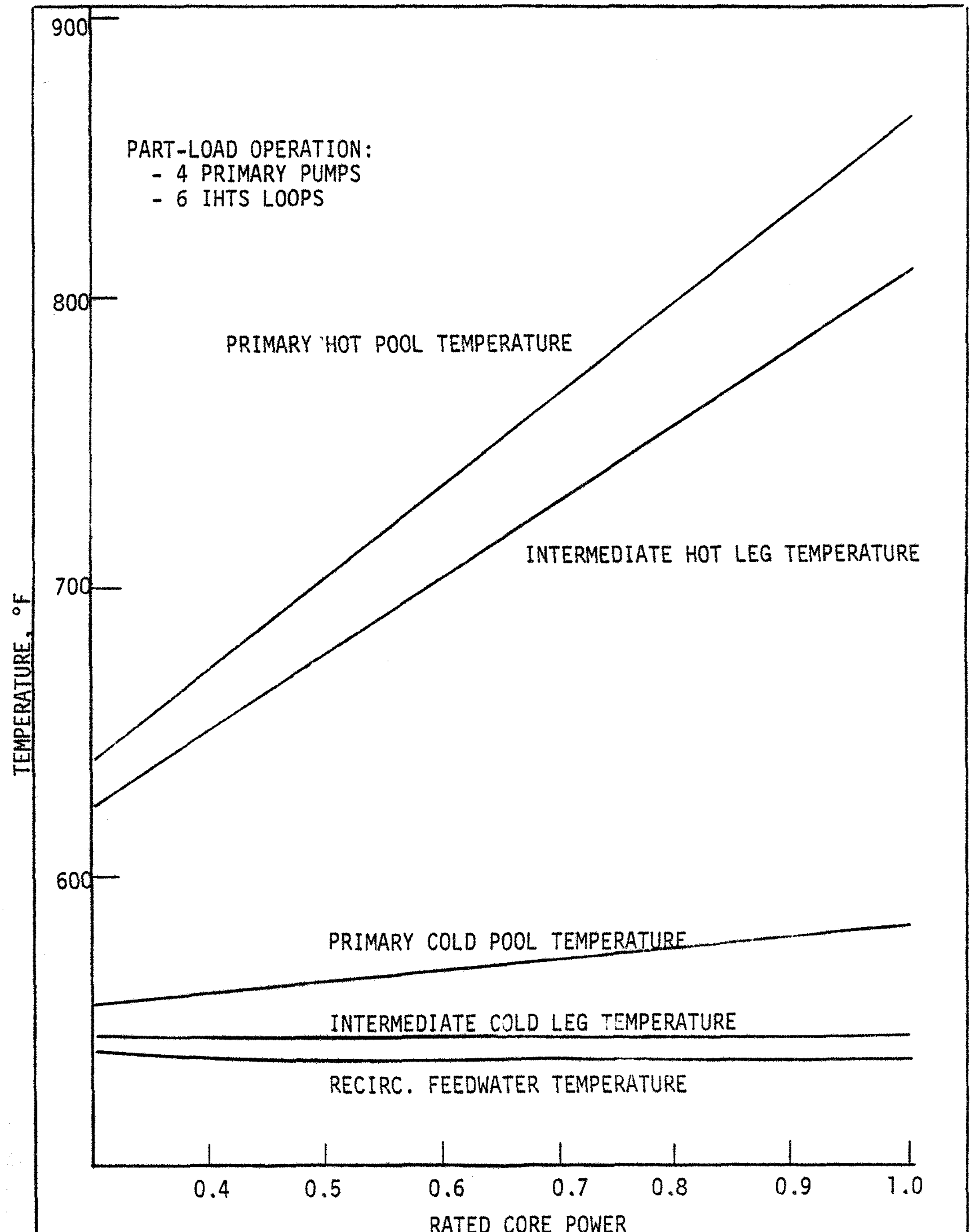

FIGURE A-6 PLANT TEMPERATURE AT PARTLOAD OPERATION

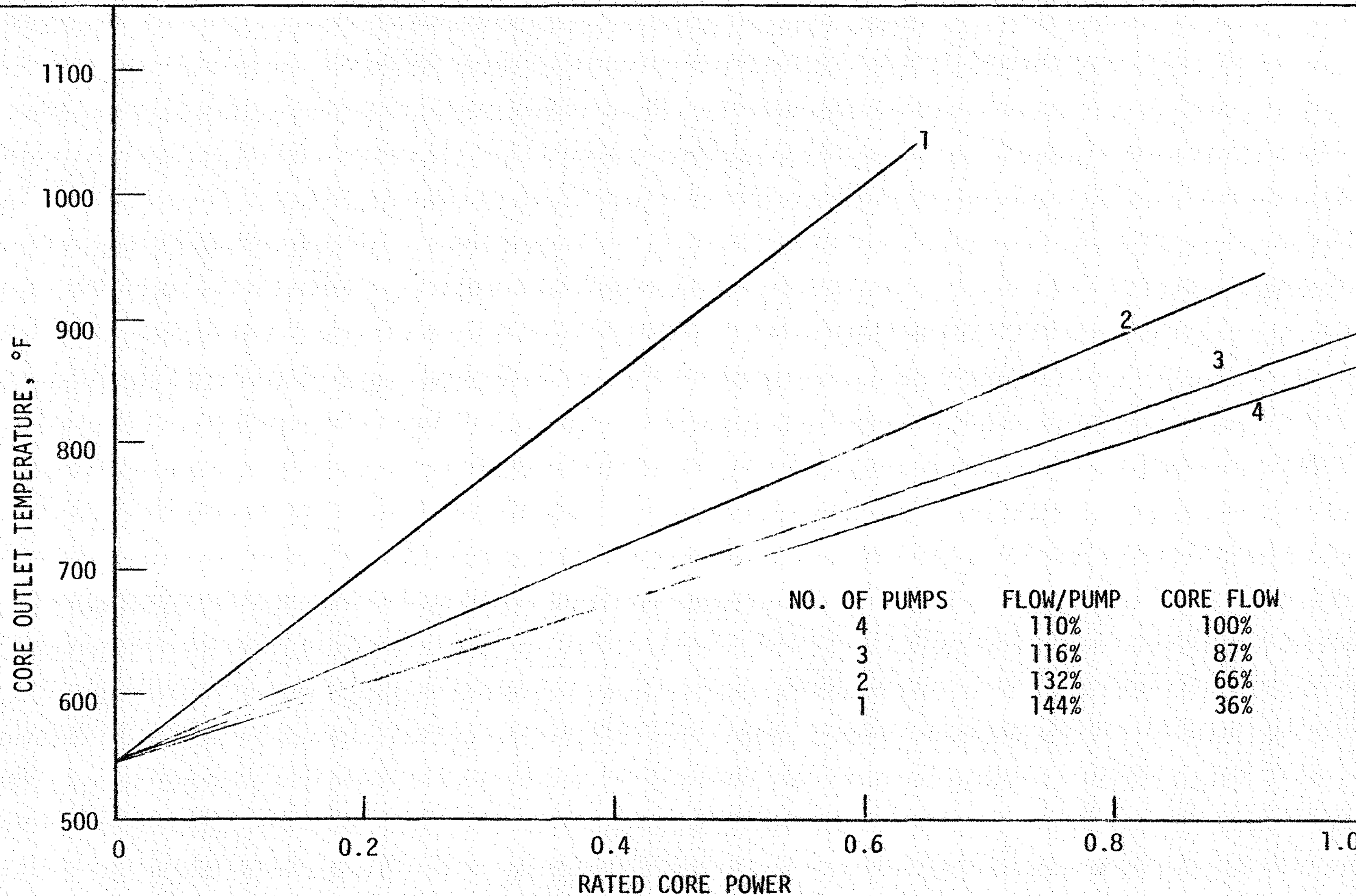

FIGURE A-7 CORE OUTLET TEMPERATURE VS. PUMP OPERATION

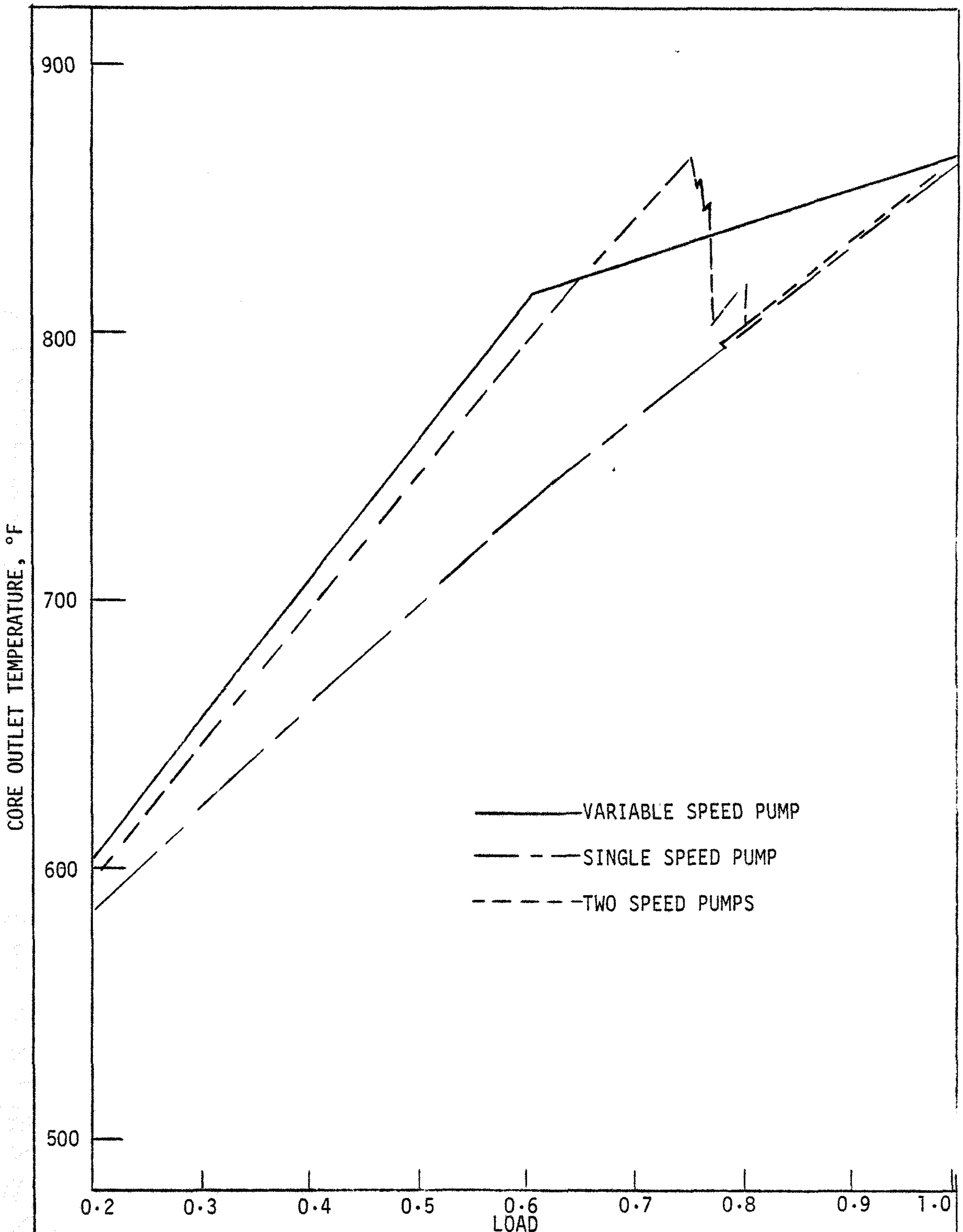

FIGURE A-8 CORE TEMPERATURE CHANGE VS. PUMP SYSTEMS

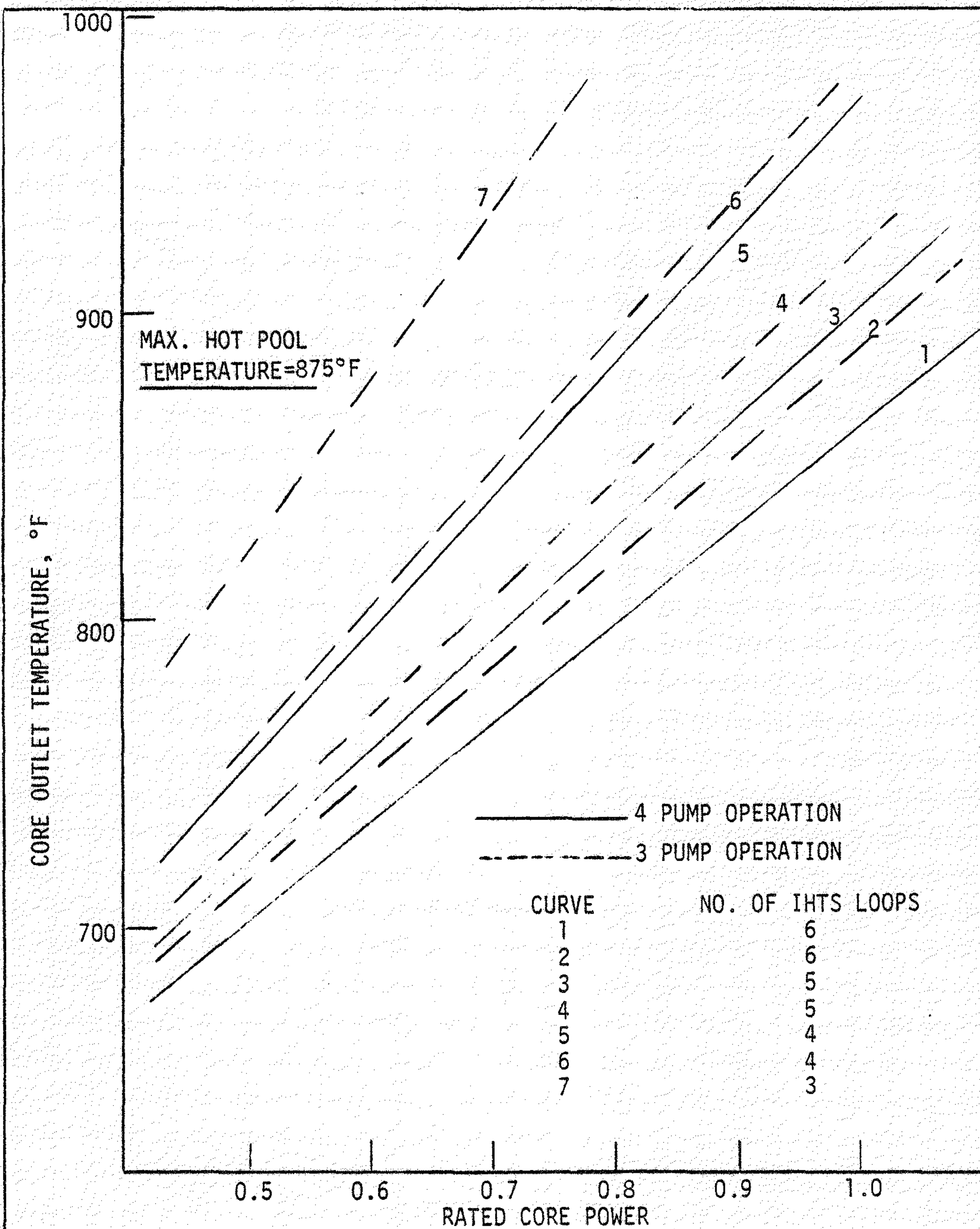

FIGURE A-9 CORE TEMPERATURE VS. COMPONENT OUTAGE

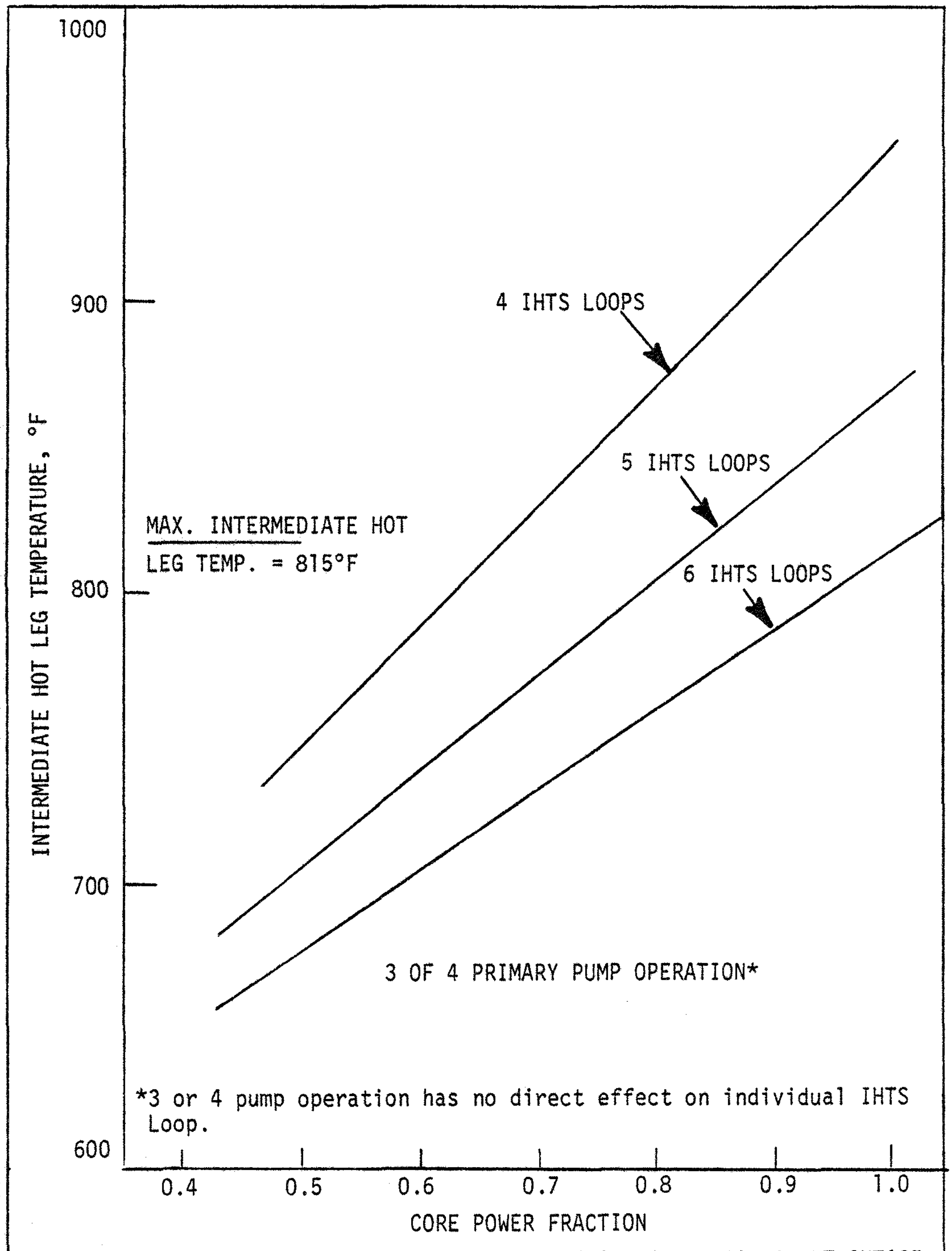

FIGURE A-10 INTERMEDIATE HOT LEG TEMPERATURE VS. COMPONENT OUTAGE

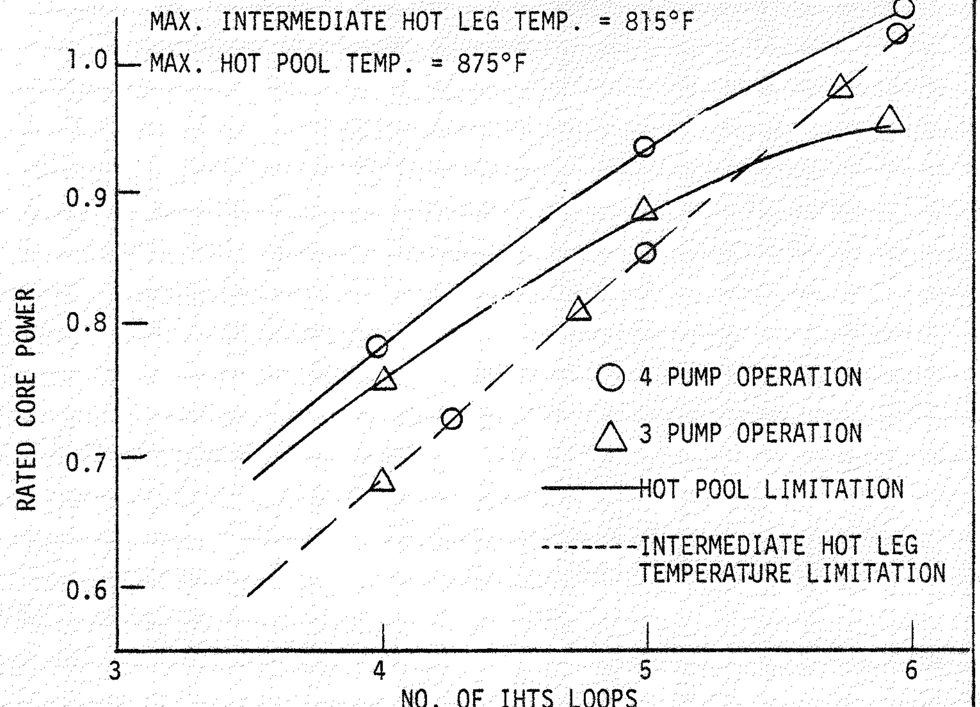

FIGURE A-11 LIMITATIONS ON CORE POWER WITH COMPONENT OUTAGE

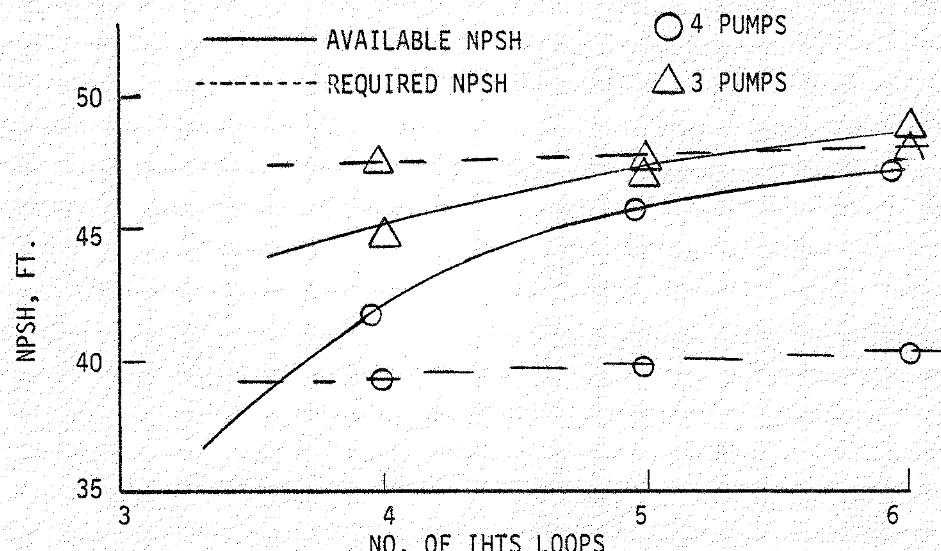

FIGURE A-12 PUMP NPSH CHARACTERISTICS

CHARGE NO. 8-51-3145	DOCUMENT NO. ND/78/35	ISSUE 1	DATE 12/8/78

FWC FORM 172 - 4

NOTATIONS IN THIS COLUMN INDICATE WHERE CHANGES HAVE BEEN MADE

APPENDIX VA

Preliminary Design of a Bent Tube IHX for the 1000 MWe Pool Reactor

Phase A, Extensions 1 and 2

B. E. Dawson 12/7/78
B. E. Dawson
Project Manager

D. H. Pai, Manager
Engineering Technology Dept.

Prepared for General Electric Company
GE Contract No. 190-K1G08
FWEC Contract No. 8-51-3145

Foster Wheeler Energy Corporation
Nuclear and Advanced Technology Operations
Livingston, New Jersey

BY	APPROVED	PAGE

TABLE OF CONTENTS

CHARGE NO. 8-51-3145	DOCUMENT NO. ND/78/35	ISSUE 1	DATE 12/8/78

LIST OF FIGURES

FWC FORM 172 - 4

NOTATIONS IN THIS COLUMN INDICATE WHERE CHANGES HAVE BEEN MADE

BY	APPROVED	PAGE

LIST OF TABLES

Drawing No. 51-3145-6-2000, Rev. A

1. INTRODUCTION

Foster Wheeler completed a 2 1/2-month preliminary design effort on an intermediate heat exchanger (IHX) for a 1000 MWe pool reactor plant in 1977. The IHX was a straight tube design with primary sodium inside the tubes and intermediate sodium in the shell. This work was summarized in Foster Wheeler report ND/77/56 dated 10/12/77.

The above-mentioned work was extended for an additional three months to make a comparative study on a bent tube IHX which would meet the same design requirements as the previous straight tube design. The design features in the bent tube unit were similar to those which were used for the British PFR and are being proposed for CFR. These features included a double sine-wave bend in each tube, an internal bore weld between the tubes and tubesheets, and a grid-type support plate. The bent tube design was summarized in Foster Wheeler report ND/78/22 dated 6/22/78. The report included comparisons between the straight tube and bent tube heat exchangers based on technical considerations and cost.

Based on the above report, the bent tube configuration was selected as the reference design. Specific areas were identified for further analysis in order to improve the design or reduce the cost. The results of these additional investigations are summarized in this report, and the general arrangement drawing is revised to show the current configuration. The report is divided into sections for each topic. This work was done during the second half of 1978.

2. DETAILED STRESS ANALYSIS OF THE LOWER TUBESHEET

A detailed ANSYS thermal and thermal stress analysis was performed on the lower tubesheet with the flow deflector ("J") and the thermal shield inner head both eliminated from the design. Reference 1 discusses the initial lower tubesheet computer analysis, which included the thermal shields. At the time of the initial lower tubesheet analysis, it was concluded that the thermal shield inner head could be removed from the design with a high probability of success in satisfying the Code limits utilizing simplified inelastic analysis techniques. The initial and the present lower tubesheet ANSYS computer analyses were performed for the controlling intermediate loop loss (upset) transient in which the primary fluid upshocks for a postulated 20 occurrences.

2.1 Thermal and Thermal Stress Analysis

The thermal boundary conditions and thermal modelling used for the present ANSYS thermal analysis are the same as those used in Reference 1 except that the thermal boundary conditions are now imposed on the inside surface of the 1/2" thick lower tubesheet hemi-head after removal of the thermal shield inner head. Figure 1 presents the lower tubesheet ANSYS thermal and thermal stress model showing dimensions and the critical regions. Tables 1 and 2 present the linearized surface thermal stresses and the peak surface thermal stresses, respectively, for the controlling sections and elements in the lower tubesheet; see Figure 2 for the thermal

2.1 Thermal and Thermal Stress Analysis (cont'd.)

stress sections and critical elements. Figures 3 and 4 present enlarged plots of the controlling inner crotch area and outer junction area of the lower tubesheet.

2.2 Comparison of Stresses

Table 3 presents a comparison of the thermal stress results at the controlling inner crotch region (spherical head-to-tubesheet junction) of the lower tubesheet, with and without the inner thermal shield head. Note that the removal of the thermal shield head has increased the gross and local volume averaged temperature (VAT) responses between the perforated and solid inner head junction regions, i.e., the thermal discontinuity bending effects have increased because the inner head has become colder. This accounts for the increased stresses in the perforated region. Also, the ΔT thermal gradient through the wall of the tubehseet inner hemi-head junction has increased from about 40°F to 110°F. This, together with the VAT rise, has increased the controlling maximum linearized thermal bending stress from 53,500 psi (Reference 1 with thermal head) to 68,800 psi (new analysis without thermal head) at the hemi-head junction cross-section 4. The peak surface thermal stresses were maximum in the perforated region of the lower tubesheet near the hemi-head junction. The peak stress intensity increased from 59,600 psi for the analysis with the thermal head, to 92,600 psi for the analysis without thermal head for the controlling perforated region element No. 254. These perforated stresses include all stress multipliers from Article A-8000 of the ASME Nuclear Vessel Code, Section III, for stresses in perforated plates.

2.3 Elastic Code Evaluation

The maximum linearized thermal stress of 68,800 psi in the solid (unperforated) region was taken as the controlling linearized surface stress for comparison with 3 Sm and inelastic strains. (This stress is similar to the perforated region linearized thermal stress of 69,800 psi from Table 1.) The linearized thermal stress of 68,800 psi exceeds the ASME Code, Section III, allowable stress limit of 3 Sm (47,000 psi) for elastically calculated secondary stress intensity range. Applying the Code simplified elastic-plastic procedures of Code Paragraph NB-3228.3 shows that the thermal range of primary (ΔP = 115 psig) plus secondary membrane plus bending stress intensity, excluding thermal bending (ΔT) stresses (calculated to be 60,000 psi), exceeds the 3 Sm allowable of 47,000 psi. However, the ratchetting criteria (NB-3222.5) is satisfied for the 68,800 psi linearized thermal elastic bending stress.

For fatigue evaluation, the controlling stress intensity is the maximum peak surface thermal stress of 92,600 psi in the perforated region of the lower tubesheet near the inner hemi-head junction; see Table 3. The Nuclear Section III fatigue evaluation of NB-3228.3c is satisfied for this peak surface thermal stress of 92,600 psi, since the controlling loop loss upshock transient occurs for only 20 cycles. However, as discussed above, the range

CHARGE NO. 8-51-3145	DOCUMENT NO. ND/78/35	ISSUE 1	DATE 12/8/78

2.3 Elastic Code Evaluation (cont'd.)

of linearized stress intensity, excluding thermal bending stresses, could not be shown to satisfy the ASME Nuclear Code, Section III, simplified elastic-plastic design procedures of Paragraph NB-3228.3a. Accordingly, inelastic analysis is required and is discussed below.

2.4 Simplified Inelastic Analysis

In order to satisfy all Code criteria, a simplified inelastic (elastic-plastic) analysis was performed for the controlling tubesheet to inner spherical head junction using the FWEC R1050 Computer Code, which performs elastic-plastic-creep analysis of long axisymmetric, circular cylindrical shells. This in-house computer program allows axisymmetric boundary conditions (loads or displacements) to be applied to the end of the finite length thin shell cylinder models, including pressures and temperature gradients.

Figure 5 presents the model and Figure 6 presents the loading histogram used to perform the simplified inelastic analysis of the lower tubesheet inner crotch region, without the thermal shield head, for the controlling loss of loop upset transient. This upshock transient is specified to occur for 20 cycles. The sphere-to-tubesheet junction (Junction A in Figure 5) was modelled as a long cylinder with half the operating pressure ($\Delta P = 1/2 \times 115$ psig = 57.5 psig) in order to obtain the same hoop stress as in the sphere. Also, the axial mechanical traction loading was input to simulate the meridional pressure stress. The ANSYS elastic stress distribution of Section 4 (Table 1) for the linearized stress intensity of 68,800 psi at the tubesheet junction A was simulated by radial (w) and rotational (θ) displacement boundary conditions applied at the end of the cylinder model. The linear through-the-wall ΔT temperature gradient was also applied to the cylinder. Thus, the pressure and thermal stress distribution at the lower tubesheet to hemi-head junction was elastically reproduced. See Figure 5 for the model and Figure 6 for the loading histogram.

The normal steady state operating condition at time step 1 (Figure 6) consists of a uniform 575°F operating temperature and the 115 psig operating pressure loading, together with the corresponding radial and rotational displacement boundary conditions due to pressure loading. The upshock transient step 2 consists of a linear through-the-wall ΔT temperature gradient of 110°F along with the corresponding radial and rotational boundary displacement conditions (w and θ) and no pressure loading (see Figure 6). This load step 2 is the quasi-steady state upshock condition for the intermediate loop loss transient. The other (lower) end of the long cylinder is modelled as a free end (see Figure 5).

2.5 Simplified Inelastic Analysis Results

Table 4 presents the material property input for the cylinder model and the results of the simplified inelastic analysis of the lower tubesheet-to-sphere inner junction. The properties are based on an average temperature of 630°F for 304 Stainless Steel. Since the maximum temperature at the inner crotch region of the tubesheet during the loss of loop upset transient (upshock) is less than 800°F, then no creep occurs.

FWC FORM 172 - 4 — NOTATIONS IN THIS COLUMN INDICATE WHERE CHANGES HAVE BEEN MADE

BY	APPROVED	PAGE 3

2.5 Simplified Inelastic Analysis Results (cont'd.)

The results of the 20 cycle elastic-plastic analysis show no fatigue damage ($4 \times 10^{-5} \approx 0$) based on an equivalent strain range of 0.2% for 20 cycles at 800°F. The linearized average (mid-fiber) and surface (inside) accumulated strains are calculated to be 0.10% and 0.16%, respectively; see Table 4. These maximum positive principal (hoop) strains satisfy the Code Case 1592 allowables for strain of 1% for average strains and 2% for surface strains. These inelastic results assume no additional fatigue damage or strain contribution due to any other transient.

It should be noted that while the results of the simplified inelastic stress analysis clearly meets the Code limits, final demonstration of structural adequacy must be shown by a detailed finite element inelastic model of the actual tubesheet junction geometry. Past experience has indicated that the results and trends of the simplified inelastic analysis are a good indication that the results of the detailed inelastic analysis will also meet the Code limits. The above simplified inelastic analysis results are based on a histogram consisting of 20 cycles of the loop loss transient. If at a later date, additional transients are shown to be critical for the lower tubesheet, then a new histogram would have to be developed for detailed inelastic evaluation.

2.6 Transient Comparison

The transient and part load data which were attached to GE Letter XL-893-87790, 10/9/78 have been qualitatively compared with the previously supplied transients which were used in the above lower tubesheet analysis. In general, the new transients are less severe than the previously supplied data and do not appear to control the analysis.

3. TUBING - 2 BENDS VERSUS 1 BEND

The feasibility of using only one tube bend instead of two bends in the IHX tube bundle was investigated. A 2-D ANSYS study, using pipe elements and the model in Figure 7, was made to evaluate the thermally induced stresses and displacements for the worst case thermal conditions. First a displacement study was made to determine the relative motion between one tube and an adjacent tube when large temperature differences exist between the tubes. The worst case for this situation arises when a tube is plugged. A conservative estimate shows that the temperature of a plugged tube may be as much as 100°F colder than its neighboring live tube, on a length averaged basis. The displacement analysis showed that with the initial tube bend geometry, for both the one bend and the two tube bend designs, tube touching would occur in the bend region between an active tube and an adjacent plugged tube.

FWC FORM 172 - 4 — NOTATIONS IN THIS COLUMN INDICATE WHERE CHANGES HAVE BEEN MADE

3. TUBING - 2 BENDS VERSUS 1 BEND (cont'd.)

Analyses were then performed to optimize the bend region geometry within the constraints of a 60 in. span length and 7 in. tube offset, in order to maximize the tube-to-tube clearance. It was found that changing the bend angle from 30° to 20° and the bend radius from 7.875 in. to 20.0 in. increased the distance between the tubes in the bend region from .072 in. to .163 in. (after subtracting out manufacturing tolerances). Figure 7 illustrates the bend region geometry changes. The finite element model of the tube was rerun with this new geometry. The results showed that the one tube bend geometry could accommodate a plugged tube to live tube temperature differential of 35°F, whereas the two bend geometry could accommodate 70°F. if the thermal expansion is distributed equally between the two bends. Present estimates show that a 100°F length averaged temperature differential may exist. This means that within the constraints of reasonable tube bend region span length and offset, a plugged tube will touch an adjacent active tube during steady state conditions whether one or two tube bends are used.

Thermal stress levels in live tubes during thermal transient events due to a 100°F temperature differential between the outer shell and the tubes were investigated for the one bend and two bend designs. It was found that for the one tube bend design, a penalty exists in terms of maximum bending stresses relative to the two tube bend geometry. However, for the one bend design the highest bending stress is 22,000 psi for the assumed upper bound 100°F suppressed thermal expansion case. The actual tube stresses depend on the maximum temperature difference between the tube and shroud. Since this 100°F case that was analyzed corresponds to the ΔT for a plugged tube, which represents a worst case, the actual stresses in the active tubes are expected to be below the yield stress. Since the single bend is located in the lower "cold" end of the bundle, elastic follow-up effects will be minimized. Therefore, it is acceptable to use the full 3 Sm ($\cong$ 46,000 psi) secondary stress range for the allowable bending stress. Hence, thermal stresses for the one bend geometry are judged not to be a significant problem.

Having concluded that thermal stresses were not a problem, the analysis effort focused its attention to the tube touching problem which occurs for the plugged tube condition. Two approaches were considered; namely, performing a wear analysis to see if the tube touching condition could lead to excessive tube wear and an investigation to see if cutting the plugged tube could relieve the tube touching.

For the wear analysis, tube contact forces were determined. The single bend tube is stiffer than the double bend tube, so the contact forces will be higher for this "interference" condition. Based on the finite element analysis, contact forces of 20 lbs develop on the single bend tube and approximately 5 lbs develop on the double bend tube. Since difficulty exists in correlating wear tests data with respect to geometry, applied motion, frequency, environment, etc., it was judged that rather than perform a tube wear analysis for these contact forces, the alternative of cutting the plugged tube should be evaluated.

3. TUBING - 2 BENDS VERSUS 1 BEND (cont'd.)

The single bend tube was analytically cut in the span immediately above the bend region. It was found this will relieve the thermal expansion stresses and tube touching will not occur for the plugged tube case. The reason is evident from Figure 8. The plugged tube temperature is most different from the active tube temperature in the upper half of the tube length. Therefore, by cutting the tube, the major "driving force" will be eliminated. Figure 9 shows that deflected shape of the plugged tube, relative to the active tube, for the cut and uncut case. It can be seen that tube touching will be eliminated in the cut plugged tube case. Therefore, tube wear will not be a problem.

It is concluded that a one-bend geometry is feasible. The bend should be in the lower region of the tube bundle. Thermal stresses were found to be acceptable for the worst case bundle to shroud temperature mismatch. Tube touching due to the plugged tube condition can be eliminated if the plugged tube is cut in the span above the bend region.

4. SEISMIC SUPPORT STUDY

General Electric studied the possibility of stiffening the IHX shell to eliminate the requirement for a seismic support in the vicinity of the upper tubesheet (using the flow shroud as a restraint). FWEC was to evaluate the GE analysis with respect to the balance of the IHX, but the GE work was not completed in time for the FWEC analysis during this report period.

5. REVIEW OF GE REPORT "DECK MAJOR COMPONENT PENETRATIONS"

The referenced report was reviewed, and the following comments noted.

Section 6 of the GE report presents the design criteria and the results of the thermal analysis. The structures analyzed are low temperature components and therefore the sum of primary and secondary stresses should not exceed the 3 Sm limit. The sum of primary stress levels due to deadweight, seismic, and other unevaluated conditions was assumed to approach the primary stress limit of 1.5 Sm. The thermal stresses therefore were limited to 1.5 Sm value. FWEC agrees with the GE approach at this stage of the continually changing design. The results presented for the IHX flow shroud and IHX casing show that thermal gradients and the associated thermal stresses for deck penetration scheme 1 and 2 are below the established 1.5 Sm criteria.

Section 7 of the GE report presents the recommendation for continued work. FWEC agrees that more work should be undertaken to eliminate reliance on the IHX flow shroud as a seismic restraint. The results of the seismic analysis performed by FWEC in the past indicated that the stresses in the tube support grids were the governing criteria used to establish the need for an additional seismic support at the upper tubesheet (and connected to the flow shroud). It was recently noted, however, that the faulted condition allowables for the tube support grid have been modified to a significantly higher value in the latest version of Code Case 1592 (1592-11). These

5. REVIEW OF GE REPORT "DECK MAJOR COMPONENT PENETRATIONS" (cont'd.)

higher allowables, in addition to the thickening of IHX shells may result in acceptable seismic loads at the grids and other regions of the IHX, without relying on the flow shroud as a seismic support. FWEC strongly agrees that proposed future work in this area is required.

6. IMPACT OF IHTS NOZZLE LOADS

The effect of the IHTS nozzle loads on the IHX top structure inner cylinders has been examined. It was found that the load controlled buckling limits for these loads (plus pressure and seismic) would be exceeded at the lower portion of the cylinder. The design options are to thicken the cylinder greatly or use radial gussets to provide a more direct load path to the IHX support flange. It has been determined that the use of gussets is the best option. These gussets must have a slight radial gap between them and the outer shell because of the large difference in temperatures between the cylinders. However, deflection controlled buckling limits at inner cylinder locations below the radial gussets will now apply, and a slight thickening of the inner cylinder will be required in combination with the gussets. Figure 10 summarizes the analysis performed and pertinent results.

FWEC sent a copy of Figure 10 to GE via telecopier on 10/3/78. GE will use this information to complete the IHX plug design, and they will specify the final configuration.

7. HOT/COLD POOL SEAL DOUBLE BELLOWS

A preliminary design and analysis for the hot/cold pool double bellows seal was conducted based on both a 60 in. and 80 in. I.D. size (original geometry was 42.0 in.). The design axial and lateral displacements acting on the bellows were obtained from Reference 2. Included in the displacements are 1/2 in. for manufacturing tolerance and an assumed 1/2 in. axial compression requirement for installation. A rotational displacement loading was also assumed acting on the bellows consisting of a 1/8 in. manufacturing tolerance across the diameter and a 10°F circumferential gradient acting on the IHX shell. The resulting displacements imposed on the bellows assembly are 1.5 in. axial, 2 in. lateral, $\pm$1.5 in. lateral due to seismic, and 0.20° to 0.25° rotational motion. The pressure acting on the bellows is the 2.5 psi primary pressure drop, acting external to the bellows.

Table 5 summarizes the resulting geometry and applied loadings applicable to both the 60 in. and 80 in. I.D. bellows. The sizing calculations utilize the EJMA formulae for determining the stresses in the bellows due to the applied displacements and pressures. In addition, the cyclic load condition of $\pm$1.5 in. of lateral motion due to a seismic occurrence was investigated with 10^6 cycles being calculated as the allowable number of cycles. The load condition of cycling between hot standby and normal operation (bellows axial motion range = 0.65 in.) was also investigated with $> 10^6$ cycles being calculated as the allowable number of cycles.

8. IRACS COIL SUPPORT

A preliminary design and analysis of an IRACS coil support structure was performed. The major objective of the analysis was to develop a support structure which would result in acceptable stress and deflection levels in the IRACS coil during seismic events.

The seismic analysis of the IRACS coil was performed by modelling the coil as a series of lumped mass and spring systems and attaching them to the overall ANSYS seismic model of the IHX. Initial analyses looked at an IRACS coil with 1) no supports, 2) supports only at the base of the vertical tube run, 3) supports at the base of the vertical tube run and at the bottom of the helical coil. The results of each of these analyses showed the IRACS coil either overstressed or with excessive displacements.

Since the above three simplified concepts were not satisfactory, the concept shown in Figure 11 was selected as the reference design. The IRACS coil is supported at four (4) circumferential locations around the helix by split support plates which extend the full length of the IRACS helical coil. These support plates are held in place on their inside diameter by a shroud which extends down from the shield plug. Based on the results of the simplified designs, it is judged that this IRACS coil support system will result in acceptable coil stresses during seismic events.

9. INTERMEDIATE SODIUM FLOW AND TEMPERATURE DISTRIBUTION

9.1 Flow Distribution in Tube Bundle

A detailed numerical flow distribution analysis on the shell side of the bent tube pool IHX has been carried out. In the previous analysis (see Reference 1), the effect of the central downcomer on the velocity distribution of the shell side inlet region was not included. A uniform velocity distribution was assumed at the bundle entrance. In the present analysis, a new flow model was set up including the central downcomer. The effect of the downcomer on the bundle entrance span was examined. A fluid velocity vector plot for the IHX unit is shown in Figure 12. As indicated in the figure, the bundle entrance velocity is far from uniform, and the velocity is much larger near the tubesheet surface. More fluid flows towards the outer edge of the bundle. The velocity tends to equalize after the second tube support structure. Flow distribution is essentially axial with little cross flow outside the inlet and the exit region. Note that the average velocity of the fluid in the downcomer is about 23 ft/sec, while the average axial velocity in the bundle is less than 3 ft/sec. The radial velocity at the bundle entrance can be as high as 15 ft/sec near the tubesheet. This velocity is about the same order of magnitude as that used in tube vibration analysis ($\simeq$ 16 ft/sec) earlier.

FWC FORM 172 - 4

NOTATIONS IN THIS COLUMN INDICATE WHERE CHANGES HAVE BEEN MADE

9.2 Tube Bundle Temperature Distribution at Full Load

In order to ensure that the tube-to-tube temperature differential of the present design is within the acceptable level, the temperature distribution of the IHX tube bundle was investigated using an axisymmetric, two-dimensional (r-z), thermal analysis code. In this investigation, the velocity distribution obtained from the above analysis (with the central downcomer included) was used. Primary side flow was assumed to be equally distributed among all tubes. Figure 13 shows the radial temperature distribution across the tube bundle at three different axial locations; namely, the shell side entrance region, middle of the bundle, and the exit bundle region. The intermediate fluid temperature difference in the inlet region between the outermost tube and the innermost tube location is about 57°F. This is due to the cross flow effect at the entrance region. The temperature near the outer radius is higher. This radial temperature differential will decrease as the intermediate sodium flows towards the shell side exit region. In the exit region, the hotter shell side sodium near the outer radius will flow towards the inner radius, thus mixing with the colder sodium. The temperature difference becomes negligible at the exit region.

Note that in the analysis reported previously in Reference 1, uniform flow is assumed after the first tube support structure. A radial temperature differential of 73°F was found in the inlet span. The effect of the central downcomer gives higher fluid velocity near the lower tubesheet region. This higher fluid momentum allows deeper penetration of fluid to the outer edge of the bundle. Therefore, the radial temperature differential is reduced.

Figure 14 shows the length averaged radial temperature distribution. The average tube bundle temperature is found to be about 712°F. The coldest tube is found near the inner bundle radius.

9.3 Alternate Flow Distribution Method

Figure 14 indicates that the temperature tends to be higher at the outer edge of the bundle. This is due to the cross flow effect at the bundle entrance region and the lack of cross flow outside the entrance and exit region. This suggests that in order to have radially uniform temperature distribution, still more intermediate flow must be diverted toward the outer edge of the bundle. This can be achieved by using variably perforated tube supports. The present tube support has a uniform perforation of about 70%. In order to get more flow on the outer edge of the bundle, it was assumed that the inner 60% of the radius had a perforation of 50%. A flow distribution analysis was performed with this tube support perforation (50% perforation for the inner 60% of the bundle width and 70% perforation for the outer 40% of the tube bundle). The resultant velocity vector plot is shown in Figure 15. The axial velocity profile at the middle of the bundle is shown in Figure 16. As expected, with this support structure perforation, more flow tends to reach the outer bundle region. The axial velocities are about 2.4 ft/sec and 3.2 ft/sec for the 50% perforated region and 70% perforated region, respectively. This velocity distribution was used to obtain

9.3 Alternate Flow Distribution Method (cont'd.)

the bundle temperature distribution. The results are shown in Figure 17 at three bundle locations. Note that at the shell side entrance region, the intermediate temperature distribution profile differs from the uniformly perforated tube support case (see Figure 13) only slightly. The difference increases as the flow proceeds upward. In the variably perforated tube support case, more fluid flows on the outer edge of the bundle. A lower intermediate temperature is found there. This effect is shown in Figure 18. The length-averaged radial temperature differential is smaller than that of the uniformly perforated tube support case.

10. PRIMARY SODIUM PRESSURE LOSS

In Reference 1, the primary side nozzle-to-nozzle pressure loss was estimated to be about 3.2 psi, which is above the 2.5 psi limit specified for the design. The exit passage nozzle contributes about 1 psi to this loss. One way to reduce the loss to an acceptable limit is to increase the exit nozzle size. The effect of the exit nozzle diameter on the primary sodium pressure loss was examined. Figure 19 shows that the total primary sodium pressure loss vs. the exit nozzle I.D. for the one- and two-tube bend design. By increasing the nozzle diameter from its present 42" I.D., the primary side pressure loss can be kept within the acceptable limit.

11. GRID TYPE SUPPORT PLATES WITH NON-UNIFORM OPEN AREA

The grid details, as shown on drawing 51-3145-5-2001 in Reference 1, show a circumferential rib between alternate rows of tubes. The circumferential rib and formed segments occupy about 30% of the free area between tubes on average. This combination produces a 70% perforation at the grid. In order to reduce the perforation an additional circumferential bar can be added to fill the space between alternate rows of tubes. The addition of the bar reduces the open area from 70% to 50% on average. However, the concept of using a non-uniform grid support was rejected because it did not have a strong effect on the intermediate temperature distribution and it would introduce a new uncertainty in flow induced vibration due to the crossflow.

12. REVISIONS TO GENERAL ARRANGEMENT DRAWING

The general arrangement drawing, 51-3145-6-2000, has been revised to incorporate design changes resulting from the current work and from GE comments. The basis for each change is discussed briefly.

12.1 Double Head and J Baffle

The detailed stress analysis of the lower tubesheet in Section 2 indicated that the current loss of intermediate loop transients can be accommodated without the double head at the bottom of the downcomer or the J baffles at the outer edge of the tubesheet. An inspection of the proposed

12.1 Double Head and J Baffle (cont'd.)

CFR transients shows that the head and baffle would probably not be required for these conditions either. The CFR transients would have to be used in the tubesheet analysis to confirm this opinion.

The outer head must be retained to provide a boundary between the primary and intermediate sodium. The inner head and the portion of the cylinder attached to the inner head are removed back to the lowest grid. This will decrease the intermediate pressure drop slightly.

12.2 Seismic Stops at Bottom Tubesheet

Due to the thermal expansion, it is not practical to consider using a seismic stop between the lower tubesheet and the cylinder between the hot and cold pool. The stop has been eliminated from the design. GE has made additional seismic analyses to determine what changes must be made in the plug region to eliminate the need for the lower seismic stop.

12.3 Hot/Cold Interface

The core support structure was originally shown to be connected to the shell. This has been corrected to show a clearance.

12.4 Change to Single Tube Bend

The single tube bend was found feasible in Section 3. The upper tube bend was eliminated and an additional tube support grid was added in place of the bend.

12.5 IRACS Coil Supports

The IRACS coil support was analyzed in Section 8. The support has been added to the drawing.

12.6 Exit Nozzle

Changing from a double bend to a single bend reduced the primary sodium pressure drop, but it still exceeded the 2.5 psi limit. By increasing the exit nozzle diameter from 42 in. to 50 in., the 2.5 psi limit can be met.

NOTATIONS IN THIS COLUMN INDICATE WHERE CHANGES HAVE BEEN MADE

References

1. Preliminary Design of an Alternate Bent Tube IHX for the 1000 MWe Pool Reactor, Foster Wheeler Report ND/78/22, June 22, 1978.

2. Pool Type LMFBR Plant, 1000 MWe, Phase A Design, General Electric Report NP-646, Volume 4, April 1978.

FWC FORM 172 - 4

NOTATIONS IN THIS COLUMN INDICATE WHERE CHANGES HAVE BEEN MADE

BY

APPROVED

FOSTER WHEELER ENERGY CORPORATION
NUCLEAR DEPARTMENT
LIVINGSTON, N. J.

CHARGE NO. 8-51-3145

DOCUMENT NO. ND/78/35

ISSUE 1

DATE 12/8/78

FIGURE 1

LOWER TUBESHEET ANSYS MODEL SHOWING DIMENSIONS AND REGIONS

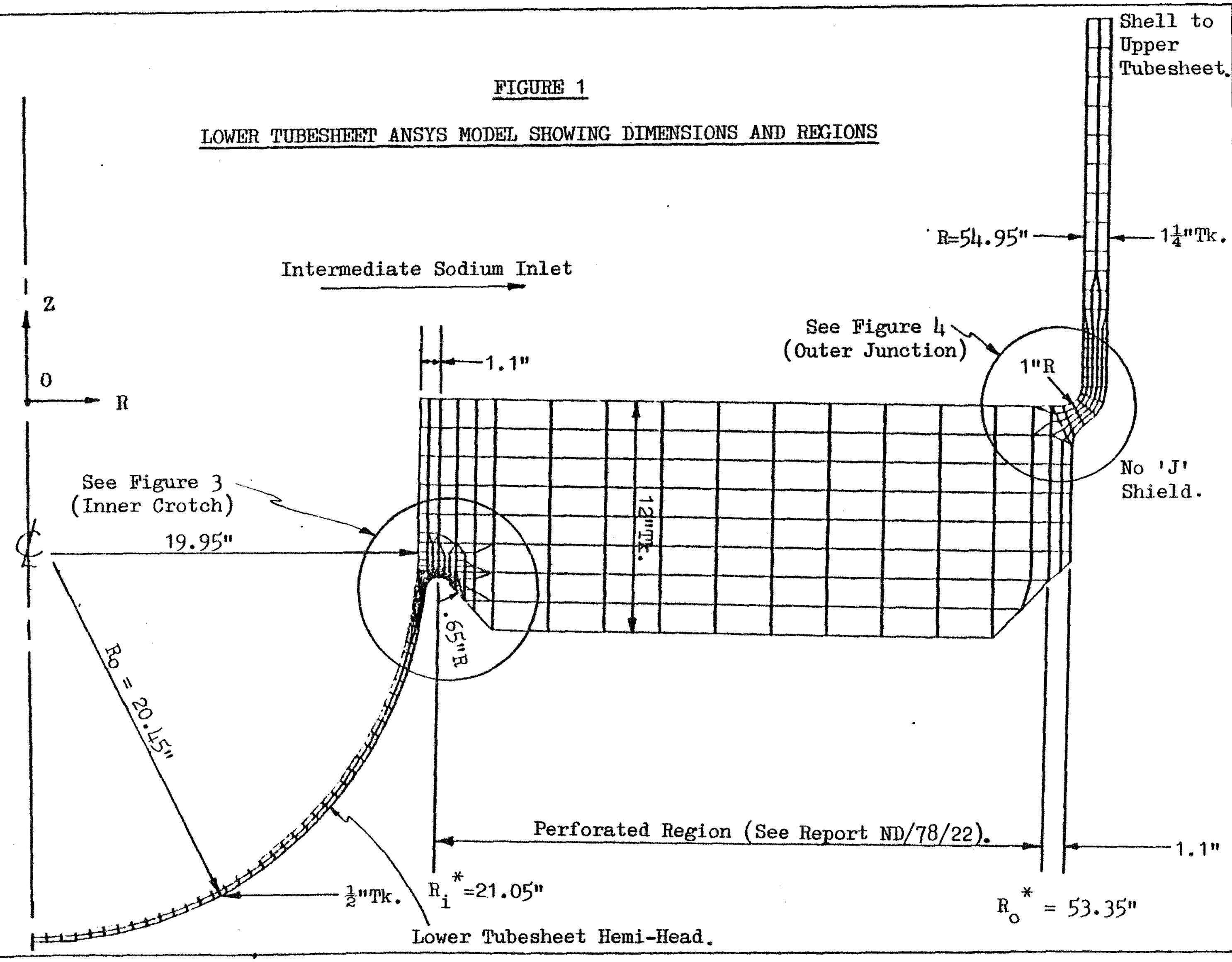

BY

APPROVED

PAGE 14

VA-14

FIGURE 2

LOWER TUBESHEET ANSYS MODEL SHOWING THERMAL STRESS SECTIONS AND CRITICAL ELEMENTS

(See Tables 1 and 2 for stresses)

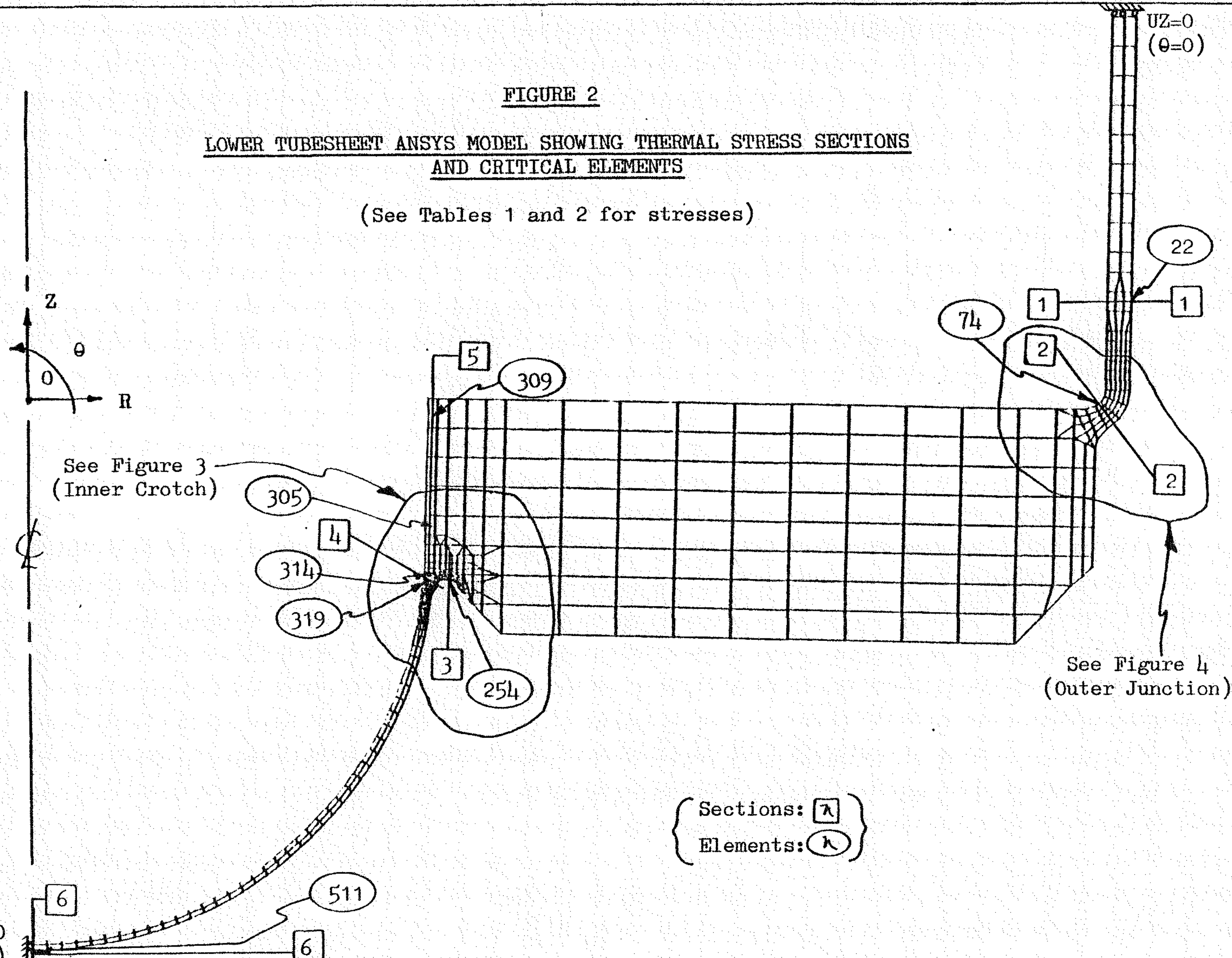

CHARGE NO. 8-51-3145 | DOCUMENT NO. ND/78/35 | ISSUE 1 | DATE 12/8/78

NUCLEAR DEPARTMENT

FOSTER WHEELER ENERGY CORPORATION

LIVINGSTON, N. J.

CHARGE NO. 8-51-3145	DOCUMENT NO. ND/78/35	ISSUE 1	DATE 12/8/78

FIGURE 3

ENLARGED PLOT OF LOWER TUBESHEET INNER CROTCH AREA SHOWING DIMENSIONS AND THERMAL SECTIONS

(See Figure 1)

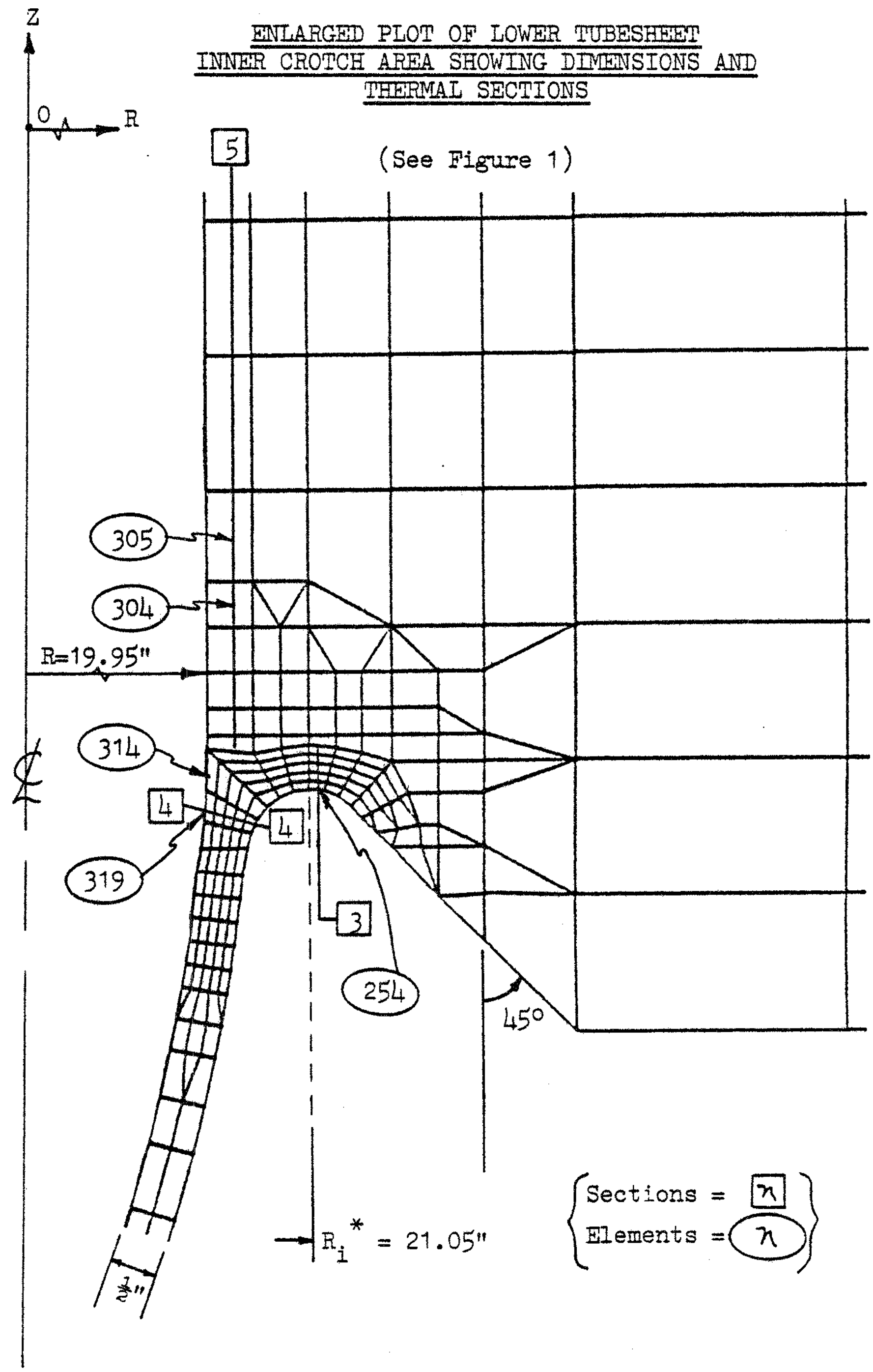

FWC FORM 172 - 4
NOTATIONS IN THIS COLUMN INDICATE WHERE CHANGES HAVE BEEN MADE

BY	APPROVED	PAGE 15

FWC FORM 172 - 4
NOTATIONS IN THIS COLUMN INDICATE WHERE CHANGES HAVE BEEN MADE

CHARGE NO. 8-51-3145	DOCUMENT NO. ND/78/35	ISSUE 1	DATE 12/8/78

FIGURE 4

ENLARGED PLOT OF LOWER TUBESHEET OUTER JUNCTION AREA SHOWING DIMENSIONS AND THERMAL SECTIONS

(See Figure 1)

Sections:
Elements: n

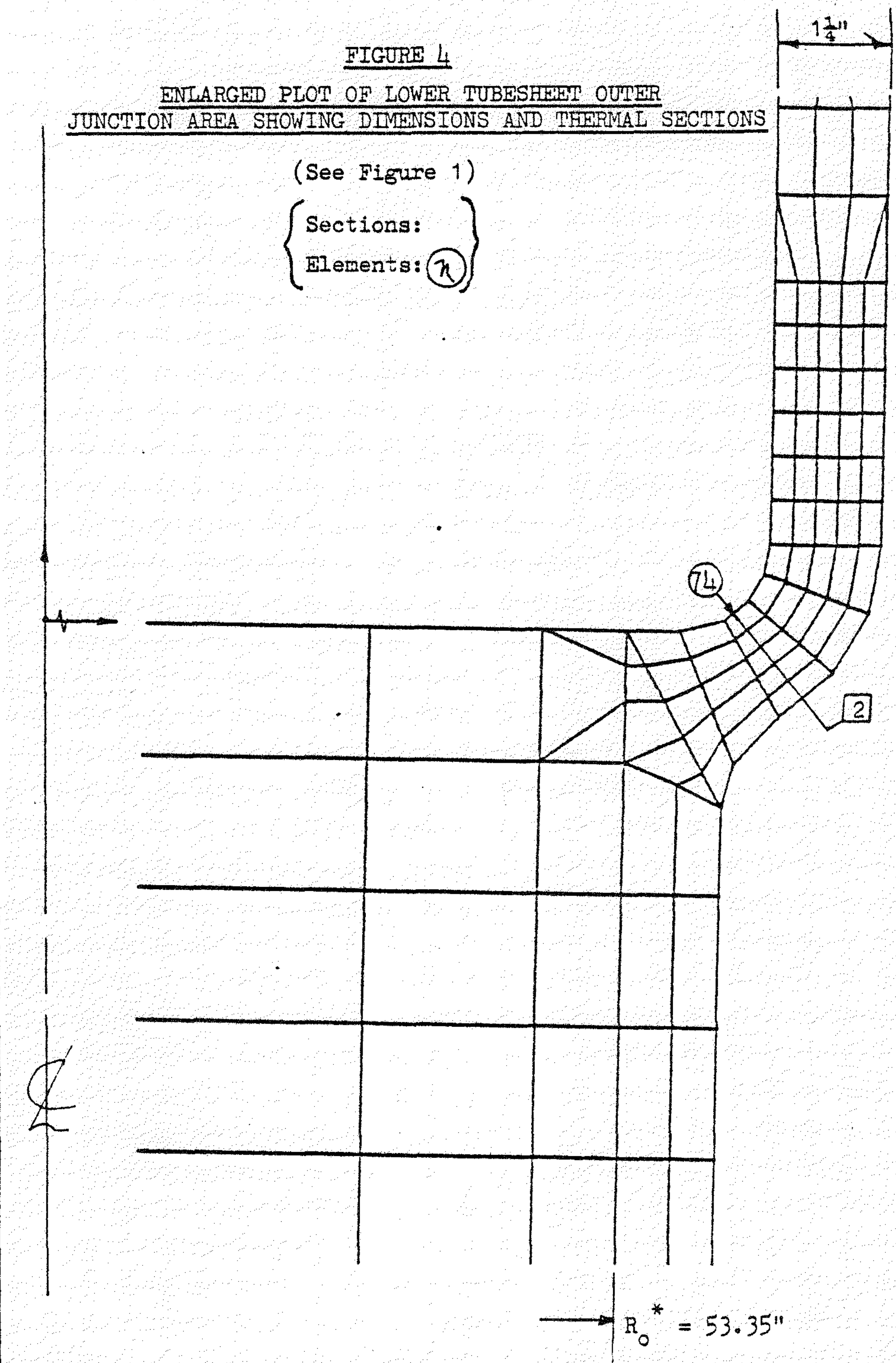

BY	APPROVED	PAGE 16

CHARGE NO. 8-51-3145	DOCUMENT NO. ND/78/35	ISSUE 1	DATE 12/8/78

FIGURE 5

LOWER TUBESHEET MODEL FOR SIMPLIFIED INELASTIC ANALYSIS OF INNER JUNCTION

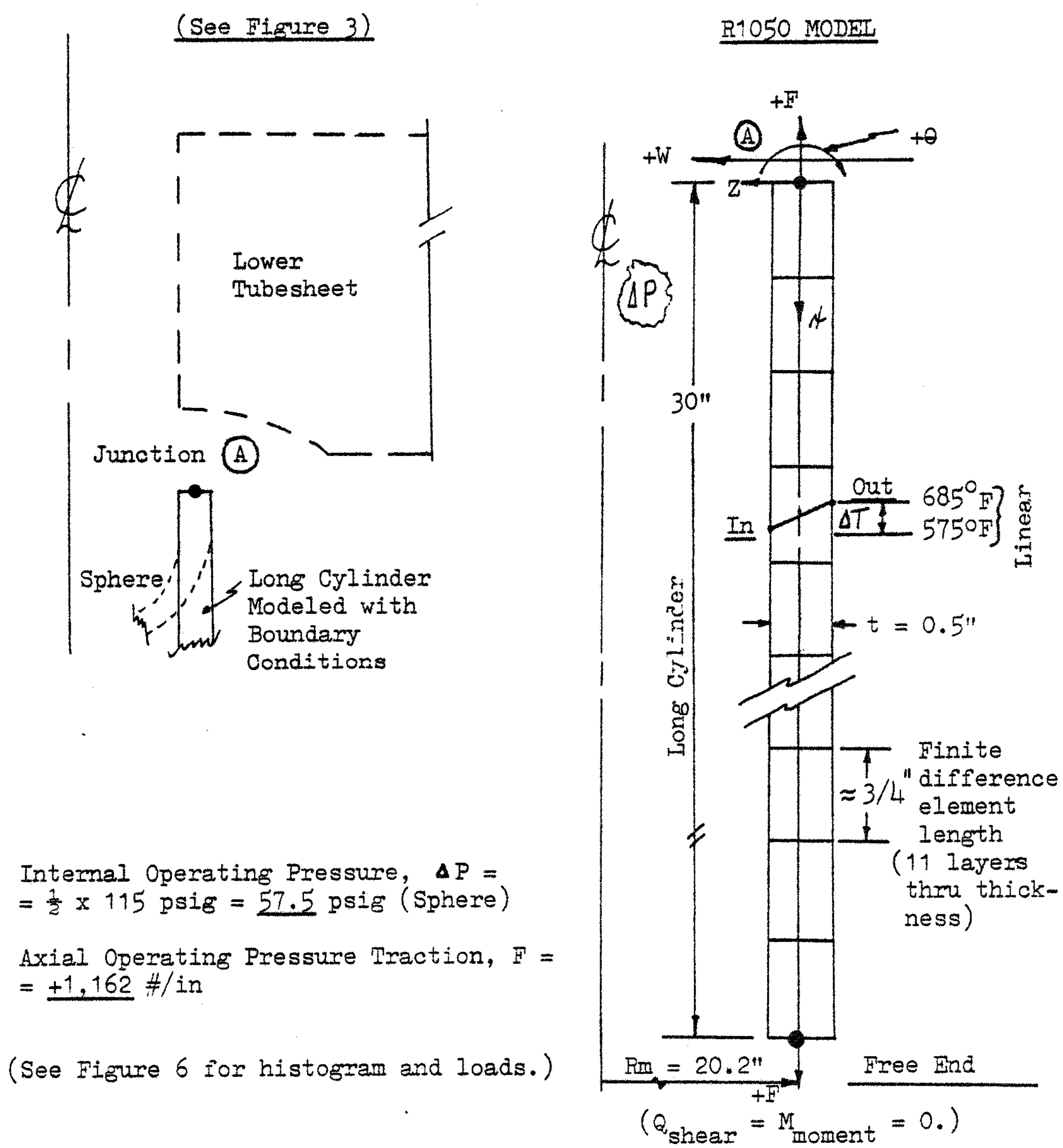

FWC FORM 172 - 4
NOTATIONS IN THIS COLUMN INDICATE WHERE CHANGES HAVE BEEN MADE

BY	APPROVED	PAGE 17

FWC FORM 172 - 4 — NOTATIONS IN THIS COLUMN INDICATE WHERE CHANGES HAVE BEEN MADE

FIGURE 6

LOADING HISTOGRAM FOR LOWER TUBESHEET LOOP LOSS TRANSIENT (1)

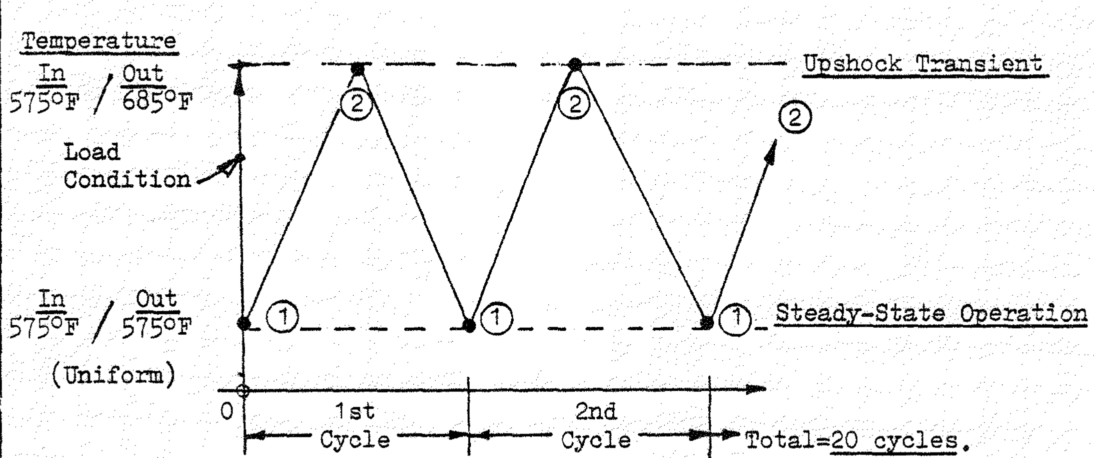

LOAD CONDITION	DESCRIPTION	INTERNAL PRESSURE ΔP (PSIG)	AXIAL TRACTION F (#/IN)	RADIAL TEMP. ΔT (°F)	RADIAL DISPLACEMENT (W-INCHES)	EDGE ROTATION (θ-RADIANS)
1	Steady-State	57.5	+1,162.	0.	-0.005	-0.001
2	Upshock Transient	0.	0.	110.	-0.0482	+0.009

NOTES: (1) See Figure 5 for inelastic cylinder model of lower tubesheet junction.

CHARGE NO. 8-51-3145	DOCUMENT NO. ND/78/35	ISSUE 1	DATE 12/8/78

FIGURE 7

TUBE BEND GEOMETRIES USED TO CALCULATE THERMAL STRESS LEVELS AND INDUCED DISPLACEMENTS

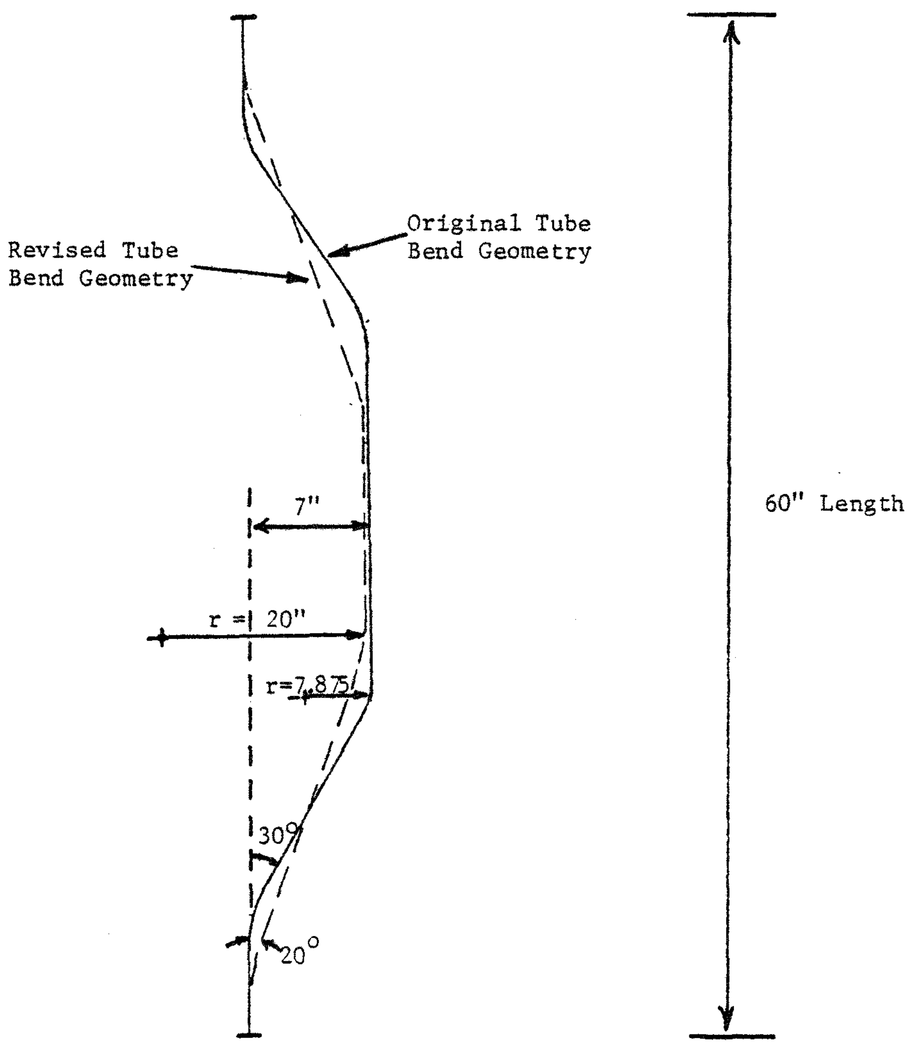

FWC FORM 172 - 4
NOTATIONS IN THIS COLUMN INDICATE WHERE CHANGES HAVE BEEN MADE

FIGURE 8

TEMPERATURE PROFILE OF PLUGGED TUBE AND ACTIVE TUBE DURING FULL POWER

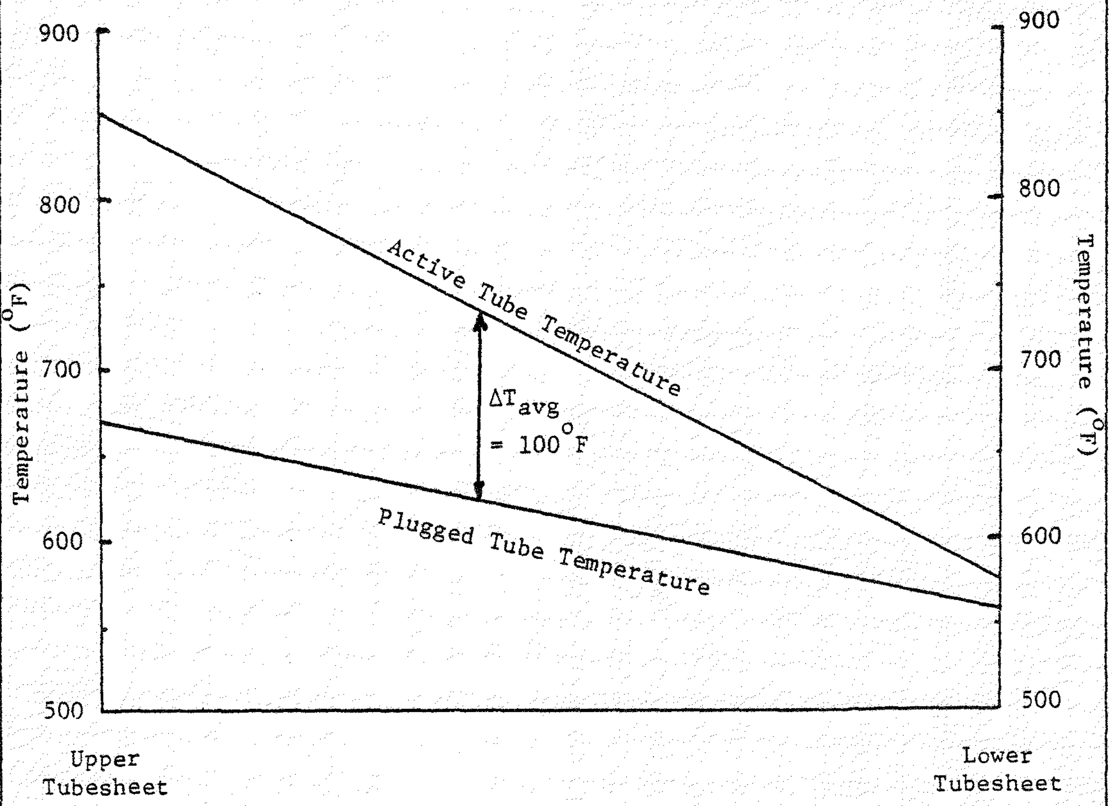

FWC FORM 172 - 4

NOTATIONS IN THIS COLUMN INDICATE WHERE CHANGES HAVE BEEN MADE

FIGURE 9

DISPLACEMENT SHAPE FOR PLUGGED TUBE RELATIVE TO THE ADJACENT ACTIVE TUBE

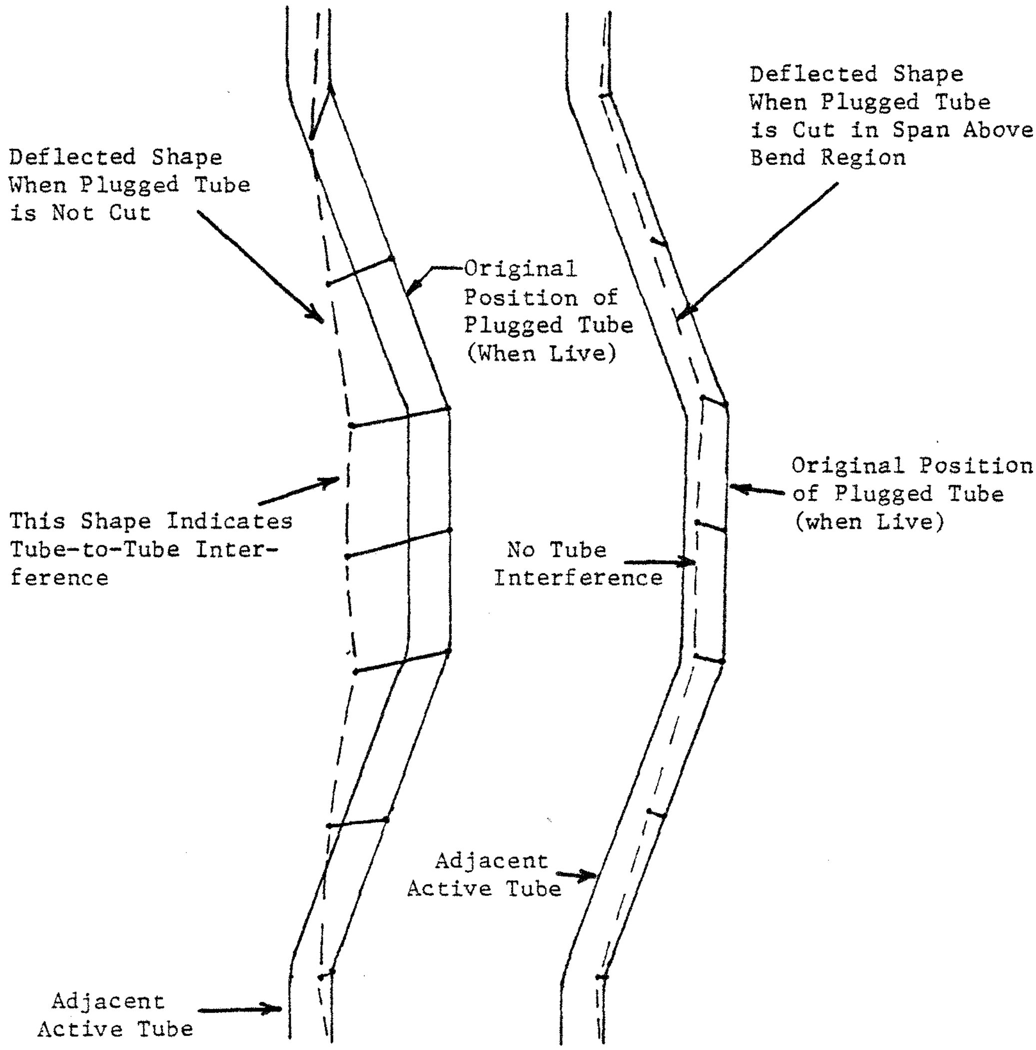

CASE 1 PLUGGED TUBE NOT CUT CASE 2 PLUGGED TUBE CUT

CHARGE NO. 8-51-3145	DOCUMENT NO. ND/78/35	ISSUE 1	DATE 12/8/78

FIGURE 10

IHTS NOZZLE LOADS

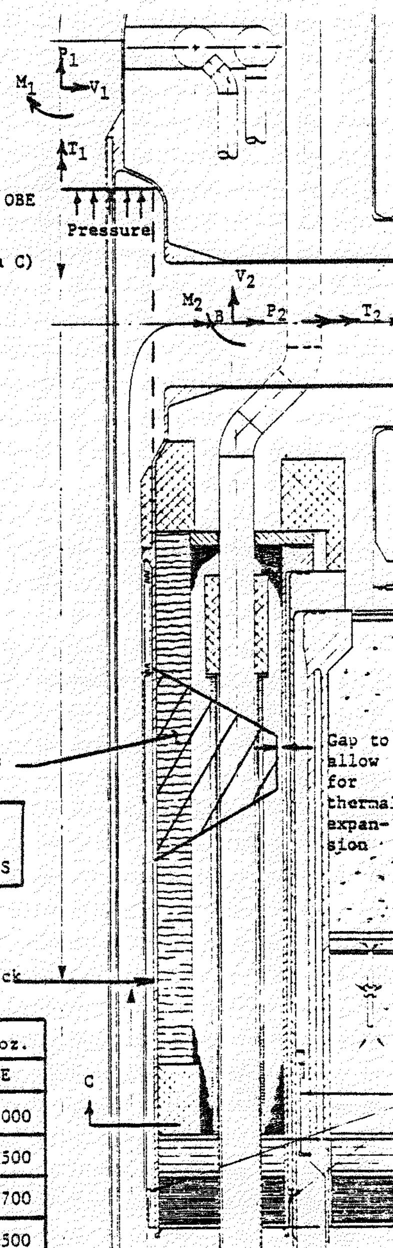

Load Combination

1. Nozzle Loads* - Use dead weight & thermal expansion & OBE
2. Pressure blow-off load (not included in buckling calculation because produces tensile stress at Section C)
3. Seismic load (from overall structural response)

Section C is controlling

Max Stress Intensity for (1 + 2 +3)

σ = 24,650 psi

S_{mt} (1 hr) = S_{mt} (300,000 hr) = 14,600 psi (at 900°F)

Max Axial Compressive Stress

σ_{ax} = -20,970 psi

σ_{allow} = -7,920 psi (load controlled - without gussets)

= -14,260 psi (deflection controlled-with gussets)

Since Section C is over-stressed, even with gussets, must either change thickness to 1.5" or change material to 316 SS

(for 316 SS, σ_{allow} = 20,950 psi for deflection controlled buckling at 900°F)

* Nozzle Loads	Interm. Inlet Noz.			Interm. Outlet Noz.		
	DW	Th Exp	OBE	DW	Th Exp	OBE
Axial (P,lbs)	13,900	32,100	900	0	12,100	34,000
Shear (V, lbs)	0	17,100	28,400	13,900	17,100	14,500
Torsion (T,ft-lbs)	32,700	49,000	81,700	32,700	49,000	81,700
Bending (M,ft-lbs)	46,200	69,400	115,500	46,240	69,400	115,500

BY	APPROVED	PAGE 22

CHARGE NO. 8-51-3145	DOCUMENT NO. ND/78/35	ISSUE 1	DATE 12/S/78

FIGURE 11

CONCEPTUAL DESIGN OF TUBE SUPPORT FOR IRACS AUXILIARY HEAT EXCHANGER

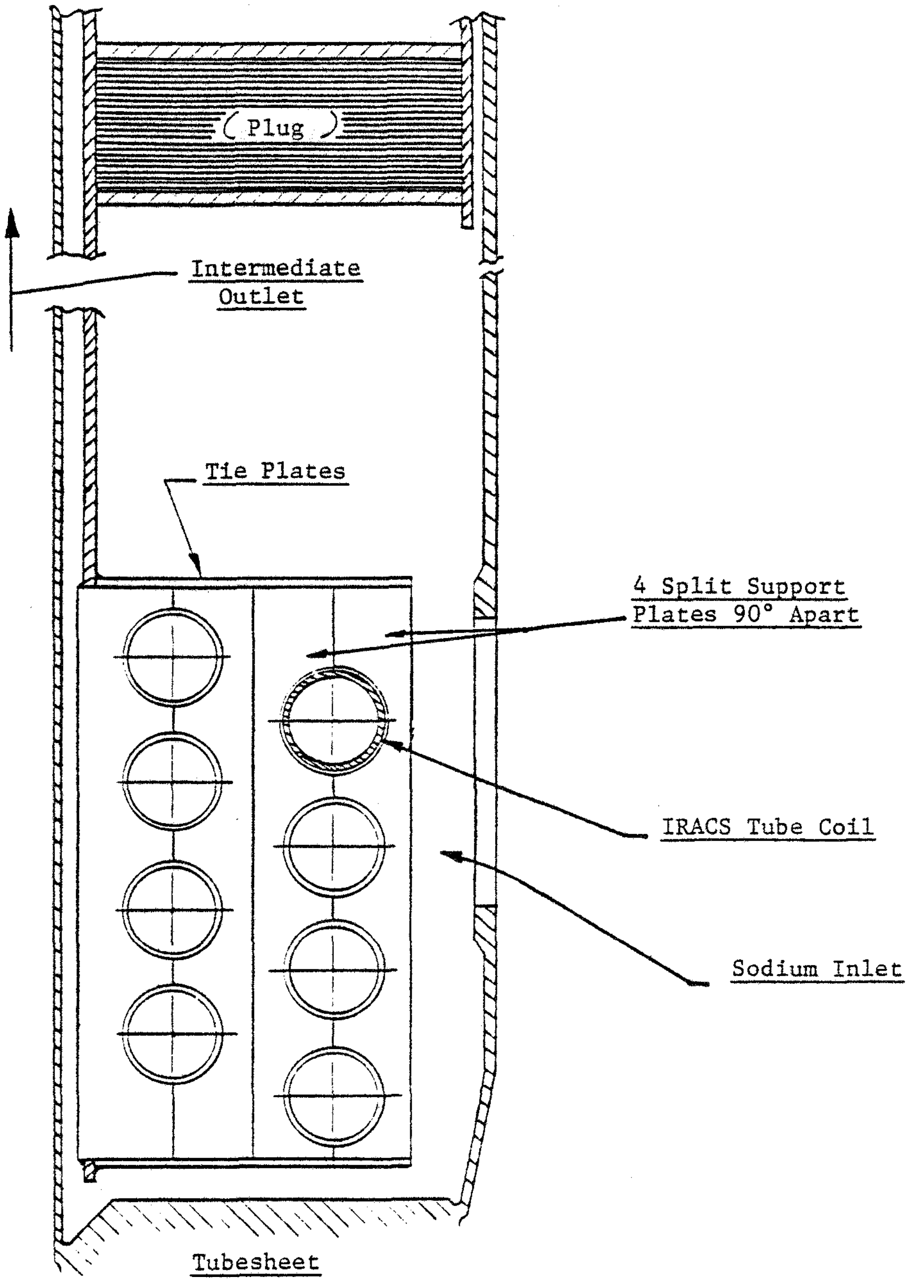

BY	APPROVED	PAGE 23

FIGURE 12

VELOCITY PROFILE WITH UNIFORMLY PERFORATED TUBE SUPPORTS

CHARGE NO. 8-51-3145	DOCUMENT NO. ND/78/35	ISSUE 1	DATE 12/8/78

FIGURE 13

TEMPERATURE DISTRIBUTION AT FULL LOAD (4860 TUBES)

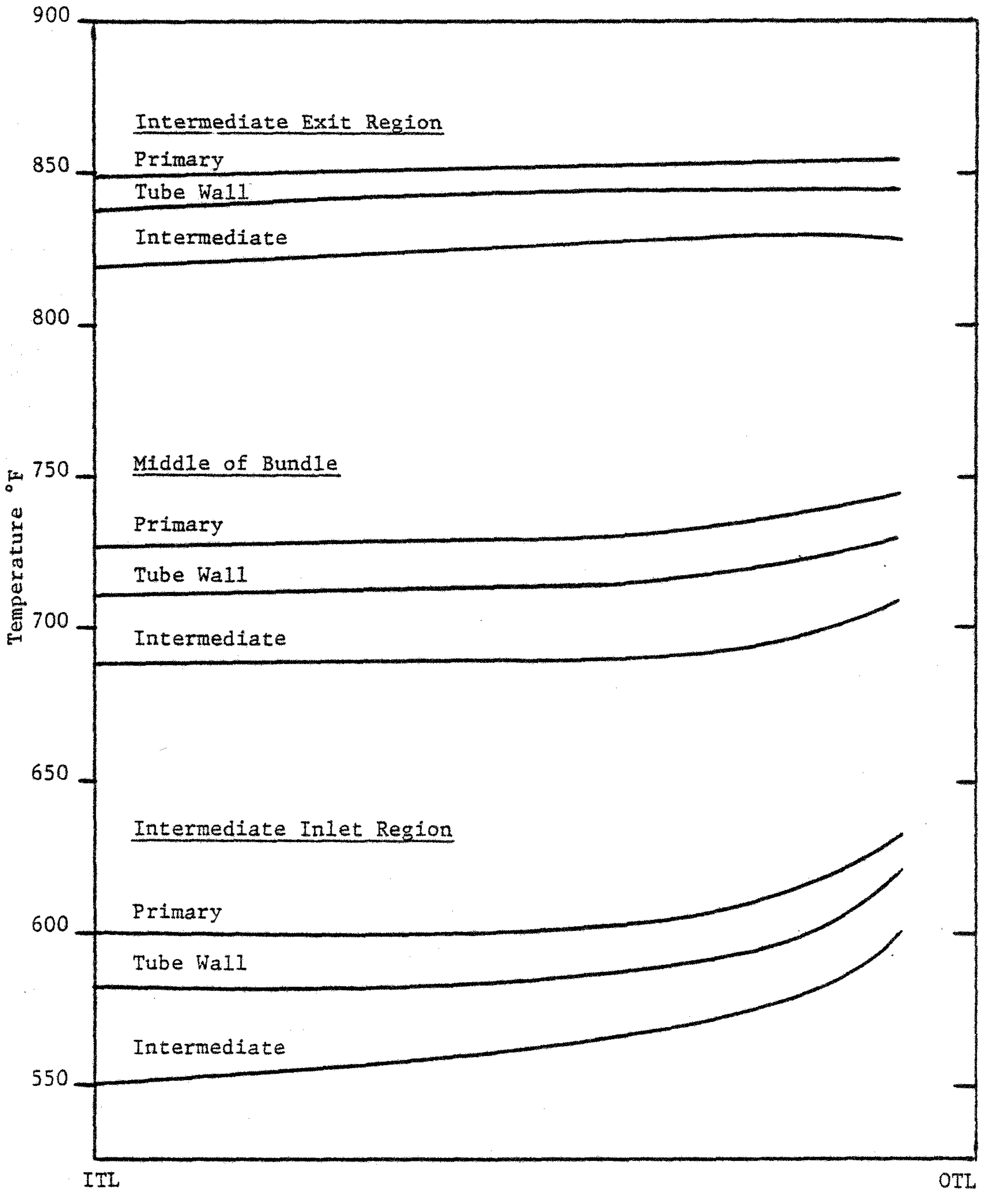

FIGURE 14

LENGTH-AVERAGED RADIAL TEMPERATURE DISTRIBUTION AT FULL LOAD

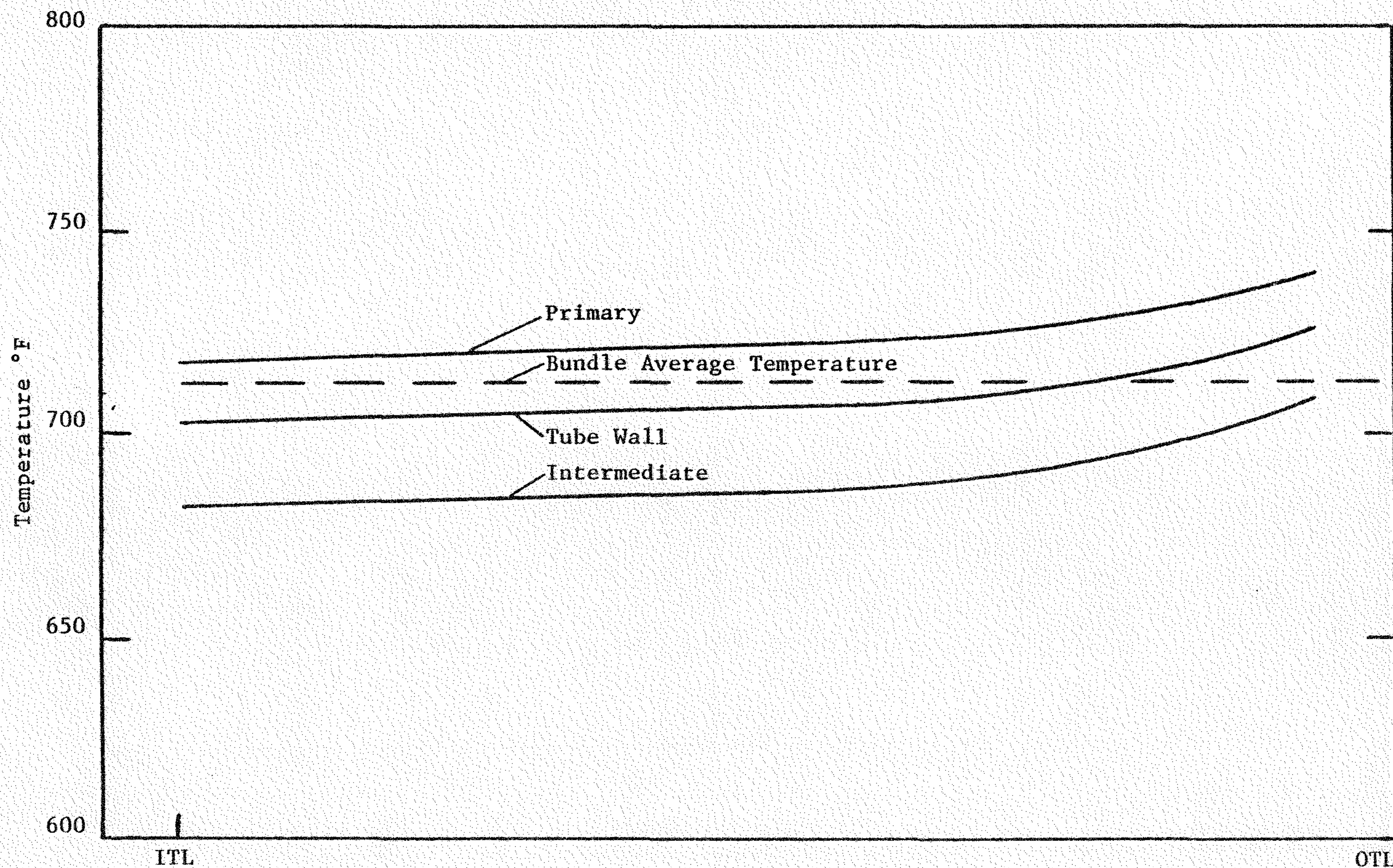

FIGURE 15

VELOCITY PROFILE WITH VARIABLY PERFORATED TUBE SUPPORTS

CHARGE NO. 8-51-3145	DOCUMENT NO. ND/78/35	ISSUE 1	DATE 12/8/78

FWC FORM 172 - 4

NOTATIONS IN THIS COLUMN INDICATE WHERE CHANGES HAVE BEEN MADE

FIGURE 16

AXIAL VELOCITY PROFILE AT MID-BUNDLE

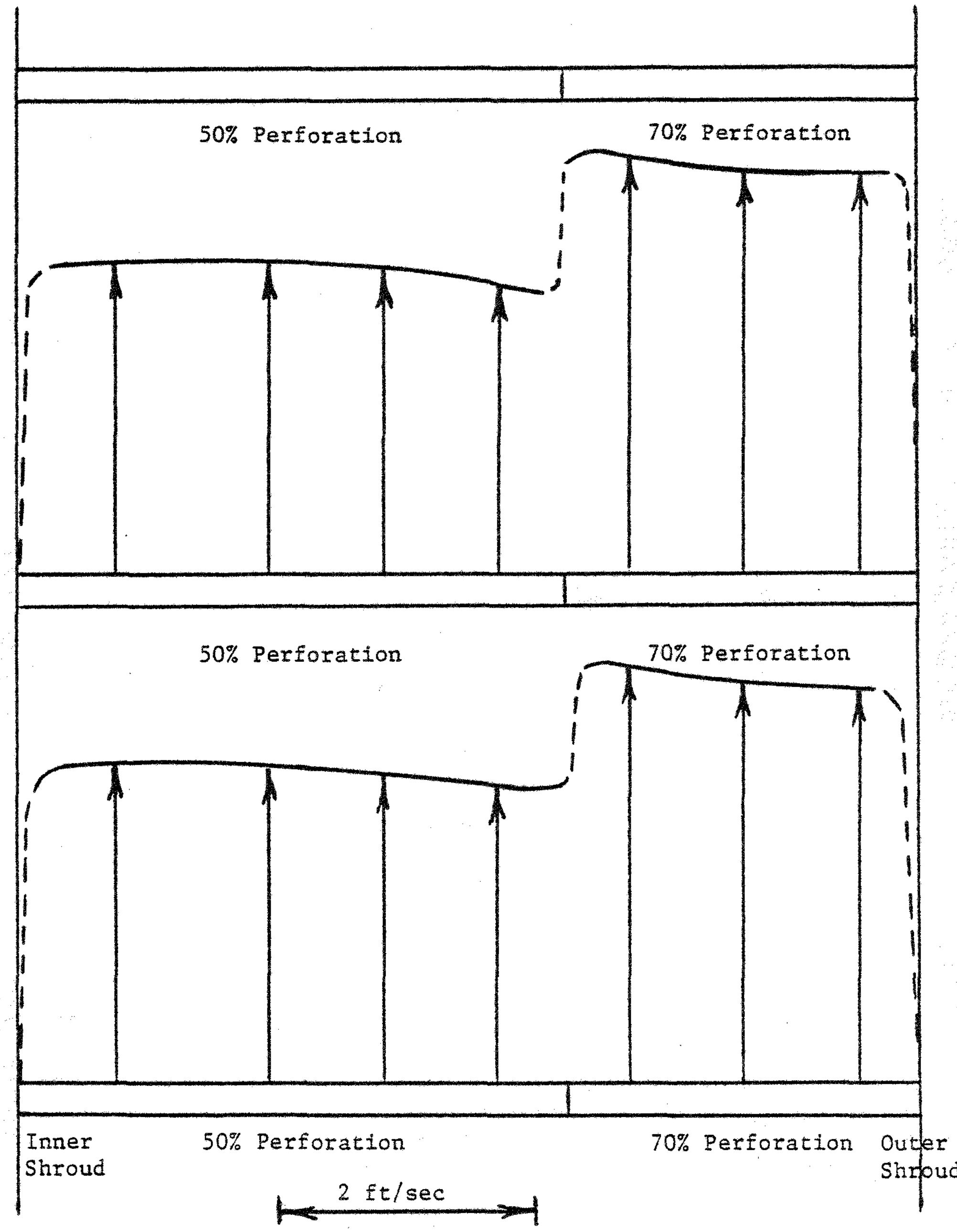

BY	APPROVED	PAGE 28

FIGURE 17

TUBE BUNDLE TEMPERATURE DISTRIBUTION AT FULL LOAD
WITH VARIABLY PERFORATED TUBE SUPPORTS

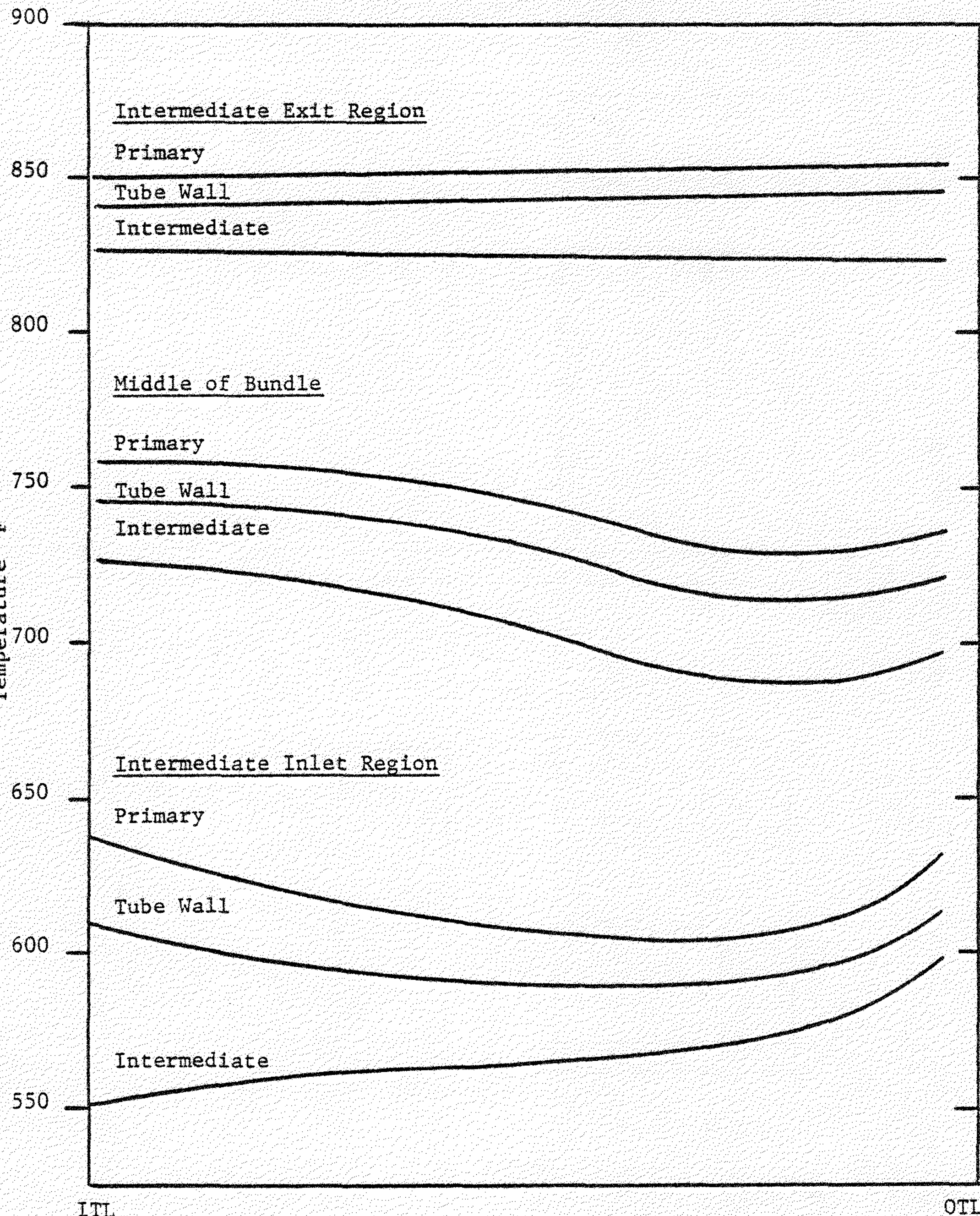

FWC FORM 172 - 4
NOTATIONS IN THIS COLUMN INDICATE WHERE CHANGES HAVE BEEN MADE

FOSTER WHEELER ENERGY CORPORATION
NUCLEAR DEPARTMENT
LIVINGSTON, N. J.

CHARGE NO. 8-51-3145 | DOCUMENT NO. ND/78/35 | ISSUE 1 | DATE 12/8/78

BY | APPROVED | PAGE 30

FIGURE 18

LENGTH-AVERAGED RADIAL TEMPERATURE DISTRIBUTION AT FULL LOAD WITH VARIABLY PERFORATED TUBE SUPPORTS

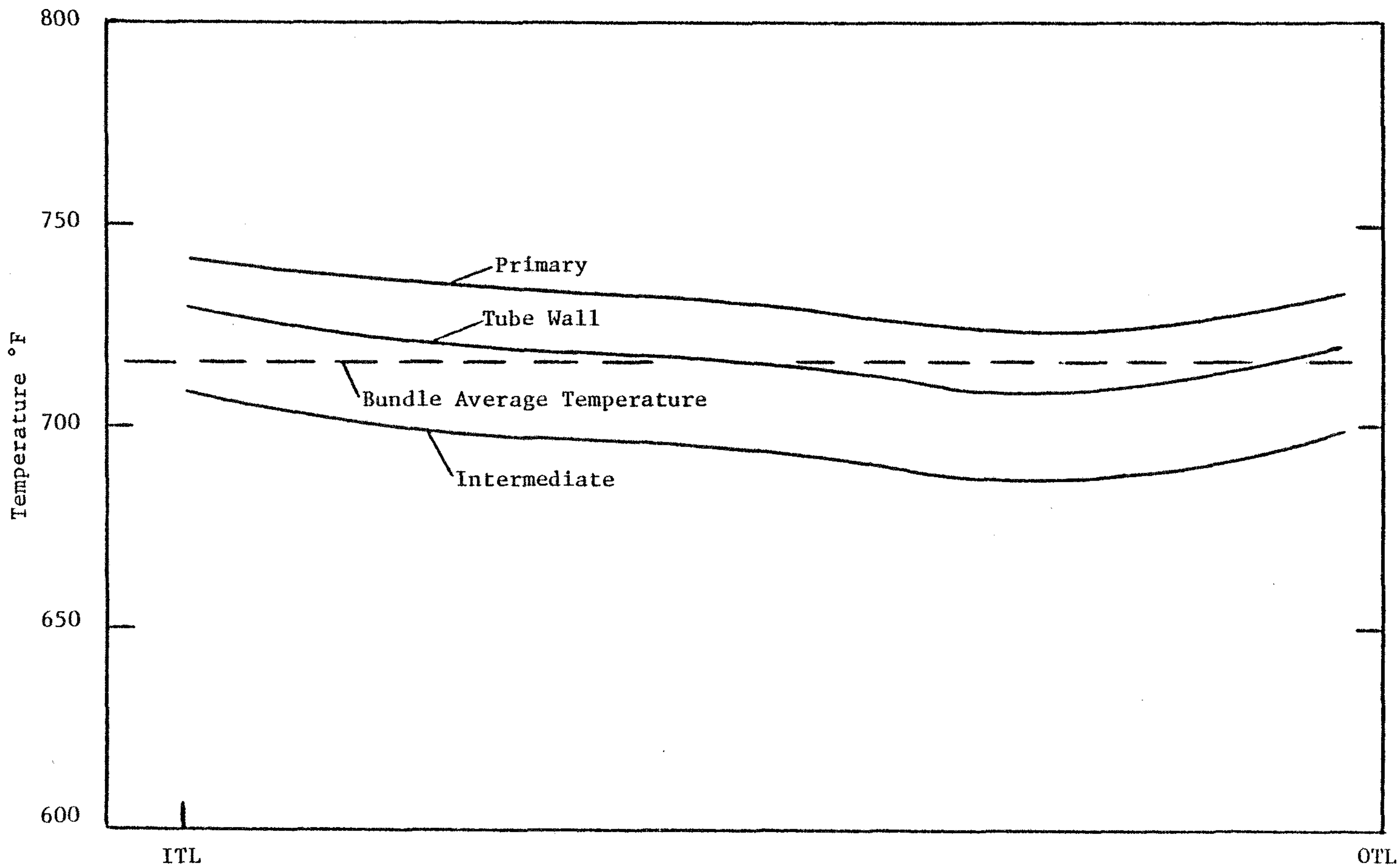

BY

APPROVED

PAGE 31

FIGURE 19

EFFECT OF EXIT NOZZLE ID ON PRIMARY PRESSURE DROP

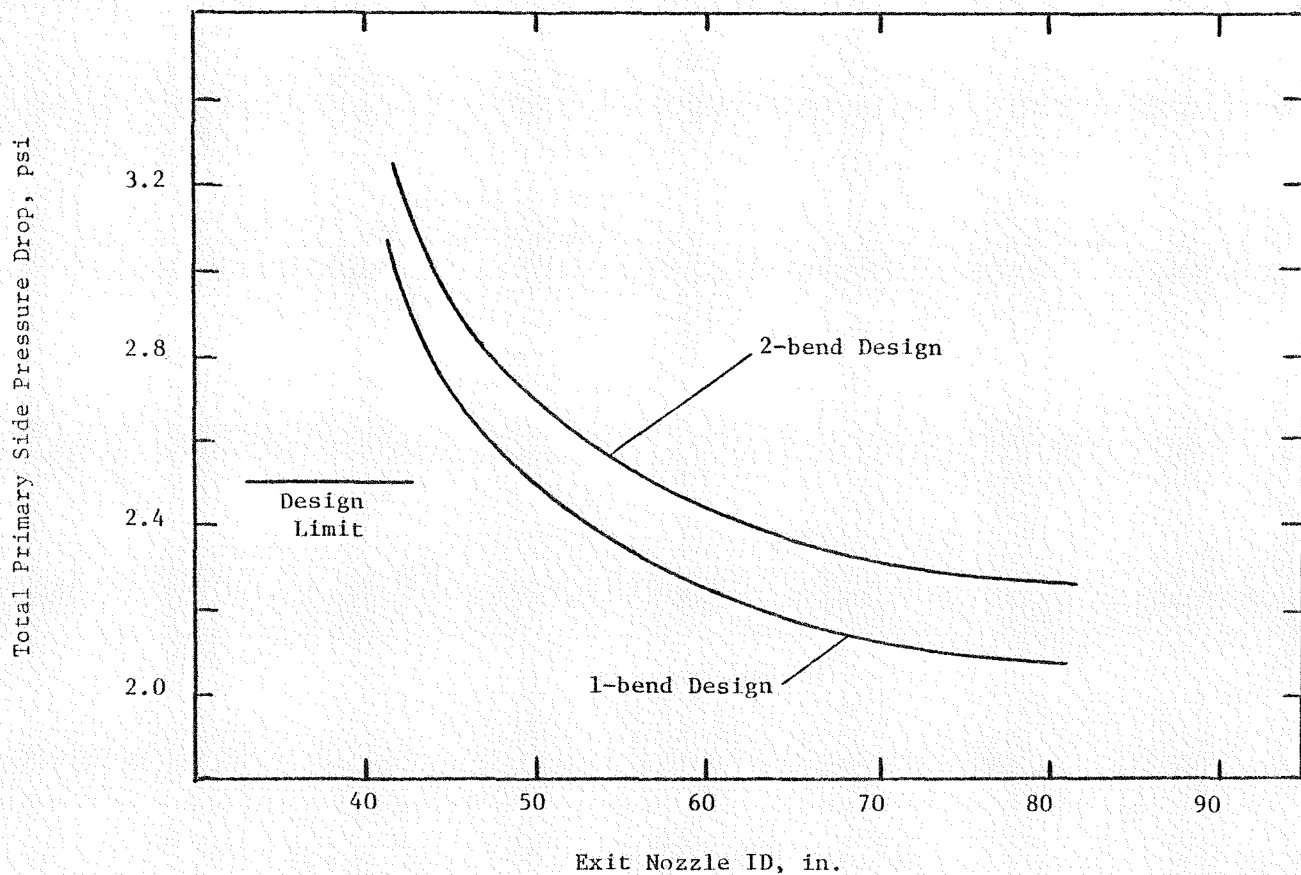

CHARGE NO. 8-51-3145
DOCUMENT NO. ND/78/35
ISSUE 1
DATE 12/8/78

NUCLEAR DEPARTMENT
FOSTER WHEELER ENERGY CORPORATION
LIVINGSTON, N. J.

CHARGE NO. 8-51-3145 | DOCUMENT NO. ND/78/35 | ISSUE 1 | DATE 12/8/78

FWC FORM 172 - 4

NOTATIONS IN THIS COLUMN INDICATE WHERE CHANGES HAVE BEEN MADE

TABLE 1

LOWER TUBESHEET LINEARIZED SURFACE THERMAL STRESSES
WITHOUT INNER THERMAL SHIELD HEAD - INTERMEDIATE LOOP LOSS TRANSIENT

SECTION (1)	ELEMENT (1)	SURFACE STRESSES (PSI)			STRESS (5) INTENSITY (PSI)
		S_1 (MERID.)	S_2 (HOOP)	S_3 (NORMAL)	
1	22	2073.	-3309.	106.	5382.
2	74	10416.	-4950.	2120.	15365.
3	254	79522. (2)	47937. (2)	9724. (2)	69799. (2),(3)
4	314	-12267.	56566.	351.	68833. (4)
	319	-15629.	52001.	-1059.	67630.
5	309	821.	55613.	8231.	54792.
	305	600.	62413.	23065.	61813.
	304	112.	60552.	16457.	60440.
6	511	16250.	16699.	263.	16436.

NOTES:

(1) See Figure 2 for element and section location.

(2) These stresses in perforated region include the stress multiplier of 2.8 and biaxiality k = 1.1, or 2.8 x 1.1 = 3.08 factor.

(3) Maximum Linearized Surface Stress in perforated region.

(4) Maximum Linearized Surface Stress in solid (unperforated) region.

(5) Allowable stress guideline is 3 x Sm - 3 x 15,600 psi = 47,000 psi at average transient temperature of 737°F between 600°F steady state and 875°F maximum upshock upset temperature. (The Sm values are 14,700 psi at 875°F and 16,400 psi at 600°F.)

BY | APPROVED | PAGE 32

FWC FORM 172 - 4

NOTATIONS IN THIS COLUMN INDICATE WHERE CHANGES HAVE BEEN MADE

TABLE 2

LOWER TUBESHEET PEAK SURFACE THERMAL STRESSES
WITHOUT INNER THERMAL SHIELD HEAD - INTERMEDIATE LOOP LOSS TRANSIENT

SECTION (1)	ELEMENT (1)	SURFACE STRESSES (PSI)			STRESS[5] INTENSITY (PSI)
		S_1 (MERID.)	S_2 (HOOP)	S_3 (NORMAL)	
1	22	2335.	-3220.	0.	5555.
2	74	14046.	-4123.	0.	18169.
3	254	92585.[2]	50472.[2]	0.	92585.[2],[3]
4	314	-7512.	57623.	0.	65135.
	319	-16863.	51875.	0.	68738.[4]
5	309	669.	55655.	0.	55655.
	305	-95.	59802.	0.	59897.
	304	521.	60169.	0.	60169.
6	511	21256.	21730.	0.	21730.

NOTES:

(1) See Figure 2 for element and section location.

(2) These stresses in perforated region include the stress multiplier of 2.8 and biaxiality k = 1.1, or 2.8 x 1.1 = 3.08 factor.

(3) Maximum Peak Surface Stress in perforated region.

(4) Maximum Peak Surface Stress in solid (unperforated) region.

(5) Allowable stress guideline is 20 cycles specified for fatigue at average transient temperature of 737°F between 600°F steady state and 875°F maximum upshock upset temperature.

CHARGE NO. 8-51-3145 | DOCUMENT NO. ND/78/35 | ISSUE 1 | DATE 12/8/78

TABLE 3

LOWER TUBESHEET REMOVAL OF INNER THERMAL SHIELD HEAD

Comparison	With Inner Thermal Shield Head (Report ND/78/22)	Without Inner Thermal Shield Head (New Analysis)
Linearized Thermal Bending Stress	53,500 psi (El. 319) (46,300 psi - Perforated El. 254)	68,800 psi (El. 314)(1) (69,800 psi - Perforated El. 254)(1)
Peak Thermal Stress in Perforated Region(3)	59,600 psi (El. 254)	92,600 psi (El. 254)(2)
Gross VAT (Total Perforated Region to Solid Inner Head)	$130^\circ F$	$145^\circ F$
Local VAT (Crotch Perforated Region to Solid Inner Junction)	$35^\circ F$	$50^\circ F$
Thermal Bending (ΔT) Sect. 315 to 319, or 314	$40^\circ F$	$110^\circ F$
Thermal Bending Stress $E\alpha\ \Delta T/2\ (1-\mu) \cong 180\Delta T$	$180 \times 40^\circ F = 7,200$ psi	$180 \times 110^\circ F = 19,800$ psi

NOTES:

(1) See Table 1 and Figure 2; stress values rounded-off.
(2) See Table 2 and Figure 2; stress values rounded-off.
(3) All Perforated Stresses include Stress Multipliers of Tables 1 and 2.

FWC FORM 172 - 4
NOTATIONS IN THIS COLUMN INDICATE WHERE CHANGES HAVE BEEN MADE

BY | APPROVED | PAGE 34

TABLE 4

LOWER TUBESHEET RESULTS OF SIMPLIFIED INELASTIC ANALYSIS
FOR INNER JUNCTION
(See Figure 5 for Model)

Material = 304 SS, Stress-Free Base Temp. = $575^{\circ}F$

Average Temperature for Material Properties = $630^{\circ}F$ ($\approx 600^{\circ}F$)

Properties: $E = 25.4 \times 10^{6}$ psi

$\mu = 0.3$

$\alpha_{Inst.} = 10.49 \times 10^{-6}$ in/in/°F

$E_{plastic} = 1.61 \times 10^{6}$ psi

$S_{yield} = 19{,}470$ psi (Average, True $S - \varepsilon$)

Kinematic Hardening for plasticity; No Creep (Max. Temp. $< 800^{\circ}F$)

Results: (Computer Output "JIGKPYJ")

For specified 20 cycles of Loop Loss operating histogram in Figure 6 (see Figure 6 for Loading Histogram):-

Fatigue Damage, $D_f = 4. \times 10^{-5} \approx 0$, based on $\varepsilon^{Eq.}_{Range} = 0.2 \times 10^{-2}$ in/in

Maximum Linearized Positive principal strains:

		Code Allowables
Average (Mid-Fiber) Hoop Strain, $\varepsilon_{\theta} \approx 0.10\% <$		0.5% Weld Material 1.0% Parent Material
Surface (Inside) Hoop Strain, $\varepsilon_{\theta} \approx 0.16\% <$		1.0% Weld Material 2.0% Parent Material

Above results assume no additional inelastic contribution from the scram transient or any other transients.

FWC FORM 172 - 4

NOTATIONS IN THIS COLUMN INDICATE WHERE CHANGES HAVE BEEN MADE

TABLE 5

HOT/COLD POOL DOUBLE BELLOWS SEAL

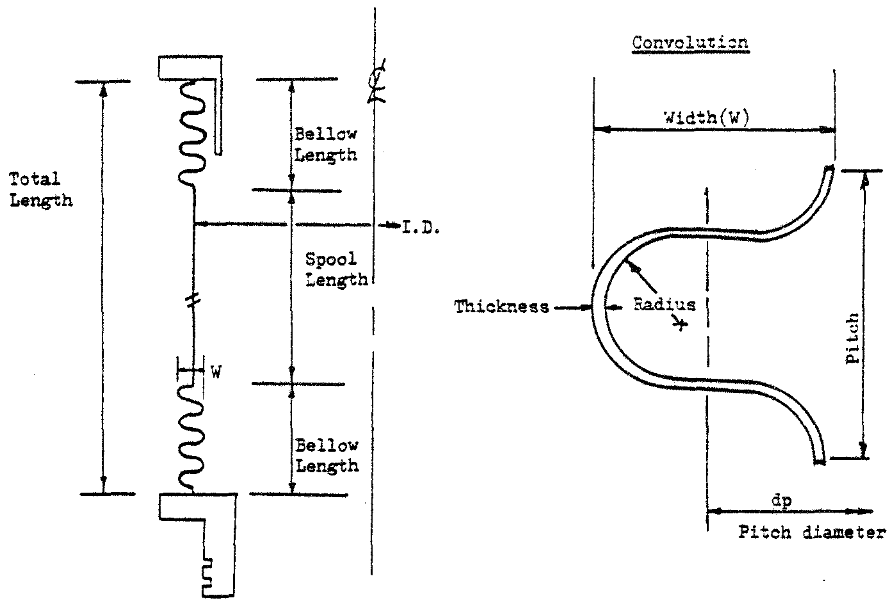

GEOMETRY	I.D. = 80"	I.D. = 60"
Total Length	60"	55"
No. Convolutions/Bellows	8	6
Total No. Convolutions	16	12
Spool Length	39"	39.5"
Convolution Width (W)	3.0"	3.0"
Pitch Diam. dp	83"	63"
Thickness	.036"(20 gage)	.036"(20 gage)
Pitch	1.3"	1.3"
Radii	0.3"	0.3"
Bellows Length (each end)	10.4"	7.8"
APPLIED MOTIONS		
Axial	1.5"	1.5"
Lateral (Seismic)	2.0" ± 1.5"	2.0" ± 2.5"
Rotational	0.20°	0.25°
Applied Pressure Differential:	2.5 psi external	2.5 psi external
Allowable Pressures: (EJMA Formulae)	Internal ΔP = 6 psi External ΔP = 19 psi	Internal ΔP = 6 psi External ΔP = 25 psi

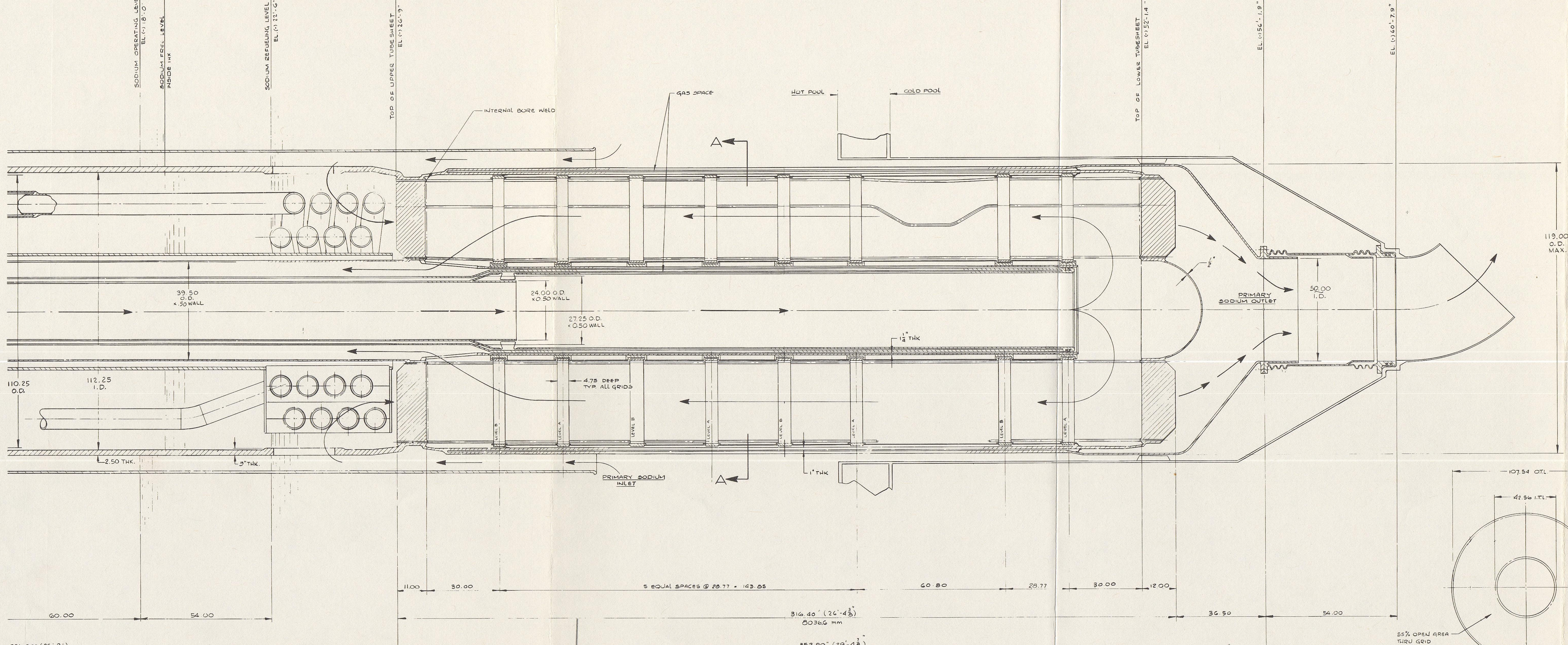

LONGITUDINAL CROSS SECTION
SCALE 3/32" = 0'-1"

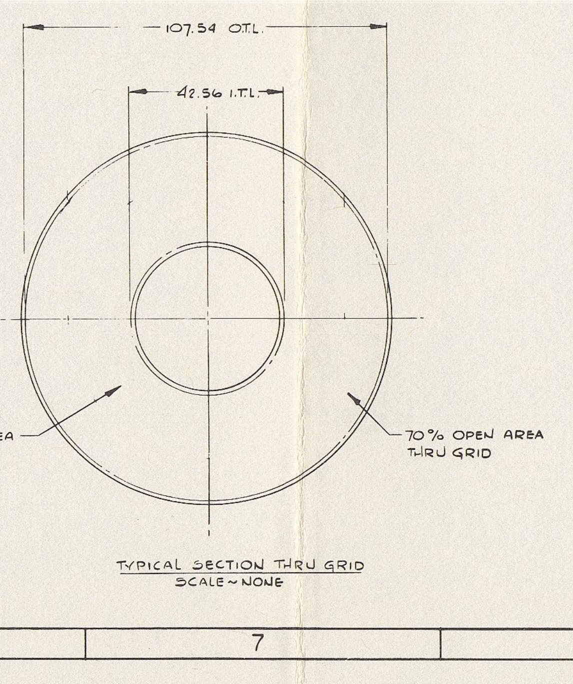

TYPICAL SECTION THRU GRID
SCALE–NONE

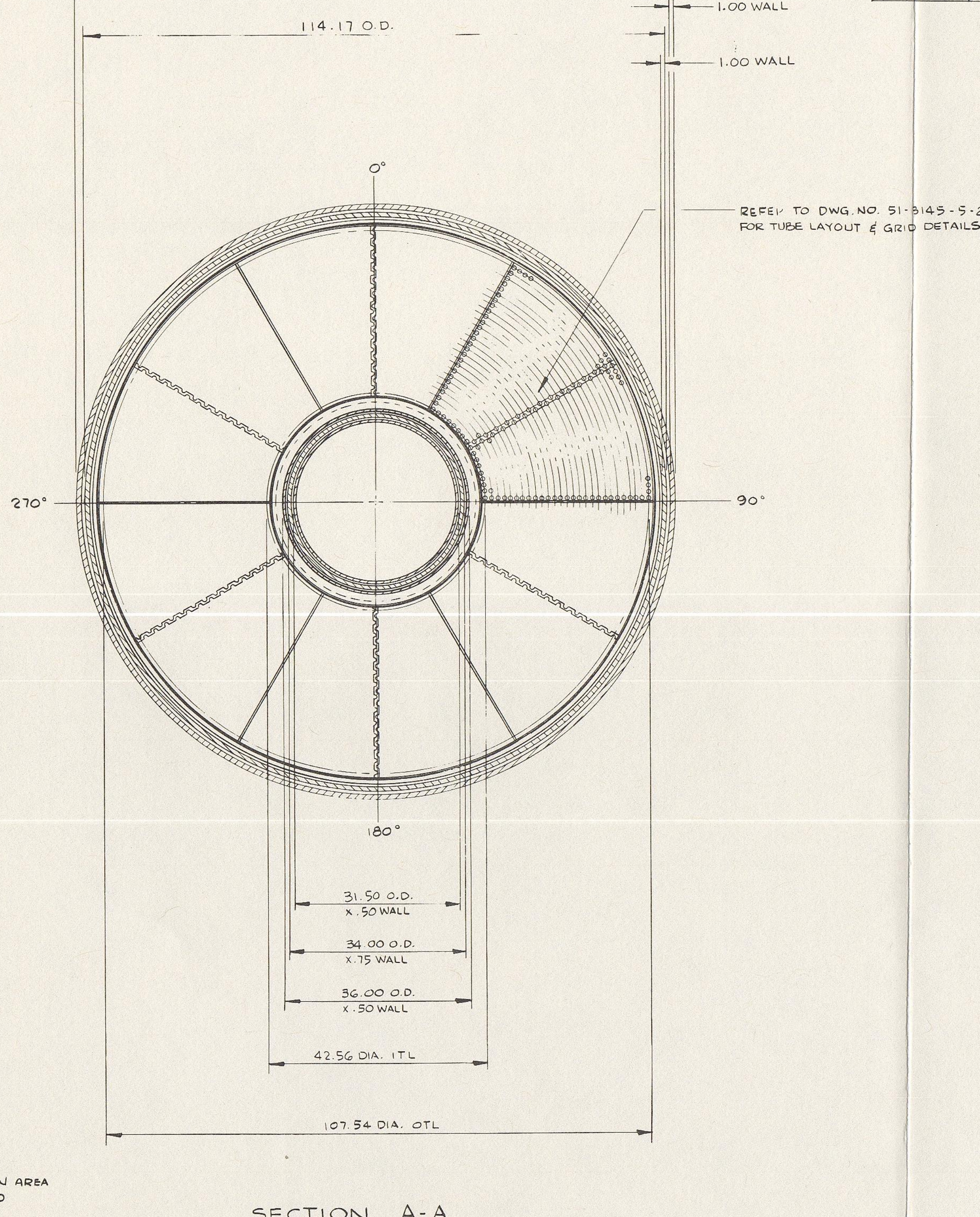

SECTION A-A
SCALE 3/32" = 0'-1"

REFERENCE DRAWINGS

DRAWING NO.	DESCRIPTION
51-3145-6-1000	DESIGN LAYOUT
51-3145-5-2001	TUBE LAYOUT & GRID DETAILS
AFS-SK-PE-002	IHX PLUG REGION (G.E.)

DESIGN AND PERFORMANCE DATA

1. PRIMARY FLOW LOCATION - TUBE SIDE
2. DESIGN TEMPERATURES:
   - PRIMARY 900°F.
   - INTERMEDIATE 835°F.
3. OPERATING TEMPERATURES:
   - PRIMARY INLET 875°F.
   - PRIMARY OUTLET 594°F.
   - INTERM. INLET 550°F.
   - INTERM. OUTLET 815°F.
   - IRACS INLET 580°F.
   - IRACS OUTLET 845°F.
4. NUMBER OF TUBES:
   - PRIMARY BUNDLE - 4860 - .875 O.D. x 0.04 MIN. WALL
   - IRACS BUNDLE - 8.625 O.D. x 0.50 WALL COIL.
5. DESIGN PRESSURE:
   - PRIMARY SIDE 10 PSIG
   - INTERM. SIDE 250 PSIG
6. THERMAL RATING:
   - PRIMARY IHX 486 MWt
   - IRAC S 3 MWt
7. FLOW RATE:
   - PRIMARY KNa · 19.25×10^6 #/HR.
   - INTERM. KNa 20.29×10^6 #/HR.
8. PRESSURE DROP:
   - TUBE SIDE 2.5 PSI
   - SHELL SIDE 27.6 PSI
9. ESTIMATED WEIGHTS:
10. OPERATING PRESSURES:
    - INTERM. SIDE 115 PSIG.

NOTES

1. VESSEL DESIGNED AND FABRICATED IN ACCORDANCE WITH ASME B&PV CODE, NUCLEAR VESSELS, SECTION III, CLASS I, 1977 EDITION.
2. DO NOT SCALE THIS DRAWING, USE FIGURE DIMENSIONS ONLY.
3. ALL DIMENSIONS APPLY AT A STANDARD TEMPERATURE OF 70°F.
4. ALL DIMENSIONS ARE IN INCHES.
5. DIMENSIONING IS IN ACCORDANCE WITH ANSI Y14.5, 1973 EDITION.
6. SURFACE FINISH SHALL BE IN ACCORDANCE WITH ANSI B46.1, UNLESS OTHERWISE SPECIFIED THE FOLLOWING SURFACE FINISHES SHALL APPLY:
   - a) MATING SURFACES 63
   - b) HEAT TRANSFER TUBES 63
   - c) TUBE SHEET HOLES 125
   - d) ALL OTHER SURFACES 250

REFER TO DWG. NO. 51-3145-5-2001 FOR TUBE LAYOUT & GRID DETAILS

PENETRATION SCHEDULE

PENETRATION NO.	DESCRIPTION	PIPE SIZE O.D.	PIPE SIZE WALL	SLEEVE SIZE O.D.	SLEEVE SIZE WALL	OPENING
P1	INTERM. SODIUM INLET	32.00	.500	—	—	—
P2	INTERM. SODIUM OUTLET	32.00	.500	—	—	—
P3	AUX. SODIUM INLET	8.625	.500	10.75	.365	—
P4	AUX. SODIUM OUTLET	8.625	.500	10.75	.365	—
P5	MANWAY	—	—	—	—	24.00
P6	ARGON GAS SUPPLY	*	*	—	—	—
P7	COOLING GAS INLET	12.750	.25	—	—	—
P8	COOLING GAS OUTLET	12.750	.25	—	—	—

* TO BE DETERMINED

MATERIAL SPECIFICATION TABLE

MAJOR PART	ASME SPEC.	FWEC SPEC.
FORGINGS	SA-336 TP304	
NOZZLES	SA-336 TP304	
HEADS	SA-240 TP304	
PLATES	SA-240 TP304	
PIPE	SA-376 TP304	
TUBING	SA-213 TP304	

LEGEND

- DENOTES STEEL
- DENOTES SHIELDING
- DENOTES INSULATION
- DENOTES STEEL SHOT

REVISIONS

LETTER	DATE	DR. INIT.	DESCRIPTION
A	11-22-78	JRG	ADDED 10'-3" DIA TO HANGING SHOP, DESIGN DATA "8" 2.5 PSI WAS 1.6 PSI SHELL THICKNESS 2½" WAS 1½", B-17 REMOVED INNER HEMI-HD AND PISTON RING AND SEISMIC STOP, AT LOWER T/S LOC. B-10. REVISED CORE SUPPORT STRUCTURE TO SHOW CLEARANCE WITH SHELL, LOC. C-18. REMOVED UPPER SIDE BEND AND ADDED ADDITIONAL GRID SUPPORT, LOC C-13. ADDED IRACS COIL SUPPORT, LOC B-16. EXIT NOZZLE, PRIMARY SODIUM 50" WAS 42", LOC. C-9. REMOVED NOTE # 7

G.E. POOL IHX
DESIGN LAYOUT

DRAWING NUMBER	SCALE: AS NOTED - 1"-0"
51-3145-6-2000	REVISION A

DWG. MADE & APPROVED BY	INITIAL	DATE	CONT. NO.
DRAFTSMAN	RMS	6-1-78	ORDER NUMBERS
CHECKER			
SQUAD LEADER			
SECTION HEAD	[signature]	6-20-78	
CONT. SUPV.			

TOP VIEW
SCALE 3/32 = 0'-1"
NOTE: SEE PENETRATION SCHEDULE FOR PENETRATION SIZES.
P1
P2
0°
P3
270°
90°
P4
P7
P8
180°
P5
P6
45°
45°
156.00
3962.4mm
DIA.
P1
P2
P3
P4
P5
P6
P7
P8
TOP OF DECK - IHX SEAT
EL. 0'-0" DATUM
SODIUM VAPOR TRAPS
EL. (-) 11'-0"
WIRE MESH
THERMAL INSULATION
PLATES
EL. (-) 13'-0"
10'-3" DIA.
JET PUMP
NITROGEN GAS
6.00
10.00
120.00
72.00
132.00
24.00
360.00 (30'-0")
762.0mm

APPENDIX VB

Primary Cold Leg Mechanical

Pump Conceptual Design

Study, Phase A Extension 2

For Pool Reactor Concept

PRIMARY COLD LEG MECHANICAL PUMP CONCEPTUAL DESIGN STUDY PHASE A EXTENSION 2

FOR

POOL REACTOR CONCEPT

PREPARED UNDER P.O. NO. 190-K3G32
FOR
GENERAL ELECTRIC COMPANY
ADVANCED REACTOR SYSTEMS DEPARTMENT

BYRON JACKSON PUMP DIVISION
BORG WARNER CORPORATION

ORDER NO. 781-G-0500

DECEMBER 1978

TABLE OF CONTENTS

LIST OF TABLES

LIST OF DRAWINGS

1.0 INTRODUCTION

This study is submitted to satisfy the specification requirements as outlined in the General Electric Company Purchase Order No. 190-K3G32. The total system pressure drop in the Phase A Study* was 90 psi but is increased to 120 psi for this Extension 2 work. The objectives of this study are to re-size and re-define the primary pump to accommodate this higher system pressure drop. Any new key features will be described.

A structural analysis, shaft dynamic analysis, and seismic analysis will be performed, as needed, to demonstrate that no insurmountable problems exist with the new pump design.

The pump selection will be made to suit either a variable speed or constant speed motor.

A response will be developed to the EPRI pump consultant comments on the Phase A Study.

Brief comments will be made regarding maintenance considerations for the pump.

*"Pool-Type LMFBR Plant, 1000 MWe Phase A Design", EPRI NP-646, Volume 1 and 2, Part II, Heat Transport Systems, April, 1978.

2.0 SUMMARY

The change in pressure drop will require a larger pump or a higher speed. The limited NPSH available remains the predominant factor in the pump selection. The 116% flow runout requirement actually places an upper limit on the pump speed.

There is no reason for changing the basic design submitted in the Phase A concept. The design will consist of two stages of a double suction impeller pumping in parallel. This is particularly applicable where the four impeller inlets are flooded, as in a pool type reactor.

Since there is a possibility of using either a variable speed or constant speed motor, a pump is selected that will be suitable for both. The pump can also be lengthened to increase the available NPSH for the flow runout condition.

Multi-stage double suction pumps with the impellers pumping in parallel have been built, tested, and are in service. Evidence appears in the report.

Consideration is given to maintenance and accessibility in the pump design. Special tools and fixtures will be supplied where required.

In conclusion, the selected pump design concept is based on experience to give reliability and long life. Development work is desirable, but would be required only to verify certain design areas.

The summary for the structural and dynamic analysis appears in the stress analysis section.

3.0 PUMP SELECTION

3.1 Type of Pump

The various possible pump design concepts were covered in Phase A, including a double suction type, an inducer type and an axial floor type. It was shown that the limited NPSH available is the prime controlling factor. Based on experience, a double suction type pump is selected. This gives the impeller two inlets and thus a lower eye velocity for a given flow. A further refinement to favor NPSH is a design utilizing more inlets. This leads to two double-suction impellers pumping in parallel. With double suction impellers, the total flow is divided into four inlets. This is particularly applicable to the pool type plant, since all of the inlets are immersed in the sodium being pumped. The suction side of the pump is no different for a multi-stage than it would be for a single stage.

The type of pump concept is the same as the one selected for Phase A. Impellers will be double suction type, which is merely two single suction impellers integrally joined back-to-back. Two double-suction impellers pumping in parallel are selected to suit the low available NPSH and to give an economical size. A single double-suction type pump was studied in the normal sequence of making a selection. For comparison, the characteristics of this single double-suction pump are shown in Table 1, Page 25.

3.2 Size of Pump

The size of the pump for this study must be changed to suit the new head and capacity requirements. In Phase A the capacity or discharge flow was 65,820 GPM. This has been increased to 68,450 GPM. The head or pressure drop in Phase A was 237 feet. For this study, this has been increased to 316 feet. In addition, a runout condition of 116% of design flow must be considered in the pump size selection.

Various speeds were considered so that a satisfactory selection could be made. In each case, such things as hydraulic parameters, size of impeller, volute area, and NPSH requirement were developed. A suitable model, if available, was selected. A curve was drawn showing performance characteristics.

As the study progressed, additional design requirements were added. One was the runout flow required from each pump for different plant conditions. Since the NPSH available does not change for this runout of 116% of design flow, the speed is limited to this requirement.

Another requirement was the consideration of a constant speed motor. This places a restriction on the speeds available. It was decided to select a speed suitable for both variable and constant speed motors. This would give flexibility to the motor selection and allow additional time for a decision without holding up the pump selection.

3.3 Speed of Pump

3.3.1 The first pump considered was a single double-suction type. A variable speed motor at 725 RPM was selected, to satisfy the available NPSH limitation. A suitable model was found so that required sizes could be determined.

The suction specific speed of the pump is satisfactory. Reliability should be good. The size, however, becomes quite large. The impeller diameter is about 50 inches. Required volute area is high. The pump will require an opening in the support deck over 7 feet in diameter. While this is perhaps acceptable, it is not desirable. The length of the pump from the discharge nozzle to the top of the motor support will be about 45 feet.

3.3.2 The next pump considered was a concept similar to the reference design selected for Phase A. It consists of two double suction impellers pumping in parallel. Each impeller supplies half the flow at the full head. The two impellers are of course identical. The impeller inlets are immersed at least one foot below the surface of sodium when the pump is operating at design speed.

For the same available NPSH, the pump speed can be increased over that required for a single stage pump. A variable speed motor of 1000 RPM maximum was selected. This satisfies the suction specific speed limitation.

Again, a suitable model is selected so that sizes and performance can be established. The required impeller would be about 36 inches in diameter. The pump length would be made to give 38 feet of NPSH. The opening in the support deck would be about 78 inches in diameter.

This speed and size would serve for the reference design using a variable speed motor. A curve is made showing the performance.

3.3.3 There would have been no need for looking at other pump speeds except for the possible use of a constant speed motor. The speed selected for a constant speed motor is subject to 300 RPM increments. A variable speed motor could be used to give the same speed. Ideally, the pump is sized for the constant speed limitation.

The first selection is for the two stage concept at 1180 RPM. The pump would have to be longer, to give 45 feet of NPSH, and satisfy the suction specific speed limitation. This speed would require a small diameter impeller, 32 inches, which would lead to an opening in the deck under 6 feet in diameter. The speed coupled with the required length of the pump is not desirable dynamically. The size of the shaft and the number and location of bearings may overcome the decrease in size. This speed could be used, but a drop to a lower constant speed would give a more conservative design. Furthermore, the run-out condition makes this speed too high.

3.3.4 The next constant speed considered is 870 RPM. The design concept is for two stages of a double suction impeller pumping in parallel.

The pump length is made to give an NPSH of 40 feet. This gives a satisfactory suction specific speed at design and runout flows. This speed would require an impeller about 42 inch diameter. The opening in the support structure for the pump would have to be slightly over 6 feet in diameter.

The selected speed combined with the relatively short pump should give a satisfactory shaft dynamic analysis. It is a conservative choice that should give the desired reliability for this type of pump.

A model with the same specific speed was selected for this pump. Using the model factor, a complete performance curve was made.

This pump speed will give an acceptable NPSH safety margin at design flow. Cavitation should be at an absolute minimum so that the expected long life can be accomplished.

4.0 PUMP SELECTION - SUMMARY

In summary, four speeds were considered in this study. For convenient comparison, the type of pump and speeds considered are tabulated in Table 1. Similarity parameters, speed, and size are shown, to assist in making the most attractive selection.

It was decided to select a speed suitable for a constant or variable speed motor. This narrowed the selection down to 870 and 1180 RPM. The slower speed of 870 RPM was selected for conservatism and reliability. The increase in size over the higher speed pump is a worthwhile trade-off. The desired critical speed should be more readily attained. Perhaps the most important factor of this speed is at the suction side of the pump. There should be very little damaging cavitation, if any, giving a long pump life expectancy.

Results of the dynamics and critical speed analysis are given in the structural and dynamics section.

5.0 KEY FEATURES OF THE PUMP

5.1 General

All parts that were covered in the Phase A study will not be repeated here. Only parts or features that are new or different will be described.

5.2 Shut-Off Valve

A shut-off valve at the outlet nozzle is used to prevent sodium backflow through a disabled pump. A conceptual valve for this purpose is shown at the bottom of the pump. The valve opens and closes with vertical motion. Two rods 180° apart, located vertically, provide the motion and actuate the valve. The rods extend vertically to the seal cartridge location. The method of providing vertical valve movement through the rods will not be a part of this study. It is merely shown that the valve could conveniently be a part of the pump.

5.3 Hydrostatic Bearing

The type of bearing has not changed from the one described in Phase A. However, the size and location has been changed. This was done as one of the things to satisfy the dynamics analysis.

The size of the bearing has been increased from 16 inch to 30 inch diameter. It should be remembered that the radial load has been increased due to the additional pump head. Also, the bearing was moved from its position at the bottom of the pump in Phase A, and located between the two impellers. At this location, the bearing has to be axially split for assembly and dismantling. This does not present any particular manufacturing problem.

Flow from discharge to the bearing pockets and return to suction is similar to the design in Phase A.

The bearing lands and end rings are hard-surfaced.

The length of the pump makes it necessary to have another hydrostatic bearing just below the lowest liquid level. This gives a satisfactory bearing span and allows the use of a smaller shaft. The size of the bearing is 16 inch diameter. Except for size, this bearing is similar to the one used in Phase A.

5.4 Radial Bearing (In Seal Area)

The span between the radial bearings in the pump and the lower radial bearing in the motor is quite long. To keep the critical speed a safe margin above the operating speed, two things can be done. First, the size of the shaft can be made large. This would penalize the size of the seals. The second method would be to place another bearing in the pump to cut down the span.

For this design, an oil lubricated radial bearing will be located in the seal area. Oil is available at this location for lubricating the bearing. In addition, the same heat exchanger required by the seal can be sized to include the requirements of the bearing.

The radial bearing is a pivoted segmental type. The bearing members of this type are tiltable shoes or pads which rest on hard steel buttons mounted on the bearing housing. The shoes are free to form automatically a wedge-shaped oil film between the shoe surface and the rotating sleeve of the shaft. The pads are babbit-lined.

5.5 Bearing Journals

The journals for the hydrostatic bearings are integral with the shaft. This eliminates a fit and gives better alignment. The journal or sleeve is made so that it can be hard-surfaced. A sleeve is also used on the hollow shaft for the journal at the liquid level. This is also integral with the shaft and can be ground accurately.

There is also an oil lubricated radial bearing in the seal area. The journal for this bearing is a part of the seal sleeve. This will allow the journal to run true to the shaft, since only one centering fit is involved. The journal does not have to be hard-surfaced, since the pads are babbeted and oil lubricated.

5.6 Pump Shaft

The type of pump shaft has not changed significantly from the one described in the Phase A study. Only the changes will be mentioned here.

The journal that was at the bottom of the shaft has been moved to a location between the two impellers. The size of the shaft is different from the one in the Phase A study since the pump has become larger and the horsepower requirement has increased.

The shaft is much too long to be made in one piece. It has a coupling at approximately the normal liquid level. The shaft size changes at the coupling, the upper portion getting larger. The shafts are joined by a rigid flanged coupling, with male and female centering fits. The flanges are bolted.

The top of the shaft has a self-centering spline. The torque from the coupling to the shaft is transmitted through the spline. The axial load tending to separate the engagement of the spline is taken by a series of fasteners. The self-centering spline-type coupling used at the top end of the pump shaft gives good accuracy and maximum load-carrying capacity. The spline teeth are cut in the solid face at the end of the shaft.

A flange with a self-centering spline to match the one on the shaft is fastened to the top of the shaft. This flange serves a double purpose. It acts as a flanged pump half coupling. In addition, it is the fan for air cooling the oil circulating in the seal cartridge.

5.7 Spacer-Type Coupling

A coupling is required between the motor shaft and pump shaft. The coupling is a spacer type. When the coupling is removed, the seal cartridge assembly can be taken out of the pump without disturbing the motor. The coupling is flanged and bolted to the motor and pump shafts.

Since the thrust bearing is in the motor, the coupling must take the axial thrust load, including the weight of the pump rotating assembly. In addition, the coupling has some flexibility. This is made possible by a diaphragm at the bottom end of the coupling. The flexibility is not required for normal operation. It is a feature required only for emergency conditions causing severe deflections of the pump that affect the alignment. It is only then that the self-aligning feature is required. The coupling is designed to Byron Jackson requirements by an experienced and well-known coupling manufacturer.

5.8 Driver Mount

The driver mount or motor support is a separate fabrication that is centered and bolted to the outer cylinder. It has openings of sufficient size to allow assembly and dismantling of the coupling and seal. The spacer type coupling can be removed. The top of the driver mount can be designed to accept a motor flange with outside or inside bolts. Interface between motor and driver mount will be worked out by mutual agreement.

The fixture for removing the coupling and seal cartridge will be fastened to the top flange of the driver mount. This fixture will be removable.

5.9 Seal Cartridge

The seal cartridge includes the two mechanical seals mounted back-to-back, the pumping ring, the oil lubricated radial bearing, and the air to oil heat exchanger. Where possible, some of the parts are made of aluminum alloy to keep the weight of the cartridge down for handling. The seal cartridge is made for convenient servicing. The seal is locked in the running position during handling, to eliminate possible damage.

A fixture will be furnished for convenient removal of the spacer coupling and seal cartridge assembly. The fixture will be temporarily fastened to the top flange of the driver mount. The spacer coupling and then the seal cartridge can be lifted and moved horizontally on rails to the outside of the driver mount. They can then be transferred to a service hoist. The fixture can of course be used for the replacement of the seal cartridge and spacer coupling. All of this is done without the removal of the motor.

6.0 Pump Material Selection

Materials of construction utilizing 2¼% Cr-1Mo; Type 304 or 316 S/S and/or 9Cr-1Mo may be used for the Pool-Type LMFBR pumps operating at 600°F in sodium. The choice of ferritic versus austenitic stainless steels would be dependent on a number of different factors, such as:

1. The lower alloy content of 2¼Cr-1Mo steel will have a lower base metal cost than the higher chromium or chrome-nickel stainless steels, especially for plate, bar, pipe and forgings, but not for castings. The lower base metal cost for wrought products is based on the assumption that the required quantity is sufficient for a mill heat and/or the required quality is available at the warehouse. Castings of 2¼Cr-1Mo will normally not result in any cost savings since the foundry problems result in costs almost equal to the cost of high alloy materials.

   Although it appears that 9Cr-1Mo has some desirable characteristics it is really too early to determine foundry and mill problems that may be incurred, it is also unknown at this time what fabrication problems may be revealed.

   The ferritic materials, including weld filler metals, will be required to meet fracture toughness of the ASME Nuclear Component Code. This requirement will narrow the cost gap between the ferritic and austenitic stainless steels, since fracture toughness is not mandatory for the latter materials.

3. The ASME Nuclear Component Code and the Elevated Temperature Code cases require that ferritic materials be preheated and post-weld heat treated. This requirement adds to manufacturing costs due to the added costs for weld qualifications and manufacturing time over that of austenitic stainless steels.

4. Cleaning costs will be higher for ferritic materials. The greater rusting problem, in atmosphere and/or during testing will require that positive anti-rusting precautions must be maintained at all times, including protection at the job site.

5. Hydraulic requirements normally dictate a design that has complex geometries. The geometries required may be obtained by such very expensive methods as (1) chemical milling; (2) contour (template) milling; precision machining; (3) precision weld fabrications and/or a combination of such methods. Historically the pump manufacturer has used static or precision castings which permits the procurement of complex geometries of acceptable quality and at a very considerable decrease in cost and procurement time.

   Material costs for ferritic steel castings, if obtainable, will probably be 2 to 3 times the cost of austenitic stainless steels, due to (a) lower demand, therefore higher cost; (b) more exacting manufacturing controls required; (c) many more foundry problems with ferritic materials; (d) maintenance of cleanliness, and (e) special procurement due to limited sources.

In summary, it is apparent that the major consideration has to be economic rather than technical. The existing state-of-the-art available for austenitic stainless steels presents no new problem areas whereas the use of ferritic materials could pose several areas requiring development programs.

After evaluation of all factors, fabrication, heat treatment, material procurement and cleanliness, it is our opinion that the pool-type pump be constructed of austenitic stainless steel.

7.0 COMMENTS ON REVIEW OF LMFBR PUMP DESIGNS

A study for a conceptual pump design for a pool type reactor was submitted to General Electric by Byron Jackson for Phase A.

An engineering design review of this pump was made by Elemer Makay, a consultant, for EPRI, dated August 31, 1978. The consultant's comments are respected and appreciated. This is an attempt to comment on some of the reviewer's concern.

It should be understood that this was a conceptual design study limited by time and budget. Some of the suggested design changes were made for the present pump study before the consultant's report was received, particularly in the dynamics and critical speed areas.

The first concern is about the basic design concept of two stages of a double suction impeller pumping in parallel. The report explains why this unique concept was selected. It lends itself particularly well to the pool type concept where all the suction inlets are flooded.

Attached separately is a Sectional Drawing D-1F-1066 showing a pump with four double suction impellers pumping in parallel. Two four-impeller and two three-impeller pumps of this type were built, tested, and are in service. Pertinent facts are shown with the Sectional.

A photograph is also enclosed showing a pump used on a hydrofoil. This pump has two double suction impellers pumping in parallel. Two of the suction nozzles are on the near side and the other two on the far side.

It is certainly agreed that careful and diligent design is required for the pump inlet geometry. A wood and plastic model has been made and tested with air for the DOE Large Scale LMFBR Pump Development Program. Results show that the suction inlets divide the flow evenly, though the suction nozzle is at the bottom of the pump. The report on this air test has been submitted to Argonne National Laboratory and is available.

The concern about axial thrust is one that is inherent in any multi-stage pump. It does not affect pump performance, only the size of the thrust bearing. The wear rings can be sized to give an upthrust that will help balance the rotor dead weight. A page from the report on axial thrust is enclosed.

The structural and dynamic analysis concludes that there are no insurmountable problems with the conceptual design. It should be understood that a design layout is made first and then analyzed. The results of the analysis may indicate certain changes that can be made to obtain satisfactory performance. For example, a bearing may be re-located or its size changed, the shaft size changed, or a bearing span altered. With these changes, the design concept would be acceptable.

Some of the suggested changes are being added to the present redesign of the pump.

The consultant asks for clarification regarding the NPSH test of the Clinch River model. This was only cited as an example. A half scale model of the Clinch River double suction pump was made and tested. The NPSH required, as measured by Hydraulic Institute standards, was 36 feet. This is the method based on a 3% loss of pump head. The model size and speed are selected to give the same head and NPSH as required by the prototype. No mention is made of cavitation. It is merely shown that for the prototype, there would be a safety margin between the required and the available NPSH. Available NPSH for the Clinch River prototype is 53 feet. The safety margin is from 36 to 53 feet, or about 147%.

The consultant indicates that the NPSH required for cavitation-free operation is 54 feet, or 150% of the 36 feet obtained by test. He infers that this safety margin is necessary to avoid cavitation erosion of the impeller eye during commercial operation. It can be seen that the example shown in the study has this margin.

For the present study a greater NPSH safety margin is used at the design or best efficiency point. This is where the pump will operate during most of its life expectancy. Lower flows will be less prone to cavitation damage.

For the runout condition, where the flow could be 116% of the design point, the safety margin is less. However, operating time at runout flow should be a small percentage of the pump life expectancy. Cavitation damage, if any, should be minimal, since it is a function of time.

Pumps with multi-stage double suction impellers pumping in parallel.

1. Size: 36 x 40 x 68 Double Suction

   4 Stages in Parallel

   Sectional Drawing D-1F-1066

   Two of these pumps were built and tested in B.J. Holland.

   User: Shell International, U.K.

   Liquid: Crude oil, with intermittent quantities of seawater.

   Four stages in parallel were used to meet the low NPSH requirement. Each stage is a double suction impeller pumping one-fourth of the total flow against the full discharge head.

   These are vertical pumps with a suction tank and underground suction. The pump is an axially split design. The suction tank is about 68" diameter. The suction is flooded, all impeller inlets being exposed to the liquid in the suction tank.

   These pumps were tested early in 1976. They have been operating in the field since then.

   Design Conditions: (4 Stage)

Capacity	44,000 GPM (total)
Head	250 ft (Sp. Gr. = 0.85)
Speed	1480 RPM (50 cy.)
NPSH	20 ft. (approx.)
Specific Speed	2460
Suction Specific Speed	16,500
BHP	2800

   Impeller Dia. - design 23½" , test 20-3/4".

2. Same pumps as above, except three stages in parallel. Two of these pumps were built and tested, for the same user as above.

Design Conditions: (3 Stage)

Capacity	22,000 GPM (total)
Head	269 ft.
Speed	1480 RPM
NPSH	16 feet
Specific Speed	1920
Suction Specific Speed	16,000
BHP	1800

Impeller dia. - design 23½" , test 20".

3. A foilborne propulsion pump was built and tested for use in a hydrofoil ship. It is a pump with two stages of double suction impellers pumping in parallel. Sectional Drawing 1F-6373 and photograph are enclosed. Liquid being pumped is sea water. Pump is axially split. The user was Boeing Company.

Design Conditions:

Capacity	28,000 GPM (total)
Head	560 ft.
Speed	1560 RPM
Specific Speed	1600
BHP	5000 (approx.)
Discharge Nozzles	10" Dia. (two)
Suction Nozzles	12" Dia. (two)
Impeller dia. design	28"

The NPSH varies with the speed of the hydrofoil.

This type of application for a pump is unique. The examples given, however, show that they can be made to operate satisfactorily.

Table No. 1

TABULATION OF
VARIOUS PUMP SPEEDS

	Single Stage	Two Impellers in Parallel		
	PUMP SPEED RPM			
	725	870	1000	1180
	Variable	Variable Constant	Variable	Variable Constant
Pump Discharge Flow - GPM	68,450			
Total Developed Head - FT	316			
NPSH Available - FT	38	40	45	38
Temperature - ^{o}F	595			
Specific Speed - N_s	2,550	2,150	2,490	2,900
Suction Specific Speed, Design. S_s	12,400	10,000	12,100	12,500
Suction Specific Speed, Runout. S_s	13,400	10,900	13,000	13,500
Pump Efficiency %	78	78	78	78
Required Pump Power (Cold) H.P.	7000			
Required Pump Power (Hot) H.P.	6150			
Impeller Diameter Inches	49½	42	36	32
Tank Diameter Inches	85	75	70	66
Pump Length Feet	45	46'-3"	45'-3"	52'-3"

AXIAL THRUST REQUIREMENTS

The pump does not have a bearing for carrying an axial thrust load. It depends on the thrust bearing used in the motor. The motor supplier must design the bearing to carry the additional load required by the pump.

The weight of the pump rotating element is estimated to be 16,000 lbs. This is of course an axial downthrust, static and at all speeds.

Double-suction impellers are theoretically balanced axially. However, actually an axial thrust is possible. This is due to slight differences in pressure on the upper and lower sides of the shrouds. This is at least in part due to the difference in actual running position between the rotating shroud and the adjacent stationary wall for the two sides of the impeller. With two impellers, this could balance out. If assumed to be additive, the axial thrust could be 15,000 lbs. in either direction. This is with the pump running at full speed. Since this load is a function of pressure, it is also a function of speed. The downthrust requirement would be lower for the slow speeds. The motor thrust bearing must be sized to take the highest load required by the pump.

The upthrust due to pressure at the impellers will not be high enough to overcome the dead weight of the pump rotating element. Even though the pump requires no axial upthrust on the motor bearing, it is anticipated that the motor thrust bearing will be designed to take some load in that direction. This is for protection due to sudden unforeseen thrust surges either by the pump or the motor rotor.

Table No. 2

WEIGHT OF MAJOR SUBASSEMBLIES

	NAME	WEIGHT, LBS.
1.	Pump Volute and Discharge Manifold	17,000
2.	Top Suction Piece	1,500
3.	Middle Suction Piece	2,000
4.	Sliding Valve	2,400
5.	Hydrostatic Bearing (Split)	1,100
6.	Lower Pump Tank	25,000
7.	Upper Pump Tank and Driver Mount	38,000
8.	Insulation Assembly	2,400
9.	Seal Assembly	2,000
10.	Rotating Assembly	13,000
	Total	104,400

Weights do not include sodium,insulation, or steel shot.

Table No. 3

PARTS LIST AND MATERIALS OF CONSTRUCTION

PRIMARY SODIUM PUMP FOR POOL TYPE CONCEPT
B.J. ORDER NO. 781-G-0500
REFERENCE DRAWINGS: 1F-8435, 1F-7589

PART NO.	QTY	NAME	MATERIAL SPECIFICATION
1		Volute Assembly	
1-1	1	Volute and Discharge Manifold	ASME SA-351 GR. CF8
1-2	1	Valve Housing	ASME SA-351 GR. CF8
2		Suction	
2-1	2	Middle Suction Piece (Split)	ASME SA-351 GR. CF8
2-2	1	Upper Suction Piece (Split)	ASME SA-351 GR. CF8
2-3	1	Hydrostatic Bearing (Pump)	ASME SA-351 GR. CF8 with Colmonoy #5 Overlay
3		Rotating Element Assembly	
3-1	1	Lower Impeller	ASTM A-351, GR. CF8
3-2	1	Upper Impeller	ASTM A-351, GR. CF8
3-3	1	Journal	ASTM A-213, Tp. 304 with #6 Colmonoy Overlay
3-4	1	Shaft Tube	ASTM A-213, Tp. 304
3-5	1	Top End - Shaft	ASTM A-182, Gr. F304
4		Middle Structure Assembly	
4-1	1	Bottom Flange	ASME SA-240, Tp. 304
4-2	1	Cone	ASME SA-240, Tp. 304
4-3	2	Bearing Support	ASME SA-240, Tp. 304
4-4	1	Hydrostatic Bearing (Middle)	ASME SA-182, GR. F304 with Colmonoy #5 Overlay
4-5	1	Top Flange	ASME SA-240, Tp. 304
4-6	1	Tube - Bearing Supply	ASME SA-213, Tp. 304
4-7	1	Insulation Container	ASME SA-240, Tp. 304

PART NO.	QTY	NAME	MATERIAL SPECIFICATION
5		Upper Structure Assembly	
5-1	1	Outer Cylinder	ASME SA-240, Tp. 304
5-2	1	Inner Cylinder	ASME SA-240, Tp. 304
5-3	1	Top Plate	ASME SA-240, Tp. 304
5-4	1	Bottom Plate	ASME SA-240, Tp. 304
5-5	1	Mounting Flange	ASME SA-240, Tp. 304
5-6	1	Seal Leakage Tank	ASME SA-240, Tp. 304
6		Driver Mount Assembly	
6-1	1	Lower Flange	ASTM A-240, Tp. 304
6-2	1	Cylinder	ASTM A-240, Tp. 304
6-3	1	Top Flange	ASTM A-240, Tp. 304
7		Valve Assembly	
7-1	1	Valve	ASME SA-351, GR. CF8
7-2	2	Valve Rods	ASTM A-479, Tp. 304
7-3	2	Valve Tubes	ASTM A-213, Tp. 304
8		Pump Coupling	
8-1	1	Spacer Type Coupling	ASTM A-322, Gr. 4140
8-2	1	Coupling Flange and Fan	ASTM A-240, Tp. 304

PART NO.	QTY	NAME	MATERIAL SPECIFICATION
12		Seal Cartridge Assembly	Reference Drawing 1F-7589
12-1	1	Seal Flange - Upper	ASME SA-182, GR. F304
12-2	1	Seal Flange - Lower	ASME SA-182, GR. F304
12-3	1	Seal Housing Assembly	ASTM A-240, Tp. 304
12-4	1	Seal Sleeve and Pumping Ring	ASTM A-182, GR. F304
12-5	1	Stand Pipe	ASTM A-182, GR. F304
12-6	2	Retainer	ASTM A-182, GR. F304
12-7	2	Rotating Face	Carbon
12-8	2	Stationary Face	316 SST with #1 Stellite Overlay
12-9	2	U-Cup	Nitrile
12-10	2	U-Cup Follower	304 SST
12-11	72	Spring	Inconel X-750
12-12	1	Drive and Thrust Collar	ASTM A-182, GR. F304
12-13	1	Split Locating Collar	ASTM A-182, GR. F304
12-14	2	Locating Pin (Removable)	ASTM A-193, GR. B6
12-15	1	Fan Cover	ASTM A-240, Tp. 304
12-16	2	Pumping Ring Bushing	ASTM A-182, GR. F304
12-17	1	Radial Bearing	Commercial
12-18	1	Seal Heat Exchanger	Aluminum 6061-76

P200R

BYRON JACKSON

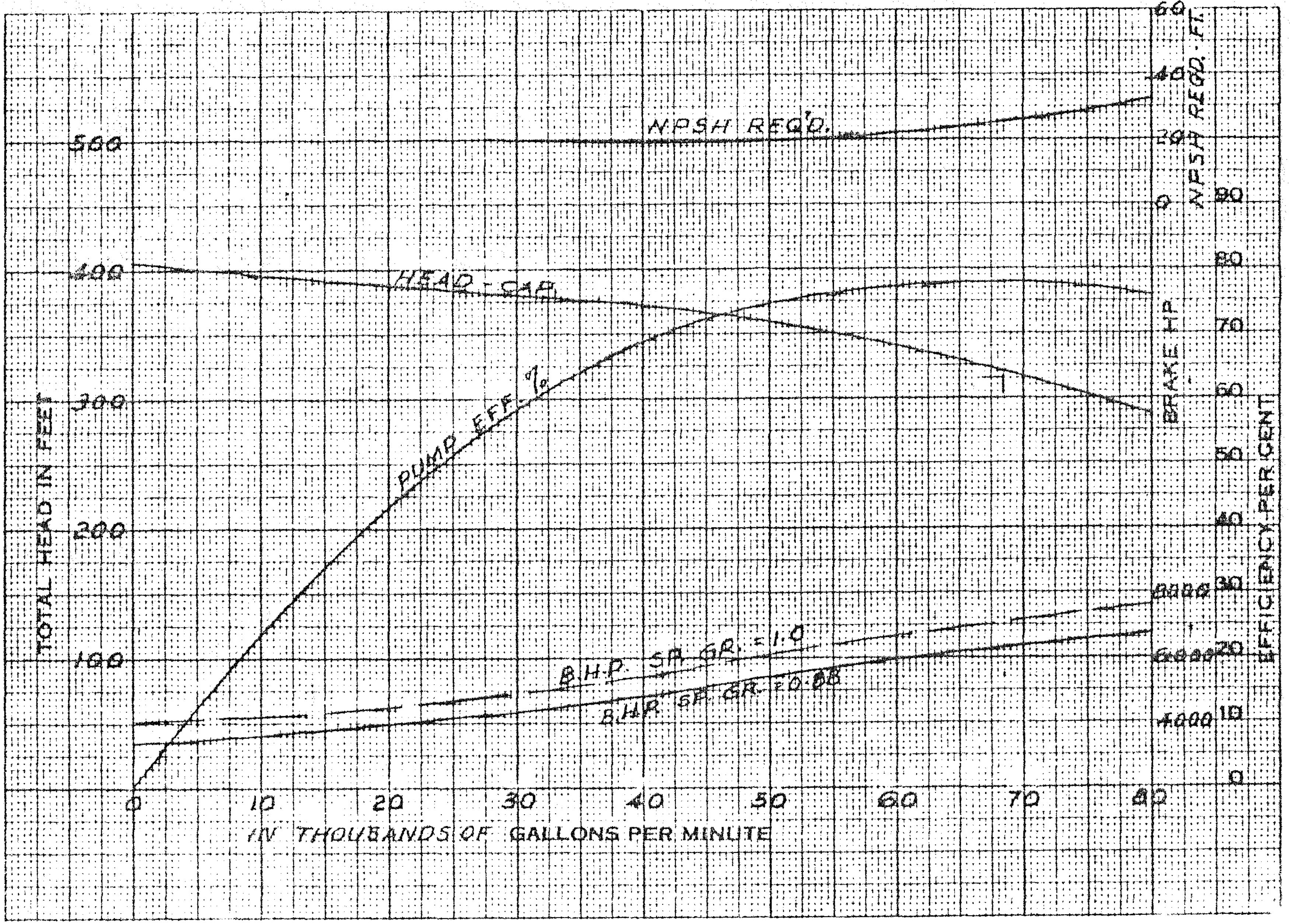

PUMP SIZE AND TYPE	RPM	CUSTOMER NO.	IMPELLER NO.	BASED ON	CASE	BYRON JACKSON NUMBER
36 × POOL × 42 D.S. TWO STAGES IN PARALLEL	870	G. S. 781-G-0500	R-3671	1-32×24×30×32 DVS		PC-33971
			BRANCH NO.	DATA BY W. S.	DRAWN BY S.W. 11-30-78	

VE-30

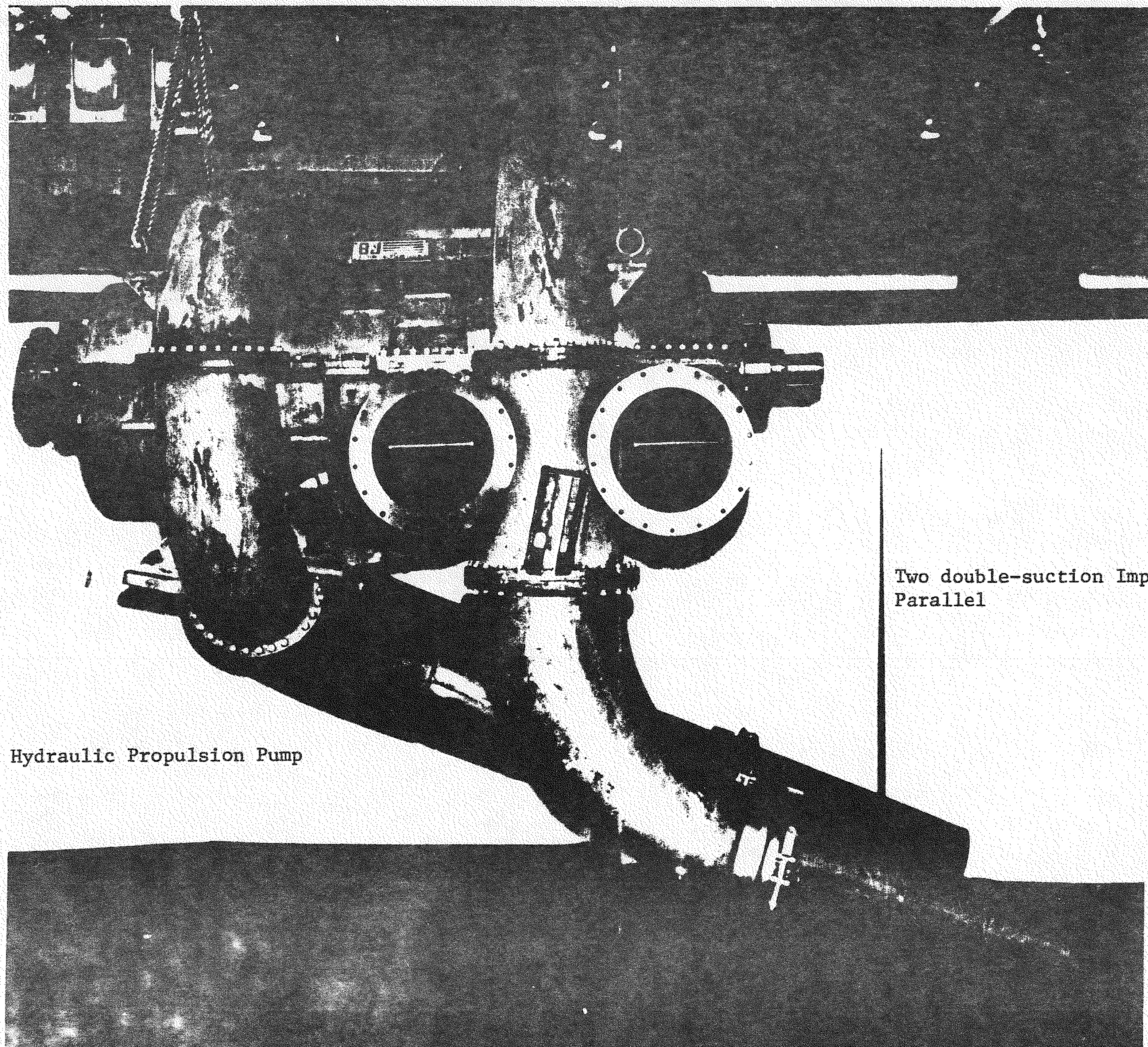
Two double-suction Impellers in Parallel
Hydraulic Propulsion Pump

BJ ORDER NO. 781-G-0500	REF. NO	BORG WARNER BYRON JACKSON® BORG-WARNER CORPORATION
DRAWN BY S WINSTEIN	DATE 12-5-78	DRAWING TITLE PRIMARY SODIUM PUMP POOL TYPE CONCEPT
CHECKED BY	DATE	
DESIGN APP'D BY	DATE	CONTRACT NO.
TITLE		
CUSTOMER APP'R		CODE IDENT. NO. / DRAWING NO. 2F-1761 / REV.
		SCALE 3/4" = 1'-0" / WEIGHT / SHEET VB-33

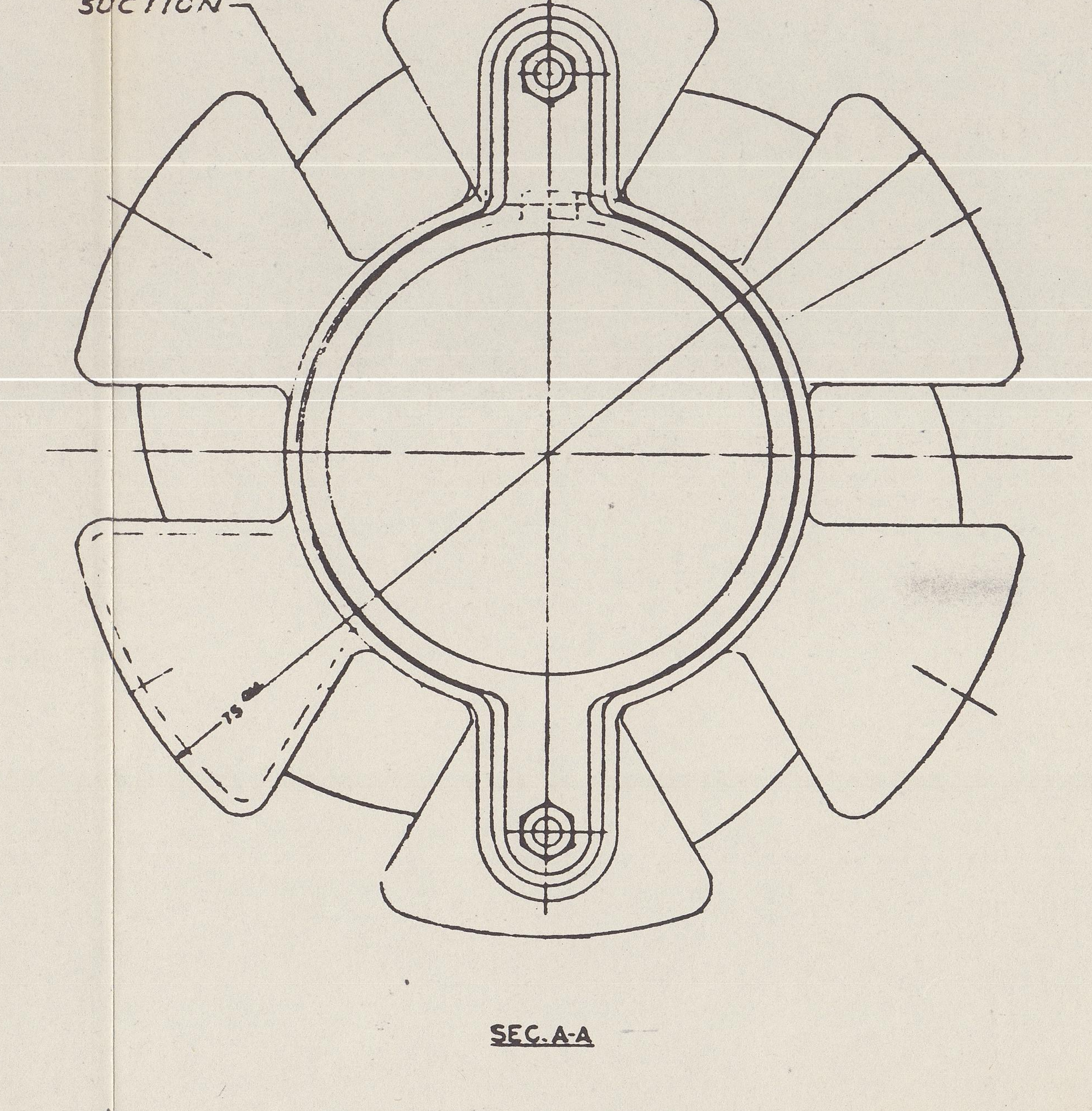

SEC. A-A

BYRON JACKSON®

BORG WARNER CORPORATION

F-8433

VB-34

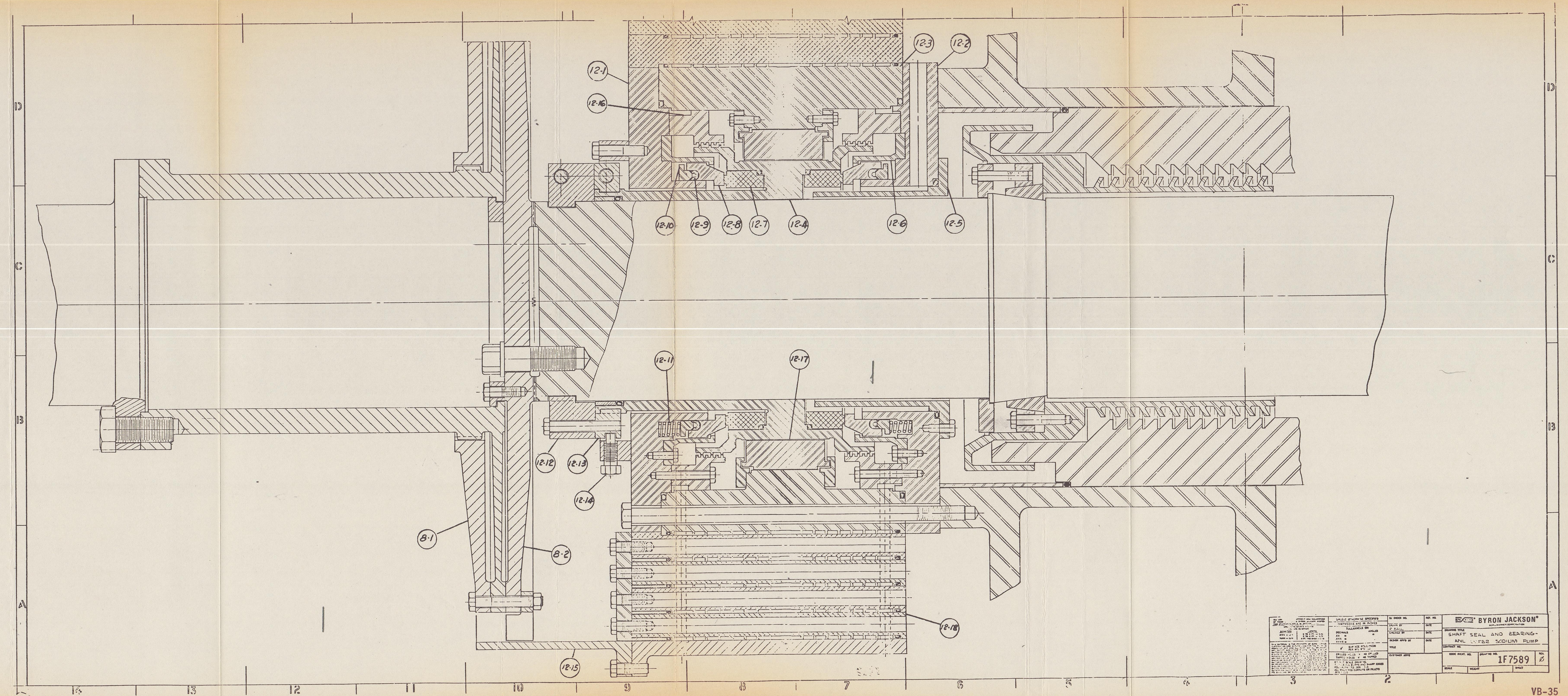

12-1
12-16
12-3
12-2
12-10
12-9
12-8
12-7
12-4
12-6
12-5
12-11
12-17
12-12
12-13
12-14
8-1
8-2
12-18
12-15
UNLESS OTHERWISE SPECIFIED
DIMENSIONS ARE IN INCHES
TOLERANCES ON
DECIMALS
ANGLES
DRILLED HOLES AS DRILLED
TAPPED HOLES AS TAPPED
DO NOT SCALE DRAWING
BJ ORDER NO.
REF. NO.
DRAWN BY
DATE
CHECKED BY
DESIGN APP'D BY
TITLE
CUSTOMER APP'R
BYRON JACKSON
BORG-WARNER CORPORATION
DRAWING TITLE
SHAFT SEAL AND BEARING-
ANL LMFBR SODIUM PUMP
CONTRACT NO.
CODE IDENT. NO.
DRAWING NO.
1F7589
REV.
Ø
SCALE
WEIGHT
SHEET

VB-35

RUNNING CLEARANCES
A 016"/ 018"
B .030"/ 034"
C 024"/ 026"
D 012 / 014

DOUBLE SUCTION IMPELLERS
FOUR STAGES IN PARALLEL

BYRON JACKSON DIVISION OF BORG WARNER B.V.

D-1F-1066

VB-36

Pool-Type LMFBR Plant
1000 MWe Phase A-Extension-2 Design

CONTENTS